Macroevolutionary patterns and drivers of morphological diversification in mammalian forelimbs

Priscila S. Rothier

MUSEUM NATIONAL D'HISTOIRE NATURELLE
Ecole Doctorale Sciences de la Nature et de l'Homme – ED 227

Année 2023 **N°attribué par la bibliothèque**

|_|_|_|_|_|_|_|_|_|_|_|_|

THESE

Pour obtenir le grade de

DOCTEUR DU MUSEUM NATIONAL D'HISTOIRE NATURELLE

Spécialité : Biologie évolutive

Présentée et soutenue publiquement par

Priscila S. Rothier

Le 07 Juillet 2023

Mécanismes macro-évolutifs et déterminants de la diversité morphologique des membres antérieurs des mammifères

---

Sous la direction de : **Anthony HERREL**, Directeur de Recherche

JURY :

Dr Géraldine VERON	**Professeure, Muséum National d'Histoire Naturelle, France**	**Présidente**
Dr Anthony HERREL	**Directeur de Recherche, Muséum National d'Histoire Naturelle, France**	**Directeur de Thèse**
Dr Bruno FRÉDÉRICH	**Chargé de cours, Université de Liège, Belgique**	**Rapporteur**
Dr Sharlene SANTANA	**Professeure, University of Washington, Etats-Unis**	**Rapportrice**
Dr Raphaël CORNETTE	**Assistant ingénieur, Muséum National d'Histoire Naturelle, France**	**Examinateur**
Dr John NYAKATURA	**Professeur, Humboldt-Universität zu Berlin, Allemagne**	**Examinateur**

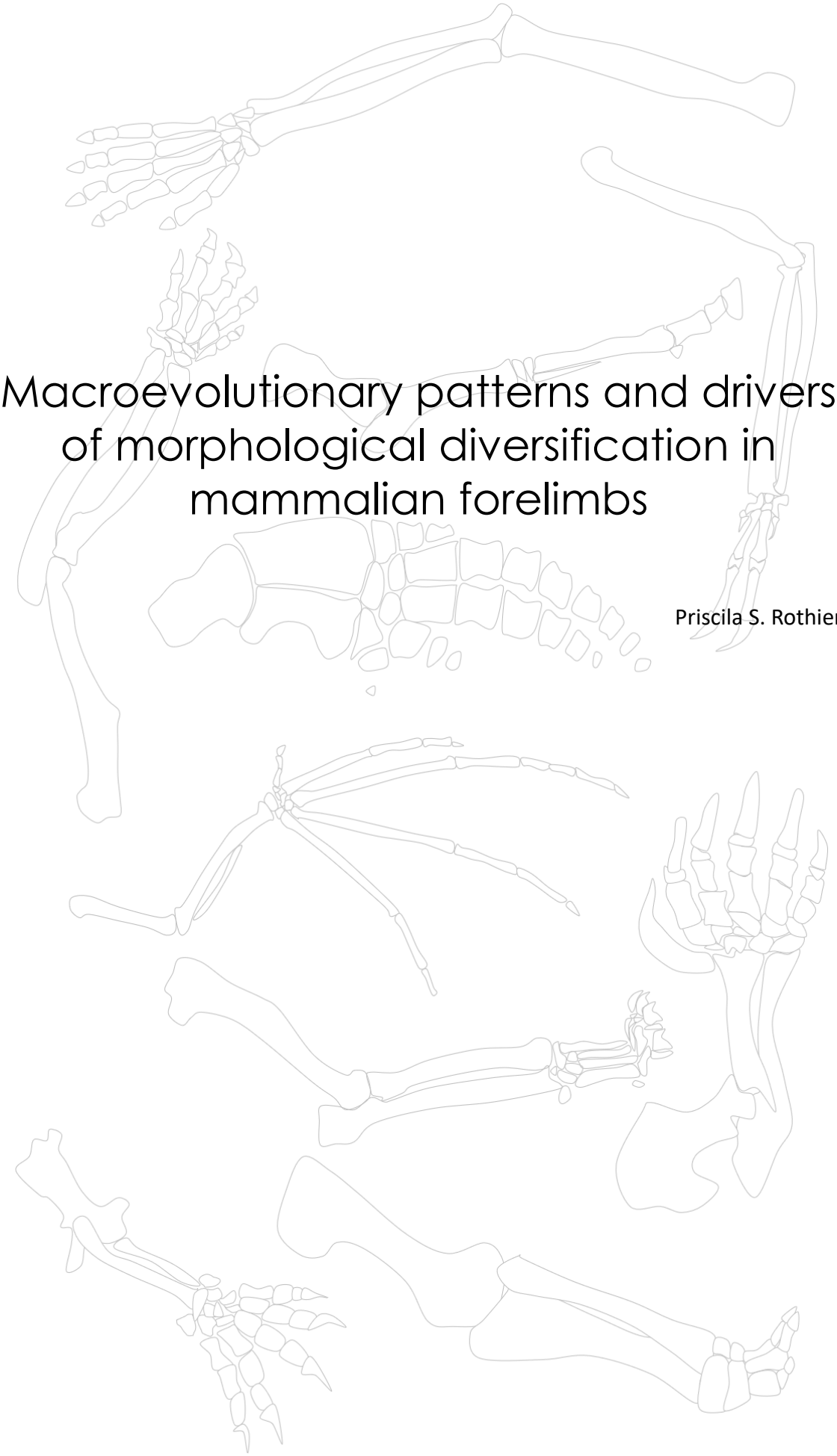

Macroevolutionary patterns and drivers of morphological diversification in mammalian forelimbs

Priscila S. Rothier

To all the mammals – humans and otherwise –
that made this work possible.

Acknowledgements

In times like these, I believe that doing science and treasuring the natural world is a powerful act of resistance. In addition to the usual challenges of producing a thesis, the research detailed in the next pages was conceived in an environment where anti-democracy and scientific denial were dictating the rules. The years that followed were marked by worldwide fear and sorrow, and the only reason this thesis thrived was due to the collective support of many incredible people. I am immensely grateful to all those who have resisted by my side and made this work possible.

Firstly, I would like to thank my supervisor, **Anthony Herrel**, for your guidance and patience during this journey. Thank you for sticking with my megalomaniac ideas! I am forever mesmerized by your superhuman power to balance a mind-blowing scientific production with such kindness and prompt support for anyone in need. I am very thankful for the way you supervised and improved this work, and for all our chats that have never failed to cheer me with your enthusiasm and positivity. You are a great inspiration to me as a scientist and as a human being.

Chapters 2 to 4 were developed in collaboration with many researchers, to whom I extend my heartfelt gratitude. Specifically, I would like to thank **Anne-Claire Fabre** for the collaboration and friendship. You have taught me so much! Thank you for always being willing to lend a hand, coming up with great ideas and opportunities, and for supporting and trusting in my work. I would also like to thank **Roger Benson** for his valuable contributions, including providing hundreds of digitized specimens and always engaging into pertinent discussions about the methods and the findings. Many thanks to **Julien Clavel**, who has always been so patient and kind in explaining the analyses and assisting with the coding. I would also like to thank **Quentin-Martinez** and **Pierre-Henri**

Fabre, who have made insightful comments and have helped with the digitalization of many specimens used in this work. I also extend my gratitude to my dear old friend **Vinicius Anelli**. I am so grateful to pursue my academic path so closely to yours, finding space to discuss life and aspirations amidst papers and analyses. Thank you for your valuable input in this thesis and for your friendship. I would also like to thank **Pedro Lorena Godoy** for his generous help with the methods, and for enthusiastically engaging in discussions about career, research and life.

Thank you so much to the following collection managers for their support during data acquisition: at the MNHN, **Aude Lalis**, **Aurélie Verguin**, **Céline Bens**, **Géraldine Veron**, **Jacques Cuisin**, **Joséphine Lesur** and **Violaine Colin**; at the AMNH, **Eleanor Hoeger**, **Marisa Surovy** and **Sara Ketelsen**; at the NHM, **Roberto Portela** and **Richard Sabin**. I also thank **Renaud Lebrun** for assisting with the CT scanning at the ISEM. Many thanks to **Silvia Castiglione** for the assistance with her R package. I also acknowledge **Anjali Goswami**, **Helder Gomes Rodrigues** and **Eric Guilbert** for their engagement during my thesis committee meetings and for their insightful contributions for the elaboration of this study. Thanks to **David Grossnickle**, **François Gould** and to an anonymous reviewer who have substantially contributed to improve the discussion of the paper that originated Chapter 2.

I would like to express my special thanks to **Tiana Kohlsdorf**, who mentored me during the early stages of my career as a biologist and played a pivotal role in training and encouraging me to pursue a PhD. It was a privilege to take my first academic steps under your guidance, and I am grateful that our collaborations have continued to flourish. I deeply value and appreciate your advice, and I am immensely thankful for your continuous support in my personal and professional development.

To my lab colleagues, thank you for the companionship and for your warm support: **Laurie Araspin**, **Soline Bettencourt**, **Loïc Kéver**, **Pablo Padilla** and **Jaleh Sarafraz**. Paris got much happier with you around – specially with **Alfred** and **Hannibal**. Thanks to my former co-bureaux and many other team colleagues for the good humor and patience while helping me transitioning to a new country and learning a new language: **Colline Brassard**, **Cyril Etienne**, **Rémi Lefebvre**, **Christophe Mallet**, **Rohan Mansuit**, **Fanny Pagès**, **Julie Soppelsa**, **Ana Phelippeau**, **Maxime Taverne**, **Marie Verheye**, **Romain Pintore**, and many others.

To my family, words can never describe my love and gratitude. To my **mother** and my **father**, thank you for your warmth and for always having encouraged me, even when my choices led me across the ocean. To my **sister**, thank you for your generosity, wisdom and friendship. To my **grandparents**, thank you for the love and for the tireless support. To my **aunt** and **cousins**, thank you for the joy and affection. To my all dear friends, whether in Brazil, France, and anywhere else, thank you for being there (you know who you are!). To **Antonin**, thank you for the beautiful partnership we share and for always believing in and encouraging me. Thanks to the **Benisti family** for warmly welcoming me, making me feel at home in this foreign beautiful – although a bit cold – country.

Finally, I would like to express my sincere gratitude to the Conselho Nacional de Desenvolvimento Científico e Tecnológico (CNPq) for having funded my PhD project (process #204841/2018-6).

Table of contents

List of figures

List of tables

Abstract

Morphological diversification is a complex process influenced by several factors, including the habitats where lineages diversify, ecological variation, developmental divergence, phylogenetic history, and chance. In this context, the vertebrate limb is an appealing system to explore the evolutionary drivers of trait diversification as it displays a remarkable morphological diversity that facilitated the dispersal of vertebrates in terrestrial environments, marking the onset of the adaptive radiation of Tetrapoda. In mammals, the morphological diversity of limbs ranges from paws to wings, flippers, hooves, and much more, and the morphology of the forearm is often suggested to be linked to the radiation of mammals into almost every habitat in the world. The objective of this thesis was to investigate the patterns of morphological evolution of the mammalian forelimb, elucidating the role of intrinsic and extrinsic drivers of morphological diversity within traits and between groups. Using phylogenetic comparative methods, a comprehensive morphological dataset of forelimb skeleton was compiled. Initially, forearm morphology was examined in terms of variation between bone segments and their timing of development. Subsequently, phenotypic variation between mammalian lineages was explored, with a focus on the influence of physical constraints associated with habitat use on forelimb disparity. Finally, the evolution of locomotor ecologies and their impact on evolutionary patterns of forelimb diversification in mammals were also investigated. The key findings of this thesis reveal that morphological variation within limb traits and between clades is uneven and influenced by ecological specialization to varying degrees. The timing of bone condensation was found to predict skeletal diversity throughout Mammalia, but developmental sequence alone does not explain all aspects of bone variation. The results suggest that the medium used for locomotion has a significant

impact on the forelimb skeletal disparity across mammal lineages, and that locomotor ecologies strongly shaped the tempo and mode of morphological evolution of the arm. The novel and insightful findings presented in this thesis significantly advance our understanding of clade-level diversity within Mammalia. Moreover, these findings shed light on the macroevolutionary patterns underlying trait diversification and provide valuable insights into the evolutionary dynamics of limb structures across different clades and ecologies.

Key-words: disparity, morphometrics, ecology, development, phenotypic convergence

Résumé

La diversification morphologique est influencée par plusieurs facteurs, comme l'habitat où les lignées se diversifient, les variations écologiques, la divergence de développement, l'histoire phylogénétique et le hasard. Dans ce contexte, les membres des vertébrés offrent un système particulièrement intéressant pour étudier les processus évolutifs qui génèrent la diversification des traits phénotypiques. Les membres présentent une diversité morphologique remarquable qui a favorisé la dispersion des vertébrés dans les environnements terrestres, marquant ainsi le début de la radiation adaptative des tétrapodes. Chez les mammifères, la diversité morphologique des membres comprend les pattes et les ailes, en passant par les nageoires, les sabots et bien plus encore. Cette variation est souvent suggérée comme étant liée à leur radiation dans presque tous les habitats du monde. L'objectif de cette thèse était d'étudier les modes d'évolution morphologique des membres antérieurs des mammifères, en élucidant le rôle des facteurs intrinsèques et extrinsèques qui sous-tendent la diversité morphologique entre les structures anatomiques et entre les groupes. En utilisant des méthodes comparatives phylogénétiques, un ensemble complet de données morphologiques de squelettes de membres antérieurs a été compilé, comprenant plus de 800 espèces et représentant 97,5 % des familles de mammifères existantes. Il s'agit de l'ensemble de données morphologiques sur les membres le plus complet du point de vue taxonomique jamais collecté pour les mammifères. Dans un premier temps, la morphologie de l’avant-bras a été examinée notamment la variation entre les segments osseux et leur séquence de développement. Par la suite, la variation phénotypique entre les lignées de mammifères a été explorée, en vue de déterminer l'influence des contraintes physiques associées à l'utilisation de l'habitat sur la disparité des membres antérieurs. L'évolution des écologies locomotrices et leur impact

sur les modes d’évolution des membres antérieurs chez les mammifères ont également été étudiés. Les principales découvertes de cette thèse révèlent que la variation morphologique entre les différents os du bras et entre les clades est inégale et influencée par la spécialisation écologique. Il a été constaté que le moment de la condensation osseuse prédit la diversité du squelette chez les mammifères, mais la séquence développementale n'est pas la seule explication. Les résultats suggèrent que le mode de locomotion a eu un impact significatif sur la disparité du squelette des membres antérieurs entre les lignées de mammifères. Aussi, les écologies locomotrices ont fortement déterminé le tempo et le mode d'évolution morphologique du membre antérieur. Les résultats novateurs présentés dans cette thèse font progresser de manière significative notre compréhension de la diversité au sein des clades des mammifères. En outre, ces résultats mettent en lumière les mécanismes macro-évolutifs qui sous-tendent la diversification des traits et fournissent des informations précieuses sur la dynamique évolutive des structures des membres à travers différents clades et écologies.

Mot clés : disparité, morphométrie, écologie, développement, convergence phénotypique

“Tudo em meu torno é o universo nu, abstrato, feito de negações noturnas. Divido-me em cansado e inquieto, e chego a tocar com a sensação do corpo um conhecimento metafísico do mistério das coisas.”

— Fernando Pessoa

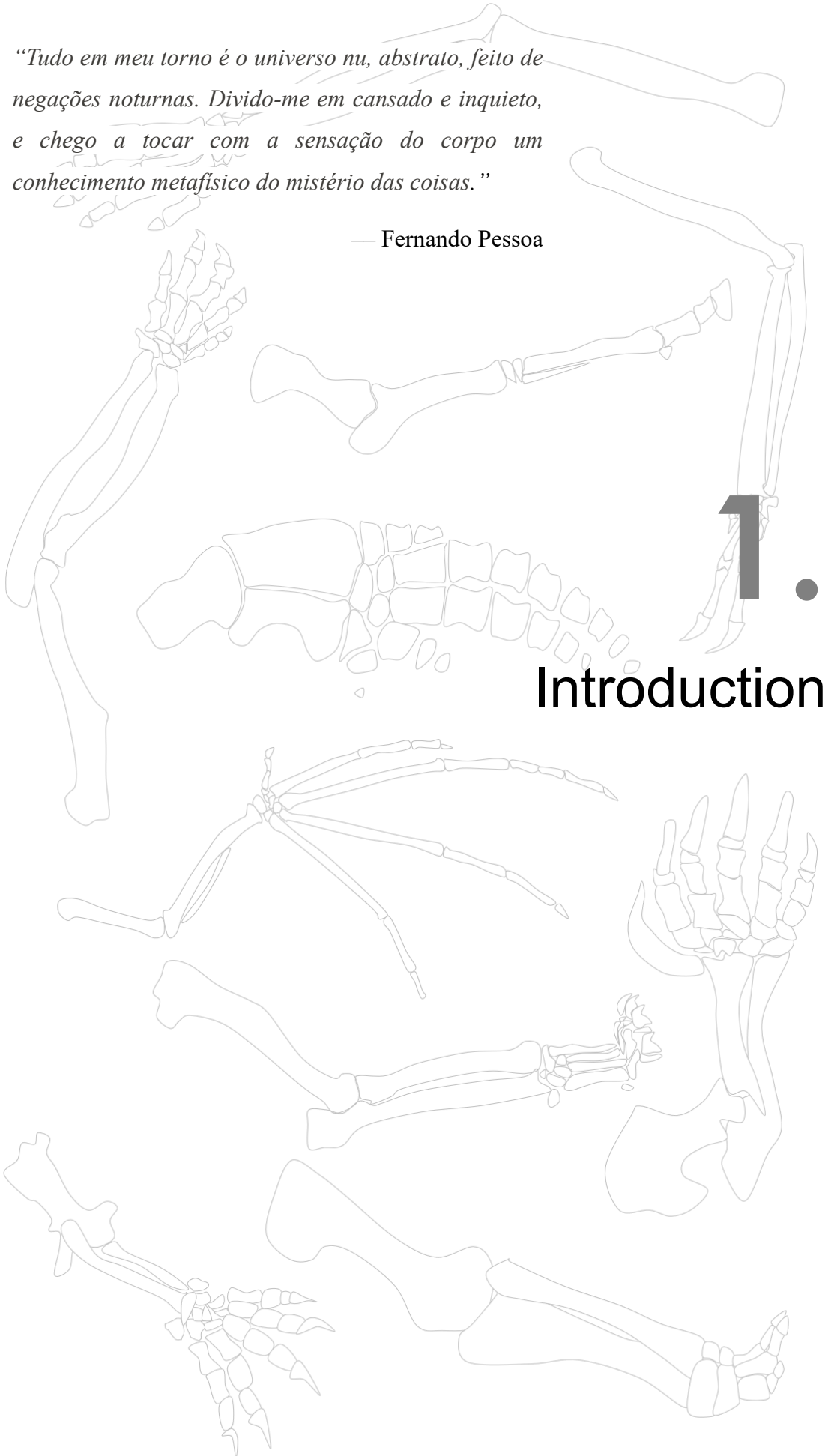

1. Introduction

1.1. The evolutionary drivers of morphological diversity

How have life forms come to be so distinct and complex? The splendor of morphological diversity of organisms has long fascinated the humankind and inspired evolutionary biologists to seek the origins and drivers of variation in a world where *endless forms most beautiful and most wonderful have been, and* are *being, evolved* (Darwin, 1859) After over a century accumulating an understanding on biological evolution, it is broadly recognized that diversity of organisms and their traits do not evolve uniformly throughout the history of life (Foote, 1997). In turn, the level at which trait diversity is being examined may impact the macroevolutionary patterns observed. Morphological diversification is subject of several overlapping factors, including the physical properties of the habitat where lineages diversify, ecological variation, developmental divergence, their underlying phylogenetic history, and pure chance (Raff, 1996). Hence, accessing biological diversity at its various levels and understanding how patterns of evolutionary change have been established is key to elucidate how distinct phenotypes and species are generated and maintained in nature (Adams, 2013).

The key determinant for organisms to thrive is determined by the way they interact with and endure in their changing environment, which is largely mediated by morphology (Arnold, 1983). Ecological specialization is then a central agent associated with the diversification of phenotypes, as it contributes to define selective agents in a given habitat and favors morphologies that interact in an adaptive manner with their surrounding environment (Schluter, 2000). How different lineages respond to similar ecological pressures, however, is highly dependent on intrinsic clade-specific factors, such as developmental variation. Through the investigation of convergent evolutionary patterns, we can better understand the interplay between functional specialization and such intrinsic constraints (Herrel et al., 2004; Losos, 2011).

The repeated independent evolution of similar forms is often used as an indicator of adaptive evolution as a result of external biomechanical constraints (Grossnickle et al., 2020; Losos, 2011; Mahler et al., 2013). The strongest examples of adaptive convergence emerge from the understanding that certain design "problems", such as overcoming mechanical limitations imposed by physical laws, can only be tackled by a limited set of morphological outcomes (Bels & Russell, 2023). For example, sharks, ichthyosaurs and dolphins have independently evolved streamlined fusiform bodies that help reduce drag when swimming, overcoming the high density and viscosity imposed by the physical properties of water (Fish, 2023). On the other hand, independent lineages facing similar environmental challenges may not fully converge due to the limited range of evolutionary pathways allowed to depart from their ancestral forms (Bels & Russell, 2023; Herrel et al., 2004). In this case, diverging evolutionary trajectories under similar ecological pressures may contribute to the diversification of many different phenotypes (Losos, 2011), exemplified by labrid fishes that produce similar suction force despite their disparate jaw structures (Alfaro et al., 2005). This further highlights the fact that selection acts on the functional output of a system and not the underlying morphological features.

Intrinsic constraints can shape the underlying structure of covariation among traits. When traits change, they most often do so in unison with other sets of traits that share a common function and/or common genetic and developmental pathways (Cheverud, 1984, 1996; Felice et al., 2018; Klingenberg, 2008). Ultimately, the structure of covariation between traits can influence the outcome of evolutionary trajectories, either facilitating or constraining the evolution of interdependent traits (Goswami et al., 2014). For example, many studies found support for a conserved structure of covariation in the mammalian skull, reinforcing the idea that relatively stable ontogenetic pathways have driven cranial variation, despite the outstanding ecological diversity present in this group

(Goswami et al., 2014; Machado et al., 2018; Porto et al., 2009). In contrast, covariation between the fore and hind limbs is much more variable, albeit sharing same developmental programs (Schmidt & Fischer, 2009; Shubin et al., 1997; Young & Hallgrímsson, 2005). In quadrupedal placentals, fore and hind limb bones exhibit strong covariation and perform similar locomotor functions, but weak covariation between limbs is observed in the presence of functional specialization, such as flying in bats and brachiation in gibbons (Schmidt & Fischer, 2009; Young & Hallgrímsson, 2005). Fore and hind limbs also display weak integration across marsupials, which might be linked to developmental heterochrony and the delayed formation of the hind limb (Bennett & Goswami, 2011; Goswami et al., 2009; Kelly & Sears, 2011; Weisbecker et al., 2008). A consequence for morphological disparity is that the underlying structure of trait covariation can impact the pattern and pace of the evolution of morphological diversity.

In an attempt to provide an integrative approach to understanding the drivers of phenotypic disparity, it is then insightful to select morphological traits with known functional relevance. In vertebrates, several studies have investigated the evolution of body size (Alencar et al., 2017; Burin et al., 2023; Clavel & Morlon, 2017; Godoy et al., 2019; Price & Hopkins, 2015; Smith & Lyons, 2011), body shape (Friedman et al., 2020, 2021; Law, 2021; Maher et al., 2022; Skinner & Lee, 2009), head shape (Bardua et al., 2019, 2021; Barros et al., 2011; Fabre et al., 2020; Gomes Rodrigues et al., 2016; Goswami et al., 2022; Jones et al., 2015; Watanabe et al., 2019) and limb shape (Collar et al., 2010; Elissamburu & Vizcaíno, 2004; Fabre et al., 2014; Fabre et al., 2019; Herrel et al., 2002; Kelly & Sears, 2011; Kohlsdorf et al., 2001; Ledbetter & Bonett, 2019; Stepanova & Womack, 2020). Notably, the evolution of limbs marks the onset of the adaptive radiation of Tetrapoda, displaying a remarkable morphological diversity that facilitated de dispersal of vertebrates in terrestrial environments (Hall, 2007; Shubin et

al., 1997). The invasion of land has led to the exploitation of diverse ecological niches, favoring the evolution of range of locomotor morphologies including: scansorial habits involving climbing (e.g. squirrels and opossums); saltatorial gaits (e.g. kangaroos and frogs); aquatic (e.g., whales, ichthyosaurs, plesiosaurs) and semi-aquatic locomotion (partial locomotion on land, such as otters and crocodiles); fossorial (e.g, moles) and semi-fossorial (e.g., armadillos) lifestyles; arboreality (e.g. primates and sloths); movement through air by gliding (e.g. colugos and flying geckos) and powered flight (bats, birds and pterosaurs); bipedalism, involving movement on two hind legs (e.g. humans and theropods), amongst others. Adaptations to many of these locomotor modes involved biomechanical constraints owing to the interaction between the organism's performance and the environment, mediated by the limb morphology (Biewener & Patek, 2018), which makes the vertebrate limb an ideal model system to investigate the evolution of morphological diversity and its interplay with intrinsic and extrinsic constraints (see Fig. 1.1)

1.2. The tetrapod limb

Richard Owen (1849) paved the way for understanding homology, showing that the vertebrate limb presents a widespread three-segment structure, despite its remarkable variation in skeletal form and arrangement across species (which Owen has attributed to variation in function). Since then, the vertebrate limb became an appealing study system for comparative anatomists. The three segments of the vertebrate limb are recognized as the proximal stylopod (humerus/ femur), the intermediate zeugopod (radius and ulna/ tibia and fibula) and the distal autopod (hand and foot, comprising the carpals/ tarsals, metacarpals/ metatarsals and phalanges). Darwin later referred to the patterns of striking

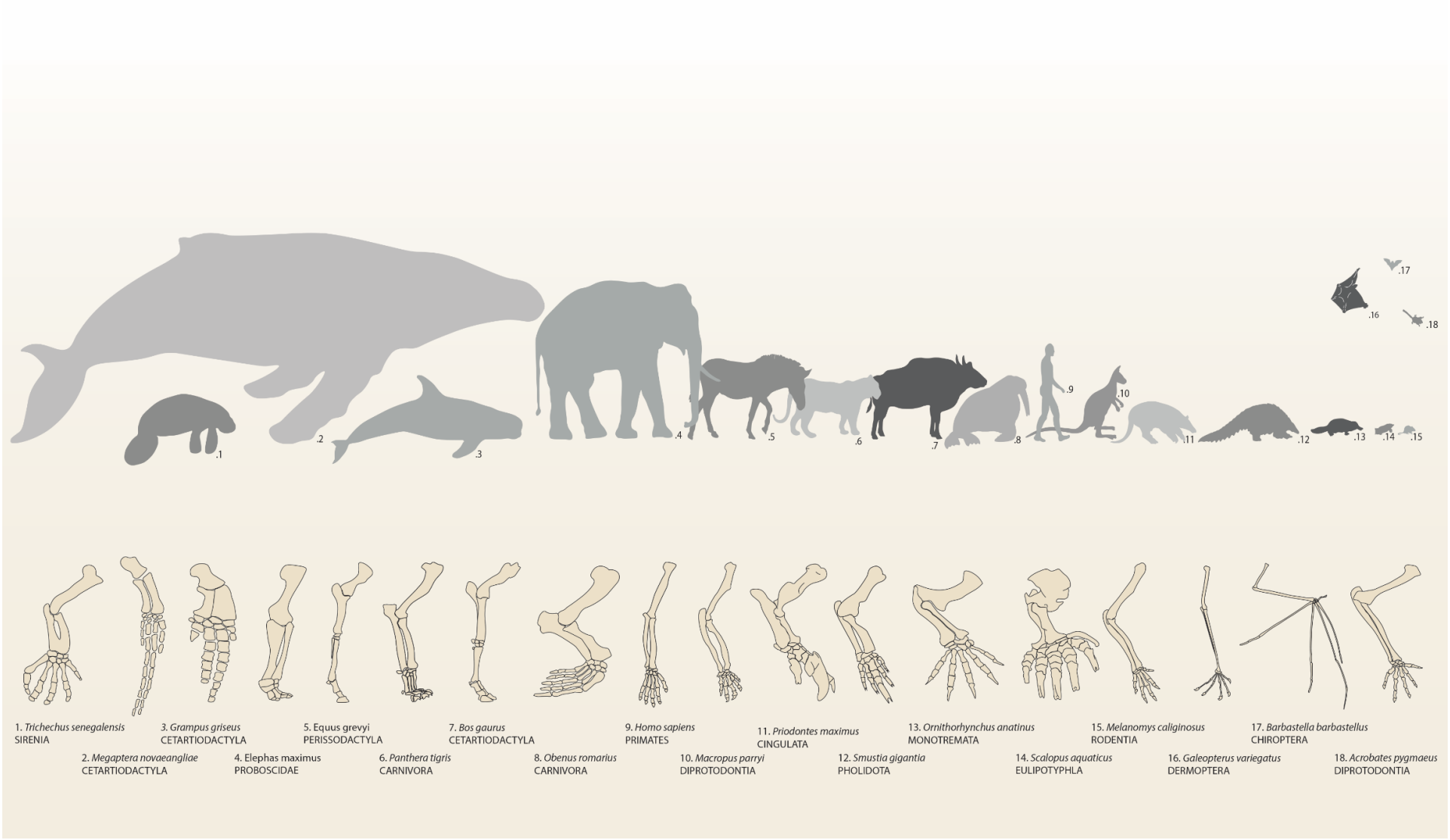

Figure 1.1. Morphological diversity in mammals. Silhouettes of diverse mammal species illustrating variation in size, as well as the corresponding skeletal morphology of the forelimbs.

similarity in structure of tetrapod limbs with vastly distinct forms and function as evidence to endorse the theory of evolution by common descent (Darwin, 1859). Because the tetrapod limb is mostly a bony structure with most of its variation concentrated in two dimensions (the proximal–distal and anterior–posterior axes), it is relatively well preserved in the fossil record, which facilitates an analytical investigation of its morphological evolution (Stopper & Wagner, 2005).

The proximal to distal organization of segments is correlated with their respective evolutionary appearance, the stylopod being the first structure to have evolved, later followed by the zeugopod and finally the autopod (Shubin et al., 1997). Although the three-segment pattern is conserved among quadrupedal tetrapods, the morphology of such structures along the proximo-distal axis does not seem to evolve in the same way (Cooper et al., 2011; Galis et al., 2001; Holder, 1983; K. Sears et al., 2007). Dramatic variation is usually observed in the distal autopod in terms of number and position of skeletal elements (i.e., fusion and loss of carpal and tarsal bones and alteration of the phalangeal formula; Cooper et al., 2011; Hamrick, 2001; Holder, 1983; Luo et al., 2015; Saxena et al., 2017). Moreover, the autopod is generally the last limb segment to condense during development (Schneider & Shubin, 2013; Shubin et al., 1997; Stopper & Wagner, 2005). Structures from the proximal limb usually condense before the autopod and they display less frequent cases of element reduction (Holder, 1983; Keeffe & Blackburn, 2022; Sears et al., 2007, 2017). The evolutionary pattern of limb reduction in some tetrapod lineages also evidences the importance of the topological skeletal position to trait disparity, as it initiates with the loss of distal skeletal elements and may later proceed with the reduction of more proximal bones, sometimes leading to complete limb loss (such as in snakes, caecilians, the hind limbs of cetaceans and sirenians, etc.; Lande, 1978; K. E. Sears et al., 2011; Wagner, 2014). Although there is an apparent conservation of the proximo-distal

timing of bone condensation throughout tetrapods, the sequence of ossification is more variable and has been shown to impact skeletal morphology and integration, such as in the late ossifying stylopod of monotremes and moles (Weisbecker, 2011). Therefore, developmental sequence is suggested to be an important feature driving macroevolutionary patterns of limb bone diversity.

1.3. Mammals as a model system

From the fingertip-sized Etruscan shrew to the largest vertebrate to have ever existed, the colossal blue whale, mammals have evolved and thrived in a variety of habitats, successfully colonizing all continents (Fig 1.2). The remarkable diversity of limb morphology in mammals is often suggested to be linked to their radiation into almost every habitat in the world (Polly, 2007). Wings, flippers, hooves, paws, and hands are just some of the many forms that mammalian limbs have taken, turning this group into one of the most popular biological models to understand how limbs have evolved, featuring studies from genetics and development to paleontology and bioengineering (Fish et al., 2008; Howenstine et al., 2021; Lungmus & Angielczyk, 2021; Polly, 2007).

Early mammaliaforms (i.e., mammals and their closest relatives) emerged within Synapsida around 220 Ma (Million years ago), in the late Triassic (Grossnickle et al., 2019; Luo, 2007; Meredith et al., 2011). These Mesozoic mammaliaforms were initially small, shrewlike, terrestrial insectivores (Grossnickle et al., 2019). The radiation of the crown Mammalia is defined by the divergence of prototherians (modern forms represented by monotremes, i.e. platypus and echidnas) and therians, around 180 Ma (Meredith et al., 2011). Clade diversity was significantly impacted later at the split of therians into Eutheria (including the living placentals) and Metatheria (marsupials and

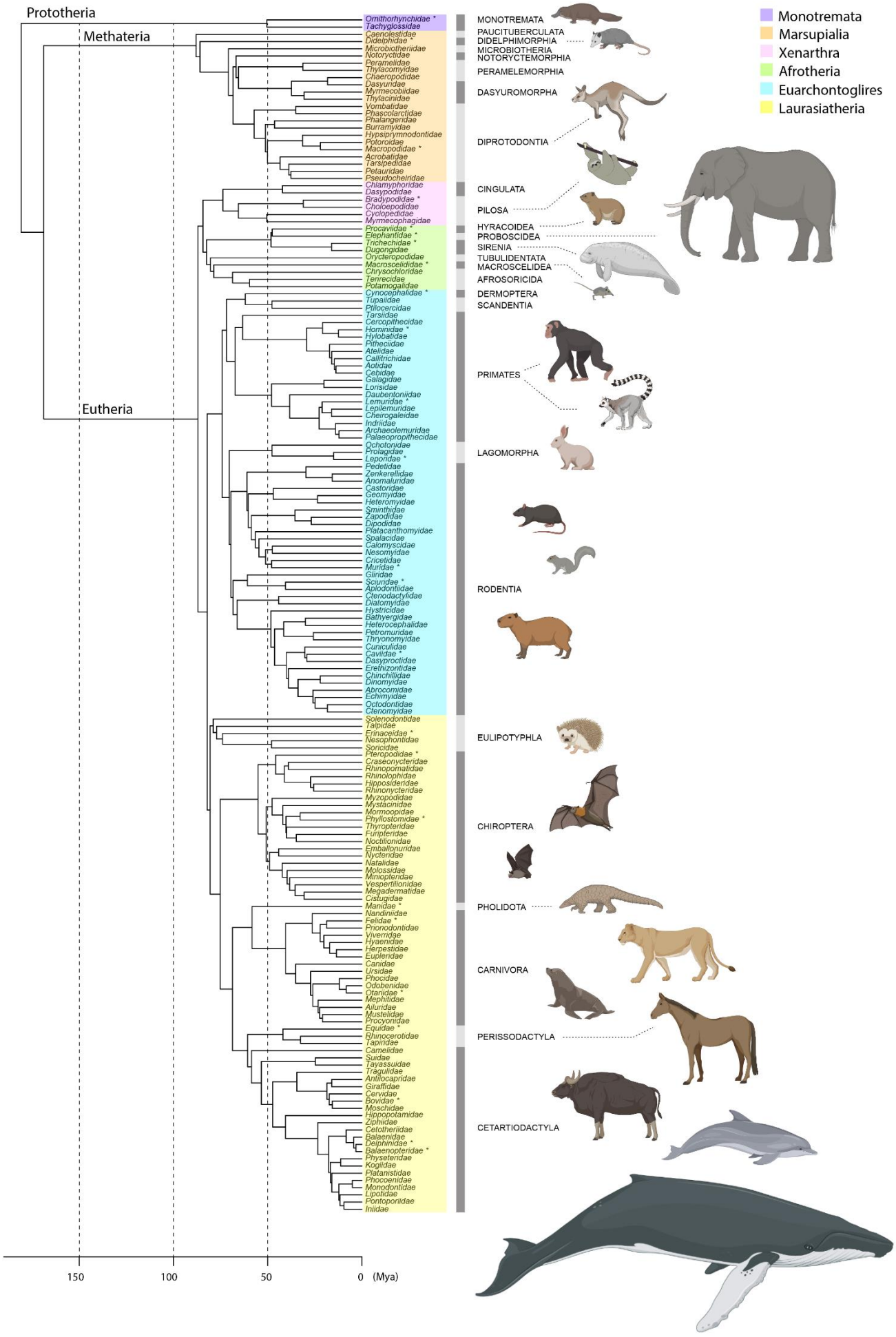
Prototheria
Methateria
Eutheria
Ornithorhynchidae *
Tachyglossidae
Caenolestidae
Didelphidae *
Microbiotheriidae
Notoryctidae
Peramelidae
Thylacomyidae
Chaeropodidae
Dasyuridae
Myrmecobiidae
Thylacinidae
Vombatidae
Phascolarctidae
Phalangeridae
Burramyidae
Hypsiprymnodontidae
Potoroidae
Macropodidae *
Acrobatidae
Tarsipedidae
Petauridae
Pseudocheiridae
Chlamyphoridae
Dasypodidae
Bradypodidae *
Cholepodidae
Cyclopedidae
Myrmecophagidae
Procaviidae *
Elephantidae *
Trichechidae *
Dugongidae
Orycteropodidae
Macroscelididae *
Chrysochloridae
Tenrecidae
Potamogalidae
Cynocephalidae *
Tupaiidae
Ptilocercidae
Tarsiidae
Cercopithecidae
Hominidae *
Hylobatidae
Pitheciidae
Atelidae
Callitrichidae
Aotidae
Cebidae
Galagidae
Lorisidae
Daubentoniidae
Lemuridae *
Lepilemuridae
Cheirogaleidae
Indriidae
Archaeolemuridae
Palaeopropithecidae
Ochotonidae
Prolagidae
Leporidae *
Pedetidae
Zenkerellidae
Anomaluridae
Castoridae
Geomyidae
Heteromyidae
Sminthidae
Zapodidae
Dipodidae
Platacanthomyidae
Spalacidae
Calomyscidae
Nesomyidae
Cricetidae
Muridae *
Gliridae
Sciuridae *
Aplodontiidae
Ctenodactylidae
Diatomyidae
Hystricidae
Bathyergidae
Heterocephalidae
Petromuridae
Thryonomyidae
Cuniculidae
Caviidae *
Dasyproctidae
Erethizontidae
Chinchillidae
Dinomyidae
Abrocomidae
Echimyidae
Octodontidae
Ctenomyidae
Solenodontidae
Talpidae
Erinaceidae *
Nesophontidae
Soricidae
Pteropodidae *
Craseonycteridae
Rhinopomatidae
Rhinolophidae
Hipposideridae
Rhinonycteridae
Myzopodidae
Mystacinidae
Mormoopidae
Phyllostomidae *
Thyropteridae
Furipteridae
Noctilionidae
Emballonuridae
Nyctenidae
Natalidae
Molossidae
Miniopteridae
Vespertilionidae
Megadermatidae
Cistugidae
Manidae *
Nandiniidae
Felidae *
Prionodontidae
Viverridae
Hyaenidae
Herpestidae
Eupleridae
Canidae
Ursidae
Phocidae
Odobenidae
Otariidae *
Mephitidae
Ailuridae
Mustelidae
Procyonidae
Equidae *
Rhinocerotidae
Tapiridae
Camelidae
Suidae
Tayassuidae
Tragulidae
Antilocapridae
Giraffidae
Cervidae
Bovidae *
Moschidae
Hippopotamidae
Ziphiidae
Cetotheriidae
Balaenidae
Delphinidae *
Balaenopteridae *
Physeteridae
Kogiidae
Platanistidae
Phocoenidae
Monodontidae
Lipotidae
Pontoporiidae
Iniidae
150
100
50
0
(Mya)
MONOTREMATA
PAUCITUBERCULATA
DIDELPHIMORPHIA
MICROBIOTHERIA
NOTORYCTEMORPHIA
PERAMELEMORPHIA
DASYUROMORPHA
DIPROTODONTIA
CINGULATA
PILOSA
HYRACOIDEA
PROBOSCIDEA
SIRENIA
TUBULIDENTATA
MACROSCELIDEA
AFROSORICIDA
DERMOPTERA
SCANDENTIA
PRIMATES
LAGOMORPHA
RODENTIA
EULIPOTYPHLA
CHIROPTERA
PHOLIDOTA
CARNIVORA
PERISSODACTYLA
CETARTIODACTYLA
Monotremata
Marsupialia
Xenarthra
Afrotheria
Euarchontoglires
Laurasiatheria

[Figure on previous page]

Figure 1.2. Evolutionary tree of living mammals. The topology (estimated using maximum clade credibility from a posterior sample of 10,000 trees from Upham et al., 2019) illustrates one possible evolutionary history underlying the diversification of mammals, with the extant or recently extinct families represented at the terminals. Orders are indicated by grey bars. All animal icons, but the sloth (illustrating the order Pilosa) and the elephant shrew (illustrating the order Macroscelidae), were obtained from BioRender.

their fossil relatives), around 160 Ma (Kemp, 2005). However, the diversification of most modern mammal groups, occurred only from the end of the Cretaceous onwards, when there was also a high rate of morphological evolution, possibly catalyzed by the great mass extinction at the Paleogene transition and coevolutionary interactions with the diversifying angiosperms (Grossnickle et al., 2019; Halliday et al., 2016; Halliday & Goswami, 2015).

The extraordinary phenotypic and ecological variation of mammals is coupled with impressive taxonomic diversity. Recent counts from the Mammalian Diversity Database, in April 2023, reports a total of 6,544 living species of mammals, in addition to 105 recently extinct species (Mammal Diversity Database, 2023). These species are classified into 27 orders, 167 families (7 recently extinct) and 1,345 genera. Placentals hold a huge proportion of the total mammalian diversity with 6,152 species. Nearly half of this taxonomic diversity is represented by rodents, and another quarter by bats. Marsupials and monotremes respectively encompass only 387 and 5 species, respectively. The investigation of the patterns of morphological evolution in mammals has been extensively addressed previously (Burin et al., 2023; Coombs et al., 2022; Fabre et al., 2021; Gomes Rodrigues et al., 2016; Law, 2021; Monteiro & Nogueira, 2011; Porto et al., 2009; and many others), but just a few studies have examined such patterns with a wide taxonomic coverage truly representative of the mammalian diversity (mostly

looking at body mass and size, and cranial shape, (Clavel & Morlon, 2017; Goswami et al., 2022; Kubo et al., 2019; Price & Hopkins, 2015). Despite the many insightful studies on limb diversity spanning particular taxonomic groups (see Bennett & Goswami, 2011; Chen & Wilson, 2015; Fabre et al., 2015, 2019; Hedrick et al., 2020; Martín-Serra & Benson, 2020; Samuels & Van Valkenburgh, 2008; Sánchez-Villagra, 2012; Weisbecker & Schmid, 2007; Weisbecker & Warton, 2006), a clade-wise study on the evolutionary patterns of morphological diversity of the mammalian limb is inexistent.

1.4. General goals

The main goal of this thesis is to investigate the patterns of morphological evolution of the mammalian forelimb, investigating the role of intrinsic and extrinsic evolutionary drivers underlying the morphological diversity between traits and between groups. To this end, I employed different phylogenetic comparative methods to study the morphology of species belonging to most of the living mammalian families under a macroevolutionary and macroecological framework. Mammals represent an ideal biological model to conduct the present study because they correspond to an exceptionally diverse group in terms of number of species, microhabitat occupancy, and limb morphology. I assessed whether forelimb elements vary and evolve differently from one another with respect to their timing of development, and whether specific microhabitats and modes of locomotion explain the pattern of morphological limb evolution. The present thesis stands out in proposing a comprehensive comparative investigation of the evolutionary processes that drive morphological diversity, using a robust and representative dataset that, to our knowledge, is the most taxonomically comprehensive for forelimb data in Mammalia. The combination of morphological, ecological, and developmental parameters on a macro

scale of investigation will certainly contribute to a deeper understanding of lineage diversification processes, elucidating key questions that underpin our understanding of evolutionary biology.

1.5. Thesis outline and specific goals

The evolutionary history of mammalian forelimb diversity is here investigated using different and complementary approaches. Forearm morphology is at first investigated in terms of within element variation and discussed under the framework of its developmental origins, moving to the physical constraints of habitat use on forelimb disparity between groups, and finishing with the evolution of modes of locomotion and their role in driving the patterns of forelimb variation in mammals. In Ch. 2, I investigated the morphological diversity of each limb bone, testing the hypothesis of the presence of developmental constraints during the proximo-to-distal limb structuration. I assessed the morphological variation, the integration and the rates of evolution of bones belonging to each limb segment. In Ch. 3, I explored whether leaving the terrestrial environment to move in continuous fluid media such as water and air, constrained the morphological variation of the forelimb. In this chapter, I examined the morphological disparity and phenotypic convergence of the absolute size and shape of the arm and its bones. In Ch.4., I tested whether locomotor modes define the evolutionary patterns of phenotypic variation in the forelimb, estimating the evolutionary transitions between modes of locomotion and testing whether such transitions are facilitated by the position of adaptive zones as predicted by the adaptive landscape model. I investigated the presence of adaptive peaks and of rate shifts while testing for different models of evolution., Finally, in Ch. 5 I summarize the main findings and discuss the contributions and limitations of this work,

concluding how future potential research would benefit from and complement the findings presented here.

1.6. An overview of the taxonomic sampling

I measured 887 specimens of mammals (552 digitally and 335 manually; Table S1.1), representing 844 species of 803 genera of 171 families. In each chapter, I used a different subset of this dataset, either because analyses were conducted before sampling all species (Ch. 2) or because individuals were removed for lacking traits that are important for the questions addressed (such as missing or fused phalanges; Ch. 4). The final dataset covers about 60% of the genus diversity of Mammalia and 97.5% of families of all living orders of this group. The proportion of genera sampled in relation to total genus diversity per order is detailed in Fig. 1.3. I sampled more than 50% of the genus diversity of most orders (except for Chiroptera and Rodentia, which correspond to the two most specious mammalian orders, and sampling consisted of 44% and 46.5% of their genus diversity, respectively), with most of them providing limb measurements for more than 75% of the described genera (following Burgin et al., 2018). Sampling varies from one to four individuals per genus, depending on the availability and state of preservation of the specimens in scientific collections. Taxa that were not sampled were either rare at zoological collections or had unpreserved post-cranial bones. That was the case for many species that had available material at the zoological collections, but which often lacked preserved autopod bones. This structure was often missing because during the preparation of specimens to be deposited in collections, the hands are usually disarticulated from the remaining limb and kept within the skin. We considered it to be extremely relevant to sample the autopod bones because this structure is often overlooked in most studies on

limb morphology, even if it displays huge amount of variation in mammals (Almécija et al., 2015; Clifford, 2010; Hamrick, 2001; Rolian, 2009; Weisbecker & Schmid, 2007; Weisbecker & Warton, 2006).

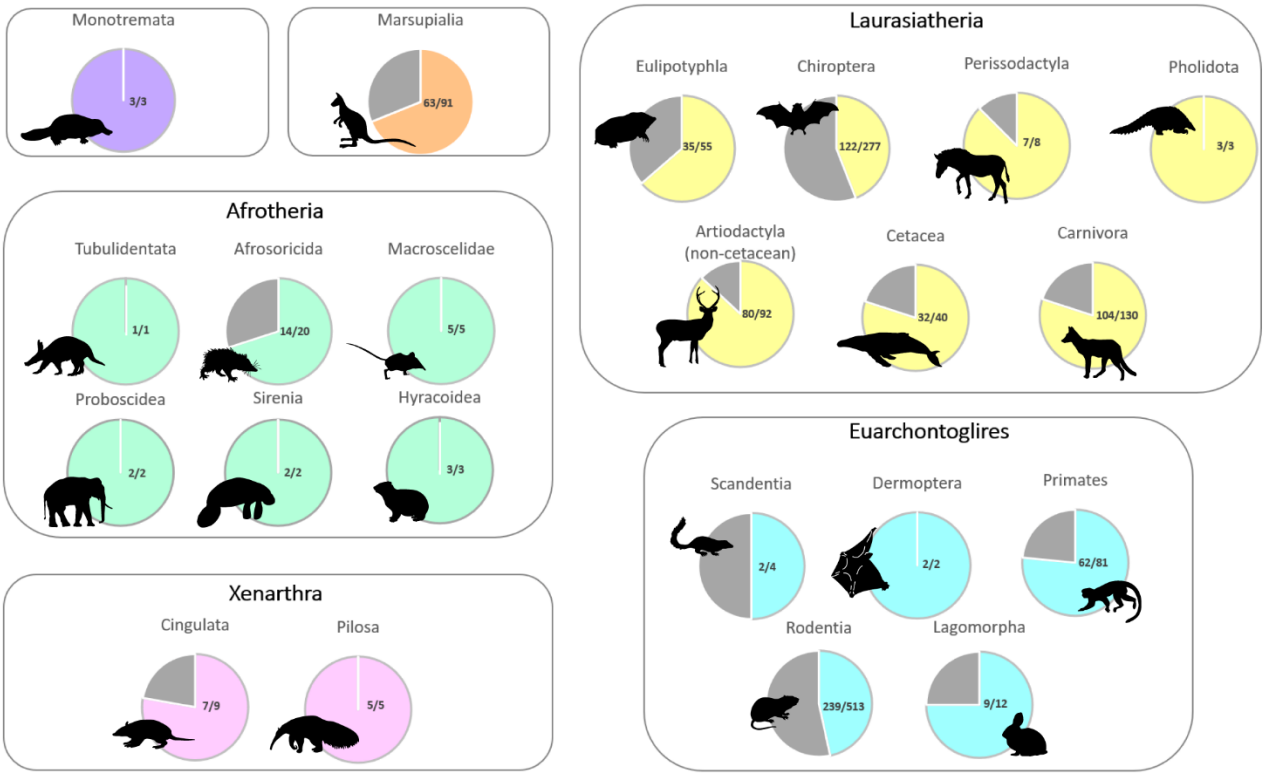

Figure 1.3. Proportion of genera sampled according to the total genus diversity per group (sampled/ total). For the four Placentalia superorders (Afrotheria, Xenarthra, Laurasiatheria and Euarchontoglires), sample effort is detailed at the order level. The colors that represent each major living Mammalia group match those from the topology illustrated in Fig. 1.2.

1.7. Morphological traits

Morphological variation was inferred combining digital and manual protocols. I CT-scanned 27 small to medium-sized specimens with an EasyTom 150 X-ray micro-

computed tomography (ISEM Institute, Montpellier, France). The digital dataset was combined with 533 meshes available on MorphoSource.org. I complemented this dataset with 334 medium to large body-sized species measured by callipers (Table S1.1). I measured 20 to 22 linear distances from the right anterior limb of each individual (depending on the phalangeal formula of the taxon and on the availability of distal phalanges preserved with the specimen). We used a subset of these measurements in Ch. 3 and 5, while in Ch. 4 all these distances were analysed. The measurements consist of length, width (proximal, central, and distal axis) and height of the tibia, radius, third metacarpal and first phalanx of digit III, as well as the length of the other phalanges of digit III to calculate the total length of the digit (the sum of 16, 21 and 22 in Fig. 1.4; Table S1.2). We opted not to include the ulna because this bone is fused to the radius in many taxa, preventing the acquisition of such measurements. The metacarpal and first phalanx of digit III were sampled because this is the only digit present in the hand of all mammalian lineages, even in groups that exhibit digit loss or fusion with other autopodial elements, such as in golden moles and ungulates (Clifford, 2010; McHorse et al., 2019; Prothero, 2009). Each individual was measured twice with the subsequent calculation of the mean and standard error in order to verify possible measurement error (see mean values in Table S1.3). In all chapters, we also assembled body mass estimates from the PanTHERIA database (Jones et al., 2009) and complemented these by literature sources when necessary (Table S1.1).

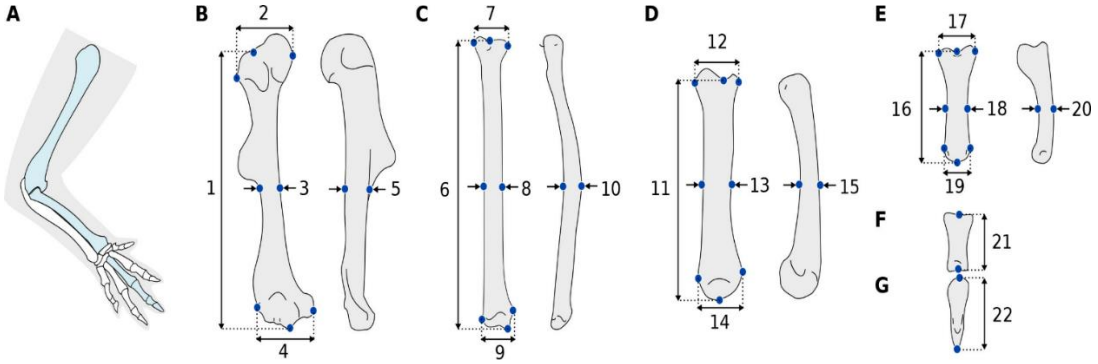

Figure 1.4. Morphological data. Right anterior limb bones illustrations of a cricetid rodent *Melanomys caliginosus*, illustrating linear morphological measurements (total of 22 distances, depending on the species' phalangeal formula) acquired either by landmark positioning in 3D models or calliper measurements on bones. **A)** schematic of the forelimb skeleton highlighting in blue the bones analysed in this study; **B)** anterior (left) and lateral (right) view of humerus; **C)** anterior (left) and lateral (right) view of the radius; **D)** dorsal (left) and lateral (right) view of the third metacarpal; **E)** dorsal (left) and lateral (right) view of the first phalanx of the third digit; **F)** dorsal view of the second phalanx of the third digit and **G)** dorsal view of the third phalanx the third digit. The description of the measurements and positioning criteria of the landmarks is detailed in Table S1.2, and mean distances per species are indicated in Table S1.3.

1.8. References

Adams, D. C. (2013). Comparing evolutionary rates for different phenotypic traits on a phylogeny using likelihood. *Systematic Biology*, *62*(2), 181–192. https://doi.org/10.1093/sysbio/sys083

Alencar, L. R. V., Martins, M., Burin, G., & Quental, T. B. (2017). Arboreality constrains morphological evolution but not species diversification in vipers. *Proceedings of the Royal Society B: Biological Sciences*, *284*(1869), 20171775. https://doi.org/10.1098/rspb.2017.1775

Alfaro, M. E., Bolnick, D. I., & Wainwright, P. C. (2005). Evolutionary consequences of many-to-one mapping of jaw norphology to mechanics in labrid fishes. *The American Naturalist*, *165*(6), E140–E154. https://doi.org/10.1086/429564

Almécija, S., Smaers, J. B., & Jungers, W. L. (2015). The evolution of human and ape hand proportions. *Nature Communications*, *6*. https://doi.org/10.1038/ncomms8717

Arnold, S. J. (1983). Morphology, performance and fitness. *American Zoologist*, *23*, 347–361. https://doi.org/10.1093/icb/23.2.347

Bardua, C., Fabre, A.-C., Clavel, J., Bon, M., Das, K., Stanley, E. L., Blackburn, D. C., & Goswami, A. (2021). Size, microhabitat, and loss of larval feeding drive cranial diversification in frogs. *Nature Communications*, *12*(1). https://doi.org/10.1038/s41467-021-22792-y

Bardua, C., Wilkinson, M., Gower, D. J., Sherratt, E., & Goswami, A. (2019). Morphological evolution and modularity of the caecilian skull. *BMC Evolutionary Biology*, *19*(1). https://doi.org/10.1186/s12862-018-1342-7

Barros, F. C., Herrel, A., & Kohlsdorf, T. (2011). Head shape evolution in Gymnophthalmidae: does habitat use constrain the evolution of cranial design in fossorial lizards? *Journal of Evolutionary Biology*, *24*(11), 2423–2433. https://doi.org/10.1111/j.1420-9101.2011.02372.x

Bels, V. L., & Russell, A. P. (2023). The concept of convergent evolution and its relationship to the understanding of form and function. In V. L. Bels & A. P. Russell (Eds.), *Convergent evolution: Animal form and function* (pp. 1–20). Springer International Publishing.

Bennett, V. C., & Goswami, A. (2011). Does developmental strategy drive limb integration in marsupials and monotremes? *Mammalian Biology*, *76*(1), 79–83. https://doi.org/10.1016/j.mambio.2010.01.004

Biewener, A. A., & Patek, S. N. (2018). *Animal locomotion* (2nd Edition.). Oxford University Press.

Burgin, C. J., Colella, J. P., Kahn, P. L., & Upham, N. S. (2018). How many species of mammals are there? *Journal of Mammalogy*, *99*(1), 1–14. https://doi.org/10.1093/jmammal/gyx147

Burin, G., Park, T., James, T. D., Slater, G. J., & Cooper, N. (2023). The dynamic adaptive landscape of cetacean body size. *Current Biology*. https://doi.org/10.1016/j.cub.2023.03.014

Chen, M., & Wilson, G. P. (2015). A multivariate approach to infer locomotor modes in Mesozoic mammals. *Paleobiology*, *21*(2), 280–312. https://doi.org/10.5061/dryad.870j3

Cheverud, J. M. (1984). Quantitative genetics and developmental constraints on evolution by selection. *Journal of Theoretical Biology*, *110*, 155–171. https://doi.org/10.1016/s0022-5193(84)80050-8

Cheverud, J. M. (1996). Developmental integration and the evolution of pleiotropy. *American Zoologist*, *36*, 44–50. https://doi.org/10.1093/icb/36.1.44

Clavel, J., & Morlon, H. (2017). Accelerated body size evolution during cold climatic periods in the Cenozoic. *Proceedings of the National Academy of Sciences of the United States of America*, *114*(16), 4183–4188. https://doi.org/10.1073/pnas.1606868114

Clifford, A. B. (2010). The evolution of the unguligrade manus in artyodactyls. *Journal of Vertebrate Paleontology*, *30*(6), 1827–1839. https://doi.org/doi.org/10.1080/02724634.2010.521216

Collar, D. C., Schulte, J. a, O'Meara, B. C., & Losos, J. B. (2010). Habitat use affects morphological diversification in dragon lizards. *Journal of Evolutionary Biology*, *23*, 1033–1049. https://doi.org/10.1111/j.1420-9101.2010.01971.x

Coombs, E. J., Felice, R. N., Clavel, J., Park, T., Bennion, R. F., Churchill, M., Geisler, J. H., Beatty, B., & Goswami, A. (2022). The tempo of cetacean cranial evolution. *Current Biology*, *32*(10), 2233-2247.e4. https://doi.org/10.1016/j.cub.2022.04.060

Cooper, K. L., Kuang-Hsien Hu, J., ten Berge, D., Fernandez-Teran, M., Ros, M. A., & Tabin, C. J. (2011). Initiation of proximal-distal patterning in the vertebrate limb by signals and growth. *Science*, *332*(6033), 1083–1086. https://doi.org/10.1126/science.1199499

Darwin, C. (1859). *On the origin of species by means of natural selection, or the preservation of favoured races in the struggle for life*. John Murray.

Elissamburu, A., & Vizcaíno, S. F. (2004). Limb proportions and adaptations in caviomorph rodents (Rodentia: Caviomorpha). *Journal of Zoology*, *262*(2), 145–159. https://doi.org/10.1017/S0952836903004485

Fabre, A.-C., Bardua, C., Bon, M., Clavel, J., Felice, R. N., Streicher, J. W., Bonnel, J., Stanley, E. L., Blackburn, D. C., & Goswami, A. (2020). Metamorphosis shapes cranial diversity and rate of evolution in salamanders. *Nature Ecology and Evolution*, *4*(8), 1129–1140. https://doi.org/10.1038/s41559-020-1225-3

Fabre, A.-C., Cornette, R., Goswami, A., & Peigné, S. (2015). Do constraints associated with the locomotor habitat drive the evolution of forelimb shape? A case study in musteloid carnivorans. *Journal of Anatomy*, *226*(6), 596–610. https://doi.org/10.1111/joa.12315

Fabre, A.-C., Dowling, C., Miguez, R. P., Fernandez, V., Noirault, E., & Goswami, A. (2021). Functional constraints during development limit jaw shape evolution in

marsupials. *Proceedings of the Royal Society B: Biological Sciences*, *288*(1949). https://doi.org/10.1098/rspb.2021.0319

Fabre, A.-C., Goswami, A., Peigné, S., & Cornette, R. (2014). Morphological integration in the forelimb of musteloid carnivorans. *Journal of Anatomy*, *225*(1), 19–30. https://doi.org/10.1111/joa.12194

Fabre, A.-C., Peckre, L., Pouydebat, E., & Wall, C. E. (2019). Does the shape of forelimb long bones co-vary with grasping behaviour in strepsirrhine primates? In *Biological Journal of the Linnean Society* (Vol. 127). https://lemur.duke.edu/discover/

Felice, R. N., Randau, M., & Goswami, A. (2018). A fly in a tube: Macroevolutionary expectations for integrated phenotypes. *Evolution*, *72*(12), 2580–2594. https://doi.org/10.1111/evo.13608

Fish, F. E. (2023). Aquatic locomotion: Environmental constraints that drive convergent evolution. In V. L. Bels & A. P. Russell (Eds.), *Convergent evolution: Animal form and function* (pp. 477–522). Springer International Publishing.

Fish, F. E., Howle, L. E., & Murray, M. M. (2008). Hydrodynamic flow control in marine mammals. *Integrative and Comparative Biology*, *48*(6), 788–800. https://doi.org/10.1093/icb/icn029

Foote, M. (1997). The evolution of morphological diversity. *Annual Review of Ecology, Evolution, and Systematics*, *28*, 129–152. www.annualreviews.org

Friedman, S. T., Price, S. A., Corn, K. A., Larouche, O., Martinez, C. M., & Wainwright, P. C. (2020). Body shape diversification along the benthic–pelagic axis in marine fishes. *Proceedings of the Royal Society B: Biological Sciences*, *287*(1931), 20201053. https://doi.org/10.1098/rspb.2020.1053

Friedman, S. T., Price, S. A., & Wainwright, P. C. (2021). The effect of locomotion mode on body shape evolution in teleost fishes. *Integrative Organismal Biology*, *3*(1). https://doi.org/10.1093/iob/obab016

Galis, F., Van Alphen, J. J. M., & Metz, J. A. J. (2001). Why five fingers? Evolutionary constraints on digit numbers. *TRENDS in Ecology & Evolution*, *16*(11). https://doi.org/10.1016/S0169-5347(01)02289-3

Godoy, P. L., Benson, R. B. J., Bronzati, M., & Butler, R. J. (2019). The multi-peak adaptive landscape of crocodylomorph body size evolution. *BMC Evolutionary Biology*, *19*(1). https://doi.org/10.1186/s12862-019-1466-4

Gomes Rodrigues, H., Šumbera, R., & Hautier, L. (2016). Life in burrows channelled the morphological evolution of the skull in rodents: The case of African mole-rats

(Bathyergidae, Rodentia). *Journal of Mammalian Evolution*, *23*(2), 175–189. https://doi.org/10.1007/s10914-015-9305-x

Goswami, A., Noirault, E., Coombs, E. J., Clavel, J., Fabre, A.-C., Halliday, T. J. D., Churchill, M., Curtis, A., Watanabe, A., Simmons, N. B., Beatty, B. L., Geisler, J. H., Fox, D. L., & Felice, R. N. (2022). Attenuated evolution of mammals through the Cenozoic. *Science*, *378*, 377–383. https://doi.org/10.1126/science.abm7525

Goswami, A., Smaers, J. B., Soligo, C., & Polly, P. D. (2014). The macroevolutionary consequences of phenotypic integration: from development to deep time. *Philosophical Transactions of the Royal Society. Series B, Biological Sciences*, *369*, 20130254. https://doi.org/10.1098/rstb.2013.0254

Goswami, A., Weisbecker, V., & Sánchez-Villagra, M. R. (2009). Developmental modularity and the marsupial-placental dichotomy. *Journal of Experimental Zoology Part B: Molecular and Developmental Evolution*, *312B*, 186–195. https://doi.org/10.1002/jez.b.21283

Grossnickle, D. M., Chen, M., Wauer, J. G. A., Pevsner, S. K., Weaver, L. N., Meng, Q. J., Liu, D., Zhang, Y. G., & Luo, Z. X. (2020). Incomplete convergence of gliding mammal skeletons. *Evolution*, *74*(12), 2662–2680. https://doi.org/10.1111/evo.14094

Grossnickle, D. M., Smith, S. M., & Wilson, G. P. (2019). Untangling the multiple ecological radiations of early mammals. *Trends in Ecology and Evolution*, *34*(10), 936–949. https://doi.org/10.1016/j.tree.2019.05.008

Hall, B. K. (2007). *Fins into Limbs: Evolution, Development, and Transformation*.

Halliday, T. J. D., & Goswami, A. (2015). Eutherian morphological disparity across the end-Cretaceous mass extinction. *Biological Journal of the Linnean Society*, *118*(1), 152–168. https://doi.org/10.1111/bij.12731

Halliday, T. J. D., Upchurch, P., & Goswami, A. (2016). Eutherians experienced elevated evolutionary rates in the immediate aftermath of the Cretaceous–Palaeogene mass extinction. *Proceedings of the Royal Society B: Biological Sciences*, *283*(1833), 20153026. https://doi.org/10.1098/rspb.2015.3026

Hamrick, M. W. (2001). Development and evolution of the mammalian limb: adaptive diversification of nails, hooves, and claws. *Evolution & Development*, *3*(5), 355–363. https://doi.org/10.1046/j.1525-142x.2001.01032.x

Hedrick, B. P., Dickson, B. V., Dumont, E. R., & Pierce, S. E. (2020). The evolutionary diversity of locomotor innovation in rodents is not linked to proximal limb morphology. *Scientific Reports*, *10*(1). https://doi.org/10.1038/s41598-019-57144-w

Herrel, A., Meyers, J. J., & Vanhooydonck, B. (2002). Relations between microhabitat use and limb shape in phrynosomatid lizards. *Biological Journal of the Linnean Society*, *77*(1), 149–163. https://doi.org/10.1046/j.1095-8312.2002.00101.x

Herrel, A., Vanhooydonck, B., & Van Damme, R. (2004). Omnivory in lacertid lizards: Adaptive evolution or constraint? *Journal of Evolutionary Biology*, *17*(5), 974–984. https://doi.org/10.1111/j.1420-9101.2004.00758.x

Holder, N. (1983). Developmental constraints and the evolution of vertebrate digit patterns. *Journal of Theoretical Biology*, *104*, 451–471. https://doi.org/10.1016/0022-5193(83)90117-0

Howenstine, A. O., Sadier, A., Anthwal, N., Lau, C. L., & Sears, K. E. (2021). Non-model systems in mammalian forelimb evo-devo. *Genetics and Development*, *69*, 65–71. https://doi.org/10.1016/j.gde.2021.01.012

Jones, K. E., Bielby, J., Cardillo, M., Fritz, S. A., O'Dell, J., David, C., Orme, L., Safi, K., Sechrest, W., Boakes, E. H., Carbone, C., Connolly, C., Cutts, M. J., Foster, J. K., Grenyer, R., Habib, M., Plaster, C. A., Price, S. A., Rigby, E. A., … Purvis, A. (2009). PanTHERIA: a species-level database of life history, ecology, and geography of extant and recently extinct mammals. *Ecology*, *90*(9), 2648-undefined. https://doi.org/10.1890/08-1494.1

Jones, K. E., Smaers, J. B., & Goswami, A. (2015). Impact of the terrestrial-aquatic transition on disparity and rates of evolution in the carnivoran skull. *BMC Evolutionary Biology*, *15*(1). https://doi.org/10.1186/s12862-015-0285-5

Keeffe, R., & Blackburn, D. C. (2022). Diversity and function of the fused anuran radioulna. *Journal of Anatomy*, *241*(4), 1026–1038. https://doi.org/10.1111/joa.13737

Kelly, E. M., & Sears, K. E. (2011). Reduced phenotypic covariation in marsupial limbs and the implications for mammalian evolution. *Biological Journal of the Linnean Society*, *102*(1), 22–36. https://doi.org/10.1111/j.1095-8312.2010.01561.x

Kemp, T. S. (2005). *The origin and evolution of mammals*. Oxford University Press.

Klingenberg, C. P. (2008). Morphological integration and developmental modularity. *Annual Review of Ecology, Evolution, and Systematics*, *39*(1), 115–132. https://doi.org/10.1146/annurev.ecolsys.37.091305.110054

Kohlsdorf, T., Garland, T., & Navas, C. A. (2001). Limb and tail lengths in relation to substrate usage in Tropidurus lizards. *Journal of Morphology*, *248*(2), 151–164. https://doi.org/10.1002/jmor.1026

Kubo, T., Sakamoto, M., Meade, A., & Venditti, C. (2019). Transitions between foot postures are associated with elevated rates of body size evolution in mammals. *Proceedings of the Proceeding of the National Academy of Sciences*, *116*(7), 2618–2623. https://doi.org/10.1073/pnas.1814329116

Lande, R. (1978). Evolutionary mechanisms of limb loss in tetrapods. *Evolution*, *32*(1), 73–92. https://doi.org/10.2307/2407411

Law, C. J. (2021). Ecological drivers of carnivoran body shape evolution. *The American Naturalist*, *198*(3), 406–420. https://doi.org/10.5061/dryad.pg4f4qrpm

Ledbetter, N. M., & Bonett, R. M. (2019). Terrestriality constrains salamander limb diversification: Implications for the evolution of pentadactyly. *Journal of Evolutionary Biology*, *32*(7), 642–652. https://doi.org/10.1111/jeb.13444

Losos, J. B. (2011). Convergence, adaptation, and constraint. *Evolution*, *65*(7), 1827–1840. https://doi.org/10.1111/j.1558-5646.2011.01289.x

Lungmus, J. K., & Angielczyk, K. D. (2021). Phylogeny, function and ecology in the deep evolutionary history of the mammalian forelimb. *Proceedings of the Royal Society B: Biological Sciences*, *288*(1949), 202104942. https://doi.org/10.1098/rspb.2021.0494

Luo, Z. X. (2007). Transformation and diversification in early mammal evolution. *Nature*, *450*(7172), 1011–1019. https://doi.org/10.1038/nature06277

Luo, Z. X., Meng, Q.-J., Ji, Q., Liu, D., Zhang, Y.-G., & Neander, A. I. (2015). Evolutionary development in basal mammaliaforms as revealed by a docodontan. *Science*, *347*(6223), 760–764. https://doi.org/10.1126/science.1260880

Machado, F. A., Zahn, T. M. G., & Marroig, G. (2018). Evolution of morphological integration in the skull of Carnivora (Mammalia): Changes in Canidae lead to increased evolutionary potential of facial traits. *Evolution*, *72*(7), 1399–1419. https://doi.org/10.1111/evo.13495

Maher, A. E., Burin, G., Cox, P. G., Maddox, T. W., Maidment, S. C. R., Cooper, N., Schachner, E. R., & Bates, K. T. (2022). Body size, shape and ecology in tetrapods. *Nature Communications*, *13*(1). https://doi.org/10.1038/s41467-022-32028-2

Mahler, D. L., Ingram, T., Revell, L. J., & Losos, J. B. (2013). Exceptional convergence on the macroevolutionary landscape in island lizard radiations. *Science*, *341*(6143), 292–295. https://doi.org/10.1126/science.1239431

Mammal Diversity Database. (2023). Mammal Diversity Database (Version 1.11) [Data set]. *Zenodo*. https://doi.org/10.5281/zenodo.7830771

Martín-Serra, A., & Benson, R. B. J. (2020). Developmental constraints do not influence long-term phenotypic evolution of marsupial forelimbs as revealed by interspecific disparity and integration patterns. *American Naturalist*, *195*(3), 547–560. https://doi.org/10.5061/dryad.900ng75

McHorse, B. K., Biewener, A. A., & Pierce, S. E. (2019). The evolution of a single toe in horses: causes, consequences, and the way forward. *Integrative and Comparative Biology*, *59*(3), 638–655. https://doi.org/10.1093/icb/icz050

Meredith, R. W., Janečka, J. E., Gatesy, J., Ryder, O. A., Fisher, C. A., Teeling, E. C., Goodbla, A., Eizirik, E., L Simão, T. L., Stadler, T., Rabosky, D. L., Honeycutt, R. L., Flynn, J. J., Ingram, C. M., Steiner, C., Williams, T. L., Robinson, T. J., Burk-Herrick, A., Westerman, M., … Murphy, W. J. (2011). Impacts of the Cretaceous terrestrial revolution and KPg extinction on mammal diversification. *Science*, *334*(524), 521. https://doi.org/10.1126/science.1211028

Monteiro, L. R., & Nogueira, M. R. (2011). Evolutionary patterns and processes in the radiation of phyllostomid bats. *BMC Evolutionary Biology*, *11*(1). https://doi.org/10.1186/1471-2148-11-137

Owen, R. (1849). *On the nature of limbs: A discourse*. John van Voorst.

Polly, D. (2007). Limbs in mammalian evolution. In B. K. Hall (Ed.), *Fins into limbs: Evolution, development, and transformation* (pp. 245–268). The University of Chicago Press.

Porto, A., de Oliveira, F. B., Shirai, L. T., de Conto, V., & Marroig, G. (2009). The evolution of modularity in the mammalian skull I: Morphological integration patterns and magnitudes. *Evolutionary Biology*, *36*(1), 118–135. https://doi.org/10.1007/s11692-008-9038-3

Price, S. A., & Hopkins, S. S. B. (2015). The macroevolutionary relationship between diet and body mass across mammals. *Biological Journal of the Linnean Society*, *115*, 173–184.

Prothero, D. R. (2009). Evolutionary transitions in the fossil record of terrestrial hoofed mammals. *Evolution: Education and Outreach*, *2*(2), 289–302. https://doi.org/10.1007/s12052-009-0136-1

Raff, R. A. (1996). *The shape of life: genes, development, and the evolution of animal form.* (J. F. C. Hanken, Ed.; 1st Edition). University of Chicago Press.

Rolian, C. (2009). Integration and evolvability in primate hands and feet. *Evolutionary Biology*, *36*(1), 100–117. https://doi.org/10.1007/s11692-009-9049-8

Samuels, J. X., & Van Valkenburgh, B. (2008). Skeletal indicators of locomotor adaptations in living and extinct rodents. *Journal of Morphology*, *269*(11), 1387–1411. https://doi.org/10.1002/jmor.10662

Sánchez-Villagra, M. R. (2012). Why are there fewer marsupials than placentals? On the relevance of geography and physiology to evolutionary patterns of mammalian diversity and disparity. *Journal of Mammalian Evolution*, *20*(4), 279–290. https://doi.org/10.1007/s10914-012-9220-3

Saxena, A., Towers, M., & Cooper, K. L. (2017). The origins, scaling and loss of tetrapod digits. *Philosophical Transactions of the Royal Society B: Biological Sciences*, *372*(1713). https://doi.org/10.1098/rstb.2015.0482

Schluter, D. (2000). *The ecology of adaptive radiation*. Oxford University Press Inc.

Schmidt, M., & Fischer, M. S. (2009). Morphological integration in Mammalian limb proportions: dissociation between function and development. *Evolution*, *63*(3), 749–776. https://doi.org/10.1111/j.l558-5646.2008.00583.x

Schneider, I., & Shubin, N. H. (2013). The origin of the tetrapod limb: From expeditions to enhancers. *Trends in Genetics*, *29*(7), 419–426. https://doi.org/10.1016/j.tig.2013.01.012

Sears, K., Behringer, R. R., Rasweiler, J. J., & Niswander, L. A. (2007). The evolutionary and developmental basis of parallel reduction in mammalian zeugopod elements. *The American Naturalist*, *169*(1), 105–117. https://doi.org/10.1086/510259

Sears, K. E., Bormet, A. K., Rockwell, A., Powers, L. E., Cooper, L. N., & Wheeler, M. B. (2011). Developmental basis of mammalian digit reduction: A case study in pigs. *Evolution and Development*, *13*(6), 533–541. https://doi.org/10.1111/j.1525-142X.2011.00509.x

Sears, K., Maier, J. A., Sadier, A., Sorensen, D., & Urban, D. J. (2017). Timing the developmental origins of mammalian limb diversity. *Genesis*, 1–14. https://doi.org/10.1002/dvg.23079

Shubin, N., Tabin, C., & Carroll, S. (1997). Fossils, genes and the evolution of animal limbs. *Nature*, *388*, 639–648. https://doi.org/10.1038/41710

Skinner, A., & Lee, M. S. Y. (2009). Body-form evolution in the scincid lizard clade Lerista and the mode of macroevolutionary transitions. *Evolutionary Biology*, *36*(3), 292–300. https://doi.org/10.1007/s11692-009-9064-9

Smith, F. A., & Lyons, S. K. (2011). How big should a mammal be? A macroecological look at mammalian body size over space and time. In *Philosophical Transactions of the Royal Society B: Biological Sciences* (Vol. 366, Issue 1576, pp. 2364–2378). https://doi.org/10.1098/rstb.2011.0067

Stepanova, N., & Womack, M. C. (2020). Anuran limbs reflect microhabitat and distal, later-developing bones are more evolutionarily labile. *Evolution*, *74*(9), 2005–2019. https://doi.org/10.1111/evo.13981

Stopper, G. F., & Wagner, G. P. (2005). Of chicken wings and frog legs: A smorgasbord of evolutionary variation in mechanisms of tetrapod limb development. *Developmental Biology*, *288*(1), 21–39. https://doi.org/10.1016/j.ydbio.2005.09.010

Upham, N. S., Esselstyn, J. A., & Jetz, W. (2019). Inferring the mammal tree: Species-level sets of phylogenies for questions in ecology, evolution, and conservation. *PLoS Biology*, *17*(12). https://doi.org/10.1371/journal.pbio.3000494

Wagner, G. P. (2014). Digits and digit identity. In *Homology, genes, and evolutionary innovation* (First Edition, pp. 356–382). Princeton UniversityPress.

Watanabe, A., Fabre, A. C., Felice, R. N., Maisano, J. A., Müller, J., Herrel, A., & Goswami, A. (2019). Ecomorphological diversification in squamates from conserved pattern of cranial integration. *Proceedings of the National Academy of Sciences of the United States of America*, *116*(29), 14688–14697. https://doi.org/10.1073/pnas.1820967116

Weisbecker, V. (2011). Monotreme ossification sequences and the riddle of mammalian skeletal development. *Evolution*, *65*(5), 1323–1335. https://doi.org/10.1111/j.1558-5646.2011.01234.x

Weisbecker, V., Goswami, A., Wroe, S., & Sánchez-Villagra, M. R. (2008). Ossification heterochrony in the therian postcranial skeleton and the marsupial-placental dichotomy. *Evolution*, *62*(8), 2027–2041. https://doi.org/10.1111/j.1558-5646.2008.00424.x

Weisbecker, V., & Schmid, S. (2007). Autopodial skeletal diversity in hystricognath rodents: Functional and phylogenetic aspects. *Mammalian Biology*, *72*(1), 27–44. https://doi.org/10.1016/j.mambio.2006.03.005

Weisbecker, V., & Warton, D. I. (2006). Evidence at hand: Diversity, functional implications, and locomotor prediction in intrinsic hand proportions of diprotodontian marsupials. *Journal of Morphology*, *267*(12), 1469–1485. https://doi.org/10.1002/jmor.10495

Young, N. M., & Hallgrímsson, B. (2005). Serial homology and the evolution of mammalian limb covariation structure. *Evolution*, *59*(12), 2691–2704. https://doi.org/10.1111/j.0014-3820.2005.tb00980.x

« Sans la curiosité de l'esprit, que serions-nous ? Telle est bien la beauté et la noblesse de la science : désir sans fin de repousser les frontières du savoir, de traquer les secrets de la matière et de la vie sans idée préconçue des conséquences éventuelles. »

— Marie Skłodowska-Curie

2.

The evolution of skeletal morphology in the mammalian forelimb:

Does developmental sequence predict bone diversity?

Adapted from: Rothier, P. S., Fabre, A.-C., Clavel, J., Benson, R. B. J., & Herrel, A. (2023). Mammalian forelimb evolution is driven by uneven proximal-to-distal morphological diversity. *eLife*, *12*. https://doi.org/10.7554/eLife.

2.1. Abstract

Vertebrate limb morphology often reflects the environment due to variation in locomotor requirements. However, proximal and distal limb segments may evolve differently from one another, reflecting an anatomical gradient of functional specialization that has been suggested to be impacted by the timing of development. Here we explore whether the temporal sequence of bone condensation predicts variation in the capacity of evolution to generate morphological diversity in proximal and distal forelimb segments across more than 600 species of mammals. Distal elements not only exhibit greater shape diversity, but also show stronger within-element integration and, on average, faster evolutionary responses than intermediate and upper limb segments. Results are consistent with the hypothesis that late developing distal bones display greater morphological variation than more proximal limb elements. However, the higher integration observed within the autopod deviates from such developmental predictions, suggesting that functional specialization plays an important role in driving within-element covariation. Proximal and distal limb segments also show different macroevolutionary patterns, albeit not showing a perfect proximo-distal gradient. The high disparity of the mammalian autopod, reported here, is consistent with the higher potential of development to generate variation in more distal limb structures, as well as functional specialization of the distal elements.

2.2. Introduction

The evolutionary origin of limbs sets the stage for the remarkable ecological diversity of Tetrapoda (Shubin et al., 1997). From delicate wings to powerful excavating claws, from slender hooved legs to wide flattened flippers, limb formation is intrinsically integrated with and constrained by the determination of the tetrapod body plan (Raff, 1996). The tetrapod limb is typically composed of three basic components: the proximal stylopod (upper arm and thigh), the intermediate zeugopod (lower arm and calf), and the distal autopod (hand and foot). The proximal to distal organization of segments is correlated with their respective evolutionary appearance, the stylopod being the first structure to evolve, later followed by the zeugopod, and finally the autopod (Shubin et al., 1997). Although the three-segment pattern is conserved among quadruped tetrapods, the morphology of these structures along the proximo-distal axis may evolve differently among groups (Cooper et al., 2011; Galis et al., 2001; Holder, 1983; Sears et al., 2007).

Limbs are often studied for their exceptional morphological and ecological diversity (Chen & Wilson, 2015; Grizante et al., 2010; Kohlsdorf et al., 2001; Ledbetter & Bonett, 2019; Polly, 2007; Rothier et al., 2017, 2022; Stepanova & Womack, 2020). In mammals, for example, the forelimb is present in all species and is typically more variable than the hind limb, possibly due to its greater number of functional roles (Fig. 2.1; Polly, 2007; Schmidt and Fischer, 2009). The meristic composition of tetrapod forelimb segments varies along the proximo-distal limb axis, where the autopod exhibits most of the diversity in terms of the number and position of skeletal elements (i.e., fusion and loss of carpal and tarsal bones and alteration of the phalangeal formula; Cooper et al., 2007; Hamrick, 2001; Holder, 1983; Luo et al., 2015; Saxena et al., 2017). Except for lineages that have undergone complete limb loss such as snakes and caecilians, the meristic composition of proximal segments is much more conserved than that of the autopod,

displaying some but less frequent cases of element reduction and partial fusion of the zeugopod bones (observed in anurans, bats, manatees, horses, etc., Holder, 1983; Keeffe and Blackburn, 2022; Sears et al., 2007). Although this meristic information is useful to quantify major evolutionary changes in element composition, most of the morphological variation observed in the limbs results from changes in the shape and relative size of individual elements (i.e. variation of form) without changing the numbers of elements, and is often associated with functional adaptation (Fabre et al., 2013, 2015; Janis & Martín-Serra, 2020; Lungmus & Angielczyk, 2021; Sears et al., 2017). Despite its importance, it remains unclear how this macroevolutionary variation of form is partitioned between the three limb segments.

Both functional and developmental factors predict that distal elements should show greater variation of form than more proximal elements. Developmental mechanisms predict this pattern due to the timing and spatial structure of morphogenesis, which has been suggested to influence the macroevolutionary outcome of adult morphologies, including that of the skull (Bardua et al., 2021; Fabre et al., 2020), the vertebrae (Adler et al., 2022), and the limbs (Holder, 1983; Stepanova & Womack, 2020). Each limb initiates as a bud that extends from the body wall and where skeletal elements are generally specified in a proximal to distal sequence that matches their evolutionary appearance during tetrapod origins: development begins with the stylopod, followed by the zeugopod, and terminating in the autopod at the distal end (Fig. 2.2 A; Schneider and Shubin, 2013; Shubin et al., 1997; Stopper and Wagner, 2005). Limb development has been notably studied in mammals, revealing that different species have more similar forelimb morphology during early development, and become more disparate during later stages of morphogenesis (Ross et al., 2013). Likewise, gene expression of different mammal species is more conserved during early phases of limb development, compared

to later phases (Maier et al., 2017), and these patterns might reflect the intrinsic temporal properties of embryogenesis (Galis et al., 2001; Sears et al., 2017).

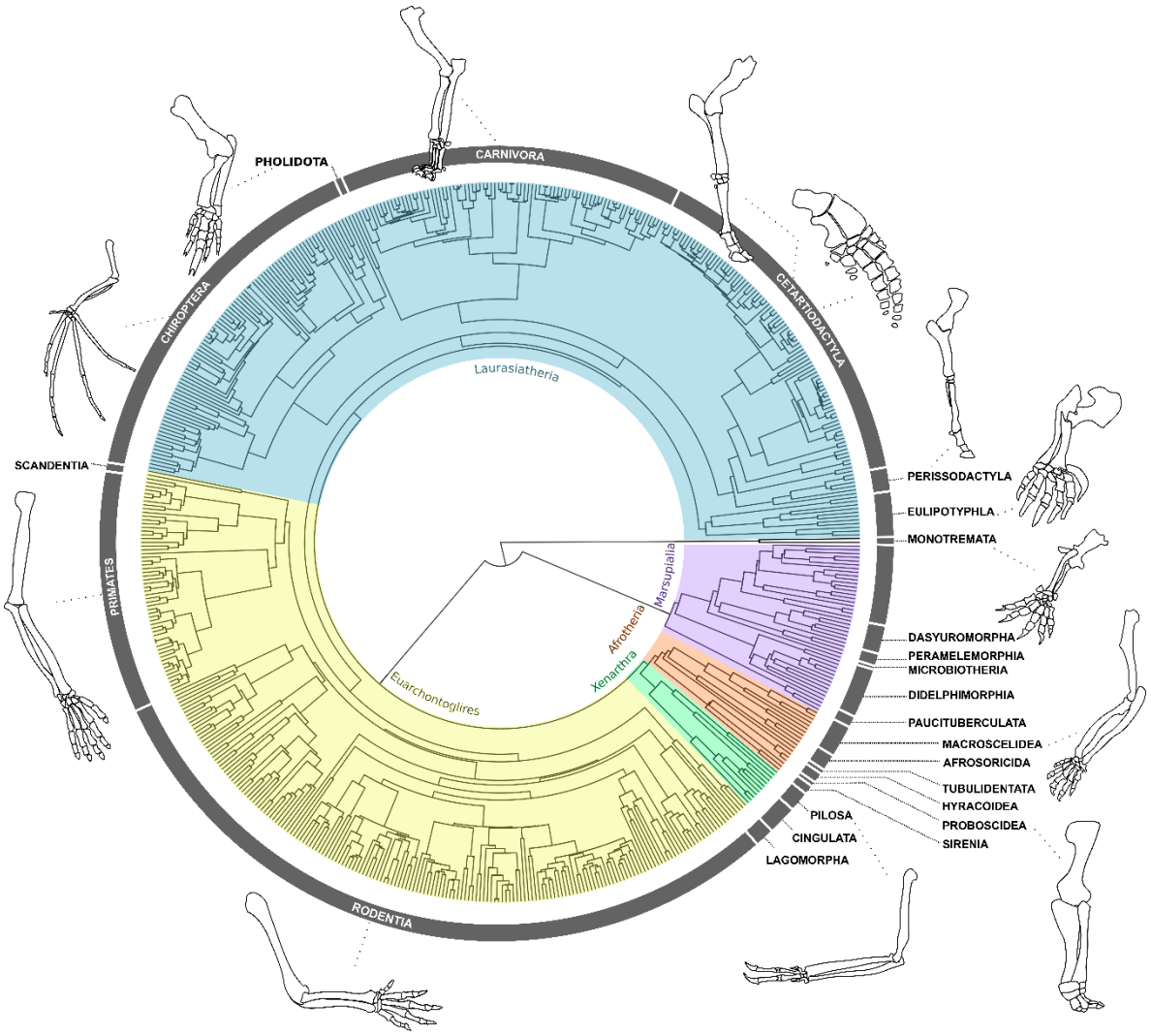

Figure 1.2. Forelimb diversity of mammals. The topology includes all genera examined in this work, representing the exceptional forelimb morphological variation for some of the species analysed. The topology was estimated using maximum clade credibility from a posterior sample of 10,000 trees published by Upham et al. (2019).

The timing of development has been already suggested to impact the uneven diversity and evolution of limb segments in frogs, with distal, late-developing bones being more variable and tending to diversify faster than proximal, early-forming elements (Stepanova & Womack, 2020). Indeed, early developmental processes mediating the initial specification of structures are generally more constrained than those governing later events, such as organ specialization (Kalinka & Tomancak, 2012). Therefore, because limb development proceeds proximo-to-distally, developmental perturbations at later phases may tend to accumulate higher morphological variation in distal elements (Hallgrímsson et al., 2002). One way to investigate the levels of developmental and functional constraints on adult morphologies is by quantifying the phenotypic integration among traits, inferred from the covariation between structures. For example, because the fore and hind limbs are serially homologous, they share genetic and developmental processes that give rise to strong phenotypic integration between and within the limbs (Ruvinsky & Gibson-Brown, 2000; Young & Hallgrímsson, 2005). In mammals, the correlation between homologous limb segments of the fore- and hind limbs (i.e., humerus with femur, radius with tibia, metacarpal with metatarsal) suggests that proximal segments are highly integrated to each other (Hallgrímsson et al., 2002; Schmidt & Fischer, 2009; Young & Hallgrímsson, 2005). In contrast, the more distal elements of the hand and foot show more variable patterns of integration, which may reflect functional specialization and the accumulation of variation during later phases of development (Hallgrímsson et al., 2002; Rolian, 2009; Young & Hallgrímsson, 2005). A consequence for limb diversification is that the patterns and pace of morphological evolution might not be the same between proximal and distal segments.

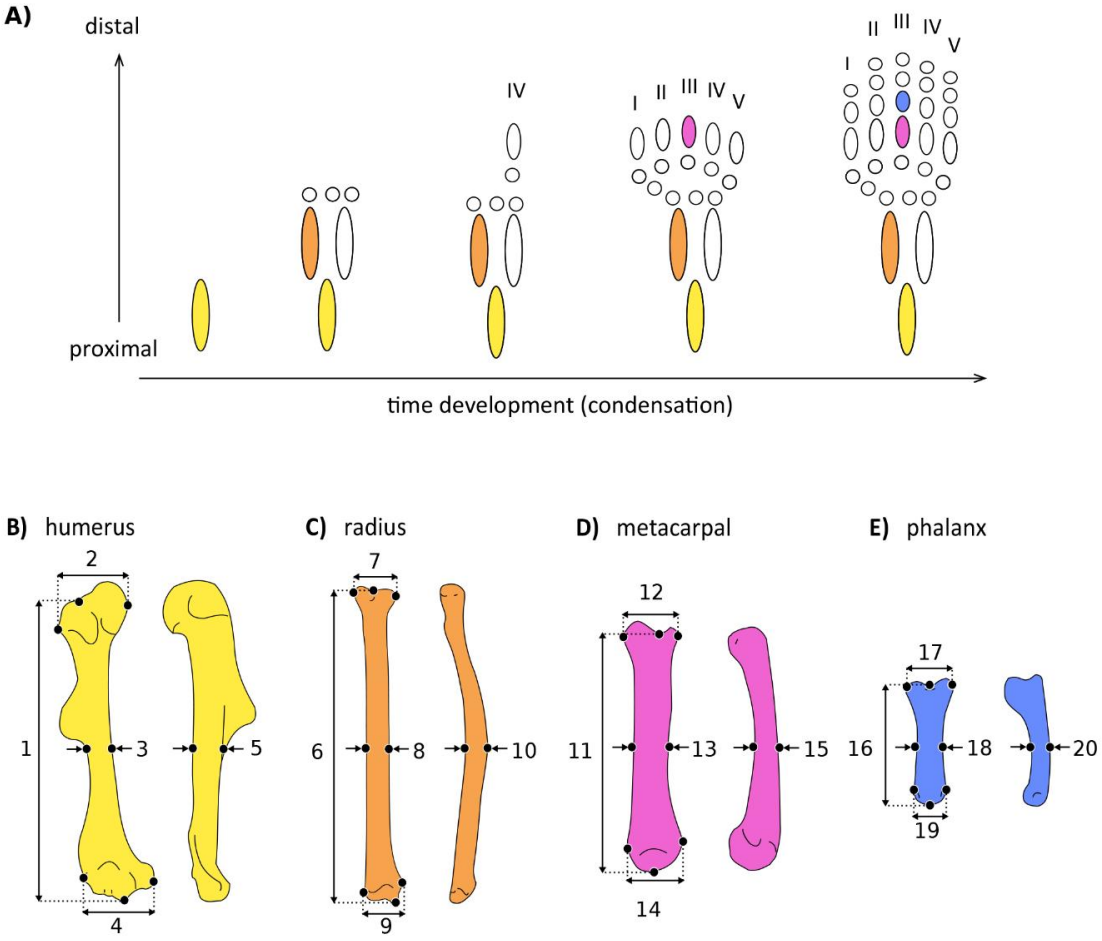

Figure 2.2. Simplified scheme of the developmental sequence of limb condensation (A), indicating the bones analysed and the linear measurements obtained. B) Humerus in anterior (right) and lateral (left) view: 1) length, 2) proximal width, 3) mid-shaft width, 4) distal width and 5) height. **C)** Radius in anterior (right) and lateral (left) view: 6) length, 7) proximal width, 8) mid-shaft width, 9) distal width and 10) height. **D)** Third metacarpal in dorsal (right) and lateral (left) view: 11) length, 12) proximal width, 13) mid-shaft width, 14) distal width and 15) height. **E)** First phalanx of the digit III in dorsal (right) and lateral (left) view: 16) length, 17) proximal width, 18) mid-shaft width, 19) distal width and 20) height. Detailed description of each measurement can be found in Table S1.2.

Here, we investigate the evolutionary patterns underlying the morphological diversification of mammalian forelimb segments along a proximal-to-distal axis, using a comprehensive data set of 638 species, capturing over 85% of Mammalia family-level diversity (Table S1.1). We ask to what extent is the temporal structure of proximo-distal bone condensation consistent with the macroevolution of limb segment morphologies. Mammals are an ideal group to address this question given their exceptional morphological and ecological diversity, combined with a substantial literature on the functional variation and the evolutionary development of their limbs (Fig. 2.1; Chen and Wilson, 2015; Grossnickle and Newham, 2016; Howenstine et al., 2021; Lungmus and Angielczyk, 2021; Maier et al., 2017; Polly, 2007; Sears et al., 2007; Weisbecker, 2011; Weisbecker et al., 2008). We examined the diversification of limb skeletal elements by quantifying morphological diversity and integration using linear measurements of four forelimb bones (Fig. 2.2 B-E, Table S1.2). We also estimated the macroevolutionary patterns of these elements using multivariate phylogenetic comparative methods. First, we quantified the morphological diversity of each segment, testing the hypothesis that distal bones are morphologically more diverse than the proximal structures as is predicted by development. Next, we investigated whether the strength of within-element integration differs between proximal and distal limb elements. We predicted that proximal elements would be more integrated than distal ones, due to their earlier condensation during development. Finally, we inferred the macroevolutionary patterns for bones belonging to all limb segments, predicting positive associations between the temporal sequence of bone condensation and the capacity for evolution to generate morphological diversity. To our knowledge, this is the first time that the evolutionary patterns observed in the form of proximal versus distal limb elements are investigated using a broad phylogenetic and ecological sample of mammals, essential to address these questions.

2.3. Results

2.3.1. Morphological diversity

Among the three different evolutionary models examined (Brownian motion, Early-Burst and Ornstein-Uhlenbeck), the Ornstein-Uhlenbeck (OU; see Hansen, 1997) process is the one that better predicts the pattern of evolution for all bones measured (Table S2.1). We inferred morphological diversity for each bone using the determinant and the trace of the original dataset (Table S2.2) and of simulated trait matrices. Determinants and traces of matrices offer different but complementary generalized metrics to describe the variation of multidimensional data. The matrix trace provides information about the accumulated trait variance, whereas the determinant provides information about the volume occupied by the multivariate data. Both show similar patterns, in which morphological variation increases along the proximo-distal axis, consistent with the timing of limb condensation during development (Fig. 2.3 A and B). The early-condensing humerus is the least variable structure (determinant = 0.0015, trace = 0.0079), and the late-condensing phalanx is the most diverse element measured (determinant = 0.0019, trace = 0.0135), followed by the third metacarpal (determinant = 0.0017, trace = 0.0101, Table S2.2). All pairwise comparisons between elements are significant (Table 2.1), although the differences of the determinant distributions of the radius and the metacarpal ($P = 0.017$) are smaller than when using the trace results ($P < 0.001$).

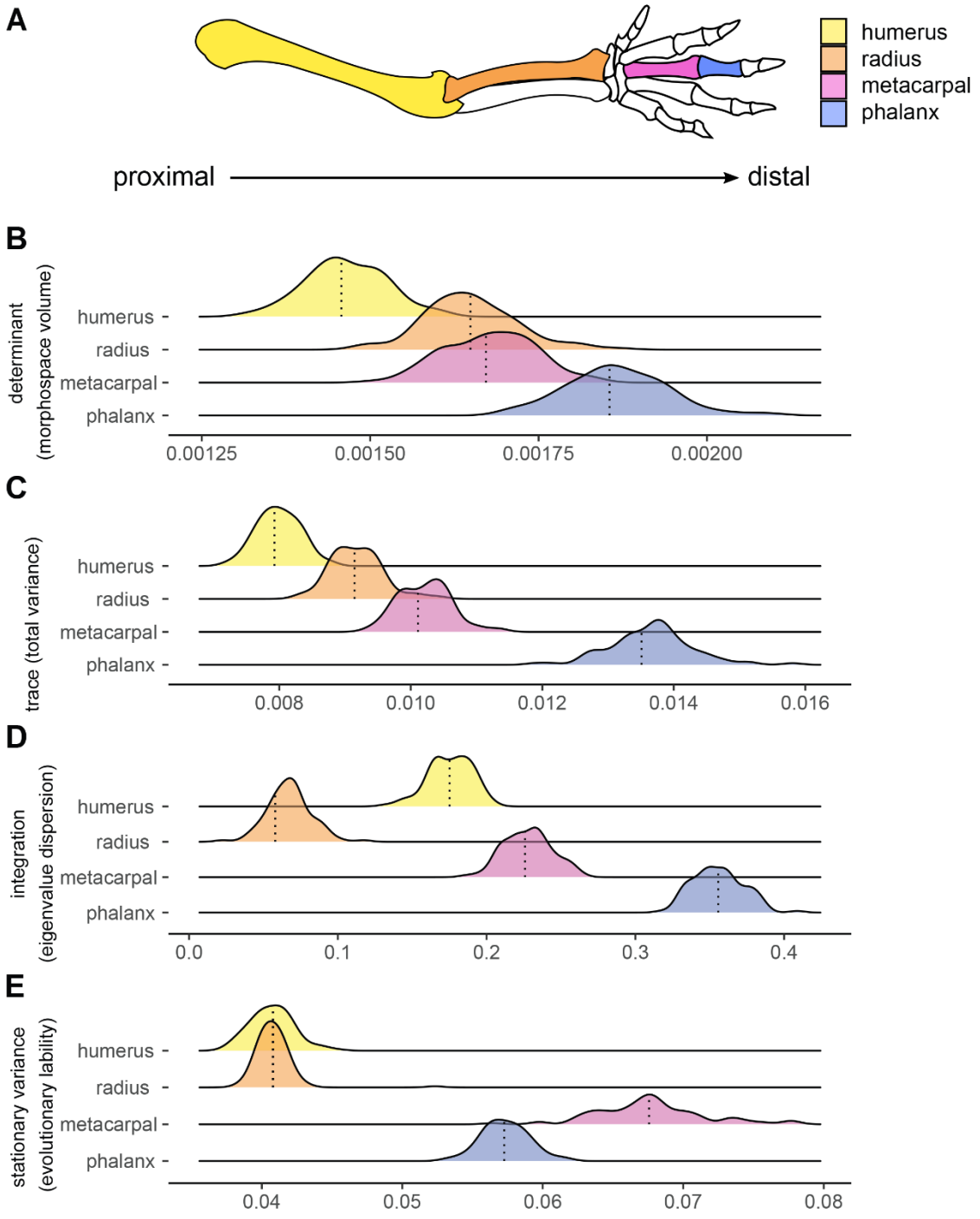

Figure 2.3. Components of the morphological evolution of forelimb skeletal elements. A) Forelimb schematic, with colours indicating bones along the proximo-distal axis: the humerus (yellow), radius (orange), third metacarpal (pink), and the first phalanx of digit III (blue). Reference lines indicate empirical values (B, C and D) or the median values (E) from 100 different topologies. replicated **B)** Morphological diversity of limb bones inferred by matrix determinant. **C)** Morphological diversity of limb bones, inferred by matrix trace. **D)** Trait integration. **E)** Stationary variance.

2.3.2. Phenotypic integration

Integration, inferred here by the values of eigenvalue dispersion, is stronger for distal elements compared to proximal ones, the phalanx being the most integrated element, followed by the metacarpal (Fig. 2.3 A and C). The values of integration do not progressively increase along the proximo-distal axis. Instead, the radius is the least integrated structure, and the more proximal humerus is the second least integrated trait. All pairwise comparisons between elements are significant (Table 2.1).

Table 2.1. Limb bone pairwise comparison of integration, determinant, trace, and stationary variance computed by a Tukey Test following an ANOVA. Pairwise differences (Diff) of each metric are indicated with the lower (Lwr) and upper (Upr) 95% CI, as well as the adjusted P-values. Hum= Humerus, Rad= Radius, Met= Metacarpus and Phal= Phalanx.

		Rad-Hum	Met-Hum	Phal-Hum	Met-Rad	Phal-Rad	Phal-Met
Determinant	Diff	1.8E-04	2.1E-04	4.0E-04	2.9E-05	2.2E-04	1.9E-04
	Lwr	1.6E-04	1.9E-04	3.8E-04	3.8E-06	1.9E-04	1.6E-04
	Upr	2.1E-04	2.4E-04	4.3E-04	5.3E-05	2.4E-04	2.1E-04
	P-value	**<0.001**	**<0.001**	**<0.001**	**0.017**	**<0.001**	**<0.001**
Trace	Diff	1.2E-03	2.2E-03	5.7E-03	1.0E-03	4.5E-03	3.4E-03
	Lwr	1.0E-03	2.1E-03	5.5E-03	8.8E-04	4.3E-03	3.3E-03
	Upr	1.4E-03	2.4E-03	5.8E-03	1.2E-03	4.6E-03	3.6E-03
	P-value	**<0.001**	**<0.001**	**<0.001**	**<0.001**	**<0.001**	**<0.001**
Integration	Diff	-0.108	0.052	0.180	0.160	0.288	0.128
	Lwr	-0.114	0.047	0.175	0.155	0.283	0.122
	Upr	-0.102	0.058	0.186	0.166	0.294	0.133
	P-value	**<0.001**	**<0.001**	**<0.001**	**<0.001**	**<0.001**	**<0.001**
Stationary variance	Diff	0.000	0.027	0.017	0.027	0.017	-0.010
	Lwr	-0.001	0.026	0.016	0.026	0.016	-0.011
	Upr	0.001	0.028	0.017	0.028	0.017	-0.009
	P-value	0.989	**<0.001**	**<0.001**	**<0.001**	**<0.001**	**<0.001**

2.3.3. Stationary variances

Traits evolving under an OU process change at a given step variance (σ^2) with a strength of constrains (α) towards an adaptive optimum (θ) (Hansen, 1997). We interpreted the tempo of evolution of traits considering the mean stationary variance ($\sigma^2/2\alpha$) of each bone, which is a measure of rate under the OU process (Hunt, 2012). The stationary variance, referred here as evolutionary lability, represents the expected variation when the OU process is at equilibrium (i.e., around the optimum): the higher the stationary variances, the greater – or more labile – is the phenotypic change around the trait optimum (see Friedman et al., 2021; Gearty et al., 2018; Hansen, 1997; Joly et al., 2018; Weaver and Grossnickle, 2020). The stationary variances are significantly higher for distal elements compared to proximal ones. The metacarpal shows the highest stationary variance, followed by the phalanx (Fig. 2.3 A and D). There are no significant differences in the stationary variances at which the humerus and the radius evolve, these values being significantly lower than those of the two autopodial elements (Table 2.1). Thus, whereas these results are in line with the predictions of the developmental hypothesis in showing greater evolutionary lability in the distal elements, they do not support the idea of a proximo-distal gradient of increasing stationary variances.

2.4. Discussion

The remarkable diversity of limb morphologies seen in mammals reflects the rich ecological and functional diversity that has evolved in this group (Polly, 2007). However, such outstanding morphological variation does not evolve uniformly among segments. Based on linear measurements of limb bones we show a general pattern of morphological diversity in Mammalia in which distal elements such as phalanges and metacarpals are in

general more disparate and show greater evolutionary lability, as indicated by our measures of stationary variance, than more proximal elements such as the humerus and radius. These results are consistent with the hypothesis that the among-species diversity of limb element morphologies is predicted by the timing of element condensation during development. Conversely, developmental constraints imposed by early versus late morphogenesis do not seem to determine differences in within-bone integration; we found that the latest-condensing elements of the hand are more integrated than the earlier-condensing humerus and radius. We hypothesize that the degree of functional specialization across segments might play a role on the levels of within-element integration, with the autopod potentially being more specialized and therefore exhibiting greater integration. We further show that distal elements evolve, on average, with greater stationary variances (i.e., faster) than the proximal limb elements.

2.4.1. Limb segments: a proximal to distal gradient of increasing diversity

Previous studies have described the exceptional meristic variation in the autopod in contrast with the proximal and intermediate limb (Holder, 1983). Here, we confirm that such diversity is also detected in the form of hand bones. A pattern of increased morphological diversity along the proximal-distal limb axis is consistent with the prediction that lower proximal diversity might have been driven by developmental canalization (Hallgrímsson et al., 2002). A similar pattern has been previously documented for anurans, in a study that compared shape variation of the humerus and the radioulna of the forelimb, as well as the femur, the tibiofibula, and the tarsus of the hind limb (Stepanova & Womack, 2020). Although this study did not include the digital elements of the hand (metacarpals and phalanges), it showed that late developing distal

structures are not only more diverse but also evolve faster than the most proximal elements belonging to the stylopod (Stepanova & Womack, 2020). Microhabitat use also explains more shape variation in the distal elements compared to the most proximal limb bones, suggesting that functional specialization evolves differently along the proximo-distal limb axis (Stepanova & Womack, 2020). Combined with our results, these findings provide evidence that the proximal-distal gradient of variation in limb structures may consist of an early conserved pattern shared across tetrapods, supporting the hypothesis that the timing of development affects the intrinsic capacity of an organism to generate variation and facilitate subsequent functional diversification.

Functional variation is often a good predictor of the pattern of morphological variation of limb bones (Chen & Wilson, 2015; Fabre et al., 2013; Grossnickle et al., 2020; Weaver & Grossnickle, 2020). The autopod is the structure that interacts directly with the surrounding environment, performing important activities such as providing support to the body during locomotion and, in some cases, digging, handling food, grooming, and mediating social interactions (Biewener & Patek, 2018; McGrew et al., 2001; Naghizadeh et al., 2020; Sustaita et al., 2013; Weisbecker & Warton, 2006). Our results corroborate the idea that the hand bones are subjected to more dynamic selective pressures that ultimately favour greater diversity and evolutionary lability compared to proximal segments. However, few studies have quantified the functional relationships driving autopod variation in mammals (Almécija et al., 2015; Rolian, 2009; Weisbecker & Schmid, 2007; Weisbecker & Warton, 2006). As the number of digits, and the number of phalanges in each digit, varies within most groups of tetrapods, including mammals, autopodial morphology is difficult to quantify in a comparable, homologous way among species. Although our data support this association, we do not explicitly test for the relationship between the variation observed in each bone and its degree of functional

specialization. Further investigations are needed to quantify the impact of these parameters on limb diversification and need to set up *a priori* testable hypotheses.

To our knowledge, our study comprises the most comprehensive taxonomic dataset on the forearm morphology of mammals. The use of linear measurements succeeded at establishing comparable topological distances and provided a robust overview for the global morphological diversity between limb segments across the mammalian tree of life. However, this method imposes some limitations on capturing detailed local shape variation. For example, the proximal joint at the humerus can encompass complex surfaces which determine the mobility of the limb (Arias-Martorell, 2019; Veeger & van der Helm, 2007), but variation therein is not captured by our measurements. Likewise, the shape and size of the deltopectoral crest of the humerus may display considerable interspecific variation (Chen & Wilson, 2015; Hopkins & Davis, 2009; Samuels & Van Valkenburgh, 2008), and is also not quantified here. Similar structures are not present at the joints or at the longitudinal surfaces of the phalanges. Thus, it is not clear whether adding such morphological features would have resulted in an increase of morphological diversity in proximal bones compared to the distal ones. Either way, previous studies that have incorporated complex geometric surfaces of the long bones detected that the robustness (that is, the correlation of length and thickness) is one of the principal factors contributing to the pattern of morphological variation (Fabre et al., 2014, 2017; Michaud et al., 2020), consistent with our results.

Having the zeugopod solely represented by the radius might as well have obscured some of the diversity present in the intermediate limb segment. The ulna is highly variable, with the olecranon particularly being a strong predictor of locomotor habit (Chen & Wilson, 2015; Lungmus & Angielczyk, 2021; Milne & Granatosky, 2021; Samuels & Van Valkenburgh, 2008; Van Valkenburgh, 1987). However, due to the high variation of

the ulna, the topological distances used to describe the skeletal morphology (length, width, and height) cannot be applied to this bone in all species as the ulna is distally reduced or fused to the radius in many taxa (Sears et al. 2007), thus preventing us from quantifying the diversity between this and other limb bones. We encourage future studies to include the ulna and to use geometric morphometrics of the joints to complement our findings with detailed information on shape variation across limb segments.

2.4.2. Functional predictors of bone integration

The high integration detected in the mammalian hand suggests that developmental constraints of early versus late bone condensation do not predict within-element covariation. These findings do not imply that development is unimportant for the individual integration of elements. Yet, in the matter of relative bone integration, the timing of condensation is unable predict which elements are the most and the least integrated. The proximal and distal humeral joints perform different functions and allow very different movements: the proximal head connects the limb to the pectoral girdle at the shoulder through a complex ball-and-socket articulation (Arias-Martorell, 2019; Veeger & van der Helm, 2007), and it distally articulates with the ulna and the radius at the elbow driving forelimb mobility and stability (Fabre et al., 2014). The radial joints are also involved in different functions, having a proximal head connected to the elbow and an enlarged distal extremity articulated at the wrist with carpals and sometimes the ulna (Macleod & Rose, 1993; Polly, 2007). Because they are involved in different functions, the articular surfaces of long bones are differently impacted by functional specialization related to locomotor habit (Fabre et al., 2014; Lungmus & Angielczyk, 2021; Macleod & Rose, 1993). In terms of within-element integration, the different functional demands at

the proximal and distal bone extremities might encompass a reduction of covariation between these traits, as detected here for the humerus and the radius. The metacarpal and the phalangeal articulations, on the other hand, work more similarly: phalanges articulate with the metacarpals at a bi-axial-joint (movement at two axes: flexion/extension, abduction/adduction) and articulate with each other at hinge joints which allow only one axis of movement (flexion and extension; Napier, 1993). The strong integration of hand bones detected for mammals indicates that these elements experience a highly correlated evolution, which in this case might also emerge from functional similarity and interdependence at the articulations.

2.4.3. Integration and evolutionary lability

The relationship between integration and morphological variation is not always consistent among traits and taxa (Felice et al., 2018). Whereas some studies have shown clear positive associations between high integration and phenotypic variation (Fabre et al., 2020, 2021; Randau & Goswami, 2017), negative associations have been also reported (Felice & Goswami, 2018; Goswami & Polly, 2010). We find no evidence for a strong correspondence of integration with morphological diversity in proximal forelimb segments: the radius exhibits greater diversity of form than the humerus but presents the weakest values of integration among the bones measured. For the distal elements, however, our results show that the highly integrated autopod, especially the phalanx, also corresponds to the most diverse structure of the limb (Fig. 2.3). These differences might reflect how selection interacts with the intrinsic and extrinsic constraints on variation. Though integration may constrain the evolution of the phenotype to a limited portion of morphospace, it may also promote variation by driving the evolution of these traits in

response to selection for functional specialization (Felice et al., 2018; Goswami et al., 2014; Hansen & Houle, 2008; Lande, 1979). Such dynamics appear to be observed in the distal elements: high integration in the phalanx and metacarpus, possibly favoured the evolution of functionally specialized autopod structures, contributes to the high variation observed in mammalian hand bones. Future studies will benefit from including extinct taxa to understand how morphological diversity and integration of limb bones evolved in deep time. Such analyses would further provide insights into whether these patterns are consistent between major taxonomic and ecological groups and through time and would provide information on when they first appeared during mammalian evolution.

2.4.4. Evolutionary lability of the autopodal elements: functional associations

The autopodial bones evolve, on average, with greater stationary variances around their optima than the stylopod and the zeugopod (Fig. 2.3). Although the developmental hypothesis predicted that the fastest evolving structures would belong to the late-condensed distal limb, evolutionary lability do not increase in a perfect proximal-to-distal pattern, and the third metacarpal is the structure with the highest stationary variances, followed by the phalanx. These findings suggest that functional selection (resulting from the direct impact of autopodial structures on locomotor performance) combined with the higher potential of development to generate variation in the morphology of more distal limb elements, facilitated the evolution of high autopodial disparity in response to varying environmental demands across mammals. Although this subject remains largely unexplored, some studies provide cues about the possible association of function with the

evolutionary lability of the autopod morphology in tetrapods (Ledbetter & Bonett, 2019; Rolian, 2009).

Notable transformations in the metacarpal and phalangeal morphology are observed in cursorial taxa that present specializations allowing for endurance running, typically involving the elongation of the distal limb in relation to proximal segments (Polly, 2007). These transformations may explain part of the results observed in our study. For example, morphological adaptations to cursoriality mostly encompass the modification of autopod posture to digitigrady (animals that stand on the distal ends of metapodials and middle phalanges, such as cats and dogs) and unguligrady (animals that stand on their hooved distal-most phalanx, such as horses and cows; Clifford, 2010; Polly, 2007; Wang, 1993). Digitigrady is observed in many carnivorans providing limb elongation and thus increasing stride length (Polly, 2007; Wang, 1993). Extant horses exhibit one of the most dramatic modifications of the third metapodial and phalanges among all unguligrade taxa: the limb is uniquely supported by the third toe, which is considerably enlarged and elongated, whilst the lateral fingers are markedly reduced (McHorse et al., 2019). One recent study suggested that the evolutionary transitions in foot and hand postures are associated with strong selection for rapid changes in increasing body size (Kubo et al., 2019). Although a digital posture presumably implies morphofunctional specialization of the distal limb, it is not clear if the acceleration of body mass evolution during autopod posture transitions has also affected the rates of morphological change of the hand and foot. Autopodial specialisations are also evident among smaller-sized mammals. For example, body size is positively associated with the tempo of evolution of postcranial morphology (hand and foot bones included) in both ground and tree dwelling animals, where medium-sized animals tend to exhibit higher stationary variances than small-sized species (Weaver & Grossnickle, 2020). Overall,

these examples suggest that functional specializations related to the locomotion and size likely played a role in driving the morphological evolution of the limb, potentially driving the accelerated evolution of hand bone morphology. Further investigations are needed to better understand the associations of body size and functional variation with the evolutionary dynamics of limb diversification.

2.5. Conclusion

This study uses a macroevolutionary framework to compare, for the first time, the general patterns of form diversification of proximal and distal limb elements in mammals. Our results reveal that the evolution of the mammalian forelimb involves different patterns of morphological diversification when comparing limb segments along a proximal–distal gradient. We detected that the diversification of autopodial elements was much more dynamic than that of the zeugopod and stylopod, involving higher morphological diversity, stronger integration, and greater evolutionary lability at distal structures. Specifically, we corroborate the premise that the late-condensing distal elements such as metacarpals and phalanges (in the autopod) exhibit higher morphological diversity than early-condensing, more proximal, elements. This pattern might emerge from different levels of constraints during the developmental succession. Yet, no proximo-distal gradient in stationary variance was observed. Furthermore, such temporal constraints of development do not explain the patterns of limb evolution alone, as functional specializations also play an important role on the diversification of the forelimb. Particularly, the strong integration of the autopodial elements most likely reflects the functional similarity and interdependence between joints in response to functional demands. We highlight the importance of considering variation induced by development

to understand the macroevolutionary outcome of adult morphologies and we hope that these results will contribute to better understand the association of limb segment variation and ecological diversity.

2.6. Material & methods

2.6.1. Taxonomic sampling and data acquisition

We sampled 638 species of mammals (670 specimens), representing 598 genera of 138 living families (Fig. 2.1). Sampling varies from one to four individuals per genus. We provided micro-CT-scans and surface scans of 58 small to medium sized-specimens from different institutions (available online at MorphoSource.org, Table S1.1), 23 of them previously used by Martín-Serra and Benson (2020). The digital dataset was combined with 351 meshes available on MorphoSource.org (Table S1.1). Image stacks were converted into three-dimensional models using Avizo 8.1.1 (1995-2014 Zuse Institute Berlin), where scale dimensions were incorporated based on the voxel size of each scan. Data collection from the digital models was also conducted in Avizo 8.1.1 (1995-2014 Zuse Institute Berlin). We complemented this dataset with measurements provided by caliper of 261 medium to large body-sized species from the mammal collection of the Muséum National d'Histoire Naturelle (Paris, France) (Table S1.1).

We measured 20 linear distances from anterior limb bones, including the humerus, the radius, the third metacarpal and the first phalanx of digit III. We acquired five measurements for each element: length, widths (proximal, mid-shaft and distal) and height (Fig. 2.2, see detailed description in Table S1.2). We opted not to include the ulna because this bone is fused to the radius in many taxa (see Sears et al. 2007), preventing the acquisition of such measurements. The metacarpal and first phalanx of digit III were

sampled because this is the only digit present in the hands of all mammalian lineages, even in groups that exhibit digit loss or fusion with other autopodial elements, such as in golden moles and ungulates (Clifford, 2010; McHorse et al., 2019; Prothero, 2009). Each individual was measured twice with the subsequent calculation of the mean and standard error in order to verify measurement error. The error estimate was most often below 1.5% regardless of an animal's size and the measurement method, demonstrating consistency and repeatability of the methods employed. Body mass values were rarely available for the individuals measured, so we assembled the average species body mass of adults from the PanTHERIA database (Jones et al., 2009) and complemented by literature sources when necessary (Table S1.1). When species level was not identified, we used the mean body mass available for the genus. Species taxonomy followed the Mammal Diversity Database published by Burgin et al. (2018).

2.6.2. Comparative analyses

Analyses were implemented in R 4.1.2 (R Core Team, 2022). We used the phangorn R package (Schliep, 2011) to estimate a maximum clade credibility (MCC) tree from a posterior sample of 10,000 trees published by Upham et al. (2019). Because the incorporation of some species was available only at the genus level, we pruned the MCC tree to genus level, according to the taxa sampled by our study, and calculated the genus mean per trait whenever we had more than one specimen measured per genus.

Allometry generally explains most of morphological variation, as body parts usually grow together, masking variation mediated by local development (Marroig, 2007; Raff, 1996). Because we are particularly interested in understanding morphological constraints imposed by the local development of the limb, we decided to remove the

allometric component of our dataset in order to reduce variation associated with other sources of development. We could not retrieve the individual body masses for most of the species included, so we calculated geometric means as a proxy for body size by including values of the individuals themselves and the average species body mass. First, we transformed body mass into linear scale by taking the cube root prior to log10-transformation (Harmon et al., 2010). We calculated the geometric means of all measurements acquired, including the linear scaled body mass, and then we fitted the log10-transformed trait means in a phylogenetic generalized least-squares (PGLS) using the geometric means as a predictor. We grouped the traits by bone and fitted the linear models for each skeletal unit with mvgls() function from mvMORPH R package (Clavel et al., 2015, 2019). We calculated the fit of three models of evolution using LASSO penalization: Brownian Motion (BM), Ornstein-Uhlenbeck (OU) and Early Burst (EB). We compared the likelihood of the model fits with Generalized Information Criterion (GIC) to establish which model provided the best fit.

The OU model of evolution had the best fit for all the linear regressions accounting for the geometric means using the MCC tree (Table S2.1). To evaluate whether using the species average value (and not the individual body mass) would bias the results, we performed supplemental PGLS removing the average body mass from the geometric means. The results between bones remained the same (Tables S2.2-S2.3), so we maintained the body mass in the geometric means for the downstream analyses. We used a parametric bootstrap approach to assess the uncertainty around point estimates for morphological diversity and integration. We first simulated 100 datasets for each bone on MCC tree using the OU process fit (that is, the best fit model on our original data) with parameters estimates from the empirical regression (function mvSIM() from mvMORPH; Clavel et al. 2015, 2019). The model (the body size PGLS under an OU process) was then

fit to these 100 simulated traits, and the distribution of parameters estimates obtained was used to assess the variability around the point estimate (for the determinant, the trace, and the measure of integration) obtained on empirical data.

2.6.3. Morphological diversity and phenotypic integration

Morphological diversity for each bone was interpreted as the values of the determinant and the trace of simulated matrices. The trace is the sum of the diagonal elements of the trait covariance matrix, that is, the sum of individual traits variance (sum(diag()), R Core Team, 2021). The determinant is a scalar measure that summarize the information contained in a square matrix (det(), R Core Team, 2021). For a covariance matrix, it corresponds to a generalized measure of variance, because contrary to the trace, the determinant account for the correlations/covariances between the traits (Rencher, 2002). We scaled the determinants by transforming their absolute value to the power of one divided by five, which is the number of dimensions of each matrix (that is, the number of measurements). Differences in the determinant and trace between skeletal elements were evaluated by ANOVA followed by Tukey Tests (function TukeyHSD() from stats R package) of the 95% confidence interval (CI).

We calculated the magnitude of integration for each bone separately, based on eigenvalue dispersion in their respective matrices. We transformed the simulated covariance matrices into correlation matrices and provided integration values as the standard deviation of eigenvalues relative to their theoretical maximum (Haber, 2011; Pavlicev et al., 2009). We calculated the integration as the dispersion of the standard deviation of eigenvalues of our trait matrices, following Pavlicev et al. (2009). For instance, highly integrated traits have most of the independent variance concentrated in

the first few eigenvalues, while uncorrelated traits have the variance similarly distributed between eigenvalues (Pavlicev et al., 2009). Eigenvalue dispersion was inferred from CalcEigenVar() function of evolqg R package (Machado et al., 2019; Melo et al., 2015), which calculates the relative eigenvalue variance of the matrix as a ratio between the observed variance and the theoretical maximum for a matrix of the same size and trace (Machado et al. 2019). Differences between distributions were computed by an ANOVA and detailed by Tukey Tests of the 95% CI.

2.6.4. Macroevolutionary patterns

Finally, we were interested in estimating the tempo of evolution of each bone. To assess variability due to the tree topology and branching times uncertainties, we replicated the body mass linear regressions with 100 randomly sampled trees from Upham et al. (2019). We fitted these linear regressions under an OU process and estimated the average rates of evolution (σ^2) per bone. Under a Brownian motion process, the tempo of evolution can be directly inferred from the σ^2, which represents the total variance of traits changes linearly, as a function of the traits covariances matrix and time (Harmon, 2019). In an OU process, however, traits evolve towards an optimum θ with an attraction α. The main difference between BM and OU, is that the trait variance changes with time in BM, while it is not related to time in OU when stationary (Hunt, 2012). Assuming that time was long enough in an OU process (so that the process is stationary, e.g., reached the optimum), its covariance matrix, equivalent to a BM matrix of traits variance and covariance, depends only on the parameters σ^2 and α (Hunt, 2012). A comparable rate metric for traits evolving under OU process is then the stationary variance ($\sigma^2/2\alpha$), representing the variance of traits distribution per evolutionary steps (or the variance of traits when lineages were

given enough time to reach their optima and the process is in equilibrium; Hansen, 1997; Hunt, 2012). Therefore, we calculated the mean stationary variance of bones from the matrices fitted under OU process (function stationary() from mvMORPH; Clavel et al. 2015). We compared their distributions using ANOVA followed by a 95% confidence interval Tukey Test.

2.7. References

Adler, K. A., Nault, D. L. de, Cardoza, C. M., & Womack, M. (2022). Evolutionary rates and shape variation along the anuran vertebral column with attention to phylogeny, body size, and ecology. *Evolution*. https://doi.org/10.1111/evo.14614

Almécija, S., Smaers, J. B., & Jungers, W. L. (2015). The evolution of human and ape hand proportions. *Nature Communications*, *6*. https://doi.org/10.1038/ncomms8717

Arias-Martorell, J. (2019). The morphology and evolutionary history of the glenohumeral joint of hominoids: A review. *Ecology and Evolution,* 9(1), 703–722. https://doi.org/10.1002/ece3.4392

Bardua, C., Fabre, A.-C., Clavel, J., Bon, M., Das, K., Stanley, E. L., Blackburn, D. C., & Goswami, A. (2021). Size, microhabitat, and loss of larval feeding drive cranial diversification in frogs. *Nature Communications*, *12*(1). https://doi.org/10.1038/s41467-021-22792-y

Biewener, A. A., & Patek, S. N. (2018). *Animal locomotion* (2nd Edition.). Oxford University Press.

Burgin, C. J., Colella, J. P., Kahn, P. L., & Upham, N. S. (2018). How many species of mammals are there? *Journal of Mammalogy*, *99*(1), 1–14. https://doi.org/10.1093/jmammal/gyx147

Chen, M., & Wilson, G. P. (2015). A multivariate approach to infer locomotor modes in Mesozoic mammals. *Paleobiology*, *21*(2), 280–312. https://doi.org/10.5061/dryad.870j3

Clavel, J., Aristide, L., & Morlon, H. (2019). A penalized likelihood framework for high-dimensional phylogenetic comparative methods and an application to new-world

monkeys brain evolution. *Systematic Biology*, *68*(1), 93–116. https://doi.org/10.1093/sysbio/syy045

Clavel, J., Escarguel, G., & Merceron, G. (2015). mvMORPH: An R package for fitting multivariate evolutionary models to morphometric data. *Methods in Ecology and Evolution*, *6*(11), 1311–1319. https://doi.org/10.1111/2041-210X.12420

Clifford, A. B. (2010). The evolution of the unguligrade manus in artyodactyls. *Journal of Vertebrate Paleontology*, *30*(6), 1827–1839. https://doi.org/doi.org/10.1080/02724634.2010.521216

Cooper, K. L., Kuang-Hsien Hu, J., ten Berge, D., Fernandez-Teran, M., Ros, M. A., & Tabin, C. J. (2011). Initiation of proximal-distal patterning in the vertebrate limb by signals and growth. *Science*, *332*(6033), 1083–1086. https://doi.org/10.1126/science.1199499

Cooper, L. N., Berta, A., Dawson, S. D., & Reidenberg, J. S. (2007). Evolution of hyperphalangy and digit reduction in the cetacean manus. *Anatomical Record*, *290*(6), 654–672. https://doi.org/10.1002/ar.20532

Fabre, A.-C., Bardua, C., Bon, M., Clavel, J., Felice, R. N., Streicher, J. W., Bonnel, J., Stanley, E. L., Blackburn, D. C., & Goswami, A. (2020). Metamorphosis shapes cranial diversity and rate of evolution in salamanders. *Nature Ecology and Evolution*, *4*(8), 1129–1140. https://doi.org/10.1038/s41559-020-1225-3

Fabre, A.-C., Cornette, R., Goswami, A., & Peigné, S. (2015). Do constraints associated with the locomotor habitat drive the evolution of forelimb shape? A case study in musteloid carnivorans. *Journal of Anatomy*, *226*(6), 596–610. https://doi.org/10.1111/joa.12315

Fabre, A.-C., Cornette, R., Slater, G., Argot, C., Peigné, S., Goswami, A., & Pouydebat, E. (2013). Getting a grip on the evolution of grasping in musteloid carnivorans: A three-dimensional analysis of forelimb shape. *Journal of Evolutionary Biology*, *26*(7), 1521–1535. https://doi.org/10.1111/jeb.12161

Fabre, A.-C., Dowling, C., Miguez, R. P., Fernandez, V., Noirault, E., & Goswami, A. (2021). Functional constraints during development limit jaw shape evolution in marsupials. *Proceedings of the Royal Society B: Biological Sciences*, *288*(1949). https://doi.org/10.1098/rspb.2021.0319

Fabre, A.-C., Goswami, A., Peigné, S., & Cornette, R. (2014). Morphological integration in the forelimb of musteloid carnivorans. *Journal of Anatomy*, *225*(1), 19–30. https://doi.org/10.1111/joa.12194

Fabre, A.-C., Marigó, J., Granatosky, M. C., & Schmitt, D. (2017). Functional associations between support use and forelimb shape in strepsirrhines and their relevance to inferring locomotor behavior in early primates. *Journal of Human Evolution*, *108*, 11–30. https://doi.org/10.1016/j.jhevol.2017.03.012

Felice, R. N., & Goswami, A. (2018). Developmental origins of mosaic evolution in the avian cranium. *Proceedings of the National Academy of Sciences of the United States of America*, *115*(3), 555–560. https://doi.org/10.1073/pnas.1716437115

Felice, R. N., Randau, M., & Goswami, A. (2018). A fly in a tube: Macroevolutionary expectations for integrated phenotypes. *Evolution*, *72*(12), 2580–2594. https://doi.org/10.1111/evo.13608

Friedman, S. T., Price, S. A., & Wainwright, P. C. (2021). The effect of locomotion mode on body shape evolution in teleost fishes. *Integrative Organismal Biology*, *3*(1). https://doi.org/10.1093/iob/obab016

Galis, F., Van Alphen, J. J. M., & Metz, J. A. J. (2001). Why five fingers? Evolutionary constraints on digit numbers. *TRENDS in Ecology & Evolution*, *16*(11). https://doi.org/10.1016/S0169-5347(01)02289-3

Gearty, W., McClain, C. R., & Payne, J. L. (2018). Energetic tradeoffs control the size distribution of aquatic mammals. *Proceedings of the National Academy of Sciences of the United States of America*, *115*(16), 4194–4199. https://doi.org/10.1073/pnas.1712629115

Goswami, A., & Polly, P. D. (2010). The influence of modularity on cranial morphological disparity in carnivora and primates (mammalia). *PLoS ONE*, *5*(3). https://doi.org/10.1371/journal.pone.0009517

Goswami, A., Smaers, J. B., Soligo, C., & Polly, P. D. (2014). The macroevolutionary consequences of phenotypic integration: from development to deep time. *Philosophical Transactions of the Royal Society. Series B, Biological Sciences*, *369*, 20130254. https://doi.org/10.1098/rstb.2013.0254

Grizante, M. B., Navas, C. A., Garland, T., & Kohlsdorf, T. (2010). Morphological evolution in Tropidurinae squamates: an integrated view along a continuum of ecological settings. *Journal of Evolutionary Biology*, *23*(1), 98–111. https://doi.org/10.1111/j.1420-9101.2009.01868.x

Grossnickle, D. M., Chen, M., Wauer, J. G. A., Pevsner, S. K., Weaver, L. N., Meng, Q. J., Liu, D., Zhang, Y. G., & Luo, Z. X. (2020). Incomplete convergence of gliding

mammal skeletons. *Evolution*, *74*(12), 2662–2680. https://doi.org/10.1111/evo.14094

Grossnickle, D. M., & Newham, E. (2016). Therian mammals experience an ecomorphological radiation during the Late Cretaceous and selective extinction at the K–Pg boundary. *Proceedings of the Royal Society B: Biological Sciences*, *283*(1832), 1–8. https://doi.org/10.1098/rspb.2016.0256

Haber, A. (2011). A comparative analysis of integration indices. *Evolutionary Biology*, *38*(4), 476–488. https://doi.org/10.1007/s11692-011-9137-4

Hallgrímsson, B., Willmore, K., & Hall, B. K. (2002). Canalization, developmental stability, and morphological integration in primate limbs. *Yearbook of Physical Anthropology*, *45*, 131–158. https://doi.org/10.1002/ajpa.10182

Hamrick, M. W. (2001). Development and evolution of the mammalian limb: adaptive diversification of nails, hooves, and claws. *Evolution & Development*, *3*(5), 355–363. https://doi.org/10.1046/j.1525-142x.2001.01032.x

Hansen, T. F. (1997). Stabilizing selection and the comparative analysis of adaptation. *Evolution*, *51*(5), 1341–1351. https://doi.org/10.1111/j.1558-5646.1997.tb01457.x

Hansen, T. F., & Houle, D. (2008). Measuring and comparing evolvability and constraint in multivariate characters. *Journal of Evolutionary Biology*, *21*(5), 1201–1219. https://doi.org/10.1111/j.1420-9101.2008.01573.x

Harmon, L. (2019). *Phylogenetic comparative methods: learning from trees*.

Harmon, L. J., Losos, J. B., Jonathan Davies, T., Gillespie, R. G., Gittleman, J. L., Bryan Jennings, W., Kozak, K. H., McPeek, M. A., Moreno-Roark, F., Near, T. J., Purvis, A., Ricklefs, R. E., Schluter, D., Schulte, J. A., Seehausen, O., Sidlauskas, B. L., Torres-Carvajal, O., Weir, J. T., & Mooers, A. T. (2010). Early bursts of body size and shape evolution are rare in comparative data. *Evolution*, *64*(8), 2385–2396. https://doi.org/10.1111/j.1558-5646.2010.01025.x

Holder, N. (1983). Developmental constraints and the evolution of vertebrate digit patterns. *Journal of Theoretical Biology*, *104*, 451–471. https://doi.org/10.1016/0022-5193(83)90117-0

Hopkins, S. S. B., & Davis, E. B. (2009). Quantitative morphological proxies for the fossoriality in small mammals. *Journal of Mammalogy*, *90*(6), 1449–1460. https://doi.org/10.1644/08-MAMM-A-262R1.1

Howenstine, A. O., Sadier, A., Anthwal, N., Lau, C. L., & Sears, K. E. (2021). Non-model systems in mammalian forelimb evo-devo. *Genetics and Development*, *69*, 65–71. https://doi.org/10.1016/j.gde.2021.01.012

Hunt, G. (2012). Measuring rates of phenotypic evolution and the inseparability of tempo and mode. *Paleobiology*, *38*(3), 351–373. https://doi.org/10.5061/dryad.c1m60s84

Janis, C. M., & Martín-Serra, A. (2020). Postcranial elements of small mammals as indicators of locomotion and habitat. *PeerJ*, *8*. https://doi.org/10.7717/peerj.9634

Joly, S., Lambert, F., Alexandre, H., Clavel, J., Léveillé-Bourret, É., & Clark, J. L. (2018). Greater pollination generalization is not associated with reduced constraints on corolla shape in Antillean plants. *Evolution*, *72*(2), 244–260. https://doi.org/10.1111/evo.13410

Kalinka, A. T., & Tomancak, P. (2012). The evolution of early animal embryos: Conservation or divergence? *Trends in Ecology and Evolution*, *27*(7), 385–393. https://doi.org/10.1016/j.tree.2012.03.007

Keeffe, R., & Blackburn, D. C. (2022). Diversity and function of the fused anuran radioulna. *Journal of Anatomy*, *241*(4), 1026–1038. https://doi.org/10.1111/joa.13737

Kohlsdorf, T., Garland, T., & Navas, C. A. (2001). Limb and tail lengths in relation to substrate usage in Tropidurus lizards. *Journal of Morphology*, *248*(2), 151–164. https://doi.org/10.1002/jmor.1026

Kubo, T., Sakamoto, M., Meade, A., & Venditti, C. (2019). Transitions between foot postures are associated with elevated rates of body size evolution in mammals. *Proceedings of the Proceeding of the National Academy of Sciences*, *116*(7), 2618–2623. https://doi.org/10.1073/pnas.1814329116

Lande, R. (1979). Quantitative genetic analysis of multivariate evolution, applied to brain: Body size allometry. *Evolution*, *33*(1), 402–416. https://doi.org/10.2307/2407630

Ledbetter, N. M., & Bonett, R. M. (2019). Terrestriality constrains salamander limb diversification: Implications for the evolution of pentadactyly. *Journal of Evolutionary Biology*, *32*(7), 642–652. https://doi.org/10.1111/jeb.13444

Lungmus, J. K., & Angielczyk, K. D. (2021). Phylogeny, function and ecology in the deep evolutionary history of the mammalian forelimb. *Proceedings of the Royal Society B: Biological Sciences*, *288*(1949), 202104942. https://doi.org/10.1098/rspb.2021.0494

Luo, Z. X., Meng, Q.-J., Ji, Q., Liu, D., Zhang, Y.-G., & Neander, A. I. (2015). Evolutionary development in basal mammaliaforms as revealed by a docodontan. *Science*, *347*(6223), 760–764. https://doi.org/10.1126/science.1260880

Machado, F. A., Hubbe, A., Melo, D., Porto, A., & Marroig, G. (2019). Measuring the magnitude of morphological integration: The effect of differences in morphometric representations and the inclusion of size. *Evolution*, *73*(12), 2518–2528. https://doi.org/10.1111/evo.13864

Macleod, N., & Rose, K. D. (1993). Inferring locomotor behavior in Paleogene mammals via eigenshape analysis. *American Journal of Science*, *293 A*, 300–355. https://doi.org/10.2475/ajs.293.A.300

Maier, J. A., Rivas-Astroza, M., Deng, J., Dowling, A., Oboikovitz, P., Cao, X., Behringer, R. R., Cretekos, C. J., Rasweiler, J. J., Zhong, S., & Sears, K. E. (2017). Transcriptomic insights into the genetic basis of mammalian limb diversity. *BMC Evolutionary Biology*, *17*(1). https://doi.org/10.1186/s12862-017-0902-6

Marroig, G. (2007). When size makes a difference: Allometry, life-history and morphological evolution of capuchins (Cebus) and squirrels (Saimiri) monkeys (Cebinae, Platyrrhini). *BMC Evolutionary Biology*, *7*(1), 20-. https://doi.org/10.1186/1471-2148-7-20

Martín-Serra, A., & Benson, R. B. J. (2020). Developmental constraints do not influence long-term phenotypic evolution of marsupial forelimbs as revealed by interspecific disparity and integration patterns. *American Naturalist*, *195*(3), 547–560. https://doi.org/10.5061/dryad.900ng75

McGrew, W. C., Marchant, L. F., Scott, S. E., & Tutin, C. E. (2001). Intergroup differences in a social custom of wild chimpanzees: The grooming hand-clasp of the Mahale Mountains. *Current Anthropology*, *42*(1), 148–153. https://doi.org/10.1086/318441

McHorse, B. K., Biewener, A. A., & Pierce, S. E. (2019). The evolution of a single toe in horses: causes, consequences, and the way forward. *Integrative and Comparative Biology*, *59*(3), 638–655. https://doi.org/10.1093/icb/icz050

Melo, D., Garcia, G., Hubbe, A., Assis, A. P., & Marroig, G. (2015). EvolQG - An R package for evolutionary quantitative genetics. *F1000Research*, *4*, 925. https://doi.org/10.1101/026518

Michaud, M., Veron, G., & Fabre, A.-C. (2020). Phenotypic integration in feliform carnivores: Covariation patterns and disparity in hypercarnivores versus generalists. *Evolution*, *74*(12), 2681–2702. https://doi.org/10.1111/evo.14112

Milne, N., & Granatosky, M. C. (2021). Ulna curvature in arboreal and terrestrial primates. *Journal of Mammalian Evolution*, *28*(3), 897–909. https://doi.org/10.1007/s10914-021-09566-5

Naghizadeh, M., Mohajerani, M. H., & Whishaw, I. Q. (2020). Mouse Arm and hand movements in grooming are reaching movements: Evolution of reaching, handedness, and the thumbnail. *Behavioural Brain Research*, *393*. https://doi.org/10.1016/j.bbr.2020.112732

Napier, J. (1993). *Hands* (R. Tuttle, Ed.). Princeton Science Library.

Pavlicev, M., Cheverud, J. M., & Wagner, G. P. (2009). Measuring morphological integration using eigenvalue variance. *Evolutionary Biology*, *36*(1), 157–170. https://doi.org/10.1007/s11692-008-9042-7

Polly, D. (2007). Limbs in mammalian evolution. In B. K. Hall (Ed.), *Fins into limbs: Evolution, development, and transformation* (pp. 245–268). The University of Chicago Press.

Prothero, D. R. (2009). Evolutionary transitions in the fossil record of terrestrial hoofed mammals. *Evolution: Education and Outreach*, *2*(2), 289–302. https://doi.org/10.1007/s12052-009-0136-1

Raff, R. A. (1996). *The shape of life: genes, development, and the evolution of animal form.* (J. F. C. Hanken, Ed.; 1st Edition). University of Chicago Press.

Randau, M., & Goswami, A. (2017). Unravelling intravertebral integration, modularity and disparity in Felidae (Mammalia). *Evolution and Development*, *19*(2), 85–95. https://doi.org/10.1111/ede.12218

R Core Team. (2022). *R: A language and environment for statistical computing. R Foundation for Statistical Computing*. URL https://www.R-project.org/.

Rencher, A. C. (2002). *Methods of multivariate analysis* (Second Edition). John Wiley & Sons, Inc.

Rolian, C. (2009). Integration and evolvability in primate hands and feet. *Evolutionary Biology*, *36*(1), 100–117. https://doi.org/10.1007/s11692-009-9049-8

Ross, D., Marcot, J. D., Betteridge, K. J., Nascone-Yoder, N., Scott Bailey, C., & Sears, K. E. (2013). Constraints on mammalian forelimb development: insights from developmental disparity. *Evolution*, *67*(12), 3645–3656. https://doi.org/10.5061/dryad.9m59b

Rothier, P. S., Brandt, R., & Kohlsdorf, T. (2017). Ecological associations of autopodial osteology in Neotropical geckos. *Journal of Morphology*, *278*(3). https://doi.org/10.1002/jmor.20635

Rothier, P. S., Simon, M. N., Marroig, G., Herrel, A., & Kohlsdorf, T. (2022). Development and function explain the modular evolution of phalanges in gecko lizards. *Proceedings of the Royal Society B: Biological Sciences*, *289*(1966), 20212300. https://doi.org/10.1098/rspb.2021.2300

Ruvinsky, I., & Gibson-Brown, J. J. (2000). Genetic and developmental bases of serial homology in vertebrate limb evolution. *Development*, *5244*, 5233–5244. https://doi.org/10.1242/dev.127.24.5233

Samuels, J. X., & Van Valkenburgh, B. (2008). Skeletal indicators of locomotor adaptations in living and extinct rodents. *Journal of Morphology*, *269*(11), 1387–1411. https://doi.org/10.1002/jmor.10662

Saxena, A., Towers, M., & Cooper, K. L. (2017). The origins, scaling and loss of tetrapod digits. *Philosophical Transactions of the Royal Society B: Biological Sciences*, *372*(1713). https://doi.org/10.1098/rstb.2015.0482

Schliep, K. P. (2011). phangorn: Phylogenetic analysis in R. *Bioinformatics*, *27*(4), 592–593. https://doi.org/10.1093/bioinformatics/btq706

Schmidt, M., & Fischer, M. S. (2009). Morphological integration in Mammalian limb proportions: dissociation between function and development. *Evolution*, *63*(3), 749–776. https://doi.org/10.1111/j.l558-5646.2008.00583.x

Schneider, I., & Shubin, N. H. (2013). The origin of the tetrapod limb: From expeditions to enhancers. *Trends in Genetics*, *29*(7), 419–426. https://doi.org/10.1016/j.tig.2013.01.012

Sears, K., Behringer, R. R., Rasweiler, J. J., & Niswander, L. A. (2007). The evolutionary and developmental basis of parallel reduction in mammalian zeugopod elements. *The American Naturalist*, *169*(1), 105–117. https://doi.org/10.1086/510259

Sears, K., Maier, J. A., Sadier, A., Sorensen, D., & Urban, D. J. (2017). Timing the developmental origins of mammalian limb diversity. *Genesis*, 1–14. https://doi.org/10.1002/dvg.23079

Shubin, N., Tabin, C., & Carroll, S. (1997). Fossils, genes and the evolution of animal limbs. *Nature*, *388*, 639–648. https://doi.org/10.1038/41710

Stepanova, N., & Womack, M. C. (2020). Anuran limbs reflect microhabitat and distal, later-developing bones are more evolutionarily labile. *Evolution*, *74*(9), 2005–2019. https://doi.org/10.1111/evo.13981

Stopper, G. F., & Wagner, G. P. (2005). Of chicken wings and frog legs: A smorgasbord of evolutionary variation in mechanisms of tetrapod limb development. *Developmental Biology*, *288*(1), 21–39. https://doi.org/10.1016/j.ydbio.2005.09.010

Sustaita, D., Pouydebat, E., Manzano, A., Abdala, V., Hertel, F., & Herrel, A. (2013). Getting a grip on tetrapod grasping: Form, function, and evolution. *Biological Reviews*, *88*(2), 380–405. https://doi.org/10.1111/brv.12010

Upham, N. S., Esselstyn, J. A., & Jetz, W. (2019). Inferring the mammal tree: Species-level sets of phylogenies for questions in ecology, evolution, and conservation. *PLoS Biology*, *17*(12). https://doi.org/10.1371/journal.pbio.3000494

Van Valkenburgh, B. (1987). Skeletal indicators of locomotor behavior in living and extinct carnivores. *Journal of Vertebrate Paleontology*, *7*(2), 162–182. https://doi.org/10.1080/02724634.1987.10011651

Veeger, H. E. J., & van der Helm, F. C. T. (2007). Shoulder function: The perfect compromise between mobility and stability. In *Journal of Biomechanics* (Vol. 40, Issue 10, pp. 2119–2129). https://doi.org/10.1016/j.jbiomech.2006.10.016

Wang, X. (1993). Transformation from plantigrady to digitigrady: Functional morphology of locomotion in Hesperocyon (Canidae: Camivora). *American Museum Novitates*, *3069*, 1–23.

Weaver, L. N., & Grossnickle, D. M. (2020). Functional diversity of small-mammal postcrania is linked to both substrate preference and body size. *Current Zoology*, *66*(5), 539–553. https://doi.org/10.1093/cz/zoaa057

Weisbecker, V. (2011). Monotreme ossification sequences and the riddle of mammalian skeletal development. *Evolution*, *65*(5), 1323–1335. https://doi.org/10.1111/j.1558-5646.2011.01234.x

Weisbecker, V., Goswami, A., Wroe, S., & Sánchez-Villagra, M. R. (2008). Ossification heterochrony in the therian postcranial skeleton and the marsupial-placental dichotomy. *Evolution*, *62*(8), 2027–2041. https://doi.org/10.1111/j.1558-5646.2008.00424.x

Weisbecker, V., & Schmid, S. (2007). Autopodial skeletal diversity in hystricognath rodents: Functional and phylogenetic aspects. *Mammalian Biology*, *72*(1), 27–44. https://doi.org/10.1016/j.mambio.2006.03.005

Weisbecker, V., & Warton, D. I. (2006). Evidence at hand: Diversity, functional implications, and locomotor prediction in intrinsic hand proportions of diprotodontian marsupials. *Journal of Morphology*, *267*(12), 1469–1485. https://doi.org/10.1002/jmor.10495

Young, N. M., & Hallgrímsson, B. (2005). Serial homology and the evolution of mammalian limb covariation structure. *Evolution*, *59*(12), 2691–2704. https://doi.org/10.1111/j.0014-3820.2005.tb00980.x

"Some of the most commonplace items in our world are also paradoxically the most improbable and wonderful."

— Rudolf Raff

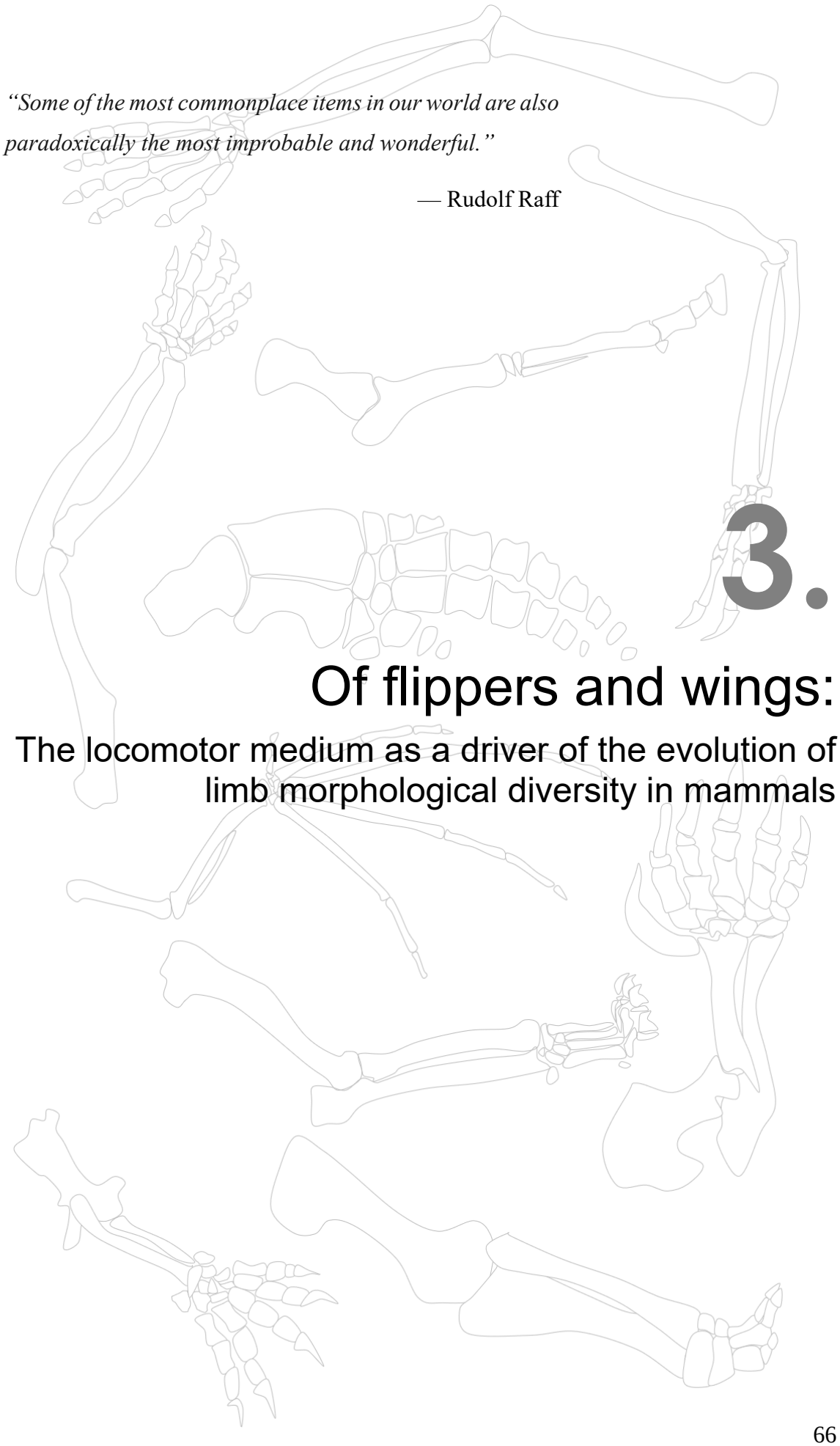

3.

Of flippers and wings:

The locomotor medium as a driver of the evolution of limb morphological diversity in mammals

3.1. Abstract

The early diversification of tetrapods in terrestrial environments involved adaptations of the locomotor apparatus allowing for weight support on heterogeneous surfaces. Many lineages later returned to the water and others conquered the aerial environment, diversifying under the physical constraints of homogeneous fluid media. We investigated whether mammals that left terrestrial environments to use air and water as the main media for locomotion experienced constraints on the morphological evolution of their forelimb. We gathered a comprehensive sample of over 800 species covering the extant family-level diversity of mammals. Results show that absolute limb size is driven by variation in body mass, with aquatic mammals being the heaviest taxa. Locomotion in both water and air limits the disparity of the absolute limb size. Once size is removed, fully-aquatic groups have the most disparate limb shapes, possibly due to the many different functional roles performed by the flippers. Air-based locomotion, in contrast, strongly restricts limb shape diversity. These results demonstrate that not all homogeneous locomotor environments exert similar selective pressures. Whereas aquatic locomotion drives limb shape diversification, aerial locomotion constrains limb diversity. We show that the locomotor environment has fostered the morphological and functional evolution of mammalian limbs.

3.2. Introduction

The evolution of an organism's phenotype is dictated by the physical properties of the surrounding environment. The medium used by animals for locomotion, such as land, air, and water, differ in density, viscosity, and in the strength imposed by gravitational constraints, therefore determining the capacity of animals to move (Biewener & Patek, 2018). With the rise of Tetrapoda, a series of morphophysiological modifications were critical during the evolutionary transition from water to land, allowing organisms to support their body weight against gravity on heterogeneous terrestrial surfaces. Most notably, adaptations in the locomotor system involved the evolution of three-segmented limbs with distal hands and feet that accommodate the substrate surface and provide the thrust for locomotion (Shubin et al., 1997), later diversifying into several morphological and locomotor specialisations (such as adaptations to cursoriality, arboreality, fossoriality, climbing, jumping, bipedalism, graviportality, amongst others; Polly, 2007). However, as tetrapods successfully radiated across the globe, some lineages independently returned to water and others conquered the aerial realm, experiencing again the constraints on locomotion imposed by fluid motion.

Although locomotion in water and air consist on moving across continuous fluids, the differences in density between these two media may constrain the locomotory biomechanics in different ways (Biewener & Patek, 2018). The high density and viscosity of water means that overcoming drag is one of the greatest challenges for aquatic locomotion. With the limbs no longer providing weight support, these traits in aquatic taxa either function to provide thrust and/or assist with controlling swim stability and manoeuvrability (Gutarra & Rahman, 2022). Moreover, a body size increase is often observed in many aquatic lineages, which, at least in mammals, is likely driven by the energetic balance between heat loss and feeding efficiency dictated by prey availability

in this environment (Gearty et al., 2018; Gutarra et al., 2022; Pyenson & Vermeij, 2016; Smith & Lyons, 2011). Unlike swimming, body weight support imposes important constraints to aerial locomotion, involving the necessity to generate sufficient lift and provide mechanical power to actively flap the arms (Biewener & Patek, 2018; Rayner, 1988). Therefore, leaving terrestrial environments to use aquatic and aerial media for locomotion likely impacted the macroevolutionary outcome of morphological diversification, involving shifts in body size and changes in the shape of the locomotor apparatus.

Several tetrapod lineages independently left the land to occupy fully-aquatic niches, with multiple other independent origins of semi-aquatic lifestyles (Howell, 1970; Vermeij & Motani, 2018). Most of these lineages (such as whales, sirenians, turtles, ichthyosaurs, plesiosaurs, etc.) share convergent morphological adaptations that are helpful to reduce drag and to overcome the high viscosity of this medium (Gutarra et al., 2022; Gutarra & Rahman, 2022; Motani & Vermeij, 2021; Vermeij & Motani, 2018). Aquatic lineages have the smallest limb sizes relative to body volume across all tetrapods (Maher et al., 2022), and most often exhibit forelimb dominance over the hind limbs, accompanied by an anterior shift of the center of mass that facilitates a horizontal posture at rest and provides fine control of buoyancy (Motani & Vermeij, 2021). Within-limb joint mobility is generally very restricted, including the loss of arm-twisting (pronation-supination), often accompanied by a modification of the limb into rigid paddle-like flippers (Cooper et al., 2007a; Motani & Vermeij, 2021). The evolution of flippers was achieved through different kinds of skeletal transformations in different groups, including hyperphalangy, evolution of supernumerary digits (in some ichthyosaurs), bone loss and/or fusion, and flattening of elbow and wrist joints (Caldwell, 2002; Cooper et al., 2007b; Fernández et al., 2020).

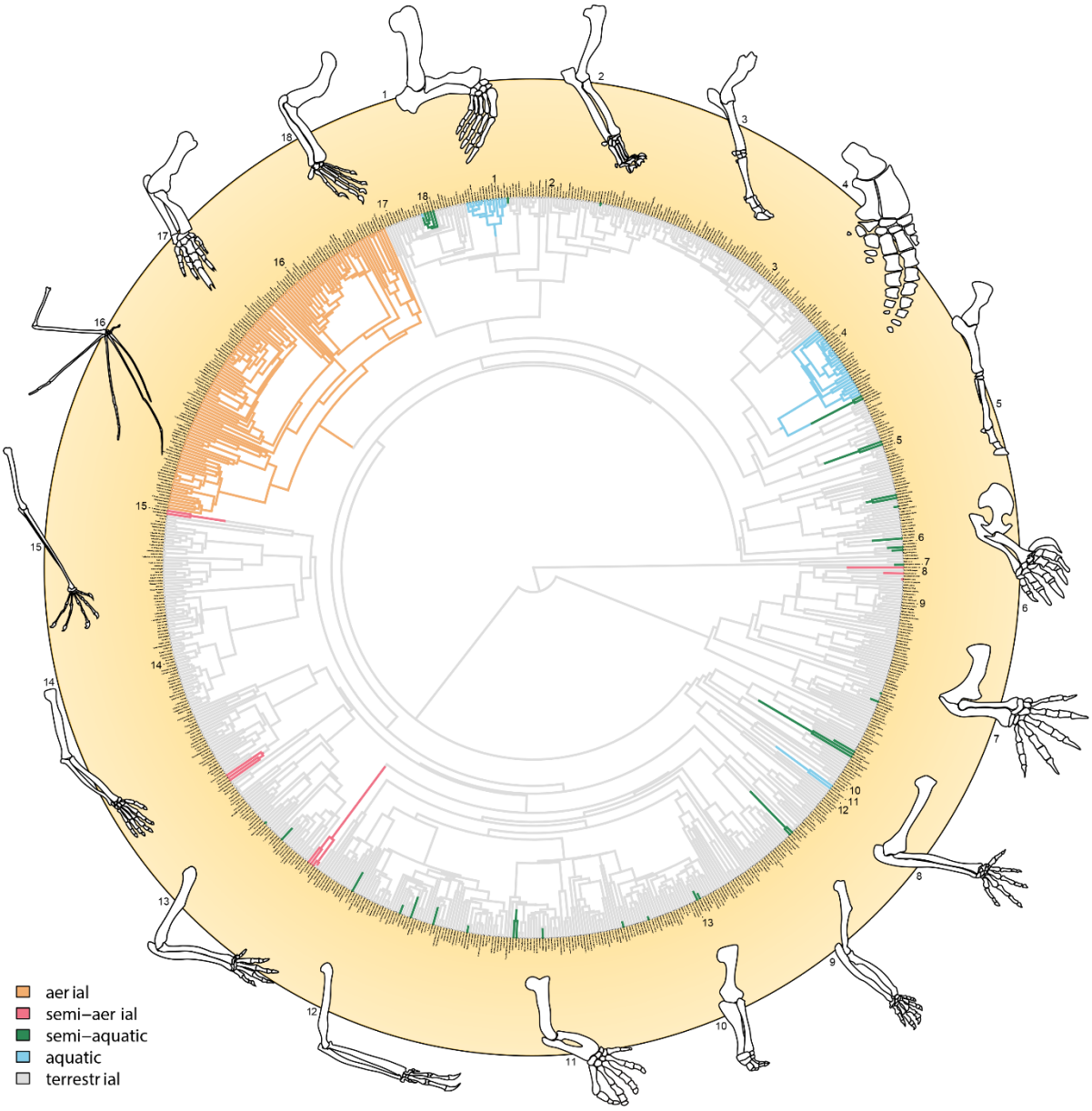

Figure 3.1. Topology of the species here examined, demonstrating the and forelimb diversity in mammals. Coloured branches indicate the media mostly used for locomotion per species. 1) *Odobenus rosmarus* (Carnivora, Odobenidae – aquatic); 2) *Panthera leo* (Carnivora, Felidae – terrestrial); 3) *Bos frontalis* (Cetartiodactyla, Bovidae – terrestrial); 4) *Tursiops truncates* (Cetartiodactyla, Delphinidae – aquatic); 5) *Equus caballus* (Perissodactyla, Equidae – terrestrial); 6) *Mogera wogura* (Eulipotyphla, Talpidae – terrestrial), 7) *Ornithorhynchus anatinus* (Monotremata, Ornithorhynchidae – semi-aquatic); 8) *Acrobates pygmaeus* (Diprotodontia, Acrobatidae – semi-aerial); 9) *Macropus giganteu** (Diprotodontia, Macropodidae – terrestrial); 10) *Elephas maximus* (Proboscidea, Elephantidae – terrestrial); 11) *Trichechus senegalensis* (Sirenia, Trichechidae – aquatic); 12) *Choloepus didactylus* (Pilosa, Megalonychidae – terrestrial); 13) *Melanomys caliginosus* (Rodentia, Cricetidae – terrestrial); 14) *Homo sapiens* (Primates, Hominidae – terrestrial); 15) *Galeopterus variegatus* (Dermoptera, Cynocephalidae – semi-aerial); 16) *Barbastella barbastellus* (Chiroptera, Vespertilionidae – aerial); 17) *Manis pentadactyla* (Pholidota, Manidae – terrestrial); 18) *Lutra lutra* (Carnivora, Mustelidae – semi-aquatic). Not scaled.

Just like in aquatic lineages, species performing aerial locomotion present several morphological convergences in response to the constraints imposed by this medium, including having a lighter body, which reduces the energetic cost of flight and provides a greater aerial maneuverability (Gatesy & Middleton, 2007; Rayner, 1988). Active flight likely evolved from gliding behavior present in arboreal ancestors and has occurred only three times in Tetrapoda, among pterosaurs, birds, and bats (Norberg, 1985). In contrast, gliding is a much less energetically costly way to move through air compared to flapping flight (Biewener & Patek, 2018), and has independently evolved in about 30 tetrapod lineages (Bishop, 2008; Dudley et al., 2007). In mammals, all flying and gliding species have a patagium, a membranous skin extension stretched laterally to the body and to the forelimbs that increases lift and slows the acceleration during descent (Bishop, 2008; Dudley et al., 2007). Elongation of the forelimb bones is a recurrent pattern detected in both flying and gliding animals, allowing to increase the surface area of the attached patagia (Gatesy & Middleton, 2007; Grossnickle et al., 2020).

Mammals are an ecologically and morphologically diversified group, displaying remarkable locomotor diversity adapted to different environments (Chen & Wilson, 2015; Polly, 2007). Most mammals use the terrestrial medium (e.g. the ground, trees, etc…) to travel. However, their evolutionary history is marked by multiple transitions from locomotion on land to fluid-based locomotion, occupying both aquatic and aerial niches (Fig. 3.1; Nowak, 1999). Here, we ask whether and how locomotion in these different physical media, terrestrial, aquatic, and aerial, as well as at their interface, fosters the morphological diversity of the forelimb skeleton, investigating the patterns of phenotypic variation, disparity and convergence in a comprehensive comparative framework based on a sample of more than 800 mammal species. We predict that the use of homogeneous media such as water and air will result in less disparate phenotypes, reflecting convergent

locomotor adaptations that overcome the physical constraints imposed by continuous fluids. To our knowledge, this is the most comprehensive study on the effect of medium use on the diversification of limbs in mammals, capturing nearly the entire extant family-level diversity of a tetrapod clade.

3.3. Material & methods

3.3.1. Taxonomic dataset and morphological inference

Our dataset consists of limb dimensions of 838 species representing most living mammalian orders (all orders except for the marsupial golden moles Notoryctemorphia, which have fused digit bones that prevented the inference of the measurements used here). Our study comprises an extended sample relative to Rothier et al. (2023), with 206 additional specimens included here. Our sample ranged from one to three individuals per species, representing 802 genera and 158 families, capturing over 60% of mammal genus diversity and nearly 95% of the modern and recently extinct mammalian families (taxonomy following Mammal Diversity Database (Burgin et al., 2018). Data acquisition was conducted by combining digital and manual methods, depending on the specimen's size.

We generated micro-CT-scans and surface scans of 134 small to medium sized-specimens from different institutions (Table S1.1). Scans were generated using a Nikon Metrology HMX ST 225 (NHMUK Natural History Museum, London) and an EasyTom 150 X-ray micro-computer tomography (ISEM Institute, Montpellier, France). Additionally, we included 415 meshes available from MorphoSource.org. We used Avizo 8.1.1 (1995-2014 Zuse Institute Berlin) to convert image stacks into three-dimensional surface models (incorporating scale dimensions based on the voxel size of each scan) later

used to obtain morphometric distances via landmark coordinates (Fig. 1.4), also in Avizo. Finally, we obtained caliper measurements of 335 limb skeletons from medium to large body-sized species, available at the French Muséum National d'Histoire Naturelle (MNHN Paris, France), the American Museum of Natural History (AMNH New York, USA), and the Natural History Museum (NHM London, UK) (Table S1.1).

We measured 21 linear distances on forelimb bones, following Rothier et al. (2023) consisting of the length, width (proximal, medial, and distal axis), and height of the humerus, radius, third metacarpal and first phalanx of digit III, in addition to the total length of the digit III (inferred as the sum of the lengths of all phalanges of the digit III, see Fig. 1.4, Table S1.2). We did not include the ulna because this bone is fused to the radius in many taxa (Sears et al., 2007), preventing the acquisition of such measurements. We chose to sample the third finger because this is the only digit present in the hands of all mammalian species, even in groups that exhibit digit loss or fusion with other autopodial elements (Clifford, 2010; McHorse et al., 2019; Prothero, 2009). We measured each individual twice with the subsequent calculation of the mean and standard error to verify measurement error. Error estimate was most often below 1.5% regardless of an animal's size and the measurement method, indicating reliability and repeatability of the methods employed. Body mass information was rarely available for the individuals analyzed, so we extracted body mass estimates per species from the PanTHERIA database (Jones et al., 2009) and from complementary literature sources when necessary (Table S1.1).

3.3.2. Classification of locomotor media

Each species was classified according to the physical medium used for long distance locomotion. We used the following classification: terrestrial (613 species), aquatic (53 species), semi-aquatic (39 species), aerial (bats only, 128 species) and semi-aerial (11 species). We consider 'terrestrial' as the medium for locomotion of all species that actively move and travel on land, including cursorial, arboreal, saltatorial, striding and fossorial mammals (following Nowak, 1999). Species classified into the 'aquatic' category are exclusively aquatic taxa, including all cetaceans, pinnipeds, sirenians and the sea otter *Enhydra lutris* (following Howell, 1970; Motani & Vermeij, 2021; Nowak, 1999). The only taxon included into "aerial" category was Chiroptera, which corresponds to the sole mammal group capable of powered flight. 'Semi-aquatic' encompasses all mammals that actively locomote in land and water: these animals, ranging from water rats to hippopotami, efficiently move both underwater and on terrestrial substrates but are highly dependent on the aquatic environment for foraging (classification based on DeBlois & Motani, 2019; Motani & Vermeij, 2021; Nowak, 1999; Vermeij & Motani, 2018). Finally, 'semi-aerial' incorporated the gliding mammals which are also active arboreal climbers (Jackson, 2000; Nowak, 1999).

3.3.3. Comparative analyses

Analyses were implemented in R 4.2.1 (R Core Team, 2022). We estimated a maximum clade credibility (MCC) tree from a posterior sample of 10,000 trees published by Upham et al. (2019), using the phangorn R package (Schliep, 2011). We interpreted our data from two different but complementary perspectives, first assembling all the distances acquired as a proxy for the whole limb morphology, and then analyzing each bone individually.

Therefore, we separated the database into two subsets, the first one comprising all measurements, and the second one excluding digit length. Sample size between subsets was not the same, because total digit length could not be calculated for all specimens since some of them lacked distal phalanges (frequently kept within the specimen's skin prior to its deposition at zoological collections), resulting in 798 species for analyses with the first subset (whole limb morphology) and 838 species for the second one (variation per bone).

3.3.4. Raw and size residual analyses

All morphological distances were log10-transformed prior to analyses. In order to understand the effect of size on limb morphology, we first analysed the absolute raw measurements, i.e., accounting for size, and then we used size residuals to investigate shape variation. First, we fitted different models of evolution using the raw log10-transformed data in a phylogenetic generalized least squares (PGLS) in the mvgls() function (mvMORPH R package; Clavel et al., 2015, 2019), repeating this procedure with all measurements (first subset) and with each bone individually (second subset). Linear regressions were replicated with LASSO penalization using the following models of trait evolution: Brownian Motion (BM), Ornstein-Uhlenbeck (OU) and Early Burst (EB). Model fit likelihood was evaluated with generalized information criterion (GIC). The OU process had the best fit for the raw data and was in the subsequent analyses as a model of regression (Table S2.1).

To account for body size on limb morphology, we transformed body mass into linear scale by calculating the cube root prior to log10-transformation (Harmon et al., 2010). We used the transformed body mass and the distance to calculate the geometric

means of each species, repeating this procedure for both subsets. We finally fitted the log10-transformed trait means in a PGLS with mvgls() function (mvMORPH R package; Clavel et al., 2015, 2019) using the geometric means as a predictor (following Rothier et al. (2023) in a BM, OU, and EB models of evolution. Again, the evolutionary model with the best support for the residual data was the OU process, which was used in the subsequent analyses. Next, we verified whether morphology of absolute size and residual morphologies varied between locomotor media via PGLS followed by multivariate analyses of variance, respectively using the functions mvgls() and mvgls.manova() from mvMORPH R package (Clavel et al., 2015, 2019). We also conducted a phylogenetic ANOVA to determine whether the transformed body mass values differed between medium categories (function phylANOVA() from phytools R package; Revell, 2012).

3.3.5. Morphological variation and ecological disparity

We used each fitted linear model into a phylogenetic principal component analyses (pPCA) with the function mvgls.pca() from mvMORPH (Clavel et al., 2015, 2019). We also fitted the first principal component (pPC1) scores of the raw pPCA against the log10 transformed body mass in a PGLS analyses in order to evaluate the effect of mass and of media use on the absolute limb bone dimensions. Then, we conducted model comparisons to estimate the impact of body mass and media use on the variation of the raw pPC1, using the function with gls() from nlme R package (Pinheiro et al., 2022) with maximum likelihood method following a Pagel correlation structure, with simultaneous estimation of the phylogenetic signal (λ). We next evaluated whether the principal components explaining most of the variation of the raw and residual data differed between locomotor media, using phylogenetic ANOVAs with post-hoc comparisons of group means (function phylANOVA() from phytools R package; Revell, 2012).

Next, we assembled all the pPC scores from each raw and residual pPCA to compute the morphological disparity of each media groups. Disparity was calculated as the mean distance between each taxon and their group centroid, using the function dispRity() followed by a PERMANOVA significance test (test.dispRity(), both from from 'dispRity' R package; Guillerme, 2018; Guillerme et al., 2020).

3.3.6. Phenotypic convergence

We used the pPC scores generated by each pPCA to calculate the morphological convergence between ecological categories. We used the function search.conv() from RRPhylo, which tests whether phenotypes of distant clades are more similar to each other than expected by chance (Castiglione et al., 2019). Morphological convergence is inferred by the significance of the angle θ between the phenotypic vectors of the species, accounting for their phylogenetic distance. Possible θ values range from 0° to 180°, with small angles implying similar phenotypes. Phenotypic convergence was explored within each media category except for 'aerial' taxa since this group is solely represented by the monophyletic order Chiroptera. Additionally, we calculated the angle of morphological convergence between aquatic and semi-aquatic taxa, as well as between aerial and semi-aerial groups.

3.4. Results

3.4.1. The limb morphology differs depending on the medium

Results from phylogenetic multivariate analyses of variance using different evolutionary models (Table S3.1) demonstrates that limb morphology is different between the

locomotor media, both in terms of absolute size and in shape (i.e., size residuals, both $P < 0.001$, Table S2.2). Morphological differences between groups are also detected for each bone when examined separately (Table S3.2). Aquatic mammals are significantly larger and heavier than any other ecological group, and the fully-aerial group, solely represented by bats, present the lowest average body mass, albeit being not statistically different from semi-aerial, terrestrial and semi-aquatic taxa (Fig. 3.2B, Table S3.3).

3.4.2. Limb form and size variation

Results here presented refer both to the absolute size of forelimb elements, i.e., derived from the raw data, and to the limb shape, calculated with size residuals. As expected, the first phylogenetic principal components (raw pPC1) from the pPCAs using raw measurements indicate a strong effect of size and explains more than 89% of the total variance (Table 3.1, Fig. 3.2A, Table S3.3 and Fig. S3.1). All raw pPC1 loadings have negative values, with larger animals having the lowest scores. We multiplied the loadings and scores by -1 to facilitate the interpretation and visualization of the results (Fig. 3.2B). We confirm that patterns of absolute limb size are largely explained by body mass variation, showing that the raw pPC1 scores are positively associated with mass ($P < 0.001$, Table S3.5). In other words, heavier animals, including elephants, cetaceans, and ungulates, have absolute larger forelimbs bones than small body-sized species. Shrews, some rodents, and some marsupials exhibit the smallest absolute limb sizes (Fig. 3.2A-B). Absolute limb size is best described by a combination of both body mass and media use (Table S3.6). Aquatic taxa have the largest limbs, which is largely the result of an increase in body mass (Fig. 3.2 B, Fig. S3.2 and Tables S3.5-3.6). However, aquatic species have a different relationship between limb proportions and body mass than terrestrial groups, presenting proportionally smaller forelimbs as body mass increases

(Fig. 3.2B, Table S3.5 and S3.7). Bats display the largest arm dimensions proportional to body mass (Fig. 3.2B).

Table 3.1. Phylogenetic principal components describing whole limb morphology. First four pPC loadings of each linear distance obtained using raw and residual size values.

	raw (absolute size)				size residuals			
	pPC1	pPC2	pPC3	pPC4	pPC1	pPC2	pPC3	pPC4
humerus								
length	0.201	0.125	-0.288	0.065	-0.156	-0.271	0.076	-0.084
proximal width	0.219	-0.084	-0.159	-0.221	0.078	-0.189	-0.166	-0.141
mid-shaft width	0.221	-0.129	-0.194	-0.308	0.117	-0.210	-0.315	0.119
distal width	0.222	-0.084	-0.051	-0.168	0.115	-0.061	-0.230	-0.028
heigth	0.234	-0.203	-0.244	-0.146	0.163	-0.305	-0.152	0.191
radius								
length	0.200	0.231	-0.388	0.222	-0.296	-0.341	0.222	-0.085
proximal width	0.224	-0.031	-0.107	-0.154	0.004	-0.122	-0.090	-0.145
mid-shaft width	0.231	-0.093	-0.293	0.024	0.021	-0.295	0.022	0.014
distal width	0.231	-0.075	-0.081	-0.020	0.020	-0.095	-0.016	-0.081
heigth	0.224	-0.102	-0.080	-0.193	0.049	-0.105	-0.185	0.328
metacarpal								
length	0.195	0.422	-0.218	0.435	-0.493	-0.057	0.498	-0.063
proximal width	0.229	-0.101	0.188	0.154	0.124	0.201	0.213	-0.243
mid-shaft width	0.224	-0.155	0.185	0.027	0.186	0.155	0.085	-0.122
distal width	0.224	-0.032	0.213	-0.102	0.093	0.191	-0.049	-0.305
heigth	0.218	-0.068	0.067	0.377	0.118	0.090	0.262	0.422
phalanx								
length	0.192	0.593	0.153	-0.271	-0.516	0.248	-0.364	-0.040
proximal width	0.220	-0.045	0.225	-0.059	0.099	0.190	-0.028	-0.314
mid-shaft width	0.223	-0.227	0.208	0.165	0.265	0.157	0.150	-0.055
distal width	0.222	-0.085	0.305	0.017	0.165	0.251	0.010	-0.136
heigth	0.218	-0.079	0.205	0.415	0.141	0.187	0.308	0.469
digit length	0.205	0.444	0.335	-0.218	-0.342	0.423	-0.277	0.297
eigen	0.0436	0.0011	0.0008	0.0004	0.0024	0.0011	0.0006	0.0005
% var	89.01%	2.15%	1.66%	0.90%	30.12%	14.28%	7.94%	6.64%

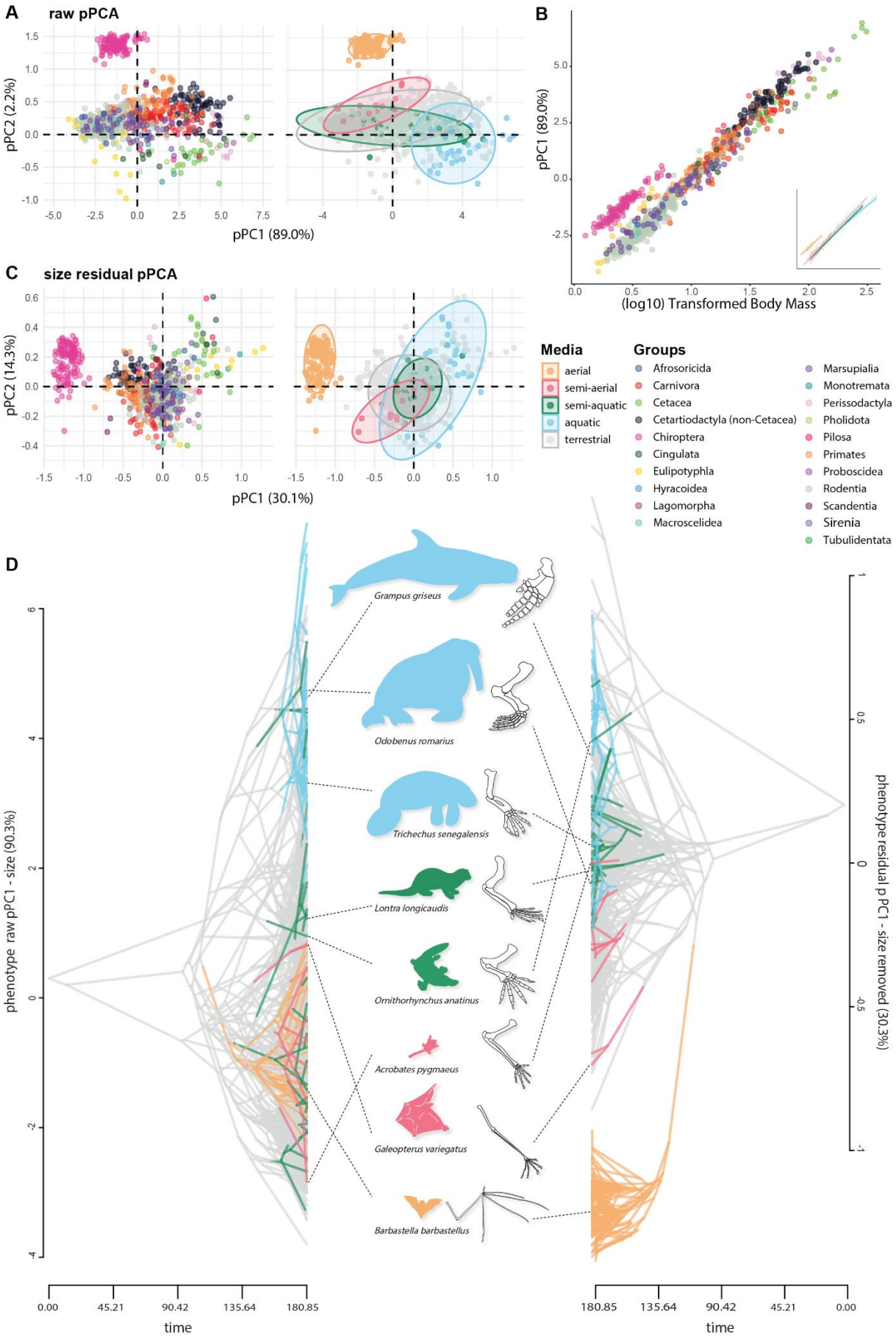
A
raw pPCA
pPC2 (2.2%)
pPC1 (89.0%)
B
pPC1 (89.0%)
(log10) Transformed Body Mass
C
size residual pPCA
pPC2 (14.3%)
pPC1 (30.1%)
Media
aerial
semi-aerial
semi-aquatic
aquatic
terrestrial
Groups
Afrosoricida
Carnivora
Cetacea
Cetartiodactyla (non-Cetacea)
Chiroptera
Cingulata
Eulipotyphla
Hyracoidea
Lagomorpha
Macroscelidea
Marsupialia
Monotremata
Perissodactyla
Pholidota
Pilosa
Primates
Proboscidea
Rodentia
Scandentia
Sirenia
Tubulidentata
D
Grampus griseus
Odobenus romarius
Trichechus senegalensis
Lontra longicaudis
Ornithorhynchus anatinus
Acrobates pygmaeus
Galeopterus variegatus
Barbastella barbastellus
phenotype raw pPC1 - size (90.3%)
phenotype residual p PC1 - size removed (30.3%)
time
time

[Figure on previous page]

Figure 3.2. Morphological variation of the mammalian limb. A) Morphospace of the first two raw principal components (pPC1 and pPC2), based on absolute limb dimensions. The taxonomic groups are highlighted on the left panel and the medium used for locomotion on the right (ellipses are 95% confidence intervals); **B)** Relationship between the first principal component scores from 'A' (raw pPC1) and the log10 values of body mass transformed to a linear scale. Regression lines per media classification are indicated in the right bottom; **C)** Morphospace of the first two size residual principal components that explain overall limb shape morphology. Taxonomic groups are highlighted on the left panel and the medium used for locomotion on the right; **D)** Mirrored phenograms indicating the evolutionary trajectories of the raw (absolute limb dimensions, from 'A') and residual (shape, from 'C'), pPC1, with colored branches indicating the ancestral state reconstruction of the medium mostly used for locomotion. Examples of species classified into non-terrestrial media are indicated (not scaled).

Considering the whole limb morphology, the raw pPC2 is similar to the size residual pPC1, showing that the greatest variation in shape is described by the relationship of length versus thickness: bone lengths vary in an opposite direction than width and height measurements (Table 3.1, Fig. S3.3). On this pPC axis, the phalanx and the metacarpal lengths are the traits with the highest loadings (see Table 3.1). Long but slender limb bones (represented by bats, primates and colugos), are positioned at one extremity of the pPC axis and short but thick arm bones are at the other extreme (illustrated by moles, cetaceans, monotremes and xenarthrans; Fig. 3.2A and C). The size residual pPC1 describing whole limb morphology indicate that the aerial taxon is significantly different from all other groups (Table S3.7). Semi-aerial species also show significantly different residual pPC1 values compared to other groups (Fig. 3.2, Table S3.7). A similar pattern is detected when analysing each bone separately: the proportionally longest humeri and radii are observed in aerial and semi-aerial taxa, while aquatic groups have shorter bones relative to body size (Fig. 3.3A-B, Table S3.7). In the

autopod, bats stand out from all other groups by having the proportionally longest metacarpals and phalanges (Fig. 3.3C-D, Table S3.7).

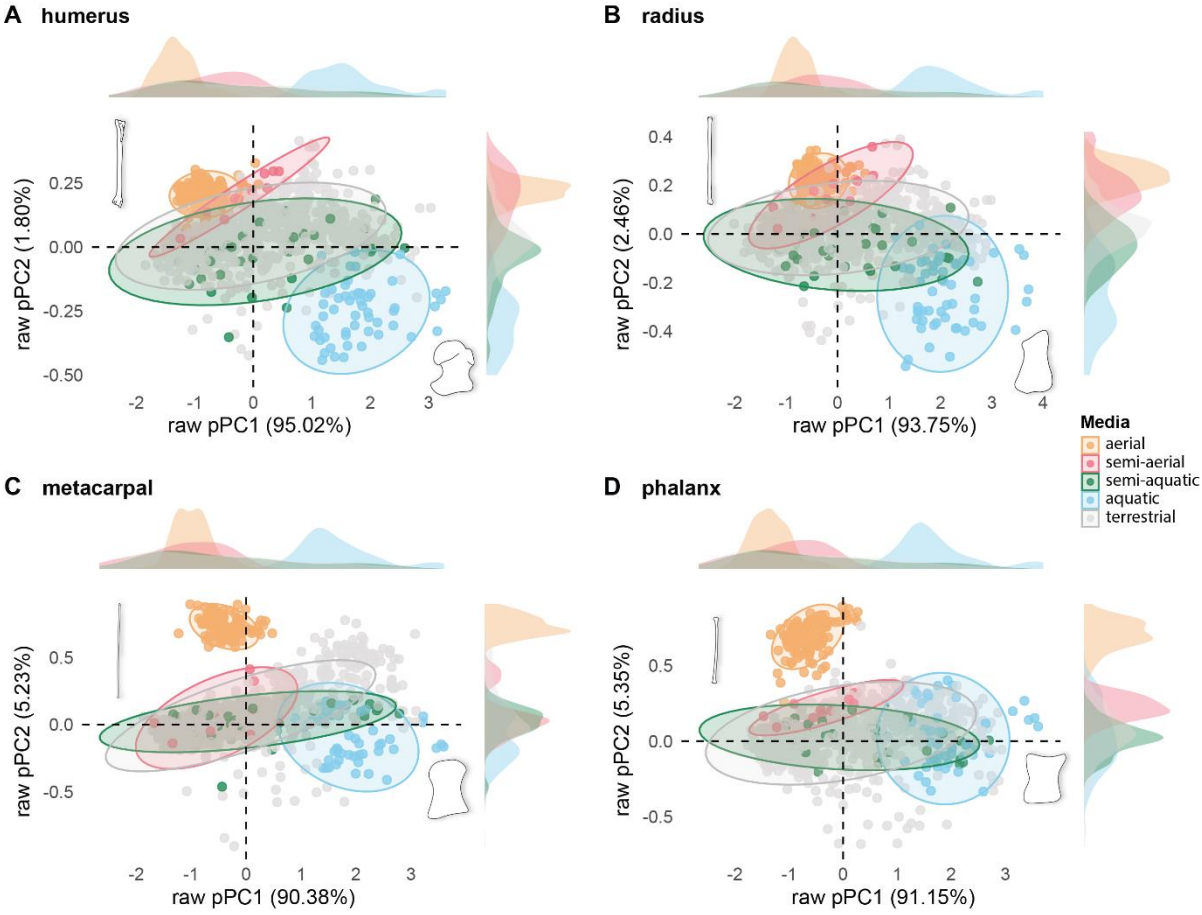

Figure 3.3. Morphospace generated by the raw pPCA of each bone separately, indicating the medium used for locomotion. In each panel, pPC1 describes the absolute bone size and pPC2 is mostly represented by length (Table S4 from SI2). Density plots on the top and right sides indicate the scores distribution per medium at each pPC. **A)** humerus; **B)** radius; **C)** metacarpal; **D)** phalanx.

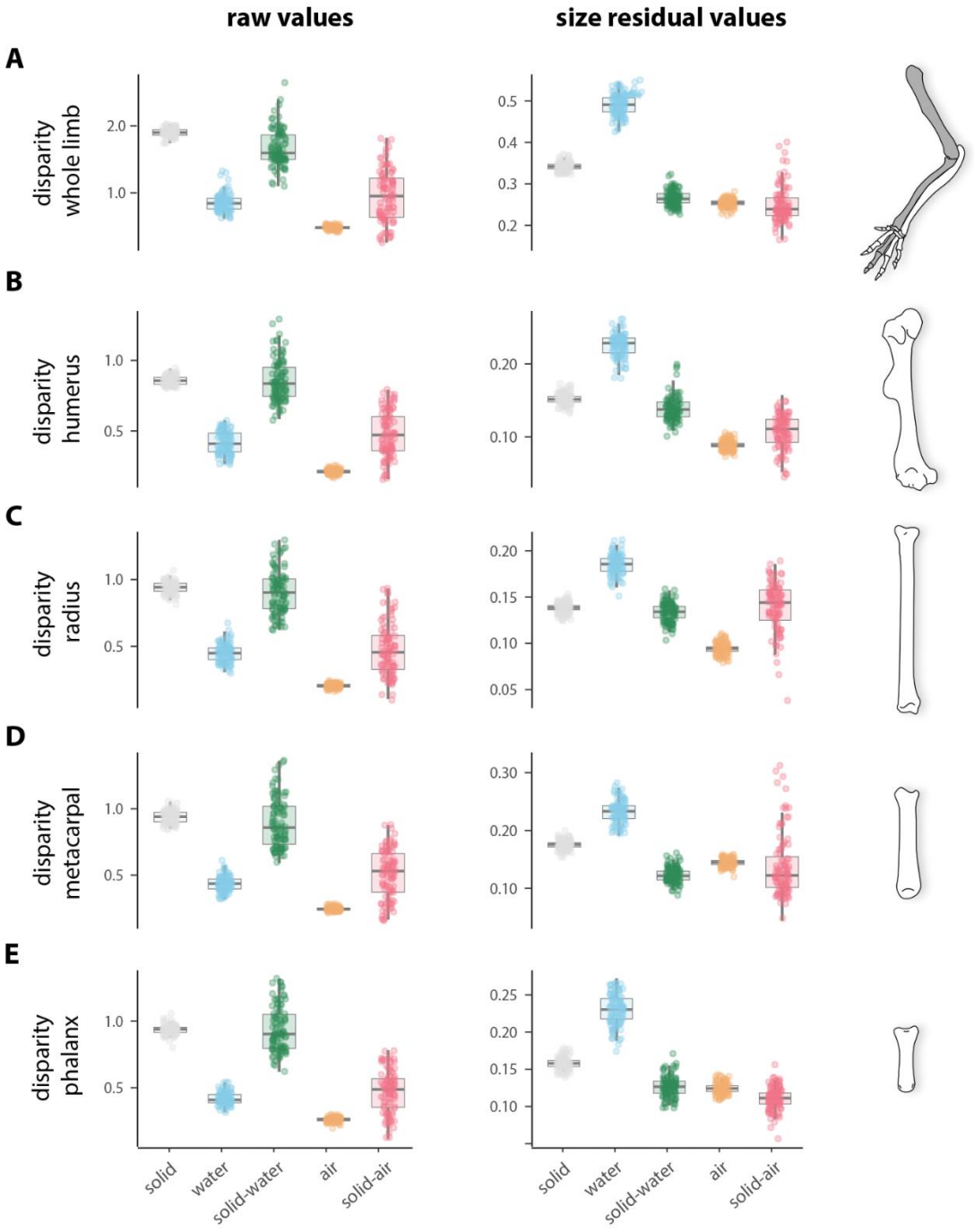

Figure 3.4. Morphological disparity across media. Left panel indicates values for the absolute raw dimensions, and size residual parameters are on the right. **A)** Whole limb morphology disparity; **B)** humerus disparity; **C)** radius disparity; **D)** metacarpal disparity; **E)** phalanx disparity.

3.4.3. Limb disparity is influenced by medium use

Taxa specialized for locomotion in continuous media (i.e., swimming and flying taxa) present the lowest disparity in absolute limb size, with aerial species exhibiting the lowest morphological diversity, followed by aquatic and semi-aerial taxa (Fig. 3.4 A). Species using terrestrial and semi-aquatic media are the most disparate ones. All pairwise comparisons are significant, except between aquatic and semi-aerial groups (Table S3.8). Similar patterns were detected while examining each bone separately; however, we did not detect significant differences in the absolute size of arm bones between the terrestrial and the semi-aquatic groups (Fig. 3.4 B-E, Table S3.8).

After removing size, aquatic taxa present a significantly higher disparity than any other ecological group (Fig. 3.4A, Table S3.8). The same result is obtained for the shape of each bone separately. Taxa using terrestrial substrates show the second most diverse morphologies, except for the radius (which is equally disparate in terrestrial, semi-aquatic, and semi-aerial groups, Fig. 3.3C, Table S3.8). The aerial taxon also presents the lowest whole-limb disparity after removing the effect of size. Differences in shape disparity between semi-aquatic, aerial, and semi-aerial species depend on the bone considered: aerial and/or semi-aerial groups have the lowest disparity in bone form except for the metacarpal, where semi-aquatic media encompass the least disparate taxa (Fig. 3.3D, Table S3.8).

3.4.4. Medium use and evolutionary convergence

Phenotypic convergence was detected for the absolute limb values within aquatic taxa, displaying a very narrow angle of morphospace convergence than expected by chance (θ=12.19°, P=0.001 Table 3.2). Absolute limb size convergence was also detected

Table 3.2. Phenotypic convergence within and between locomotor media. Angles and significance of morphospace convergence (of absolute size and size residual values) are indicated for the whole limb as well as per bone. Significant p-values are highlighted in bold.

			raw (absolute size)		size residual	
	State 1	State 2	angle	p-value	angle	p-value
whole limb	terrestrial		84.31	1.000	86.73	1.000
	aquatic	-	12.19	**0.001**	55.82	1.000
	semi-aquatic	-	87.03	0.922	84.86	0.955
	semi-aerial	-	56.72	0.026	45.62	**0.001**
	aerial	semi-aerial	48.30	**0.010**	69.26	**0.010**
	semi-aquatic	aquatic	102.69	1.000	87.03	0.990
humerus	terrestrial		88.60	0.450	84.23	0.981
	aquatic	-	9.09	**0.001**	47.62	1.000
	semi-aquatic	-	91.20	0.900	88.97	0.997
	semi-aerial	-	70.61	0.720	36.98	**0.001**
	aerial	semi-aerial	47.01	**0.010**	70.73	**0.010**
	semi-aquatic	aquatic	95.02	0.980	89.51	1.000
radius	terrestrial		89.73	0.131	85.54	1.000
	aquatic	-	8.32	**0.001**	36.07	1.000
	semi-aquatic	-	90.08	0.792	77.66	0.868
	semi-aerial	-	78.36	0.900	43.89	**0.001**
	aerial	semi-aerial	61.90	**0.010**	41.96	**0.010**
	semi-aquatic	aquatic	95.95	0.990	85.69	0.970
metacarpal	terrestrial		88.59	0.965	88.47	1.000
	aquatic	-	8.87	**0.001**	76.56	1.000
	semi-aquatic	-	90.99	0.890	91.30	0.998
	semi-aerial	-	71.77	0.601	51.27	**0.007**
	aerial	semi-aerial	75.80	**0.010**	108.48	0.140
	semi-aquatic	aquatic	99.01	1.000	89.25	1.000
phalanx	terrestrial		89.22	0.980	88.47	1.000
	aquatic	-	9.08	**0.001**	75.91	1.000
	semi-aquatic	-	90.62	0.842	90.58	0.988
	semi-aerial	-	62.77	0.216	39.57	**0.002**
	aerial	semi-aerial	46.98	**0.010**	35.64	**0.010**
	semi-aquatic	aquatic	99.24	1.000	90.40	0.970

between aerial and semi-aerial taxa, but with larger angles (θ=48.30°, *P*=0.01, Table 3.2). We did not detect convergence of absolute limb dimensions within terrestrial, semi-aquatic, and semi-aerial, nor between aquatic and semi-aquatic taxa. Convergence between aerial and semi-aerial taxa was also detected for the limb dimensions irrespective of size (θ=69.26°, *P*=0.01). This was not the case for aquatic species (θ=55.82°, *P*=1, Table 3.2). We also detected significant limb shape convergence among semi-aerial mammals (θ=45.62°, *P*=0.001). The pattern of phenotypic convergence detected for the absolute limb size and limb shape was confirmed when examining each bone separately, except for the metacarpal of semi-aerial and aerial groups (i.e., gliders and powered flight), which do not show significant convergence (θ=108.48, *P*=0.14).

3.5. Discussion

Solids, water, and air compose the surrounding world of living organisms. Each medium exhibits particular physical properties that constrain the ability of animals to move, ultimately imposing macroevolutionary limitations on the morphological diversity of locomotor systems (Biewener & Patek, 2018). Using a dataset that represents a comprehensive coverage of the extant mammalian diversity, we show that the use of fluid media predicts the variation of limb size and shape. We specifically demonstrate that fully aquatic habitat, involving the locomotion in a dense and viscous media, drives convergent evolution of larger absolute limb sizes, which is facilitated by the evolution of larger body masses in these groups. Aquatic taxa also display a low morphological disparity of the absolute limb size compared to terrestrial substrate users. Variation is evidenced once size is removed, and aquatic species exhibit the most disparate forearm shapes across Mammalia. Our findings indicate that water media constrains animal size but not the

shape of the forelimb. Aerial locomotion restricts limb disparity in terms of size and shape, explaining the partial phenotypic convergence of limb bones in gliding mammals and bats.

Absolute limb size is directly correlated with body mass, and the latter is a predictor of body size. Therefore, the low phenotypic disparity and the strong evolutionary convergence detected for the absolute limb size in groups that move in continuous fluids ultimately reflect the disparity and convergence of their overall body sizes. However, the different physical properties between water an air, particularly involving fluid density and the influence of buoyancy, constrain limb variation into opposite morphotypes. Aerial taxa show smaller sizes but proportionally larger limbs, and exclusively aquatic mammals show larger sizes but proportionally smaller limbs. Gliding airspeed varies in proportion to the wing loading, which is the ratio of the body mass to the wing area (Dudley et al., 2007). Therefore, larger body masses promote larger descent speeds, unless compensated by an increased wing surface area. However, high wing loadings affect maneuverability in air, implying an upper limit to body mass in gliding and flying animals (Dudley et al., 2007). Conversely, the strong pattern of phenotypic convergence detected for the absolute limb dimensions among fully-aquatic mammals strongly reflects the convergent evolution of larger body size in aquatic mammals. Aquatic mammals evolved towards an adaptive peak of increasing body mass that is much more constrained than for their terrestrial relatives (Gearty et al., 2018). Albeit the energetic advantages on having large body size, this may impact drag (Gutarra et al., 2022). Strategies for drag reduction are consequently diverse in aquatic tetrapods which might explain the high degree of morphological disparity in the limb shape of aquatic mammals.

Aside from flippers, fully aquatic animals often present fusiform body shapes, hypodermal fat deposits, integument modifications (such as fur loss), fluke-shaped tails, etc. (Fish, 1996; Gutarra & Rahman, 2022). These different adaptations are associated with the evolution of different swimming modes and may impact the role of the forearm during underwater locomotion. Mammals use two general swimming strategies to provide thrust, one through the movement of the axial skeleton – as in sea otters and true seals, that use undulatory pelvic movements, and dolphins and whales, that mostly swim through dorsoventral fluke movements – and the other one through appendicular thrust provided by the limbs, observed in fur seals and sea lions (Biewener & Patek, 2018; Fish, 1996; Gutarra & Rahman, 2022). The functional role of flippers, therefore, varies in function of the swimming mode (Fish, 1996; Hocking et al., 2021; Kuhn & Frey, 2012). For example, in cetaceans, fore fins mostly function as control surfaces and assist rotation and surging, with the thrust being mostly provided by the tail (Fish, 1996; Gutarra & Rahman, 2022). The flippers in this group encompass a very rigid structure with limited within-limb flexibility (Cooper et al., 2007b; DeBlois & Motani, 2019). Therefore, within-limb proportions are likely less constrained than overall limb dimensions relative to body mass. This in turn could favor the observed diversity of skeletal shapes. In sea lions, for instance, the flippers provide surface control in addition to the propulsive thrust (Fish, 1996). Such biomechanical diversity reflects on the shape of the forelimb elements, as propulsive-flipper tetrapods (including otariid seals, marine turtles, and penguins) tend to have less dense and robust arm bones compared to the cetacean surface control flippers. This results in limbs that are more flexible and more efficient to produce thrust (DeBlois & Motani, 2019).

Bats are the only mammal group capable of powered flight and are included here as the single representative of strict aerial locomotion. The phenotypic disparity of bat

wings is extremely low in terms of size and shape, possibly reflecting the monophyletic origin of the group. Therefore, we do not provide much statistical power to evaluate the relationship between fully-aerial locomotion with the distinct morphospace occupied by bat limb morphology due to their single evolutionary origin. Yet, when compared to pterosaurs and birds, bats also have the least disparate wings among all flying tetrapods, occupying a restricted morphospace of limb bone proportions (Gatesy & Middleton, 2007). Low skeletal disparity is consistent with the hypothesis that wing morphology reached a constrained adaptive optimum for flight. This is believed to have favored the group diversification while maintaining low diversity of limb morphology (Amador et al., 2019; Burtner et al., 2022). Except for the metacarpal, we observed that most of the limb bones of bats and gliding mammals present wide but significantly convergent angles in the morphospace. Our findings are consistent with previous descriptions of incomplete convergence of the postcranial skeleton among gliding mammals, which showed that gliding adaptations are more linked to the lengthening of proximal long bones (Grossnickle et al., 2020). The similarities detected between bats and gliding mammals have been recently suggested to support a gliding ancestor in Chiroptera, with volant animals exhibiting intermediate morphologies between arboreal mammals and bats (Burtner et al., 2022).

The hand bones of bats stand out for having extremely elongated metacarpals, a unique feature that is not shared with any other gliding taxa. The lack of evolutionary convergence in metacarpal shape may reflect distinct evolutionary regimes regulating proximal and distal variation. The length of long bones of bats and volant groups likely evolved towards adaptive peaks that are much closer to each other compared to the metacarpal and digit length (Burtner et al., 2022). Higher variation in the autopod is also expected given the uneven nature of morphological variation between proximal and distal

limb segments. The autopod dimensions are more variable than those from the proximal bones, possibly due to a combination of its functional diversity and later formation during development, showing much faster evolutionary changes (Rothier et al., 2023).

Locomotion on terrestrial substrates and at the interface of water and land characterizes the groups occupying the center of the morphospace, in between taxa specialized in fluid-based locomotion. Phenotypic disparity of absolute limb size is the highest among these groups, with species using solid substrates having the second most diverse limb shape after aquatic taxa. These patterns are not surprising considering that terrestrial medium category encompasses groups that use many different types of micro-habitats and display a variety of modes of locomotion. Semi-aquatic taxa, for instance, present a more generalist locomotor apparatus capable of moving in both media and often showing intermediate and less constrained biomechanical specializations for movement on both land and in water (Botton-Divet et al., 2017; Gutarra & Rahman, 2022; Hood, 2020; Motani & Vermeij, 2021). Besides showing a relatively high disparity, semi-aquatic taxa do not exhibit phenotypic convergence neither for limb size nor for shape, which may reflect the many different degrees of adaptation to aquatic environments and the different modes used to swim (Motani & Vermeij, 2021). For example, the muskrat *Ondatra* uses pelvic paddling during swimming with limbs oriented in the vertical parasagittal plane, whereas platypuses execute mostly pectoral rowing, with limbs positioned horizontal to the body plane (Fish, 1993, 1996). Otters, use both pelvic paddling and body undulation for propulsion (Fish, 1993), illustrating the diversity of locomotor modes in this group.

Among terrestrial modes of locomotion, a great heterogeneity of limb bone morphology is observed for small to medium-sized mammals, particularly related to constraints for fossoriality and arboreality (Chen & Wilson, 2015; Fabre et al., 2015;

Hedrick et al., 2020; Weaver & Grossnickle, 2020; Weisbecker & Schmid, 2007; Weisbecker & Warton, 2006). Mammals with fossorial habits also move in dense substrates but that are typically very heterogenous. Fossoriality and semi-fossoriality in many lineages of primarily diggers have resulted in the convergence of bulky and short proximal bones and robust autopods (Chen & Wilson, 2015; Fabre et al., 2015; Hedrick et al., 2020; Nevo, 1979, 1995). Conversely, arboreality seems to drive the convergent evolution of more gracile limb bones and slender phalanges, a pattern consistently observed for many mammalian lineages (Chen & Wilson, 2015; Fabre et al., 2015; Weisbecker & Schmid, 2007; Weisbecker & Warton, 2006). Although some works have started to transpose these associations from the lineage level comparison to a higher macroevolutionary context (Maher et al., 2022), further investigation is necessary to understand how morphological evolution across distant taxa responds to similar ecological drivers.

3.6. Conclusion

We here describe the relationships of limb morphological diversity and the medium use based on a taxonomically comprehensive dataset of mammals. We demonstrate that leaving terrestrial substrates contributed to the diversification of the mammalian limb form into new parts of the morphospace. At the same time, the evolution of some morphologies may be limited by the way that habitat physical conditions act on locomotion, with fluid-based locomotion, represented by aquatic and aerial media imposing different types of constraints on limb bone diversity. Water constrains the disparity of absolute limb dimensions which reflects the strong convergent evolution of larger body masses in aquatic mammals. However, once size is removed, the use of

aquatic environments evidenced the diversification of limb shape, which may reflect the variety of functional roles exhibited by the pectoral limb while swimming. Conversely, aerial locomotion imposes more strict constraints on limb shape, with bats and gliding mammals exhibiting similar patterns of convergence mostly involving the elongation of the proximal limb segments, supporting the findings from previous studies (Burtner et al., 2022; Grossnickle et al., 2020). We show that the outstanding forelimb diversity in mammals is uneven according to the physical properties of the locomotor environment, highlighting the important role of the forelimb in the evolutionary radiation of mammals. Overall, we demonstrate that not all media can be traversed with the same set of forms and functions and, that the locomotor environment has driven much of the morphological and functional evolution of the mammalian limb during the Cenozoic.

3.7. References

Amador, L. I., Simmons, N. B., & Giannini, N. P. (2019). Aerodynamic reconstruction of the primitive fossil bat *Onychonycteris finneyi* (Mammalia: Chiroptera). *Biology Letters*, *15*(3). https://doi.org/10.1098/rsbl.2018.0857

Biewener, A. A., & Patek, S. N. (2018). *Animal locomotion* (2nd Edition.). Oxford University Press.

Bishop, K. L. (2008). The evolution of flight in bats: narrowing the field of plausible hypothesis. *The Quaternary Review of Biology*, *83*(2), 153–169. https://doi.org/10.1086/587825

Botton-Divet, L., Cornette, R., Houssaye, A., Fabre, A.-C., & Herrel, A. (2017). Swimming and running: a study of the convergence in long bone morphology among semi-aquatic mustelids (Carnivora: Mustelidae). *Biological Journal of the Linnean Society*, *121*, 38–49. https://doi.org/10.1093/biolinnean/blw027

Burgin, C. J., Colella, J. P., Kahn, P. L., & Upham, N. S. (2018). How many species of mammals are there? *Journal of Mammalogy*, *99*(1), 1–14. https://doi.org/10.1093/jmammal/gyx147

Burtner, A. E., Grossnickle, D. M., Santana, S. E., & Law, C. J. (2022). Gliding towards an understanding of the origin of flight in bats. *BioRxiv*. https://doi.org/10.1101/2022.09.26.509622

Caldwell, M. W. (2002). From fins to limbs to fins: Limb evolution in fossil marine reptiles. *American Journal of Medical Genetics*, *112*(3), 236–249. https://doi.org/10.1002/ajmg.10773

Castiglione, S., Serio, C., Tamagnini, D., Melchionna, M., Mondanaro, A., di Febbraro, M., Profico, A., Piras, P., Barattolo, F., & Raia, P. (2019). A new, fast method to search for morphological convergence with shape data. *PLoS ONE*, *14*(12). https://doi.org/10.1371/journal.pone.0226949

Chen, M., & Wilson, G. P. (2015). A multivariate approach to infer locomotor modes in Mesozoic mammals. *Paleobiology*, *21*(2), 280–312. https://doi.org/10.5061/dryad.870j3

Clavel, J., Aristide, L., & Morlon, H. (2019). A penalized likelihood framework for high-dimensional phylogenetic comparative methods and an application to new-world monkeys brain evolution. *Systematic Biology*, *68*(1), 93–116. https://doi.org/10.1093/sysbio/syy045

Clavel, J., Escarguel, G., & Merceron, G. (2015). mvMORPH: An R package for fitting multivariate evolutionary models to morphometric data. *Methods in Ecology and Evolution*, *6*(11), 1311–1319. https://doi.org/10.1111/2041-210X.12420

Clifford, A. B. (2010). The evolution of the unguligrade manus in artiodactyls. *Journal of Vertebrate Paleontology*, *30*(6), 1827–1839. https://doi.org/doi.org/10.1080/02724634.2010.521216

Cooper, L. N., Berta, A., Dawson, S. D., & Reidenberg, J. S. (2007a). Evolution of hyperphalangy and digit reduction in the cetacean manus. *Anatomical Record*, *290*(6), 654–672. https://doi.org/10.1002/ar.20532

Cooper, L. N., Dawson, S. D., Reidenberg, J. S., & Berta, A. (2007b). Neuromuscular anatomy and evolution of the cetacean forelimb. *Anatomical Record*, *290*(9), 1121–1137. https://doi.org/10.1002/ar.20571

DeBlois, M. C., & Motani, R. (2019). Flipper bone distribution reveals flexible trailing edge in underwater flying marine tetrapods. *Journal of Morphology*, *280*(6), 908–924. https://doi.org/10.1002/jmor.20992

Dudley, R., Byrnes, G., Yanoviak, S. P., Borrell, B., Brown, R. M., & Mcguire, J. A. (2007). Gliding and the functional origins of flight: Biomechanical novelty or

necessity? *Annual Review of Ecology, Evolution, and Systematics*, *38*, 179–201. https://doi.org/10.1146/annurev.ecolsys.37.091305.110014

Fabre, A. C., Cornette, R., Goswami, A., & Peigné, S. (2015). Do constraints associated with the locomotor habitat drive the evolution of forelimb shape? A case study in musteloid carnivorans. *Journal of Anatomy*, *226*(6), 596–610. https://doi.org/10.1111/joa.12315

Fernández, M. S., Vlachos, E., Buono, M. R., Alzugaray, L., Campos, L., Sterli, J., Herrera, Y., & Paolucci, F. (2020). Fingers zipped up or baby mittens? Two main tetrapod strategies to return to the sea. *Biology Letters*, *16*(8). https://doi.org/10.1098/rsbl.2020.0281

Fish, F. E. (1993). Influence of hydrodynamic design and propulsive mode on mammalian swimming energetics. *Australian Journal of Zoology*, *42*, 79–101. https://doi.org/10.1071/ZO9940079

Fish, F. E. (1996). Transitions from drag-based to lift-based propulsion in mammalian swimming. *American Zoologist*, *36*(6), 628–641. https://doi.org/10.1093/icb/36.6.628

Gatesy, S. M., & Middleton, K. M. (2007). Skeletal adaptations for flight. In B. K. Hall (Ed.), *Fins into limbs: Evolution, development, and transformation* (pp. 269–283). The University of Chicago Press.

Gearty, W., McClain, C. R., & Payne, J. L. (2018). Energetic tradeoffs control the size distribution of aquatic mammals. *Proceedings of the National Academy of Sciences*, *115*(16), 4194–4199. https://doi.org/10.1073/pnas.1712629115

Grossnickle, D. M., Chen, M., Wauer, J. G. A., Pevsner, S. K., Weaver, L. N., Meng, Q. J., Liu, D., Zhang, Y. G., & Luo, Z. X. (2020). Incomplete convergence of gliding mammal skeletons. *Evolution*, *74*(12), 2662–2680. https://doi.org/10.1111/evo.14094

Guillerme, T. (2018). dispRity: A modular R package for measuring disparity. *Methods in Ecology and Evolution*, *9*(7), 1755–1763. https://doi.org/10.1111/2041-210X.13022

Guillerme, T., Cooper, N., Brusatte, S. L., Davis, K. E., Jackson, A. L., Gerber, S., Goswami, A., Healy, K., Hopkins, M. J., Jones, M. E. H., Lloyd, G. T., O'Reilly, J. E., Pate, A., Puttick, M. N., Rayfield, E. J., Saupe, E. E., Sherratt, E., Slater, G. J., Weisbecker, V., … Donoghue, P. C. J. (2020). Disparities in the analysis of

morphological disparity. *Biology Letters*, *16*(7), 20200199. https://doi.org/10.1098/rsbl.2020.0199

Gutarra, S., & Rahman, I. A. (2022). The locomotion of extinct secondarily aquatic tetrapods. *Biological Reviews*, *97*(1), 67–98. https://doi.org/10.1111/brv.12790

Gutarra, S., Stubbs, T. L., Moon, B. C., Palmer, C., & Benton, M. J. (2022). Large size in aquatic tetrapods compensates for high drag caused by extreme body proportions. *Communications Biology*, *5*(1). https://doi.org/10.1038/s42003-022-03322-y

Harmon, L. J., Losos, J. B., Jonathan Davies, T., Gillespie, R. G., Gittleman, J. L., Bryan Jennings, W., Kozak, K. H., McPeek, M. A., Moreno-Roark, F., Near, T. J., Purvis, A., Ricklefs, R. E., Schluter, D., Schulte, J. A., Seehausen, O., Sidlauskas, B. L., Torres-Carvajal, O., Weir, J. T., & Mooers, A. T. (2010). Early bursts of body size and shape evolution are rare in comparative data. *Evolution*, *64*(8), 2385–2396. https://doi.org/10.1111/j.1558-5646.2010.01025.x

Hedrick, B. P., Dickson, B. V., Dumont, E. R., & Pierce, S. E. (2020). The evolutionary diversity of locomotor innovation in rodents is not linked to proximal limb morphology. *Scientific Reports*, *10*(1). https://doi.org/10.1038/s41598-019-57144-w

Hocking, D. P., Marx, F. G., Wang, S., Burton, D., Thompson, M., Park, T., Burville, B., Richards, H. L., Sattler, R., Robbins, J., Miguez, R. P., Fitzgerald, E. M. G., Slip, D. J., & Evans, A. R. (2021). Convergent evolution of forelimb-propelled swimming in seals. *Current Biology*, *31*(11), 2404-2409.e2. https://doi.org/10.1016/j.cub.2021.03.019

Hood, G. A. (2020). *Semi-aquatic mammals: Ecology and biology*. John Hopkins University Press.

Howell, A. B. (1970). *Aquatic mammals: Their adaptations to life in the water*. Dover Publication Inc.

Jackson, S. M. (2000). Glide angle in the genus Petaurus and a review of gliding in mammals. In *Mammal Review* (Vol. 30, Issue 1, pp. 9–30). Blackwell Publishing Ltd. https://doi.org/10.1046/j.1365-2907.2000.00056.x

Jones, K. E., Bielby, J., Cardillo, M., Fritz, S. A., O'Dell, J., David, C., Orme, L., Safi, K., Sechrest, W., Boakes, E. H., Carbone, C., Connolly, C., Cutts, M. J., Foster, J. K., Grenyer, R., Habib, M., Plaster, C. A., Price, S. A., Rigby, E. A., … Purvis, A. (2009). PanTHERIA: a species-level database of life history, ecology, and

geography of extant and recently extinct mammals. *Ecology*, *90*(9), 2648-undefined. https://doi.org/10.1890/08-1494.1

Kuhn, C., & Frey, E. (2012). Walking like caterpillars, flying like bats-pinniped locomotion. *Palaeobiodiversity and Palaeoenvironments*, *92*(2), 197–210. https://doi.org/10.1007/s12549-012-0077-5

Maher, A. E., Burin, G., Cox, P. G., Maddox, T. W., Maidment, S. C. R., Cooper, N., Schachner, E. R., & Bates, K. T. (2022). Body size, shape and ecology in tetrapods. *Nature Communications*, *13*(1). https://doi.org/10.1038/s41467-022-32028-2

McHorse, B. K., Biewener, A. A., & Pierce, S. E. (2019). The evolution of a single toe in horses: causes, consequences, and the way forward. *Integrative and Comparative Biology*, *59*(3), 638–655. https://doi.org/10.1093/icb/icz050

Motani, R., & Vermeij, G. J. (2021). Ecophysiological steps of marine adaptation in extant and extinct non-avian tetrapods. *Biological Reviews*, *96*(5), 1769–1798. https://doi.org/10.1111/brv.12724

Nevo, E. (1979). Adaptive convergence and divergence of subterranean mammals. *Annual Reviews of Ecology and Systematics*. https://doi.org/10.1146/annurev.es.10.110179.001413

Nevo, E. (1995). Mammalian evolution underground. The ecological-genetic-phenetic interfaces. *Acta Theriologica*, *3*, 9–31. https://doi.org/10.4098/AT.ARCH.95-43

Norberg, U. M. (1985). Evolution of vertebrate flight: An aerodynamic model for the transition from gliding to active flight. *The American Naturalist*, *126*(3), 303–327. https://doi.org/10.1086/284419

Nowak, R. M. (1999). *Walker's mammals of the world*. Johns Hopkins University Press.

Pinheiro, J., Bates, D., & R Core Team. (2022). *nlme: Linear and Nonlinear Mixed Effects Models* (R package version 3.1-161).

Polly, D. (2007). Limbs in mammalian evolution. In B. K. Hall (Ed.), *Fins into limbs: Evolution, development, and transformation* (pp. 245–268). The University of Chicago Press.

Prothero, D. R. (2009). Evolutionary transitions in the fossil record of terrestrial hoofed mammals. *Evolution: Education and Outreach*, *2*(2), 289–302. https://doi.org/10.1007/s12052-009-0136-1

Pyenson, N. D., & Vermeij, G. J. (2016). The rise of ocean giants: Maximum body size in Cenozoic marine mammals as an indicator for productivity in the Pacific and Atlantic oceans. *Biology Letters*, *12*(7). https://doi.org/10.1098/rsbl.2016.0186

Rayner, J. M. V. (1988). The evolution of vertebrate flight. *Biological Journal of the Linnean Society*, *34*(3), 269–287. https://doi.org/10.1111/j.1095-8312.1988.tb01963.x

R Core Team. (2022). *R: A language and environment for statistical computing. R Foundation for Statistical Computing*. URL https://www.R-project.org/.

Revell, L. J. (2012). phytools: An R package for phylogenetic comparative biology (and other things). *Methods in Ecology and Evolution*, *3*(2), 217–223. https://doi.org/10.1111/j.2041-210X.2011.00169.x

Rothier, P. S., Fabre, A. C., Clavel, J., Benson, R. B. J., & Herrel, A. (2023). Mammalian forelimb evolution is driven by uneven proximal-to-distal morphological diversity. *ELife*, *12*. https://doi.org/10.7554/eLife.81492

Schliep, K. P. (2011). phangorn: Phylogenetic analysis in R. *Bioinformatics*, *27*(4), 592–593. https://doi.org/10.1093/bioinformatics/btq706

Sears, K., Behringer, R. R., Rasweiler, J. J., & Niswander, L. A. (2007). The evolutionary and developmental basis of parallel reduction in mammalian zeugopod elements. *The American Naturalist*, *169*(1), 105–117. https://doi.org/10.1086/510259

Shubin, N., Tabin, C., & Carroll, S. (1997). Fossils, genes and the evolution of animal limbs. *Nature*, *388*, 639–648. https://doi.org/10.1038/41710

Smith, F. A., & Lyons, S. K. (2011). How big should a mammal be? A macroecological look at mammalian body size over space and time. In *Philosophical Transactions of the Royal Society B: Biological Sciences* (Vol. 366, Issue 1576, pp. 2364–2378). https://doi.org/10.1098/rstb.2011.0067

Upham, N. S., Esselstyn, J. A., & Jetz, W. (2019). Inferring the mammal tree: Species-level sets of phylogenies for questions in ecology, evolution, and conservation. *PLoS Biology*, *17*(12). https://doi.org/10.1371/journal.pbio.3000494

Vermeij, G. J., & Motani, R. (2018). Land to sea transitions in vertebrates: The dynamics of colonization. *Paleobiology*, *44*(2), 237–250. https://doi.org/10.1017/pab.2017.37

Weaver, L. N., & Grossnickle, D. M. (2020). Functional diversity of small-mammal postcrania is linked to both substrate preference and body size. *Current Zoology*, *66*(5), 539–553. https://doi.org/10.1093/cz/zoaa057

Weisbecker, V., & Schmid, S. (2007). Autopodial skeletal diversity in hystricognath rodents: Functional and phylogenetic aspects. *Mammalian Biology*, *72*(1), 27–44. https://doi.org/10.1016/j.mambio.2006.03.005

Weisbecker, V., & Warton, D. I. (2006). Evidence at hand: Diversity, functional implications, and locomotor prediction in intrinsic hand proportions of diprotodontian marsupials. *Journal of Morphology*, *267*(12), 1469–1485. https://doi.org/10.1002/jmor.10495

"Palavra puxa palavra, uma ideia traz outra, e assim se faz um livro, um governo, ou uma revolução, alguns dizem mesmo que assim é que a natureza compôs as suas espécies."

— Machado de Assis

4.

Unravelling the adaptive landscape of limb morphology in mammals:

The role of locomotor ecologies

4.1. Abstract

The metaphor of the phenotypic adaptive landscape has contributed to our understanding of the macroevolutionary patterns underlying morphological diversity. The outstanding phenotypic variation of mammals has been understood to be impacted by a series of selective regimes, notably for the direct links between limb morphology and the environment where locomotion takes place. However, these associations have been rather addressed across a somewhat limited taxonomic diversity. We tested whether locomotor mode defines phenotypic variation of mammals using the adaptive landscape model while covering the family-level diversity of Mammalia. We show that the diversity of body mass and, most remarkably, forelimb morphology is best explained by a multi-peak structure of adaptive zones driven by locomotor mode. Terrestrial locomotor modes exhibit nearby optima rendering transitions between locomotor modes simpler. Highly specialized locomotion in fluids or dense media, including flight, aquatic, and fossorial locomotion, drives the most extreme morphologies associated with the most isolated adaptive optima, indicating that shifts towards these specializations are possibly irreversible and extremely rare. The degree of locomotor specialization did not present a clear association with the rates of morphological evolution, with different functional constraints likely driving different evolutionary dynamics. These findings contribute to our understanding of how mammalian morphology adapted in diverse environments and highlight the significance of adaptive landscapes in elucidating selective regimes driving phenotypic diversity.

4.2. Introduction

Animals move and interact with their environment in a variety of ways, with functionally relevant phenotypes playing a crucial role in individual performance and often serving as a direct target of natural selection (Arnold, 1983). However, assessing the effect of morphology and performance on fitness requires extensive populational observations, which may impose limitations on studying and understanding the evolution of diversity through time. Nonetheless, natural selection may leave signatures in the morphological diversity that can be detectable on a macroevolutionary scale, shaping the phenotypic variation into adaptive zones that differ from patterns predicted by chance.

The idea behind phenotypic adaptive zones is rooted in the metaphor of adaptive landscapes. Originally conceived within the conceptual framework of population genetics (Wright, 1932), adaptive landscapes draw an analogy to topographic maps where peaks and valleys correspond to the fitness of individuals or populations (Fig. 4.1; Dietrich & Skipper Jr, 2012). A conceptual bridge between micro and macroevolutionary studies was later proposed by Simpson (1944), who transposed the genetic dimensions of the landscapes into phenotypic traits (Arnold et al., 2001). According to this model, peak positions can change through time and, if variation is present, lineages might transit from one adaptive peak to another in response to selection induced by environmental change or genetic drift (Lande, 1986). However, peak shifts are limited by the depth of the adaptive valleys, where phenotypes have the lowest fitness (Lande, 1986). Therefore, morphological transformation is more likely to occur across a series of peak shifts passing by shallow adaptive valleys than experiencing a single shift across a deep valley (Lande, 1986). A consequence for morphological evolution is that transitions between certain ecological regimes may occur more easily than between others.

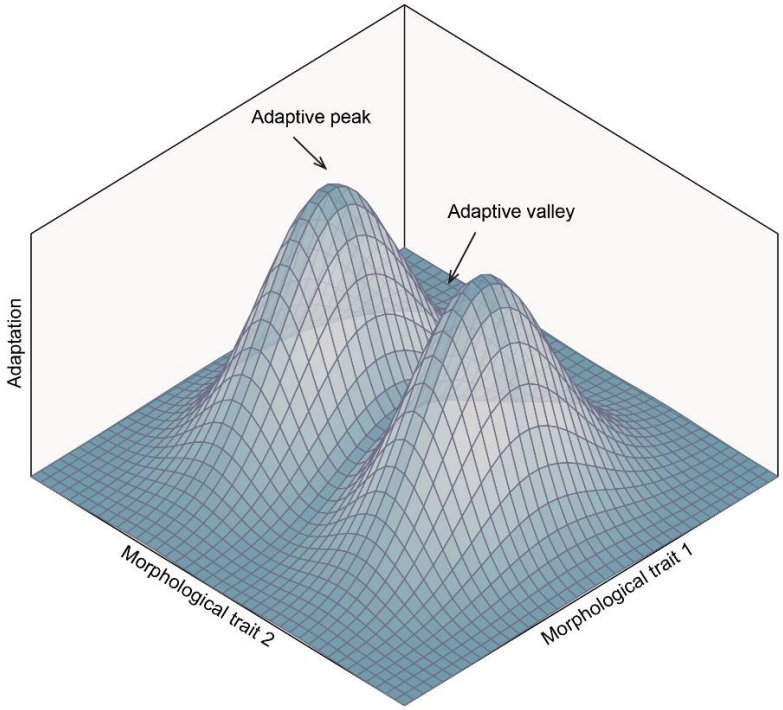

Figure 4.1. Conceptual representation of a phenotypic adaptive landscape.

Despite its metaphorical nature, ecological factors such as modes of locomotion and habitat use have been demonstrated to define adaptive zones and constrain the outcome of the evolution of morphological diversity (Friedman et al., 2021; Godoy et al., 2019; Mahler et al., 2013), particularly in mammals (Gearty et al., 2018; Weaver & Grossnickle, 2020). The remarkable morphological variation in mammals has long been linked to the diversity of locomotor behaviors which have independently evolved multiple times in this group (Chen & Wilson, 2015; Polly, 2007; Samuels & Van Valkenburgh, 2008; Van Valkenburgh, 1987) – except for powered flight with a single origin in bats. Particularly, the evolution of highly specialized types of locomotion such as swimming or flight is supported by adaptive models which have respectively driven a body mass increase in aquatic mammals (Gearty et al., 2018) and forelimb elongation in bats

(Burtner et al., 2022). How easily less specialized morphologies shifted to these peaks, however, remains unclear. Furthermore, no studies to date have conducted a clade-wise comparison to estimate if the different modes of locomotion of mammals together conform to the idea of an adaptive landscape facilitating the transitions between specific sets of locomotor modes situated closer together on the adaptive landscape.

Here, we reconstructed the patterns and process of the morphological evolution of forelimb morphology and body mass testing the hypothesis that locomotor ecologies have shaped an adaptive landscape of phenotypic diversification in mammals. We provide a comprehensibly characterized diversity of mammals by quantifying forelimb morphology for nearly 800 species, capturing over 60% of the mammal genus diversity and nearly 95% of the modern and recently extinct familial diversity (Burgin et al., 2018) (Table S1.1). We first explored the patterns of morphological variation associated with locomotor ecologies and then used a model-comparison approach to test for the support of a multi-peak adaptive model of evolution, posteriorly estimating the evolutionary transitions between regimes and the rates and shifts of the tempo of evolution throughout the evolutionary history of mammals.

4.3. Results & discussion

4.3.1. Ecological associates of body mass and limb shape

Before testing the hypothesis that locomotor regimes drive the macroevolutionary phenotypic landscape in mammals, we first investigated the patterns of variation in locomotor traits across different ecological regimes. We specifically quantified the variation in body mass and forelimb dimensions. We classified species into ten categories to describe their modes of locomotion (Table S1.1): 1) aquatic (44 species), 2) arboreal

(123 species), 3) flight (127 species), 4) fossorial (28 species), 5) gliding (11 species), 6) scansorial (65 species), 7) semiaquatic (41 species), 8) semifossorial (81 species), 9) terrestrial biped (20 species), and 10) terrestrial quadruped (257 species).

Body mass and the morphology of the forelimb are distinguishable between some, but not all locomotor categories. We found that body mass extremes tend to be characterized by species that move in fluids, such as in water, air and dense media like soil (underground), with aquatic mammals exhibiting the greatest body mass, and flying and fossorial habits encompassing, on average, the lightest animals (Fig. 4.2A, Table S4.1). Increased body mass in aquatic lineages has been exhaustively reported and is linked to the energetic balance between heat loss and feeding efficiency dictated by prey availability in this environment (Gearty et al., 2018; Pyenson & Vermeij, 2016). The lighter bodies of flying mammals may reduce the energetic cost of flight and provide a greater aerial maneuverability in bats (Rayner, 1988), while in fossorial animals, reduces the energetic cost of tunnel construction and facilitates the displacement through complex and narrow tunnels (Navas et al., 2004; Zelová et al., 2010). Besides locomotion, previous studies have demonstrated that diet plays an important role on body mass, particularly for terrestrial mammals, with herbivores being substantially heavier than omnivores and carnivores (Price & Hopkins, 2015). Semiaquatic species present on average the second heaviest body masses, but significant differences are only detected between few groups (mostly those also using fluid-based locomotion, such as flight, aquatic, fossorial and semi-fossorial). Terrestrial animals present average values of body mass, without significant differences between different locomotor groups.

The limb shape morphospace is likewise characterized by clusters of groups specialized in fluid locomotion. A phylogenetic principal component analysis reveals that the major axis of variation (pPC1 27.48% of total variation) corresponds to bone lengths

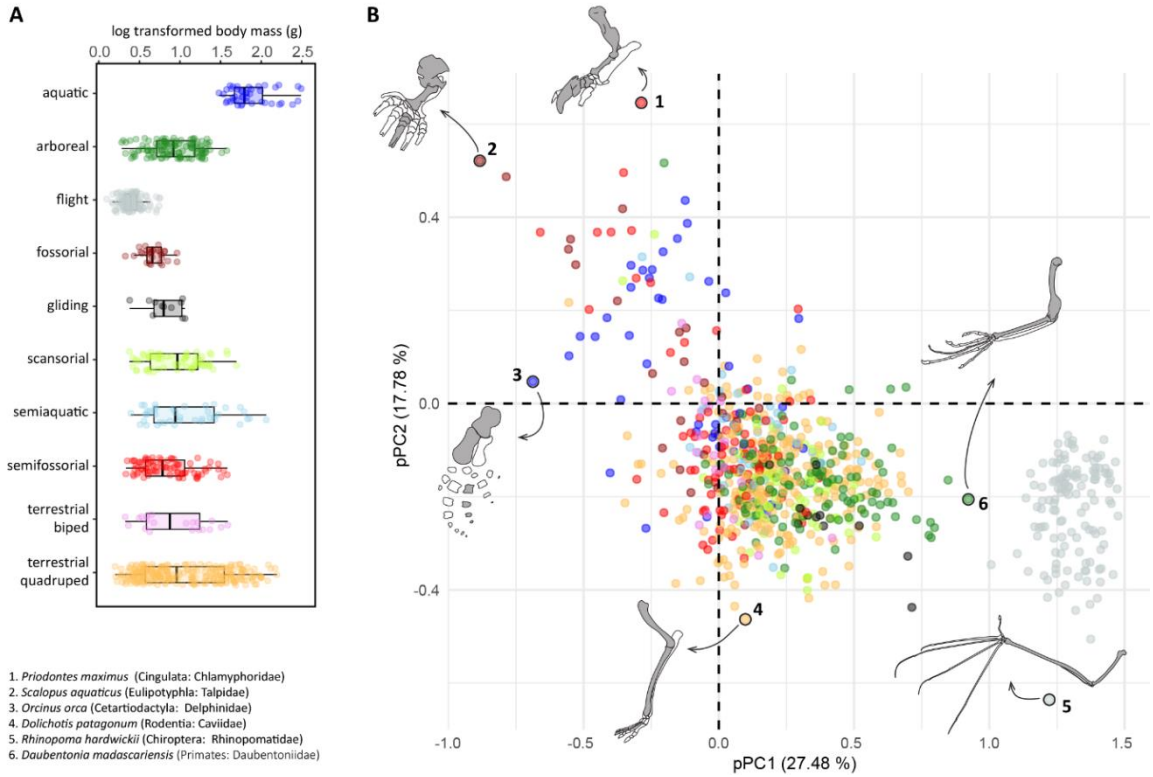

Figure 4.2. Body mass and limb shape variation across locomotor modes. A) Body mass variation (log10-transfomed g values in linear scale) represented by different locomotor modes. B) Limb morphospace represented by the two axes of highest variation (pPC1 and pPC2), indicating the taxa occupying extremes (bones examined in grey). Scatter colors correspond to the locomotory categories represented in A.

varying in opposition to width and height, with the highest loadings corresponding to the length of autopod structures (metacarpal, phalanx, and digit; Fig. 4.2B, Table 4.1). Flyers are clustered at one extreme of the pPC1 and present the most slender limbs with long and narrow bones and long hands. This morphology allows the increase of the surface area for the membranous wing, which provides lift and reduces acceleration during descent (Bishop, 2008; Gatesy & Middleton, 2007; Grossnickle et al., 2020). Many arboreal species are distributed close to the flight cluster, with the aye-aye *Daubentonia madascariensis* being positioned in between the flyers and other arboreal specialists.

Gracile bones have repeatedly evolved in many arboreal mammals, favoring greater joint mobility and more agile interaction with narrow supports (Chen & Wilson, 2015; Fabre et al., 2015). However, aye-ayes have a highly modified and elongated middle digit which is not specialized for locomotion, but for foraging. These primates use their elongated skinny finger to tap tree trunks and detect and extract insects from inside the woods (Lhota et al., 2008).

The other pPC1 extreme is described by species with the most robust limbs (short but thick bones) and the shortest hands, which is dominated by an overlap of many aquatic and fossorial taxa, as well as some semifossorial species. The Eastern mole *Scalopus aquaticus* and the killer whale *Orcinus orca* define this end of the pPC1 axis, displaying the most robust limbs and shortest hands for fossorial and aquatic taxa, respectively (Fig. 4.2B). The variation associated with the pPC1 has strong phylogenetic signal ($\lambda = 0.97$). The second major axis of variation (pPC2, 17.78% of total variation) mostly describes the length of proximal bones (humerus and radius) versus digit length. Fossorial and some semifossorial mammals are again positioned at one extreme and show great overlap with many aquatic groups: these species share relatively short proximal bones that are proportionally similar to the digit length. This maximum axis is represented by the semifossorial giant armadillo *Priodontes maximus* and by the Eastern mole. This region of morphospace is also occupied by a few non-fossorial and non-aquatic species: the arboreal silky anteater (*Cyclopes didactylus*, Pilosa: Cyclopedidae), the scansorial tree pangolin (*Phataginus tricuspis*, Pholidota: Manidae) and southern Tamandua (*Tamandua tetradactyla*, Pilosa: Myrmecophagidae), and the terrestrial long-nosed echidna (*Zaglossus sp*., Monotremata: Tachyglossidae). All these species share close ancestry with semifossorial or fossorial taxa, suggesting that high phylogenetic signal and not locomotor specialization contributes to their positioning in this part of morphospace ($\lambda =$

0.94). Despite not presenting fossorial behavior, all these species feed on ants and termites, using their bulky, long-clawed hands to excavate the nests and extract the insects from within (Nowak, 1999). These results suggest that other factors besides locomotion, such as phylogenetic history, and foraging strategy relying on forceful limb retraction may also drive patterns of limb shape diversity.

Table 4.1. Phylogenetic principal components of residual limb morphology. First four pPC loadings of each linear distance obtained using size residual values.

		pPC1	pPC2	pPC3	pPC4
humerus					
	Length	0.228	**-0.685**	-0.007	0.024
	Width	-0.325	-0.234	**0.530**	-0.180
	Height	-0.498	-0.324	0.272	-0.371
radius					
	Length	0.351	**-0.757**	-0.203	-0.009
	Width	-0.253	-0.476	0.027	0.055
	Height	-0.270	0.039	0.421	**-0.526**
metacarpus					
	Length	**0.642**	-0.394	-0.429	-0.113
	Width	-0.364	0.376	-0.038	0.414
	Height	-0.214	0.238	**-0.503**	**-0.526**
phalanx					
	Length	**0.863**	0.165	0.239	0.033
	Width	**-0.553**	0.375	-0.250	0.342
	Height	-0.200	0.426	**-0.570**	-0.338
digit					
	Length	**0.693**	**0.512**	0.151	-0.175
	Eigenvalues	0.00103	0.00066	0.00041	0.00029
	Var explained %	27.49	17.78	11.04	7.74

The minimum pPC2 extreme is defined by animals having digit lengths that are much shorter than their elongated proximal bones. This axis end does not present a clear cluster

of locomotor modes and is occupied by species as diverse as the lesser mouse-tailed bat *Rhinopoma hardwickii* (representing the monogeneric family Rhinopomatidae, with reduced phalangeal formula, 2-2-2-2-2, and extremally curved distal phalanx) and the Patagonian mara *Dolichotis patagonum* (a large long-legged rodent with reduced digits and ungulate-like body posture).

Overall, mammals that use fluid media for locomotion present the most distinct and specialized morphologies. Our previous findings demonstrate that leaving the terrestrial environment to locomote in homogeneous fluids, such as water and air, involved the evolution of highly modified morphological features (Ch. 3), which is also showed here by the distribution of flying and many aquatic species in distinct parts of morphospace. Soil, on the other hand, is a much more discontinuous fluid than water or air, varying in compaction due to composition, humidity, granulometry, etc. (Biewener & Patek, 2018). The mechanical constraints of moving underground are linked to the recurrent convergent evolution of robust forelimb bones in many fossorial lineages, often possessing wide robust claws (Chen & Wilson, 2015; Hedrick et al., 2020; Montoya-Sanhueza et al., 2022; Samuels & Van Valkenburgh, 2008). Such robust bones provide an increase of the skeletal surface where powerful musculature is attached, generating the mechanical power for digging (Fabre et al., 2015). A similar morphological pattern is also observed in many aquatic species, suggesting that locomotion in water and soil share some common constraints. It has, for example, been previously demonstrated that aquatic and semifossorial mustelids have convergent humeral morphologies (Fabre et al., 2015). Our results show that skeletal robustness is also shared across many distally related aquatic and fossorial mammals, a pattern that is detected here for the overall forelimb shape.

It is important to highlight, however, that not all fossorial and aquatic mammals occupy extreme parts of limb mophospace as many of these species display limb shape

variation that is distributed more centrally or along the pPC2 continuum. Such variation is potentially involved with the biomechanical diversity in both fossorial and aquatic locomotion (Ch. 3; Sansalone et al., 2020). Many subterranean mammals mainly dig their burrows with their incisors, and not with their forelimbs (for example, the naked mole rat *Heterocephalus glaber*) imposing functional constraints on skull rather than limb morphology (Gomes Rodrigues et al., 2016). Likewise, swimming can be achieved through caudal or flipper propulsion, implying in different roles performed by the forearm (Fish, 1996). These biomechanical differences are associated with morphological variation in the tetrapod flipper (DeBlois & Motani, 2019), and might be linked to the outstanding morphological disparity of the forelimb bones in aquatic mammals (see Ch. 3).

4.3.2. The adaptive evolution of locomotor morphologies

We tested the hypothesis that locomotion influenced the evolutionary patterns the forelimb morphology in mammals. The variation of phenotypes relies on complex relationships revealed by the interrelation of traits. The way phenotypic traits vary is seldom completely independent from each other because they may share developmental constraints, pleiotropic effects and genetic linkages (Cheverud, 1984, 1996). Therefore, the nature of phenotypic variation is multivariate and consequently we conducted our analyses favoring multivariate approaches over univariate ones in order to better capture the complex nature of trait interrelatedness. We first examined the overall size variation across locomotor categories, combining body mass with the absolute values of forelimb measurements. We then analyzed the variation of the forelimb traits removing size to

provide a more precise understanding of the relationship between locomotion and trait proportions, that is, limb shape.

A multi-peak adaptive landscape is the best supported scenario underlying the morphological evolution of locomotor traits in mammals (Table S4.2). In other words, we detected a strong pattern of adaptive evolution for the body mass and forelimb morphology driven by locomotion. The generalized information criterion (GIC) revealed that, for both cases, the best model of continuous trait evolution is an Ornstein-Uhlenbeck model with multiple trait optima (OUM), each represented by a locomotory regime (Table S4.2, Fig. S4.1: GIC_{size} = -274749.0; $GIC_{residual}$ = -30124.9). In this model, the rates of morphological evolution and the attraction towards each optimum are constant – more complex OU models could not be calculated in a multivariate framework because they are either inexistent or present computational limitations when implemented for large datasets (Clavel et al., 2015). As a way to compare and visualize the different adaptive peaks, we calculated the sum of the traits' optima for each locomotor regime. The optima detected for the overall size recovered the patterns of body mass variation: aquatic animals exhibit the highest values of the optimum, isolated from other peaks (Fig. 4.3A, Table S4.3) and semiaquatic taxa show the second highest optimum. Arboreal species and terrestrial quadrupeds share a similar adaptive optimum of overall body size, without significant differences between one another. There is considerable overlap in the optima for groups with more generalist locomotion, indicating that terrestrial bipeds, semifossorial, gliding and scansorial lineages evolve towards the same body size peak (Table S4.3). Flying taxa exhibit the lowest values, followed by fossorial taxa.

The differences between the locomotory optima are much more obvious for limb shape, after removing the effect of size (Fig. 4.3A). All trait optima are significantly different. Moreover, the extremes are defined by highly specialized locomotion in fluids:

flying species are isolated in one end with the highest peak values for limb shape, contrasting with fossorial and aquatic groups towards the other end. Most groups sharing less specialized forelimb morphologies, including scansorial, terrestrial quadrupeds and bipeds, semiaquatic, and semifossorial taxa present intermediate and nearby values of their shape optima.

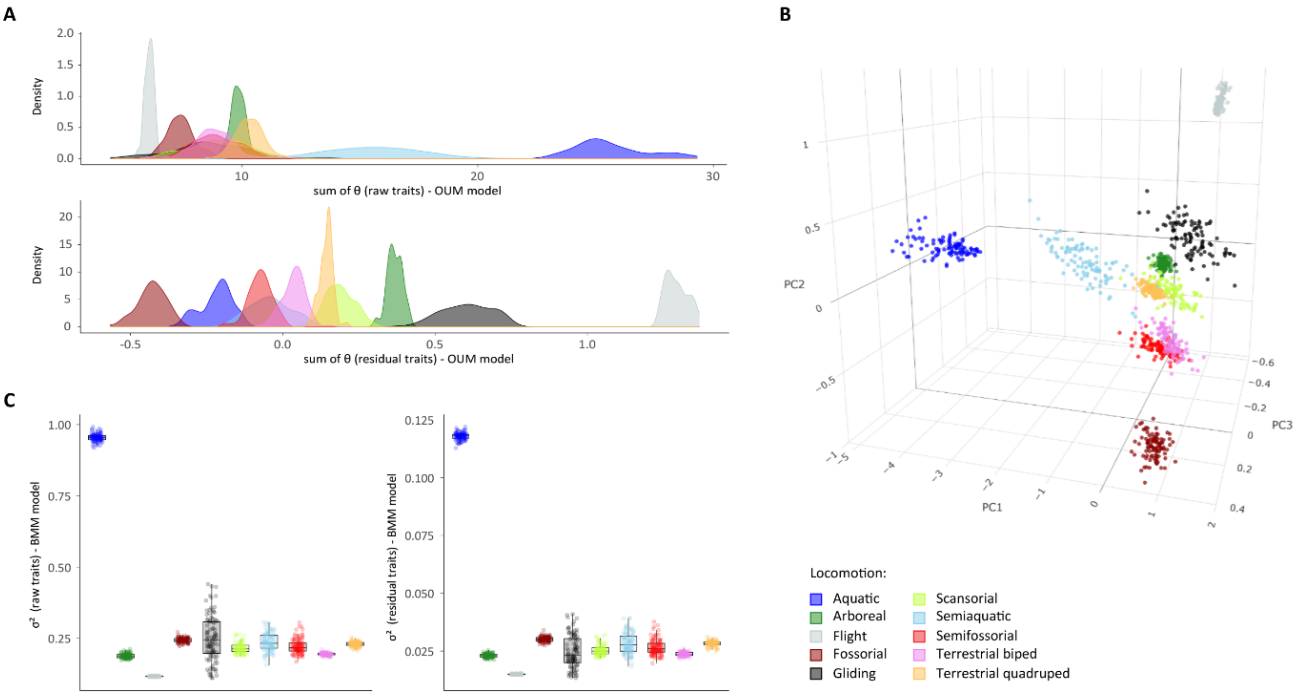

Figure 4.3. Morphological trait optima and rates across locomotory regimes. A) Sum of trait optima calculated from raw (top) and size residual data (bottom). B) Morphospace of trait optima for the different locomotor modes (calculated with raw data). C) Rates of morphological evolution of raw (left) and size residual (right) traits.

Although providing the sum of all trait optima is informative, it hides the contribution of each trait to the absolute optima value. Therefore, we summarized the

variation of all trait peaks in a PCA and visualized the first three axes in a three-dimensional plot. Results evidenced that the aquatic, flying and fossorial regimes as the three major isolated optima, occupying the morphospace extremes (Fig. 4.3B). The first axis describes the peaks towards overall size, isolating aquatic taxa from all other regimes. The second and third axis are explained by limb proportions irrespective of size, and are mostly influenced by the lengths of the autopod in the PC2 and of proximal bones (humerus and radius) in the PC3 (Table S4.4).

The three-dimensional plot reveals that the optima of locomotor modes displaying intermediate specialization in fluids or dense media (i.e. semiaquatic, semifossorial, and gliding) lean from the morphospace center towards the adaptive peaks of their corresponding fully specialized regimes. Such trend was already evident in the optima sums (Fig. 4.3A) and is reinforced here. Scansorial, arboreal, and terrestrial quadrupeds and bipeds have more similar and closer adaptive peaks, positioned in the center of the morphospace.

Detecting a high support for multi-peak adaptive model reinforces the important role of locomotion as a driver of body size and limb shape. These results confirm that convergent locomotor styles experience similar selective pressures on limb morphology throughout the whole mammalian radiation. Nevertheless, we do observe that many taxa diverge from their optima, illustrated by the overlap in morphospace between groups with distinct locomotor modes. As previously mentioned, other factors besides locomotion, such as foraging behaviour and ancestry, also seem to play an important role in explaining the limb morphology of some taxa. Therefore, it is expected to detect differences between the morphospace occupation and the distributions of the optima, as effectively reaching the adaptive zones might be impossible given environmental fluctuation, functional trade-offs, genetic drift, and selection on genetically correlated traits (Hansen, 1997;

Mongiardino Koch, 2021). We also detected that most locomotor styles have central nearby optima, with adaptive peaks being positioned gradually further as specialization increases. Such variation suggests that central adaptive zones experience more similar selective pressures than the extremes, where specialization likely evolved thorough an ordered pathway.

4.3.3. Evolutionary transitions across modes of locomotion

We tested whether transitions between specific sets of locomotor ecologies are more facilitated than others by examining the likelihood of character evolution in different possible scenarios (Lewis, 2001). The best supported scenario indicates that the evolution to fluid specialized regimes is ordinated and directional, with more transitions arriving to and departing from the terrestrial quadrupedal mode (Fig. 4.4, directional model 2, see Fig. S4.1 and Table S4.5). Combined with the distributions of the phenotypic adaptive zones previously described (Fig. 4.3A-B), these results demonstrate that the fastest transitions are more likely to occur between adjacent optima. Such a phenomenon is notably observed in the rapid transitions from both semiaquatic and scansorial to terrestrial quadrupedal styles, as well as from scansorial to arboreal modes, all consisting of nearby phenotypic zones.

Although peak distances have been demonstrated to have little impact in the rate shift of populational models, valley depth is critical for limiting such changes (Lande, 1986). The patterns detected here suggest that the limb morphology presents a central landscape with shallower adaptive valleys, where intermediate phenotypes, for example, between terrestrial quadruped and scansorial taxa, do not present a strongly reduced fitness. Therefore, transitions between land-based locomotion occur more easily than

transition to more specialized modes including those involving water, air, or underground environments. These results are not surprising considering that the quadrupedal body posture is a plesiomorphic condition in mammals (Grossnickle et al., 2019), and it would be expected for such forms to occupy more central adaptive optima, where transitions to other modes may depart from and return to.

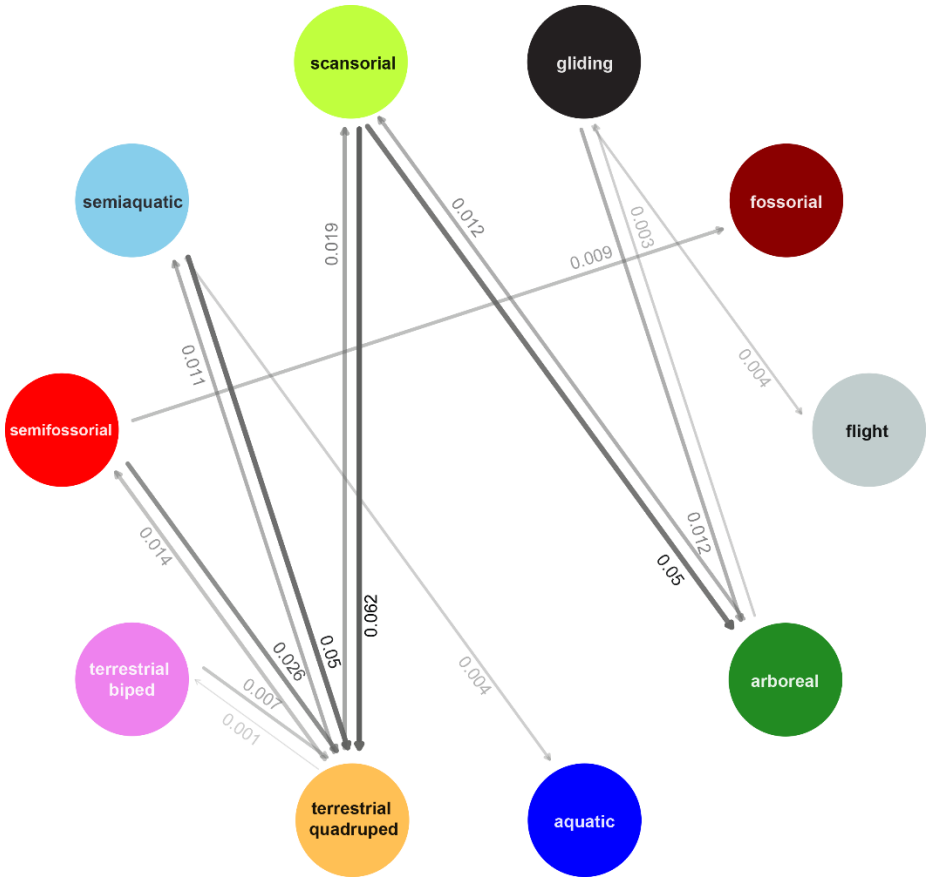

Figure 4.4. Transition rates between locomotor models. Diagram representing the evolutionary rates (*q*) of character transitions according to a best-fitted ordered model of increasing locomotory specialization (directional model 2).

In contrast, transitions to distant specialized peaks including flight, aquatic locomotion and strict fossoriality are rare and occurred under low rates, with a low to inexistent chance of returning to the previous evolutionary stage. Results revealed that these transitions are likely to occur stepwise and compulsorily involve passing through semi-specialized morphologies, which may thus facilitate shifts to the three distant fully-specialized zones (Fig. 4.4). The evolution of cetaceans widely recovers this stepwise pattern, where the exquisite fossil record points to gradual transition from a terrestrial quadrupedal ancestor, to semi-aquatic riverine and deltaic environments, to fully aquatic marine forms (with some later reinvasions to freshwater systems, Pyenson, 2017). Pinnipeds and sirenians also evolved towards aquatic locomotion passing by less specialized semi-aquatic forms, although their fossil record is not as well documented as for cetaceans (Benoit et al., 2013; Rybczynski et al., 2009). The evolution of flight in bats is not fully understood given the absence of intermediate phenotypes in the fossil record, but it is widely suggested to have evolved from gliding ancestors (Bishop, 2008). In fact, models of morphological evolution suggest that the origin of bat flight likely resulted from a "tree-down" transition from arboreality to gliding to flight (Burtner et al., 2022), a pattern that is also detected here.

Once locomotor phenotypes transitioned to specialized fluid locomotion, our data suggest that lineages are limited to shift to any other locomotor mode or even to return to the plesiomorphic state. Indeed, there is no fossil record suggesting that a reversal from fully aquatic, fossorial or flight modes to a terrestrial quadrupedal mode ever occurred in Mammalia. One possible explanation for this phenomenon is that, in the long term, high specialization may lead to profound genetic and developmental changes, such as irreversible trait loss, ultimately constraining the amount of heritable variation (Gould, 1970; Lande, 1986). The reduced available variation in specialists may sometimes limit

the lineage to persist and adapt under rapidly changing environments, leading to higher extinction rates (Day et al., 2016). Fossorial specialization, for example, encompasses an evolutionary dead-end for snakes, which exhibit reduced speciation rates and increased extinction (Cyriac & Kodandaramaiah, 2018). The same pattern, however, is not detected for lizards| (Cyriac & Kodandaramaiah, 2018). For mammals, it is not clear whether irreversibility of these specialized regimes is linked to an increase in the likelihood of extinction. Nevertheless, it does not seem to be the case for bats, for which the evolution of flight seems to be linked to a radiation that resulted in the second most specious mammalian order, after rodents (Burgin et al., 2018). Further studies on speciation dynamics are required to appropriately address these questions, however.

4.3.4. Shifts and rates of morphological evolution

From our previous results, it was unclear whether the degree of locomotor specialization impacted the tempo of morphological evolution. Therefore, we provided estimates of the rates of phenotypic change generated by a multi-rate Brownian motion model (BMM, Table S4.2), which displayed the second-best fit for the evolution of locomotor traits. This model assumes that traits evolved by random walk, but at varying rates, depending on the locomotor category. One of the caveats of the multivariate method employed here is that we were unable to test for more complex OU models, such as those with variable rates of evolution and peak attraction. Therefore, we decided to additionally consider the results provided by the BMM model in order to understand the degree of variation in the rates of evolution across locomotor regimes.

Locomotor specialization can be either associated with an increase or a decrease in the rates of morphological evolution. The fastest rates of evolution are observed in

aquatic taxa, exhibiting remarkable differences from any other locomotor mode and opposed to flying species that show the slowest rate changes (Fig. 4.2C, Table S4.6). Fossorial lineages present the second highest rates while arboreal groups show the second slowest evolutionary change. All these patterns were recovered while both considering and removing body size. However, we did not detect a clear correspondence between the rates of morphological change and the ordination of locomotor transitions: specialized modes might have low or fast rates, while less specialized morphologies show more average values.

The differences observed in the rate values reveal different evolutionary dynamics according to the environment where locomotion takes place. Aquatic lineages also present the fastest rates of skull morphological evolution throughout Mammalia, most notably in cetaceans (Goswami et al., 2022). After early cetaceans transitioned to the oceans and experienced a peak shift towards larger body sizes, their morphological evolution was marked by a rather flat adaptive landscape of increasing variation through time (Burin et al., 2023). This suggests that the release of terrestrial constraints favoured more relaxed selective pressures on aquatic morphologies once they have increased in size, resulting in rapid evolution that triggered remarkably disparate phenotypes (Coombs et al., 2022; Jones et al., 2015; see Ch.3). Locomotion in air, on the other hand, imposes more powerful constraints on morphological diversification, as previously shown, and resulted in a low morphological diversity of limb shape (Ch. 3). The slow changes of morphological evolution in flying species suggests that strong stabilizing forces might have favoured the diversification of Chiroptera resulting in low diversity of limb morphology (Amador et al., 2019). However, these results must be interpreted with caution, as mammals performing powered flight have a single origin, meaning that we lack of statistical power to determine the degree of functional constraint for flight on the bat wing.

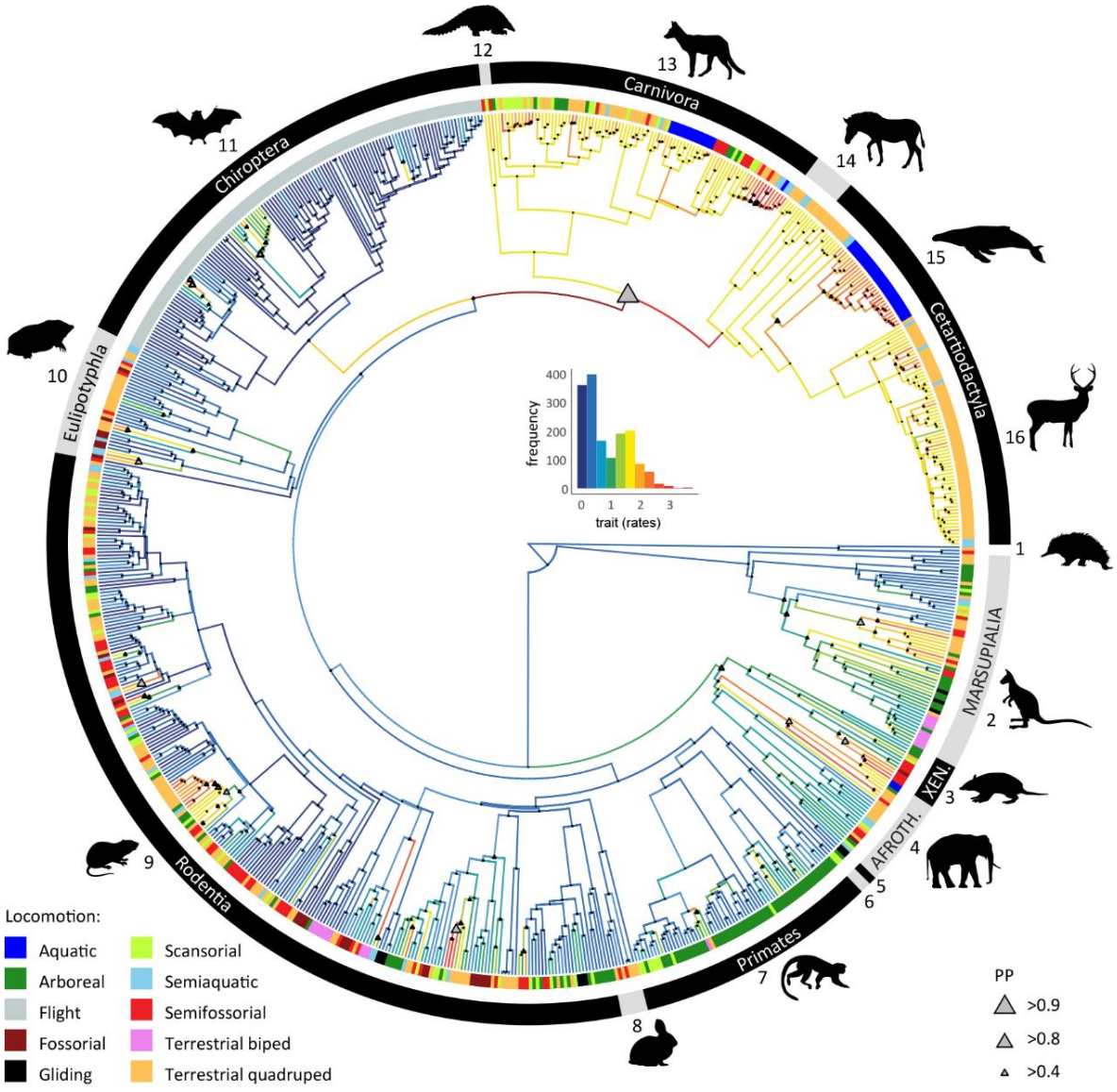

Figure 4.5. Evolutionary rates and rate shifts of body mass mammals. Color gradients indicate the rate of trait evolution, with faster rates represented by warmer colors and slower rates by the cooler ones. Shifts in morphological rates with high probabilities are represented by grey triangles of relative size proportional to their posterior probabilities. Tip colors represent the prevalent locomotor mode used by each species here examined. 1. *Tachyglossus aculeatus* (Monotremata: Tachyglossidae); 2. *Macropus parryi* (Diprotodontia: Macropodidae); 3. *Euphractus sexcinctus* (Cingulata: Chlamyphoridae); 4. *Elephas maximus* (Proboscidea: Elephantidae); 5. Dermoptera; 6. Scandentia; 7. Saimiri sciureus (Primates: Cebidae); 8. *Sylvilagus bachmani* (Lagomrpha: Leporidae); 9. *Nesokia indica* (Rodentia: Muridae); 10. *Mogera wogura* (Eulipotyphla: Talpidae); 11. *Carollia brevicauda* (Chiroptera: Phyllostomidae); 12. *Smustia gigantia* (Pholidota: Manidae); 13. *Lycalopex vetulus* (Carnivora: Canidae); 14. *Equus grevyi* (Perissodactyla: Equidae); 15. *Megaptera novaeangliae* (Cetartiodactyla: Balaenopteridae); 16. *Cervus unicolor* (Cetartiodactyla: Cervidae).

Finally, we reconstructed the evolutionary history of morphological rates and shifts in the rate of evolution of body mass and limb shape throughout the mammalian radiation to verify whether rate shifts correspond to major ecological transitions (Table S4.7, Fig. S4.3 and S4.4). We identified a single major rate shift of body mass in the node of Ferungulata, which groups Carnivora, Perissodactyla and Cetartiodactyla (Fig. 4.5). Accelerated evolution of body mass is particularly evidenced in Cetacea and mustelids (warmer branch colors evidenced in Fig. 4.5). Outside Ferungulata, fast morphological changes were also detected within Afrotheria (specifically Paenungulata, that is, elephants, manatees, and hyraxes), in dasyurid marsupials (including the terrestrial quadrupeds Tasmanian devil and thylacine) and Chlamyphoridae armadillos. A previous study has demonstrated that shifts in body size evolution in terrestrial mammals is associated with transitions between foot postures (Kubo et al., 2019). Ferungulata is also the mammalian clade with the most diversity of foot postures, such as unguligrady in horses and deer, digitigrady in cats and rhinos, and plantigrady in bears, which might explain why we detected a rate shift of body mass at the lineage node.

The evolution of the shape of mammal limbs has been marked by several episodes of significant rate shifts, which were more prevalent than rate shifts in body mass. (Fig. 4.6). The aquatic transitions in cetaceans and pinnipeds, for instance, are marked by independent rate shifts in the form of the flipper. We also recovered rate shifts in moles, which might be linked to the modifications required for fossoriality. Apart from these examples, many other clade level shifts have been identified. We detected a major shift in the node of Boreoeutheria (Laurasiatheria and Euarchontoglires), as well as in Xenarthra, Carnivora, and in the dichotomy of Perissodactyla and Cetartiodactyla. These shifts were followed by accelerated morphological diversification, but without clear associations with locomotor regime transitions. Similar to body mass, transitions in digit

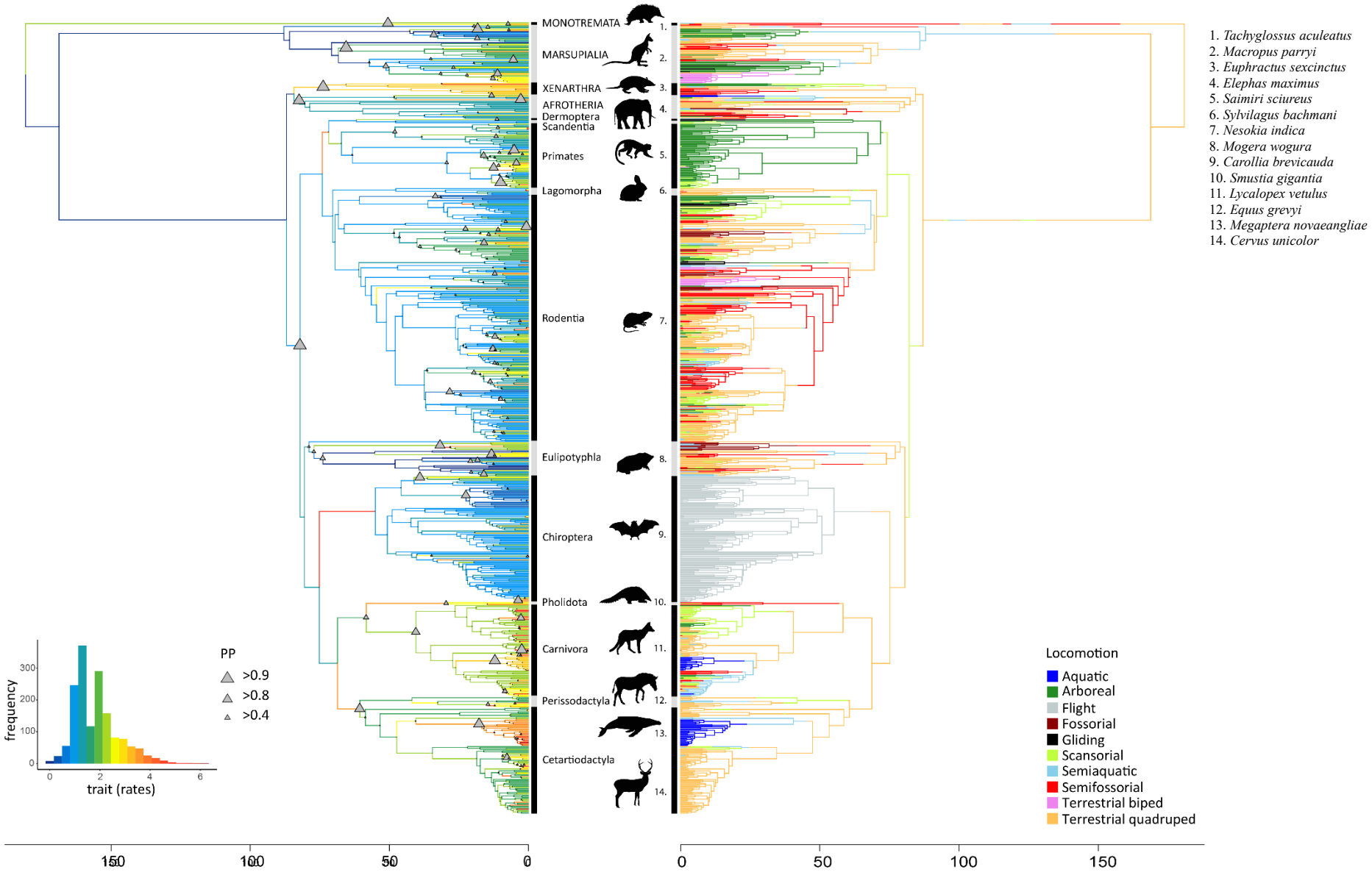
MONOTREMATA
MARSUPIALIA
XENARTHRA
AFROTHERIA
Dermoptera
Scandentia
Primates
Lagomorpha
Rodentia
Eulipotyphla
Chiroptera
Pholidota
Carnivora
Perissodactyla
Cetartiodactyla
1.
2.
3.
4.
5.
6.
7.
8.
9.
10.
11.
12.
13.
14.
1. Tachyglossus aculeatus
2. Macropus parryi
3. Euphractus sexcinctus
4. Elephas maximus
5. Saimiri sciureus
6. Sylvilagus bachmani
7. Nesokia indica
8. Mogera wogura
9. Carollia brevicauda
10. Smustia gigantia
11. Lycalopex vetulus
12. Equus grevyi
13. Megaptera novaeangliae
14. Cervus unicolor
frequency
trait (rates)
PP
>0.9
>0.8
>0.4
Locomotion
Aquatic
Arboreal
Flight
Fossorial
Gliding
Scansorial
Semiaquatic
Semifossorial
Terrestrial biped
Terrestrial quadruped
150
100
50
0
0
50
100
150

[Figure on previous page]

Figure 4.6. Evolutionary rates of limb shape in mammals and ancestral state reconstruction of locomotor modes. Topology on the left with color gradients indicating the rate of trait evolution, with faster rates indicated by warmer colors and slower rates by cooler colors. Shifts in morphological rates with high probabilities are represented by grey triangles of relative size proportional to their posterior probabilities. Topology on the right illustrates one example of stochastically mapped ancestral reconstruction of locomotor modes.

posture may have played an important role for the shifts detected within ferungulates. Most of the species with derived foot postures such as digitigrady and unguligrady were classified in our study as terrestrial quadrupeds, which to some extent reduces the morphological complexity of these taxa into a single generalized category. Future research detailing the nuances of terrestrial quadruped locomotion, such as the impact of digit posture and the gait (for example, the degree of cursoriality) may provide further insights into the patterns of morphological shifts during limb shape evolution.

4.4. Conclusion

The metaphor of phenotypic adaptive landscapes has greatly contributed to the understanding of macroevolutionary patterns, as well as of the selective regimes driving phenotypic diversity (Arnold et al., 2001). Here, we show that the morphological diversity of locomotor traits in mammals strongly recovers the multi-peak structure of an adaptive landscape, meaning that functional constraints involving the biomechanics of locomotion drive the evolution of phenotypes. Highly specialized locomotor modes such as aquatic locomotion, flight and fossorial locomotion, consistently stand out as defining the most extreme morphologies. Adaptive zones are more evident for limb shape compared to overall size and body mass. Faster and more frequent transitions occur between modes of

locomotion that occupy rather central and nearby adaptive optima, with a low degree of specialization in fluid locomotion. Locomotor shifts to specialized media, however, are likely irreversible and extremely rare, compulsorily passing by semi-specialized modes as previously suggested by the fossil record and evolutionary models (Bishop, 2008; Pyenson, 2017). The level of locomotor specialization did not present a clear association with the rates of morphological evolution, as aquatic and fossorial taxa exhibit the fastest evolving morphologies, while flyers and arboreal species evolve at slowest rates. We suggest that the evolutionary dynamics of locomotor morphologies depend on the different functional constraints required to move in a given environment. Further research using fossil data is needed to shed light on the evolutionary patterns of such transitions and on the impact of functional specialization for clade diversity. Our findings contribute to a better understanding of how mammals have adapted their limbs to thrive in diverse environments and highlight the significance of adaptive landscapes in elucidating macroevolutionary patterns and selective regimes driving phenotypic diversity.

4.5. Material & methods

4.5.1. Taxonomic sampling and morphological data

We sampled the limb dimensions of 830 specimens, comprising a total of 797 species representing all living orders except for the marsupial golden moles Notoryctemorphia (which display fused phalanges in their third digits, preventing the acquisition for some of the measurements used). This study used part of the dataset sampled in the previous chapters (also see Rothier et al., 2023). Our sample ranged from one to three individuals per species, representing 761 genera and 152 families (taxonomy following Mammal

Diversity Database; Burgin et al., 2018). Data acquisition was conducted by combining digital and manual methods, depending on the specimen's size.

We generated micro-CT-scans and surface scans of 126 small to medium sized-specimens from different institutions (Table S1.1). Scans were generated using a Nikon Metrology HMX ST 225 (NHMUK Natural History Museum, London) and an EasyTom 150 X-ray micro-computer tomography (ISEM Institute, Montpellier, France). We combined this digital dataset with an additional 414 meshes available in MorphoSource.org. We used Avizo 8.1.1 (1995-2014 Zuse Institute Berlin) to convert image stacks into three-dimensional surface models (incorporating scale dimensions based on the voxel size of each scan) later used to obtain morphometric distances via landmark coordinates, also in Avizo. Finally, we obtained caliper measurements of 290 limb skeletons from medium to large body-sized species from the French Muséum National d'Histoire Naturelle (MNHN Paris, France), the American Museum of Natural History (AMNH New York, USA), and the Natural History Museum (NHM London, UK) (Table S1.1).

We obtained 13 linear distances on forelimb bones consisting of the length, medial width, and height of the humerus, radius, third metacarpal and first phalanx of digit III, in addition to the total length of the digit III (inferred as the sum of the lengths of all digit III phalanges). We did not include the ulna because this bone is fused to the radius in many taxa, preventing the acquisition of such measurements (Sears et al., 2007). The third finger was sampled because this is the only digit present in the hands of all mammalian species. We measured each individual twice and calculated each trait's mean and standard error to verify measurement error. Error estimate was most often below 1.5% regardless of an animal's size and the measurement method, indicating reliability and repeatability of the methods employed. Because body mass information was rarely available for the

individuals analyzed, we compiled body mass estimates per species from the PanTHERIA database (Jones et al., 2009) and from complementary literature sources when necessary (Table S1.1).

4.5.2. Classification of locomotor ecologies

We classified each species according to the most predominant type of locomotion. We conducted an exhaustive literature review based on the ecological descriptions provided by Nowak (1999) and complemented by other relevant sources (see Table S1.1). We assigned ten locomotor categories taking into account the type of substrate species use the most for traveling, foraging, and resting: 1) aquatic (present limbs modified into flippers, travel and forage principally or entirely in water); 2) arboreal (use arboreal surfaces most of the time for foraging, resting, traveling, although capable of moving on the ground); 3) flight (travel by powered flight); 4) fossorial (construct their own borrows, spending most of the time underground for traveling, foraging, and resting); 5) gliding (arboreal species capable of moving through air with the help of a patagium); 6) scansorial (spend considerable time both on the ground and in trees for foraging, escaping, or leisure activities); 7) semi-aquatic (efficiently move both in water and on the ground but are highly dependent on the aquatic environment for foraging); 8) semi-fossorial (make considerable use of subterranean and ground substrates. Might be capable of digging for foraging and shelter, but do not construct complex burrows); 9) terrestrial biped (ground locomotion on land on the two hind limbs, by hopping, saltation or walking); 10) terrestrial quadruped (locomotion takes place in majority or entirely on the ground, such as in grass, sand, rock, leaf litter, etc., where the animal's weight is supported by both fore and hind limbs).

4.5.3. Topology and stochastic character mapping

Analyses were implemented in R 4.2.2 (R Core Team, 2022). We estimated a maximum clade credibility (MCC) tree from a posterior sample of 10,000 trees published by Upham et al. (2019), using the phangorn R package (Schliep, 2011). We pruned the MCC topology into a tree with 797 tips corresponding to the species we present morphometric data. We then used stochastic character mapping to reconstruct the evolution of the modes of locomotion of mammals by assigning the locomotor categories into the internal branches of the MCC tree. We calculated 100 mapped trees (simmap, Bollback, 2006) using the make.simmap() function from phytools R package (Revell, 2012), with a model of asymmetric character change (ARD model).

4.5.4. Comparative analyses and model fit

All morphological distances were log10-transformed prior to analyses, and body mass values transformed into linear scale by calculating the cube root prior to log10-transformation (Harmon et al., 2010). First, we conducted a phylogenetic ANOVA (function phylANOVA() from phytools R package, Revell, 2012) to determine whether the transformed body mass values differed between locomotor categories. Next, we calculated the geometric means of each species using the log-transformed limb distances as well as body mass values in linear scale. In order to obtain the relative dimensions of limb shape, we calculated the size residuals of each trait by implementing a phylogenetic regression with the geometric means as a predictor. We calculated the regression with the function phyl.resid() from phytools (Revell, 2012) using the lambda method for the correlation structure. We next conducted a phylogenetic principal component analysis (pPCA) using the covariance matrix of the size residuals to visualize limb shape

morphospace occupancy by each locomotory category (function phyl.pca() from phytools; Revell, 2012).

We evaluated the likelihood of different models of evolution of raw (limb distances and body mass) and size residual trait values in a phylogenetic generalized least squares (PGLS), using the mvgls() function (mvMORPH R package; Clavel et al., 2015). Linear regressions were estimated using maximum likelihood and LASSO penalized likelihood (Clavel et al., 2015, 2019). We examined the fitting of the following models: 1) BM (Brownian motion with single rate of evolution, σ^2, per trait), 2) OU (Ornstein-Uhlenbeck with single peak θ, attraction α and rate σ^2 per trait), 3) EB (Early Burst of uniform accelerated evolution), 4) BMM (multi-rates Brownian motion, i.e., allowing σ^2 to vary between regimes) and 5) OUM (multi-peak Ornstein-Uhlenbeck, i.e., allowing trait optima θ to vary between regimes, but traits have fixed α and σ^2). We repeated the OUM and BMM regression in all simulated 100 simmap trees to incorporate mapping uncertainty. Model fit likelihood was evaluated with generalized information criterion (GIC; with average values for the OUM and BMM). To better visualize the variation of the adaptive optima and the rates generated by the OUM and BMM models, respectively, we first provided the sums of the θ and σ^2 of all traits of each locomotor category, obtaining a single value per regime in both cases. We repeated this calculation for each fitted map regression. We conducted an ANOVA followed by Tukey test to verify the distance and significance between the distributions of the θ and σ^2 sums. Although obtaining the θ sum is helpful to summarize the overall optima variation across the modes of locomotion, we were also interested to visualize the multidimensional distribution of traits' optima. Therefore we concatenated each trait's θ from all stochastic maps and conducted a principal component analyses (prcomp() from stats R package; R Core Team, 2022) on the covariance matrix of trait optima.

The OUM models exhibited the best fit for both raw and residual values (Table S4.2). To determine whether we had the power to accurately differentiate the complex OU models from Brownian motion, we simulated trait evolution under Brownian motion using the empirical parameters obtained from the OUM regressions. We recovered the parameters of the fitted OUM models for 10 stochastic maps and simulated 10 datasets per tree (function mvSIM() from mvMORPH R package, Clavel et al., 2015), resulting in 100 simulated datasets. We repeated the PGLS model fits using the datasets to verify whether the analyses using simulated values recover the empirical results, and they largely do (Fig. S4.1). We repeated this protocol for both raw and size residual datasets.

4.5.5. Modelling evolutionary transitions of modes of locomotion

We simulated the evolutionary transitions between locomotor modes using the Mk model (i.e., discrete k-state Markov process; Lewis, 2001). Evolution occurring by Mk process assumes that changes can occur between discrete states at any time, and its rate (q value) is dependent only on the current state (thus, with no historical memory concerning changes that occurred previously). When q value is high, the rate of change between two states is fast, while small q values denote less frequent changes (Revell & Harmon, 2022).

We simulated six different models of evolutionary transitions (Table S4.5). The first model (Equal-rates, or ER model) relies on transition rates between all pairs of states as the same. The second model (SYM, symmetric model), assumes that transition rates can vary between different pairs of states; however, transition rate from state *a* to state *b* is equal to transition rate from *b* to *a*. The third model ('All-rates-different', or ARD model) allows every transition to have a different rate. The three remaining models (Directional model 1 to 3) are variations of ARD model, but assuming different

hypotheses regarding the evolution of locomotion modes in mammals (see in Table S4.5 the transition pairs allowed in each Directional model). We fitted all six models of discrete character evolution using the function fitMk() in the R package phytools (Revell 2012). We compared all six models using the Akaike Information Criterion (AIC) and Akaike weight, as lowest AIC value with higher weight support best-fit model. We also plotted the Mk models using the function plot.fitMk() to graphically represent the transition rates (q values) using arrows to connect pairs of states that change between one to another.

4.5.6. Mapping shifts in rates of morphological evolution

Finally, we were interested in uncovering the presence of rate shifts during the evolution of body mass and limb morphology. Shifts in the rate of continuous trait evolution were modelled by a Brownian process using a reversible-jump Markov chain Monte Carlo algorithm in BayesTraits v.3 (http://www.evolution.rdg.ac.uk/), allowing rates to vary through time. We conducted this analysis first using the single value of linear transformed body mass and then the limb shape data, the latter using as input the size residual phylogenetic principal components corresponding to 95% of total variation. For each analysis, we ran twenty independent chains with 200,000,000 iterations, sampling every 10,000 iterations and discarding the first 25,000,000 as burn-in. We examined the trace plots from every chain and retained two independent chains that were stationary after burn-in. We checked the effective sample size and the convergence of the chains with a Gelman and Rubin's convergence diagnostic, using the functions effectiveSize() and and gelman.diag() from the R coda package (Table S4.7; Plummer et al., 2006). Results were plotted with the function mytreebybranch() (https://github.com/anjgoswami/salamanders/blob/master/mytreerateplotter.R) and the branch-specific average rate and the posterior probability of rate shifts were summarized from the posterior samples using the rjpp() and plotShift() functions from BTRTools R package (Fabre et al., 2020, 2021).

4.6. References

Amador, L. I., Simmons, N. B., & Giannini, N. P. (2019). Aerodynamic reconstruction of the primitive fossil bat *Onychonycteris finneyi* (Mammalia: Chiroptera). *Biology Letters*, *15*(3). https://doi.org/10.1098/rsbl.2018.0857

Arnold, S. J. (1983). Morphology, performance and fitness. *American Zoologist*, *23*, 347–361. https://doi.org/10.1093/icb/23.2.347

Arnold, S. J., Pfrender, M. E., & Jones, A. G. (2001). The adaptive landscape as a conceptual bridge between micro- and macroevolution. *Genetica*, *112–113*, 9–32. https://doi.org/10.1023/A:1013373907708

Benoit, J., Adnet, S., El Mabrouk, E., Khayati, H., Ben Haj Ali, M., Marivaux, L., Merzeraud, G., Merigeaud, S., Vianey-Liaud, M., & Tabuce, R. (2013). Cranial remain from Tunisia provides new clues for the origin and evolution of Sirenia (Mammalia, Afrotheria) in Africa. *PLoS ONE*, *8*(1). https://doi.org/10.1371/journal.pone.0054307

Biewener, A. A., & Patek, S. N. (2018). *Animal locomotion* (2nd Edition.). Oxford University Press.

Bishop, K. L. (2008). The evolution of flight in bats: narrowing the field of plausible hypothesis. *The Quaternary Review of Biology*, *83*(2), 153–169. https://doi.org/10.1086/587825

Bollback, J. P. (2006). SIMMAP: Stochastic character mapping of discrete traits on phylogenies. *BMC Bioinformatics*, *7*(88), 1–7. https://doi.org/10.1186/1471-2105-7-88

Burgin, C. J., Colella, J. P., Kahn, P. L., & Upham, N. S. (2018). How many species of mammals are there? *Journal of Mammalogy*, *99*(1), 1–14. https://doi.org/10.1093/jmammal/gyx147

Burin, G., Park, T., James, T. D., Slater, G. J., & Cooper, N. (2023). The dynamic adaptive landscape of cetacean body size. *Current Biology*. https://doi.org/10.1016/j.cub.2023.03.014

Burtner, A. E., Grossnickle, D. M., Santana, S. E., & Law, C. J. (2022). Gliding towards an understanding of the origin of flight in bats. *BioRxiv*. https://doi.org/10.1101/2022.09.26.509622

Chen, M., & Wilson, G. P. (2015). A multivariate approach to infer locomotor modes in Mesozoic mammals. *Paleobiology*, *21*(2), 280–312. https://doi.org/10.5061/dryad.870j3

Cheverud, J. M. (1984). Quantitative genetics and developmental constraints on evolution by selection. *Journal of Theoretical Biology*, *110*, 155–171. https://doi.org/10.1016/s0022-5193(84)80050-8

Cheverud, J. M. (1996). Developmental integration and the evolution of pleiotropy. *American Zoologist*, *36*, 44–50. https://doi.org/10.1093/icb/36.1.44

Clavel, J., Aristide, L., & Morlon, H. (2019). A penalized likelihood framework for high-dimensional phylogenetic comparative methods and an application to new-world monkeys brain evolution. *Systematic Biology*, *68*(1), 93–116. https://doi.org/10.1093/sysbio/syy045

Clavel, J., Escarguel, G., & Merceron, G. (2015). mvMORPH: An R package for fitting multivariate evolutionary models to morphometric data. *Methods in Ecology and Evolution*, *6*(11), 1311–1319. https://doi.org/10.1111/2041-210X.12420

Coombs, E. J., Felice, R. N., Clavel, J., Park, T., Bennion, R. F., Churchill, M., Geisler, J. H., Beatty, B., & Goswami, A. (2022). The tempo of cetacean cranial evolution. *Current Biology*, *32*(10), 2233-2247.e4. https://doi.org/10.1016/j.cub.2022.04.060

Cyriac, V. P., & Kodandaramaiah, U. (2018). Digging their own macroevolutionary grave: fossoriality as an evolutionary dead end in snakes. *Journal of Evolutionary Biology*, *31*(4), 587–598. https://doi.org/10.1111/jeb.13248

Day, E. H., Hua, X., & Bromham, L. (2016). Is specialization an evolutionary dead end? Testing for differences in speciation, extinction and trait transition rates across diverse phylogenies of specialists and generalists. *Journal of Evolutionary Biology*, *29*(6), 1257–1267. https://doi.org/10.1111/jeb.12867

DeBlois, M. C., & Motani, R. (2019). Flipper bone distribution reveals flexible trailing edge in underwater flying marine tetrapods. *Journal of Morphology*, *280*(6), 908–924. https://doi.org/10.1002/jmor.20992

Dietrich, M. R., & Skipper Jr, R. A. (2012). A shifting terrain: A brief history of the adaptive landscape. In E. I. Svensson & R. Calsbeek (Eds.), *The adaptive landscape in Evolutionary Biology* (1st ed., pp. 3–14). Oxford University Press.

Fabre, A. C., Bardua, C., Bon, M., Clavel, J., Felice, R. N., Streicher, J. W., Bonnel, J., Stanley, E. L., Blackburn, D. C., & Goswami, A. (2020). Metamorphosis shapes

cranial diversity and rate of evolution in salamanders. *Nature Ecology and Evolution*, *4*(8), 1129–1140. https://doi.org/10.1038/s41559-020-1225-3

Fabre, A. C., Cornette, R., Goswami, A., & Peigné, S. (2015). Do constraints associated with the locomotor habitat drive the evolution of forelimb shape? A case study in musteloid carnivorans. *Journal of Anatomy*, *226*(6), 596–610. https://doi.org/10.1111/joa.12315

Fabre, A. C., Dowling, C., Miguez, R. P., Fernandez, V., Noirault, E., & Goswami, A. (2021). Functional constraints during development limit jaw shape evolution in marsupials. *Proceedings of the Royal Society B: Biological Sciences*, *288*(1949). https://doi.org/10.1098/rspb.2021.0319

Fish, F. E. (1996). Transitions from drag-based to lift-based propulsion in mammalian swimming. *American Zoologist*, *36*(6), 628–641. https://doi.org/10.1093/icb/36.6.628

Friedman, S. T., Price, S. A., & Wainwright, P. C. (2021). The effect of locomotion mode on body shape evolution in teleost fishes. *Integrative Organismal Biology*, *3*(1). https://doi.org/10.1093/iob/obab016

Gatesy, S. M., & Middleton, K. M. (2007). Skeletal adaptations for flight. In B. K. Hall (Ed.), *Fins into limbs: Evolution, development, and transformation* (pp. 269–283). The University of Chicago Press.

Gearty, W., McClain, C. R., & Payne, J. L. (2018). Energetic tradeoffs control the size distribution of aquatic mammals. *Proceedings of the National Academy of Sciences*, *115*(16), 4194–4199. https://doi.org/10.1073/pnas.1712629115

Godoy, P. L., Benson, R. B. J., Bronzati, M., & Butler, R. J. (2019). The multi-peak adaptive landscape of crocodylomorph body size evolution. *BMC Evolutionary Biology*, *19*(1). https://doi.org/10.1186/s12862-019-1466-4

Gomes Rodrigues, H., Šumbera, R., & Hautier, L. (2016). Life in burrows channelled the morphological evolution of the skull in rodents: The case of African mole-rats (Bathyergidae, Rodentia). *Journal of Mammalian Evolution*, *23*(2), 175–189. https://doi.org/10.1007/s10914-015-9305-x

Goswami, A., Noirault, E., Coombs, E. J., Clavel, J., Fabre, A.-C., Halliday, T. J. D., Churchill, M., Curtis, A., Watanabe, A., Simmons, N. B., Beatty, B. L., Geisler, J. H., Fox, D. L., & Felice, R. N. (2022). Attenuated evolution of mammals through the Cenozoic. *Science*, *378*, 377–383. https://doi.org/10.1126/science.abm7525

Gould, S. J. (1970). Dollo on Dollo's Law: Irreversibility and the Status of Evolutionary Laws. *Journal of the History of Biology*, *3*(2), 189–212. https://doi.org/10.1007/BF00137351

Grossnickle, D. M., Chen, M., Wauer, J. G. A., Pevsner, S. K., Weaver, L. N., Meng, Q. J., Liu, D., Zhang, Y. G., & Luo, Z. X. (2020). Incomplete convergence of gliding mammal skeletons. *Evolution*, *74*(12), 2662–2680. https://doi.org/10.1111/evo.14094

Grossnickle, D. M., Smith, S. M., & Wilson, G. P. (2019). Untangling the multiple ecological radiations of early mammals. *Trends in Ecology and Evolution*, *34*(10), 936–949. https://doi.org/10.1016/j.tree.2019.05.008

Hansen, T. F. (1997). Stabilizing selection and the comparative analysis of adaptation. *Evolution*, *51*(5), 1341–1351. https://doi.org/10.1111/j.1558-5646.1997.tb01457.x

Harmon, L. J., Losos, J. B., Jonathan Davies, T., Gillespie, R. G., Gittleman, J. L., Bryan Jennings, W., Kozak, K. H., McPeek, M. A., Moreno-Roark, F., Near, T. J., Purvis, A., Ricklefs, R. E., Schluter, D., Schulte, J. A., Seehausen, O., Sidlauskas, B. L., Torres-Carvajal, O., Weir, J. T., & Mooers, A. T. (2010). Early bursts of body size and shape evolution are rare in comparative data. *Evolution*, *64*(8), 2385–2396. https://doi.org/10.1111/j.1558-5646.2010.01025.x

Hedrick, B. P., Dickson, B. V., Dumont, E. R., & Pierce, S. E. (2020). The evolutionary diversity of locomotor innovation in rodents is not linked to proximal limb morphology. *Scientific Reports*, *10*(1). https://doi.org/10.1038/s41598-019-57144-w

Jones, K. E., Bielby, J., Cardillo, M., Fritz, S. A., O'Dell, J., David, C., Orme, L., Safi, K., Sechrest, W., Boakes, E. H., Carbone, C., Connolly, C., Cutts, M. J., Foster, J. K., Grenyer, R., Habib, M., Plaster, C. A., Price, S. A., Rigby, E. A., … Purvis, A. (2009). PanTHERIA: a species-level database of life history, ecology, and geography of extant and recently extinct mammals. *Ecology*, *90*(9), 2648-undefined. https://doi.org/10.1890/08-1494.1

Jones, K. E., Smaers, J. B., & Goswami, A. (2015). Impact of the terrestrial-aquatic transition on disparity and rates of evolution in the carnivoran skull. *BMC Evolutionary Biology*, *15*(1). https://doi.org/10.1186/s12862-015-0285-5

Kubo, T., Sakamoto, M., Meade, A., & Venditti, C. (2019). Transitions between foot postures are associated with elevated rates of body size evolution in mammals. *Proceedings of the Proceeding of the National Academy of Sciences*, *116*(7), 2618–2623. https://doi.org/10.1073/pnas.1814329116

Lande, R. (1986). The dynamics of peak shifts and the pattern of morphological evolution. *Paleobiology*, *12*(4), 343–354. https://doi.org/10.1017/S0094837300003092

Lewis, P. O. (2001). A likelihood approach to estimating phylogeny from discrete morphological character data. *Systematic Biology*, *50*(6), 913–925. https://doi.org/10.1080/106351501753462876

Lhota, S., Jůnek, T., Bartos, L., & Kuběna, A. A. (2008). Specialized use of two fingers in free-ranging aye-ayes (*Daubentonia madagascariensis*). *American Journal of Primatology*, *70*(8), 786–795. https://doi.org/10.1002/ajp.20548

Mahler, D. L., Ingram, T., Revell, L. J., & Losos, J. B. (2013). Exceptional convergence on the macroevolutionary landscape in island lizard radiations. *Science*, *341*(6143), 292–295. https://doi.org/10.1126/science.1239431

Mongiardino Koch, N. (2021). Exploring adaptive landscapes across deep time: A case study using echinoid body size. *Evolution*, *75*(6), 1567–1581. https://doi.org/10.1111/evo.14219

Montoya-Sanhueza, G., Šaffa, G., Šumbera, R., Chinsamy, A., Jarvis, J. U. M., & Bennett, N. C. (2022). Fossorial adaptations in African mole-rats (Bathyergidae) and the unique appendicular phenotype of naked mole-rats. *Communications Biology*, *5*(1). https://doi.org/10.1038/s42003-022-03480-z

Navas, C. A., Antoniazzi, M. M., Carvalho, J. E., Chaui-Berlink, J. G., James, R. S., Jared, C., Kohlsdorf, T., Pai-Silva, M. D., & Wilson, R. S. (2004). Morphological and physiological specialization for digging in amphisbaenians, an ancient lineage of fossorial vertebrates. *Journal of Experimental Biology*, *207*(14), 2433–2441. https://doi.org/10.1242/jeb.01041

Nowak, R. M. (1999). *Walker's mammals of the world*. Johns Hopkins University Press.

Plummer, M., Best, N., Cowles, K., & Vines, K. (2006). CODA: Convergence Diagnosis and Output Analysis for MCMC. *R News*, *6*(1), 7–11. http://CRAN.

Polly, D. (2007). Limbs in mammalian evolution. In B. K. Hall (Ed.), *Fins into limbs: Evolution, development, and transformation* (pp. 245–268). The University of Chicago Press.

Price, S. A., & Hopkins, S. S. B. (2015). The macroevolutionary relationship between diet and body mass across mammals. *Biological Journal of the Linnean Society*, *115*, 173–184.

Pyenson, N. D. (2017). The ecological rise of whales chronicled by the fossil record. *Current Biology*, *27*(11), R558–R564. https://doi.org/10.1016/j.cub.2017.05.001

Pyenson, N. D., & Vermeij, G. J. (2016). The rise of ocean giants: Maximum body size in Cenozoic marine mammals as an indicator for productivity in the Pacific and Atlantic oceans. *Biology Letters*, *12*(7). https://doi.org/10.1098/rsbl.2016.0186

Rayner, J. M. V. (1988). The evolution of vertebrate flight. *Biological Journal of the Linnean Society*, *34*(3), 269–287. https://doi.org/10.1111/j.1095-8312.1988.tb01963.x

R Core Team. (2022). *R: A language and environment for statistical computing. R Foundation for Statistical Computing*. URL https://www.R-project.org/.

Revell, L. J. (2012). phytools: An R package for phylogenetic comparative biology (and other things). *Methods in Ecology and Evolution*, *3*(2), 217–223. https://doi.org/10.1111/j.2041-210X.2011.00169.x

Revell, L. J., & Harmon, L. J. (2022). *Phylogenetic comparative methods in R*. Princeton University Press.

Rothier, P. S., Fabre, A. C., Clavel, J., Benson, R. B. J., & Herrel, A. (2023). Mammalian forelimb evolution is driven by uneven proximal-to-distal morphological diversity. *ELife*, *12*. https://doi.org/10.7554/eLife.81492

Rybczynski, N., Dawson, M. R., & Tedford, R. H. (2009). A semi-aquatic Arctic mammalian carnivore from the Miocene epoch and origin of Pinnipedia. *Nature*, *458*(7241), 1021–1024. https://doi.org/10.1038/nature07985

Samuels, J. X., & Van Valkenburgh, B. (2008). Skeletal indicators of locomotor adaptations in living and extinct rodents. *Journal of Morphology*, *269*(11), 1387–1411. https://doi.org/10.1002/jmor.10662

Sansalone, G., Castiglione, S., Raia, P., Archer, M., Dickson, B., Hand, S., Piras, P., Profico, A., & Wroe, S. (2020). Decoupling functional and morphological convergence, the study case of fossorial Mammalia. *Frontiers in Earth Science*, *8*. https://doi.org/10.3389/feart.2020.00112

Schliep, K. P. (2011). phangorn: Phylogenetic analysis in R. *Bioinformatics*, *27*(4), 592–593. https://doi.org/10.1093/bioinformatics/btq706

Sears, K., Behringer, R. R., Rasweiler, J. J., & Niswander, L. A. (2007). The evolutionary and developmental basis of parallel reduction in mammalian zeugopod elements. *The American Naturalist*, *169*(1), 105–117. https://doi.org/10.1086/510259

Simpson, G. G. (1944). *Tempo and mode in evolution*. Columbia University Press.

Van Valkenburgh, B. (1987). Skeletal indicators of locomotor behavior in living and extinct carnivores. *Journal of Vertebrate Paleontology*, *7*(2), 162–182. https://doi.org/10.1080/02724634.1987.10011651

Weaver, L. N., & Grossnickle, D. M. (2020). Functional diversity of small-mammal postcrania is linked to both substrate preference and body size. *Current Zoology*, *66*(5), 539–553. https://doi.org/10.1093/cz/zoaa057

Wright, S. (1932). The roles of mutation, inbreeding, crossbreeding and selection in evolution. *Proceedings of the Sixth Annual Congress of Genetics*, 356–366.

Zelová, J., Šumbera, R., Okrouhlík, J., & Burda, H. (2010). Cost of digging is determined by intrinsic factors rather than by substrate quality in two subterranean rodent species. *Physiology and Behavior*, *99*(1), 54–58. https://doi.org/10.1016/j.physbeh.2009.10.007

« Je ne suis sûr d'absolument rien, nous ne sommes pas mis au monde pour être sûrs. »

— Romain Gary

5.
General discussion & conclusion

The limb is a remarkable structure for investigating the drivers of trait evolution, given its essential role during the occupation of novel habitats (Hall, 2007; Shubin, 2002). Particularly, the extraordinary variation of the forelimb in mammals has long inspired evolutionary biologists to seek for the developmental and functional patterns underlying the morphological diversification of this structure. The main goal of this thesis was to unravel the evolution of the morphological diversity of the fore arm in Mammalia, identifying the presence of major intrinsic and extrinsic evolutionary drivers, such as developmental timing and habitat use, respectively, underlying phenotypic diversification. I addressed these questions using an unprecedent dataset that comprises more than 800 living and recently extinct mammal species. The novel and insightful findings presented in this thesis on the clade-level diversity of Mammalia significantly advance our understanding of the macroevolutionary patterns underlying trait diversification and shed light on how limb structures have evolved among clades and ecologies. In the subsequent sessions, I present an overview of the main findings and their contributions to the field of comparative biology. I also present new results that link the last three chapters and raise new questions on the evolutionary drivers for limb diversification in Mammalia.

5.1 Variation between traits and between groups: linking intrinsic to extrinsic constrains

In this thesis I presented that the evolution of limb diversity is uneven at two levels of observation: between limb traits and between taxa. I showed in Ch. 2 that developmental timing is a strong predictor of the macroevolutionary outcome of trait diversity, in which a pattern of an increase in proximal to distal bone variation corresponds to the sequence

of evolutionary appearance and of developmental condensation. Although previous studies have noticed a meristic pattern of uneven variation between limb regions with the most notable divergence being observed in the late-forming autopod (Holder, 1983), this is the first time that this premise has been formally tested using continuous morphometric data in mammals. This pattern represents a general and widespread trend governing the mammalian limb evolution, which is endorsed by the exhaustive taxonomic coverage provided in this work. However, such proximal to distal gradient is not clearly evidenced for parameters such as within element integration and rates of morphological evolution, suggesting that factors other than the timing of development, such as function, likewise contribute to the mosaic evolution of skeletal limb elements.

In order to investigate the strength of functional associations with limb variation, in the subsequent two chapters I explored the patterns and processes driving the forearm morphology across different groups, defined by ecological criteria. Separating species into ecological categories revealed the impact of ecology on trait diversity, with aquatic taxa presenting the most disparate limb and bone shapes compared to any other group, and the flying bats encompassing the least disparate forms. Furthermore, evolutionary models indicated a strong support for adaptive evolution of limb morphology linked to the interface of locomotor mode and habitat use.

To better understand whether the above patters hold on a clade-wise basis, I replicated the analyses described in Ch. 2, but this time using an expanded dataset of 837 species. I first compared Marsupials and super ordinal placental groups (Fig. 5.1) and then examined such patterns across some of the most diverse placental orders (Fig. 5.2). Monotremes were not included because of they are solely represented by three species, providing results with low statistical power.

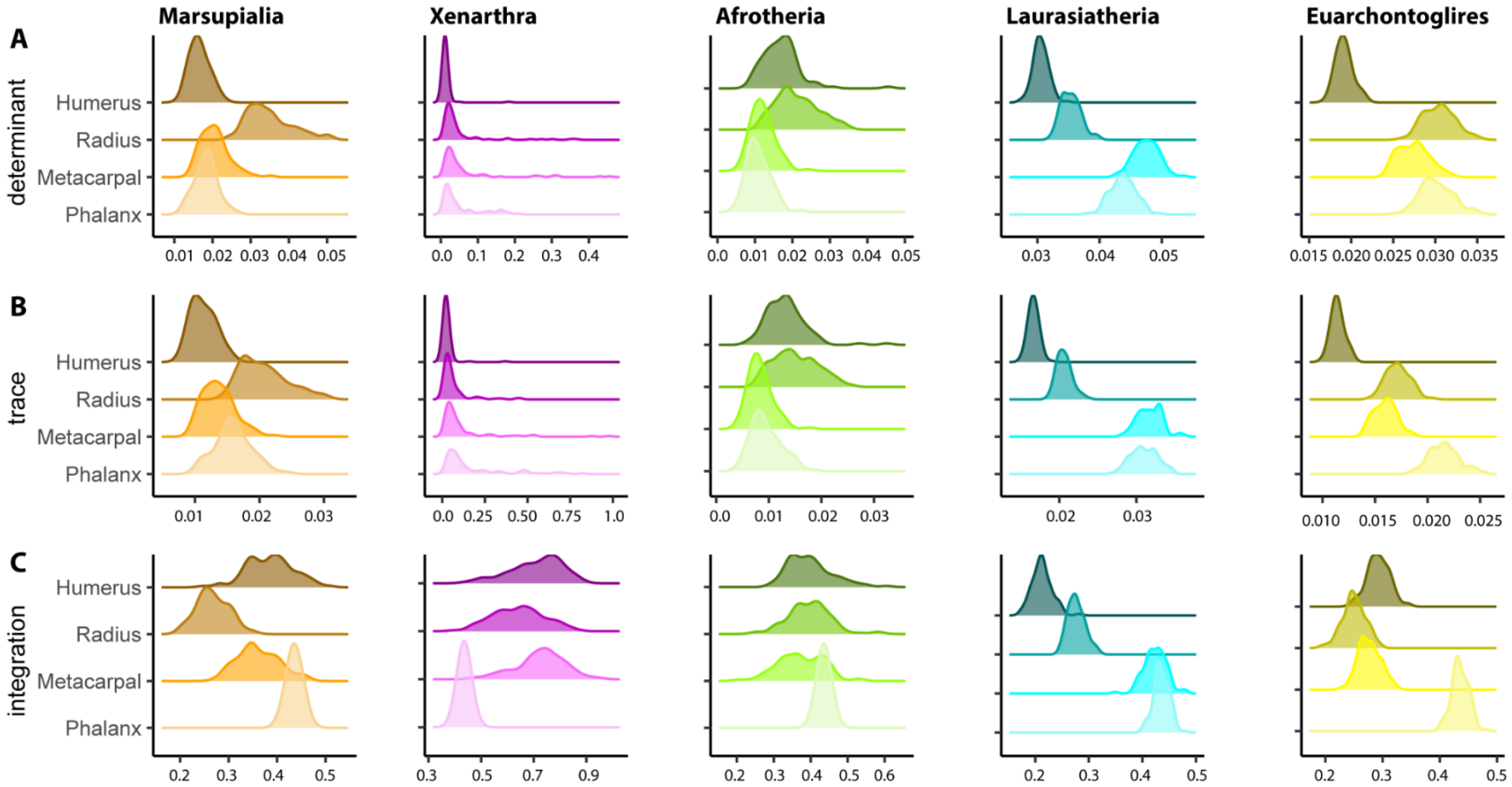

Figure 5.1. Forelimb bone variation across super ordinal mammalian groups. A) Morphological diversity calculated from matrix determinant (multiplicated by 100 to facilitate interpretation); **B)** Morphological diversity calculated from matrix trace (multiplicated by 10 to facilitate interpretation); **C)** integration inferred from eigenvalue dispersion.

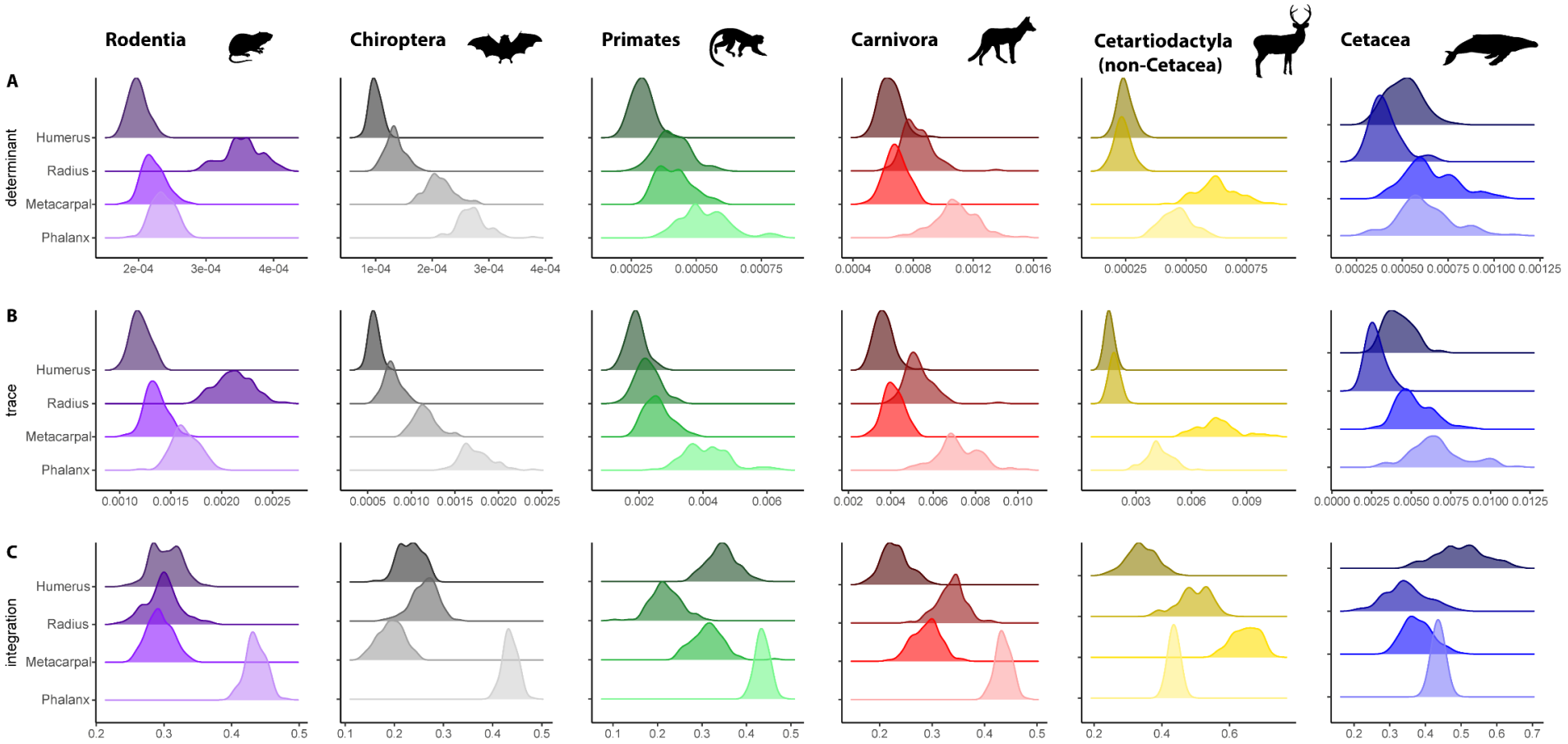

Figure 5.2. Forelimb bone variation across the most specious placental orders. A) Morphological diversity calculated from matrix determinant; **B)** Morphological diversity calculated from matrix trace; **C)** integration inferred from eigenvalue dispersion.

Surprisingly, the pattern of proximal to distal increasing limb trait diversity was not observed for several mammalian clades, being only recovered for Chiroptera and Primates. The humerus was, however, most often the least diverse structure across subclades in accordance to the patterns detected among the whole Mammalia radiation, except within Afrotheria and Cetacea (Fig. 5.1-5.2). The structure of integration is also variable between groups, but, similar to the findings reported in Ch. 2, the phalanx is the most integrated structure for the majority of mammalian taxa (except for xenarthrans and cetartiodactyls). These findings complement the results published from Ch. 2 (Rothier et al., 2023), indicating that while developmental timing predicts variation across the whole Mammalia radiation, a closer examination of different mammal subgroups reveals that ontogenetic sequence alone cannot explain the within limb variation. Further investigation into the developmental diversity of these groups (e.g., accounting for heterochrony and developmental modes, such as altriciality and precociality, see Fabre et al., 2021 and White et al., 2023), along with a more detailed analysis of the ecological and functional diversity among these clades, may provide additional insights to explain the uneven variation and evolution of limb morphology.

I then compared the forelimb morphological disparity among major mammalian clades, employing the analysis described in Ch. 3. Since my main focus here was to understand the variation in forelimb shape – and not overall size – between ecological groups, I used size residual values to calculate disparity of the overall forelimb form and then of each bone (analysis detailed in Ch. 3).

Marsupials, i.e., living Metatheria, are much less disparate than placentals (living Eutheria; Fig 5.3). These results recover the findings from previous works, which demonstrated that marsupials exhibit less morphological diversity in the forelimbs when compared to placentals (Cooper & Steppan, 2010; Pevsner et al., 2022). Different from

placentals such as whales and bats, marsupials have never evolved fully aquatic life-styles or active flight, respectively. Developmental constraints have been long attributed as an explanation to the lower morphological diversity in metatherians. Specifically, marsupials are born without being fully developed and need to move from the uterus to the mother's teat using their forelimbs (Gemmel et al., 2002). However, marsupials also had less biogeographical opportunity to diversify into as many ecological niches as placentals (Sánchez-Villagra, 2013). Developmental constraints, ecological limitations, or both in combination therefore are believed to have restricted not only the morphological diversity of the forelimbs of marsupials, but also of their skulls and the jaws (Bennett and Goswami, 2013; Cooper and Steppan, 2010; Fabre et al., 2021; Pevsner et al., 2022; Sánchez-Villagra, 2013; Sears, 2004).

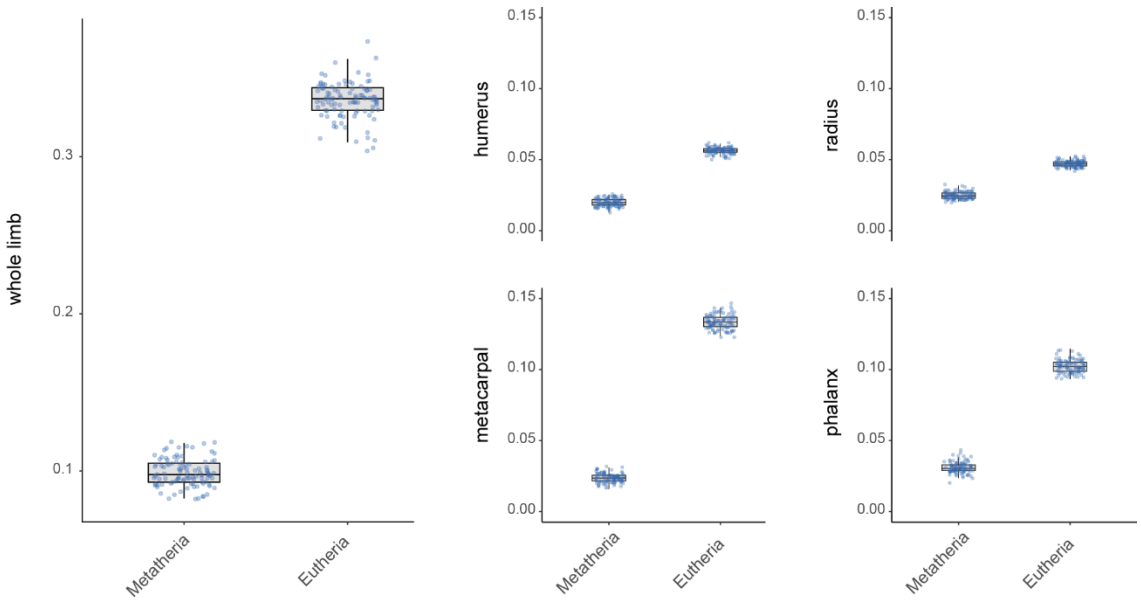

Figure 5.3. Morphological limb shape disparity in Eutheria and Metatheria. Left panel shows disparity of the whole limb morphology, intermediate and right panels indicate variation of the different forelimb bones.

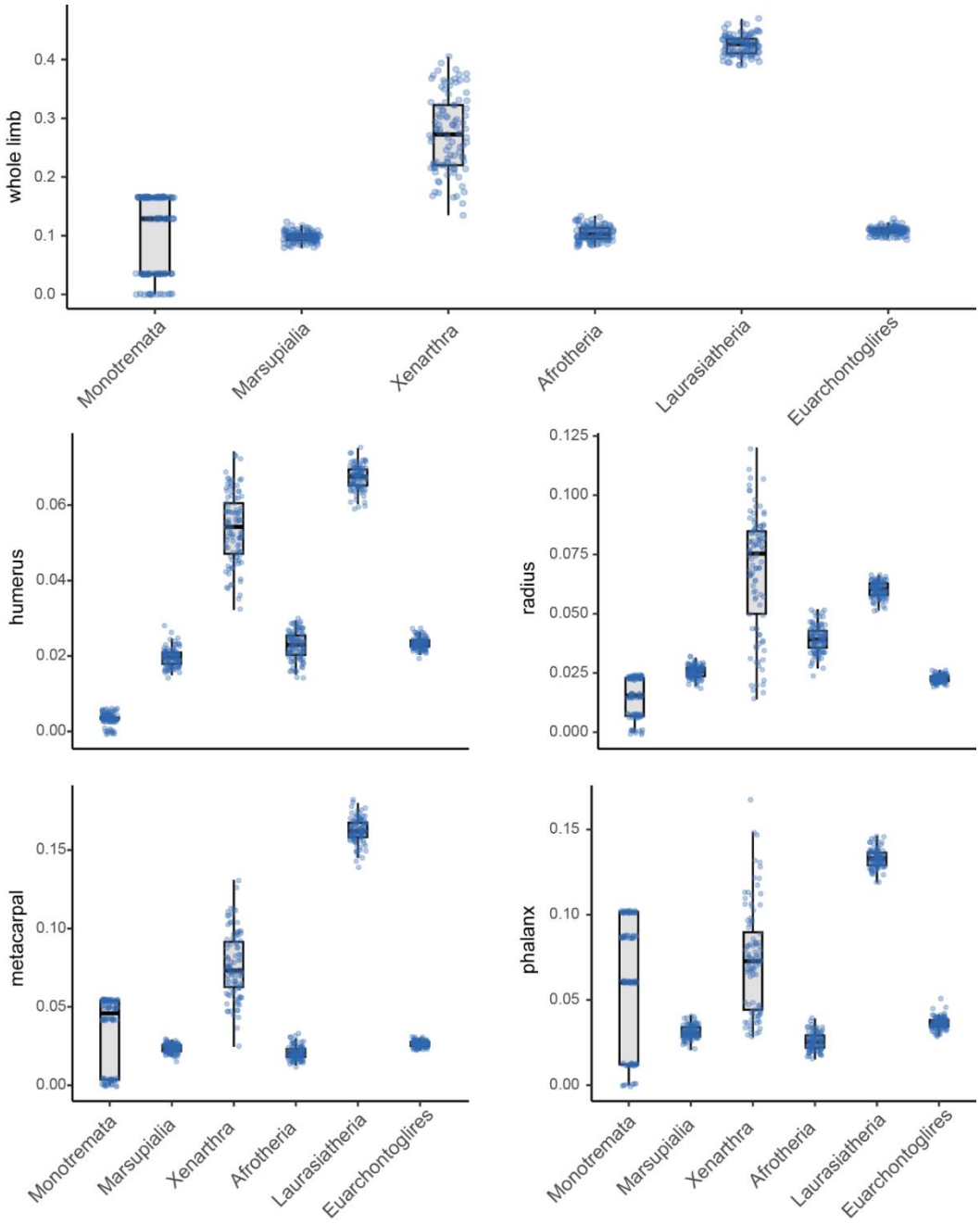

Figure 5.4. Morphological disparity between mammalian clades. Upper panel shows disparity of the whole limb morphology, and intermediate and lower panels indicate variation of the different forelimb bones.

Among placentals, Laurasiatherians exhibited the most disparate forelimbs, a pattern recovered for all bones but the radius, for which the highest disparity is observed

in Xenarthra (Fig 5.4). Xenarthrans also consistently demonstrated a substantial high level of disparity, often ranking as the second most disparate group. Among the most specious placental orders, the order Eulipothyphla displays the most disparate limb morphologies (Fig 5.5), followed by Cetacea. Cetaceans also display the most disparate radius and phalanx. The lowest limb disparity is detected among hares and rabbits (Lagomorpha), with bats representing the second lowest overall variation.

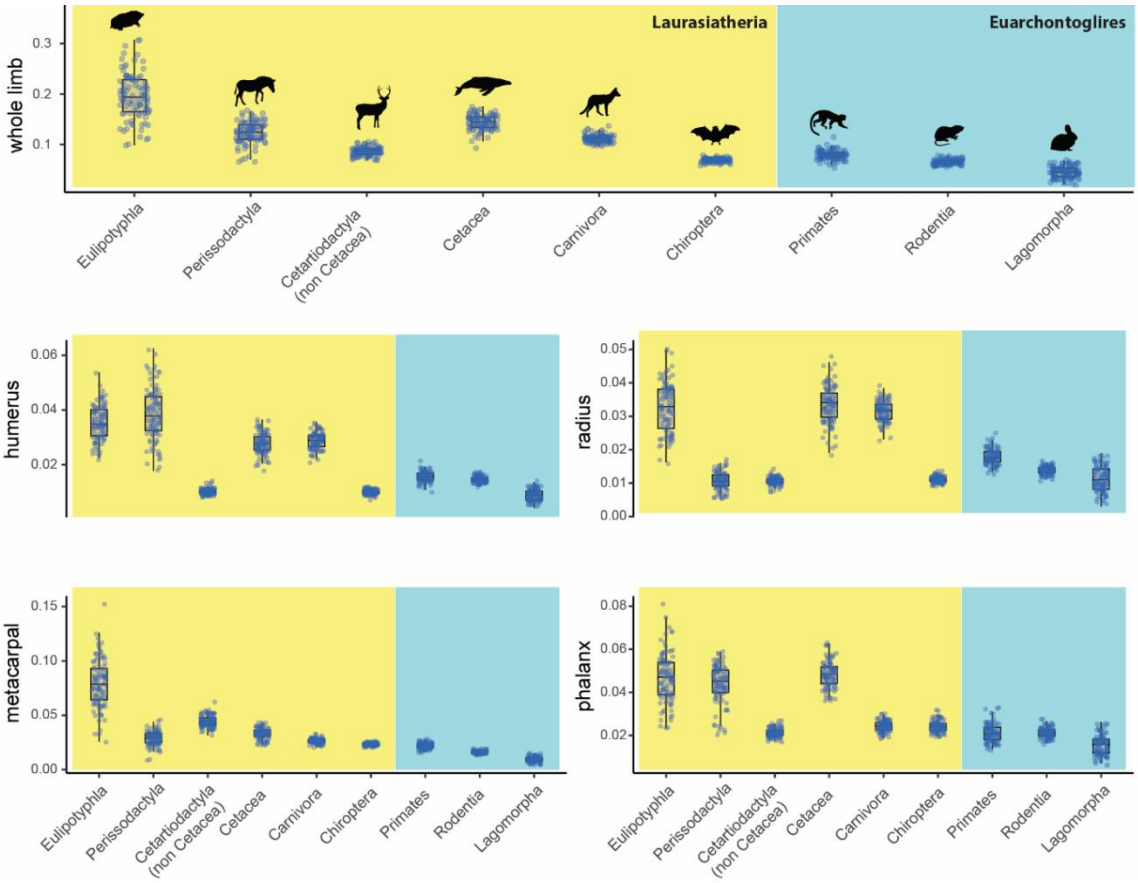

Figure 5.5. Morphological disparity between major Boreoeutheria orders. Upper panel shows disparity of the whole limb morphology, and intermediate and lower panels indicate variation of the different forelimb bones.

Morphological diversity among afrotherians ranges from small tenrecs to giant elephants, so it would be expected to detect a high degree of phenotypic disparity in their forelimb shape. Surprisingly, I did not find an elevated disparity in the afrotherian forelimb (Fig 5.4). It is important to highlight that although I had access to morphological data for the afrotherian family of African moles (Chrysochloridae), I excluded them from the analyses due to their reduced phalangeal formula in which the third digit only bears a single robust ungual phalanx. Such distinct morphology prevented the acquisition of the morphometric distances applied for typically proximal phalanges. Therefore, further examination of disparity between groups, including Chrysochloridae, should be considered to obtain a more comprehensive understanding of disparity across Afrotheria.

Next, I compared the arm shape disparity between the locomotor ecologies previously described in Ch. 4. The results are consistent with those obtained in Ch. 3, indicating that aquatic mammals display the highest level of disparity in limb shape, and the flyers the lowest (Fig 5.6). It is important to emphasize, however, that the low disparity in flying animals is detected with also low statistical power since this group solely corresponds to the monophyletic order Chiroptera. This more detailed classification across terrestrial-based modes of locomotion revealed that fossorial mammals also exhibit high disparity. These findings complement previous results and suggest that, although shown in Ch. 4 that the model of adaptive landscape best predicts the patterns of morphological evolution of the forelimb, each adaptive optimum "allows" for a different degree of variation. Particularly, the adaptive evolution towards aquatic and fossorial lifestyles is likely less constrained and therefore permits greater limb shape diversity than, for example, arboreality. Although multivariate methods allowing for the estimation of more complex adaptive models already exist (for example, allowing for evolutionary rates and peak attraction to vary between regimes, see Clavel et al., 2015),

they demand high computational power to estimate such parameters in large datasets, meaning that they are not yet easily implemented for the dataset examined in this thesis. Hopefully, the advances in phylogenetic comparative methods to estimate morphological evolution may in the near future enable more refined analyses and more realistic interpretation of the evolutionary patterns of the limb diversification in mammals.

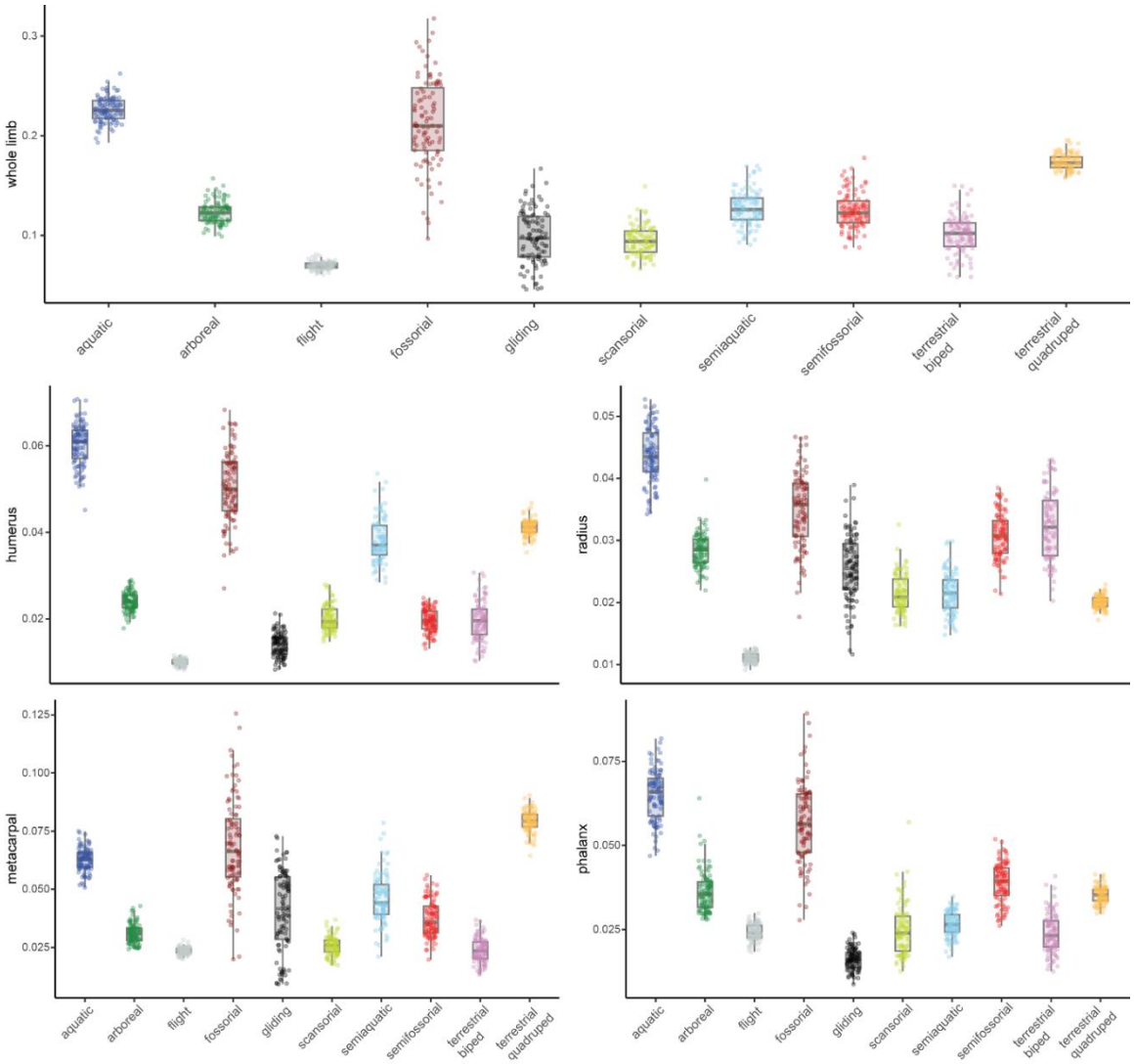

Figure 5.6. Morphological disparity between ecologies. Upper panel shows disparity of the whole limb morphology, and intermediate and lower panels indicate variation of the different forelimb bones.

5.2 Major contributions and future directions

One of the major contributions of this thesis is the unique and comprehensive dataset on forearm morphology, fully capturing extant mammalian diversity. Although previous studies have significantly contributed to understanding the patterns of limb variation in mammals, they have done so by investigating at lower taxonomic levels, such as in carnivores (Fabre et al., 2015; Van Valkenburgh, 1987) and rodents (Samuels & Van Valkenburgh, 2008), or excluding medium to large-sized species (Chen & Wilson, 2015; Janis & Martín-Serra, 2020; Weaver & Grossnickle, 2020). The findings in this thesis significantly improve the current knowledge on mammalian forelimb evolution, while paving the road for a more extensive investigation of phenotypic diversification in tetrapods over the deep time. It is essential to note that, like any other work, data collection and methods employed here have certain limitations that require further attention. I discuss some of these limitations below and propose potential future directions derived from the findings presented by the thesis.

5.1.1 Morphological and taxonomic sample

Studying exclusively living taxa may hide the underlying phenotypic diversity that structures the tree of life, thus biasing biological interpretation. Therefore, including fossils may improve the resolution of the estimated evolutionary rates (see Burin et al., 2023; Slater, 2013), and may provide insights on the patterns of limb transformation during ecological transitions. Because limb morphology was here estimated with two-dimensional data, the same metrics may be applied to many fossils, facilitating the understanding of mammalian forelimb transformation from deep time to modern forms.

Moreover, the morphological distances examined here can be replicated to the limbs of not only extinct mammals, but in other tetrapod groups. Our study revealed that aquatic mammals have relatively small limbs (Ch. 3), a trend that has also been reported for aquatic frogs and salamanders (Ledbetter & Bonett, 2019; Stepanova & Womack, 2020). However, while in mammals the forearm morphology evolved at the fastest rates across aquatic lineages (Ch. 4), a similar pattern was only observed for salamanders and not for frogs. Since all three studies, including ours, used different methods to quantify various aspects of limb morphology (Stepanova & Womack, 2020 used geometric morphometrics but excluded the autopod, and Ledbetter & Bonett, 2019 combined limb length distance to digit number), it is necessary to standardize a protocol for data acquisition to properly compare limb evolution across these different groups. By standardizing such a dataset, researchers would be able to determine whether certain evolutionary patterns that structure limb evolution are unique to mammals or follow a generalized trend of developmental and functional constraints shared across Tetrapoda.

The use of linear measurements has been proven to be a fast and effective method for quantifying the global morphological diversity of limb skeleton across the mammalian tree of life. However, this approach presents some limitations in capturing detailed local shape variation. To obtain a more comprehensive analysis of form, geometric morphometrics may offer additional insights that 2D data fails to account for. Geometric morphometrics, for example, may reveal details in articulation joints that differ considerably among groups and modes of locomotion (Arias-Martorell, 2019; Fabre et al., 2015, 2019; Veeger & van der Helm, 2007), and capture refined aspects of shape variation in ungual phalanges. For instance, while ungulates possess short and flat distal phalanges that bear hooves, sloths and anteaters possess long and curved ungual phalanges that similarly support long-curled claws (Hamrick, 2001). Utilizing length

alone, as employed in this thesis, overlooks the substantial shape disparity in this structure across lineages, which could serve as an indicator of functional specialization (Baeckens et al., 2020; Zani, 2000). Therefore, combining geometric morphometrics with the present dataset would be beneficial for future studies in order to provide a more comprehensive understanding of shape variation in limb elements at an evolutionary macroscale.

As discussed in Ch. 2, having the zeugopod solely represented by the radius might as well have obscured some of the diversity present in the intermediate limb segment. The ulna is highly variable, and its olecranon is particularly a strong indication of locomotor modes (Chen & Wilson, 2015; Lungmus & Angielczyk, 2021; Milne & Granatosky, 2021; Samuels & Van Valkenburgh, 2008; Van Valkenburgh, 1987), which, as already mentioned, was not included here due to difficulty for assessing the same topological distances captured for the other bones. Likewise, variation between digits such as reduction in phalangeal formula and digit loss, can certainly provide additional insights on the role of ecological specialization in the evolution of the autopod, as well as the associations between meristic composition with skeletal shape. Future research interested in understanding the overall pattern of limb evolution would definitely benefit from including the ulna and the phalangeal formula for a deeper understanding of the transformations involving the mammalian forelimb.

5.1.2 Morphological evolution and lineage diversification

Establishing a direct link between morphological rates and lineage diversification is not always straightforward. For example, the rate of body size evolution is positively correlated with of rates of species diversification across ray-finned fishes (Rabosky et al., 2013), but not across birds (Crouch & Ricklefs, 2019). Therefore, speciation may be

promoted either by trait divergence (fast rates of morphological evolution) and by trait conservatism (slow rates of morphological evolution; Barreto et al., 2023).

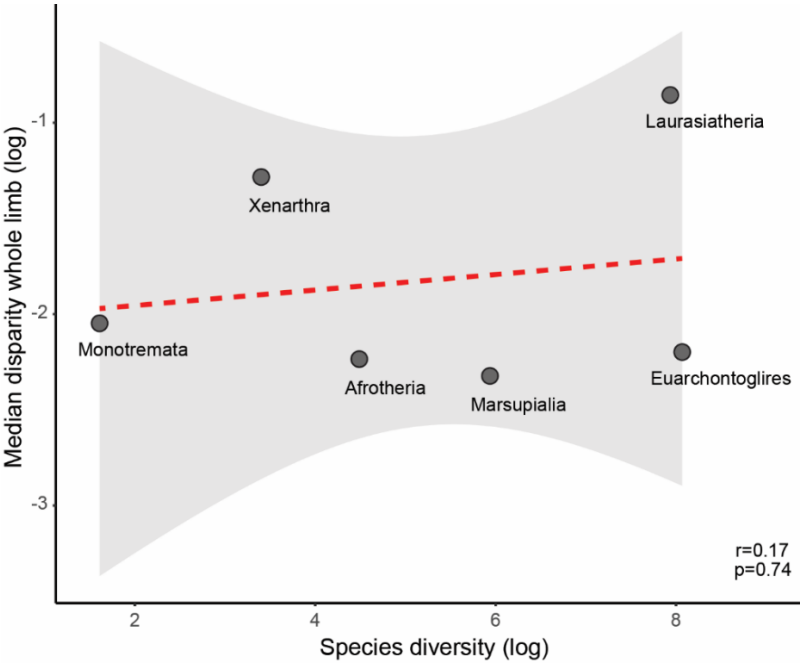

Figure 5.7. Taxonomic diversity and mean limb disparity across mammal clades. Person correlation (r) and p-value (p) are indicated in the bottom left.

The limb phenotypic diversity is often suggested as playing a crucial role in mammalian diversification (Polly, 2007; Shubin & Davis, 2004), but these associations have been never formally tested. Particularly, findings from Ch. 4 do not suggest a positive relationship between the morphological evolution of limbs and lineage diversification. For example, despite the remarkable taxonomic diversity of bats and rodents, the methods employed here did not identify increased rate shifts of forelimb evolution, nor disparity (Fig 4.6 and 5.5). A simple correlation test evaluating clade diversity (inferred by species number) and forelimb disparity (previously calculated in

session 5.1 of this chapter) demonstrates that these two features have a weak association (Fig. 5.7), showing that, overall, the morphological variation of the forelimb is independent of taxonomic diversity. Formal tests are required to confirm the validity of these observation and further explore the particularities of the interplay of the rates of morphological evolution and species diversification in mammals (see Alencar et al., 2017; Gillet et al., 2019).

5.1.3. The genomic revolution

A novel genomic dataset of protein-coding alignment of 427 mammals and whole aligned genomes of 240 placental species – the Zoonomia Consortium (Christmas et al., 2023; Zoonomia Consortium, 2020) – has recently improved our understanding of mammalian evolution. This large-scale genomic assessment provides a valuable opportunity to investigate how mammals have adapted to various niches and to identify the genomic basis for the evolution of phenotypic innovation. With Zoonomia's unprecedented database, Christmas et al. (2023) were able to pinpoint the genomic elements that underlie exceptional mammalian traits, including olfaction, hibernation, brain size, and vocal learning. The use of genomic data is certainly stimulating for better understanding the evolutionary patterns of limb transformation, as well as to uncover the genetic basis leading to functional similarity observed in convergent patterns of locomotor modes. As Tomas S. Kemp (2005) predicted in his textbook on mammal evolution two decades ago, these are indeed exciting times to be a mammologist.

5.3 Conclusion

Through the examination of limb evolution within a diverse taxonomic group characterized by disparate morphologies, sizes, ecologies and evolutionary histories, this thesis explored the influences of selection and constraint in the evolution of the mammalian forelimb. With an unparalleled dataset comprising over 800 extant mammal species, this thesis demonstrates the importance of considering variation related to development and function to understand the macroevolutionary outcome of adult morphologies. The key findings of the thesis revealed that variation between limb traits and between clades is uneven and influenced to varying degrees by ecological specialization. Specifically, the timing of bone condensation was found to predict skeletal diversity throughout the Mammalia, although additional analyses show that this pattern is not fully observed at lower taxonomic levels. These findings highlight the need for further investigation into patterns of diversity between traits across different taxonomic and ecological groups. Furthermore, the results revealed that leaving terrestrial substrates contributed to the diversification of mammalian limb forms in previously unexplored regions of morphospace. While specialization in homogenous and continuous media (i.e. fluids) constrained the disparity of absolute forelimb size, these substrates may either favour or constrain limb shape variation, with locomotion in water promoting disparity and locomotion in air limiting such variation. This work also showed that mammalian forelimb morphology is better explained by a model of multipeak adaptive landscape defined by locomotor ecologies. Terrestrial locomotor ecologies exhibit nearby optima, while highly specialized locomotion in fluids, such as water and air as well as underground (fossoriality) drive the most extreme morphologies explained with isolated adaptive optima. These findings indicate that shifts towards such locomotor specializations are rare and possibly irreversible. Overall, this thesis contributes to our

understanding of mammalian morphology and provides a framework for addressing broader questions regarding limb evolution in tetrapods. The findings here reported paves the way for future studies to integrate fossil and genetic data and provide a more comprehensive perspective on the macroevolutionary patterns underlying the phenotypic diversification of mammals.

5.4 References

Alencar, L. R. V., Martins, M., Burin, G., & Quental, T. B. (2017). Arboreality constrains morphological evolution but not species diversification in vipers. *Proceedings of the Royal Society B: Biological Sciences*, *284*(1869), 20171775. https://doi.org/10.1098/rspb.2017.1775

Arias-Martorell, J. (2019). The morphology and evolutionary history of the glenohumeral joint of hominoids: A review. *Ecology and Evolution*, 9(1), 703–722. https://doi.org/10.1002/ece3.4392

Baeckens, S., Goeyers, C., & van Damme, R. (2020). Convergent evolution of claw shape in a transcontinental lizard radiation. *Integrative and Comparative Biology*, *60*(1), 10–23. https://doi.org/10.1093/icb/icz151

Barreto, E., Lim, M. C. W., Rojas, D., Dávalos, L. M., Wüest, R. O., Machac, A., & Graham, C. H. (2023). Morphology and niche evolution influence hummingbird speciation rates. *Proceedings of the Royal Society B: Biological Sciences*, *290*(1997), 20221793. https://doi.org/10.1098/rspb.2022.1793

Bennett, C. V., & Goswami, A. (2013). Statistical support for the hypothesis of developmental constraint in marsupial skull evolution. *BMC Biology*, *11*(1), 1–14. https://doi.org/10.1186/1741-7007-11-52

Burin, G., Park, T., James, T. D., Slater, G. J., & Cooper, N. (2023). The dynamic adaptive landscape of cetacean body size. *Current Biology*. https://doi.org/10.1016/j.cub.2023.03.014

Chen, M., & Wilson, G. P. (2015). A multivariate approach to infer locomotor modes in Mesozoic mammals. *Paleobiology*, *21*(2), 280–312. https://doi.org/10.5061/dryad.870j3

Christmas, M. J., Kaplow, I. M., Genereux, D. P., Dong, M. X., Hughes, G. M., Li, X., Sullivan, P. F., Hindle, A. G., Andrews, G., Armstrong, J. C., Bianchi, M., Breit, A. M., Diekhans, M., Fanter, C., Foley, N. M., Goodman, D. B., Goodman, L., Keough, K. C., Kirilenko, B., … Zhang, X. (2023). Evolutionary constraint and innovation across hundreds of placental mammals. *Science*, *380*(6643). https://doi.org/10.1126/science.abn3943

Clavel, J., Escarguel, G., & Merceron, G. (2015). mvMORPH: An R package for fitting multivariate evolutionary models to morphometric data. *Methods in Ecology and Evolution*, *6*(11), 1311–1319. https://doi.org/10.1111/2041-210X.12420

Cooper, W. J., & Steppan, S. J. (2010). Developmental constraint on the evolution of marsupial forelimb morphology. *Australian Journal of Zoology*, *58*(1), 1–15. https://doi.org/10.1071/ZO09102

Crouch, N. M. A., & Ricklefs, R. E. (2019). Speciation rate is independent of the rate of evolution of morphological size, shape, and absolute morphological specialization in a large clade of birds. *American Naturalist*, *193*(4), E78–E91. https://doi.org/10.5061/dryad.8fq4mf6

Fabre, A.-C., Cornette, R., Goswami, A., & Peigné, S. (2015). Do constraints associated with the locomotor habitat drive the evolution of forelimb shape? A case study in musteloid carnivorans. *Journal of Anatomy*, *226*(6), 596–610. https://doi.org/10.1111/joa.12315

Fabre, A.-C., Dowling, C., Miguez, R. P., Fernandez, V., Noirault, E., & Goswami, A. (2021). Functional constraints during development limit jaw shape evolution in marsupials. *Proceedings of the Royal Society B: Biological Sciences*, *288*(1949). https://doi.org/10.1098/rspb.2021.0319

Fabre, A.-C., Peckre, L., Pouydebat, E., & Wall, C. E. (2019). Does the shape of forelimb long bones co-vary with grasping behaviour in strepsirrhine primates? In *Biological Journal of the Linnean Society* (Vol. 127). https://lemur.duke.edu/discover/

Gemmel, R. T., Veitch, C., & Nelso, J. (2002). Birth in marsupials. *Comparative Biochemistry and Physiology Part B*, *131*(4), 621–650. https://doi.org/10.1016/S1096-4959(02)00016-7

Gillet, A., Frédérich, B., & Parmentier, E. (2019). Divergent evolutionary morphology of the axial skeleton as a potential key innovation in modern cetaceans. *Proceedings of the Royal Society B: Biological Sciences*, *286*(1916). https://doi.org/10.1098/rspb.2019.1771

Hall, B. K. (2007). *Fins into Limbs: Evolution, Development, and Transformation*.

Hamrick, M. W. (2001). Development and evolution of the mammalian limb: adaptive diversification of nails, hooves, and claws. *Evolution & Development*, *3*(5), 355–363. https://doi.org/10.1046/j.1525-142x.2001.01032.x

Holder, N. (1983). Developmental constraints and the evolution of vertebrate digit patterns. *Journal of Theoretical Biology*, *104*, 451–471. https://doi.org/10.1016/0022-5193(83)90117-0

Janis, C. M., & Martín-Serra, A. (2020). Postcranial elements of small mammals as indicators of locomotion and habitat. *PeerJ*, *8*. https://doi.org/10.7717/peerj.9634

Kemp, T. S. (2005). *The origin and evolution of mammals*. Oxford University Press.

Ledbetter, N. M., & Bonett, R. M. (2019). Terrestriality constrains salamander limb diversification: Implications for the evolution of pentadactyly. *Journal of Evolutionary Biology*, *32*(7), 642–652. https://doi.org/10.1111/jeb.13444

Lungmus, J. K., & Angielczyk, K. D. (2021). Phylogeny, function and ecology in the deep evolutionary history of the mammalian forelimb. *Proceedings of the Royal Society B: Biological Sciences*, *288*(1949), 202104942. https://doi.org/10.1098/rspb.2021.0494

Milne, N., & Granatosky, M. C. (2021). Ulna curvature in arboreal and terrestrial primates. *Journal of Mammalian Evolution*, *28*(3), 897–909. https://doi.org/10.1007/s10914-021-09566-5

Pevsner, S. K., Grossnickle, D. M., & Luo, Z.-X. (2022). The functional diversity of marsupial limbs is influenced by both ecology and developmental constraint. *Biological Journal of the Linnean Society*, *135*, 569–585. www.phylopic.

Polly, D. (2007). Limbs in mammalian evolution. In B. K. Hall (Ed.), *Fins into limbs: Evolution, development, and transformation* (pp. 245–268). The University of Chicago Press.

Rabosky, D. L., Santini, F., Eastman, J., Smith, S. A., Sidlauskas, B., Chang, J., & Alfaro, M. E. (2013). Rates of speciation and morphological evolution are correlated across the largest vertebrate radiation. *Nature Communications*, *4*, 1–8. https://doi.org/10.1038/ncomms2958

Rothier, P. S., Fabre, A.-C., Clavel, J., Benson, R. B. J., & Herrel, A. (2023). Mammalian forelimb evolution is driven by uneven proximal-to-distal morphological diversity. *ELife*, *12*. https://doi.org/10.7554/eLife.81492

Samuels, J. X., & Van Valkenburgh, B. (2008). Skeletal indicators of locomotor adaptations in living and extinct rodents. *Journal of Morphology*, *269*(11), 1387–1411. https://doi.org/10.1002/jmor.10662

Sánchez-Villagra, M. R. (2013). Why are there fewer marsupials than placentals? On the relevance of geography and physiology to evolutionary patterns of mammalian diversity and disparity. In *Journal of Mammalian Evolution* (Vol. 20, Issue 4, pp. 279–290). https://doi.org/10.1007/s10914-012-9220-3

Sears, K. (2004). Constraints on the morphological evolution of marsupial shoulder girdles. *Evolution*, *58*(10), 2353. https://doi.org/10.1554/03-669

Shubin, N. H. (2002). Origin of evolutionary novelty: Examples from limbs. *Journal of Morphology*, *252*(1), 15–28. https://doi.org/10.1002/jmor.10017

Shubin, N. H., & Davis, M. C. (2004). Modularity in the evolution of vertebrate appendages. In *Modularity in development and evolution* (pp. 429–442). University of Chicago Press.

Slater, G. J. (2013). Phylogenetic evidence for a shift in the mode of mammalian body size evolution at the Cretaceous-Palaeogene boundary. *Methods in Ecology and Evolution*, *4*(8), 734–744. https://doi.org/10.1111/2041-210X.12084

Stepanova, N., & Womack, M. C. (2020). Anuran limbs reflect microhabitat and distal, later-developing bones are more evolutionarily labile. *Evolution*, *74*(9), 2005–2019. https://doi.org/10.1111/evo.13981

Van Valkenburgh, B. (1987). Skeletal indicators of locomotor behavior in living and extinct carnivores. *Journal of Vertebrate Paleontology*, *7*(2), 162–182. https://doi.org/10.1080/02724634.1987.10011651

Veeger, H. E. J., & van der Helm, F. C. T. (2007). Shoulder function: The perfect compromise between mobility and stability. In *Journal of Biomechanics* (Vol. 40, Issue 10, pp. 2119–2129). https://doi.org/10.1016/j.jbiomech.2006.10.016

Weaver, L. N., & Grossnickle, D. M. (2020). Functional diversity of small-mammal postcrania is linked to both substrate preference and body size. *Current Zoology*, *66*(5), 539–553. https://doi.org/10.1093/cz/zoaa057

White, H. E., Tucker, A. S., Fernandez, V., Portela Miguez, R., Hautier, L., Herrel, A., Urban, D. J., Sears, K. E., & Goswami, A. (2023). Pedomorphosis in the ancestry of marsupial mammals. *Current Biology*. https://doi.org/10.1016/j.cub.2023.04.009

Zani, P. A. (2000). The comparative evolution of lizard claw and toe morphology and clinging performance. *Journal of Evolutionary Biology*, *13*(2), 316–325. https://doi.org/10.1046/j.1420-9101.2000.00166.x

Zoonomia Consortium. (2020). A comparative genomics multitool for scientific discovery and conservation. *Nature*, *587*(7833), 240–245. https://doi.org/10.1038/s41586-020-2876-6

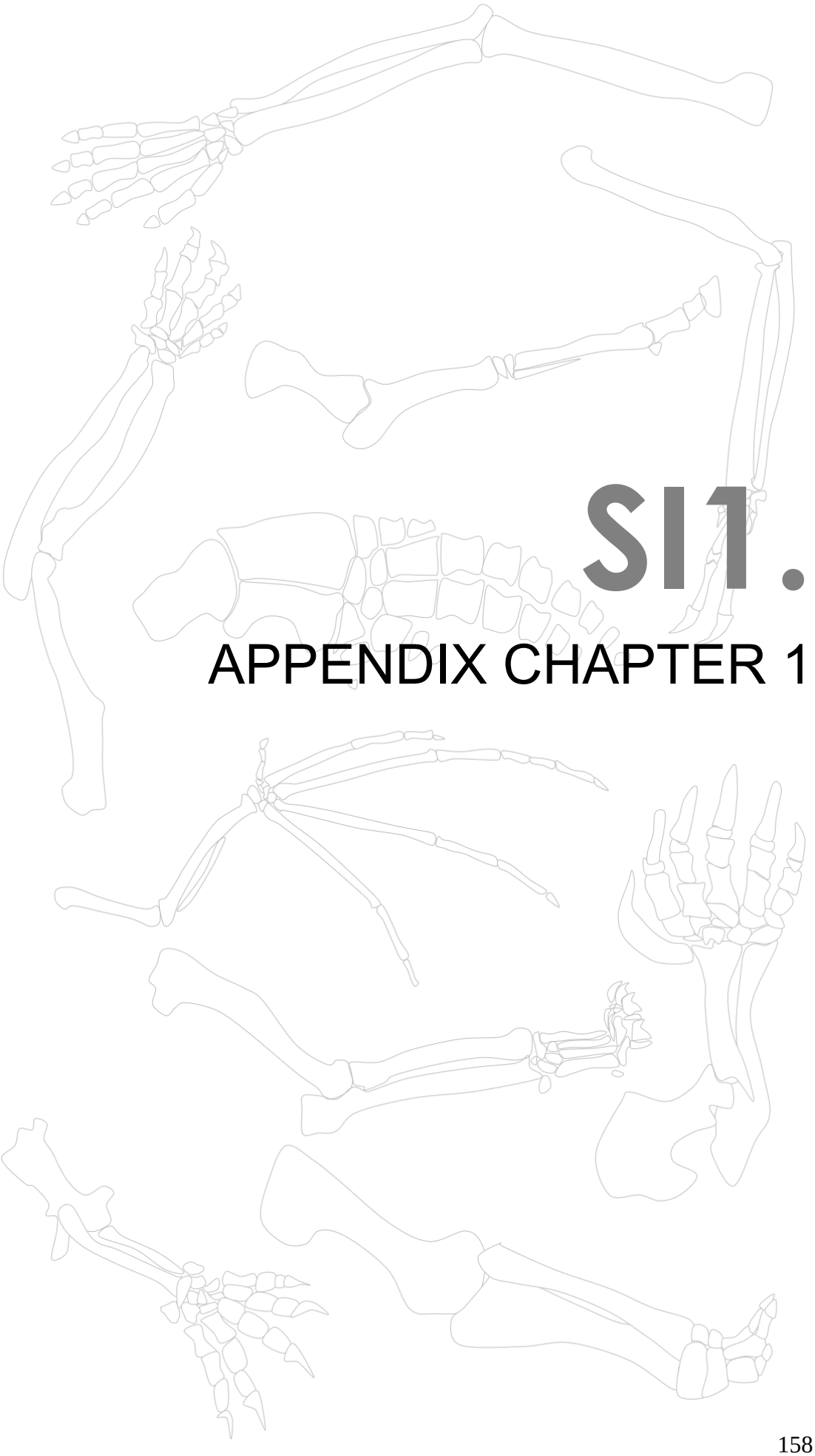

SI1.
APPENDIX CHAPTER 1

Table S1.1. Specimens and ecological classifications. Method of data acquisition is stated alongside the specimen (digital or by caliper), as well as the ecological classification adopted in Ch. 3 and 4. Specimens used per chapter are indicated by an asterisk (*).

	Superord. group	Order	Family	Species	Institution Voucher	Method	MorpoSouce ID	Mass (g)	OBS	Body mass additional reference (if not Jones et al., 2009)	Medium (Ch3)	Locomotor ecology (Ch4)	Ecology reference	Ch2	Ch3	Ch4
1	Afrotheria	Afrosoricida	Chrysochloridae	Amblysomus_hottentotus	MCZ:Mamm:57045	Digital	ark:/87602/m4/M80637	62.60			terrestrial	fossorial	Chen & Wilson, 2015			
2	Afrotheria	Afrosoricida	Chrysochloridae	Chrysochloris_asiatica	MVZ:Mamm:183379	Digital	ark:/87602/m4/M85283	37.16			terrestrial	fossorial	Bronner, 2013			
3	Afrotheria	Afrosoricida	Chrysochloridae	Eremitalpa_granti	MVZ:Mamm:183384	Digital	ark:/87602/m4/M85284	22.04			terrestrial	fossorial	Hopkins & Davis, 2009			
4	Afrotheria	Afrosoricida	Chrysochloridae	Huetia_leucorhina	MNHN-ZM-MO-1982-1026	Digital	Montpellier	41.00		Smith et al., 2018	terrestrial	fossorial	Bronner, 2013			
5	Afrotheria	Afrosoricida	Potamogalidae	Micropotamogale_ruwenzorii	NHMUK:67.213	Digital	ark:/87602/m4/M155019	109.13			semiaquatic	semiaquatic	Hood, 2020	*	*	*
6	Afrotheria	Afrosoricida	Potamogalidae	Potamogale_velox	YPM:VZ:Mamm 014396	Digital	ark:/87602/m4/M64570	670.99			semiaquatic	semiaquatic	Hood, 2020	*	*	*
7	Afrotheria	Afrosoricida	Potamogalidae	Potamogale_velox	UMCZ:vertebrates:e.5425.f	Digital	ark:/87602/m4/M140882	670.99			semiaquatic	semiaquatic	Hood, 2020	*	*	*
8	Afrotheria	Afrosoricida	Tenrecidae	Echinops_telfairi	UMMZ:Mamm:175912	Digital	10.17602/M2/M55753	152.25			terrestrial	scansorial	Chen & Wilson, 2015	*	*	*
9	Afrotheria	Afrosoricida	Tenrecidae	Geogale_aurita	UMMZ:Mamm:167220	Digital	doi:10.17602/M2/M64406	6.69			terrestrial	terrestrialquad	Nielsen, 2005	*	*	*
10	Afrotheria	Afrosoricida	Tenrecidae	Hemicentetes_semispinosus	YPM:VZ:Mamm 005783	Digital	ark:/87602/m4/M64841	134.00			terrestrial	semifossorial	Chen & Wilson, 2015	*	*	*
11	Afrotheria	Afrosoricida	Tenrecidae	Microgale_longicaudata	UMMZ:Mamm:174711	Digital	doi:10.17602/M2/M64408	8.08			terrestrial	arboreal	Nowak, 1999	*	*	*
12	Afrotheria	Afrosoricida	Tenrecidae	Microgale_mergulus	mcz:Mamm:45533	Digital	ark:/87602/m4/M81743	76.86	Same as Limnogale mergulus in MorphoSource.		semiaquatic	semiaquatic	Benstead et al., 2011	*	*	*
13	Afrotheria	Afrosoricida	Tenrecidae	Nesogale_sp	NHMUK:ZD:1948.120-122	Digital	ark:/87602/m4/M164551	42.84	Genus average body mass of species Nesogale talazaci (old taxonomy Microgale talazaci, in PanTHERIA) and N. dobsoni (old taxonomy Microgale dobsoni, from Stephenson at al., 1994).	Speakman et al., 1994	terrestrial	scansorial	Nowak, 1999		*	*
14	Afrotheria	Afrosoricida	Tenrecidae	Oryzorictes_tetradactylus	UMZC:vertebrates:e.5453.c	Digital	ark:/87602/m4/M141014	35.99			terrestrial	fossorial	Nowak, 1999		*	*
15	Afrotheria	Afrosoricida	Tenrecidae	Setifer_setosus	UMMZ:Mamm:174775	Digital	doi:10.17602/M2/M55759	185.00			terrestrial	terrestrialquad	Owens, 2014	*	*	*
16	Afrotheria	Afrosoricida	Tenrecidae	Tenrec_ecaudatus	YPM:VZ:Mamm 006029	Digital	ark:/87602/m4/M65199	887.59			terrestrial	semifossorial	Nowak, 1999	*	*	*
17	Afrotheria	Afrosoricida	Tenrecidae	Tenrec_ecaudatus	UMMZ:Mamm:138441	Digital	ark:/87602/m4/M141220	887.59			terrestrial	semifossorial	Nowak, 1999	*	*	*
18	Afrotheria	Hyracoidea	Procaviidae	Dendrohyrax_arboreus	MNHN-ZM-MO-1977-255	Caliper	-	2981.11			terrestrial	arboreal	Milner & Gaylard, 2013	*	*	*
19	Afrotheria	Hyracoidea	Procaviidae	Dendrohyrax_arboreus	MNHN-ZM-MO-1977-258	Caliper	-	2981.11			terrestrial	arboreal	Milner & Gaylard, 2013	*	*	*
20	Afrotheria	Hyracoidea	Procaviidae	Heterohyrax_brucei	MNHN-1934-92	Caliper	-	2453.66			terrestrial	scansorial	Barry & Hoeck, 2013	*	*	*
21	Afrotheria	Hyracoidea	Procaviidae	Heterohyrax_brucei	MNHN-1934-94	Caliper	-	2453.66			terrestrial	scansorial	Barry & Hoeck, 2013	*	*	*
22	Afrotheria	Hyracoidea	Procaviidae	Procavia_capensis	MNHN-1934-95	Caliper	-	2952.48			terrestrial	terrestrialquad	Hopkins & Davis, 2009	*	*	*
23	Afrotheria	Hyracoidea	Procaviidae	Procavia_capensis	NHM-69-2-2-4	Caliper	-	2952.48			terrestrial	terrestrialquad	Hopkins & Davis, 2009	*	*	*
24	Afrotheria	Macroscelidea	Macroscelididae	Elephantulus_brachyrhynchus	NHMUK:1963.1004	Digital	ark:/87602/m4/M157351	45.11			terrestrial	terrestrialquad	Perrin, 2013	*	*	*
25	Afrotheria	Macroscelidea	Macroscelididae	Macroscelides_micus	CAS:mam:30345	Digital	ark:/87602/m4/M83184	38.64			terrestrial	terrestrialquad	Dumbacher et al., 2014	*	*	*
26	Afrotheria	Macroscelidea	Macroscelididae	Macroscelides_proboscideus	FMNH:Mamm:137045	Digital	ark:/87602/m4/M157790	38.64			terrestrial	terrestrialquad	Perrin & Rathbun, 2013b	*	*	*
27	Afrotheria	Macroscelidea	Macroscelididae	Petrodromus_tetradactylus	CAS:mam:28177	Digital	ark:/87602/m4/M83183	201.00			terrestrial	terrestrialquad	Chen & Wilson, 2015	*	*	*
28	Afrotheria	Macroscelidea	Macroscelididae	Petrosaltator_rozeti	NHMUK:1891.10.15.11	Digital	ark:/87602/m4/M157363	43.07			terrestrial	terrestrialquad	Perrin & Rathbun, 2013a		*	*
29	Afrotheria	Macroscelidea	Macroscelididae	Rhynchocyon_petersi	NHMUK:zoo:1886.9.21.1	Digital	ark:/87602/m4/M157403	423.99			terrestrial	terrestrialquad	Rathbun, 2013	*	*	*
30	Afrotheria	Proboscidea	Elephantidae	Elephas_maximus	MNHN-ZM-AC-1900-492	Caliper	-	3269794.34			terrestrial	terrestrialquad	Nowak, 1999	*	*	*
31	Afrotheria	Proboscidea	Elephantidae	Loxodonta_africana	NHM-58-11-15-1	Caliper	-	3824539.93			terrestrial	terrestrialquad	Poole et al., 2013		*	*
32	Afrotheria	Sirenia	Dugongidae	Dugong_dugon	MNHN-ZM-AC-1875-279	Caliper	-	295000.00			aquatic	aquatic	Nowak, 1999	*	*	*
33	Afrotheria	Sirenia	Dugongidae	Dugong_dugon	MNHN-ZM-AC-1883-241	Caliper	-	295000.00			aquatic	aquatic	Nowak, 1999	*	*	*
34	Afrotheria	Sirenia	Trichechidae	Trichechus_senegalensis	MNHN-ZM-AC-1924-354	Caliper	-	454000.00			aquatic	aquatic	Nowak, 1999	*	*	*
35	Afrotheria	Tubulidentata	Orycteropodidae	Orycteropus_afer	MNHN-1919-16	Caliper	-	56175.20			terrestrial	semifossorial	Hopkins & Davis, 2009	*	*	*
36	Afrotheria	Tubulidentata	Orycteropodidae	Orycteropus_afer	MNHN-1919-19	Caliper	-	56175.20			terrestrial	semifossorial	Hopkins & Davis, 2009	*	*	*
37	Euarchontoglires	Lagomorpha	Leporidae	Lepus_sp	MNHN-1902-809	Caliper	-	2554.35	Body mass of genus average.		terrestrial	terrestrialquad	Nowak, 1999	*	*	*
38	Euarchontoglires	Lagomorpha	Leporidae	Nesolagus_netscheri	NHM-1921-1-181	Caliper	-	1511.67			terrestrial	terrestrialquad	Nowak, 1999		*	*

	Superord. group	Order	Family	Species	Institution Voucher	Method	MorpoSouce ID	Mass (g)	OBS	Body mass additional reference (if not Jones et al., 2009)	Medium (Ch3)	Locomotor ecology (Ch4)	Ecology reference	Ch2	Ch3	Ch4
39	Euarchontoglires	Lagomorpha	Leporidae	Oryctolagus_cuniculus	MNHN-1985-1836	Caliper	-	1590.57			terrestrial	semifossorial	Nowak, 1999	*	*	*
40	Euarchontoglires	Lagomorpha	Leporidae	Pentalagus_furnessi	NHM-76-1366	Caliper	-	2240.00		Yamada & Cervantes, 2005	terrestrial	terrestrialquad	Nowak, 1999		*	
41	Euarchontoglires	Lagomorpha	Leporidae	Poelagus_marjorita	NHM-1929-5-14-31	Caliper	-	2509.70			terrestrial	terrestrialquad	GBIF Secretariat, 2022e		*	*
42	Euarchontoglires	Lagomorpha	Leporidae	Pronolagus_rupestris	FMNH:Mamm:177246	Digital	ark:/87602/m4/M157945	2249.99			terrestrial	terrestrialquad	Nowak, 1999	*	*	
43	Euarchontoglires	Lagomorpha	Leporidae	Romerolagus_diazi	NHM-84-20-98	Caliper	-	465.58			terrestrial	semifossorial	Nowak, 1999		*	*
44	Euarchontoglires	Lagomorpha	Leporidae	Sylvilagus_bachmani	UMMZ:Mamm:93557	Digital	ark:/87602/m4/M164470	714.53			terrestrial	terrestrialquad	GBIF Secretariat, 2022h	*	*	*
45	Euarchontoglires	Lagomorpha	Ochotonidae	Ochotona_alpina	UMMZ:Mamm:123059	Digital	ark:/87602/m4/M89554	150.00			terrestrial	terrestrialquad	Nowak, 1999	*	*	*
46	Euarchontoglires	Primates	Atelidae	Alouatta_seniculus	AMNH:Mamm:m-200550	Digital	ark:/87602/m4/M24485	6398.31			terrestrial	arboreal	Granatosky, 2018	*	*	*
47	Euarchontoglires	Primates	Atelidae	Ateles_belzebuth	AMNH:Mamm:m-188125	Digital	ark:/87602/m4/M26328	6692.42			terrestrial	arboreal	Granatosky, 2018	*	*	*
48	Euarchontoglires	Primates	Atelidae	Ateles_fusciceps	AMNH:Mamm:m-188141	Digital	ark:/87602/m4/M23454	9067.94			terrestrial	arboreal	Nowak, 1999	*	*	*
49	Euarchontoglires	Primates	Atelidae	Lagothrix_sp	AMNH:Mamm:m-202801	Digital	ark:/87602/m4/M24482	6263.69	L. lagotricha body mass.		terrestrial	arboreal	Nowak, 1999	*	*	*
50	Euarchontoglires	Primates	Atelidae	Lagothrix_sp	AMNH:Mamm:m-201386	Digital	ark:/87602/m4/M22689	6263.69	L. lagotricha body mass.		terrestrial	arboreal	Nowak, 1999	*	*	*
51	Euarchontoglires	Primates	Cebidae	Aotus_trivirgatus	MNHN-ZM-AC-1935-114	Caliper	-	912.40			terrestrial	arboreal	Nowak, 1999	*	*	*
52	Euarchontoglires	Primates	Cebidae	Callimico_goeldii	AMNH:Mamm:m-183285	Digital	ark:/87602/m4/M25372	558.00			terrestrial	arboreal	Granatosky, 2018	*	*	*
53	Euarchontoglires	Primates	Cebidae	Callithrix_jacchus	MNHN-ZM-AC-1912-453	Caliper	-	290.21			terrestrial	arboreal	Nowak, 1999	*	*	*
54	Euarchontoglires	Primates	Cebidae	Callithrix_sp	DU:EA:197	Digital	doi:10.17602/M2/M28929	345.22	Body mass of genus average.		terrestrial	arboreal	Chen & Wilson, 2015	*	*	*
55	Euarchontoglires	Primates	Cebidae	Cebus_albifrons	MNHN-ZM-AC-1896-467	Caliper	-	2509.68			terrestrial	arboreal	Nowak, 1999	*	*	*
56	Euarchontoglires	Primates	Cebidae	Leontopithecus_rosalia	AMNH:Mamm:m-235274	Digital	ark:/87602/m4/M27304	592.52			terrestrial	arboreal	Granatosky, 2018	*	*	*
57	Euarchontoglires	Primates	Cebidae	Saguinus_sp	DU:EA:203	Digital	doi:10.17602/M2/M49203	493.42	Body mass of genus average.		terrestrial	arboreal	Nowak, 1999	*	*	*
58	Euarchontoglires	Primates	Cebidae	Saimiri_sciureus	MCZ:Mamm:4245	Digital	ark:/87602/m4/M73027	749.47			terrestrial	arboreal	Chen & Wilson, 2015	*	*	*
59	Euarchontoglires	Primates	Cebidae	Sapajus_apella	MNHN-ZM-AC-1880-1380	Caliper	-	2758.38	Same as Cebus apella in PanTHERIA (old taxonomy).		terrestrial	arboreal	Granatosky, 2018	*	*	*
60	Euarchontoglires	Primates	Cercopithecidae	Cercocebus_atys	MNHN-ZM-AC-1933-309	Caliper	-	6941.24			terrestrial	scansorial	McGraw, 2013	*	*	*
61	Euarchontoglires	Primates	Cercopithecidae	Cercopithecus_albogularis	MNHN-ZM-AC-1871-54	Caliper	-	5033.33		Makhasi, 2013	terrestrial	arboreal	Granatosky, 2018	*	*	*
62	Euarchontoglires	Primates	Cercopithecidae	Chlorocebus_pygerythrus	MNHN-ZM-AC-1894-544	Caliper	-	3695.99	Chlorocebus aethiops body mass.		terrestrial	scansorial	Isbell & Jaffe, 2013	*	*	*
63	Euarchontoglires	Primates	Cercopithecidae	Colobus_polykomos	MNHN-ZM-MO-1961-1017	Caliper	-	8797.29			terrestrial	arboreal	Granatosky, 2018	*	*	*
64	Euarchontoglires	Primates	Cercopithecidae	Erythrocebus_patas	MNHN-ZM-AC-1934-535	Caliper	-	7966.30			terrestrial	scansorial	Isbell, 2013	*	*	*
65	Euarchontoglires	Primates	Cercopithecidae	Lophocebus_aterrimus	MNHN-ZM-AC-1935-61	Caliper	-	6510.37			terrestrial	arboreal	Nowak, 1999	*	*	*
66	Euarchontoglires	Primates	Cercopithecidae	Macaca_mulatta	UCD:31692	Digital	ark:/87602/m4/M63132	6455.19			terrestrial	scansorial	Nowak, 1999	*	*	*
67	Euarchontoglires	Primates	Cercopithecidae	Macaca_mulatta	UCD:37477	Digital	ark:/87602/m4/M73328	6455.19			terrestrial	scansorial	Nowak, 1999	*	*	*
68	Euarchontoglires	Primates	Cercopithecidae	Mandrillus_leucophaeus	MNHN-1892-30	Caliper	-	14253.30			terrestrial	scansorial	Schaaf et al., 2013	*	*	*
69	Euarchontoglires	Primates	Cercopithecidae	Miopithecus_talapoin	MNHN-ZM-AC-A3863	Caliper	-	1248.86			terrestrial	arboreal	Frederick, 2002	*	*	*
70	Euarchontoglires	Primates	Cercopithecidae	Nasalis_larvatus	MNHN-ZM-MO-1897-1301	Caliper	-	12265.65			terrestrial	arboreal	Woltanski, 2004	*	*	*
71	Euarchontoglires	Primates	Cercopithecidae	Papio_sp	AMNH:Mamm:m-200689	Digital	ark:/87602/m4/M49138	16662.66	Body mass of genus average.		terrestrial	scansorial	Nowak, 1999	*	*	*
72	Euarchontoglires	Primates	Cercopithecidae	Piliocolobus_badius	MNHN-ZM-MO-1961-1018	Caliper	-	8430.40			terrestrial	arboreal	Granatosky, 2018		*	*
73	Euarchontoglires	Primates	Cercopithecidae	Presbytis_sp	DU:EA:259	Digital	doi:10.17602/M2/M64272	6419.29	Body mass of genus average.		terrestrial	arboreal	Granatosky, 2018	*	*	*
74	Euarchontoglires	Primates	Cercopithecidae	Procolobus_verus	MNHN-1962-178	Caliper	-	3977.86			terrestrial	arboreal	Granatosky, 2018		*	*
75	Euarchontoglires	Primates	Cercopithecidae	Semnopithecus_entellus	MNHN-ZM-AC-1881-140	Caliper	-	12679.29			terrestrial	scansorial	Semke, 2011	*	*	*
76	Euarchontoglires	Primates	Cercopithecidae	Trachypithecus_phayrei	MNHN-ZM-AC-1934-546	Caliper	-	7681.72			terrestrial	arboreal	Nowak, 1999	*	*	*
77	Euarchontoglires	Primates	Cheirogaleidae	Cheirogaleus_medius	DLC:1653f	Digital	doi:10.17602/M2/M26259	196.76			terrestrial	arboreal	Granatosky, 2018	*	*	*
78	Euarchontoglires	Primates	Cheirogaleidae	Microcebus_murinus	DLC:7024m	Digital	doi:10.17602/M2/M17961	69.00			terrestrial	arboreal	Granatosky, 2018		*	*
79	Euarchontoglires	Primates	Cheirogaleidae	Mirza_zaza	DLC:2304m	Digital	doi:10.17602/M2/M16436	280.90		Rode-Margono et al., 2015	terrestrial	arboreal	Nowak, 1999		*	*
80	Euarchontoglires	Primates	Daubentoniidae	Daubentonia_madagascariensis	DLC:6454f	Digital	doi:10.17602/M2/M32055	2731.37			terrestrial	arboreal	Granatosky, 2018	*	*	*
81	Euarchontoglires	Primates	Daubentoniidae	Daubentonia_madagascariensis	DLC:6941m	Digital	doi:10.17602/M2/M24659	2731.37			terrestrial	arboreal	Granatosky, 2018	*	*	*
82	Euarchontoglires	Primates	Galagidae	Euoticus_elegantulus	AMNH:Mamm:m-269906	Digital	ark:/87602/m4/M16449	295.48			terrestrial	arboreal	Ambrose, 2013		*	*
83	Euarchontoglires	Primates	Galagidae	Galago_senegalensis	DU:EA:195	Digital	doi:10.17602/M2/M28595	215.20			terrestrial	arboreal	Nowak, 1999	*	*	*
84	Euarchontoglires	Primates	Galagidae	Galagoides_demidovii	DLC:3022m	Digital	doi:10.17602/M2/M26216	66.04	Same as Galago demidoff in PanTHERIA.		terrestrial	arboreal	Granatosky, 2018	*	*	*
85	Euarchontoglires	Primates	Galagidae	Otolemur_garnettii	DLC:NN_Og01	Digital	doi:10.17602/M2/M15702	811.17			terrestrial	arboreal	Nowak, 1999	*	*	*
86	Euarchontoglires	Primates	Galagidae	Sciurocheirus_alleni	AMNH:Mamm:m-201448	Digital	ark:/87602/m4/M20544	266.03	Same as Galago alleni in PanTHERIA.		terrestrial	arboreal	Nowak, 1999	*	*	*
87	Euarchontoglires	Primates	Hominidae	Gorilla_gorilla	YPM:VZ:Mamm:014997	Digital	ark:/87602/m4/M54448	112588.99			terrestrial	terrestrialquad	Granatosky, 2018	*	*	*
88	Euarchontoglires	Primates	Hominidae	Homo_sapiens	MNHN-ZM-AC-1928-273	Caliper	-	58540.63			terrestrial	terrestrialbip	Nowak, 1999	*	*	*
89	Euarchontoglires	Primates	Hominidae	Pan_paniscus	AMNH:Mamm:m-202870	Digital	ark:/87602/m4/M38741	35119.95			terrestrial	arboreal	Granatosky, 2018	*	*	*
90	Euarchontoglires	Primates	Hominidae	Pongo_pygmaeus	MNHN-ZM-2014-574	Caliper	-	53408.29			terrestrial	arboreal	Granatosky, 2018	*	*	*
91	Euarchontoglires	Primates	Hylobatidae	Hoolock_leuconedys	AMNH:Mamm:m-201743	Digital	ark:/87602/m4/M49863	6699.00	Same as Bunopithecus hoolock in PanTHERIA.		terrestrial	arboreal	Nowak, 1999	*	*	*
92	Euarchontoglires	Primates	Hylobatidae	Hylobates_sp	MNHN-ZM-AC-1880-1170	Caliper	-	5757.16	Body mass of genus average.		terrestrial	arboreal	Granatosky, 2018	*	*	*
93	Euarchontoglires	Primates	Hylobatidae	Nomascus_concolor	MNHN-ZM-AC-1944-47	Caliper	-	6410.47			terrestrial	arboreal	Nowak, 1999	*	*	*
94	Euarchontoglires	Primates	Hylobatidae	Symphalangus_syndactylus	AMNH:Mamm:m-202326	Digital	ark:/87602/m4/M24484	10839.00			terrestrial	arboreal	Granatosky, 2018	*	*	*
95	Euarchontoglires	Primates	Indriidae	Avahi_laniger	AMNH:Mamm:m-170451	Digital	ark:/87602/m4/M20898	1092.28			terrestrial	arboreal	Nowak, 1999	*	*	*
96	Euarchontoglires	Primates	Indriidae	Indri_indri	MNHN-A-3813	Caliper	-	8565.48			terrestrial	arboreal	Nowak, 1999	*	*	*
97	Euarchontoglires	Primates	Indriidae	Propithecus_verreauxi	MNHN-ZM-AC-1939-330	Caliper	-	3588.26			terrestrial	arboreal	Granatosky, 2018	*	*	*
98	Euarchontoglires	Primates	Lemuridae	Eulemur_coronatus	DLC:6177f	Digital	doi:10.17602/M2/M31062	1699.85			terrestrial	arboreal	Granatosky, 2018	*	*	*
99	Euarchontoglires	Primates	Lemuridae	Hapalemur_griseus	DLC:1302f	Digital	doi:10.17602/M2/M15955	916.00			terrestrial	arboreal	Granatosky, 2018	*	*	*
100	Euarchontoglires	Primates	Lemuridae	Lemur_catta	DLC:7142f	Digital	doi:10.17602/M2/M32220	2626.48			terrestrial	scansorial	Nowak, 1999	*	*	*
101	Euarchontoglires	Primates	Lemuridae	Varecia_variegata	AMNH:Mamm:m-201395	Digital	ark:/87602/m4/M22685	3849.99			terrestrial	arboreal	Granatosky, 2018	*	*	*
102	Euarchontoglires	Primates	Lemuridae	Varecia_variegata	AMNH:Mamm:m-200578	Digital	ark:/87602/m4/M24491	3849.99			terrestrial	arboreal	Granatosky, 2018	*	*	*
103	Euarchontoglires	Primates	Lepilemuridae	Lepilemur_mustelinus	AMNH:Mamm:m-170790	Digital	ark:/87602/m4/M24493	669.03			terrestrial	arboreal	Nowak, 1999	*	*	*

	Superord. group	Order	Family	Species	Institution Voucher	Method	MorpoSouce ID	Mass (g)	OBS	Body mass additional reference (if not Jones et al., 2009)	Medium (Ch3)	Locomotor ecology (Ch4)	Ecology reference	Ch2	Ch3	Ch4
104	Euarchontoglires	Primates	Lorisidae	Arctocebus_aureus	YPM:VZ:Mamm 014401	Digital	ark:/87602/m4/M57009	234.16			terrestrial	arboreal	Nowak, 1999	*	*	*
105	Euarchontoglires	Primates	Lorisidae	Arctocebus_calabarensis	YPM:VZ:Mamm 014402	Digital	ark:/87602/m4/M50832	258.01			terrestrial	arboreal	Nowak, 1999	*	*	*
106	Euarchontoglires	Primates	Lorisidae	Loris_tardigradus	DLC:2930m	Digital	doi:10.17602/M2/M16454	249.22			terrestrial	arboreal	Granatosky, 2018	*	*	*
107	Euarchontoglires	Primates	Lorisidae	Nycticebus_coucang	DU:EA:193	Digital	doi:10.17602/M2/M28832	924.55			terrestrial	arboreal	Granatosky, 2018	*	*	*
108	Euarchontoglires	Primates	Lorisidae	Nycticebus_pygmaeus	DLC:2901f	Digital	doi:10.17602/M2/M14935	342.32			terrestrial	arboreal	Nowak, 1999	*	*	*
109	Euarchontoglires	Primates	Lorisidae	Perodicticus_potto	YPM:VZ:Mamm 014912	Digital	ark:/87602/m4/M48709	1081.81			terrestrial	arboreal	Granatosky, 2018	*	*	*
110	Euarchontoglires	Primates	Pitheciidae	Cacajao_calvus	MNHN-ZM-AC1884-319	Caliper	-	3421.04			terrestrial	arboreal	Granatosky, 2018	*	*	*
111	Euarchontoglires	Primates	Pitheciidae	Cheracebus_torquatus	NHM-1948-450	Caliper	-	1209.57			terrestrial	arboreal	Granatosky, 2018		*	
112	Euarchontoglires	Primates	Pitheciidae	Chiropotes_sp	SBU:Blue Pin	Digital	ark:/87602/m4/M53814	2967.27	C. satanas body mass.		terrestrial	arboreal	Nowak, 1999	*	*	*
113	Euarchontoglires	Primates	Pitheciidae	Pithecia_pithecia	SBU:White Pin	Digital	ark:/87602/m4/M55604	1667.19			terrestrial	arboreal	Granatosky, 2018	*	*	*
114	Euarchontoglires	Primates	Tarsiidae	Carlito_syrichta	AMNH:Mamm:m-150143	Digital	ark:/87602/m4/M19566	115.91	Same as Tarsius stricta in MorphoSource and PanTHERIA.		terrestrial	arboreal	Granatosky, 2018		*	*
115	Euarchontoglires	Primates	Tarsiidae	Tarsius_sp	DU:EA:032	Digital	doi:10.17602/M2/M27280	139.79	Body mass of genus average.		terrestrial	arboreal	Granatosky, 2018	*	*	*
116	Euarchontoglires	Rodentia	Abrocomidae	Abrocoma_cinerea	UMMZ:Mamm:120621	Digital	ark:/87602/m4/M141118	193.64			terrestrial	terrestrialquad	Hopkins & Davis, 2009	*	*	*
117	Euarchontoglires	Rodentia	Anomaluridae	Anomalurus_beecrofti	NHMUK:zoo:zd 1989.174	Digital	ark:/87602/m4/M52927	479.07			semiaerial	gliding	Jackson, 2000	*	*	*
118	Euarchontoglires	Rodentia	Anomaluridae	Anomalurus_sp	YPM:VZ:Mamm 014526	Digital	ark:/87602/m4/M95047	250.00	A. pusillus body mass.		semiaerial	gliding	Jackson, 2000	*	*	*
119	Euarchontoglires	Rodentia	Anomaluridae	Idiurus_zenkeri	UMZC:Vertebrates:e.1421	Digital	ark:/87602/m4/M52943	100.00			semiaerial	gliding	Jackson, 2000		*	*
120	Euarchontoglires	Rodentia	Aplodontiidae	Aplodontia_rufa	FMNH:Mamm:57831	Digital	ark:/87602/m4/M162923	806.21			terrestrial	fossorial	Nowak, 1999		*	*
121	Euarchontoglires	Rodentia	Bathyergidae	Bathyergus_suillus	MNHN-A3351	Caliper	-	777.38			terrestrial	fossorial	Weisbecker & Schmid, 2007	*	*	*
122	Euarchontoglires	Rodentia	Bathyergidae	Cryptomys_hottentotus	UF:Mammal:24603	Digital	ark:/87602/m4/M140423	75.13			terrestrial	fossorial	Chen & Wilson, 2015	*	*	*
123	Euarchontoglires	Rodentia	Bathyergidae	Fukomys_mechowi	CBUN-4372	Digital	Montpellier	271.54			terrestrial	fossorial	Nowak, 1999		*	*
124	Euarchontoglires	Rodentia	Bathyergidae	Georychus_capensis	MVZ:Mamm:117769	Digital	ark:/87602/m4/M98695	188.36			terrestrial	fossorial	Samuels & Van Valkenburgh, 2018	*	*	*
125	Euarchontoglires	Rodentia	Bathyergidae	Heliophobius_argenteocinereus	MCZ:Mamm:59825	Digital	ark:/87602/m4/M84238	159.46			terrestrial	fossorial	Samuels & Van Valkenburgh, 2018	*	*	*
126	Euarchontoglires	Rodentia	Calomyscidae	Calomyscus_bailwardi	UMMZ:Mamm:167649	Digital	doi:10.17602/M2/M64407	21.38			terrestrial	terrestrialquad	Hopkins & Davis, 2009	*	*	*
127	Euarchontoglires	Rodentia	Calomyscidae	Calomyscus_baluchi	UF:Mammal:28671	Digital	ark:/87602/m4/M140390	21.38	C. bailwardi body mass.		terrestrial	terrestrialquad	Hopkins & Davis, 2009	*	*	*
128	Euarchontoglires	Rodentia	Capromyidae	Capromys_pilorides	MNHN-ZM-AC-1869-407	Caliper	-	5200.00			terrestrial	scansorial	Weisbecker & Schmid, 2007	*	*	*
129	Euarchontoglires	Rodentia	Castoridae	Castor_canadensis	MNHN-1901-262	Caliper	-	18124.41			semiaquatic	semiaquatic	Severud et al., 2013		*	*
130	Euarchontoglires	Rodentia	Castoridae	Castor_fiber	MNHN-1893-461	Caliper	-	19000.00			semiaquatic	semiaquatic	Severud et al., 2014	*	*	*
131	Euarchontoglires	Rodentia	Caviidae	Cavia_fulgida	UMZC:vertebrates:e.3705	Digital	ark:/87602/m4/M140710	282.50			terrestrial	terrestrialquad	Nowak, 1999	*	*	*
132	Euarchontoglires	Rodentia	Caviidae	Dolichotis_patagonum	MNHN-ZM-AC-1894-574	Caliper	-	8000.00			terrestrial	terrestrialquad	Weisbecker & Schmid, 2007	*	*	*
133	Euarchontoglires	Rodentia	Caviidae	Galea_musteloides	UMMZ:Mamm:134539	Digital	ark:/87602/m4/M68599	386.64			terrestrial	terrestrialquad	Weisbecker & Schmid, 2007	*	*	*
134	Euarchontoglires	Rodentia	Caviidae	Hydrochoerus_hydrochaeris	MNHN-ZM-AC-1929-492	Caliper	-	48144.91			semiaquatic	semiaquatic	Desbiez et al., 2011	*	*	*
135	Euarchontoglires	Rodentia	Caviidae	Kerodon_rupestris	MNHN-ZM-MO-1982-646	Caliper	-	799.15			terrestrial	scansorial	Weisbecker & Schmid, 2007	*	*	*
136	Euarchontoglires	Rodentia	Chinchillidae	Chinchilla_lanigera	UMMZ:Mamm:93493	Digital		480.28			terrestrial	scansorial	Weisbecker & Schmid, 2007	*	*	*
137	Euarchontoglires	Rodentia	Chinchillidae	Lagidium_sp	MNHN-1871-163	Caliper	-	1814.00	Body mass of genus average.		terrestrial	scansorial	Weisbecker & Schmid, 2007	*	*	*
138	Euarchontoglires	Rodentia	Cricetidae	Abrothrix_longipilis	MVZ:Mamm:163725	Digital	ark:/87602/m4/M99364	38.86			terrestrial	semifossorial	Nowak, 1999	*	*	*
139	Euarchontoglires	Rodentia	Cricetidae	Akodon_boliviensis	UMMZ:Mamm:160805	Digital	doi:10.17602/M2/M68610	27.50			terrestrial	terrestrialquad	Nowak, 1999	*	*	*
140	Euarchontoglires	Rodentia	Cricetidae	Allocricetulus_eversmanni	UMMZ:Mamm:111194	Digital	ark:/87602/m4/M68570	50.00		Ushakova et al., 2012	terrestrial	terrestrialquad	Verde Arregoitia et al., 2017	*	*	*
141	Euarchontoglires	Rodentia	Cricetidae	Alticola_argentatus	UF:Mammal:27219	Digital	ark:/87602/m4/M133925	37.69			terrestrial	semifossorial	Nowak, 1999	*	*	*
142	Euarchontoglires	Rodentia	Cricetidae	Andalgalomys_pearsoni	UMMZ:Mamm:134386	Digital	ark:/87602/m4/M65520	25.40			terrestrial	terrestrialquad	Nowak, 1999	*	*	*
143	Euarchontoglires	Rodentia	Cricetidae	Andinomys_edax	AMNH:Mamm:m-278180	Digital	ark:/87602/m4/M101247	69.75	A. edax body mass.		terrestrial	scansorial	Nowak, 1999	*	*	*
144	Euarchontoglires	Rodentia	Cricetidae	Arvicola_amphibius	UMMZ:Mamm:138456	Digital	ark:/87602/m4/M65521	120.00			semiaquatic	semiaquatic	Hood, 2020	*	*	*
145	Euarchontoglires	Rodentia	Cricetidae	Auliscomys_pictus	MVZ:Mamm:174309	Digital	ark:/87602/m4/M85271	48.97			terrestrial	terrestrialquad	Dunnum et al., 2016	*	*	*
146	Euarchontoglires	Rodentia	Cricetidae	Baiomys_taylori	UMMZ:Mamm:108722	Digital	ark:/87602/m4/M68560	7.43			terrestrial	terrestrialquad	Nowak, 1999	*	*	*
147	Euarchontoglires	Rodentia	Cricetidae	Calomys_laucha	UMMZ:Mamm:134402	Digital	ark:/87602/m4/M68595	14.00			terrestrial	terrestrialquad	Nowak, 1999	*	*	*
148	Euarchontoglires	Rodentia	Cricetidae	Chilomys_instans	UMMZ:Mamm:155796	Digital	doi:10.17602/M2/M64403	19.00			terrestrial	terrestrialquad	Nowak, 1999	*	*	*
149	Euarchontoglires	Rodentia	Cricetidae	Chinchillula_sahamae	AMNH:Mamm:m-249019	Digital	ark:/87602/m4/M101240	169.74	C. sahamae body mass.		terrestrial	terrestrialquad	Nowak, 1999	*	*	*
150	Euarchontoglires	Rodentia	Cricetidae	Chionomys_nivalis	MNHN-ZM-2005-1004	Digital	Montpellier	42.01			terrestrial	terrestrialquad	Nowak, 1999		*	*
151	Euarchontoglires	Rodentia	Cricetidae	Cricetulus_barabensis	UMMZ:Mamm:111191	Digital	doi:10.17602/M2/M68568	33.50		Freudenthal & Suárez, 2013	terrestrial	semifossorial	Verde Arregoitia et al., 2017	*	*	*
152	Euarchontoglires	Rodentia	Cricetidae	Cricetus_cricetus	UMMZ:Mamm:108463	Digital	ark:/87602/m4/M64394	428.95			terrestrial	semifossorial	Verde Arregoitia et al., 2017	*	*	*
153	Euarchontoglires	Rodentia	Cricetidae	Dicrostonyx_richardsoni	UMMZ:Mamm:114757	Digital	ark:/87602/m4/M57196	62.50		Freudenthal & Suárez, 2013	terrestrial	semifossorial	Nowak, 1999	*	*	*
154	Euarchontoglires	Rodentia	Cricetidae	Eligmodontia_typus	UMMZ:Mamm:115506	Digital	ark:/87602/m4/M65517	17.37			terrestrial	terrestrialquad	Nowak, 1999	*	*	*
155	Euarchontoglires	Rodentia	Cricetidae	Ellobius_alaicus	UMMZ:Mamm:123043	Digital	doi:10.17602/M2/M65519	60.00	Body mass of genus average.		terrestrial	fossorial	Nowak, 1999	*	*	*
156	Euarchontoglires	Rodentia	Cricetidae	Eolagurus_luteus	MSB:Mamm:249169	Digital	ark:/87602/m4/M165495	26.00			terrestrial	semifossorial	Nowak, 1999		*	*
157	Euarchontoglires	Rodentia	Cricetidae	Eothenomys_melanogaster	MVZ:Mamm:180936	Digital	ark:/87602/m4/M85279	19.59			terrestrial	semifossorial	Nowak, 1999	*	*	*
158	Euarchontoglires	Rodentia	Cricetidae	Euryoryzomys_macconnelli	UF:Mammal:30789	Digital	ark:/87602/m4/M140444	66.49	Same as Oryzomys macconnelli in PanTHERIA.		terrestrial	terrestrialquad	Nowak, 1999	*	*	*
159	Euarchontoglires	Rodentia	Cricetidae	Geoxus_valdivianus	MVZ:Mamm:158411	Digital	ark:/87602/m4/M85266	30.80			terrestrial	fossorial	Samuels & Van Valkenburgh, 2008	*	*	*

	Superord. group	Order	Family	Species	Institution Voucher	Method	MorpoSouce ID	Mass (g)	OBS	Body mass additional reference (if not Jones et al., 2009)	Medium (Ch3)	Locomotor ecology (Ch4)	Ecology reference	Ch2	Ch3	Ch4
160	Euarchontoglires	Rodentia	Cricetidae	Graomys_griseoflavus	UMMZ:Mamm:109231	Digital	ark:/87602/m4/M68561	68.32			terrestrial	scansorial	Nowak, 1999	*	*	*
161	Euarchontoglires	Rodentia	Cricetidae	Habromys_lepturus	UMMZ:Mamm:113793	Digital	ark:/87602/m4/M68575	84.99			terrestrial	scansorial	Contreras-Medina et al., 2022	*	*	*
162	Euarchontoglires	Rodentia	Cricetidae	Handleyomys_alfaroi	UMMZ:Mamm:116889	Digital	ark:/87602/m4/M113722	33.30	Same as Oryzomys alfaroi in PanTHERIA.		terrestrial	terrestrialquad	Timm et al., 2016	*	*	*
163	Euarchontoglires	Rodentia	Cricetidae	Hodomys_alleni	UMMZ:Mamm:113820	Digital	ark:/87602/m4/M68576	367.59			terrestrial	terrestrialquad	Nowak, 1999	*	*	*
164	Euarchontoglires	Rodentia	Cricetidae	Hyperacrius_wynnei	UMMZ:Mamm:167666	Digital	ark:/87602/m4/M57218	52.60			terrestrial	fossorial	Nowak, 1999	*	*	*
165	Euarchontoglires	Rodentia	Cricetidae	Lasiopodomys_brandtii	MSB:Mamm:267271	Digital	ark:/87602/m4/M165499	46.05		Zhang & Wang, 2006	terrestrial	semifossorial	Nowak, 1999		*	*
166	Euarchontoglires	Rodentia	Cricetidae	Lemmiscus_curtatus	UMMZ:Mamm:115494	Digital	ark:/87602/m4/M68580	20.60			terrestrial	semifossorial	Nowak, 1999		*	*
167	Euarchontoglires	Rodentia	Cricetidae	Lemmus_lemmus	UMMZ:Mamm:57801	Digital	ark:/87602/m4/M64410	67.62			terrestrial	semifossorial	Nowak, 1999	*	*	*
168	Euarchontoglires	Rodentia	Cricetidae	Lemmus_sibiricus	UMMZ:Mamm:110403	Digital	ark:/87602/m4/M57192	53.81			terrestrial	semifossorial	Nowak, 1999	*	*	*
169	Euarchontoglires	Rodentia	Cricetidae	Lenoxus_apicalis	MVZ:Mamm:172346	Digital	ark:/87602/m4/M85198	53.60			terrestrial	terrestrialquad	Nowak, 1999	*	*	*
170	Euarchontoglires	Rodentia	Cricetidae	Loxodontomys_micropus	MVZ:Mamm:176761	Digital	ark:/87602/m4/M85201	70.76			terrestrial	scansorial	Nowak, 1999	*	*	*
171	Euarchontoglires	Rodentia	Cricetidae	Megadontomys_thomasi	UMMZ:Mamm:114816	Digital	ark:/87602/m4/M68579	110.52			terrestrial	terrestrialquad	Verde Arregoitia et al., 2017	*	*	*
172	Euarchontoglires	Rodentia	Cricetidae	Melanomys_caliginosus	UMMZ:Mamm:174810	Digital	ark:/87602/m4/M68618	41.00			terrestrial	terrestrialquad	Cassola, 2016c	*	*	*
173	Euarchontoglires	Rodentia	Cricetidae	Microryzomys_minutus	UMMZ:Mamm:156399	Digital	ark:/87602/m4/M68604	13.49			terrestrial	scansorial	Nowak, 1999	*	*	*
174	Euarchontoglires	Rodentia	Cricetidae	Microtus_afghanus	UMMZ:Mamm:110407	Digital	ark:/87602/m4/M68563	30.00	Synonym Blanfordimys afghanus	Freudenthal & Suárez, 2013	terrestrial	semifossorial	Molur, 2016	*	*	*
175	Euarchontoglires	Rodentia	Cricetidae	Microtus_chrotorrhinus	UMMZ:Mamm:138423	Digital	ark:/87602/m4/M57210	38.99			terrestrial	semifossorial	Nowak, 1999	*	*	*
176	Euarchontoglires	Rodentia	Cricetidae	Myodes_rutilus	UMMZ:Mamm:62533	Digital	ark:/87602/m4/M70180	19.94			terrestrial	terrestrialquad	Hopkins & Davis, 2009	*	*	*
177	Euarchontoglires	Rodentia	Cricetidae	Myopus_schisticolor	MVZ:Mamm:173692	Digital	ark:/87602/m4/M85199	29.99			terrestrial	terrestrialquad	Nowak, 1999	*	*	*
178	Euarchontoglires	Rodentia	Cricetidae	Neacomys_sp	UMMZ:Mamm:156291	Digital	ark:/87602/m4/M68603	15.87	N. guianae body mass.		terrestrial	terrestrialquad	Nowak, 1999	*	*	*
179	Euarchontoglires	Rodentia	Cricetidae	Necromys_lasiurus	UMMZ:Mamm:134432	Digital	ark:/87602/m4/M68596	39.93			terrestrial	terrestrialquad	Nowak, 1999	*	*	*
180	Euarchontoglires	Rodentia	Cricetidae	Nectomys_squamipes	UMMZ:Mamm:126275	Digital	ark:/87602/m4/M68594	184.98			semiaquatic	semiaquatic	Okihiro, 2011	*	*	*
181	Euarchontoglires	Rodentia	Cricetidae	Neofiber_alleni	UF:Mammal:13931	Digital	ark:/87602/m4/M140579	265.38			semiaquatic	semiaquatic	Hood, 2020	*	*	*
182	Euarchontoglires	Rodentia	Cricetidae	Neotoma_mexicana	UMMZ:Mamm:113819	Digital	ark:/87602/m4/M57194	203.00			terrestrial	terrestrialquad	Verde Arregoitia et al., 2017	*	*	*
183	Euarchontoglires	Rodentia	Cricetidae	Neotomodon_alstoni	UMMZ:Mamm:111938	Digital	ark:/87602/m4/M68572	44.64			terrestrial	terrestrialquad	Verde Arregoitia et al., 2017	*	*	*
184	Euarchontoglires	Rodentia	Cricetidae	Neusticomys_oyapocki	UM-V1647	Digital	Montpellier	47.00			semiaquatic	semiaquatic	Hood, 2020		*	*
185	Euarchontoglires	Rodentia	Cricetidae	Nyctomys_sumichrasti	UMMZ:Mamm:113823	Digital	ark:/87602/m4/M68577	59.99			terrestrial	arboreal	Verde Arregoitia et al., 2017	*	*	*
186	Euarchontoglires	Rodentia	Cricetidae	Ochrotomys_nuttalli	UMMZ:Mamm:93497	Digital	ark:/87602/m4/M68627	22.81			terrestrial	scansorial	Nowak, 1999	*	*	*
187	Euarchontoglires	Rodentia	Cricetidae	Oecomys_rutilus	UM-V1123	Digital	Montpellier	73.40			terrestrial	scansorial	Nowak, 1999		*	*
188	Euarchontoglires	Rodentia	Cricetidae	Oligoryzomys_fulvescens	UMMZ:Mamm:123200	Digital	ark:/87602/m4/M68592	25.00			terrestrial	terrestrialquad	Verde Arregoitia et al., 2017	*	*	*
189	Euarchontoglires	Rodentia	Cricetidae	Ondatra_zibethicus	CBGP	Digital	Montpellier	991.31			semiaquatic	semiaquatic	Hood, 2020		*	*
190	Euarchontoglires	Rodentia	Cricetidae	Onychomys_leucogaster	UMMZ:Mamm:62316	Digital	doi:10.17602/M2/M68621	30.00			terrestrial	terrestrialquad	Samuels & Van Valkenburgh, 2008	*	*	*
191	Euarchontoglires	Rodentia	Cricetidae	Oryzomys_palustris	UMMZ:Mamm:110387	Digital	ark:/87602/m4/M68562	53.26			semiaquatic	semiaquatic	Hood, 2020	*	*	*
192	Euarchontoglires	Rodentia	Cricetidae	Osgoodomys_banderanus	UMMZ:Mamm:113787	Digital	ark:/87602/m4/M68574	49.99			terrestrial	arboreal	Verde Arregoitia et al., 2017	*	*	*
193	Euarchontoglires	Rodentia	Cricetidae	Ototylomys_phyllotis	UMMZ:Mamm:63549	Digital	ark:/87602/m4/M68624	86.94			terrestrial	arboreal	Verde Arregoitia et al., 2017	*	*	*
194	Euarchontoglires	Rodentia	Cricetidae	Oxymycterus_rufus	UMMZ:Mamm:115500	Digital	ark:/87602/m4/M70168	82.01			terrestrial	semifossorial	Nowak, 1999	*	*	*
195	Euarchontoglires	Rodentia	Cricetidae	Peromyscus_leucopus	UMMZ:Mamm:175564	Digital	ark:/87602/m4/M57267	18.07			terrestrial	scansorial	Aguilar, 2011	*	*	*
196	Euarchontoglires	Rodentia	Cricetidae	Peromyscus_truei	UMMZ:Mamm:59361	Digital	ark:/87602/m4/M76617	27.00			terrestrial	scansorial	Gumas, 2004	*	*	*
197	Euarchontoglires	Rodentia	Cricetidae	Phodopus_roborovskii	UMMZ:Mamm:124118	Digital	ark:/87602/m4/M68593	21.00		Freudenthal & Suárez, 2013	terrestrial	semifossorial	Verde Arregoitia et al., 2017	*	*	*
198	Euarchontoglires	Rodentia	Cricetidae	Phyllotis_sp	UMMZ:Mamm:156344	Digital	ark:/87602/m4/M70173	50.08	Body mass of genus average.		terrestrial	terrestrialquad	Nowak, 1999	*	*	*
199	Euarchontoglires	Rodentia	Cricetidae	Podomys_floridanus	UMMZ:Mamm:103733	Digital	ark:/87602/m4/M64393	30.74			terrestrial	terrestrialquad	Nowak, 1999	*	*	*
200	Euarchontoglires	Rodentia	Cricetidae	Prometheomys_schaposchnikowi	UMMZ:Mamm:110414	Digital	ark:/87602/m4/M68564	75.00			terrestrial	fossorial	Nowak, 1999	*	*	*
201	Euarchontoglires	Rodentia	Cricetidae	Pseudoryzomys_simplex	UMMZ:Mamm:134387	Digital	ark:/87602/m4/M64402	45.20			terrestrial	terrestrialquad	Nowak, 1999	*	*	*
202	Euarchontoglires	Rodentia	Cricetidae	Reithrodon_auritus	NHMUK:ZD:1925.5.6.2	Digital	ark:/87602/m4/M164545	79.73			terrestrial	semifossorial	Nowak, 1999		*	*
203	Euarchontoglires	Rodentia	Cricetidae	Reithrodontomys_megalotis	UMMZ:Mamm:55891	Digital	ark:/87602/m4/M68620	10.72			terrestrial	terrestrialquad	Verde Arregoitia et al., 2017	*	*	*
204	Euarchontoglires	Rodentia	Cricetidae	Rhipidomys_fulviventer	UMMZ:Mamm:156377	Digital	doi:10.17602/M2/M70174	89.00			terrestrial	arboreal	Nowak, 1999	*	*	*
205	Euarchontoglires	Rodentia	Cricetidae	Scapteromys_tumidus	UMMZ:Mamm:134434	Digital	ark:/87602/m4/M68597	146.00			semiaquatic	semiaquatic	Hood, 2020	*	*	*
206	Euarchontoglires	Rodentia	Cricetidae	Scotinomys_teguina	UMMZ:Mamm:123113	Digital	ark:/87602/m4/M68591	11.59			terrestrial	terrestrialquad	Verde Arregoitia et al., 2017	*	*	*
207	Euarchontoglires	Rodentia	Cricetidae	Sigmodon_hispidus	UMMZ:Mamm:164639	Digital	ark:/87602/m4/M68612	110.65			terrestrial	terrestrialquad	Samuels & Van Valkenburgh, 2008	*	*	*
208	Euarchontoglires	Rodentia	Cricetidae	Thalpomys_lasiotis	MSU:MR:MR.29355	Digital	ark:/87602/m4/M86161	23.99			terrestrial	terrestrialquad	Nowak, 1999	*	*	*
209	Euarchontoglires	Rodentia	Cricetidae	Thaptomys_nigrita	UMMZ:Mamm:134511	Digital	ark:/87602/m4/M68598	19.90			terrestrial	semifossorial	Patton et al., 2017	*	*	*
210	Euarchontoglires	Rodentia	Cricetidae	Thomasomys_aureus	UMMZ:Mamm:156177	Digital	doi:10.17602/M2/M70171	87.99			terrestrial	arboreal	Pacheco, 2016	*	*	*
211	Euarchontoglires	Rodentia	Cricetidae	Transandinomys_bolivaris	MSB:Mamm:130077	Digital	ark:/87602/m4/M161366	60.50			terrestrial	scansorial	Gómez-Laverde & Pino, 2016		*	*
212	Euarchontoglires	Rodentia	Cricetidae	Zygodontomys_brevicauda	UMMZ:Mamm:111960	Digital	ark:/87602/m4/M68573	52.22			terrestrial	terrestrialquad	Nowak, 1999	*	*	*
213	Euarchontoglires	Rodentia	Ctenodactylidae	Ctenodactylus_sp	AMNH:Mamm:m-239586	Digital	ark:/87602/m4/M101290	231.01	Body mass of genus average.		terrestrial	terrestrialquad	Nowak, 1999	*	*	*
214	Euarchontoglires	Rodentia	Ctenodactylidae	Felovia_vae	MNHN-ZM-MO-2001-773	Digital	Montpellier	205.00			terrestrial	terrestrialquad	Nowak, 1999		*	*
215	Euarchontoglires	Rodentia	Ctenodactylidae	Massoutiera_mzabi	MNHN-ZM-AC-1936-21	Caliper	-	194.00			terrestrial	terrestrialquad	Nowak, 1999	*	*	*

	Superord. group	Order	Family	Species	Institution Voucher	Method	MorpoSouce ID	Mass (g)	OBS	Body mass additional reference (if not Jones et al., 2009)	Medium (Ch3)	Locomotor ecology (Ch4)	Ecology reference	Ch2	Ch3	Ch4
216	Euarchontoglires	Rodentia	Ctenodactylidae	Pectinator_spekei	MNHN-ZM-MO-1995-20	Digital	Montpellier	169.70			terrestrial	terrestrialquad	Nowak, 1999		*	*
217	Euarchontoglires	Rodentia	Ctenomyidae	Ctenomys_maulinus	UF:Mammal:15021	Digital	ark:/87602/m4/M140433	215.00			terrestrial	fossorial	Weisbecker & Schmid, 2007	*	*	*
218	Euarchontoglires	Rodentia	Cuniculidae	Cuniculus_paca	MNHN-1889-138	Caliper	-	1590.57			terrestrial	terrestrialquad	Weisbecker & Schmid, 2007	*	*	*
219	Euarchontoglires	Rodentia	Cuniculidae	Cuniculus_taczanowskii	FMNH:Mamm:70804	Digital	ark:/87602/m4/M141347	8999.95			terrestrial	terrestrialquad	Weisbecker & Schmid, 2007	*	*	
220	Euarchontoglires	Rodentia	Dasyproctidae	Dasyprocta_prymnolopha	MNHN-1934-599	Caliper	-	2900.00			terrestrial	terrestrialquad	Weisbecker & Schmid, 2007	*	*	*
221	Euarchontoglires	Rodentia	Dasyproctidae	Dasyprocta_punctata	FMNH:Mamm:60569	Digital	ark:/87602/m4/M141358	2309.12			terrestrial	terrestrialquad	Weisbecker & Schmid, 2007	*	*	
222	Euarchontoglires	Rodentia	Dasyproctidae	Myoprocta_acouchy	MNHN-1924-357	Caliper	-	954.87			terrestrial	terrestrialquad	Weisbecker & Schmid, 2007	*	*	*
223	Euarchontoglires	Rodentia	Diatomyidae	Laonastes_aenigmamus	NHMUK:zoo:zd 1999.74	Digital	ark:/87602/m4/M155040	374.00		Jenkins, et al. 2005b	terrestrial	terrestrialquad	Jenkins et al., 2005	*	*	*
224	Euarchontoglires	Rodentia	Dipodidae	Allactaga_elater	UF:Mammal:30045	Digital	ark:/87602/m4/M133921	59.00			terrestrial	terrestrialbip	Chen & Wilson, 2015	*	*	*
225	Euarchontoglires	Rodentia	Dipodidae	Dipus_sagitta	MVZ:Mamm:176844	Digital	ark:/87602/m4/M85272	89.00			terrestrial	terrestrialbip	Verde Arregoitia et al., 2017		*	*
226	Euarchontoglires	Rodentia	Dipodidae	Euchoreutes_naso	MVZ:Mamm:179169	Digital	ark:/87602/m4/M85278	30.70		Stubbe, et al. 2007	terrestrial	terrestrialbip	Verde Arregoitia et al., 2017		*	*
227	Euarchontoglires	Rodentia	Dipodidae	Jaculus_jaculus	UMMZ:Mamm:120204	Digital	doi:10.17602/M2/M64399	59.80			terrestrial	terrestrialbip	Chen & Wilson, 2015	*	*	*
228	Euarchontoglires	Rodentia	Dipodidae	Pygeretmus_pumilio	MSB:Mamm:268220	Digital	ark:/87602/m4/M125126	52.24			terrestrial	terrestrialbip	Samuels & Van Valkenburgh, 2008		*	*
229	Euarchontoglires	Rodentia	Dipodidae	Salpingotus_crassicauda	UMMZ:Mamm:120123	Digital	ark:/87602/m4/M68587	9.50		Freudenthal & Suárez, 2013	terrestrial	terrestrialbip	Verde Arregoitia et al., 2017	*	*	*
230	Euarchontoglires	Rodentia	Dipodidae	Stylodipus_andrewsi	MVZ:Mamm:176848	Digital	ark:/87602/m4/M98701	75.32		Shenbrot, et al 2017	terrestrial	terrestrialbip	Verde Arregoitia et al., 2017	*	*	*
231	Euarchontoglires	Rodentia	Echimyidae	Hoplomys_gymnurus	MSB:Mamm:263519	Digital	ark:/87602/m4/M158897	281.42			terrestrial	semifossorial	Nowak, 1999		*	*
232	Euarchontoglires	Rodentia	Echimyidae	Hoplomys_gymnurus	MSB:Mamm:263528	Digital	ark:/87602/m4/M158898	281.42			terrestrial	semifossorial	Nowak, 1999		*	*
233	Euarchontoglires	Rodentia	Echimyidae	Isothrix_bistriata	MVZ:Mamm:191300	Digital	ark:/87602/m4/M85288	444.99			terrestrial	arboreal	Nowak, 1999	*	*	*
234	Euarchontoglires	Rodentia	Echimyidae	Lonchothrix_emiliae	AMNH:Mamm:m-95787	Digital	ark:/87602/m4/M101252	138.20			terrestrial	arboreal	Nowak, 1999	*	*	*
235	Euarchontoglires	Rodentia	Echimyidae	Makalata_didelphoides	UM-861-V	Digital	Montpellier	398.66			terrestrial	arboreal	Nowak, 1999		*	*
236	Euarchontoglires	Rodentia	Echimyidae	Myocastor_coypus	MNHN-ZM-AC-1906-45	Caliper	-	6361.55			semiaquatic	semiaquatic	Guichón et al., 2003	*	*	*
237	Euarchontoglires	Rodentia	Echimyidae	Phyllomys_brasiliensis	MNHN-ZM-MO-1898-1848	Digital	Montpellier	312.49			terrestrial	arboreal	Emmons et al., 2002		*	*
238	Euarchontoglires	Rodentia	Echimyidae	Proechimys_guyannensis	NHMUK:79.322	Digital	ark:/87602/m4/M154965	314.03			terrestrial	terrestrialquad	Hopkins & Davis, 2009	*	*	*
239	Euarchontoglires	Rodentia	Echimyidae	Proechimys_semispinosus	UMMZ:Mamm:115393	Digital	ark:/87602/m4/M82215	353.32			terrestrial	terrestrialquad	Hopkins & Davis, 2009	*	*	*
240	Euarchontoglires	Rodentia	Erethizontidae	Coendou_prehensilis	MNHN-ZM-AC-1959-119	Caliper	-	4116.20			terrestrial	arboreal	Weisbecker & Schmid, 2007	*	*	*
241	Euarchontoglires	Rodentia	Geomyidae	Cratogeomys_castanops	MSB:Mamm:63804	Digital	ark:/87602/m4/M165468	266.83			terrestrial	fossorial	Verde Arregoitia et al., 2017		*	*
242	Euarchontoglires	Rodentia	Geomyidae	Geomys_pinetis	UF:Mammal:10349	Digital	ark:/87602/m4/M140446	201.15			terrestrial	fossorial	Chen & Wilson, 2015	*	*	*
243	Euarchontoglires	Rodentia	Geomyidae	Thomomys_mazama	UWMB:Mammal:38906	Digital	ark:/87602/m4/M140852	93.07			terrestrial	fossorial	Hopkins & Davis, 2009	*	*	*
244	Euarchontoglires	Rodentia	Gliridae	Dryomys_nitedula	UMMZ:Mamm:123085	Digital	doi:10.17602/M2/M64400	29.50			terrestrial	arboreal	Verde Arregoitia et al., 2017	*	*	*
245	Euarchontoglires	Rodentia	Gliridae	Eliomys_sp	E14	Digital	Montpellier	107.49	Body mass of genus average.		terrestrial	arboreal	Verde Arregoitia et al., 2017		*	*
246	Euarchontoglires	Rodentia	Gliridae	Glis_glis	UMMZ:Mamm:113304	Digital	doi:10.17602/M2/M64395	128.09			terrestrial	arboreal	Chen & Wilson, 2015	*	*	*
247	Euarchontoglires	Rodentia	Gliridae	Graphiurus_murinus	YPM:VZ:Mamm 014485	Digital	ark:/87602/m4/M89787	20.07			terrestrial	arboreal	Nowak, 1999	*	*	*
248	Euarchontoglires	Rodentia	Gliridae	Muscardinus_avellanarius	UMMZ:Mamm:103438	Digital	doi:10.17602/M2/M64392	29.19			terrestrial	arboreal	Verde Arregoitia et al., 2017	*	*	*
249	Euarchontoglires	Rodentia	Heterocephalidae	Heterocephalus_glaber	UMMZ:Mamm:172915	Digital	ark:/87602/m4/M68614	39.36			terrestrial	fossorial	Samuels & Van Valkenburgh, 2008	*	*	*
250	Euarchontoglires	Rodentia	Heterocephalidae	Heterocephalus_glaber	UF:Mammal:6289	Digital	ark:/87602/m4/M140449	39.36			terrestrial	fossorial	Samuels & Van Valkenburgh, 2008	*	*	*
251	Euarchontoglires	Rodentia	Heteromyidae	Chaetodipus_penicillatus	UF:Mammal:10053	Digital	ark:/87602/m4/M140401	15.57			terrestrial	terrestrialquad	Nowak, 1999	*	*	*
252	Euarchontoglires	Rodentia	Heteromyidae	Dipodomys_deserti	UWMB:Mammal:38049	Digital	ark:/87602/m4/M140434	107.63			terrestrial	terrestrialbip	Chen & Wilson, 2015	*	*	*
253	Euarchontoglires	Rodentia	Heteromyidae	Dipodomys_merriami	UF:Mamm:23955	Digital	ark:/87602/m4/M140438	37.91			terrestrial	terrestrialbip	Nowak, 1999		*	*
254	Euarchontoglires	Rodentia	Heteromyidae	Heteromys_nelsoni	UMMZ:Mamm:114492	Digital	ark:/87602/m4/M64396	67.55			terrestrial	semifossorial	Nowak, 1999	*	*	*
255	Euarchontoglires	Rodentia	Heteromyidae	Microdipodops_megacephalus	MVZ:Mamm:171003	Digital	ark:/87602/m4/M85197	12.30			terrestrial	terrestrialbip	Nowak, 1999	*	*	*
256	Euarchontoglires	Rodentia	Heteromyidae	Perognathus_fasciatus	UMMZ:Mamm:75340	Digital	ark:/87602/m4/M68625	11.29			terrestrial	semifossorial	Nowak, 1999	*	*	*
257	Euarchontoglires	Rodentia	Hystricidae	Atherurus_macrourus	MVZ:Mamm:186560	Digital	ark:/87602/m4/M99369	2000.00			terrestrial	terrestrialquad	Nowak, 1999	*	*	*
258	Euarchontoglires	Rodentia	Hystricidae	Hystrix_cristata	MNHN-ZM-AC-1933-35	Caliper	-	13406.27			terrestrial	semifossorial	Samuels & Van Valkenburgh, 2008	*	*	*
259	Euarchontoglires	Rodentia	Hystricidae	Trichys_fasciculata	UMZC:Vertebrates:e.3496	Digital	ark:/87602/m4/M164559	1750.00			terrestrial	scansorial	Reister, 2006	*	*	*
260	Euarchontoglires	Rodentia	Muridae	Acomys_cahirinus	YPM:VZ:Mamm 005794	Digital	ark:/87602/m4/M64826	41.16			terrestrial	terrestrialquad	Nowak, 1999	*	*	*
261	Euarchontoglires	Rodentia	Muridae	Apodemus_agrarius	UMMZ:Mamm:62380	Digital	ark:/87602/m4/M68622	21.11			terrestrial	terrestrialquad	Verde Arregoitia et al., 2017	*	*	*
262	Euarchontoglires	Rodentia	Muridae	Apomys_littoralis	UMMZ:Mamm:160321	Digital	ark:/87602/m4/M70176	30.95			terrestrial	terrestrialquad	Nowak, 1999	*	*	*
263	Euarchontoglires	Rodentia	Muridae	Arvicanthis_niloticus	UMMZ:Mamm:157598	Digital	ark:/87602/m4/M68606	95.80			terrestrial	semifossorial	John, 2005	*	*	*
264	Euarchontoglires	Rodentia	Muridae	Bandicota_bengalensis	UF:Mamm:27601	Digital	ark:/87602/m4/M140386	226.99			terrestrial	semifossorial	Nowak, 1999		*	*
265	Euarchontoglires	Rodentia	Muridae	Chiropodomys_gliroides	FMNH:Mamm:46730	Digital	ark:/87602/m4/M162901	23.68			terrestrial	arboreal	Nowak, 1999		*	*
266	Euarchontoglires	Rodentia	Muridae	Chrotomys_gonzalesi	FMNH:Mamm:147175	Digital	ark:/87602/m4/M159896	140.20			terrestrial	semifossorial	Martinez et al., 2018	*	*	*
267	Euarchontoglires	Rodentia	Muridae	Chrotomys_whiteheadi	UMMZ:Mamm:174496	Digital	ark:/87602/m4/M70178	54.33			terrestrial	semifossorial	Martinez et al., 2018		*	*
268	Euarchontoglires	Rodentia	Muridae	Colomys_goslingi	FMNH:Mamm:227792	Digital	ark:/87602/m4/M162903	62.50			semiaquatic	semiaquatic	Hood, 2020		*	*

	Superord. group	Order	Family	Species	Institution Voucher	Method	MorpoSouce ID	Mass (g)	OBS	Body mass additional reference (if not Jones et al., 2009)	Medium (Ch3)	Locomotor ecology (Ch4)	Ecology reference	Ch2	Ch3	Ch4
269	Euarchontoglires	Rodentia	Muridae	Dasymys_incomtus	FMNH:Mamm:21260	Digital	ark:/87602/m4/M159916	127.75			semiaquatic	semiaquatic	Hood, 2020		*	*
270	Euarchontoglires	Rodentia	Muridae	Deomys_ferrugineus	MNHN-ZM-MO-1996-707	Digital	Montpellier	57.60			semiaquatic	semiaquatic	Hood, 2020		*	*
271	Euarchontoglires	Rodentia	Muridae	Desmodillus_auricularis	UMMZ:Mamm:111122	Digital	ark:/87602/m4/M68567	54.81			terrestrial	semifossorial	Nowak, 1999	*	*	*
272	Euarchontoglires	Rodentia	Muridae	Desmomys_yaldeni	CBUN-ETH1422	Digital	Montpellier	47.00		Lavrenchenko, 2003	terrestrial	scansorial	Nowak, 1999		*	*
273	Euarchontoglires	Rodentia	Muridae	Gerbilliscus_kempi	MNHN-ZM-MO-1992-1714	Digital	Montpellier	100.83			terrestrial	semifossorial	Nowak, 1999		*	*
274	Euarchontoglires	Rodentia	Muridae	Gerbillus_gerbillus	UMMZ:Mamm:156635	Digital	ark:/87602/m4/M68605	26.99			terrestrial	semifossorial	Nowak, 1999	*	*	*
275	Euarchontoglires	Rodentia	Muridae	Golunda_ellioti	NHMUK:ZD:1887.3.4.7	Digital	ark:/87602/m4/M164547	60.73			terrestrial	terrestrialquad	Nowak, 1999		*	*
276	Euarchontoglires	Rodentia	Muridae	Grammomys_dolichurus	MVZ:Mamm:220992	Digital	ark:/87602/m4/M85203	41.85			terrestrial	arboreal	Nowak, 1999	*	*	*
277	Euarchontoglires	Rodentia	Muridae	Hapalomys_longicaudatus	AMNH:Mamm:m-242685	Digital	ark:/87602/m4/M101291	70.00			terrestrial	arboreal	Nowak, 1999		*	*
278	Euarchontoglires	Rodentia	Muridae	Hybomys_univittatus	MVZ:Mamm:196296	Digital	ark:/87602/m4/M85202	54.46			terrestrial	terrestrialquad	Nowak, 1999	*	*	*
279	Euarchontoglires	Rodentia	Muridae	Hydromys_chrysogaster	MVZ:Mamm:175330	Digital	ark:/87602/m4/M99366	626.17			semiaquatic	semiaquatic	Hood, 2020	*	*	*
280	Euarchontoglires	Rodentia	Muridae	Hylomyscus_stella	NHMUK:Zoo:1976.1611	Digital	ark:/87602/m4/M164548	18.99			terrestrial	arboreal	Nowak, 1999		*	*
281	Euarchontoglires	Rodentia	Muridae	Hyorhinomys_stuempkei	C37198	Digital	Montpellier	202.75		Esselstyn et al., 2015	terrestrial	terrestrialquad	Rowe & Kennerley, 2019		*	*
282	Euarchontoglires	Rodentia	Muridae	Leggadina_forresti	MV-C9362	Digital	Montpellier	23.88			terrestrial	terrestrialquad	Verde Arregoitia et al., 2017		*	*
283	Euarchontoglires	Rodentia	Muridae	Lenothrix_canus	AMNH:Mamm:m-240359	Digital	ark:/87602/m4/M100502	150.00			terrestrial	arboreal	Nowak, 1999		*	*
284	Euarchontoglires	Rodentia	Muridae	Leopoldamys_sabanus	UMMZ:Mamm:174506	Digital	ark:/87602/m4/M68617	347.61			terrestrial	terrestrialquad	Nowak, 1999	*	*	*
285	Euarchontoglires	Rodentia	Muridae	Lophuromys_flavopunctatus	UMMZ:Mamm:114774	Digital	ark:/87602/m4/M68578	57.07			terrestrial	terrestrialquad	Nowak, 1999	*	*	*
286	Euarchontoglires	Rodentia	Muridae	Lorentzimys_nouhuysi	AMNH:Mamm:279098	Digital	ark:/87602/m4/M100505	14.44			terrestrial	arboreal	Verde Arregoitia et al., 2017		*	*
287	Euarchontoglires	Rodentia	Muridae	Malacomys_longipes	UMZC:Vertebrates:e.2265	Digital	ark:/87602/m4/M140841	95.64			terrestrial	terrestrialquad	Nowak, 1999		*	*
288	Euarchontoglires	Rodentia	Muridae	Mastacomys_fuscus	MV-C10003	Digital	Montpellier	125.72			terrestrial	terrestrialquad	Verde Arregoitia et al., 2017		*	*
289	Euarchontoglires	Rodentia	Muridae	Mastomys_sp	UMMZ:Mamm:120407	Digital	ark:/87602/m4/M70169	51.56	Body mass of genus average.		terrestrial	terrestrialquad	Verde Arregoitia et al., 2017	*	*	*
290	Euarchontoglires	Rodentia	Muridae	Melasmothrix_naso	AMNH:Mamm:m-223965	Digital	ark:/87602/m4/M100500	47.70		Esselstyn et al., 2015	terrestrial	terrestrialquad	Nowak, 1999		*	*
291	Euarchontoglires	Rodentia	Muridae	Melomys_burtoni	MV-C26645	Digital	Montpellier	71.29			terrestrial	terrestrialquad	Nowak, 1999		*	*
292	Euarchontoglires	Rodentia	Muridae	Meriones_tamariscinus	UMMZ:Mamm:119320	Digital	ark:/87602/m4/M68583	120.00		Tchabovsky & Bazykin, 2004	terrestrial	semifossorial	Nowak, 1999	*	*	*
293	Euarchontoglires	Rodentia	Muridae	Micaelamys_namaquensis	CBUN-ANG001	Digital	Montpellier	57.10			terrestrial	scansorial	Nowak, 1999		*	*
294	Euarchontoglires	Rodentia	Muridae	Micromys_minutus	UMMZ:Mamm:108469	Digital	ark:/87602/m4/M82214	6.99			terrestrial	arboreal	Verde Arregoitia et al 2017	*	*	*
295	Euarchontoglires	Rodentia	Muridae	Millardia_meltada	MVZ:Mamm:182980	Digital	ark:/87602/m4/M99367	67.17			terrestrial	semifossorial	Nowak, 1999	*	*	*
296	Euarchontoglires	Rodentia	Muridae	Mus_musculus	YPM:VZ:Mamm 005792	Digital	ark:/87602/m4/M64828	19.30			terrestrial	terrestrialquad	Verde Arregoitia et al., 2017	*	*	*
297	Euarchontoglires	Rodentia	Muridae	Mus_musculus	UMMZ:Mamm:57532	Digital	ark:/87602/m4/M82217	19.30			terrestrial	terrestrialquad	Verde Arregoitia et al., 2017	*	*	*
298	Euarchontoglires	Rodentia	Muridae	Nesokia_indica	UMMZ:Mamm:120203	Digital	ark:/87602/m4/M68588	178.08			terrestrial	semifossorial	Nowak, 1999	*	*	*
299	Euarchontoglires	Rodentia	Muridae	Niviventer_rapit	UMMZ:Mamm:174433	Digital	ark:/87602/m4/M70177	79.73			terrestrial	scansorial	Wilson et al., 2017		*	*
300	Euarchontoglires	Rodentia	Muridae	Oenomys_hypoxanthus	AMNH:Mamm:m-55684	Digital	ark:/87602/m4/M101251	89.84			terrestrial	terrestrialquad	Wilson et al., 2017		*	*
301	Euarchontoglires	Rodentia	Muridae	Otomys_irroratus	MVZ:Mamm:117728	Digital	ark:/87602/m4/M85262	114.45			terrestrial	terrestrialquad	Nowak, 1999	*	*	*
302	Euarchontoglires	Rodentia	Muridae	Pachyuromys_duprasi	YPM:VZ:Mamm 005826	Digital	ark:/87602/m4/M85263	47.50			terrestrial	terrestrialquad	Nowak, 1999	*	*	*
303	Euarchontoglires	Rodentia	Muridae	Pachyuromys_duprasi	UMMZ:Mamm:119424	Digital	ark:/87602/m4/M82770	47.50			terrestrial	terrestrialquad	Nowak, 1999	*	*	*
304	Euarchontoglires	Rodentia	Muridae	Paraleptomys_wilhelmina	AMNH:Mamm:m-152744	Digital	ark:/87602/m4/M101283	33.68			terrestrial	terrestrialquad	Nowak, 1999		*	*
305	Euarchontoglires	Rodentia	Muridae	Paruromys_dominator	MVZ:Mamm:225789	Digital	ark:/87602/m4/M85291	325.31			terrestrial	terrestrialquad	Nowak, 1999	*	*	*
306	Euarchontoglires	Rodentia	Muridae	Pelomys_fallax	CBUN-RS1371	Digital	Montpellier	120.46			semiaquatic	semiaquatic	Hood, 2020		*	*
307	Euarchontoglires	Rodentia	Muridae	Pogonomys_loriae	AMNH:Mamm:m-193163	Digital	ark:/87602/m4/M101284	95.39			terrestrial	scansorial	Nowak, 1999		*	*
308	Euarchontoglires	Rodentia	Muridae	Praomys_sp	MCZ:Mamm:62412	Digital	ark:/87602/m4/M84303	37.75	Body mass of genus average.		terrestrial	scansorial	Nowak, 1999	*	*	*
309	Euarchontoglires	Rodentia	Muridae	Psammomys_obesus	UMMZ:Mamm:119326	Digital	ark:/87602/m4/M68584	102.15			terrestrial	semifossorial	Nowak, 1999	*	*	*
310	Euarchontoglires	Rodentia	Muridae	Pseudomys_hermannsburgensis	NHMUK:Zoo:zd 1970.1117	Digital	ark:/87602/m4/M154978	13.38			terrestrial	terrestrialquad	Verde Arregoitia et al., 2017		*	*
311	Euarchontoglires	Rodentia	Muridae	Pseudomys_higginsi	YPM:VZ:Mamm 005701	Digital	ark:/87602/m4/M90672	63.16			terrestrial	terrestrialquad	Verde Arregoitia et al.,	*	*	*
312	Euarchontoglires	Rodentia	Muridae	Rattus_norvegicus	UMMZ:Mamm:167022	Digital	doi:10.17602/M2/M82216	282.89			terrestrial	terrestrialquad	Samuels & Van Valkenburgh, 2008	*	*	*
313	Euarchontoglires	Rodentia	Muridae	Rhabdomys_pumilio	MVZ:Mamm:117451	Digital	ark:/87602/m4/M98041	40.73			terrestrial	terrestrialquad	Nowak, 1999	*	*	*
314	Euarchontoglires	Rodentia	Muridae	Rhombomys_opimus	UMMZ:Mamm:108460	Digital	ark:/87602/m4/M68559	192.50		Freudenthal & Suárez, 2013	terrestrial	semifossorial	Nowak, 1999	*	*	*
315	Euarchontoglires	Rodentia	Muridae	Rhynchomys_isarogensis	USNM11XXX	Digital	Montpellier	122.29			terrestrial	terrestrialquad	GBIF Secretariat, 2022f		*	*
316	Euarchontoglires	Rodentia	Muridae	Sekeetamys_calurus	UMMZ:Mamm:119351	Digital	ark:/87602/m4/M68585	56.61			terrestrial	semifossorial	Nowak, 1999	*	*	*
317	Euarchontoglires	Rodentia	Muridae	Stenocephalemys_albocaudata	CM:Mamm:52575	Digital	ark:/87602/m4/M95877	144.00			terrestrial	terrestrialquad	GBIF Secretariat, 2022g	*	*	*
318	Euarchontoglires	Rodentia	Muridae	Stenocephalemys_griseicauda	CM:Mamm:48632	Digital	ark:/87602/m4/M96127	85.75			terrestrial	terrestrialquad	GBIF Secretariat, 2022h	*	*	*
319	Euarchontoglires	Rodentia	Muridae	Sundamys_muelleri	UMMZ:Mamm:174437	Digital	ark:/87602/m4/M68616	356.48			terrestrial	terrestrialquad	Nowak, 1999	*	*	*
320	Euarchontoglires	Rodentia	Muridae	Taeromys_celebensis	AMNH:Mamm:m-223291	Digital	ark:/87602/m4/M100499	252.70		Fabre et al., 2018	terrestrial	scansorial	Nowak, 1999		*	*
321	Euarchontoglires	Rodentia	Muridae	Tateomys_rhinogradoides	AMNH:Mamm:m-223968	Digital	ark:/87602/m4/M101289	86.50		Rowe et al., 2016	terrestrial	terrestrialquad	Nowak, 1999		*	*
322	Euarchontoglires	Rodentia	Muridae	Tatera_indica	UMMZ:Mamm:119378	Digital	ark:/87602/m4/M68586	138.28			terrestrial	terrestrialquad	Chen & Wilson, 2015	*	*	*
323	Euarchontoglires	Rodentia	Muridae	Taterillus_emini	UMMZ:Mamm:122871	Digital	ark:/87602/m4/M70170	52.50	Synonym T. harringtoni	Freudenthal & Suárez, 2013	terrestrial	semifossorial	Nowak, 1999	*	*	*
324	Euarchontoglires	Rodentia	Muridae	Thallomys_sp	CBUN-ANG0157	Digital	Montpellier	101.10	Body mass of genus average.		terrestrial	scansorial	Nowak, 1999		*	*
325	Euarchontoglires	Rodentia	Muridae	Tokudaia_muenninki	MSU:MR:MR.12513	Digital	ark:/87602/m4/M86158	148.40		Yamada et al., 2010	terrestrial	terrestrialquad	Nowak, 1999	*	*	*
326	Euarchontoglires	Rodentia	Muridae	Uromys_sp	MV-C16497	Digital	Montpellier	628.46	Body mass of genus average.		terrestrial	arboreal	Verde Arregoitia et al., 2017		*	*
327	Euarchontoglires	Rodentia	Muridae	Vandeleuria_oleracea	AMNH:Mamm:m-241515	Digital	ark:/87602/m4/M100503	10.00		Smith et al., 2018	terrestrial	arboreal	Nowak, 1999		*	*
328	Euarchontoglires	Rodentia	Muridae	Zyzomys_argurus	AMNH:Mamm:m-197322	Digital	ark:/87602/m4/M100498	40.42			terrestrial	terrestrialquad	Verde Arregoitia et al., 2017		*	*

	Superord. group	Order	Family	Species	Institution Voucher	Method	MorpoSouce ID	Mass (g)	OBS	Body mass additional reference (if not Jones et al., 2009)	Medium (Ch3)	Locomotor ecology (Ch4)	Ecology reference	Ch2	Ch3	Ch4
329	Euarchontoglires	Rodentia	Nesomyidae	Brachytarsomys_albicauda	MVZ:Mamm:223935	Digital	ark:/87602/m4/M85290	200.00			terrestrial	arboreal	Verde Arregoitia et al., 2017	*	*	*
330	Euarchontoglires	Rodentia	Nesomyidae	Cricetomys_gambianus	NHMUK:ZD:1890.3.27.2	Digital	ark:/87602/m4/M155027	1267.52			terrestrial	semifossorial	Nowak, 1999	*	*	*
331	Euarchontoglires	Rodentia	Nesomyidae	Gymnuromys_roberti	FMNH:Mamm:161906	Digital	ark:/87602/m4/M159926	97.50			terrestrial	terrestrialquad	Verde Arregoitia et al., 2017	*	*	*
332	Euarchontoglires	Rodentia	Nesomyidae	Hypogeomys_antimena	FMNH:Mamm:151994	Digital	ark:/87602/m4/M159947	1175.93			terrestrial	semifossorial	Nowak, 1999	*	*	
333	Euarchontoglires	Rodentia	Nesomyidae	Macrotarsomys_bastardi	FMNH:Mamm:179397	Digital	ark:/87602/m4/M159959	28.45			terrestrial	terrestrialquad	Nowak, 1999	*	*	*
334	Euarchontoglires	Rodentia	Nesomyidae	Malacothrix_typica	UMMZ:Mamm:117815	Digital	ark:/87602/m4/M141168	17.02			terrestrial	semifossorial	Nowak, 1999	*	*	*
335	Euarchontoglires	Rodentia	Nesomyidae	Monticolomys_koopmani	FMNH:Mamm:161705	Digital	ark:/87602/m4/M159972	25.00			terrestrial	scansorial	Nowak, 1999	*	*	*
336	Euarchontoglires	Rodentia	Nesomyidae	Nesomys_rufus	FMNH:Mamm:173271	Digital	ark:/87602/m4/M159987	163.96			terrestrial	terrestrialquad	Chen & Wilson, 2015	*	*	*
337	Euarchontoglires	Rodentia	Nesomyidae	Saccostomus_campestris	MVZ:Mamm:118603	Digital	ark:/87602/m4/M98043	50.33			terrestrial	semifossorial	Nowak, 1999	*	*	*
338	Euarchontoglires	Rodentia	Nesomyidae	Steatomys_pratensis	MSU:MR:MR.24868	Digital	ark:/87602/m4/M86528	30.58			terrestrial	semifossorial	Nowak, 1999	*	*	*
339	Euarchontoglires	Rodentia	Octodontidae	Octodon_degus	MSB:Mamm:132851	Digital	ark:/87602/m4/M125080	203.27			terrestrial	semifossorial	Chen & Wilson, 2015		*	*
340	Euarchontoglires	Rodentia	Octodontidae	Spalacopus_cyanus	FMNH:Mamm:49943	Digital	ark:/87602/m4/M157846	100.86			terrestrial	fossorial	Weisbecker & Schmid, 2007		*	*
341	Euarchontoglires	Rodentia	Platacanthomyidae	Typhlomys_chapensis	UM	Digital	Montpellier	16.93		Cheng et al., 2017	terrestrial	arboreal	Smith, 2017		*	*
342	Euarchontoglires	Rodentia	Sciuridae	Belomys_pearsonii	AMNH:Mamm:m-274181	Digital	ark:/87602/m4/M101246	217.00		Smith et al., 2018	semiaerial	gliding	Jackson, 2000		*	*
343	Euarchontoglires	Rodentia	Sciuridae	Callosciurus_notatus	NHMUK:Zoo:1975.1337	Digital	ark:/87602/m4/M157332	209.49			terrestrial	arboreal	Nowak, 1999		*	*
344	Euarchontoglires	Rodentia	Sciuridae	Cynomys_ludovicianus	MNHN-ZM-AC-1895-4	Caliper		797.05			terrestrial	semifossorial	Chen & Wilson, 2015	*	*	*
345	Euarchontoglires	Rodentia	Sciuridae	Dremomys_pernyi	MVZ:Mamm:180961	Digital	ark:/87602/m4/M85281	198.63			terrestrial	scansorial	Nowak, 1999	*	*	*
346	Euarchontoglires	Rodentia	Sciuridae	Funambulus_pennantii	UF:Mamm:29482	Digital	ark:/87602/m4/M140445	102.49			terrestrial	scansorial	Stalder, 2009		*	*
347	Euarchontoglires	Rodentia	Sciuridae	Funisciurus_anerythrus	YPM:VZ:Mamm 014449	Digital	ark:/87602/m4/M91244	223.54			terrestrial	arboreal	Nowak, 1999	*	*	*
348	Euarchontoglires	Rodentia	Sciuridae	Glaucomys_volans	YPM:VZ:Mamm 005215	Digital	ark:/87602/m4/M65302	71.90			semiaerial	gliding	Chen & Wilson, 2015	*	*	*
349	Euarchontoglires	Rodentia	Sciuridae	Heliosciurus_rufobrachium	YPM:VZ:Mamm 014455	Digital	ark:/87602/m4/M95040	332.88			terrestrial	scansorial	Chen & Wilson, 2015	*	*	*
350	Euarchontoglires	Rodentia	Sciuridae	Hyosciurus_heinrichi	AMNH:Mamm:m-223548	Digital	ark:/87602/m4/M101288	296.00		Hayssen, 2008	terrestrial	terrestrialquad	Cassola, 2016b		*	*
351	Euarchontoglires	Rodentia	Sciuridae	Lariscus_insignis	MVZ:Mamm:192194	Digital	ark:/87602/m4/M85289	174.41			terrestrial	terrestrialquad	Nowak, 1999	*	*	*
352	Euarchontoglires	Rodentia	Sciuridae	Marmota_marmota	MNHN-1919-60	Caliper	-	4059.15			terrestrial	semifossorial	Nowak, 1999	*	*	*
353	Euarchontoglires	Rodentia	Sciuridae	Paraxerus_cepapi	MVZ:Mamm:120841	Digital	ark:/87602/m4/M84951	222.85			terrestrial	arboreal	Pronga, 2017	*	*	*
354	Euarchontoglires	Rodentia	Sciuridae	Petaurista_petaurista	MNHN-ZM-AC-1958-102	Caliper	-	1533.84			semiaerial	gliding	Jackson, 2000	*	*	*
355	Euarchontoglires	Rodentia	Sciuridae	Prosciurillus_leucomus	AMNH:Mamm:m-223534	Digital	ark:/87602/m4/M101287	158.27		Hayssen, 2008	terrestrial	scansorial	Nowak, 1999		*	*
356	Euarchontoglires	Rodentia	Sciuridae	Ratufa_indica	MNHN-ZM-AC-1966-65	Caliper	-	1060.00			terrestrial	arboreal	Nowak, 1999	*	*	*
357	Euarchontoglires	Rodentia	Sciuridae	Rubrisciurus_rubriventer	AMNH:Mamm:m-223024	Digital	ark:/87602/m4/M101286	688.10		Hayssen, 2008	terrestrial	arboreal	Nowak, 1999		*	*
358	Euarchontoglires	Rodentia	Sciuridae	Sciurus_vulgaris	UMMZ:Mamm:80280	Digital	doi:10.17602/M2/M97682	333.00			terrestrial	arboreal	Verde Arregoitia et al., 2017	*	*	*
359	Euarchontoglires	Rodentia	Sciuridae	Spermophilopsis_leptodactylus	UMMZ:Mamm:119250	Digital	ark:/87602/m4/M141258	600.00		Smith et al., 2018	terrestrial	semifossorial	Hopkins & Davis 2008		*	*
360	Euarchontoglires	Rodentia	Sciuridae	Spermophilus_sp	DU:EA:166	Digital	doi:10.17602/M2/M27306	353.19	Body mass of genus average.		terrestrial	semifossorial	Samuels & Van Valkenburgh, 2008; Verde Arregoitia et al., 2017	*	*	*
361	Euarchontoglires	Rodentia	Sciuridae	Tamias_striatus	YPM:VZ:Mamm 014464	Digital	ark:/87602/m4/M64827	154.00		Freudenthal & Suárez, 2013	terrestrial	scansorial	Kroll, 2013	*	*	*
362	Euarchontoglires	Rodentia	Sciuridae	Tamiasciurus_hudsonicus	UMMZ:Mamm:113549	Digital	ark:/87602/m4/M164465	200.24			terrestrial	scansorial	Nowak, 1999		*	*
363	Euarchontoglires	Rodentia	Sciuridae	Tamiops_maritimus	MVZ:Mamm:180950	Digital	ark:/87602/m4/M85280	66.77			terrestrial	arboreal	Hopkins & Davis 2008	*	*	*
364	Euarchontoglires	Rodentia	Sciuridae	Xerus_erythropus	NHMUK:Zoo:1890.6.15.1	Digital	ark:/87602/m4/M164546	602.23			terrestrial	semifossorial	Hopkins & Davis, 2009		*	*
365	Euarchontoglires	Rodentia	Sminthidae	Sicista_concolor	UF:Mamm:27336	Digital	ark:/87602/m4/M140651	10.00		Smith et al., 2018	terrestrial	semifossorial	Nowak, 1999		*	*
366	Euarchontoglires	Rodentia	Spalacidae	Myospalax_myospalax	UMMZ:Mamm:110401	Digital	ark:/87602/m4/M141236	356.50		Poor, 2005	terrestrial	fossorial	Nowak, 1999		*	*
367	Euarchontoglires	Rodentia	Spalacidae	Nannospalax_ehrenbergi	MNHN-ZM-MO-1879-1615	Digital	Montpellier	164.35			terrestrial	fossorial	Nowak, 1999		*	*
368	Euarchontoglires	Rodentia	Spalacidae	Spalax_leucodon	UMMZ:Mamm:110416	Digital	ark:/87602/m4/M65513	188.67			terrestrial	fossorial	Samuels & Van Valkenburgh, 2008	*	*	*
369	Euarchontoglires	Rodentia	Spalacidae	Tachyoryctes_splendens	FMNH:Mamm:173826-173827	Digital	ark:/87602/m4/M157876	210.00		Hrouzková et al., 2013	terrestrial	fossorial	Samuels & Van Valkenburgh, 2008	*	*	*
370	Euarchontoglires	Rodentia	Spalacidae	Tachyoryctes_splendens	MVZ:Mamm:183905	Digital	ark:/87602/m4/M98048	227.13			terrestrial	fossorial	Samuels & Van Valkenburgh, 2008		*	*
371	Euarchontoglires	Rodentia	Zapodidae	Napaeozapus_insignis	MSB:Mamm:309389	Digital	ark:/87602/m4/M125073	22.25			terrestrial	terrestrialquad	Samuels & Van Valkenburgh, 2008	*	*	*
372	Euarchontoglires	Rodentia	Zapodidae	Zapus_hudsonius	YPM:VZ:Mamm 005659	Digital	ark:/87602/m4/M64824	18.43			terrestrial	terrestrialquad	Smith, 1999	*	*	*
373	Euarchontoglires	Rodentia	Zenkerellidae	Zenkerella_insignis	NHMUK:5.5.23.27	Digital	ark:/87602/m4/M154996	200.00			terrestrial	arboreal	Nowak, 1999		*	*
374	Euarchontoglires	Scandentia	Cynocephalidae	Cynocephalus_volans	MNHN-A3959	Caliper		1250.00			semiaerial	gliding	Jackson, 2000		*	*
375	Euarchontoglires	Scandentia	Cynocephalidae	Galeopterus_variegatus	NHM-67-1481	Caliper	-	1112.20			semiaerial	gliding	Jackson, 2000		*	*
376	Euarchontoglires	Scandentia	Ptilocercidae	Ptilocercus_lowii	FMNH:Mamm:57450	Digital	ark:/87602/m4/M57402	42.50			terrestrial	arboreal	Nowak, 1999	*	*	*
377	Euarchontoglires	Scandentia	Tupaiidae	Tupaia_dorsalis	UMMZ:Mamm:174427	Digital	ark:/87602/m4/M68615	168.05			terrestrial	scansorial	Nowak, 1999	*	*	*
378	Euarchontoglires	Scandentia	Tupaiidae	Tupaia_sp	DU:EA:179	Digital	doi:10.17602/M2/M28441	156.27	Body mass of genus average.		terrestrial	scansorial	Nowak, 1999	*	*	*
379	Laurasiatheria	Carnivora	Ailuridae	Ailurus_fulgens	MNHN-1960-84	Caliper	-	5170.08			terrestrial	arboreal	Fabre et al., 2015	*	*	*
380	Laurasiatheria	Carnivora	Canidae	Atelocynus_microtis	AMNH-100095	Caliper	-	8363.22			terrestrial	terrestrialquad	Samuels et al., 2013		*	*
381	Laurasiatheria	Carnivora	Canidae	Canis_lupus	MNHN-1962-4165	Caliper	-	31756.51			terrestrial	terrestrialquad	Samuels et al., 2013	*	*	*
382	Laurasiatheria	Carnivora	Canidae	Cerdocyon_thous	MNHN-1973-289	Caliper	-	5741.66			terrestrial	terrestrialquad	Chen & Wilson, 2015; Samuels et al., 2013	*	*	*
383	Laurasiatheria	Carnivora	Canidae	Cerdocyon_thous	MNHN-1921-56	Caliper	-	5741.66			terrestrial	terrestrialquad	Chen & Wilson, 2015; Samuels et al., 2013	*	*	*
384	Laurasiatheria	Carnivora	Canidae	Chrysocyon_brachyurus	AMNH-133941	Caliper	-	23325.00			terrestrial	terrestrialquad	Samuels et al., 2013		*	
385	Laurasiatheria	Carnivora	Canidae	Cuon_alpinus	MNHN-1963-330	Caliper	-	15800.00			terrestrial	terrestrialquad	Samuels et al., 2013	*	*	*
386	Laurasiatheria	Carnivora	Canidae	Lycalopex_gymnocercus	MNHN-1897-410	Caliper	-	4542.67			terrestrial	terrestrialquad	Samuels et al., 2013		*	*
387	Laurasiatheria	Carnivora	Canidae	Lycaon_pictus	MNHN-1902-629	Caliper	-	21999.99			terrestrial	terrestrialquad	Samuels et al., 2013	*	*	*

	Superord. group	Order	Family	Species	Institution Voucher	Method	MorpoSouce ID	Mass (g)	OBS	Body mass additional reference (if not Jones et al., 2009)	Medium (Ch3)	Locomotor ecology (Ch4)	Ecology reference	Ch2	Ch3	Ch4
388	Laurasiatheria	Carnivora	Canidae	Nyctereutes_procyonoides	MNHN-1943-65	Caliper	-	4214.99			terrestrial	terrestrialquad	Samuels et al., 2013	*	*	*
389	Laurasiatheria	Carnivora	Canidae	Otocyon_megalotis	MNHN-1935-115	Caliper	-	4098.12			terrestrial	terrestrialquad	Samuels et al., 2013	*	*	
390	Laurasiatheria	Carnivora	Canidae	Speothos_venaticus	MNHN-2000-368	Caliper	-	6324.54			terrestrial	semifossorial	Samuels et al., 2013	*	*	*
391	Laurasiatheria	Carnivora	Canidae	Urocyon_cinereoargenteus	MNHN-1865-202	Caliper	-	3833.71			terrestrial	scansorial	Chen & Wilson, 2015	*	*	*
392	Laurasiatheria	Carnivora	Canidae	Vulpes_lagopus	MNHN-1909-380	Caliper	-	3584.37			terrestrial	terrestrialquad	Middlebrook, 2007	*	*	*
393	Laurasiatheria	Carnivora	Eupleridae	Cryptoprocta_ferox	MNHN-1963-248	Caliper	-	9500.00			terrestrial	arboreal	Samuels et al., 2013	*	*	*
394	Laurasiatheria	Carnivora	Eupleridae	Eupleres_goudotii	MNHN-ZM-MO-1962-2105	Caliper	-	2763.34			terrestrial	terrestrialquad	Nowak, 1999	*	*	*
395	Laurasiatheria	Carnivora	Eupleridae	Fossa_fossana	MNHN-ZM-MO-1882-1586	Caliper	-	1853.98			terrestrial	terrestrialquad	Samuels et al., 2013	*	*	*
396	Laurasiatheria	Carnivora	Eupleridae	Galidia_elegans	MNHN-ZM-MO-1992-1684	Caliper	-	810.00			terrestrial	scansorial	Samuels et al., 2013	*	*	*
397	Laurasiatheria	Carnivora	Eupleridae	Galidictis_fasciata	MNHN-ZM-MO-1882-1615	Caliper	-	549.99			terrestrial	terrestrialquad	Samuels et al., 2013	*	*	
398	Laurasiatheria	Carnivora	Eupleridae	Mungotictis_decemlineata	MNHN-ZM-MO-1992-1670	Caliper	-	657.03			terrestrial	scansorial	Nowak, 1999	*	*	*
399	Laurasiatheria	Carnivora	Eupleridae	Salanoia_concolor	MNHN-ZM-MO-1961-974	Caliper	-	711.49			terrestrial	terrestrialquad	Nowak, 1999	*	*	
400	Laurasiatheria	Carnivora	Felidae	Acinonyx_jubatus	MNHN-1933-124	Caliper	-	50577.92			terrestrial	terrestrialquad	Samuels et al., 2013	*	*	*
401	Laurasiatheria	Carnivora	Felidae	Caracal_aurata	AMNH-51994	Caliper	-	11277.17			terrestrial	terrestrialquad	Law, 2021		*	
402	Laurasiatheria	Carnivora	Felidae	Caracal_caracal	MNHN-1883-1576	Caliper	-	11964.38			terrestrial	scansorial	Law, 2021	*	*	*
403	Laurasiatheria	Carnivora	Felidae	Catopuma_temminckii	MNHN-1941-293	Caliper	-	7726.46			terrestrial	terrestrialquad	Law, 2021	*	*	*
404	Laurasiatheria	Carnivora	Felidae	Felis_catus	MNHN-squelette monté	Caliper	-	2884.80			terrestrial	scansorial	Anna Toenjes, 2014	*	*	*
405	Laurasiatheria	Carnivora	Felidae	Leopardus_pardalis	MNHN-1873-258	Caliper	-	11880.00			terrestrial	scansorial	Law, 2021	*	*	*
406	Laurasiatheria	Carnivora	Felidae	Leptailurus_serval	MNHN-1888-545	Caliper	-	11999.96			terrestrial	scansorial	Law, 2021	*	*	*
407	Laurasiatheria	Carnivora	Felidae	Lynx_rufus	MNHN-1895-50	Caliper	-	6374.47			terrestrial	scansorial	Samuels et al., 2013	*	*	*
408	Laurasiatheria	Carnivora	Felidae	Neofelis_nebulosa	AMNH-22919	Caliper	-	14945.05			terrestrial	arboreal	Samuels et al., 2013		*	
409	Laurasiatheria	Carnivora	Felidae	Panthera_leo	MNHN-ZM-2020-1586	Caliper	-	158623.93			terrestrial	terrestrialquad	Samuels et al., 2013	*	*	*
410	Laurasiatheria	Carnivora	Felidae	Pardofelis_marmorata	MNHN-ZM-AC-A3424	Caliper	-	2826.68			terrestrial	arboreal	Samuels et al., 2013	*	*	
411	Laurasiatheria	Carnivora	Felidae	Prionailurus_bengalensis	MNHN-1883-1588	Caliper	-	2780.97			terrestrial	scansorial	Law, 2021	*	*	*
412	Laurasiatheria	Carnivora	Felidae	Puma_concolor	AMNH-70409	Caliper	-	53954.05			terrestrial	scansorial	Samuels et al., 2013		*	*
413	Laurasiatheria	Carnivora	Herpestidae	Atilax_paludinosus	MNHN-ZM-AC-1902-37	Caliper	-	3600.16			semiaquatic	semiaquatic	Hood, 2020; Samuels et al., 2013	*	*	*
414	Laurasiatheria	Carnivora	Herpestidae	Crossarchus_sp	AMNH-208107	Caliper	-	1395.09	Body mass of genus average.		terrestrial	terrestrialquad	Chen & Wilson, 2015; Samuels et al., 2013		*	*
415	Laurasiatheria	Carnivora	Herpestidae	Cynictis_penicillata	MNHN-ZM-AC-A3451	Caliper	-	694.41			terrestrial	terrestrialquad	Samuels et al., 2013	*	*	
416	Laurasiatheria	Carnivora	Herpestidae	Dologale_dybowskii	AMNH-51608	Caliper	-	361.92			terrestrial	terrestrialquad	Nowak, 1999		*	
417	Laurasiatheria	Carnivora	Herpestidae	Galerella_sanguinea	MNHN-ZM-AC-1858-27	Caliper	-	543.83			terrestrial	terrestrialquad	Samuels et al., 2013		*	*
418	Laurasiatheria	Carnivora	Herpestidae	Herpestes_ichneumon	MNHN-1882-49	Caliper	-	2980.02			terrestrial	terrestrialquad	Samuels et al., 2013	*	*	*
419	Laurasiatheria	Carnivora	Herpestidae	Ichneumia_albicauda	MNHN-ZM-MO-1939-185	Caliper	-	3628.40			terrestrial	terrestrialquad	Samuels et al., 2013	*	*	*
420	Laurasiatheria	Carnivora	Herpestidae	Ichneumia_albicauda	MNHN-ZM-MO-1918-17B	Caliper	-	3628.40			terrestrial	terrestrialquad	Samuels et al., 2013	*	*	*
421	Laurasiatheria	Carnivora	Herpestidae	Mungos_mungo	MNHN-ZM-AC-1894-414	Caliper	-	1260.00			terrestrial	terrestrialquad	Samuels et al., 2013	*	*	*
422	Laurasiatheria	Carnivora	Herpestidae	Suricata_suricatta	MNHN-A3439	Caliper	-	729.99			terrestrial	semifossorial	van Staaden, 1994	*	*	*
423	Laurasiatheria	Carnivora	Herpestidae	Urva_auropunctata	MNHN-1895-164	Caliper	-	559.50	synonym Herpestes javanicus	Horst et al., 2001	terrestrial	terrestrialquad	Lutz, 2003		*	*
424	Laurasiatheria	Carnivora	Hyaenidae	Crocuta_crocuta	MNHN-1938-87	Caliper	-	63369.98			terrestrial	terrestrialquad	Samuels et al., 2013	*	*	*
425	Laurasiatheria	Carnivora	Hyaenidae	Hyaena_hyaena	MNHN-ZM-AC-1883-1570	Caliper	-	35070.51			terrestrial	terrestrialquad	Samuels et al., 2013	*	*	*
426	Laurasiatheria	Carnivora	Hyaenidae	Proteles_cristata	MNHN-ZM-AC-A3467	Caliper	-	8139.39			terrestrial	terrestrialquad	Samuels et al., 2013	*	*	*
427	Laurasiatheria	Carnivora	Mephitidae	Conepatus_chinga	MNHN-ZM-AC-1897-431	Caliper	-	3400.00		Afflerbaugh, 2002	terrestrial	semifossorial	Fabre et al., 2015	*	*	*
428	Laurasiatheria	Carnivora	Mephitidae	Mephitis_mephitis	MVZ:Mamm:126784	Digital	ark:/87602/m4/M98696	2399.99			terrestrial	semifossorial	Fabre et al., 2015	*	*	*
429	Laurasiatheria	Carnivora	Mephitidae	Mydaus_javanensis	UMZC:Vertebrates:k.1802	Digital	ark:/87602/m4/M164558	2500.00			terrestrial	semifossorial	Fabre et al., 2015	*	*	*
430	Laurasiatheria	Carnivora	Mephitidae	Spilogale_gracilis	UMMZ:Mamm:103458	Digital	-	444.75		Verts et al., 2001	terrestrial	semifossorial	Fabre et al., 2015	*	*	*
431	Laurasiatheria	Carnivora	Mustelidae	Aonyx_capensis	MNHN-ZM-AC-A3388	Caliper	-	19322.22			semiaquatic	semiaquatic	Hood, 2020	*	*	*
432	Laurasiatheria	Carnivora	Mustelidae	Arctonyx_collaris	MNHN-1961-196	Caliper	-	8166.52			terrestrial	semifossorial	Samuels et al., 2013	*	*	*
433	Laurasiatheria	Carnivora	Mustelidae	Eira_barbara	MNHN-1896-361	Caliper	-	4134.99			terrestrial	scansorial	Fabre et al., 2015	*	*	*
434	Laurasiatheria	Carnivora	Mustelidae	Enhydra_lutris	MNHN-ZM-AC-A12503	Caliper	-	27410.93			aquatic	aquatic	Howell 1970; Nowak, 1999	*	*	*
435	Laurasiatheria	Carnivora	Mustelidae	Galictis_vittata	MNHN-ZM-AC-1878-515	Caliper	-	2600.00		Gregg, 2013	terrestrial	terrestrialquad	Fabre et al., 2015	*	*	*
436	Laurasiatheria	Carnivora	Mustelidae	Gulo_gulo	MNHN-ZM-MO-1995-1208	Caliper	-	12792.49			terrestrial	terrestrialquad	Fabre et al., 2015	*	*	*
437	Laurasiatheria	Carnivora	Mustelidae	Ictonyx_striatus	MNHN-ZM-AC-A3402	Caliper	-	811.02			terrestrial	semifossorial	Fabre et al., 2015	*	*	*
438	Laurasiatheria	Carnivora	Mustelidae	Lontra_longicaudis	MNHN-ZM-MO-1976-339	Caliper	-	6554.97			semiaquatic	semiaquatic	Chen & Wilson, 2015; Hood, 2020	*	*	*
439	Laurasiatheria	Carnivora	Mustelidae	Lutra_lutra	MNHN-1962-274	Caliper	-	8868.69			semiaquatic	semiaquatic	Hood, 2020	*	*	*
440	Laurasiatheria	Carnivora	Mustelidae	Lyncodon_patagonicus	MNHN-1897-570	Caliper	-	225.00			terrestrial	terrestrialquad	Malek, 2003	*	*	*
441	Laurasiatheria	Carnivora	Mustelidae	Martes_foina	MNHN-ZM-MO-1992-2030	Caliper	-	1675.00			terrestrial	scansorial	Fabre et al., 2015	*	*	*
442	Laurasiatheria	Carnivora	Mustelidae	Meles_meles	MNHN-1976-333	Caliper	-	11884.03			terrestrial	semifossorial	Fabre et al., 2015	*	*	*
443	Laurasiatheria	Carnivora	Mustelidae	Mellivora_capensis	MNHN-2006-511	Caliper	-	8999.99			terrestrial	semifossorial	Fabre et al., 2015	*	*	*
444	Laurasiatheria	Carnivora	Mustelidae	Melogale_moschata	MNHN-ZM-AC-1892-1015	Caliper	-	938.50			terrestrial	semifossorial	Fabre et al., 2015	*	*	*
445	Laurasiatheria	Carnivora	Mustelidae	Mustela_erminea	UMMZ:Mamm:175894	Digital	doi:10.17602/M2/M57242	284.50			terrestrial	terrestrialquad	Chen & Wilson, 2015	*	*	*
446	Laurasiatheria	Carnivora	Mustelidae	Mustela_frenata	YPM:VZ:Mamm 014733	Digital	ark:/87602/m4/M64575	190.03			terrestrial	terrestrialquad	Samuels et al., 2013	*	*	*
447	Laurasiatheria	Carnivora	Mustelidae	Pteronura_brasiliensis	MNHN-A1618	Caliper	-	26000.00			semiaquatic	semiaquatic	Hood, 2020	*	*	*
448	Laurasiatheria	Carnivora	Mustelidae	Taxidea_taxus	MNHN-ZM-AC-1895-417	Caliper	-	7842.15			terrestrial	semifossorial	Chen & Wilson, 2015	*	*	
449	Laurasiatheria	Carnivora	Nandiniidae	Nandinia_binotata	MNHN-ZM-AC-1896-482	Caliper	-	2167.20			terrestrial	arboreal	Chen & Wilson, 2015	*	*	*
450	Laurasiatheria	Carnivora	Odobenidae	Odobenus_rosmarus	MNHN-ZM-AC-1913-490	Caliper	-	1042996.25			aquatic	aquatic	Nowak, 1999	*	*	*
451	Laurasiatheria	Carnivora	Otariidae	Arctocephalus_galapagoensis	AMNH-100341	Caliper	-	39448.04			aquatic	aquatic	Nowak, 1999		*	
452	Laurasiatheria	Carnivora	Otariidae	Callorhinus_ursinus	MNHN-ZM-AC-1900-165	Caliper	-	55464.82			aquatic	aquatic	Nowak, 1999	*	*	*
453	Laurasiatheria	Carnivora	Otariidae	Eumetopias_jubatus	AMNH-71170	Caliper	-	382466.74			aquatic	aquatic	Nowak, 1999		*	
454	Laurasiatheria	Carnivora	Otariidae	Otaria_byronia	MNHN-ZM-AC-1891-1083	Caliper	-	193670.53			aquatic	aquatic	Nowak, 1999	*	*	*

	Superord. group	Order	Family	Species	Institution Voucher	Method	MorpoSouce ID	Mass (g)	OBS	Body mass additional reference (if not Jones et al., 2009)	Medium (Ch3)	Locomotor ecology (Ch4)	Ecology reference	Ch2	Ch3	Ch4
455	Laurasiatheria	Carnivora	Otariidae	Phocarctos_hookeri	NHM-333-B	Caliper	-	273499.99			aquatic	aquatic	Nowak, 1999		*	
456	Laurasiatheria	Carnivora	Otariidae	Zalophus_californianus	MNHN-ZM-AC-1882-190	Caliper	-	137194.86			aquatic	aquatic	Nowak, 1999	*	*	*
457	Laurasiatheria	Carnivora	Phocidae	Cystophora_cristata	NHM-1956-11-7-1	Caliper	-	278896.81			aquatic	aquatic	Nowak, 1999		*	*
458	Laurasiatheria	Carnivora	Phocidae	Erignathus_barbatus	AMNH-19347	Caliper	-	279999.99			aquatic	aquatic	Nowak, 1999		*	*
459	Laurasiatheria	Carnivora	Phocidae	Halichoerus_grypus	MNHN-squelette monté	Caliper	-	197570.01			aquatic	aquatic	Nowak, 1999	*	*	*
460	Laurasiatheria	Carnivora	Phocidae	Histriophoca_fasciata	NHM-1966-12-7-2	Caliper	-	90000.00			aquatic	aquatic	Nowak, 1999		*	*
461	Laurasiatheria	Carnivora	Phocidae	Hydrurga_leptonyx	MNHN-ZM-AC-1970-325	Caliper	-	352675.48			aquatic	aquatic	Nowak, 1999	*	*	*
462	Laurasiatheria	Carnivora	Phocidae	Neomonachus_tropicalis	AMNH-77741	Caliper	-	197758.36			aquatic	aquatic	Nowak, 1999		*	*
463	Laurasiatheria	Carnivora	Phocidae	Ommatophoca_rossii	NHM-1965-8-21	Caliper	-	208252.12			aquatic	aquatic	Nowak, 1999		*	*
464	Laurasiatheria	Carnivora	Phocidae	Pagophilus_groenlandicus	NHM-1938-12-10	Caliper	-	132250.00			aquatic	aquatic	Nowak, 1999		*	*
465	Laurasiatheria	Carnivora	Phocidae	Phoca_vitulina	MNHN-ZM-AC-1934-603	Caliper	-	87316.66			aquatic	aquatic	Nowak, 1999	*	*	*
466	Laurasiatheria	Carnivora	Phocidae	Pusa_hispida	MNHN-ZM-AC-A7954	Caliper	-	70963.60			aquatic	aquatic	Nowak, 1999	*	*	*
467	Laurasiatheria	Carnivora	Prionodontidae	Prionodon_pardicolor	NHM-1879-11-21-241	Caliper	-	1142.68			terrestrial	scansorial	Nowak, 1999		*	*
468	Laurasiatheria	Carnivora	Procyonidae	Bassariscus_astutus	MNHN-ZM-AC-1854-128	Caliper	-	1010.37			terrestrial	arboreal	Samuels et al., 2013	*	*	*
469	Laurasiatheria	Carnivora	Procyonidae	Nasua_narica	MNHN-ZM-AC-1888-846	Caliper	-	4578.43			terrestrial	scansorial	Fabre et al., 2015	*	*	*
470	Laurasiatheria	Carnivora	Procyonidae	Potos_flavus	MNHN-ZM-AC-1889-109	Caliper	-	2441.81			terrestrial	arboreal	Fabre et al., 2015	*	*	*
471	Laurasiatheria	Carnivora	Procyonidae	Procyon_lotor	MNHN-ZM-AC-1910-252	Caliper	-	6373.72			terrestrial	scansorial	Fabre et al., 2015	*	*	*
472	Laurasiatheria	Carnivora	Ursidae	Ailuropoda_melanoleuca	MNHN-1870-293	Caliper	-	117999.99			terrestrial	terrestrialquad	Samuels et al., 2013	*	*	*
473	Laurasiatheria	Carnivora	Ursidae	Helarctos_malayanus	MNHN-ZM-AC-1932-5	Caliper	-	57075.78			terrestrial	scansorial	Samuels et al., 2013		*	*
474	Laurasiatheria	Carnivora	Ursidae	Melursus_ursinus	MNHN-ZM-AC-1871-85	Caliper	-	99999.99			terrestrial	terrestrialquad	Samuels et al., 2013	*	*	*
475	Laurasiatheria	Carnivora	Ursidae	Tremarctos_ornatus	MNHN-1990-696	Caliper	-	123176.97			terrestrial	scansorial	Samuels et al., 2013		*	*
476	Laurasiatheria	Carnivora	Ursidae	Ursus_maritimus	MNHN-1012-139	Caliper	-	371703.81			semiaquatic	semiaquatic	Howell, 1970	*	*	*
477	Laurasiatheria	Carnivora	Viverridae	Arctictis_binturong	MNHN-ZM-AC-1975-78	Caliper	-	12999.99			terrestrial	arboreal	Samuels et al., 2013	*	*	*
478	Laurasiatheria	Carnivora	Viverridae	Arctogalidia_trivirgata	MNHN-ZM-MO-2001-495	Caliper	-	2323.79			terrestrial	arboreal	Law, 2021	*	*	*
479	Laurasiatheria	Carnivora	Viverridae	Chrotogale_owstoni	MVZ:Mamm:186572	Digital	ark:/87602/m4/M85286	3267.71			terrestrial	scansorial	Law, 2021	*	*	*
480	Laurasiatheria	Carnivora	Viverridae	Civettictis_civetta	MNHN-ZM-AC-1890-3920	Caliper	-	12075.58			terrestrial	terrestrialquad	Samuels et al., 2013	*	*	*
481	Laurasiatheria	Carnivora	Viverridae	Genetta_angolensis	FMNH:Mamm:163777	Digital	ark:/87602/m4/M141402	1859.64			terrestrial	scansorial	Law, 2021		*	
482	Laurasiatheria	Carnivora	Viverridae	Genetta_genetta	MNHN-ZM-AC-1886-30	Caliper	-	1756.17			terrestrial	scansorial	Samuels et al., 2013	*	*	*
483	Laurasiatheria	Carnivora	Viverridae	Paguma_larvata	MNHN-ZM-AC-1876-214	Caliper	-	4300.00			terrestrial	arboreal	Chen & Wilson, 2015	*	*	*
484	Laurasiatheria	Carnivora	Viverridae	Paradoxurus_hermaphroditus	MNHN-ZM-AC-1894-159	Caliper	-	3200.00			terrestrial	arboreal	Chen & Wilson, 2015	*	*	*
485	Laurasiatheria	Carnivora	Viverridae	Poiana_richardsonii	YPM:VZ:Mamm 014715	Digital	ark:/87602/m4/M95043	570.08			terrestrial	arboreal	Gillette, 2005	*	*	*
486	Laurasiatheria	Carnivora	Viverridae	Viverra_zibetha	MNHN-ZM-AC-A12952	Caliper	-	9148.77			terrestrial	terrestrialquad	Samuels et al., 2013	*	*	*
487	Laurasiatheria	Carnivora	Viverridae	Viverricula_indica	MNHN-ZM-AC-1895-209	Caliper	-	2918.88			terrestrial	terrestrialquad	Samuels et al., 2013	*	*	*
488	Laurasiatheria	Cetartiodactyla	Antilocapridae	Antilocapra_americana	MNHN-ZM-AC-1964-272	Caliper	-	47450.01			terrestrial	terrestrialquad	Nowak, 1999		*	*
489	Laurasiatheria	Cetartiodactyla	Antilocapridae	Antilocapra_americana	MNHN-ZM-AC-1964-273	Caliper	-	47450.01			terrestrial	terrestrialquad	Nowak, 1999		*	*
490	Laurasiatheria	Cetartiodactyla	Balaenidae	Eubalaena_australis	MNHN-ZM-AC-1921-123	Caliper	-	22999999.91			aquatic	aquatic	Nowak, 1999		*	*
491	Laurasiatheria	Cetartiodactyla	Balaenidae	Eubalaena_glacialis	NHM-1914-6-30-1	Caliper	-	22999999.91			aquatic	aquatic	Nowak, 1999		*	*
492	Laurasiatheria	Cetartiodactyla	Balaenopteridae	Balaenoptera_acutorostrata	MNHN-ZM-AC-1881-1225	Caliper	-	5587093.59			aquatic	aquatic	Nowak, 1999	*	*	*
493	Laurasiatheria	Cetartiodactyla	Balaenopteridae	Megaptera_novaeangliae	MNHN-ZM-AC-A2931	Caliper	-	30000000.01			aquatic	aquatic	Nowak, 1999	*	*	*
494	Laurasiatheria	Cetartiodactyla	Bovidae	Addax_nasomaculatus	MNHN-1970-277	Caliper	-	96077.36			terrestrial	terrestrialquad	Nowak, 1999	*	*	*
495	Laurasiatheria	Cetartiodactyla	Bovidae	Aepyceros_melampus	MNHN-1973-39	Caliper	-	52591.69			terrestrial	terrestrialquad	Nowak, 1999	*	*	*
496	Laurasiatheria	Cetartiodactyla	Bovidae	Alcelaphus_buselaphus	MNHN-1862-58	Caliper	-	168695.66			terrestrial	terrestrialquad	Nowak, 1999	*	*	*
497	Laurasiatheria	Cetartiodactyla	Bovidae	Ammodorcas_clarkei	NHM-1935-12-13-6	Caliper	-	28049.81			terrestrial	terrestrialquad	Nowak, 1999		*	
498	Laurasiatheria	Cetartiodactyla	Bovidae	Ammotragus_lervia	MNHN-ZM-AC-1896-439	Caliper	-	94202.22			terrestrial	terrestrialquad	Nowak, 1999	*	*	*
499	Laurasiatheria	Cetartiodactyla	Bovidae	Antidorcas_marsupialis	MNHN-1971-89	Caliper	-	33571.24			terrestrial	terrestrialquad	Nowak, 1999	*	*	*
500	Laurasiatheria	Cetartiodactyla	Bovidae	Antilope_cervicapra	MNHN-1886-321	Caliper	-	36301.10			terrestrial	terrestrialquad	Nowak, 1999	*	*	*
501	Laurasiatheria	Cetartiodactyla	Bovidae	Beatragus_hunteri	NHM-1938-7-11-1	Caliper	-	79132.17			terrestrial	terrestrialquad	Nowak, 1999		*	*
502	Laurasiatheria	Cetartiodactyla	Bovidae	Bison_bonasus	MNHN-ZM-AC-1962-222	Caliper	-	675876.70			terrestrial	terrestrialquad	Nowak, 1999	*	*	*
503	Laurasiatheria	Cetartiodactyla	Bovidae	Bos_frontalis	MNHN-ZM-AC-1970-280	Caliper	-	800143.05			terrestrial	terrestrialquad	Nowak, 1999	*	*	*
504	Laurasiatheria	Cetartiodactyla	Bovidae	Bos_grunniens	MNHN-2008-107	Caliper	-	500000.00			terrestrial	terrestrialquad	Nowak, 1999	*	*	*
505	Laurasiatheria	Cetartiodactyla	Bovidae	Boselaphus_tragocamelus	MNHN-ZM-AC-1907-146	Caliper	-	182253.04			terrestrial	terrestrialquad	Nowak, 1999	*	*	*
506	Laurasiatheria	Cetartiodactyla	Bovidae	Bubalus_bubalis	MNHN-ZM-AC-1902-905	Caliper	-	929500.97			terrestrial	terrestrialquad	Nowak, 1999	*	*	*
507	Laurasiatheria	Cetartiodactyla	Bovidae	Budorcas_taxicolor	MNHN-ZM-AC-1925-240	Caliper	-	294515.33			terrestrial	terrestrialquad	Nowak, 1999	*	*	*
508	Laurasiatheria	Cetartiodactyla	Bovidae	Capra_hircus	MNHN-1921-30	Caliper	-	47386.47			terrestrial	terrestrialquad	Nowak, 1999	*	*	*
509	Laurasiatheria	Cetartiodactyla	Bovidae	Capra_ibex	MNHN-ZM-2019-1646	Caliper	-	43500.00	Body mass of specimen provided by collection.		terrestrial	terrestrialquad	Nowak, 1999	*	*	*
510	Laurasiatheria	Cetartiodactyla	Bovidae	Capricornis_sumatraensis	MNHN-ZM-AC-1937-314	Caliper	-	110942.22			terrestrial	terrestrialquad	Nowak, 1999	*	*	*
511	Laurasiatheria	Cetartiodactyla	Bovidae	Cephalophus_dorsalis	MNHN-1971-306	Caliper	-	20000.00			terrestrial	terrestrialquad	Nowak, 1999	*	*	*
512	Laurasiatheria	Cetartiodactyla	Bovidae	Connochaetes_taurinus	MNHN-1938-86	Caliper	-	198619.68			terrestrial	terrestrialquad	Nowak, 1999	*	*	*
513	Laurasiatheria	Cetartiodactyla	Bovidae	Damaliscus_pygargus	MNHN-1970-384	Caliper	-	77784.55			terrestrial	terrestrialquad	Nowak, 1999	*	*	*
514	Laurasiatheria	Cetartiodactyla	Bovidae	Dorcatragus_megalotis	NHM-1895-5-21	Caliper	-	10918.12			terrestrial	terrestrialquad	Nowak, 1999		*	
515	Laurasiatheria	Cetartiodactyla	Bovidae	Eudorcas_thomsonii	MNHN-1961-41	Caliper	-	22907.43			terrestrial	terrestrialquad	Nowak, 1999	*	*	*
516	Laurasiatheria	Cetartiodactyla	Bovidae	Gazella_sp	MNHN-1923-2137	Caliper	-	20951.41	Body mass of genus average.		terrestrial	terrestrialquad	Nowak, 1999	*	*	*
517	Laurasiatheria	Cetartiodactyla	Bovidae	Hemitragus_jemlahicus	MNHN-1991-693	Caliper	-	68616.43			terrestrial	terrestrialquad	Nowak, 1999	*	*	*
518	Laurasiatheria	Cetartiodactyla	Bovidae	Hippotragus_equinus	MNHN-ZM-AC-1995-147	Caliper	-	264173.96			terrestrial	terrestrialquad	Nowak, 1999	*	*	*
519	Laurasiatheria	Cetartiodactyla	Bovidae	Kobus_ellipsiprymnus	MNHN-1935-637	Caliper	-	204393.48			terrestrial	terrestrialquad	Nowak, 1999	*	*	*
520	Laurasiatheria	Cetartiodactyla	Bovidae	Litocranius_walleri	NHM-1935-7-24-1	Caliper	-	38804.37			terrestrial	terrestrialquad	Nowak, 1999		*	*
521	Laurasiatheria	Cetartiodactyla	Bovidae	Madoqua_phillipsi	NHM-1895-10-13-3	Caliper	-	3424.47	Body mass of M. saltiana at Pantheria.		terrestrial	terrestrialquad	Nowak, 1999		*	*
522	Laurasiatheria	Cetartiodactyla	Bovidae	Nanger_dama	MNHN-1882-264	Caliper	-	71424.81			terrestrial	terrestrialquad	Nowak, 1999	*	*	*
523	Laurasiatheria	Cetartiodactyla	Bovidae	Nemorhaedus_goral	MNHN-1963-320	Caliper	-	28796.51			terrestrial	terrestrialquad	Nowak, 1999		*	*

	Superord. group	Order	Family	Species	Institution Voucher	Method	MorpoSouce ID	Mass (g)	OBS	Body mass additional reference (if not Jones et al., 2009)	Medium (Ch3)	Locomotor ecology (Ch4)	Ecology reference	Ch2	Ch3	Ch4
524	Laurasiatheria	Cetartiodactyla	Bovidae	Neotragus_moschatus	NHM-1936-3-30-3	Caliper	-	5639.01			terrestrial	terrestrialquad	Nowak, 1999		*	
525	Laurasiatheria	Cetartiodactyla	Bovidae	Oreamnos_americanus	MNHN-ZM-AC-1925-437	Caliper	-	72105.40			terrestrial	terrestrialquad	Nowak, 1999	*	*	*
526	Laurasiatheria	Cetartiodactyla	Bovidae	Oryx_gazella	MNHN-ZM-2005-712	Caliper	-	188404.45			terrestrial	terrestrialquad	Nowak, 1999	*	*	*
527	Laurasiatheria	Cetartiodactyla	Bovidae	Ourebia_ourebi	NHM-1934-5-1-3	Caliper	-	17186.09			terrestrial	terrestrialquad	Nowak, 1999		*	
528	Laurasiatheria	Cetartiodactyla	Bovidae	Ovibos_moschatus	NHM-612-F	Caliper	-	312500.00			terrestrial	terrestrialquad	Nowak, 1999		*	*
529	Laurasiatheria	Cetartiodactyla	Bovidae	Ovis_aries	MNHN-1907-579	Caliper	-	39097.89			terrestrial	terrestrialquad	Nowak, 1999	*	*	*
530	Laurasiatheria	Cetartiodactyla	Bovidae	Pantholops_hodgsonii	NHM-70-191	Caliper	-	32733.12			terrestrial	terrestrialquad	Nowak, 1999		*	
531	Laurasiatheria	Cetartiodactyla	Bovidae	Pelea_capreolus	MNHN-A11898	Caliper	-	22731.33			terrestrial	terrestrialquad	Nowak, 1999	*	*	*
532	Laurasiatheria	Cetartiodactyla	Bovidae	Philantomba_maxwellii	MNHN-ZM-AC-1921-223	Caliper	-	8557.69			terrestrial	terrestrialquad	Nowak, 1999	*	*	*
533	Laurasiatheria	Cetartiodactyla	Bovidae	Pseudois_nayaur	MNHN-1995-197	Caliper	-	52334.57			terrestrial	terrestrialquad	Nowak, 1999	*	*	*
534	Laurasiatheria	Cetartiodactyla	Bovidae	Raphicerus_melanotis	NHM-1862-3-13-13	Caliper	-	11661.53			terrestrial	terrestrialquad	Nowak, 1999		*	*
535	Laurasiatheria	Cetartiodactyla	Bovidae	Redunca_redunca	MNHN-ZM-AC-1924-45	Caliper	-	43288.95			terrestrial	terrestrialquad	Nowak, 1999	*	*	*
536	Laurasiatheria	Cetartiodactyla	Bovidae	Rupicapra_rupicapra	MNHN-ZM-AC-1924-262	Caliper	-	33266.35			terrestrial	terrestrialquad	Nowak, 1999	*	*	*
537	Laurasiatheria	Cetartiodactyla	Bovidae	Saiga_tatarica	MNHN-1965-128	Caliper	-	37734.01			terrestrial	terrestrialquad	Nowak, 1999	*	*	*
538	Laurasiatheria	Cetartiodactyla	Bovidae	Sylvicapra_grimmia	MNHN-1906-86	Caliper	-	15639.15			terrestrial	terrestrialquad	Nowak, 1999	*	*	*
539	Laurasiatheria	Cetartiodactyla	Bovidae	Syncerus_caffer	MNHN-1936-72	Caliper	-	592665.98			terrestrial	terrestrialquad	Nowak, 1999	*	*	*
540	Laurasiatheria	Cetartiodactyla	Bovidae	Taurotragus_oryx	MNHN-ZM-AC-A7983	Caliper	-	562592.69			terrestrial	terrestrialquad	Nowak, 1999		*	*
541	Laurasiatheria	Cetartiodactyla	Bovidae	Tetracerus_quadricornis	MNHN-ZM-AC-1909-150	Caliper	-	19282.12			terrestrial	terrestrialquad	Nowak, 1999	*	*	*
542	Laurasiatheria	Cetartiodactyla	Bovidae	Tragelaphus_strepsiceros	MNHN-ZM-AC-1992-1462	Caliper	-	206056.41			terrestrial	terrestrialquad	Nowak, 1999	*	*	*
543	Laurasiatheria	Cetartiodactyla	Camelidae	Camelus_bactrianus	MNHN-ZM-AC-1898239	Caliper	-	554515.91			terrestrial	terrestrialquad	Nowak, 1999	*	*	*
544	Laurasiatheria	Cetartiodactyla	Camelidae	Camelus_dromedarius	MNHN-ZM-AC-1876-259	Caliper	-	492714.47			terrestrial	terrestrialquad	Nowak, 1999	*	*	*
545	Laurasiatheria	Cetartiodactyla	Camelidae	Lama_glama	MNHN-ZM-AC-1987-16	Caliper	-	78322.67			terrestrial	terrestrialquad	Nowak, 1999	*	*	*
546	Laurasiatheria	Cetartiodactyla	Camelidae	Lama_guanicoe	MNHN-ZM-AC-1925-200	Caliper	-	115000.00		Hoffman, 2014	terrestrial	terrestrialquad	Nowak, 1999	*	*	*
547	Laurasiatheria	Cetartiodactyla	Cervidae	Alces_alces	MNHN-2019-1315	Caliper	-	461900.76			terrestrial	terrestrialquad	Nowak, 1999	*	*	*
548	Laurasiatheria	Cetartiodactyla	Cervidae	Axis_axis	MNHN-ZM-AC-1860-187	Caliper	-	69499.99			terrestrial	terrestrialquad	Nowak, 1999	*	*	*
549	Laurasiatheria	Cetartiodactyla	Cervidae	Capreolus_capreolus	MNHN-ZM-AC-1993-266	Caliper	-	22502.01			terrestrial	terrestrialquad	Nowak, 1999	*	*	*
550	Laurasiatheria	Cetartiodactyla	Cervidae	Cervus_elaphus	MNHN-1980-4026	Caliper	-	240867.13			terrestrial	terrestrialquad	Nowak, 1999	*	*	*
551	Laurasiatheria	Cetartiodactyla	Cervidae	Dama_dama	MNHN-ZM-AC-1882-128	Caliper	-	57224.61			terrestrial	terrestrialquad	Nowak, 1999	*	*	*
552	Laurasiatheria	Cetartiodactyla	Cervidae	Elaphurus_davidianus	MNHN-ZM-AC-1972-67	Caliper	-	165989.17			terrestrial	semiaquatic	Hood, 2020	*	*	*
553	Laurasiatheria	Cetartiodactyla	Cervidae	Hydropotes_inermis	MNHN-ZM-AC-1948-87	Caliper	-	12760.04			terrestrial	semiaquatic	Hood, 2020	*	*	*
554	Laurasiatheria	Cetartiodactyla	Cervidae	Mazama_sp	MNHN-ZM-AC-1974-93	Caliper	-	17891.79	Body mass of genus average.		terrestrial	terrestrialquad	Nowak, 1999	*	*	*
555	Laurasiatheria	Cetartiodactyla	Cervidae	Muntiacus_muntjak	MNHN-1856-62	Caliper	-	17611.59			terrestrial	terrestrialquad	Nowak, 1999	*	*	*
556	Laurasiatheria	Cetartiodactyla	Cervidae	Odocoileus_virginianus	MNHN-ZM-AC-1876-312	Caliper	-	75901.25			terrestrial	terrestrialquad	Nowak, 1999	*	*	*
557	Laurasiatheria	Cetartiodactyla	Cervidae	Panolia_eldii	MNHN-ZM-AC-1985-41	Caliper	-	95471.61			terrestrial	terrestrialquad	Nowak, 1999		*	*
558	Laurasiatheria	Cetartiodactyla	Cervidae	Pudu_puda	MNHN-ZM-2017-1205	Caliper	-	9642.62			terrestrial	terrestrialquad	Nowak, 1999	*	*	*
559	Laurasiatheria	Cetartiodactyla	Cervidae	Rangifer_tarandus	MNHN-ZM-AC-1945-29	Caliper	-	109088.50			terrestrial	terrestrialquad	Nowak, 1999	*	*	*
560	Laurasiatheria	Cetartiodactyla	Cervidae	Rucervus_duvaucelii	MNHN-ZM-2013-1075	Caliper	-	171223.86			terrestrial	terrestrialquad	Nowak, 1999	*	*	*
561	Laurasiatheria	Cetartiodactyla	Cervidae	Rusa_unicolor	MNHN-ZM-AC-1886-09	Caliper	-	177522.90			terrestrial	terrestrialquad	Nowak, 1999	*	*	*
562	Laurasiatheria	Cetartiodactyla	Delphinidae	Cephalorhynchus_commersonii	MNHN-ZM-AC-1983-56	Caliper	-	72400.00			aquatic	aquatic	Nowak, 1999	*	*	*
563	Laurasiatheria	Cetartiodactyla	Delphinidae	Cephalorhynchus_commersonii	MNHN-ZM-1983-58	Caliper	-	72400.00			aquatic	aquatic	Nowak, 1999	*	*	*
564	Laurasiatheria	Cetartiodactyla	Delphinidae	Delphinus_delphis	MNHN-ZM-AC-1934-367	Caliper	-	79271.69			aquatic	aquatic	Nowak, 1999	*	*	*
565	Laurasiatheria	Cetartiodactyla	Delphinidae	Globicephala_melas	MNHN-ZM-AC-1902-902	Caliper	-	800000.00			aquatic	aquatic	Nowak, 1999	*	*	*
566	Laurasiatheria	Cetartiodactyla	Delphinidae	Grampus_griseus	MNHN-ZM-AC-1881-1186	Caliper	-	387500.00			aquatic	aquatic	Nowak, 1999	*	*	*
567	Laurasiatheria	Cetartiodactyla	Delphinidae	Lagenorhynchus_acutus	MNHN-ZM-AC-1881-1226	Caliper	-	186517.55			aquatic	aquatic	Nowak, 1999	*	*	*
568	Laurasiatheria	Cetartiodactyla	Delphinidae	Lissodelphis_borealis	AMNH-31422	Caliper	-	113000.00			aquatic	aquatic	Nowak, 1999		*	
569	Laurasiatheria	Cetartiodactyla	Delphinidae	Orcaella_brevirostris	MNHN-ZM-AC-1888-388	Caliper	-	189999.99			aquatic	aquatic	Nowak, 1999	*	*	*
570	Laurasiatheria	Cetartiodactyla	Delphinidae	Orcinus_orca	MNHN-ZM-AC-1885-427	Caliper	-	2441000.50		Clark et al., 2000	aquatic	aquatic	Nowak, 1999	*	*	*
571	Laurasiatheria	Cetartiodactyla	Delphinidae	Peponocephala_electra	NHM-1965-6-21	Caliper	-	206000.00			aquatic	aquatic	Nowak, 1999		*	*
572	Laurasiatheria	Cetartiodactyla	Delphinidae	Pseudorca_crassidens	AMNH-99681	Caliper	-	1360000.00			aquatic	aquatic	Nowak, 1999		*	*
573	Laurasiatheria	Cetartiodactyla	Delphinidae	Stenella_longirostris	MNHN-ZM-AC-1882-104	Caliper	-	50500.00			aquatic	aquatic	Nowak, 1999	*	*	*
574	Laurasiatheria	Cetartiodactyla	Delphinidae	Steno_bredanensis	MNHN-ZM-AC-1885-300	Caliper	-	130000.00			aquatic	aquatic	Nowak, 1999	*	*	*
575	Laurasiatheria	Cetartiodactyla	Delphinidae	Tursiops_truncatus	MNHN-1978-09	Caliper	-	281040.55			aquatic	aquatic	Nowak, 1999	*	*	*
576	Laurasiatheria	Cetartiodactyla	Eschrichtiidae	Eschrichtius_robustus	AMNH-34260	Caliper	-	27324024.19			aquatic	aquatic	Nowak, 1999		*	
577	Laurasiatheria	Cetartiodactyla	Giraffidae	Giraffa_camelopardalis	MNHN-A8012	Caliper	-	964654.73			terrestrial	terrestrialquad	Nowak, 1999	*	*	*
578	Laurasiatheria	Cetartiodactyla	Giraffidae	Okapia_johnstoni	MNHN-ZM-AC-1904-57	Caliper	-	230001.14			terrestrial	terrestrialquad	Nowak, 1999	*	*	*
579	Laurasiatheria	Cetartiodactyla	Hippopotamidae	Choeropsis_liberiensis	MNHN-ZM-AC-1944-146	Caliper	-	235001.16			semiaquatic	semiaquatic	Hood, 2020	*	*	*
580	Laurasiatheria	Cetartiodactyla	Hippopotamidae	Choeropsis_liberiensis	MNHN-ZM-AC-1982-10	Caliper	-	235001.16			semiaquatic	semiaquatic	Hood, 2020	*	*	*
581	Laurasiatheria	Cetartiodactyla	Hippopotamidae	Hippopotamus_amphibius	MNHN-ZM-AC-1897-33	Caliper	-	1536310.40			semiaquatic	semiaquatic	Hood, 2020	*	*	*
582	Laurasiatheria	Cetartiodactyla	Hippopotamidae	Hippopotamus_amphibius	MNHN-ZM-AC-1943-27	Caliper	-	1536310.40			semiaquatic	semiaquatic	Hood, 2020	*	*	*
583	Laurasiatheria	Cetartiodactyla	Iniidae	Inia_geoffrensis	MNHN-ZM-AC-1865-154	Caliper	-	121430.76			aquatic	aquatic	Nowak, 1999	*	*	*
584	Laurasiatheria	Cetartiodactyla	Kogiidae	Kogia_breviceps	NHM-1981-109	Caliper	-	431500.00			aquatic	aquatic	Nowak, 1999		*	*
585	Laurasiatheria	Cetartiodactyla	Monodontidae	Delphinapterus_leucas	MNHN-ZM-AC-A3246	Caliper	-	1381640.73			aquatic	aquatic	Nowak, 1999	*	*	*
586	Laurasiatheria	Cetartiodactyla	Monodontidae	Monodon_monoceros	MNHN-ZM-AC-A12536	Caliper	-	938126.44			aquatic	aquatic	Nowak, 1999	*	*	*
587	Laurasiatheria	Cetartiodactyla	Moschidae	Moschus_moschiferus	MNHN-ZM-AC-1961-294	Caliper	-	13315.57			terrestrial	terrestrialquad	Nowak, 1999	*	*	*
588	Laurasiatheria	Cetartiodactyla	Moschidae	Moschus_sp	MNHN-ZM-AC-VI-1402	Caliper	-	13297.20	Body mass of genus average.		terrestrial	terrestrialquad	Nowak, 1999	*	*	*
589	Laurasiatheria	Cetartiodactyla	Neobalaenidae	Caperea_marginata	AMNH-36692	Caliper	-	4500000.00		Cover, 2000	aquatic	aquatic	Nowak, 1999		*	*
590	Laurasiatheria	Cetartiodactyla	Phocoenidae	Neophocaena_phocaenoides	AMNH-141150	Caliper	-	32500.00			aquatic	aquatic	Nowak, 1999		*	
591	Laurasiatheria	Cetartiodactyla	Phocoenidae	Phocoena_phocoena	MNHN-B11209	Caliper	-	52730.93			aquatic	aquatic	Nowak, 1999	*	*	*
592	Laurasiatheria	Cetartiodactyla	Phocoenidae	Phocoenoides_dalli	AMNH-90802	Caliper	-	106042.53			aquatic	aquatic	Nowak, 1999		*	*
593	Laurasiatheria	Cetartiodactyla	Physeteridae	Physeter_macrocephalus	AMNH-34872	Caliper	-	14540959.82			aquatic	aquatic	Nowak, 1999		*	*
594	Laurasiatheria	Cetartiodactyla	Platanistidae	Platanista_gangetica	MNHN-ZM-AC-A7943	Caliper	-	93481.96			aquatic	aquatic	Nowak, 1999	*	*	*

	Superord. group	Order	Family	Species	Institution Voucher	Method	MorpoSouce ID	Mass (g)	OBS	Body mass additional reference (if not Jones et al., 2009)	Medium (Ch3)	Locomotor ecology (Ch4)	Ecology reference	Ch2	Ch3	Ch4
595	Laurasiatheria	Cetartiodactyla	Pontoporiidae	Pontoporia_blainvillei	MNHN-ZM-AC-1928-278	Caliper	-	40499.99			aquatic	aquatic	Nowak, 1999	*	*	*
596	Laurasiatheria	Cetartiodactyla	Pontoporiidae	Pontoporia_blainvillei	MNHN-1828-167	Caliper	-	40499.99			aquatic	aquatic	Nowak, 1999	*	*	*
597	Laurasiatheria	Cetartiodactyla	Suidae	Babyrousa_babyrussa	AMNH-152858	Caliper	-	92950.09			terrestrial	semiaquatic	Hood, 2020; Nowak, 1999		*	
598	Laurasiatheria	Cetartiodactyla	Suidae	Hylochoerus_meinertzhageni	AMNH-53673	Caliper	-	198130.47			terrestrial	terrestrialquad	Nowak, 1999		*	*
599	Laurasiatheria	Cetartiodactyla	Suidae	Phacochoerus_africanus	MNHN-ZM-AC-1923-2433	Caliper	-	82499.99			terrestrial	terrestrialquad	Nowak, 1999	*	*	*
600	Laurasiatheria	Cetartiodactyla	Suidae	Phacochoerus_africanus	MNHN-1900-49	Caliper	-	82499.99			terrestrial	terrestrialquad	Nowak, 1999	*	*	*
601	Laurasiatheria	Cetartiodactyla	Suidae	Potamochoerus_larvatus	MNHN-ZM-AC-1876-454	Caliper	-	69063.79			terrestrial	terrestrialquad	Nowak, 1999	*	*	*
602	Laurasiatheria	Cetartiodactyla	Suidae	Sus_sp	MNHN-1938-70	Caliper	-	107579.38	Body mass of genus average.		terrestrial	terrestrialquad	Nowak, 1999	*	*	*
603	Laurasiatheria	Cetartiodactyla	Tayassuidae	Pecari_tajacu	MNHN-ZM-AC-1909-492	Caliper	-	21133.69			terrestrial	terrestrialquad	Nowak, 1999	*	*	*
604	Laurasiatheria	Cetartiodactyla	Tayassuidae	Pecari_tajacu	MNHN-1879-192	Caliper	-	21133.69			terrestrial	terrestrialquad	Nowak, 1999	*	*	*
605	Laurasiatheria	Cetartiodactyla	Tayassuidae	Tayassu_pecari	MNHN-1892-1107	Caliper	-	31798.71			terrestrial	terrestrialquad	Nowak, 1999	*	*	*
606	Laurasiatheria	Cetartiodactyla	Tragulidae	Hyemoschus_aquaticus	MNHN-1914-97	Caliper	-	10850.00			terrestrial	semiaquatic	Hart, 2013	*	*	*
607	Laurasiatheria	Cetartiodactyla	Tragulidae	Hyemoschus_aquaticus	MNHN-1892-33	Caliper	-	10850.00			terrestrial	semiaquatic	Hart, 2013	*	*	*
608	Laurasiatheria	Cetartiodactyla	Tragulidae	Moschiola_meminna	MNHN-1925-15	Caliper	-	3130.95			terrestrial	terrestrialquad	Nowak, 1999	*	*	*
609	Laurasiatheria	Cetartiodactyla	Tragulidae	Tragulus_javanicus	MNHN-1976-392	Caliper	-	1889.93			terrestrial	terrestrialquad	Nowak, 1999	*	*	*
610	Laurasiatheria	Cetartiodactyla	Tragulidae	Tragulus_sp	MNHN-1880-1000	Caliper	-	3581.80	Body mass of genus average.		terrestrial	terrestrialquad	Nowak, 1999	*	*	*
611	Laurasiatheria	Cetartiodactyla	Ziphiidae	Berardius_arnuxii	MNHN-ZM-AC-1875-712	Caliper	-	7000000.02			aquatic	aquatic	Nowak, 1999	*	*	
612	Laurasiatheria	Cetartiodactyla	Ziphiidae	Hyperoodon_ampullatus	MNHN-ZM-AC-A3236	Caliper	-	3393361.08			aquatic	aquatic	Nowak, 1999	*	*	
613	Laurasiatheria	Cetartiodactyla	Ziphiidae	Mesoplodon_bidens	MNHN-ZM-AC-1909-81	Caliper	-	3400000.00			aquatic	aquatic	Nowak, 1999	*	*	*
614	Laurasiatheria	Cetartiodactyla	Ziphiidae	Ziphius_cavirostris	AMNH-40015	Caliper	-	4774999.99			aquatic	aquatic	Nowak, 1999		*	*
615	Laurasiatheria	Chiroptera	Craseonycteridae	Craseonycteris_thonglongyai	USNM:528306	Digital	ark:/87602/m4/M170681	1.96			aerial	flight	Nowak, 1999		*	*
616	Laurasiatheria	Chiroptera	Emballonuridae	Balantiopteryx_plicata	UMMZ:Mamm:109740	Digital	doi:10.17602/M2/M57255	6.57			aerial	flight	Nowak, 1999	*	*	*
617	Laurasiatheria	Chiroptera	Emballonuridae	Coleura_afra	MCZ:Mamm:59781	Digital	ark:/87602/m4/M79516	10.68			aerial	flight	Nowak, 1999	*	*	*
618	Laurasiatheria	Chiroptera	Emballonuridae	Cormura_brevirostris	UMMZ:Mamm:175633	Digital	ark:/87602/m4/M55751	9.26			aerial	flight	Nowak, 1999	*	*	*
619	Laurasiatheria	Chiroptera	Emballonuridae	Emballonura_alecto	UMMZ:Mamm:156850	Digital	ark:/87602/m4/M55755	5.25			aerial	flight	Nowak, 1999	*	*	*
620	Laurasiatheria	Chiroptera	Emballonuridae	Mosia_nigrescens	UMZC:Vertebrates:e.5805.a	Digital	ark:/87602/m4/M164555	3.33			aerial	flight	Nowak, 1999		*	*
621	Laurasiatheria	Chiroptera	Emballonuridae	Peropteryx_kappleri	UMMZ:Mamm:168863	Digital	ark:/87602/m4/M58365	9.85			aerial	flight	Nowak, 1999	*	*	*
622	Laurasiatheria	Chiroptera	Emballonuridae	Rhynchonycteris_naso	UMMZ:Mamm:115887	Digital	ark:/87602/m4/M58343	4.14			aerial	flight	Nowak, 1999	*	*	*
623	Laurasiatheria	Chiroptera	Emballonuridae	Saccolaimus_saccolaimus	MVZ:Mamm:174626	Digital	ark:/87602/m4/M99365	43.00			aerial	flight	Nowak, 1999		*	*
624	Laurasiatheria	Chiroptera	Emballonuridae	Saccopteryx_leptura	UMMZ:Mamm:115892	Digital	ark:/87602/m4/M68582	5.75	Body mass of genus average.		aerial	flight	Nowak, 1999	*	*	*
625	Laurasiatheria	Chiroptera	Furipteridae	Amorphochilus_schnablii	YPM:VZ:Mamm 005693	Digital	ark:/87602/m4/M64836	3.30		Cover, 2000	aerial	flight	Nowak, 1999	*	*	*
626	Laurasiatheria	Chiroptera	Furipteridae	Furipterus_horrens	UMMZ:Mamm:175646	Digital	doi:10.17602/M2/M57236	3.15			aerial	flight	Nowak, 1999	*	*	*
627	Laurasiatheria	Chiroptera	Hipposideridae	Asellia_tridens	UMMZ:Mamm:160968	Digital	ark:/87602/m4/M55749	12.94			aerial	flight	Nowak, 1999	*	*	*
628	Laurasiatheria	Chiroptera	Hipposideridae	Asellia_tridens	YPM:VZ:Mamm 005514	Digital	ark:/87602/m4/M65077	12.94			aerial	flight	Nowak, 1999	*	*	*
629	Laurasiatheria	Chiroptera	Hipposideridae	Hipposideros_speoris	YPM:VZ:Mamm 005627	Digital	ark:/87602/m4/M65071	10.39			aerial	flight	Nowak, 1999	*	*	*
630	Laurasiatheria	Chiroptera	Megadermatidae	Cardioderma_cor	YPM:VZ:Mamm 005622	Digital	ark:/87602/m4/M64568	26.45			aerial	flight	Nowak, 1999	*	*	*
631	Laurasiatheria	Chiroptera	Megadermatidae	Lavia_frons	MCZ:Mamm:52243	Digital	ark:/87602/m4/M84553	23.80			aerial	flight	Nowak, 1999	*	*	*
632	Laurasiatheria	Chiroptera	Megadermatidae	Megaderma_spasma	UMMZ:Mamm:163615	Digital	ark:/87602/m4/M57216	24.71			aerial	flight	Nowak, 1999	*	*	*
633	Laurasiatheria	Chiroptera	Miniopteridae	Miniopterus_australis	UMMZ:Mamm:160356	Digital	ark:/87602/m4/M61959	7.40			aerial	flight	Nowak, 1999	*	*	*
634	Laurasiatheria	Chiroptera	Molossidae	Chaerephon_plicatus	YPM:VZ:Mamm: 005625	Digital	ark:/87602/m4/M89771	21.83			aerial	flight	Nowak, 1999		*	*
635	Laurasiatheria	Chiroptera	Molossidae	Chaerephon_pumilus	YPM:VZ:Mamm: 005519	Digital	ark:/87602/m4/M89768	10.98			aerial	flight	Nowak, 1999		*	*
636	Laurasiatheria	Chiroptera	Molossidae	Cheiromeles_torquatus	UMMZ:Mamm:174627	Digital	ark:/87602/m4/M57225	169.43			aerial	flight	Nowak, 1999	*	*	*
637	Laurasiatheria	Chiroptera	Molossidae	Eumops_dabbenei	UMMZ:Mamm:134251	Digital	ark:/87602/m4/M57257	67.27			aerial	flight	Nowak, 1999	*	*	*
638	Laurasiatheria	Chiroptera	Molossidae	Molossops_temminckii	UMMZ:Mamm:134262	Digital	ark:/87602/m4/M57261	5.86			aerial	flight	Nowak, 1999	*	*	*
639	Laurasiatheria	Chiroptera	Molossidae	Molossus_molossus	UMMZ:Mamm:175614	Digital	ark:/87602/m4/M57232	13.70			aerial	flight	Nowak, 1999	*	*	*
640	Laurasiatheria	Chiroptera	Molossidae	Mops_mops	UMMZ:Mamm:174631	Digital	ark:/87602/m4/M57227	31.12			aerial	flight	Nowak, 1999	*	*	*
641	Laurasiatheria	Chiroptera	Molossidae	Mormopterus_acetabulosus	UMMZ:Mamm:115818	Digital	ark:/87602/m4/M58342	7.30		Goodman et al., 2008	aerial	flight	Nowak, 1999		*	*
642	Laurasiatheria	Chiroptera	Molossidae	Nyctinomops_femorosaccus	MVZ:Mamm:186401	Digital	ark:/87602/m4/M85285	15.04			aerial	flight	Nowak, 1999		*	*
643	Laurasiatheria	Chiroptera	Molossidae	Otomops_martiensseni	UMMZ:Mamm:175808	Digital	ark:/87602/m4/M57240	34.92			aerial	flight	Nowak, 1999	*	*	*
644	Laurasiatheria	Chiroptera	Molossidae	Promops_centralis	UMMZ:Mamm:134253	Digital	ark:/87602/m4/M57259	29.80			aerial	flight	Nowak, 1999	*	*	*
645	Laurasiatheria	Chiroptera	Molossidae	Tadarida_australis	UMMZ:Mamm:164676	Digital	ark:/87602/m4/M57249	36.40			aerial	flight	Nowak, 1999	*	*	*
646	Laurasiatheria	Chiroptera	Mormoopidae	Mormoops_megalophylla	UMMZ:Mamm:111721	Digital	ark:/87602/m4/M58337	16.09			aerial	flight	Nowak, 1999	*	*	*
647	Laurasiatheria	Chiroptera	Mormoopidae	Pteronotus_davyi	YPM:VZ:Mamm 005812	Digital	ark:/87602/m4/M64825	9.52			aerial	flight	Nowak, 1999	*	*	*
648	Laurasiatheria	Chiroptera	Mormoopidae	Pteronotus_parnellii	UMMZ:Mamm:175621	Digital	doi:10.17602/M2/M57270	19.59			aerial	flight	Nowak, 1999	*	*	*
649	Laurasiatheria	Chiroptera	Mystacinidae	Mystacina_tuberculata	MVZ:Mamm:173919	Digital	ark:/87602/m4/M85200	13.14			aerial	flight	Nowak, 1999		*	*
650	Laurasiatheria	Chiroptera	Myzopodidae	Myzopoda_aurita	MNHN-ZM-MO-1985-654	Digital	Montpellier	9.10			aerial	flight	Nowak, 1999		*	*
651	Laurasiatheria	Chiroptera	Natalidae	Natalus_stramineus	UMMZ:Mamm:122343	Digital	ark:/87602/m4/M57199	5.68			aerial	flight	Nowak, 1999	*	*	*
652	Laurasiatheria	Chiroptera	Noctilionidae	Noctilio_albiventris	UMMZ:Mamm:175795	Digital	doi:10.17602/M2/M57238	31.46			aerial	flight	Nowak, 1999	*	*	*
653	Laurasiatheria	Chiroptera	Nycteridae	Nycteris_thebaica	UMMZ:Mamm:164963	Digital	ark:/87602/m4/M96231	9.20			aerial	flight	Nowak, 1999	*	*	*
654	Laurasiatheria	Chiroptera	Phyllostomidae	Ametrida_centurio	YPM:VZ:Mamm 015120	Digital	ark:/87602/m4/M64842	10.61			aerial	flight	Nowak, 1999	*	*	*
655	Laurasiatheria	Chiroptera	Phyllostomidae	Anoura_caudifer	UMMZ:Mamm:168870	Digital	ark:/87602/m4/M57220	10.81			aerial	flight	Nowak, 1999	*	*	*
656	Laurasiatheria	Chiroptera	Phyllostomidae	Anoura_geoffroyi	YPM:VZ:Mamm 014593	Digital	ark:/87602/m4/M64829	15.15			aerial	flight	Nowak, 1999	*	*	*
657	Laurasiatheria	Chiroptera	Phyllostomidae	Ardops_nichollsi	MVZ:Mamm:166215	Digital	ark:/87602/m4/M98045	19.23			aerial	flight	Nowak, 1999		*	*
658	Laurasiatheria	Chiroptera	Phyllostomidae	Artibeus_planirostris	UMMZ:Mamm:156082	Digital	ark:/87602/m4/M57263	54.50		Hollis, 2005	aerial	flight	Nowak, 1999	*	*	*
659	Laurasiatheria	Chiroptera	Phyllostomidae	Brachyphylla_cavernarum	YPM:VZ:Mamm 006022	Digital	ark:/87602/m4/M64569	45.50			aerial	flight	Nowak, 1999	*	*	*
660	Laurasiatheria	Chiroptera	Phyllostomidae	Carollia_brevicauda	UMMZ:Mamm:93471	Digital	ark:/87602/m4/M58375	14.85			aerial	flight	Nowak, 1999		*	*
661	Laurasiatheria	Chiroptera	Phyllostomidae	Centurio_senex	UMMZ:Mamm:115176	Digital	ark:/87602/m4/M58341	23.09			aerial	flight	Nowak, 1999	*	*	*
662	Laurasiatheria	Chiroptera	Phyllostomidae	Chiroderma_villosum	UMMZ:Mamm:168883	Digital	ark:/87602/m4/M57265	23.81			aerial	flight	Nowak, 1999	*	*	*
663	Laurasiatheria	Chiroptera	Phyllostomidae	Choeroniscus_godmani	UMMZ:Mamm:113583	Digital	ark:/87602/m4/M58338	7.90			aerial	flight	Nowak, 1999	*	*	*
664	Laurasiatheria	Chiroptera	Phyllostomidae	Choeronycteris_mexicana	UMMZ:Mamm:77751	Digital	ark:/87602/m4/M58373	17.26			aerial	flight	Nowak, 1999	*	*	*

	Superord. group	Order	Family	Species	Institution Voucher	Method	MorpoSouce ID	Mass (g)	OBS	Body mass additional reference (if not Jones et al., 2009)	Medium (Ch3)	Locomotor ecology (Ch4)	Ecology reference	Ch2	Ch3	Ch4
665	Laurasiatheria	Chiroptera	Phyllostomidae	Chrotopterus_auritus	UMMZ:Mamm:175769	Digital	ark:/87602/m4/M58371	78.26			aerial	flight	Nowak, 1999	*	*	*
666	Laurasiatheria	Chiroptera	Phyllostomidae	Desmodus_rotundus	UMMZ:Mamm:175606	Digital	ark:/87602/m4/M58370	33.16			aerial	flight	Nowak, 1999	*	*	*
667	Laurasiatheria	Chiroptera	Phyllostomidae	Diphylla_ecaudata	MVZ:Mamm:167939	Digital	ark:/87602/m4/M98046	28.11			aerial	flight	Nowak, 1999		*	*
668	Laurasiatheria	Chiroptera	Phyllostomidae	Ectophylla_alba	UMMZ:Mamm:125633	Digital	ark:/87602/m4/M58349	5.55			aerial	flight	Nowak, 1999	*	*	*
669	Laurasiatheria	Chiroptera	Phyllostomidae	Enchisthenes_hartii	UMMZ:Mamm:114485	Digital	ark:/87602/m4/M58340	16.99			aerial	flight	Nowak, 1999	*	*	*
670	Laurasiatheria	Chiroptera	Phyllostomidae	Glossophaga_soricina	YPM:VZ:Mamm 005536	Digital	ark:/87602/m4/M64822	9.97			aerial	flight	Nowak, 1999	*	*	*
671	Laurasiatheria	Chiroptera	Phyllostomidae	Glossophaga_soricina	UMMZ:Mamm:160901	Digital	ark:/87602/m4/M58359	9.97			aerial	flight	Nowak, 1999	*	*	*
672	Laurasiatheria	Chiroptera	Phyllostomidae	Hsunycteris_thomasi	UMMZ:Mamm:175572	Digital	ark:/87602/m4/M58369	10.00		Santoro, 2004	aerial	flight	Nowak, 1999		*	*
673	Laurasiatheria	Chiroptera	Phyllostomidae	Lampronycteris_brachyotis	UMMZ:Mamm:122288	Digital	ark:/87602/m4/M58347	10.39			aerial	flight	Nowak, 1999	*	*	*
674	Laurasiatheria	Chiroptera	Phyllostomidae	Lionycteris_spurrelli	UMMZ:Mamm:160890	Digital	ark:/87602/m4/M58358	8.85			aerial	flight	Nowak, 1999	*	*	*
675	Laurasiatheria	Chiroptera	Phyllostomidae	Lonchorhina_aurita	UMMZ:Mamm:111319	Digital	ark:/87602/m4/M58336	15.38			aerial	flight	Nowak, 1999	*	*	*
676	Laurasiatheria	Chiroptera	Phyllostomidae	Lophostoma_brasiliense	UMMZ:Mamm:116152	Digital	ark:/87602/m4/M58346	9.76			aerial	flight	Nowak, 1999		*	*
677	Laurasiatheria	Chiroptera	Phyllostomidae	Macrophyllum_macrophyllum	UMMZ:Mamm:116026	Digital	ark:/87602/m4/M58344	8.02			aerial	flight	Nowak, 1999	*	*	*
678	Laurasiatheria	Chiroptera	Phyllostomidae	Macrotus_waterhousii	UMMZ:Mamm:79945	Digital	ark:/87602/m4/M58374	8.02			aerial	flight	Nowak, 1999		*	*
679	Laurasiatheria	Chiroptera	Phyllostomidae	Mesophylla_macconnelli	MVZ:Mamm:155282	Digital	ark:/87602/m4/M84952	6.86			aerial	flight	Nowak, 1999		*	*
680	Laurasiatheria	Chiroptera	Phyllostomidae	Mimon_cozumelae	UMMZ:Mamm:103429	Digital	ark:/87602/m4/M58333	23.00		Ávila-Palma et al., 2019	aerial	flight	Nowak, 1999	*	*	*
681	Laurasiatheria	Chiroptera	Phyllostomidae	Monophyllus_redmani	MVZ:Mamm:166164	Digital	ark:/87602/m4/M98044	8.79			aerial	flight	Nowak, 1999		*	*
682	Laurasiatheria	Chiroptera	Phyllostomidae	Musonycteris_harrisoni	UMMZ:Mamm:110686	Digital	ark:/87602/m4/M58335	11.64		Tschapka et al., 2008	aerial	flight	Nowak, 1999	*	*	*
683	Laurasiatheria	Chiroptera	Phyllostomidae	Phyllonycteris_poeyi	MVZ:Mamm:166161	Digital	ark:/87602/m4/M98066	22.00		Mancina, 2010	aerial	flight	Nowak, 1999		*	*
684	Laurasiatheria	Chiroptera	Phyllostomidae	Phyllops_falcatus	UMMZ:Mamm:124092	Digital	ark:/87602/m4/M58372	19.50		Tavares & Mancina, 2008	aerial	flight	Nowak, 1999	*	*	*
685	Laurasiatheria	Chiroptera	Phyllostomidae	Phyllostomus_discolor	UMMZ:Mamm:116027	Digital	ark:/87602/m4/M58345	36.70			aerial	flight	Nowak, 1999	*	*	*
686	Laurasiatheria	Chiroptera	Phyllostomidae	Platalina_genovensium	MCZ:Mamm:49468	Digital	ark:/87602/m4/M82933	18.38		Velazco et al., 2013	aerial	flight	Nowak, 1999	*	*	*
687	Laurasiatheria	Chiroptera	Phyllostomidae	Platyrrhinus_helleri	UMMZ:Mamm:168986	Digital	ark:/87602/m4/M58366	13.44			aerial	flight	Nowak, 1999	*	*	*
688	Laurasiatheria	Chiroptera	Phyllostomidae	Pygoderma_bilabiatum	UMMZ:Mamm:134227	Digital	ark:/87602/m4/M58353	18.50			aerial	flight	Nowak, 1999	*	*	*
689	Laurasiatheria	Chiroptera	Phyllostomidae	Rhinophylla_pumilio	YPM:VZ:Mamm 014632	Digital	ark:/87602/m4/M64838	9.58			aerial	flight	Nowak, 1999	*	*	*
690	Laurasiatheria	Chiroptera	Phyllostomidae	Stenoderma_rufum	UMMZ:Mamm:156616	Digital	ark:/87602/m4/M58354	21.10			aerial	flight	Nowak, 1999	*	*	*
691	Laurasiatheria	Chiroptera	Phyllostomidae	Sturnira_ludovici	UMMZ:Mamm:113642	Digital	ark:/87602/m4/M58339	21.00			aerial	flight	Nowak, 1999	*	*	*
692	Laurasiatheria	Chiroptera	Phyllostomidae	Trachops_cirrhosus	UMMZ:Mamm:164884	Digital	ark:/87602/m4/M58363	36.90			aerial	flight	Nowak, 1999	*	*	*
693	Laurasiatheria	Chiroptera	Phyllostomidae	Uroderma_bilobatum	UMMZ:Mamm:127216	Digital	ark:/87602/m4/M58350	16.28			aerial	flight	Nowak, 1999	*	*	*
694	Laurasiatheria	Chiroptera	Phyllostomidae	Vampyressa_pusilla	UMMZ:Mamm:134119	Digital	ark:/87602/m4/M58352	8.77			aerial	flight	Nowak, 1999	*	*	*
695	Laurasiatheria	Chiroptera	Phyllostomidae	Vampyrodes_caraccioli	UMMZ:Mamm:158066	Digital	ark:/87602/m4/M58357	35.89			aerial	flight	Nowak, 1999	*	*	*
696	Laurasiatheria	Chiroptera	Phyllostomidae	Vampyrum_spectrum	MVZ:Mamm:165941	Digital	ark:/87602/m4/M85268	171.61			aerial	flight	Nowak, 1999		*	*
697	Laurasiatheria	Chiroptera	Pteropodidae	Aethalops_alecto	UMMZ:Mamm:174565	Digital	ark:/87602/m4/M58367	15.00			aerial	flight	Nowak, 1999	*	*	*
698	Laurasiatheria	Chiroptera	Pteropodidae	Balionycteris_maculata	UMMZ:Mamm:174571	Digital	ark:/87602/m4/M58368	14.43			aerial	flight	Nowak, 1999	*	*	*
699	Laurasiatheria	Chiroptera	Pteropodidae	Chironax_melanocephalus	NHMUK:ZD:1975.1233	Digital	ark:/87602/m4/M164553	17.70			aerial	flight	Nowak, 1999		*	*
700	Laurasiatheria	Chiroptera	Pteropodidae	Cynopterus_brachyotis	UMMZ:Mamm:130388	Digital	ark:/87602/m4/M58351	33.87			aerial	flight	Nowak, 1999	*	*	*
701	Laurasiatheria	Chiroptera	Pteropodidae	Eonycteris_spelaea	UMMZ:Mamm:161208	Digital	ark:/87602/m4/M58361	58.70			aerial	flight	Nowak, 1999	*	*	*
702	Laurasiatheria	Chiroptera	Pteropodidae	Epomophorus_gambianus	MVZ:Mamm:149185	Digital	ark:/87602/m4/M85265	134.59			aerial	flight	Nowak, 1999		*	*
703	Laurasiatheria	Chiroptera	Pteropodidae	Haplonycteris_fischeri	UMMZ:Mamm:157351	Digital	ark:/87602/m4/M58355	18.25			aerial	flight	Nowak, 1999	*	*	*
704	Laurasiatheria	Chiroptera	Pteropodidae	Harpyionycteris_whiteheadi	UMMZ:Mamm:161303	Digital	ark:/87602/m4/M68611	135.48			aerial	flight	Nowak, 1999	*	*	*
705	Laurasiatheria	Chiroptera	Pteropodidae	Macroglossus_minimus	YPM:VZ:Mamm 005631	Digital	ark:/87602/m4/M65078	16.30			aerial	flight	Nowak, 1999	*	*	*
706	Laurasiatheria	Chiroptera	Pteropodidae	Macroglossus_minimus	UMMZ:Mamm:162913	Digital	ark:/87602/m4/M58362	16.30			aerial	flight	Nowak, 1999	*	*	*
707	Laurasiatheria	Chiroptera	Pteropodidae	Megaerops_ecaudatus	MVZ:Mamm:173803	Digital	ark:/87602/m4/M85269	26.29			aerial	flight	Nowak, 1999		*	*
708	Laurasiatheria	Chiroptera	Pteropodidae	Micropteropus_pusillus	UMMZ:Mamm:124088	Digital	ark:/87602/m4/M58348	25.38			aerial	flight	Nowak, 1999	*	*	*
709	Laurasiatheria	Chiroptera	Pteropodidae	Micropteropus_pusillus	YPM:VZ:Mamm 014564	Digital	ark:/87602/m4/M64572	25.38			aerial	flight	Nowak, 1999	*	*	*
710	Laurasiatheria	Chiroptera	Pteropodidae	Myonycteris_torquata	YPM:VZ:Mamm 014565	Digital	ark:/87602/m4/M64573	44.92			aerial	flight	Nowak, 1999	*	*	*
711	Laurasiatheria	Chiroptera	Pteropodidae	Nanonycteris_veldkampii	YPM:VZ:Mamm: 014567	Digital	ark:/87602/m4/M89779	21.89			aerial	flight	Nowak, 1999		*	*
712	Laurasiatheria	Chiroptera	Pteropodidae	Nyctimene_rabori	UMMZ:Mamm:158890	Digital	ark:/87602/m4/M63739	68.25			aerial	flight	Nowak, 1999	*	*	*
713	Laurasiatheria	Chiroptera	Pteropodidae	Paranyctimene_raptor	YPM:VZ:Mamm 005629	Digital	ark:/87602/m4/M64832	24.94			aerial	flight	Nowak, 1999	*	*	*
714	Laurasiatheria	Chiroptera	Pteropodidae	Penthetor_lucasi	UMMZ:Mamm:174604	Digital	ark:/87602/m4/M61965	35.39			aerial	flight	Nowak, 1999	*	*	*
715	Laurasiatheria	Chiroptera	Pteropodidae	Ptenochirus_jagori	UMMZ:Mamm:156741	Digital	ark:/87602/m4/M61951	79.18			aerial	flight	Nowak, 1999	*	*	*
716	Laurasiatheria	Chiroptera	Pteropodidae	Pteropus_pumilus	UMMZ:Mamm:156775	Digital	doi:10.17602/M2/M61952	184.05			aerial	flight	Nowak, 1999	*	*	*
717	Laurasiatheria	Chiroptera	Pteropodidae	Rousettus_aegyptiacus	YPM:VZ:Mamm 014576	Digital	ark:/87602/m4/M64574	134.00			aerial	flight	Nowak, 1999	*	*	*
718	Laurasiatheria	Chiroptera	Pteropodidae	Sphaerias_blanfordi	MVZ:Mamm:173806	Digital	ark:/87602/m4/M85270	28.88			aerial	flight	Nowak, 1999		*	*
719	Laurasiatheria	Chiroptera	Pteropodidae	Syconycteris_hobbit	YPM:VZ:Mamm: 005640	Digital	ark:/87602/m4/M89775	20.06			aerial	flight	Nowak, 1999		*	*
720	Laurasiatheria	Chiroptera	Rhinolophidae	Rhinolophus_arcuatus	UMMZ:Mamm:158869	Digital	ark:/87602/m4/M63738	8.98			aerial	flight	Nowak, 1999	*	*	*
721	Laurasiatheria	Chiroptera	Rhinolophidae	Rhinolophus_clivosus	YPM:VZ:Mamm: 005621	Digital	ark:/87602/m4/M89770	18.00		Jacobs et al., 2007	aerial	flight	Nowak, 1999		*	*
722	Laurasiatheria	Chiroptera	Rhinolophidae	Rhinolophus_cornutus	UMMZ:Mamm:165959	Digital	ark:/87602/m4/M96232	7.27			aerial	flight	Nowak, 1999		*	*
723	Laurasiatheria	Chiroptera	Rhinonycteridae	Triaenops_persicus	UMMZ:Mamm:164967	Digital	ark:/87602/m4/M55765	13.18			aerial	flight	Nowak, 1999	*	*	*
724	Laurasiatheria	Chiroptera	Rhinopomatidae	Rhinopoma_hardwickii	UMMZ:Mamm:157595	Digital	ark:/87602/m4/M61957	13.10			aerial	flight	Nowak, 1999	*	*	*
725	Laurasiatheria	Chiroptera	Thyropteridae	Thyroptera_tricolor	UMMZ:Mamm:120402	Digital	doi:10.17602/M2/M63736	4.52			aerial	flight	Nowak, 1999	*	*	*
726	Laurasiatheria	Chiroptera	Vespertilionidae	Antrozous_pallidus	UMMZ:Mamm:101281	Digital	ark:/87602/m4/M61946	22.24			aerial	flight	Nowak, 1999	*	*	*
727	Laurasiatheria	Chiroptera	Vespertilionidae	Barbastella_barbastellus	UMMZ:Mamm:113297	Digital	ark:/87602/m4/M61948	8.31			aerial	flight	Nowak, 1999	*	*	*
728	Laurasiatheria	Chiroptera	Vespertilionidae	Chalinolobus_gouldii	UMMZ:Mamm:164680	Digital	ark:/87602/m4/M63740	14.24			aerial	flight	Nowak, 1999	*	*	*
729	Laurasiatheria	Chiroptera	Vespertilionidae	Eptesicus_fuscus	UMMZ:Mamm:110759	Digital	ark:/87602/m4/M96224	17.49			aerial	flight	Nowak, 1999		*	*
730	Laurasiatheria	Chiroptera	Vespertilionidae	Euderma_maculatum	MVZ:Mamm:61931	Digital	ark:/87602/m4/M85274	16.17			aerial	flight	Nowak, 1999	*	*	*
731	Laurasiatheria	Chiroptera	Vespertilionidae	Glischropus_tylopus	MVZ:Mamm:129207	Digital	ark:/87602/m4/M98065	4.59			aerial	flight	Nowak, 1999		*	*
732	Laurasiatheria	Chiroptera	Vespertilionidae	Hesperoptenus_tickelli	UMMZ:Mamm:172252	Digital	ark:/87602/m4/M61962	16.30			aerial	flight	Nowak, 1999	*	*	*
733	Laurasiatheria	Chiroptera	Vespertilionidae	Histiotus_velatus	MCZ:Mamm:4184	Digital	ark:/87602/m4/M89510	11.32			aerial	flight	Nowak, 1999		*	*
734	Laurasiatheria	Chiroptera	Vespertilionidae	Kerivoula_picta	UMMZ:Mamm:172244	Digital	ark:/87602/m4/M63742	4.50			aerial	flight	Nowak, 1999	*	*	*
735	Laurasiatheria	Chiroptera	Vespertilionidae	Lasionycteris_noctivagans	UMMZ:Mamm:55198	Digital	ark:/87602/m4/M63742	11.02			aerial	flight	Nowak, 1999	*	*	*

	Superord. group	Order	Family	Species	Institution Voucher	Method	MorpoSouce ID	Mass (g)	OBS	Body mass additional reference (if not Jones et al., 2009)	Medium (Ch3)	Locomotor ecology (Ch4)	Ecology reference	Ch2	Ch3	Ch4
736	Laurasiatheria	Chiroptera	Vespertilionidae	Lasiurus_borealis	YPM:VZ:Mamm 005667	Digital	ark:/87602/m4/M65076	12.33			aerial	flight	Nowak, 1999	*	*	*
737	Laurasiatheria	Chiroptera	Vespertilionidae	Myotis_lucifugus	UMMZ:Mamm:58828	Digital	doi:10.17602/M2/M63746	7.80			aerial	flight	Nowak, 1999	*	*	*
738	Laurasiatheria	Chiroptera	Vespertilionidae	Neoromicia_nana	YPM:VZ:Mamm: 005696	Digital	ark:/87602/m4/M89777	3.88			aerial	flight	Nowak, 1999		*	*
739	Laurasiatheria	Chiroptera	Vespertilionidae	Nycticeius_humeralis	UMMZ:Mamm:81282	Digital	ark:/87602/m4/M63747	9.12			aerial	flight	Nowak, 1999	*	*	*
740	Laurasiatheria	Chiroptera	Vespertilionidae	Nyctophilus_geoffroyi	UMMZ:Mamm:164682	Digital	ark:/87602/m4/M64404	8.90		Turbill & Geiser, 2006	aerial	flight	Nowak, 1999	*	*	*
741	Laurasiatheria	Chiroptera	Vespertilionidae	Plecotus_auritus	UMMZ:Mamm:113298	Digital	ark:/87602/m4/M63734	8.19			aerial	flight	Nowak, 1999	*	*	*
742	Laurasiatheria	Chiroptera	Vespertilionidae	Rhogeessa_tumida	UMMZ:Mamm:114489	Digital	ark:/87602/m4/M63735	4.58			aerial	flight	Nowak, 1999	*	*	*
743	Laurasiatheria	Chiroptera	Vespertilionidae	Scotophilus_kuhlii	UMMZ:Mamm:156908	Digital	ark:/87602/m4/M61955	20.31			aerial	flight	Nowak, 1999	*	*	*
744	Laurasiatheria	Chiroptera	Vespertilionidae	Vespadelus_sp	YPM:VZ:Mamm: 005574	Digital	ark:/87602/m4/M89769	5.05	Body mass of genus average.		aerial	GBIF	Nowak, 1999		*	*
745	Laurasiatheria	Chiroptera	Vespertilionidae	Vespertilio_murinus	MCZ:Mamm:3131	Digital	ark:/87602/m4/M95923	15.42			aerial	flight	Nowak, 1999		*	*
746	Laurasiatheria	Eulipotyphla	Erinaceidae	Atelerix_albiventris	MNHN-ZM-MO-1992-1490	Digital	Montpellier	293.44			terrestrial	terrestrialquad	Happold, 2013		*	*
747	Laurasiatheria	Eulipotyphla	Erinaceidae	Echinosorex_gymnura	UMZC:E.5111.C-E	Digital	ark:/87602/m4/M164562	756.53			terrestrial	terrestrialquad	Chen & Wilson, 2015		*	*
748	Laurasiatheria	Eulipotyphla	Erinaceidae	Erinaceus_europaeus	UMMZ:Mamm:138469	Digital	doi:10.17602/M2/M63737	777.95			terrestrial	fossorial	Hopkins & Davis, 2009	*	*	*
749	Laurasiatheria	Eulipotyphla	Erinaceidae	Hemiechinus_auritus	UMMZ:Mamm:101315	Digital	doi:10.17602/M2/M64391	322.04			terrestrial	semifossorial	Ballenger, 1999	*	*	*
750	Laurasiatheria	Eulipotyphla	Erinaceidae	Neotetracus_sinensis	NHMUK:ZD:1933.4.1.134	Digital	ark:/87602/m4/M154934	87.00		Smith et al., 2018	terrestrial	terrestrialquad	Nowak, 1999		*	*
751	Laurasiatheria	Eulipotyphla	Erinaceidae	Paraechinus_aethiopicus	MNHN-ZM-MO-2000-312	Digital	Montpellier	352.40			terrestrial	terrestrialquad	Nowak, 1999		*	*
752	Laurasiatheria	Eulipotyphla	Erinaceidae	Podogymnura_truei	FMNH:Mamm:146591	Digital	ark:/87602/m4/M159150	67.00		Heaney et al., 2006	terrestrial	terrestrialquad	Rasmussen, 2007		*	*
753	Laurasiatheria	Eulipotyphla	Solenodontidae	Solenodon_paradoxus	TCWC:Mamm:28881	Digital	ark:/87602/m4/M81935	899.99			terrestrial	semifossorial	Chen & Wilson, 2015		*	*
754	Laurasiatheria	Eulipotyphla	Soricidae	Anourosorex_squamipes	NHMUK:ZD:1933.4.1.165	Digital	ark:/87602/m4/M157300	20.00			terrestrial	fossorial	Nowak, 1999		*	*
755	Laurasiatheria	Eulipotyphla	Soricidae	Blarina_brevicauda	UMMZ:Mamm:47268	Digital	doi:10.17602/M2/M68619	18.56			terrestrial	semifossorial	GBIF Secretariat, 2022a	*	*	*
756	Laurasiatheria	Eulipotyphla	Soricidae	Chimarrogale_himalayica	AMNH:Mamm:m-272282	Digital	ark:/87602/m4/M101243	33.50			semiaquatic	semiaquatic	Hood, 2020		*	*
757	Laurasiatheria	Eulipotyphla	Soricidae	Congosorex_verheyeni	MNHN-ZM-MO-2018-570	Digital	Montpellier	7.10		Stanley et al., 2005	terrestrial	terrestrialquad	Barrière & Hutterer, 2013		*	*
758	Laurasiatheria	Eulipotyphla	Soricidae	Crocidura_russula	UMMZ:Mamm:157845	Digital	doi:10.17602/M2/M68608	9.89			terrestrial	terrestrialquad	Aulagnier & Vogel, 2013	*	*	*
759	Laurasiatheria	Eulipotyphla	Soricidae	Cryptotis_mexicana	UMMZ:Mamm:113138	Digital	ark:/87602/m4/M164466	7.00			terrestrial	terrestrialquad	Cassola, 2016a		*	*
760	Laurasiatheria	Eulipotyphla	Soricidae	Diplomesodon_pulchellum	MVZ:Mamm:179157	Digital	ark:/87602/m4/M85273	11.00			terrestrial	terrestrialquad	Nowak, 1999		*	*
761	Laurasiatheria	Eulipotyphla	Soricidae	Episoriculus_caudatus	UMMZ:Mamm:122889	Digital	doi:10.17602/M2/M68589	6.00		Freudenthal & Suárez, 2013	terrestrial	terrestrialquad	Molur, 2016b	*	*	*
762	Laurasiatheria	Eulipotyphla	Soricidae	Episoriculus_caudatus	FMNH:Mamm:114227	Digital	ark:/87602/m4/M141380	6.00		Freudenthal & Suárez, 2013	terrestrial	terrestrialquad	Molur, 2016b		*	*
763	Laurasiatheria	Eulipotyphla	Soricidae	Myosorex_kihaulei	FMNH:Mamm:209072-209073	Digital	ark:/87602/m4/M157935	9.50		Peterhans et al., 2008	terrestrial	terrestrialquad	Stanley, 2013a		*	*
764	Laurasiatheria	Eulipotyphla	Soricidae	Nectogale_elegans	AMNH:Mamm:m-115571	Digital	ark:/87602/m4/M101239	38.82			semiaquatic	semiaquatic	Hood, 2020		*	*
765	Laurasiatheria	Eulipotyphla	Soricidae	Neomys_fodiens	UMMZ:Mamm:157664	Digital	ark:/87602/m4/M68607	15.26			semiaquatic	semiaquatic	Hood, 2020	*	*	*
766	Laurasiatheria	Eulipotyphla	Soricidae	Notiosorex_crawfordi	MNHN-ZM-MO-1985-645	Digital	Montpellier	4.79			terrestrial	terrestrialquad	Allen, 2000		*	*
767	Laurasiatheria	Eulipotyphla	Soricidae	Paracrocidura_schoutedeni	FMNH:Mamm:227382	Digital	ark:/87602/m4/M157801	12.18			terrestrial	terrestrialquad	Ray & Hutterer, 2013		*	*
768	Laurasiatheria	Eulipotyphla	Soricidae	Scutisorex_somereni	FMNH:Mamm:160182	Digital	ark:/87602/m4/M157824	91.49			terrestrial	terrestrialquad	Nowak, 1999		*	*
769	Laurasiatheria	Eulipotyphla	Soricidae	Sorex_cinereus	UMMZ:Mamm:175520	Digital	doi:10.17602/M2/M64409	4.20			terrestrial	terrestrialquad	Nowak, 1999	*	*	*
770	Laurasiatheria	Eulipotyphla	Soricidae	Soriculus_nigrescens	UMMZ:Mamm:122888	Digital	doi:10.17602/M2/M141210	14.58			terrestrial	terrestrialquad	Nowak, 1999		*	*
771	Laurasiatheria	Eulipotyphla	Soricidae	Suncus_murinus	UMMZ:Mamm:115820	Digital	ark:/87602/m4/M68581	43.76			terrestrial	terrestrialquad	Nowak, 1999	*	*	*
772	Laurasiatheria	Eulipotyphla	Soricidae	Surdisorex_norae	FMNH:Mamm:190260	Digital	ark:/87602/m4/M164407	23.57			terrestrial	semifossorial	Happold, 2013b		*	*
773	Laurasiatheria	Eulipotyphla	Soricidae	Sylvisorex_howelli	FMNH:Mamm:198205-198206	Digital	ark:/87602/m4/M157866	4.00		Smith et al., 2018	terrestrial	terrestrialquad	Stanley, 2013b		*	*
774	Laurasiatheria	Eulipotyphla	Talpidae	Condylura_cristata	YPM:VZ:Mamm 014548	Digital	ark:/87602/m4/M64579	48.15			semiaquatic	semiaquatic	Hood, 2020; Nowak, 1999	*	*	*
775	Laurasiatheria	Eulipotyphla	Talpidae	Desmana_moschata	UMMZ:Mamm:124125	Digital	ark:/87602/m4/M159827	427.64			semiaquatic	semiaquatic	Hood, 2020		*	*
776	Laurasiatheria	Eulipotyphla	Talpidae	Euroscaptor_micrura	NHMUK:99.10.25.1	Digital	ark:/87602/m4/M157383	60.46			terrestrial	fossorial	Nowak, 1999		*	*
777	Laurasiatheria	Eulipotyphla	Talpidae	Galemys_pyrenaicus	MCZ:Mamm:28163	Digital	ark:/87602/m4/M82658	60.17			semiaquatic	semiaquatic	Chen & Wilson, 2015; Hood, 2020	*	*	*
778	Laurasiatheria	Eulipotyphla	Talpidae	Galemys_pyrenaicus	OUMNH:9427	Digital	ark:/87602/m4/M158328	60.17			semiaquatic	semiaquatic	Chen & Wilson 2015; Hood, 2020		*	*
779	Laurasiatheria	Eulipotyphla	Talpidae	Mogera_wogura	CM:Mamm:94705	Digital	ark:/87602/m4/M95876	96.88			terrestrial	fossorial	Nowak, 1999		*	*
780	Laurasiatheria	Eulipotyphla	Talpidae	Neurotrichus_gibbsii	UMMZ:Mamm:114715	Digital	ark:/87602/m4/M65515	9.56			terrestrial	fossorial	Gochis, 2002	*	*	*
781	Laurasiatheria	Eulipotyphla	Talpidae	Scalopus_aquaticus	YPM:VZ:Mamm: 005709	Digital	ark:/87602/m4/M90673	87.15			terrestrial	fossorial	Hopkins & Davis, 2009		*	*
782	Laurasiatheria	Eulipotyphla	Talpidae	Scapanus_latimanus	UMMZ:Mamm:74584	Digital	ark:/87602/m4/M160076	62.46			terrestrial	fossorial	Nowak, 1999		*	*
783	Laurasiatheria	Perissodactyla	Equidae	Equus_asinus	MHNH-ZM-AC-1893-634	Caliper	-	164998.49			terrestrial	terrestrialquad	Nowak, 1999	*	*	*
784	Laurasiatheria	Perissodactyla	Equidae	Equus_caballus	MNHN-ZM-AC-1911-145	Caliper	-	403598.53			terrestrial	terrestrialquad	Nowak, 1999	*	*	*
785	Laurasiatheria	Perissodactyla	Equidae	Equus_grevyi	MNHN-ZM-AC-1913-58	Caliper	-	408000.35			terrestrial	terrestrialquad	Nowak, 1999	*	*	*
786	Laurasiatheria	Perissodactyla	Equidae	Equus_hemionus	MHNH-ZM-AC-1902-487	Caliper	-	235248.07			terrestrial	terrestrialquad	Nowak, 1999	*	*	*
787	Laurasiatheria	Perissodactyla	Rhinocerotidae	Ceratotherium_simum	MNHN-ZM-AC-A7968	Caliper	-	2285939.43			terrestrial	terrestrialquad	Nowak, 1999	*	*	*
788	Laurasiatheria	Perissodactyla	Rhinocerotidae	Dicerorhinus_sumatrensis	MNHN-ZM-AC-A7967	Caliper	-	1046156.04			terrestrial	terrestrialquad	Nowak, 1999	*	*	*
789	Laurasiatheria	Perissodactyla	Rhinocerotidae	Diceros_bicornis	MNHN-ZM-AC-1944-278	Caliper	-	995940.54			terrestrial	terrestrialquad	Nowak, 1999	*	*	*
790	Laurasiatheria	Perissodactyla	Rhinocerotidae	Rhinoceros_sondaicus	MNHN-ZM-AC-A7971	Caliper	-	1750000.00			terrestrial	terrestrialquad	Nowak, 1999	*	*	*
791	Laurasiatheria	Perissodactyla	Rhinocerotidae	Rhinoceros_unicornis	MNHN-ZM-AC-1960-59	Caliper	-	1843655.80			terrestrial	terrestrialquad	Nowak, 1999	*	*	*
792	Laurasiatheria	Perissodactyla	Tapiridae	Acrocodia_indicus	MNHN-ZM-AC-1944-267	Caliper	-	311209.19			semiaquatic	semiaquatic	García et al., 2012; Nowak, 1999		*	*
793	Laurasiatheria	Perissodactyla	Tapiridae	Tapirus_pinchaque	MNHN-ZM-AC-1982-34	Caliper	-	156923.40			semiaquatic	semiaquatic	García et al., 2012; Nowak, 1999	*	*	
794	Laurasiatheria	Perissodactyla	Tapiridae	Tapirus_terrestris	MNHN-ZM-AC-1937-1	Caliper	-	169496.64			semiaquatic	semiaquatic	García et al., 2012; Nowak, 1999	*	*	*
795	Laurasiatheria	Pholidota	Manidae	Manis_pentadactyla	MNHN-1872-64	Caliper	-	4675.00			terrestrial	semifossorial	GBIF Secretariat, 2022b; Raynor, 2000	*	*	*
796	Laurasiatheria	Pholidota	Manidae	Phataginus_tricuspis	MNHN-1972-173	Caliper	-	1539.31			terrestrial	scansorial	GBIF Secretariat 2022d	*	*	*
797	Laurasiatheria	Pholidota	Manidae	Smutsia_gigantea	MNHN-1869-760	Caliper	-	32999.70			terrestrial	semifossorial	Nowak, 1999,GBIF Secretariat, 2022b	*	*	*
798	Laurasiatheria	Pholidota	Manidae	Smutsia_gigantea	NHM-1965-5-12-1	Caliper	-	32999.70			terrestrial	semifossorial	Nowak, 1999; GBIF Secretariat, 2022b		*	*

	Superord. group	Order	Family	Species	Institution Voucher	Method	MorpoSouce ID	Mass (g)	OBS	Body mass additional reference (if not Jones et al., 2009)	Medium (Ch3)	Locomotor ecology (Ch4)	Ecology reference	Ch2	Ch3	Ch4
799	Marsupialia	Dasyuromorpha	Dasyuridae	Antechinomys_laniger	NHMUK:zoo:zd 1932.2.11.23	Digital	ark:/87602/m4/M82407	25.57			terrestrial	terrestrialquad	Nowak, 1999		*	*
800	Marsupialia	Dasyuromorpha	Dasyuridae	Antechinus_stuartii	FMNH:Mamm:129556	Digital	ark:/87602/m4/M82261	29.01			terrestrial	terrestrialquad	Nowak, 1999	*	*	*
801	Marsupialia	Dasyuromorpha	Dasyuridae	Dasycercus_cristicauda	NHMUK:Zoo:1897.11.3.4	Digital	ark:/87602/m4/M82423	99.54			terrestrial	semifossorial	Nowak, 1999		*	*
802	Marsupialia	Dasyuromorpha	Dasyuridae	Dasyuroides_byrnei	NHMUK:zoo:1992.02	Digital	ark:/87602/m4/M164550	109.47			terrestrial	terrestrialquad	Chen & Wilson, 2015	*	*	*
803	Marsupialia	Dasyuromorpha	Dasyuridae	Dasyurus_maculatus	UMZC:Vertebrates:a6. 10/3	Digital	ark:/87602/m4/M68239	3284.15			terrestrial	terrestrialquad	Nowak, 1999	*	*	*
804	Marsupialia	Dasyuromorpha	Dasyuridae	Dasyurus_maculatus	MVZ:Mamm:126999	Digital	ark:/87602/m4/M98700	3284.15			terrestrial	terrestrialquad	Nowak, 1999	*	*	*
805	Marsupialia	Dasyuromorpha	Dasyuridae	Phascogale_pirata	NHM-304c	Caliper	-	179.88		Aplin et al., 2015	terrestrial	arboreal	Woinarski et al., 2019		*	*
806	Marsupialia	Dasyuromorpha	Dasyuridae	Sarcophilus_harrisii	AMNH-150211	Caliper	-	8202.25			terrestrial	terrestrialquad	Nowak, 1999		*	
807	Marsupialia	Dasyuromorpha	Dasyuridae	Sminthopsis_crassicaudata	FMNH:Mamm:72923	Digital	ark:/87602/m4/M82320	15.98			terrestrial	terrestrialquad	Nowak, 1999	*	*	*
808	Marsupialia	Dasyuromorpha	Myrmecobiidae	Myrmecobius_fasciatus	UMZC:Vertebrates:a6. 41/8	Digital	ark:/87602/m4/M68247	511.44			terrestrial	semifossorial	Chen & Wilson, 2015; Cooper & Withers, 2002		*	*
809	Marsupialia	Dasyuromorpha	Thylacidae	Thylacinus_cynocephalus	NRM:566599	Digital	doi:10.17602/M2/M158442	29999.99			terrestrial	terrestrialquad	Hopkins & Davis, 2009	*	*	*
810	Marsupialia	Didelphimorphia	Didelphidae	Caluromys_derbianus	UMMZ:Mamm:114856	Digital	doi:10.17602/M2/M82350	326.72			terrestrial	arboreal	Chen & Wilson, 2015	*	*	*
811	Marsupialia	Didelphimorphia	Didelphidae	Caluromys_sp	DU:EA:181	Digital	doi:10.17602/M2/M28455	307.84	Body mass of genus average.		terrestrial	arboreal	Chen & Wilson, 2015	*	*	*
812	Marsupialia	Didelphimorphia	Didelphidae	Caluromysiops_irrupta	FMNH:Mamm:60698	Digital	ark:/87602/m4/M82280	257.48			terrestrial	arboreal	Nowak, 1999	*	*	*
813	Marsupialia	Didelphimorphia	Didelphidae	Chironectes_minimus	UMMZ:Mamm:155686	Digital	ark:/87602/m4/M75118	974.33			semiaquatic	semiaquatic	Hood, 2020	*	*	*
814	Marsupialia	Didelphimorphia	Didelphidae	Didelphis_sp	DU:EA:204	Digital	doi:10.17602/M2/M29046	1428.30	Body mass of genus average.		terrestrial	scansorial	Chen & Wilson 2016	*	*	*
815	Marsupialia	Didelphimorphia	Didelphidae	Glironia_venusta	UMMZ:Mamm:156021	Digital	ark:/87602/m4/M68601	114.00	Same as Marmosa venusta in MorphoSource.		terrestrial	arboreal	Nowak, 1999	*	*	*
816	Marsupialia	Didelphimorphia	Didelphidae	Gracilinanus_agilis	UMMZ:Mamm:134557	Digital	doi:10.17602/M2/M82358	22.03			terrestrial	arboreal	Nowak, 1999	*	*	*
817	Marsupialia	Didelphimorphia	Didelphidae	Lutreolina_crassicaudata	UMMZ:Mamm:134562	Digital	doi:10.17602/M2/M82375	554.77			semiaquatic	semiaquatic	Hood, 2020 Nowak, 1999	*	*	*
818	Marsupialia	Didelphimorphia	Didelphidae	Marmosa_robinsoni	UMMZ:Mamm:117236	Digital	ark:/87602/m4/M64398	60.57			terrestrial	arboreal	Chen & Wilson, 2015	*	*	*
819	Marsupialia	Didelphimorphia	Didelphidae	Marmosops_incanus	FMNH:Mamm:145325	Digital	ark:/87602/m4/M164404	59.88			terrestrial	arboreal	Nowak, 1999	*	*	*
820	Marsupialia	Didelphimorphia	Didelphidae	Metachirus_nudicaudatus	UMMZ:Mamm:155687	Digital	doi:10.17602/M2/M68600	363.77			terrestrial	terrestrialquad	Chen & Wilson, 2015	*	*	*
821	Marsupialia	Didelphimorphia	Didelphidae	Metachirus_nudicaudatus	UMMZ:Mamm:117229	Digital	ark:/87602/m4/M64397	363.77			terrestrial	terrestrialquad	Chen & Wilson, 2015	*	*	*
822	Marsupialia	Didelphimorphia	Didelphidae	Monodelphis_domestica	UMMZ:Mamm:165514	Digital	doi:10.17602/M2/M68214	93.45			terrestrial	terrestrialquad	Nowak, 1999	*	*	*
823	Marsupialia	Didelphimorphia	Didelphidae	Philander_opossum	UMMZ:Mamm:114855	Digital	doi:10.17602/M2/M82596	425.81			terrestrial	terrestrialquad	Nowak, 1999		*	*
824	Marsupialia	Didelphimorphia	Didelphidae	Thylamys_venustus	UMMZ:Mamm:156033	Digital	doi:10.17602/M2/M82399	17.80		Amador & Giannini, 2016	terrestrial	scansorial	Nowak, 1999	*	*	*
825	Marsupialia	Diprotodontia	Acrobatidae	Acrobates_pygmaeus	NHMUK:82.7.29.23	Digital	ark:/87602/m4/M52800	13.84			semiaerial	gliding	Jackson, 2000	*	*	*
826	Marsupialia	Diprotodontia	Acrobatidae	Acrobates_pygmaeus	MCZ:Mamm:19480	Digital	ark:/87602/m4/M83740	13.84			semiaerial	gliding	Jackson, 2000	*	*	*
827	Marsupialia	Diprotodontia	Burramyidae	Cercartetus_concinnus	NHMUK:zoo:zd 1897.11.18.1	Digital	ark:/87602/m4/M82415	15.96	Same as Dromicia concinna in MorphoSource.		terrestrial	arboreal	Nowak, 1999	*	*	*
828	Marsupialia	Diprotodontia	Hypsiprymnodontidae	Hypsiprymnodon_moschatus	NHM-1981-100	Caliper	-	534.25			terrestrial	terrestrialquad	Nowak, 1999		*	*
829	Marsupialia	Diprotodontia	Hypsiprymnodontidae	Hypsiprymnodon_moschatus	NHM-1694a	Caliper	-	534.25			terrestrial	terrestrialquad	Nowak, 1999		*	*
830	Marsupialia	Diprotodontia	Hypsiprymnodontidae	Hypsiprymnodon_moschatus	AMNH:Mamm:m-65340	Digital	doi:10.17602/M2/M370249	534.25			terrestrial	terrestrialquad	Nowak, 1999		*	*
831	Marsupialia	Diprotodontia	Macropodidae	Dendrolagus_lumholtzi	AMNH-35623	Caliper	-	6649.97			terrestrial	arboreal	Nowak, 1999		*	*
832	Marsupialia	Diprotodontia	Macropodidae	Dorcopsis_muelleri	AMNH-222626	Caliper	-	5370.79			terrestrial	terrestrialbip	Nowak, 1999		*	
833	Marsupialia	Diprotodontia	Macropodidae	Macropus_giganteus	MNHN-1970-11	Caliper	-	33409.89			terrestrial	terrestrialbip	Nowak, 1999	*	*	*
834	Marsupialia	Diprotodontia	Macropodidae	Notamacropus_parryi	MNHN-1932-579	Caliper	-	12629.83			terrestrial	terrestrialbip	Nowak, 1999		*	*
835	Marsupialia	Diprotodontia	Macropodidae	Onychogalea_fraenata	UMZC:Vertebrates:a12. 59/3	Digital	ark:/87602/m4/M82448	4952.05			terrestrial	terrestrialbip	Nowak, 1999		*	*
836	Marsupialia	Diprotodontia	Macropodidae	Petrogale_penicillata	MNHN-1874-77	Caliper	-	6931.60			terrestrial	terrestrialbip	Nowak, 1999	*	*	*
837	Marsupialia	Diprotodontia	Macropodidae	Setonix_brachyurus	AMNH-35744	Caliper	-	3027.67			terrestrial	terrestrialbip	Nowak, 1999		*	*
838	Marsupialia	Diprotodontia	Macropodidae	Thylogale_stigmatica	UMZC:Vertebrates:a12. 44/1	Digital	ark:/87602/m4/M82466	4511.47			terrestrial	terrestrialbip	Nowak, 1999	*	*	*
839	Marsupialia	Diprotodontia	Macropodidae	Wallabia_bicolor	AMNH-70264	Caliper	-	14999.95			terrestrial	terrestrialbip	Nowak, 1999		*	*
840	Marsupialia	Diprotodontia	Petauridae	Dactylopsila_trivirgata	NHMUK:1897.8.7.79	Digital	ark:/87602/m4/M68263	413.41			terrestrial	arboreal	Nowak, 1999	*	*	*
841	Marsupialia	Diprotodontia	Petauridae	Petaurus_breviceps	FMNH:129430	Digital	ark:/87602/m4/M52791	120.76			semiaerial	gliding	Jackson, 2000	*	*	*
842	Marsupialia	Diprotodontia	Phalangeridae	Ailurops_ursinus	AMNH-153372	Caliper	-	10000.00			terrestrial	arboreal	Seaton, 2002		*	*
843	Marsupialia	Diprotodontia	Phalangeridae	Phalanger_orientalis	NHMUK:1867.4.12.413	Digital	ark:/87602/m4/M160191	2487.50			terrestrial	arboreal	Nowak, 1999	*	*	*
844	Marsupialia	Diprotodontia	Phalangeridae	Spilocuscus_maculatus	FMNH:Mamm:31752	Digital	ark:/87602/m4/M164405	4060.46			terrestrial	arboreal	Nowak, 1999	*	*	
845	Marsupialia	Diprotodontia	Phalangeridae	Strigocuscus_pelengensis	AMNH-107999	Caliper	-	1000.00		Moe, 2007	terrestrial	arboreal	Nowak, 1999		*	
846	Marsupialia	Diprotodontia	Phalangeridae	Trichosurus_vulpecula	YPM:VZ:Mamm 005643	Digital	ark:/87602/m4/M68288	2685.39			terrestrial	arboreal	Chen & Wilson, 2015	*	*	*
847	Marsupialia	Diprotodontia	Phascolarctidae	Phascolarctos_cinereus	MNHN-1879-60	Caliper	-	6528.74			terrestrial	arboreal	Hopkins & Davis, 2009	*	*	*
848	Marsupialia	Diprotodontia	Potoroidae	Aepyprymnus_rufescens	MSU:MR:MR.4680	Digital	ark:/87602/m4/M112448	2810.31			terrestrial	terrestrialbip	Chen & Wilson, 2015	*	*	*
849	Marsupialia	Diprotodontia	Potoroidae	Bettongia_gaimardi	MNHN-1883-1517	Caliper	-	1667.55			terrestrial	terrestrialbip	Nowak, 1999	*	*	*
850	Marsupialia	Diprotodontia	Potoroidae	Potorous_tridactylus	FMNH:Mamm:57805	Digital	ark:/87602/m4/M68179	1054.67			terrestrial	terrestrialbip	Chen & Wilson, 2015	*	*	
851	Marsupialia	Diprotodontia	Pseudocheiridae	Hemibelideus_lemuroides	MSU:MR:MR.4678	Digital	ark:/87602/m4/M86530	993.59			terrestrial	arboreal	Chen & Wilson, 2015	*	*	*
852	Marsupialia	Diprotodontia	Pseudocheiridae	Petauroides_volans	NHMUK:zoo:1926.3.11.225	Digital	ark:/87602/m4/M52207	1257.17			semiaerial	gliding	Jackson, 2000	*	*	*
853	Marsupialia	Diprotodontia	Pseudocheiridae	Pseudocheirus_peregrinus	YPM:VZ:Mamm 014395	Digital	ark:/87602/m4/M91603	895.22			terrestrial	arboreal	Chen & Wilson, 2015	*	*	*
854	Marsupialia	Diprotodontia	Tarsipedidae	Tarsipes_rostratus	UMMZ:Mamm:122547	Digital	doi:10.17602/M2/M82391	9.66			terrestrial	arboreal	Nowak, 1999	*	*	*
855	Marsupialia	Diprotodontia	Vombatidae	Lasiorhinus_latifrons	MNHN-1869-761	Caliper	-	26163.80			terrestrial	semifossorial	Green, 2006	*	*	*
856	Marsupialia	Diprotodontia	Vombatidae	Vombatus_ursinus	UMZC:Vertebrates:a10. 10/2	Digital	ark:/87602/m4/M83581	26000.00			terrestrial	semifossorial	Hopkins & Davis, 2009	*	*	*
857	Marsupialia	Microbiotheria	Microbiotheriidae	Dromiciops_gliroides	UMMZ:Mamm:156354	Digital	doi:10.17602/M2/M68206	25.00	Same as Dromiciops australis.		terrestrial	scansorial	Nowak, 1999	*	*	*
858	Marsupialia	Notoryctemorphia	Notoryctidae	Notoryctes_typhlops	MCZ:Mamm:28158	Digital	ark:/87602/m4/M81856	55.00			terrestrial	fossorial	Hopkins & Davis, 2009			
859	Marsupialia	Paucituberculata	Caenolestidae	Caenolestes_fuliginosus	UMZC:Vertebrates:a8. 2/3	Digital	ark:/87602/m4/M164556	28.64			terrestrial	terrestrialquad	Nowak, 1999	*	*	*
860	Marsupialia	Paucituberculata	Caenolestidae	Lestoros_inca	UMMZ:Mamm:160733	Digital	doi:10.17602/M2/M82366	23.07			terrestrial	terrestrialquad	Siciliano Martina, 2013	*	*	*
861	Marsupialia	Paucituberculata	Caenolestidae	Rhyncholestes_raphanurus	FMNH:Mamm:127476	Digital	ark:/87602/m4/M82330	21.94			terrestrial	terrestrialquad	Patterson et al., 1990	*	*	*
862	Marsupialia	Peramelemorphia	Chaeropodidae	Chaeropus_ecaudatus	UMZC:Vertebrates:a7. 19/1	Digital	ark:/87602/m4/M164560	219.51			terrestrial	terrestrialquad	Normile, 1999; Nowak, 1999	*	*	*
863	Marsupialia	Peramelemorphia	Peramelidae	Echymipera_kalubu	MVZ:Mamm:138479	Digital	ark:/87602/m4/M85264	825.16			terrestrial	terrestrialquad	Nowak, 1999	*	*	*
864	Marsupialia	Peramelemorphia	Peramelidae	Isoodon_obesulus	UMZC:Vertebrates:a7. 4/5	Digital	ark:/87602/m4/M82439	824.76			terrestrial	semifossorial	Nowak, 1999; Warburton et al., 2013	*	*	*

	Superord. group	Order	Family	Species	Institution Voucher	Method	MorpoSouce ID	Mass (g)	OBS	Body mass additional reference (if not Jones et al., 2009)	Medium (Ch3)	Locomotor ecology (Ch4)	Ecology reference	Ch2	Ch3	Ch4
865	Marsupialia	Peramelemorphia	Peramelidae	Isoodon_obesulus	MVZ:Mamm:132249	Digital	ark:/87602/m4/M99361	824.76			terrestrial	semifossorial	Nowak, 1999; Warburton et al., 2013	*	*	*
866	Marsupialia	Peramelemorphia	Peramelidae	Perameles_nasuta	AMNH-48189	Caliper	-	720.26			terrestrial	terrestrialquad	Chen & Wilson, 2015		*	*
867	Marsupialia	Peramelemorphia	Peramelidae	Peroryctes_raffrayana	AMNH-152487	Caliper	-	905.63			terrestrial	terrestrialquad	Nowak, 1999		*	*
868	Marsupialia	Peramelemorphia	Thylacomyidae	Macrotis_lagotis	MNHN-ZM-AC-1872-172	Caliper	-	1229.58			terrestrial	semifossorial	Nowak, 1999; Warburton et al., 2013	*	*	*
869	Marsupialia	Peramelemorphia	Thylacomyidae	Macrotis_lagotis	MNHN-1872-309	Caliper	-	1229.58			terrestrial	semifossorial	Nowak, 1999; Warburton et al., 2013	*	*	*
870	Xenarthra	Cingulata	Chlamyphoridae	Cabassous_chacoensis	UF:Mamm:20650	Digital	ark:/87602/m4/M40499	1490.01			terrestrial	semifossorial	Nowak, 1999	*	*	*
871	Xenarthra	Cingulata	Chlamyphoridae	Chaetophractus_villosus	MNHN-1884-911	Caliper	-	4372.80			terrestrial	semifossorial	Nowak, 1999	*	*	*
872	Xenarthra	Cingulata	Chlamyphoridae	Chlamyphorus_truncatus	FMNH:Mamm:39468	Digital	ark:/87602/m4/M54401	83.53			terrestrial	fossorial	Hopkins & Davis, 2009	*	*	*
873	Xenarthra	Cingulata	Chlamyphoridae	Chlamyphorus_truncatus	NHMUK:1911.9.6.1	Digital	ark:/87602/m4/M154858	83.53			terrestrial	fossorial	Hopkins & Davis, 2009	*	*	*
874	Xenarthra	Cingulata	Chlamyphoridae	Euphractus_sexcinctus	UMMZ:Mamm:80276	Digital	doi:10.17602/M2/M64414	4731.16			terrestrial	semifossorial	Hopkins & Davis, 2009	*	*	*
875	Xenarthra	Cingulata	Chlamyphoridae	Priodontes_maximus	MNHN-1885-389	Caliper	-	40641.89			terrestrial	semifossorial	Hopkins & Davis, 2009	*	*	*
876	Xenarthra	Cingulata	Chlamyphoridae	Tolypeutes_matacus	UMMZ:Mamm:125621	Digital	doi:10.17602/M2/M64401	1303.47			terrestrial	semifossorial	Hopkins & Davis, 2009	*	*	*
877	Xenarthra	Cingulata	Dasypodidae	Dasypus_sp	DU:EA:164	Digital	doi:10.17602/M2/M49221	4149.37	Body mass of genus average.		terrestrial	semifossorial	Hopkins & Davis, 2009	*	*	*
878	Xenarthra	Pilosa	Bradypodidae	Bradypus_tridactylus	MNHN-1955-112	Caliper	-	4375.80			terrestrial	arboreal	Nowak, 1999	*	*	*
879	Xenarthra	Pilosa	Cyclopedidae	Cyclopes_didactylus	UMMZ:Mamm:99169	Digital	ark:/87602/m4/M64415	263.95			terrestrial	arboreal	Hopkins & Davis, 2009	*	*	*
880	Xenarthra	Pilosa	Cyclopedidae	Cyclopes_didactylus	UMZC:Vertebrates:e.621	Digital	ark:/87602/m4/M140748	263.95			terrestrial	arboreal	Hopkins & Davis, 2009	*	*	*
881	Xenarthra	Pilosa	Megalonychidae	Choloepus_didactylus	MNHN-ZM-MO-1996-594	Caliper	-	6646.50			terrestrial	arboreal	Hopkins & Davis, 2009	*	*	*
882	Xenarthra	Pilosa	Myrmecophagidae	Myrmecophaga_tridactyla	MNHN-ZM-AC-1880-1433	Caliper	-	29531.83			terrestrial	terrestrialquad	Hopkins & Davis, 2009	*	*	*
883	Xenarthra	Pilosa	Myrmecophagidae	Tamandua_tetradactyla	MNHN-ZM-AC-1917-219	Caliper	-	4800.00			terrestrial	scansorial	Hayssen, 2011	*	*	*
884		Monotremata	Ornithorhynchidae	Ornithorhynchus_anatinus	MVZ:Mamm:32885	Digital	ark:/87602/m4/M65299	1484.25			semiaquatic	semiaquatic	Hood, 2020	*	*	*
885		Monotremata	Ornithorhynchidae	Ornithorhynchus_anatinus	UMZC:Vertebrates:a2. 2/10	Digital	ark:/87602/m4/M141006	1484.25			semiaquatic	semiaquatic	Hood, 2020	*	*	*
886		Monotremata	Tachyglossidae	Tachyglossus_aculeatus	YPM:VZ:Mamm 014872	Digital	doi:10.17602/M2/M64577	4499.97			terrestrial	semifossorial	Cason, 2009	*	*	*
887		Monotremata	Tachyglossidae	Zaglossus_sp	TCSA:940136	Digital	ark:/87602/m4/359989	8951.71	Z. brujini body mass.		terrestrial	terrestrialquad	Hopkins & Davis, 2009		*	*

Table S1.2. Description of linear measurements. Acquisitions were made either by landmark positioning in 3D digital models or by direct caliper measurements (illustrated in Fig. 1.4).

I) Humerus length

Landmark 1 - Midpoint of the intertubercular groove

Landmark 2 - Distal end of the trochlea

II) Humerus proximal width

Landmark 3 - Right edge just above the neck of the humerus

Landmark 4 - Left edge just above the neck of the humerus

III) Humerus mid shaft width

Landmark 5 - Right edge of central axis in anterior view

Landmark 6 - Left edge of central axis in anterior view

IV) Humerus distal width

Landmark 7 - Right edge of lateral epicondyle

Landmark 8 - Left edge of medial epicondyle

V) Humerus height

Landmark 9 - Right edge of central axis in lateral view

Landmark 10 - Left edge of central axis in lateral view

VI) Radius length

Landmark 11 – Sulcus in the radius head

Landmark 12 – Distal end of styloid process

VII) Radius proximal width

Landmark 13 – Rightest edge under epiphysis suture of radius head

Landmark 14 – Leftist edge under epiphysis suture of radius head

VIII) Radius mid shaft width

Landmark 15 - Right edge of central axis in anterior view

Landmark 16 - Left edge of central axis in anterior view

IX) Radius distal width

Landmark 17 – Rightest edge above epiphysis suture of distal radius

Landmark 18 – Leftist edge above epiphysis suture of distal radius

X) Radius height

Landmark 9 - Right edge of central axis in lateral view

Landmark 10 - Left edge of central axis in lateral view

XI) Third metacarpal length

Landmark 21 – Sulcus of articulation with magnum carpal

Landmark 22 – Proximal-most tip of epiphysis

XII) Third metacarpal proximal width

Landmark 23 – Rightest edge under the suture of the proximal epiphysis

Landmark 24 – Leftist edge under the suture of the proximal epiphysis

XIII) Third metacarpal mid shaft width

Landmark 25 - Right edge of central axis in dorsal view

Landmark 26 - Left edge of central axis in dorsal view

XIV) Third metacarpal distal width

Landmark 27 – Rightest edge above distal epiphysis suture

Landmark 28 – Leftist edge above distal epiphysis suture

Table S1.2. [continued].

XV) Third metacarpal height

Landmark 29 - Right edge of central axis in lateral view

Landmark 30 - Left edge of central axis in lateral view

XVI) Digit III phalanx I length

Landmark 31 – Sulcus of articulation with third metacarpal

Landmark 32 – Sulcus of articulation with second phalanx

XVII) Digit III phalanx proximal width

Landmark 23 – Rightest edge under the suture of the distal epiphysis

Landmark 24 – Leftist edge under the suture of the distal epiphysis

XVIII) Digit III phalanx mid shaft width

Landmark 29 - Right edge of central axis in dorsal view

Landmark 30 - Left edge of central axis in dorsal view

XIX) Digit III phalanx distal width

Landmark 37 – Rightest edge above distal epiphysis suture

Landmark 38 – Leftist edge above distal epiphysis suture

XX) Digit III phalanx height

Landmark 39 - Right edge of central axis in lateral view

Landmark 40 - Left edge of central axis in lateral view

XXIII) Digit III length

Sum of the length measurements all phalanges belonging to digit III.

Table S1.3. Morphological data. Table contain the mean values of mass (g) and bone distances (mm) all species measured. L= length; PW= proximal width; MW= mid-shaft width; DW= distal width; H= height.

						Humerus					Radius					Metacarpal					Phalanx					
	Superord. group	Order	Family	Species	Mass	L	PW	MW	DW	H	L	PW	MW	DW	H	L	PW	MW	DW	H	L	PW	MW	DW	H	DL
1		Monotremata	Tachyglossidae	Zaglossus_sp	8951.71	76.75	36.97	16.57	55.85	18.23	79.73	16.99	9.81	16.73	4.79	11.00	11.51	11.02	10.71	8.17	6.00	10.88	11.36	11.10	6.22	45.81
2		Monotremata	Tachyglossidae	Tachyglossus_aculeatus	4499.97	52.93	26.48	12.10	45.91	10.65	45.35	12.21	5.25	10.63	4.64	6.98	8.06	7.27	7.73	4.85	3.63	8.26	9.01	7.95	6.09	33.15
3		Monotremata	Ornithorhynchidae	Ornithorhynchus_anatinus	1484.25	34.43	16.75	9.17	26.91	7.77	30.84	6.31	2.88	6.09	2.71	10.87	4.59	3.01	4.32	3.38	8.46	4.88	4.65	5.23	2.71	26.95
4	Laurasiatheria	Eulipotyphla	Solenodontidae	Solenodon_paradoxus	899.99	49.46	12.00	5.77	18.26	7.83	40.30	5.59	5.74	8.68	3.05	16.86	2.76	2.32	3.57	2.57	9.01	3.93	2.79	3.06	2.65	26.27
5	Laurasiatheria	Eulipotyphla	Talpidae	Neurotrichus_gibbsii	9.56	6.63	3.82	1.74	3.97	1.57	7.96	1.59	0.89	1.48	0.54	1.52	0.99	0.73	0.89	0.69	1.33	0.99	0.64	0.83	0.65	5.21
6	Laurasiatheria	Eulipotyphla	Talpidae	Galemys_pyrenaicus	60.17	12.12	4.53	2.16	6.35	1.97	15.40	1.92	1.13	1.90	1.00	3.57	1.01	0.69	0.80	0.86	3.08	0.96	0.79	0.82	0.82	8.75
7	Laurasiatheria	Eulipotyphla	Talpidae	Desmana_moschata	427.64	21.95	9.09	4.80	13.49	4.09	24.67	3.55	2.67	4.35	1.80	6.98	2.12	1.52	1.45	1.54	5.64	1.56	1.32	1.39	1.53	14.67
8	Laurasiatheria	Eulipotyphla	Talpidae	Euroscaptor_micrura	60.46	11.71	9.55	4.03	8.11	3.00	8.72	2.73	1.66	3.77	1.25	2.48	2.17	1.47	1.75	1.33	1.90	1.85	1.69	1.70	0.74	8.92
9	Laurasiatheria	Eulipotyphla	Talpidae	Mogera_wogura	96.88	17.78	13.78	6.07	12.14	4.33	12.07	4.25	2.47	5.62	2.01	3.49	3.06	2.24	2.52	2.21	2.65	2.95	2.52	2.96	1.48	13.01
10	Laurasiatheria	Eulipotyphla	Talpidae	Condylura_cristata	48.15	10.82	8.23	2.88	7.67	3.32	12.22	2.82	1.18	3.33	1.10	2.85	2.22	1.30	1.68	1.32	2.79	1.72	1.17	1.44	1.11	10.07
11	Laurasiatheria	Eulipotyphla	Talpidae	Scalopus_aquaticus	87.15	12.44	11.69	5.85	10.73	4.07	9.64	3.44	2.53	5.50	1.66	1.36	3.01	2.68	2.77	1.54	1.44	2.95	2.89	2.90	1.39	12.77
12	Laurasiatheria	Eulipotyphla	Talpidae	Scapanus_latimanus	62.46	11.75	10.12	4.72	9.39	3.67	8.39	2.76	1.83	4.56	1.24	1.31	2.40	2.03	2.15	1.41	1.50	2.19	2.17	2.28	1.14	10.65
13	Laurasiatheria	Eulipotyphla	Soricidae	Myosorex_kihaulei	9.50	9.00	2.18	0.99	3.17	1.26	8.40	0.92	0.51	1.08	0.41	3.12	0.52	0.41	0.62	0.46	1.67	0.71	0.46	0.55	0.39	4.49
14	Laurasiatheria	Eulipotyphla	Soricidae	Congosorex_verheyeni	7.10	7.61	2.14	0.86	2.99	0.96	6.50	0.94	0.51	0.75	0.34	2.47	0.53	0.38	0.64	0.41	1.32	0.74	0.39	0.51	0.43	3.75
15	Laurasiatheria	Eulipotyphla	Soricidae	Sylvisorex_howelli	4.00	7.29	1.53	0.59	2.10	0.84	6.85	0.68	0.46	0.72	0.35	3.01	0.36	0.30	0.50	0.28	1.61	0.52	0.29	0.38	0.26	3.32
16	Laurasiatheria	Eulipotyphla	Soricidae	Scutisorex_somereni	91.49	16.90	4.14	1.61	5.52	2.45	14.55	1.69	1.08	1.86	0.75	6.24	0.94	0.95	1.26	0.70	3.27	1.27	0.74	0.84	0.64	7.70
17	Laurasiatheria	Eulipotyphla	Soricidae	Suncus_murinus	43.76	11.98	2.87	1.70	3.69	1.49	10.82	1.21	0.77	1.63	0.68	5.03	0.68	0.49	0.91	0.70	3.04	1.02	0.63	0.83	0.63	5.57
18	Laurasiatheria	Eulipotyphla	Soricidae	Diplomesodon_pulchellum	11.00	8.95	2.27	0.90	2.90	1.03	8.64	0.85	0.56	1.07	0.42	3.46	0.51	0.43	0.65	0.39	1.94	0.78	0.40	0.49	0.42	5.01
19	Laurasiatheria	Eulipotyphla	Soricidae	Crocidura_russula	9.89	8.79	2.09	0.88	2.61	0.99	8.00	0.89	0.56	0.93	0.38	3.16	0.52	0.38	0.58	0.37	1.71	0.63	0.35	0.46	0.30	4.03
20	Laurasiatheria	Eulipotyphla	Soricidae	Paracrocidura_schoutedeni	12.18	8.89	2.52	1.11	2.80	1.31	7.56	0.93	0.68	0.94	0.47	3.28	0.55	0.45	0.59	0.45	1.62	0.71	0.42	0.54	0.44	4.02
21	Laurasiatheria	Eulipotyphla	Soricidae	Neomys_fodiens	15.26	9.56	2.41	1.03	3.46	1.08	9.41	1.08	0.69	0.79	0.54	4.08	0.47	0.41	0.63	0.50	2.34	0.75	0.37	0.51	0.47	5.52
22	Laurasiatheria	Eulipotyphla	Soricidae	Episoriculus_caudatus	6.00	6.73	1.79	0.69	2.18	0.77	7.84	0.74	0.40	0.83	0.32	2.72	0.38	0.34	0.50	0.32	1.56	0.56	0.33	0.39	0.32	3.64
23	Laurasiatheria	Eulipotyphla	Soricidae	Soriculus_nigrescens	14.58	16.77	4.07	1.50	5.43	2.26	14.45	1.62	0.98	1.78	0.67	6.25	0.93	0.80	1.16	0.63	3.25	1.24	0.64	0.85	0.57	7.54
24	Laurasiatheria	Eulipotyphla	Soricidae	Nectogale_elegans	38.82	9.39	2.81	1.43	4.23	1.34	10.16	1.15	0.61	1.48	0.53	4.27	0.55	0.46	0.66	0.46	2.24	0.79	0.48	0.56	0.43	5.49
25	Laurasiatheria	Eulipotyphla	Soricidae	Chimarrogale_himalayica	33.50	12.31	2.73	1.58	4.71	1.57	10.87	1.42	0.89	1.64	0.61	4.64	0.72	0.57	0.87	0.65	3.26	1.02	0.56	0.70	0.59	7.11
26	Laurasiatheria	Eulipotyphla	Soricidae	Surdisorex_norae	23.57	9.98	3.50	2.10	5.96	2.37	9.75	1.42	0.82	1.71	0.75	3.59	0.93	0.73	1.08	0.74	1.90	1.25	0.80	0.98	0.76	6.68
27	Laurasiatheria	Eulipotyphla	Soricidae	Notiosorex_crawfordi	4.79	6.85	1.81	0.78	2.38	0.78	6.17	0.72	0.39	0.67	0.36	2.36	0.35	0.29	0.46	0.31	1.41	0.51	0.28	0.36	0.31	3.55
28	Laurasiatheria	Eulipotyphla	Soricidae	Anourosorex_squamipes	20.00	10.66	2.96	1.31	4.02	1.37	9.36	1.22	0.72	1.18	0.52	3.19	0.64	0.52	0.80	0.47	1.84	0.92	0.49	0.57	0.43	4.78
29	Laurasiatheria	Eulipotyphla	Soricidae	Blarina_brevicauda	18.56	9.32	2.37	1.08	3.61	1.14	8.41	1.02	0.64	0.93	0.43	3.16	0.59	0.42	0.69	0.49	1.77	0.77	0.41	0.50	0.48	4.75
30	Laurasiatheria	Eulipotyphla	Soricidae	Cryptotis_mexicana	7.00	7.66	2.54	1.02	3.61	1.05	7.60	0.97	0.56	1.05	0.43	2.58	0.53	0.41	0.62	0.44	1.43	0.79	0.42	0.52	0.50	3.99
31	Laurasiatheria	Eulipotyphla	Soricidae	Sorex_cinereus	4.20	5.67	1.24	0.60	1.82	0.61	6.37	0.59	0.32	0.51	0.25	2.45	0.23	0.23	0.41	0.28	1.34	0.46	0.25	0.32	0.25	3.08
32	Laurasiatheria	Eulipotyphla	Erinaceidae	Neotetracus_sinensis	87.00	17.88	2.88	1.36	3.97	1.99	15.17	1.59	1.01	1.80	0.67	6.59	0.75	0.61	0.99	0.57	3.52	1.08	0.54	0.65	0.55	7.37
33	Laurasiatheria	Eulipotyphla	Erinaceidae	Podogymnura_truei	67.00	20.42	3.92	1.66	5.06	2.78	20.13	2.16	1.22	2.18	0.70	8.14	0.99	0.67	1.32	0.69	3.95	1.29	0.65	0.93	0.62	8.93
34	Laurasiatheria	Eulipotyphla	Erinaceidae	Echinosorex_gymnura	756.53	53.00	10.42	4.76	13.92	6.44	43.37	6.78	3.16	6.50	2.13	19.20	2.66	2.20	3.53	2.09	8.96	3.54	2.03	1.91	1.77	19.52
35	Laurasiatheria	Eulipotyphla	Erinaceidae	Erinaceus_europaeus	777.95	32.33	9.26	3.52	10.09	4.33	25.23	5.67	3.11	3.72	2.08	9.63	2.33	1.96	3.09	1.97	4.15	2.63	1.91	2.20	1.81	11.65
36	Laurasiatheria	Eulipotyphla	Erinaceidae	Paraechinus_aethiopicus	352.40	35.55	7.30	2.63	8.15	4.24	37.00	3.78	2.14	4.28	1.38	9.19	1.70	1.21	2.06	0.85	3.41	2.13	1.37	1.44	0.89	9.12
37	Laurasiatheria	Eulipotyphla	Erinaceidae	Hemiechinus_auritus	322.04	29.77	6.52	2.83	7.92	3.27	29.87	3.76	1.78	2.83	1.54	8.28	1.76	1.60	1.94	1.10	3.44	2.09	1.36	1.49	1.06	9.84
38	Laurasiatheria	Eulipotyphla	Erinaceidae	Atelerix_albiventris	293.44	28.72	6.34	2.35	6.02	3.64	29.31	3.53	2.08	3.54	1.54	7.71	1.20	1.02	1.33	1.04	2.08	1.44	1.10	1.26	0.81	6.75
39	Laurasiatheria	Perissodactyla	Equidae	Equus_asinus	164998.49	254.06	86.33	35.06	71.59	41.71	305.33	74.51	34.53	70.03	23.34	209.07	46.33	29.47	40.50	23.70	75.93	41.33	25.86	38.02	21.23	144.51
40	Laurasiatheria	Perissodactyla	Equidae	Equus_hemionus	235248.07	231.56	81.18	31.32	65.60	37.89	281.01	64.73	31.16	39.86	20.72	215.67	41.39	25.71	38.03	21.50	68.84	38.45	24.64	36.35	20.97	139.39
41	Laurasiatheria	Perissodactyla	Equidae	Equus_grevyi	408000.35	284.97	97.69	44.53	80.29	53.18	323.42	88.26	42.49	78.08	30.72	237.66	51.58	32.88	46.07	28.04	83.57	46.47	30.36	44.00	25.68	153.70
42	Laurasiatheria	Perissodactyla	Equidae	Equus_caballus	403598.53	170.34	84.62	30.89	68.55	40.34	306.79	72.58	31.63	66.01	23.15	199.97	44.72	28.43	41.23	20.68	72.97	47.70	29.98	42.76	21.33	155.15
43	Laurasiatheria	Perissodactyla	Tapiridae	Acrocodia_indicus	311209.19	230.21	91.00	34.64	77.04	39.34	215.25	51.18	24.70	44.78	25.28	110.77	31.01	25.97	36.07	13.38	31.59	33.24	25.42	29.71	10.49	73.70
44	Laurasiatheria	Perissodactyla	Tapiridae	Tapirus_terrestris	169496.64	231.00	82.37	35.42	66.32	41.83	209.91	50.05	25.34	36.10	25.23	113.12	28.15	28.57	34.42	15.80	29.53	28.47	24.61	25.89	11.28	75.17
45	Laurasiatheria	Perissodactyla	Tapiridae	Tapirus_pinchaque	156923.40	236.94	77.43	27.76	67.27	32.17	207.86	48.17	20.37	34.18	17.46	114.93	28.56	23.61	31.15	9.60	31.42	28.56	22.58	25.58	12.63	NA
46	Laurasiatheria	Perissodactyla	Rhinocerotidae	Rhinoceros_unicornis	1843655.80	427.00	199.52	83.17	169.96	75.97	403.99	121.07	59.95	116.67	35.11	201.18	68.45	57.00	72.73	29.85	43.65	64.26	62.21	62.32	21.22	112.98
47	Laurasiatheria	Perissodactyla	Rhinocerotidae	Rhinoceros_sondaicus	1750000.00	391.73	172.04	89.95	133.49	73.06	344.47	107.07	51.72	106.05	38.02	159.71	65.15	59.12	67.10	19.11	38.01	57.87	53.87	51.71	22.51	99.88
48	Laurasiatheria	Perissodactyla	Rhinocerotidae	Dicerorhinus_sumatrensis	1046156.04	327.85	116.86	73.99	108.60	44.27	281.22	71.31	35.32	72.82	26.80	134.41	43.12	42.63	52.97	13.84	34.69	43.24	40.97	39.50	14.88	87.45

						Humerus					Radius					Metacarpal					Phalanx					
	Superord. group	Order	Family	Species	Mass	L	PW	MW	DW	H	L	PW	MW	DW	H	L	PW	MW	DW	H	L	PW	MW	DW	H	DL
49	Laurasiatheria	Perissodactyla	Rhinocerotidae	Diceros_bicornis	995940.54	275.35	165.90	51.11	139.49	79.39	378.40	98.16	48.13	87.57	32.77	161.97	46.17	45.30	64.50	23.02	34.40	58.01	55.37	54.41	22.32	81.83
50	Laurasiatheria	Perissodactyla	Rhinocerotidae	Ceratotherium_simum	2285939.43	358.78	159.39	68.33	168.62	155.24	389.90	117.81	61.09	114.55	38.50	160.29	54.20	52.52	36.41	24.51	41.16	49.70	47.93	45.90	26.17	91.50
51	Laurasiatheria	Cetartiodactyla	Camelidae	Lama_guanicoe	115000.00	237.78	68.06	27.48	49.95	30.00	274.92	45.39	27.68	43.59	15.18	219.91	19.30	10.25	18.42	14.03	66.77	18.73	10.86	15.09	13.42	117.00
52	Laurasiatheria	Cetartiodactyla	Camelidae	Lama_glama	78322.67	228.89	66.32	25.34	50.37	29.40	265.41	47.47	28.59	45.76	15.86	215.62	27.30	11.72	21.37	14.49	70.22	20.00	11.72	13.91	15.06	123.55
53	Laurasiatheria	Cetartiodactyla	Camelidae	Camelus_dromedarius	492714.47	320.75	117.65	52.71	84.11	56.19	444.08	87.57	49.90	85.09	30.66	312.31	45.19	19.39	35.88	27.37	86.58	36.02	21.46	26.98	22.20	160.03
54	Laurasiatheria	Cetartiodactyla	Camelidae	Camelus_bactrianus	554515.91	385.85	120.85	59.13	99.85	57.87	473.51	95.74	52.50	98.98	35.26	334.39	52.22	18.52	43.46	28.67	100.59	43.04	22.14	28.30	24.90	194.31
55	Laurasiatheria	Cetartiodactyla	Tayassuidae	Tayassu_pecari	31798.71	121.77	33.75	12.74	27.12	17.60	90.73	19.26	12.34	20.46	11.87	50.47	11.27	8.07	10.05	8.64	26.40	9.95	9.75	8.37	9.21	62.26
56	Laurasiatheria	Cetartiodactyla	Tayassuidae	Pecari_tajacu	21133.69	124.90	31.96	12.71	27.86	17.53	98.10	19.28	11.88	20.66	11.80	51.37	12.08	8.48	10.51	7.96	23.77	9.11	8.11	10.00	9.26	60.22
57	Laurasiatheria	Cetartiodactyla	Suidae	Potamochoerus_larvatus	69063.79	175.77	53.36	25.49	49.84	29.19	144.55	30.59	18.75	35.58	17.27	67.41	21.31	15.48	18.41	11.84	31.85	18.01	13.75	15.10	11.85	75.93
58	Laurasiatheria	Cetartiodactyla	Suidae	Sus_sp	107579.38	183.63	64.00	19.63	41.09	30.36	157.73	30.08	18.97	37.58	15.20	62.75	25.01	16.42	18.57	12.16	31.61	18.52	16.04	17.36	15.60	80.45
59	Laurasiatheria	Cetartiodactyla	Suidae	Phacochoerus_africanus	82499.99	142.07	50.71	14.29	38.03	18.11	128.35	25.40	13.18	31.25	10.90	68.26	20.23	11.86	14.17	10.12	32.58	11.77	9.34	10.67	11.12	69.42
60	Laurasiatheria	Cetartiodactyla	Suidae	Hylochoerus_meinertzhageni	198130.47	213.29	71.38	24.54	55.50	33.81	165.20	35.68	24.13	43.02	16.94	77.24	24.10	19.33	21.04	11.70	38.28	18.74	15.87	18.58	14.92	90.97
61	Laurasiatheria	Cetartiodactyla	Suidae	Babyrousa_babyrussa	92950.09	167.71	55.51	20.92	42.19	28.29	152.94	26.00	17.37	30.90	13.27	66.70	14.73	12.17	15.81	8.39	28.07	14.90	12.01	12.79	10.65	NA
62	Laurasiatheria	Cetartiodactyla	Hippopotamidae	Hippopotamus_amphibius	1536310.40	393.29	146.92	74.73	130.42	66.56	275.41	99.02	48.75	91.12	42.85	144.81	47.06	41.35	49.64	25.40	63.64	48.21	34.98	39.77	24.47	134.74
63	Laurasiatheria	Cetartiodactyla	Hippopotamidae	Choeropsis_liberiensis	235001.16	213.17	76.67	40.78	59.36	31.13	153.08	45.20	22.48	44.75	21.41	83.71	25.12	20.30	28.72	11.19	41.01	26.62	21.05	22.30	13.58	78.08
64	Laurasiatheria	Cetartiodactyla	Balaenidae	Eubalaena_australis	22999999.91	526.41	306.81	213.37	263.78	143.33	539.33	215.98	226.07	335.21	89.36	163.59	116.30	96.83	124.01	70.03	176.49	114.40	72.53	105.92	54.96	642.49
65	Laurasiatheria	Cetartiodactyla	Balaenidae	Eubalaena_glacialis	22999999.91	429.38	151.61	177.18	301.96	142.59	470.24	235.60	198.68	333.52	88.32	141.20	116.97	82.34	98.57	75.20	153.91	96.08	57.77	93.20	60.58	517.18
66	Laurasiatheria	Cetartiodactyla	Delphinidae	Lissodelphis_borealis	113000.00	60.12	30.15	26.63	38.71	26.87	74.67	25.47	26.27	29.23	13.41	31.13	14.43	14.16	16.21	9.04	21.41	16.33	14.14	15.50	6.78	NA
67	Laurasiatheria	Cetartiodactyla	Neobalaenidae	Caperea_marginata	4500000.00	143.98	82.12	64.94	83.89	48.43	211.85	57.60	45.61	47.13	24.69	45.03	19.32	13.23	20.13	12.99	26.76	17.19	11.82	16.48	9.03	61.74
68	Laurasiatheria	Cetartiodactyla	Eschrichtiidae	Eschrichtius_robustus	27324024.19	458.55	245.93	220.59	271.09	126.96	707.44	177.34	188.94	260.72	84.29	163.35	115.20	105.91	138.89	72.22	165.66	119.33	79.35	122.66	59.94	NA
69	Laurasiatheria	Cetartiodactyla	Balaenopteridae	Megaptera_novaeangliae	30000000.01	323.18	267.30	211.65	257.76	126.69	740.19	193.01	122.17	232.00	85.12	194.89	81.52	54.98	78.69	47.90	186.77	91.38	46.79	93.43	45.06	772.37
70	Laurasiatheria	Cetartiodactyla	Balaenopteridae	Balaenoptera_acutorostrata	5587093.59	215.80	150.17	135.80	158.41	87.89	446.45	114.08	88.95	118.86	49.98	78.75	42.98	28.97	45.46	30.74	74.36	46.07	25.17	43.26	21.24	196.15
71	Laurasiatheria	Cetartiodactyla	Kogiidae	Kogia_breviceps	431500.00	79.76	45.12	40.21	51.84	25.82	59.30	35.51	30.47	37.02	15.74	29.61	16.54	10.41	18.35	10.20	23.23	17.35	13.10	14.98	9.88	83.06
72	Laurasiatheria	Cetartiodactyla	Physeteridae	Physeter_macrocephalus	14540959.82	445.95	231.84	191.14	249.07	116.35	330.37	198.60	156.80	210.11	97.84	180.25	95.59	51.84	79.00	43.30	138.27	76.20	46.70	69.71	31.86	371.37
73	Laurasiatheria	Cetartiodactyla	Ziphiidae	Mesoplodon_bidens	3400000.00	139.77	59.24	62.07	67.94	42.82	142.92	47.68	44.00	46.78	28.32	36.49	22.59	21.40	21.18	11.81	28.09	16.77	14.04	15.83	7.52	47.74
74	Laurasiatheria	Cetartiodactyla	Ziphiidae	Ziphius_cavirostris	4774999.99	141.13	64.92	63.24	59.44	39.81	163.30	45.77	41.91	46.37	25.00	50.14	23.03	18.01	24.36	10.58	41.16	22.62	15.27	24.03	7.96	101.55
75	Laurasiatheria	Cetartiodactyla	Ziphiidae	Hyperoodon_ampullatus	3393361.08	217.89	102.25	98.81	107.92	61.63	225.71	78.70	66.36	73.83	45.17	67.01	39.31	30.69	33.67	21.70	43.34	30.97	23.85	29.33	13.30	NA
76	Laurasiatheria	Cetartiodactyla	Ziphiidae	Berardius_arnuxii	7000000.02	214.16	101.57	95.16	99.19	64.93	199.38	83.50	63.64	76.32	43.89	73.75	30.81	22.92	36.15	15.35	42.61	31.00	25.79	28.51	11.94	NA
77	Laurasiatheria	Cetartiodactyla	Monodontidae	Monodon_monoceros	938126.44	131.38	63.79	36.59	62.12	32.05	121.67	41.07	40.54	51.23	21.77	35.80	28.28	19.99	25.97	12.57	25.57	20.41	14.00	20.99	10.08	81.17
78	Laurasiatheria	Cetartiodactyla	Monodontidae	Delphinapterus_leucas	1381640.73	132.32	55.74	40.20	69.61	35.82	113.20	50.31	51.27	67.91	26.53	35.55	35.10	28.50	34.02	13.69	25.47	29.48	22.23	29.44	10.47	128.15
79	Laurasiatheria	Cetartiodactyla	Phocoenidae	Phocoenoides_dalli	106042.53	52.23	27.14	22.30	32.61	19.61	57.64	28.20	28.29	32.66	11.08	21.05	13.53	13.94	16.35	6.56	13.60	15.98	14.04	14.51	5.27	26.97
80	Laurasiatheria	Cetartiodactyla	Phocoenidae	Phocoena_phocoena	52730.93	54.04	26.35	19.71	28.93	17.02	59.36	22.98	24.85	30.02	10.58	18.67	12.56	11.40	13.19	6.83	13.28	12.04	11.37	11.50	5.70	34.05
81	Laurasiatheria	Cetartiodactyla	Phocoenidae	Neophocaena_phocaenoides	32500.00	54.14	26.08	20.51	34.51	17.90	62.17	26.73	28.07	27.76	9.67	24.17	14.18	13.33	16.34	5.59	17.04	15.35	13.81	14.39	4.86	NA
82	Laurasiatheria	Cetartiodactyla	Delphinidae	Lagenorhynchus_acutus	186517.55	64.92	43.16	35.77	50.65	31.00	78.17	37.46	39.61	44.89	14.60	40.41	23.86	23.68	25.79	12.45	32.90	22.99	18.96	22.30	9.56	68.52
83	Laurasiatheria	Cetartiodactyla	Delphinidae	Orcinus_orca	2441000.50	180.56	99.26	83.07	127.83	66.60	174.98	91.70	85.64	119.72	40.67	42.83	49.50	42.66	52.01	18.98	28.92	50.94	44.33	48.98	16.31	66.64
84	Laurasiatheria	Cetartiodactyla	Delphinidae	Orcaella_brevirostris	189999.99	83.60	32.99	24.44	42.47	24.14	79.77	28.06	38.12	41.20	17.39	48.72	23.66	21.93	25.01	11.88	25.08	24.44	19.92	22.74	7.43	76.04
85	Laurasiatheria	Cetartiodactyla	Delphinidae	Grampus_griseus	387500.00	94.40	56.86	47.83	70.68	42.11	114.61	54.37	53.63	65.00	26.81	63.73	33.96	31.25	38.67	18.74	41.13	35.06	28.71	33.30	15.84	214.03
86	Laurasiatheria	Cetartiodactyla	Delphinidae	Pseudorca_crassidens	1360000.00	116.26	62.50	47.69	90.94	45.38	118.59	69.06	70.38	88.90	25.55	59.17	40.74	28.60	39.64	16.61	47.59	43.76	29.12	37.84	11.92	116.65
87	Laurasiatheria	Cetartiodactyla	Delphinidae	Peponocephala_electra	206000.00	50.82	29.78	25.44	34.13	22.32	61.22	27.74	30.20	36.57	10.29	31.42	17.20	15.06	19.11	8.88	21.08	18.11	15.21	18.42	6.66	NA
88	Laurasiatheria	Cetartiodactyla	Delphinidae	Globicephala_melas	800000.00	137.74	71.54	60.01	99.49	58.37	152.31	74.72	76.79	109.77	31.70	77.01	55.03	38.13	52.95	21.75	54.04	48.59	37.64	50.16	21.26	259.61
89	Laurasiatheria	Cetartiodactyla	Delphinidae	Steno_bredanensis	130000.00	75.88	51.88	33.57	52.14	27.96	92.49	38.94	44.85	50.85	15.04	39.09	23.12	22.06	27.28	5.10	22.48	27.64	22.86	22.16	4.78	49.31
90	Laurasiatheria	Cetartiodactyla	Delphinidae	Tursiops_truncatus	281040.55	77.09	40.25	39.51	56.68	31.85	98.22	39.70	45.28	56.52	18.39	43.81	27.21	22.87	30.03	12.71	34.78	31.13	24.51	30.89	10.70	112.44
91	Laurasiatheria	Cetartiodactyla	Delphinidae	Stenella_longirostris	50500.00	43.92	31.65	23.79	35.15	20.20	60.58	26.47	26.21	32.37	8.80	29.50	14.37	13.39	19.12	6.67	13.05	17.97	16.19	18.74	5.14	45.80
92	Laurasiatheria	Cetartiodactyla	Delphinidae	Delphinus_delphis	79271.69	58.74	33.08	29.93	42.72	28.41	75.58	30.78	33.47	39.07	11.83	31.68	15.97	13.65	18.20	7.94	20.12	18.51	15.72	18.40	6.86	57.63
93	Laurasiatheria	Cetartiodactyla	Delphinidae	Cephalorhynchus_commersonii	72400.00	54.37	33.19	24.97	35.61	18.76	65.90	25.05	24.50	30.49	9.77	24.44	16.14	14.98	17.16	8.24	20.23	16.47	14.04	15.86	5.33	66.93
94	Laurasiatheria	Cetartiodactyla	Iniidae	Inia_geoffrensis	121430.76	99.84	46.92	47.43	61.17	31.09	79.03	50.75	50.41	55.39	25.53	30.41	30.47	23.80	24.58	9.09	29.84	22.94	18.67	20.00	11.40	103.46
95	Laurasiatheria	Cetartiodactyla	Pontoporiidae	Pontoporia_blainvillei	40499.99	48.59	23.72	21.02	31.23	16.35	33.52	19.64	17.62	28.22	10.30	20.24	15.25	12.60	12.77	6.38	12.92	9.55	7.69	8.33	4.28	20.84
96	Laurasiatheria	Cetartiodactyla	Platanistidae	Platanista_gangetica	93481.96	60.69	31.55	23.92	38.13	15.38	37.52	25.11	20.54	19.90	11.38	28.48	21.28	13.93	17.60	7.14	25.25	15.12	9.44	14.39	5.91	57.10
97	Laurasiatheria	Cetartiodactyla	Tragulidae	Moschiola_meminna	3130.95	65.79	11.83	5.54	11.42	7.31	55.26	9.33	5.80	8.58	3.87	36.94	4.52	2.97	3.77	3.07	9.44	4.81	3.40	3.62	3.68	26.81
98	Laurasiatheria	Cetartiodactyla	Tragulidae	Tragulus_sp	3581.80	60.81	11.74	4.25	9.32	5.84	56.51	7.88	5.28	7.30	2.99	40.17	3.37	2.74	3.56	3.07	7.75	3.57	2.58	2.71	2.62	19.20
99	Laurasiatheria	Cetartiodactyla	Tragulidae	Tragulus_javanicus	1889.93	56.00	11.30	4.09	9.06	5.33	51.95	7.59	4.72	6.87	3.30	34.89	4.09	2.63	3.48	2.60	8.38	4.09	3.18	3.26	3.69	21.53

						Humerus					Radius					Metacarpal					Phalanx					
	Superord. group	Order	Family	Species	Mass	L	PW	MW	DW	H	L	PW	MW	DW	H	L	PW	MW	DW	H	L	PW	MW	DW	H	DL
100	Laurasiatheria	Cetartiodactyla	Tragulidae	Hyemoschus_aquaticus	10850.00	88.79	21.74	7.52	17.84	10.63	68.64	14.78	8.32	13.82	6.44	40.70	9.71	6.56	8.44	4.89	12.87	7.83	6.27	5.69	6.41	37.09
101	Laurasiatheria	Cetartiodactyla	Giraffidae	Okapia_johnstoni	230001.14	277.13	84.25	40.26	92.65	46.82	349.77	80.04	42.83	66.04	29.09	307.13	37.26	16.43	33.34	28.41	75.67	29.06	22.31	25.37	23.05	156.13
102	Laurasiatheria	Cetartiodactyla	Giraffidae	Giraffa_camelopardalis	964654.73	436.63	115.15	54.57	119.92	63.37	712.56	123.68	56.16	101.05	43.70	635.64	66.73	25.11	44.90	41.38	109.74	40.84	33.62	43.82	41.15	225.22
103	Laurasiatheria	Cetartiodactyla	Antilocapridae	Antilocapra_americana	47450.01	167.81	51.21	17.30	32.88	22.00	195.40	33.98	19.86	31.39	12.52	200.91	22.08	7.36	13.67	12.97	43.40	13.06	9.03	11.26	12.01	95.10
104	Laurasiatheria	Cetartiodactyla	Cervidae	Muntiacus_muntjak	17611.59	111.95	27.69	11.79	22.93	13.20	110.23	21.99	12.76	19.95	8.06	90.54	14.82	4.96	9.30	9.20	19.76	8.57	7.71	7.41	9.13	52.12
105	Laurasiatheria	Cetartiodactyla	Cervidae	Dama_dama	57224.61	159.94	45.82	21.45	37.92	22.81	186.59	35.48	22.21	33.56	12.62	180.99	20.53	9.19	13.25	12.78	33.39	11.69	9.55	10.81	12.30	89.12
106	Laurasiatheria	Cetartiodactyla	Cervidae	Panolia_eldii	95471.61	184.31	54.91	24.10	43.50	25.33	219.30	43.05	27.03	39.04	17.75	214.21	24.44	9.90	17.04	16.39	47.46	13.81	11.16	12.36	14.59	112.38
107	Laurasiatheria	Cetartiodactyla	Cervidae	Elaphurus_davidianus	165989.17	208.08	66.85	38.20	54.27	35.46	240.84	54.70	29.27	47.31	22.55	225.09	30.90	12.78	22.95	18.39	59.12	19.82	17.04	15.80	21.20	159.43
108	Laurasiatheria	Cetartiodactyla	Cervidae	Cervus_elaphus	240867.13	236.75	73.67	27.11	53.87	33.46	264.17	55.15	32.97	48.02	17.60	229.60	29.18	12.37	20.21	18.84	47.97	19.13	14.71	17.16	17.99	134.05
109	Laurasiatheria	Cetartiodactyla	Cervidae	Rusa_unicolor	177522.90	218.62	67.14	30.85	52.02	32.10	226.64	51.23	30.95	46.41	18.40	211.63	27.34	10.25	18.16	17.32	48.21	15.29	14.70	15.21	18.08	132.04
110	Laurasiatheria	Cetartiodactyla	Cervidae	Rucervus_duvaucelii	171223.86	226.72	73.22	30.77	52.21	35.81	244.90	50.94	31.27	48.83	23.56	239.41	30.12	12.51	19.40	19.41	56.74	16.47	14.94	15.96	18.67	142.74
111	Laurasiatheria	Cetartiodactyla	Cervidae	Axis_axis	69499.99	161.70	46.57	18.85	40.12	20.65	178.97	41.01	22.16	37.15	14.88	166.46	24.24	9.08	14.84	15.16	35.15	12.48	10.95	11.13	15.46	93.33
112	Laurasiatheria	Cetartiodactyla	Cervidae	Rangifer_tarandus	109088.50	200.68	54.14	17.88	42.04	21.87	243.46	42.77	18.85	38.59	14.37	182.27	25.39	7.81	18.49	14.06	43.81	21.10	13.47	15.05	12.70	114.13
113	Laurasiatheria	Cetartiodactyla	Cervidae	Pudu_puda	9642.62	104.49	24.67	9.82	20.32	11.31	86.26	18.21	10.34	15.77	6.91	58.35	9.51	4.77	7.02	5.42	19.41	6.78	6.05	5.97	6.45	52.53
114	Laurasiatheria	Cetartiodactyla	Cervidae	Mazama_sp	17891.79	141.72	33.97	15.91	29.13	17.28	145.20	28.22	18.81	26.57	10.96	129.07	15.97	7.05	11.85	10.57	29.62	9.18	8.75	8.78	9.35	78.12
115	Laurasiatheria	Cetartiodactyla	Cervidae	Odocoileus_virginianus	75901.25	166.41	46.12	19.31	34.45	21.25	199.90	32.71	22.20	31.42	12.34	182.70	20.25	7.77	14.45	13.64	35.30	10.75	10.64	10.02	14.28	94.42
116	Laurasiatheria	Cetartiodactyla	Cervidae	Hydropotes_inermis	12760.04	109.32	26.02	10.02	20.03	13.40	121.30	18.73	12.38	18.75	8.34	119.12	9.30	5.68	8.82	8.27	29.34	7.20	5.77	6.44	7.82	69.03
117	Laurasiatheria	Cetartiodactyla	Cervidae	Capreolus_capreolus	22502.01	147.14	34.17	13.55	27.71	16.89	163.45	25.67	16.27	25.36	9.39	156.82	16.64	6.10	10.84	10.10	30.18	10.04	7.90	8.94	8.97	75.57
118	Laurasiatheria	Cetartiodactyla	Cervidae	Alces_alces	461900.76	353.29	100.15	39.93	79.00	46.37	417.65	77.13	41.67	70.09	29.66	336.47	43.52	16.57	29.71	25.19	68.98	29.53	23.39	26.00	26.91	200.23
119	Laurasiatheria	Cetartiodactyla	Moschidae	Moschus_moschiferus	13315.57	133.83	24.71	9.79	21.54	11.84	137.16	18.52	11.62	19.20	6.78	120.94	13.03	5.09	8.82	7.55	23.95	8.81	5.53	6.13	6.09	56.69
120	Laurasiatheria	Cetartiodactyla	Moschidae	Moschus_sp	13297.20	123.74	25.57	9.48	21.07	11.60	119.94	19.43	11.75	21.02	8.05	90.84	12.80	4.92	9.67	8.25	26.16	9.16	6.40	7.68	6.90	66.65
121	Laurasiatheria	Cetartiodactyla	Bovidae	Bos_frontalis	800143.05	280.50	124.69	47.32	85.41	59.17	282.52	92.15	48.46	87.77	33.40	197.04	48.30	23.21	32.62	30.07	61.91	30.06	28.91	31.36	31.44	166.30
122	Laurasiatheria	Cetartiodactyla	Bovidae	Bison_bonasus	675876.70	327.56	97.78	44.92	86.64	53.92	348.35	87.36	47.88	77.73	29.23	219.40	48.53	21.24	33.49	25.70	67.06	31.50	29.62	33.00	26.85	177.56
123	Laurasiatheria	Cetartiodactyla	Bovidae	Bos_grunniens	500000.00	282.19	117.18	45.96	81.84	59.82	288.43	89.19	53.48	80.96	29.84	155.05	49.20	29.21	35.94	24.89	56.55	36.07	36.32	34.33	31.78	149.69
124	Laurasiatheria	Cetartiodactyla	Bovidae	Syncerus_caffer	592665.98	274.28	102.37	45.60	83.53	51.93	297.29	92.01	46.54	84.52	30.26	189.75	45.42	21.69	33.05	28.25	61.30	31.39	29.40	31.74	28.97	171.25
125	Laurasiatheria	Cetartiodactyla	Bovidae	Ammodorcas_clarkei	28049.81	146.83	33.91	14.30	31.12	18.21	210.57	28.11	17.61	27.32	10.94	253.02	10.42	7.50	11.98	12.97	48.16	10.23	7.93	8.53	10.76	NA
126	Laurasiatheria	Cetartiodactyla	Bovidae	Bubalus_bubalis	929500.97	285.64	109.29	54.61	78.44	55.19	301.67	85.90	52.89	82.23	31.54	189.06	46.87	21.04	34.30	29.00	59.41	34.13	32.14	33.97	29.14	165.66
127	Laurasiatheria	Cetartiodactyla	Bovidae	Taurotragus_oryx	562592.69	307.18	104.84	42.02	84.64	50.72	343.48	86.37	41.43	75.66	29.51	256.81	46.08	17.27	32.32	30.03	59.59	27.81	26.30	28.51	26.45	162.90
128	Laurasiatheria	Cetartiodactyla	Bovidae	Tragelaphus_strepsiceros	206056.41	259.13	75.53	28.58	64.36	36.25	313.47	67.30	36.29	61.64	20.66	307.06	37.62	14.65	23.88	23.89	68.34	19.66	17.43	19.43	21.79	155.09
129	Laurasiatheria	Cetartiodactyla	Bovidae	Tetracerus_quadricornis	19282.12	119.57	33.99	11.90	26.56	13.47	143.39	24.95	13.85	23.02	8.52	139.12	14.16	5.77	10.63	9.85	35.05	7.20	7.10	7.40	9.82	74.70
130	Laurasiatheria	Cetartiodactyla	Bovidae	Boselaphus_tragocamelus	182253.04	246.16	89.97	32.78	59.78	38.84	304.80	62.90	36.70	57.18	20.99	261.61	35.36	13.85	22.62	21.88	68.44	20.55	18.97	20.48	22.84	160.53
131	Laurasiatheria	Cetartiodactyla	Bovidae	Neotragus_moschatus	5639.01	78.82	17.21	6.79	14.52	8.55	83.50	13.72	8.26	12.21	4.66	82.51	6.21	3.61	5.03	5.04	12.58	4.77	4.19	3.73	5.19	NA
132	Laurasiatheria	Cetartiodactyla	Bovidae	Aepyceros_melampus	52591.69	168.45	56.90	19.77	37.31	25.86	227.83	38.02	22.44	35.85	15.13	232.97	24.15	9.96	14.83	16.69	48.71	11.75	11.44	11.28	13.97	104.69
133	Laurasiatheria	Cetartiodactyla	Bovidae	Pelea_capreolus	22731.33	146.95	40.70	15.25	29.24	18.82	174.77	30.08	19.34	28.23	12.66	175.21	19.07	7.67	12.16	13.13	38.29	10.01	9.02	9.49	12.58	85.95
134	Laurasiatheria	Cetartiodactyla	Bovidae	Redunca_redunca	43288.95	139.77	43.74	14.45	31.08	18.47	175.11	31.53	17.91	27.83	13.34	182.24	20.63	6.60	11.82	11.46	45.61	11.17	9.37	8.91	10.53	94.73
135	Laurasiatheria	Cetartiodactyla	Bovidae	Kobus_ellipsiprymnus	204393.48	221.22	76.62	34.53	62.08	36.16	255.58	62.61	36.91	50.81	21.70	230.83	33.09	12.84	21.66	20.25	56.37	20.07	19.05	19.71	21.63	142.72
136	Laurasiatheria	Cetartiodactyla	Bovidae	Ourebia_ourebi	17186.09	104.29	25.11	10.41	22.01	12.27	133.14	19.44	14.42	18.95	7.74	165.49	9.87	5.35	8.43	9.15	35.88	7.33	6.57	6.65	8.57	NA
137	Laurasiatheria	Cetartiodactyla	Bovidae	Raphicerus_melanotis	11661.53	99.34	19.97	7.96	18.56	9.46	119.32	15.97	9.35	16.06	6.34	124.90	7.29	4.15	7.12	6.39	24.25	6.52	5.24	5.56	6.40	61.01
138	Laurasiatheria	Cetartiodactyla	Bovidae	Madoqua_phillipsi	3424.47	66.89	12.63	5.38	11.75	6.81	83.79	9.84	6.72	9.61	3.86	80.24	3.84	2.50	4.49	3.85	19.17	4.30	3.67	3.94	4.07	42.80
139	Laurasiatheria	Cetartiodactyla	Bovidae	Dorcatragus_megalotis	10918.12	111.12	22.75	9.80	19.73	11.99	141.59	17.66	11.83	18.31	6.40	132.63	7.96	5.99	7.83	7.45	33.07	7.49	6.60	6.83	7.20	NA
140	Laurasiatheria	Cetartiodactyla	Bovidae	Saiga_tatarica	37734.01	143.78	46.17	16.88	31.04	20.79	170.89	31.09	17.89	28.40	10.56	153.47	18.73	7.09	11.66	11.79	42.16	10.36	8.10	8.55	9.73	88.48
141	Laurasiatheria	Cetartiodactyla	Bovidae	Nanger_dama	71424.81	173.05	56.19	19.40	38.79	23.43	253.47	38.89	22.49	36.35	13.48	270.22	23.91	9.61	14.23	15.31	60.70	12.28	10.48	11.78	13.30	127.24
142	Laurasiatheria	Cetartiodactyla	Bovidae	Eudorcas_thomsonii	22907.43	111.76	32.41	12.38	23.02	12.59	148.52	23.74	14.20	21.22	8.31	163.79	16.72	6.06	9.50	9.20	41.79	8.66	6.25	6.57	7.47	79.39
143	Laurasiatheria	Cetartiodactyla	Bovidae	Gazella_sp	20951.41	116.46	36.64	12.24	26.49	13.51	148.28	25.33	14.34	23.56	8.22	162.11	16.52	5.72	9.34	9.41	35.71	7.15	6.67	8.23	8.45	70.52
144	Laurasiatheria	Cetartiodactyla	Bovidae	Antilope_cervicapra	36301.10	106.17	34.17	11.95	27.36	12.95	130.03	27.78	13.94	26.72	8.82	142.19	17.76	6.47	12.96	9.94	40.00	9.12	6.72	8.06	10.68	83.75
145	Laurasiatheria	Cetartiodactyla	Bovidae	Litocranius_walleri	38804.37	170.04	40.55	17.93	36.12	19.76	247.90	34.66	21.44	32.87	12.34	294.97	14.40	9.95	14.68	13.80	56.97	11.24	9.84	9.93	13.95	115.50
146	Laurasiatheria	Cetartiodactyla	Bovidae	Antidorcas_marsupialis	33571.24	142.74	47.66	16.11	28.52	18.11	194.62	31.95	17.34	29.18	10.94	224.16	21.29	7.69	12.26	13.04	53.08	11.27	9.66	10.57	12.06	109.29
147	Laurasiatheria	Cetartiodactyla	Bovidae	Philantomba_maxwellii	8557.69	86.44	23.10	8.87	20.38	9.86	91.62	17.74	12.01	24.10	6.08	100.63	12.30	5.76	8.71	7.75	21.49	7.38	5.90	6.85	8.26	53.96
148	Laurasiatheria	Cetartiodactyla	Bovidae	Sylvicapra_grimmia	15639.15	94.77	21.26	8.47	19.90	9.31	94.72	18.62	10.84	19.55	5.28	98.60	11.59	4.33	7.38	6.65	23.50	6.51	5.60	6.31	6.36	55.77
149	Laurasiatheria	Cetartiodactyla	Bovidae	Cephalophus_dorsalis	20000.00	107.99	28.69	13.12	24.06	14.53	108.09	21.54	14.10	20.27	8.92	89.64	13.61	5.84	10.05	8.77	23.43	8.52	7.31	8.09	9.07	57.70
150	Laurasiatheria	Cetartiodactyla	Bovidae	Pantholops_hodgsonii	32733.12	159.00	39.06	16.85	33.13	21.04	194.29	34.72	18.46	30.70	10.83	178.52	14.02	7.37	13.22	11.49	42.30	12.26	10.19	12.37	12.24	NA

						Humerus					Radius					Metacarpal					Phalanx					
	Superord. group	Order	Family	Species	Mass	L	PW	MW	DW	H	L	PW	MW	DW	H	L	PW	MW	DW	H	L	PW	MW	DW	H	DL
151	Laurasiatheria	Cetartiodactyla	Bovidae	Ovibos_moschatus	312500.00	288.87	89.41	40.95	73.14	48.07	294.84	74.61	39.75	73.02	24.00	153.74	28.74	21.00	33.35	20.91	54.70	29.98	30.23	31.66	22.18	133.54
152	Laurasiatheria	Cetartiodactyla	Bovidae	Nemorhaedus_goral	28796.51	147.01	38.45	14.73	26.75	17.04	150.75	27.71	16.35	28.58	11.88	113.41	16.95	8.88	13.22	9.98	30.07	11.74	11.03	11.20	11.62	78.05
153	Laurasiatheria	Cetartiodactyla	Bovidae	Capricornis_sumatraensis	110942.22	191.05	40.32	19.71	41.24	23.78	190.01	30.59	20.27	35.42	13.73	149.54	21.97	9.14	17.96	13.35	42.27	16.33	12.91	13.69	14.52	102.41
154	Laurasiatheria	Cetartiodactyla	Bovidae	Ovis_aries	39097.89	144.40	47.13	17.79	31.33	18.64	170.79	35.10	20.05	32.88	9.94	142.69	19.00	8.40	13.45	11.94	36.83	12.05	11.17	12.47	11.10	89.50
155	Laurasiatheria	Cetartiodactyla	Bovidae	Hemitragus_jemlahicus	68616.43	176.86	51.87	20.32	40.06	23.33	186.22	39.27	21.68	38.11	14.66	120.84	22.65	8.56	16.37	13.06	37.14	14.57	11.91	13.93	11.11	89.22
156	Laurasiatheria	Cetartiodactyla	Bovidae	Capra_ibex	43500.00	191.75	67.31	26.51	41.96	29.12	205.72	48.10	26.85	43.05	16.83	137.17	30.31	12.13	20.27	15.73	47.07	20.11	15.41	16.70	15.64	119.40
157	Laurasiatheria	Cetartiodactyla	Bovidae	Capra_hircus	47386.47	187.27	55.01	22.43	37.14	27.71	193.08	37.16	26.17	38.62	15.25	125.42	22.59	11.32	16.32	13.81	41.17	16.04	14.77	15.45	13.79	97.04
158	Laurasiatheria	Cetartiodactyla	Bovidae	Pseudois_nayaur	52334.57	195.01	57.62	22.24	40.44	27.08	219.95	41.53	25.50	39.49	14.28	162.36	17.77	12.93	18.79	15.41	41.95	15.88	14.13	15.94	14.12	106.56
159	Laurasiatheria	Cetartiodactyla	Bovidae	Budorcas_taxicolor	294515.33	273.77	87.99	36.03	64.92	40.31	255.80	58.95	33.22	59.29	24.05	116.42	34.30	22.26	28.46	19.62	39.26	28.75	26.16	23.58	21.74	120.48
160	Laurasiatheria	Cetartiodactyla	Bovidae	Oreamnos_americanus	72105.40	201.71	54.12	18.49	40.60	24.06	188.29	40.27	22.87	39.98	13.98	98.69	24.59	13.03	20.51	12.75	38.24	18.49	16.65	16.77	17.18	94.63
161	Laurasiatheria	Cetartiodactyla	Bovidae	Rupicapra_rupicapra	33266.35	164.80	42.70	15.59	32.09	18.23	181.63	30.53	18.03	30.10	11.53	142.45	21.08	8.04	16.07	10.96	42.80	14.03	10.97	12.27	11.38	103.26
162	Laurasiatheria	Cetartiodactyla	Bovidae	Ammotragus_lervia	94202.22	209.70	60.57	28.70	48.11	33.61	237.29	47.76	32.85	46.55	19.01	157.24	28.12	12.42	20.90	16.53	45.48	19.04	16.69	17.22	14.83	100.48
163	Laurasiatheria	Cetartiodactyla	Bovidae	Connochaetes_taurinus	198619.68	226.78	76.87	29.21	54.43	33.92	310.10	64.99	34.00	52.27	20.15	212.62	37.73	12.05	20.17	19.32	62.53	18.69	15.58	17.12	18.27	149.68
164	Laurasiatheria	Cetartiodactyla	Bovidae	Damaliscus_pygargus	77784.55	169.14	58.62	21.16	36.08	23.00	235.36	40.47	21.65	33.93	13.10	214.44	24.04	9.14	15.71	13.91	52.97	13.63	10.53	10.72	12.84	116.77
165	Laurasiatheria	Cetartiodactyla	Bovidae	Beatragus_hunteri	79132.17	197.75	59.22	24.96	45.46	31.06	299.29	45.25	29.27	44.04	17.43	252.79	18.19	11.40	17.38	17.85	62.54	16.52	13.76	13.90	17.37	138.72
166	Laurasiatheria	Cetartiodactyla	Bovidae	Alcelaphus_buselaphus	168695.66	191.58	70.01	21.80	41.69	27.86	260.99	46.30	23.23	38.10	14.53	219.30	27.54	9.26	16.60	17.73	46.51	14.95	11.83	11.35	15.16	112.40
167	Laurasiatheria	Cetartiodactyla	Bovidae	Hippotragus_equinus	264173.96	243.03	93.22	35.15	60.73	35.15	317.81	63.35	36.54	58.94	21.76	240.23	36.69	14.07	25.44	23.03	70.94	20.82	18.50	27.17	22.79	164.21
168	Laurasiatheria	Cetartiodactyla	Bovidae	Oryx_gazella	188404.45	209.03	63.45	24.51	45.96	32.07	277.36	54.41	27.61	46.28	16.55	212.86	26.95	10.52	18.52	18.11	48.61	17.38	14.48	16.62	16.27	116.88
169	Laurasiatheria	Cetartiodactyla	Bovidae	Addax_nasomaculatus	96077.36	192.85	68.30	26.10	45.40	28.70	255.00	49.45	26.30	44.29	16.86	184.43	27.26	10.03	18.43	16.13	46.14	21.11	15.70	19.68	15.05	114.46
170	Laurasiatheria	Carnivora	Viverridae	Arctogalidia_trivirgata	2323.79	83.99	15.06	6.36	18.81	8.23	58.40	7.22	4.73	9.01	3.31	19.05	3.00	2.06	4.75	2.09	12.70	4.41	3.02	3.91	1.74	31.36
171	Laurasiatheria	Carnivora	Viverridae	Paguma_larvata	4300.00	89.50	16.02	6.69	20.68	9.15	73.05	9.50	9.72	11.71	3.53	19.57	3.82	2.65	4.63	2.33	12.54	5.22	3.07	3.70	2.42	32.62
172	Laurasiatheria	Carnivora	Viverridae	Paradoxurus_hermaphroditus	3200.00	86.71	10.62	7.42	20.83	8.19	67.89	8.08	4.48	10.24	3.73	20.09	4.35	2.66	4.33	2.57	11.78	3.88	3.36	3.43	2.11	28.02
173	Laurasiatheria	Carnivora	Viverridae	Arctictis_binturong	12999.99	142.34	25.72	12.92	38.21	14.28	117.85	13.26	8.67	19.23	7.07	30.91	6.23	4.11	7.94	3.51	17.60	7.25	5.44	5.49	3.40	50.00
174	Laurasiatheria	Carnivora	Viverridae	Chrotogale_owstoni	3267.71	51.00	8.92	4.48	12.84	4.81	41.84	5.61	3.18	7.52	3.08	14.65	2.21	1.81	2.73	1.74	7.94	3.00	2.47	2.10	1.43	19.16
175	Laurasiatheria	Carnivora	Viverridae	Viverricula_indica	2918.88	70.06	12.85	4.88	14.12	7.40	59.83	6.99	4.17	9.15	3.12	45.73	3.28	3.03	4.28	2.57	8.59	3.90	2.61	3.37	3.04	20.08
176	Laurasiatheria	Carnivora	Viverridae	Civettictis_civetta	12075.58	91.78	20.64	7.88	25.85	9.11	87.47	10.77	6.51	17.85	5.08	38.76	6.03	3.87	5.60	4.06	13.83	6.06	4.42	4.26	2.72	30.73
177	Laurasiatheria	Carnivora	Viverridae	Viverra_zibetha	9148.77	108.08	19.33	8.05	23.89	10.23	96.71	10.27	6.00	15.58	4.93	34.83	5.83	3.73	6.69	3.76	13.81	6.11	4.05	4.76	2.75	31.63
178	Laurasiatheria	Carnivora	Viverridae	Genetta_genetta	1756.17	77.52	12.01	4.70	14.27	6.23	65.98	6.31	3.36	8.48	3.53	20.79	2.76	2.36	4.58	2.10	12.07	4.05	2.56	3.22	2.69	27.46
179	Laurasiatheria	Carnivora	Viverridae	Poiana_richardsonii	570.08	45.83	7.62	3.27	11.83	5.13	34.96	4.97	2.42	6.24	2.86	13.20	2.60	1.35	2.59	1.78	9.26	3.28	2.06	2.23	1.64	21.10
180	Laurasiatheria	Carnivora	Viverridae	Genetta_angolensis	1859.64	67.94	10.56	4.78	13.20	5.77	55.34	5.90	3.32	8.22	3.25	17.26	2.64	1.93	3.27	1.89	8.77	3.36	2.34	2.55	1.64	NA
181	Laurasiatheria	Carnivora	Eupleridae	Eupleres_goudotii	2763.34	70.80	15.33	5.76	19.02	7.53	74.61	7.53	3.95	8.80	4.47	23.10	3.74	2.90	4.43	2.61	9.57	4.77	3.18	3.22	3.17	29.14
182	Laurasiatheria	Carnivora	Eupleridae	Fossa_fossana	1853.98	68.15	10.14	4.94	12.22	6.14	68.64	5.99	3.28	7.99	3.22	22.18	3.76	2.37	3.55	1.90	7.99	3.68	2.22	2.77	1.87	18.81
183	Laurasiatheria	Carnivora	Eupleridae	Galidictis_fasciata	549.99	56.44	9.51	4.16	9.54	5.31	48.03	4.77	2.54	6.07	2.69	17.38	2.37	1.49	2.57	1.62	8.52	2.71	1.57	1.88	1.51	NA
184	Laurasiatheria	Carnivora	Eupleridae	Salanoia_concolor	711.49	48.25	6.66	2.92	8.50	4.32	44.56	3.83	2.22	4.60	2.02	15.53	1.58	1.21	2.33	1.33	6.78	2.40	1.47	0.83	1.49	NA
185	Laurasiatheria	Carnivora	Eupleridae	Mungotictis_decemlineata	657.03	47.20	7.69	2.66	7.37	3.10	48.00	3.76	2.28	5.51	1.90	16.49	1.69	1.25	2.22	1.22	7.46	2.48	1.37	1.67	1.12	20.86
186	Laurasiatheria	Carnivora	Eupleridae	Galidia_elegans	810.00	49.45	8.06	3.50	10.13	4.10	42.28	4.64	2.48	5.48	2.18	17.39	2.24	1.39	2.87	1.56	9.07	2.77	1.58	2.25	1.51	21.72
187	Laurasiatheria	Carnivora	Eupleridae	Cryptoprocta_ferox	9500.00	112.35	21.08	8.28	24.22	10.68	85.80	13.08	5.90	14.27	4.52	27.47	5.36	3.29	6.64	2.93	14.37	6.16	3.33	4.46	2.97	37.07
188	Laurasiatheria	Carnivora	Herpestidae	Cynictis_penicillata	694.41	57.28	10.65	4.33	11.24	4.48	49.79	5.15	2.59	7.42	2.05	18.97	2.35	1.98	2.84	1.93	7.18	2.64	1.54	2.31	1.25	NA
189	Laurasiatheria	Carnivora	Herpestidae	Ichneumia_albicauda	3628.40	88.38	15.07	6.30	17.61	7.95	79.87	7.83	4.80	10.79	4.33	33.98	4.13	3.43	4.89	2.97	11.85	4.80	3.21	3.80	2.78	28.68
190	Laurasiatheria	Carnivora	Herpestidae	Herpestes_ichneumon	2980.02	65.16	14.56	5.89	17.64	8.14	53.15	8.26	4.66	10.13	4.03	24.73	4.46	3.02	5.34	2.62	11.39	4.68	3.29	3.86	2.42	29.18
191	Laurasiatheria	Carnivora	Ailuridae	Galerella_sanguinea	543.83	50.79	7.85	3.53	9.65	6.35	37.32	4.78	2.36	6.18	2.36	14.97	2.53	1.46	2.44	1.86	7.86	2.34	1.87	2.28	2.06	16.17
192	Laurasiatheria	Carnivora	Herpestidae	Urva_auropunctata	559.50	45.23	8.67	4.23	10.60	4.13	35.91	4.70	2.34	5.55	2.10	15.25	2.63	1.66	2.95	1.52	7.30	2.73	2.23	2.16	2.28	18.29
193	Laurasiatheria	Carnivora	Herpestidae	Atilax_paludinosus	3600.16	80.91	15.60	6.43	19.38	7.18	71.34	9.47	5.43	10.12	4.41	31.19	4.45	3.36	5.34	2.96	14.25	5.13	2.93	3.70	3.07	31.82
194	Laurasiatheria	Carnivora	Herpestidae	Suricata_suricatta	729.99	50.27	9.09	3.92	11.56	5.87	49.99	4.93	2.23	6.42	2.37	16.59	1.95	1.66	2.68	1.32	6.51	2.81	1.35	1.86	1.47	21.84
195	Laurasiatheria	Carnivora	Herpestidae	Mungos_mungo	1260.00	51.35	11.16	4.75	13.17	6.32	40.99	5.36	3.79	7.64	2.81	17.09	3.27	2.05	3.39	2.05	7.95	3.26	2.23	2.51	2.12	23.41
196	Laurasiatheria	Carnivora	Herpestidae	Dologale_dybowskii	361.92	41.87	8.34	2.96	10.92	4.77	34.28	4.16	2.45	5.32	2.01	14.62	1.92	1.45	2.56	1.25	6.53	2.61	1.65	1.87	1.26	NA
197	Laurasiatheria	Carnivora	Herpestidae	Crossarchus_sp	1395.09	51.14	9.77	4.54	13.61	5.18	43.05	5.10	3.57	6.99	2.57	16.73	2.55	1.99	3.23	1.64	8.82	3.62	2.27	2.62	1.71	22.54
198	Laurasiatheria	Carnivora	Hyaenidae	Hyaena_hyaena	35070.51	194.75	34.65	17.48	41.47	22.11	220.14	22.73	16.50	30.52	10.19	84.30	9.39	8.11	10.21	8.91	27.50	9.42	6.53	7.77	6.26	61.99
199	Laurasiatheria	Carnivora	Hyaenidae	Proteles_cristata	8139.39	121.53	21.73	8.31	23.18	9.36	126.51	13.33	9.72	19.51	5.06	60.79	5.29	5.16	6.85	4.43	19.18	6.84	4.50	5.15	4.01	42.61
200	Laurasiatheria	Carnivora	Hyaenidae	Crocuta_crocuta	63369.98	194.65	35.09	14.90	42.04	21.33	224.89	20.58	15.25	30.97	10.29	86.08	8.87	7.70	7.24	7.13	24.74	9.27	6.57	7.31	5.69	57.93
201	Laurasiatheria	Carnivora	Prionodontidae	Prionodon_pardicolor	1142.68	46.45	7.71	3.12	9.55	4.08	35.80	4.14	2.27	5.82	1.99	13.16	2.78	1.56	2.40	1.27	8.34	2.89	1.86	1.91	1.53	19.48

						Humerus					Radius					Metacarpal					Phalanx					
	Superord. group	Order	Family	Species	Mass	L	PW	MW	DW	H	L	PW	MW	DW	H	L	PW	MW	DW	H	L	PW	MW	DW	H	DL
202	Laurasiatheria	Carnivora	Felidae	Leptailurus_serval	11999.96	95.04	19.32	7.51	23.56	11.67	89.12	9.47	6.58	16.07	5.13	42.57	6.10	3.75	7.24	3.80	17.84	6.04	4.71	4.80	4.09	40.79
203	Laurasiatheria	Carnivora	Felidae	Caracal_aurata	11277.17	142.23	26.07	12.03	31.11	14.48	122.70	12.99	10.74	20.93	6.22	49.14	7.66	5.51	8.37	4.98	22.21	8.23	5.85	6.87	4.40	NA
204	Laurasiatheria	Carnivora	Felidae	Caracal_caracal	11964.38	134.50	24.87	9.30	25.70	11.32	120.75	12.15	8.49	18.28	4.85	48.05	5.73	4.76	8.81	3.78	21.30	7.36	4.75	5.45	3.96	50.89
205	Laurasiatheria	Carnivora	Felidae	Leopardus_pardalis	11880.00	133.17	25.45	11.38	30.96	13.32	119.35	14.22	9.48	21.67	6.14	46.82	8.55	5.31	8.10	4.74	20.90	6.54	5.81	6.06	3.68	47.62
206	Laurasiatheria	Carnivora	Felidae	Prionailurus_bengalensis	2780.97	40.34	7.74	3.62	9.98	3.77	33.20	4.49	2.39	6.69	2.19	14.62	2.42	2.07	2.80	2.20	8.48	2.57	2.21	2.87	1.78	18.85
207	Laurasiatheria	Carnivora	Felidae	Felis_catus	2884.80	88.23	15.74	16.11	16.75	7.15	83.86	9.28	5.15	10.59	3.55	30.27	4.65	2.91	4.44	2.88	12.75	4.02	3.21	3.70	2.36	30.49
208	Laurasiatheria	Carnivora	Felidae	Lynx_rufus	6374.47	125.79	19.58	8.69	24.34	10.21	116.55	10.72	7.27	16.69	4.18	45.14	6.31	4.09	6.64	3.73	20.39	6.15	4.10	4.93	3.00	48.74
209	Laurasiatheria	Carnivora	Felidae	Pardofelis_marmorata	2826.68	103.86	17.14	7.25	20.51	9.62	88.49	10.27	6.11	14.49	3.82	29.93	4.38	3.17	5.35	3.34	18.43	4.74	3.11	4.15	2.47	NA
210	Laurasiatheria	Carnivora	Felidae	Catopuma_temminckii	7726.46	146.51	25.00	12.13	29.46	15.21	130.44	13.79	10.16	21.34	5.92	48.98	5.96	4.81	7.97	4.56	23.32	7.04	5.22	5.97	4.09	51.73
211	Laurasiatheria	Carnivora	Felidae	Acinonyx_jubatus	50577.92	222.12	33.27	13.48	35.77	21.94	208.12	21.46	17.58	26.76	11.61	78.91	10.25	7.05	11.48	6.04	29.36	10.12	6.42	7.38	6.15	68.23
212	Laurasiatheria	Carnivora	Felidae	Puma_concolor	53954.05	201.56	40.25	17.59	47.53	23.00	166.03	21.29	18.31	33.49	9.15	72.56	13.61	7.67	13.84	7.20	32.51	12.46	8.81	10.49	6.19	82.46
213	Laurasiatheria	Carnivora	Felidae	Panthera_leo	158623.93	283.48	66.09	25.90	73.89	37.78	262.14	31.81	23.49	47.56	14.57	94.98	17.30	11.78	19.39	10.71	39.70	16.38	12.20	15.38	10.37	108.00
214	Laurasiatheria	Carnivora	Felidae	Neofelis_nebulosa	14945.05	159.40	29.83	13.42	41.66	16.44	126.20	17.28	11.01	25.27	6.38	44.09	10.33	5.97	10.74	5.29	26.77	10.39	6.74	8.51	4.73	NA
215	Laurasiatheria	Carnivora	Nandiniidae	Nandinia_binotata	2167.20	77.52	14.46	6.50	18.55	8.51	59.44	6.82	6.11	9.46	3.06	18.71	2.91	2.11	4.38	2.01	14.70	3.86	2.92	3.49	1.99	29.66
216	Laurasiatheria	Carnivora	Canidae	Urocyon_cinereoargenteus	3833.71	130.02	23.25	7.99	22.87	8.97	125.60	12.35	7.92	16.72	4.48	51.63	4.48	3.91	6.31	3.75	22.58	5.74	3.57	4.69	3.41	54.22
217	Laurasiatheria	Carnivora	Canidae	Vulpes_lagopus	3584.37	88.26	16.77	5.67	16.54	6.48	87.31	9.30	5.88	11.62	4.71	34.56	4.54	3.10	5.30	2.82	14.22	4.67	3.20	3.66	2.87	39.47
218	Laurasiatheria	Carnivora	Canidae	Nyctereutes_procyonoides	4214.99	100.59	20.37	8.32	21.69	10.24	91.07	11.18	6.37	15.25	6.11	41.83	4.34	4.13	5.51	3.53	12.74	4.18	3.15	3.94	3.04	33.66
219	Laurasiatheria	Carnivora	Canidae	Otocyon_megalotis	4098.12	95.48	16.41	6.07	16.64	7.32	102.51	9.13	5.85	12.86	3.54	40.21	3.62	2.78	4.49	2.57	13.49	4.39	2.56	3.33	2.59	NA
220	Laurasiatheria	Carnivora	Canidae	Cerdocyon_thous	5741.66	102.38	18.19	7.64	19.88	9.54	101.31	11.04	7.36	14.45	4.82	47.82	4.99	4.15	5.31	3.59	12.27	5.27	3.97	4.61	4.25	30.47
221	Laurasiatheria	Carnivora	Canidae	Speothos_venaticus	6324.54	104.84	22.52	9.21	24.88	9.77	86.07	12.80	7.08	15.46	6.27	42.59	5.61	5.25	7.10	3.29	18.33	5.91	3.57	4.79	3.66	45.47
222	Laurasiatheria	Carnivora	Canidae	Atelocynus_microtis	8363.22	112.50	23.64	8.17	24.99	11.31	105.96	12.86	8.14	18.13	5.87	43.51	6.29	4.07	6.62	4.09	16.75	6.07	3.98	5.22	3.40	NA
223	Laurasiatheria	Carnivora	Canidae	Lycalopex_gymnocercus	4542.67	102.31	15.96	10.98	18.17	6.90	97.25	9.93	6.82	14.20	3.80	44.72	4.72	3.28	5.99	3.43	17.58	5.14	2.92	4.16	3.09	41.04
224	Laurasiatheria	Carnivora	Canidae	Lycaon_pictus	21999.99	187.70	36.09	12.55	35.08	18.70	203.42	20.65	15.17	26.08	8.55	80.06	8.27	6.77	9.42	6.61	27.47	8.62	5.68	7.12	5.12	63.37
225	Laurasiatheria	Carnivora	Canidae	Chrysocyon_brachyurus	23325.00	255.57	38.50	15.59	41.35	17.42	273.96	20.48	16.20	26.94	10.50	115.59	9.27	7.17	9.60	8.54	23.41	8.60	6.30	6.94	7.52	NA
226	Laurasiatheria	Carnivora	Canidae	Canis_lupus	31756.51	187.41	38.15	14.41	38.36	18.28	193.65	20.69	15.76	32.55	9.73	78.94	9.37	6.97	10.18	5.86	26.14	9.58	6.02	8.10	5.89	64.43
227	Laurasiatheria	Carnivora	Canidae	Cuon_alpinus	15800.00	153.04	32.75	11.85	31.06	14.35	135.63	16.90	11.24	23.36	8.80	63.05	9.31	6.19	9.60	6.31	27.08	8.39	5.32	7.09	5.47	57.85
228	Laurasiatheria	Carnivora	Ursidae	Ailuropoda_melanoleuca	117999.99	273.31	54.88	24.79	77.35	32.73	204.94	32.20	17.36	43.01	16.30	46.41	7.67	7.58	11.30	6.86	24.30	11.70	9.63	9.52	7.37	71.67
229	Laurasiatheria	Carnivora	Ursidae	Tremarctos_ornatus	123176.97	229.23	48.64	25.23	63.54	27.52	189.06	25.88	15.87	34.91	11.20	49.92	9.75	7.46	12.74	7.58	22.56	11.12	7.36	9.62	6.90	81.15
230	Laurasiatheria	Carnivora	Ursidae	Helarctos_malayanus	57075.78	175.33	38.42	21.19	54.58	23.00	152.37	20.93	17.01	32.65	10.39	36.44	7.71	7.09	10.04	6.21	20.91	10.34	7.77	8.95	8.32	78.76
231	Laurasiatheria	Carnivora	Ursidae	Melursus_ursinus	99999.99	212.95	49.94	26.47	70.33	28.87	183.97	28.00	19.40	44.33	14.59	45.96	9.90	8.71	11.94	8.44	20.75	12.58	9.32	11.46	7.14	88.97
232	Laurasiatheria	Carnivora	Ursidae	Ursus_maritimus	371703.81	367.92	66.99	28.72	112.45	38.09	300.75	51.77	25.09	62.38	15.32	87.13	19.35	12.14	22.41	11.26	33.28	22.12	12.41	16.24	8.88	95.36
233	Laurasiatheria	Carnivora	Otariidae	Eumetopias_jubatus	382466.74	273.92	92.38	57.58	111.68	75.16	238.96	59.71	48.93	74.40	25.06	93.67	26.65	19.31	25.57	12.61	78.74	21.95	13.86	17.51	9.25	NA
234	Laurasiatheria	Carnivora	Otariidae	Zalophus_californianus	137194.86	134.50	45.46	24.17	59.22	44.37	146.98	25.68	30.67	45.97	11.56	53.60	9.45	7.36	13.15	8.30	38.16	12.35	8.36	9.21	5.68	83.08
235	Laurasiatheria	Carnivora	Otariidae	Otaria_byronia	193670.53	156.55	51.50	27.76	65.67	52.40	165.57	26.36	34.20	49.29	16.36	55.71	11.95	9.13	15.13	9.31	46.76	13.84	9.21	11.27	5.78	102.04
236	Laurasiatheria	Carnivora	Otariidae	Arctocephalus_galapagoensis	39448.04	131.92	38.25	20.40	48.41	38.89	159.73	29.64	14.07	23.34	10.53	41.50	10.36	7.83	13.60	6.32	38.50	13.38	6.05	10.98	3.81	NA
237	Laurasiatheria	Carnivora	Otariidae	Phocarctos_hookeri	273499.99	168.47	62.60	34.85	69.15	56.89	190.34	36.50	38.04	56.94	14.73	56.56	11.96	8.30	14.28	10.15	44.43	15.67	9.01	11.77	4.86	NA
238	Laurasiatheria	Carnivora	Otariidae	Callorhinus_ursinus	55464.82	110.08	33.10	20.29	39.03	36.53	123.97	24.57	21.68	36.23	12.04	43.86	8.15	6.99	11.18	8.09	40.59	9.85	6.90	8.35	4.24	84.78
239	Laurasiatheria	Carnivora	Odobenidae	Odobenus_rosmarus	1042996.25	349.85	126.06	61.83	137.94	66.89	266.36	66.05	52.64	85.55	29.65	75.98	16.34	18.30	25.10	17.63	70.88	22.89	15.92	18.57	11.13	137.16
240	Laurasiatheria	Carnivora	Phocidae	Neomonachus_tropicalis	197758.36	155.11	45.84	24.49	53.81	32.52	133.57	27.73	28.61	43.00	13.76	47.11	10.53	8.50	12.86	7.60	47.22	12.87	8.60	11.01	5.99	117.24
241	Laurasiatheria	Carnivora	Phocidae	Ommatophoca_rossii	208252.12	116.37	53.74	32.48	51.69	43.20	140.46	31.45	43.22	45.91	19.23	51.92	12.63	11.05	15.74	10.86	62.99	15.86	10.55	14.08	6.58	139.95
242	Laurasiatheria	Carnivora	Phocidae	Hydrurga_leptonyx	352675.48	173.83	74.76	37.28	67.16	54.88	185.64	39.11	60.80	66.06	19.16	68.19	15.02	11.12	16.91	13.40	78.99	18.27	12.26	16.33	8.56	174.28
243	Laurasiatheria	Carnivora	Phocidae	Erignathus_barbatus	279999.99	164.11	52.37	25.80	63.29	34.96	155.04	30.86	28.02	46.06	16.00	51.71	9.97	10.95	15.42	11.87	32.96	16.22	11.87	14.26	10.30	107.23
244	Laurasiatheria	Carnivora	Phocidae	Halichoerus_grypus	197570.01	76.31	30.65	12.86	34.41	26.93	76.21	16.48	12.59	26.89	7.00	25.11	6.66	5.60	8.66	5.63	22.11	8.57	5.61	8.47	4.17	70.34
245	Laurasiatheria	Carnivora	Phocidae	Pusa_hispida	70963.60	99.20	35.59	16.17	35.52	29.04	101.80	20.06	26.94	38.83	8.63	31.60	7.35	6.69	9.61	6.65	25.10	9.13	7.05	7.89	5.76	68.98
246	Laurasiatheria	Carnivora	Phocidae	Phoca_vitulina	87316.66	85.63	29.47	14.27	35.51	25.27	80.82	16.72	20.70	28.75	7.50	27.28	6.61	5.90	8.47	7.59	21.40	6.94	6.35	7.48	5.06	63.92
247	Laurasiatheria	Carnivora	Phocidae	Pagophilus_groenlandicus	132250.00	127.70	43.31	26.09	43.93	43.97	126.13	22.14	34.82	42.52	14.44	37.23	9.63	9.03	11.89	8.39	29.47	12.62	10.09	12.61	8.62	98.43
248	Laurasiatheria	Carnivora	Phocidae	Histriophoca_fasciata	90000.00	118.16	42.31	23.16	45.15	36.96	102.34	25.15	27.03	36.82	10.63	34.21	7.98	7.91	10.54	8.71	27.61	11.50	8.91	11.94	7.30	78.77
249	Laurasiatheria	Carnivora	Phocidae	Cystophora_cristata	278896.81	151.41	52.87	35.28	53.67	56.08	144.45	29.03	43.19	53.43	16.31	45.48	9.62	10.62	12.87	10.96	40.04	13.86	11.84	12.97	9.85	105.79
250	Laurasiatheria	Carnivora	Ailuridae	Ailurus_fulgens	5170.08	112.46	18.25	7.51	25.64	10.56	90.74	10.57	6.26	14.65	5.16	27.44	5.03	3.28	5.37	3.25	18.80	5.97	4.41	5.30	3.61	43.47
251	Laurasiatheria	Carnivora	Procyonidae	Procyon_lotor	6373.72	103.71	17.29	7.34	23.40	11.26	103.04	9.88	6.37	14.12	4.99	30.08	3.71	2.81	4.62	2.69	14.65	3.85	2.74	3.50	2.87	31.89
252	Laurasiatheria	Carnivora	Procyonidae	Bassariscus_astutus	1010.37	67.60	11.98	5.34	14.50	7.31	54.47	6.78	4.12	8.65	3.34	17.84	3.27	2.18	4.40	2.28	10.04	4.25	2.54	2.71	2.22	23.24

						Humerus					Radius					Metacarpal					Phalanx					
	Superord. group	Order	Family	Species	Mass	L	PW	MW	DW	H	L	PW	MW	DW	H	L	PW	MW	DW	H	L	PW	MW	DW	H	DL
253	Laurasiatheria	Carnivora	Procyonidae	Nasua_narica	4578.43	84.94	18.11	8.10	24.94	12.33	74.85	10.15	7.56	15.44	4.99	23.00	3.89	3.28	4.08	2.83	11.41	4.15	3.20	2.84	2.98	35.82
254	Laurasiatheria	Carnivora	Procyonidae	Potos_flavus	2441.81	82.50	14.92	7.11	23.32	9.94	64.89	8.13	5.55	11.17	4.25	19.71	3.56	2.93	4.60	2.78	14.79	4.16	3.15	3.54	2.79	36.42
255	Laurasiatheria	Carnivora	Mustelidae	Taxidea_taxus	7842.15	90.75	19.88	8.88	30.18	11.03	72.00	11.25	5.29	17.05	5.70	22.35	7.34	4.26	7.12	4.49	14.82	6.73	5.56	6.67	4.71	NA
256	Laurasiatheria	Carnivora	Mustelidae	Meles_meles	11884.03	71.11	22.67	8.69	27.75	10.10	55.51	11.77	6.03	14.79	4.60	21.26	5.03	3.62	6.38	3.57	10.55	5.49	4.28	5.18	3.08	30.38
257	Laurasiatheria	Carnivora	Mustelidae	Arctonyx_collaris	8166.52	120.59	21.75	11.94	40.20	14.42	96.87	14.83	10.15	22.18	6.30	32.41	8.37	5.31	8.33	4.01	13.45	7.42	5.19	6.00	4.33	50.64
258	Laurasiatheria	Carnivora	Mustelidae	Melogale_moschata	938.50	47.97	10.88	4.34	13.44	5.62	37.80	5.83	3.86	7.30	2.43	14.09	2.89	1.88	3.23	1.81	7.51	3.33	2.45	2.79	1.98	20.26
259	Laurasiatheria	Carnivora	Mustelidae	Lyncodon_patagonicus	225.00	33.74	7.03	2.42	8.34	3.67	23.32	3.68	1.64	4.69	2.21	10.74	1.58	1.29	2.10	1.15	6.82	2.16	1.33	1.69	1.21	18.24
260	Laurasiatheria	Carnivora	Mustelidae	Galictis_vittata	2600.00	59.88	11.55	3.91	15.89	5.49	40.39	7.59	3.14	8.13	3.04	16.92	3.38	2.58	4.01	1.99	10.15	3.99	2.52	3.17	2.56	26.07
261	Laurasiatheria	Carnivora	Mustelidae	Ictonyx_striatus	811.02	53.63	10.32	4.03	14.13	4.87	40.98	5.52	2.59	7.20	2.66	15.30	2.46	1.96	3.23	1.93	10.12	3.76	2.34	3.19	1.84	29.35
262	Laurasiatheria	Carnivora	Mustelidae	Pteronura_brasiliensis	26000.00	102.03	27.56	9.05	35.75	14.30	73.63	13.93	8.55	21.85	7.27	39.41	8.56	6.64	9.51	5.75	24.96	9.69	6.62	6.99	4.52	58.06
263	Laurasiatheria	Carnivora	Mustelidae	Lontra_longicaudis	6554.97	72.17	15.44	5.91	21.57	11.20	47.72	9.53	4.71	11.04	4.94	21.54	4.05	3.45	5.09	2.94	12.71	4.91	3.43	3.99	2.64	31.86
264	Laurasiatheria	Carnivora	Mustelidae	Lutra_lutra	8868.69	61.78	16.59	5.95	22.95	10.04	44.82	9.38	4.50	11.95	4.08	21.72	5.08	2.63	4.86	3.26	12.20	4.55	3.37	3.76	2.23	31.61
265	Laurasiatheria	Carnivora	Mustelidae	Aonyx_capensis	19322.22	86.82	22.95	7.77	29.95	11.34	71.86	11.83	6.01	13.87	5.49	29.08	5.44	3.57	6.28	3.65	20.75	5.70	3.57	4.79	2.88	40.88
266	Laurasiatheria	Carnivora	Mustelidae	Enhydra_lutris	27410.93	108.99	28.85	10.88	32.39	22.28	86.03	14.77	11.85	18.86	5.29	24.00	4.42	5.01	6.25	6.31	13.93	6.15	4.58	5.05	3.71	32.97
267	Laurasiatheria	Carnivora	Mustelidae	Mustela_erminea	284.50	21.83	3.70	1.55	4.07	1.71	14.05	1.92	1.12	2.43	0.97	7.12	0.72	0.78	1.05	0.67	3.87	1.14	0.73	0.91	0.68	8.83
268	Laurasiatheria	Carnivora	Mustelidae	Mustela_frenata	190.03	26.67	4.50	1.74	4.87	1.84	18.07	2.37	1.20	2.98	1.09	8.89	0.82	1.04	1.06	0.78	5.12	1.30	0.82	1.01	0.87	12.29
269	Laurasiatheria	Carnivora	Mustelidae	Gulo_gulo	12792.49	141.89	30.28	11.67	38.97	13.96	115.91	16.62	8.24	22.45	7.01	48.64	6.42	5.76	9.58	5.34	22.39	9.17	5.42	6.92	4.78	59.84
270	Laurasiatheria	Carnivora	Mustelidae	Martes_foina	1675.00	68.19	11.94	5.66	15.60	6.51	50.41	6.49	3.71	8.75	3.22	22.20	3.13	2.55	3.82	2.52	12.46	3.94	2.58	3.05	2.09	31.13
271	Laurasiatheria	Carnivora	Mustelidae	Eira_barbara	4134.99	62.92	17.51	6.26	20.74	9.37	53.82	9.93	7.33	11.06	3.35	22.73	4.26	3.06	5.08	2.68	12.59	4.73	3.08	3.22	2.74	33.60
272	Laurasiatheria	Carnivora	Mustelidae	Mellivora_capensis	8999.99	94.40	20.73	8.63	29.63	9.47	76.72	12.01	7.31	17.64	4.70	26.22	4.56	4.17	6.69	3.51	13.80	5.78	4.34	5.35	4.23	52.73
273	Laurasiatheria	Carnivora	Mephitidae	Conepatus_chinga	3400.00	39.92	9.87	3.57	13.15	5.36	34.37	4.98	1.98	6.89	2.96	10.55	2.17	1.53	2.57	1.84	4.87	2.13	1.94	2.22	1.72	25.90
274	Laurasiatheria	Carnivora	Mephitidae	Mephitis_mephitis	2399.99	58.07	13.19	5.03	17.05	7.65	47.21	6.48	3.26	9.68	3.84	15.19	2.84	2.36	3.62	2.37	6.71	3.87	2.58	2.46	2.36	24.87
275	Laurasiatheria	Carnivora	Mephitidae	Spilogale_gracilis	444.75	41.93	9.39	3.57	11.43	5.55	33.73	4.78	2.73	6.76	2.41	10.93	1.59	1.54	2.27	1.79	5.41	2.39	1.65	1.69	1.42	16.79
276	Laurasiatheria	Carnivora	Mephitidae	Mydaus_javanensis	2500.00	69.23	15.17	6.56	23.91	8.58	54.10	8.24	4.18	10.80	5.02	16.59	3.29	2.89	3.88	2.67	5.17	4.06	3.39	2.65	2.36	26.12
277	Laurasiatheria	Pholidota	Manidae	Manis_pentadactyla	4675.00	77.50	24.44	9.86	37.61	14.49	48.88	12.48	4.80	12.19	11.55	13.27	10.03	6.26	7.88	6.98	5.39	7.48	7.68	7.51	7.15	56.06
278	Laurasiatheria	Pholidota	Manidae	Smutsia_gigantea	32999.70	111.48	29.87	17.79	50.33	19.08	74.01	19.97	11.63	19.54	9.43	13.41	14.14	11.35	11.53	13.26	8.14	12.06	10.93	10.74	11.30	78.19
279	Laurasiatheria	Pholidota	Manidae	Phataginus_tricuspis	1539.31	44.99	11.29	7.48	19.50	9.03	35.62	7.93	3.17	8.16	5.90	8.33	6.93	4.35	4.78	3.67	6.55	5.10	4.84	4.50	3.53	38.18
280	Laurasiatheria	Chiroptera	Nycteridae	Nycteris_thebaica	9.20	20.10	3.66	1.50	4.99	1.59	41.45	2.00	1.16	2.40	1.11	33.39	1.04	0.57	1.62	0.62	22.94	1.30	0.52	0.84	0.51	43.88
281	Laurasiatheria	Chiroptera	Emballonuridae	Saccolaimus_saccolaimus	43.00	38.88	6.02	2.31	4.52	2.47	66.90	4.12	2.07	4.01	2.03	69.09	1.28	1.09	1.69	0.88	27.60	1.42	0.89	1.14	0.73	54.75
282	Laurasiatheria	Chiroptera	Emballonuridae	Balantiopteryx_plicata	6.57	23.71	3.18	1.23	2.62	1.21	42.35	2.15	1.08	2.13	1.09	40.55	0.98	0.58	0.94	0.60	11.64	1.05	0.41	0.69	0.42	32.72
283	Laurasiatheria	Chiroptera	Emballonuridae	Mosia_nigrescens	3.33	19.28	2.39	0.98	2.33	0.97	33.48	1.70	0.95	2.19	0.79	32.69	0.59	0.32	0.64	0.44	9.07	0.60	0.24	0.42	0.27	21.14
284	Laurasiatheria	Chiroptera	Emballonuridae	Peropteryx_kappleri	9.85	27.77	3.48	1.31	3.15	1.29	49.09	2.54	1.22	2.13	1.09	45.89	1.01	0.59	0.90	0.57	14.70	1.17	0.43	0.65	0.46	39.01
285	Laurasiatheria	Chiroptera	Emballonuridae	Cormura_brevirostris	9.26	25.69	3.79	1.39	3.07	1.40	43.85	2.35	1.30	2.32	1.19	41.03	0.91	0.52	0.88	0.62	13.16	0.86	0.44	0.60	0.43	34.41
286	Laurasiatheria	Chiroptera	Emballonuridae	Saccopteryx_leptura	5.75	20.51	2.69	1.23	2.85	1.17	38.48	2.24	1.10	1.98	1.00	39.46	0.78	0.47	0.81	0.56	11.30	0.86	0.39	0.60	0.41	29.74
287	Laurasiatheria	Chiroptera	Emballonuridae	Rhynchonycteris_naso	4.14	19.87	2.72	1.06	2.46	1.09	35.42	2.06	1.05	2.03	0.93	37.88	0.63	0.54	0.70	0.37	11.36	0.84	0.31	0.43	0.30	26.54
288	Laurasiatheria	Chiroptera	Emballonuridae	Emballonura_alecto	5.25	24.85	3.26	1.26	2.81	1.27	43.92	2.09	1.10	2.23	1.07	42.50	0.95	0.59	1.01	0.61	12.07	1.20	0.44	0.72	0.44	35.00
289	Laurasiatheria	Chiroptera	Emballonuridae	Coleura_afra	10.68	25.98	3.52	1.30	3.07	1.41	46.37	2.37	1.22	2.01	1.15	43.11	0.91	0.56	0.95	0.59	16.39	1.04	0.47	0.61	0.49	33.11
290	Laurasiatheria	Chiroptera	Natalidae	Natalus_stramineus	5.68	14.17	3.00	1.13	3.42	1.12	23.04	2.34	1.11	2.35	1.04	23.92	1.02	0.71	1.16	0.41	14.59	0.87	0.37	0.68	0.41	32.66
291	Laurasiatheria	Chiroptera	Molossidae	Cheiromeles_torquatus	169.43	48.28	8.39	3.55	6.27	3.27	69.23	6.09	3.15	6.33	2.61	78.82	2.66	1.54	2.84	1.94	45.84	2.93	1.50	1.14	1.15	83.26
292	Laurasiatheria	Chiroptera	Molossidae	Chaerephon_pumilus	10.98	17.79	2.87	1.05	2.14	1.14	29.46	2.00	1.05	2.00	1.04	31.03	0.77	0.56	1.04	0.60	12.44	0.87	0.52	0.49	0.42	25.22
293	Laurasiatheria	Chiroptera	Molossidae	Chaerephon_plicatus	21.83	26.64	4.51	1.71	3.53	1.67	41.06	3.19	1.66	3.08	1.57	43.32	1.37	0.95	1.54	0.86	18.73	1.36	0.74	0.78	0.58	34.37
294	Laurasiatheria	Chiroptera	Molossidae	Mops_mops	31.12	28.41	4.81	1.65	3.52	1.80	43.93	3.37	1.83	3.13	1.72	47.48	1.45	1.02	1.59	0.90	21.54	1.93	0.88	0.77	0.64	38.05
295	Laurasiatheria	Chiroptera	Molossidae	Tadarida_australis	36.40	32.84	5.58	1.89	3.81	2.11	55.39	3.28	1.71	3.38	1.90	59.41	1.59	1.17	1.98	0.97	24.11	2.55	0.88	0.91	0.63	48.81
296	Laurasiatheria	Chiroptera	Molossidae	Mormopterus_acetabulosus	7.30	21.22	3.00	1.26	2.44	1.20	39.02	2.19	1.30	2.22	1.20	40.79	0.65	0.81	1.15	0.59	15.16	1.38	0.50	0.48	0.34	28.05
297	Laurasiatheria	Chiroptera	Molossidae	Nyctinomops_femorosaccus	15.04	26.16	3.97	1.37	2.83	1.55	43.40	2.58	1.43	2.32	1.44	45.18	0.97	0.77	1.27	0.80	19.18	1.74	0.61	0.58	0.44	36.65
298	Laurasiatheria	Chiroptera	Molossidae	Molossops_temminckii	5.86	17.29	2.87	1.12	2.21	1.16	28.51	2.05	1.03	2.22	1.04	31.91	0.81	0.55	1.00	0.62	12.00	1.15	0.54	0.57	0.32	25.24
299	Laurasiatheria	Chiroptera	Molossidae	Promops_centralis	29.80	31.14	4.94	1.97	3.40	1.92	48.99	3.42	1.73	3.00	1.67	53.73	1.46	1.07	1.75	0.90	23.69	2.23	0.85	0.86	0.56	43.53
300	Laurasiatheria	Chiroptera	Molossidae	Molossus_molossus	13.70	23.73	3.89	1.45	2.75	1.53	35.90	2.54	1.48	2.47	1.44	40.30	1.59	0.95	1.25	0.84	18.00	1.62	0.75	0.59	0.51	26.14
301	Laurasiatheria	Chiroptera	Molossidae	Eumops_dabbenei	67.27	41.80	7.08	3.05	4.91	2.93	71.22	4.41	2.84	4.51	2.77	77.54	2.29	1.90	2.48	1.41	32.90	2.12	1.07	1.26	1.14	65.00
302	Laurasiatheria	Chiroptera	Molossidae	Otomops_martiensseni	34.92	37.31	6.03	2.14	3.94	2.27	68.26	4.04	1.94	3.35	1.90	73.17	1.67	1.25	1.88	1.02	26.45	2.13	0.93	1.03	0.57	55.27
303	Laurasiatheria	Chiroptera	Vespertilionidae	Hesperoptenus_tickelli	16.30	34.33	4.79	2.03	3.58	1.87	54.24	3.47	1.93	3.68	1.82	53.19	1.14	0.87	1.19	1.04	22.78	1.62	0.69	1.06	0.81	45.72

						Humerus					Radius					Metacarpal					Phalanx					
	Superord. group	Order	Family	Species	Mass	L	PW	MW	DW	H	L	PW	MW	DW	H	L	PW	MW	DW	H	L	PW	MW	DW	H	DL
304	Laurasiatheria	Chiroptera	Vespertilionidae	Glischropus_tylopus	4.59	17.01	2.53	1.04	2.53	0.97	25.14	1.87	1.03	2.32	0.89	25.87	0.80	0.63	1.07	0.45	13.43	0.97	0.42	0.58	0.39	26.00
305	Laurasiatheria	Chiroptera	Vespertilionidae	Vespertilio_murinus	15.42	26.89	3.67	1.48	2.84	1.53	42.58	2.28	1.43	2.70	1.45	41.37	0.94	0.86	1.16	0.78	17.33	1.12	0.57	0.77	0.70	29.46
306	Laurasiatheria	Chiroptera	Vespertilionidae	Neoromicia_nana	3.88	18.52	2.48	1.06	2.28	0.98	29.78	1.69	0.99	2.13	0.95	29.53	0.59	0.61	0.82	0.55	10.93	0.70	0.35	0.59	0.41	20.31
307	Laurasiatheria	Chiroptera	Vespertilionidae	Nyctophilus_geoffroyi	8.90	18.12	2.49	0.94	2.17	0.94	30.00	1.71	0.94	2.01	0.79	28.98	0.60	0.46	0.79	0.58	11.20	0.77	0.36	0.48	0.39	22.38
308	Laurasiatheria	Chiroptera	Vespertilionidae	Vespadelus_sp	5.05	18.45	2.60	1.03	2.20	0.98	30.12	1.71	1.09	2.08	0.93	28.72	0.63	0.59	0.83	0.57	10.30	0.81	0.40	0.52	0.47	18.74
309	Laurasiatheria	Chiroptera	Vespertilionidae	Chalinolobus_gouldii	14.24	27.42	3.90	1.59	2.96	1.68	41.65	2.51	1.43	2.67	1.50	43.81	0.96	0.69	1.15	0.78	18.27	1.23	0.54	0.81	0.59	33.78
310	Laurasiatheria	Chiroptera	Vespertilionidae	Eptesicus_fuscus	17.49	26.98	3.59	1.47	3.18	1.46	40.34	2.52	1.48	2.93	1.40	39.87	0.90	0.68	1.12	0.78	14.97	1.08	0.54	0.67	0.54	27.86
311	Laurasiatheria	Chiroptera	Vespertilionidae	Histiotus_velatus	11.32	25.52	3.52	1.49	2.98	1.53	43.71	2.63	1.40	3.02	1.33	43.20	0.86	0.66	1.03	0.80	13.67	1.04	0.56	0.66	0.51	28.75
312	Laurasiatheria	Chiroptera	Vespertilionidae	Lasionycteris_noctivagans	11.02	25.24	3.42	1.22	2.84	1.38	37.91	2.19	1.37	2.60	1.30	38.01	0.73	0.73	0.93	0.76	14.86	0.94	0.48	0.64	0.54	27.28
313	Laurasiatheria	Chiroptera	Vespertilionidae	Euderma_maculatum	16.17	28.67	3.82	1.49	3.31	1.61	47.38	2.57	1.52	2.96	1.37	43.87	0.82	0.66	1.08	0.65	13.95	1.08	0.54	0.79	0.58	33.78
314	Laurasiatheria	Chiroptera	Vespertilionidae	Plecotus_auritus	8.19	23.62	3.22	1.31	2.99	1.27	39.65	2.23	1.14	2.67	0.93	36.68	0.86	0.55	0.91	0.56	13.71	0.93	0.36	0.58	0.47	27.70
315	Laurasiatheria	Chiroptera	Vespertilionidae	Barbastella_barbastellus	8.31	23.86	2.99	1.41	2.77	1.27	36.23	2.08	1.20	2.52	1.24	35.58	0.79	0.64	0.90	0.55	12.38	0.99	0.39	0.56	0.53	27.08
316	Laurasiatheria	Chiroptera	Vespertilionidae	Rhogeessa_tumida	4.58	17.82	2.75	1.10	2.55	1.09	28.60	2.08	1.05	2.37	0.94	28.68	0.67	0.57	0.84	0.54	10.51	0.78	0.42	0.48	0.43	20.79
317	Laurasiatheria	Chiroptera	Vespertilionidae	Antrozous_pallidus	22.24	31.16	4.63	1.75	4.37	1.77	50.82	3.17	1.72	3.73	1.54	46.71	1.13	0.87	1.31	0.63	14.60	1.15	0.60	0.65	0.55	28.45
318	Laurasiatheria	Chiroptera	Vespertilionidae	Lasiurus_borealis	12.33	24.77	3.27	1.39	2.56	1.31	35.88	2.55	1.21	2.50	1.16	41.06	1.04	0.65	0.91	0.56	16.61	1.01	0.42	0.53	0.51	32.99
319	Laurasiatheria	Chiroptera	Vespertilionidae	Scotophilus_kuhlii	20.31	31.71	4.63	1.58	3.42	1.66	48.03	2.82	1.61	3.37	1.50	49.93	1.00	0.78	1.32	0.74	16.07	1.40	0.52	0.73	0.62	28.52
320	Laurasiatheria	Chiroptera	Vespertilionidae	Nycticeius_humeralis	9.12	22.58	3.14	1.18	2.60	1.16	35.57	1.92	1.19	2.59	1.02	34.34	0.80	0.59	0.97	0.66	12.99	0.92	0.45	0.55	0.45	24.91
321	Laurasiatheria	Chiroptera	Vespertilionidae	Kerivoula_picta	4.50	19.31	2.79	1.20	2.69	1.08	32.83	2.21	1.06	2.70	0.96	36.70	0.91	0.85	1.29	0.45	15.68	1.24	0.51	0.60	0.40	35.85
322	Laurasiatheria	Chiroptera	Vespertilionidae	Myotis_lucifugus	7.80	21.69	2.92	1.17	2.63	1.13	34.96	2.10	1.23	2.55	0.99	34.70	0.76	0.57	0.88	0.63	11.14	0.84	0.35	0.52	0.46	21.70
323	Laurasiatheria	Chiroptera	Miniopteridae	Miniopterus_australis	7.40	19.78	3.00	0.90	2.17	1.08	34.06	2.10	1.02	2.01	0.92	31.83	0.81	0.49	0.97	0.62	8.39	1.06	0.40	0.67	0.44	32.18
324	Laurasiatheria	Chiroptera	Myzopodidae	Myzopoda_aurita	9.10	24.04	3.26	1.47	3.82	1.26	45.74	2.61	1.39	3.07	1.26	39.67	1.11	0.50	1.31	0.80	17.68	1.26	0.47	0.71	0.63	48.02
325	Laurasiatheria	Chiroptera	Thyropteridae	Thyroptera_tricolor	4.52	17.13	2.41	1.02	2.66	0.93	33.85	1.96	0.90	2.64	0.89	34.34	1.20	0.53	0.97	0.49	13.82	1.06	0.36	0.48	0.33	26.46
326	Laurasiatheria	Chiroptera	Noctilionidae	Noctilio_albiventris	31.46	33.06	5.20	2.19	5.57	2.06	59.16	3.81	2.08	4.06	1.82	57.71	2.48	1.31	1.81	1.19	13.82	2.06	0.97	1.22	0.71	54.83
327	Laurasiatheria	Chiroptera	Furipteridae	Furipterus_horrens	3.15	18.33	2.87	0.99	2.45	0.91	33.69	1.85	1.02	1.74	0.82	31.99	0.98	0.46	0.88	0.57	5.44	0.84	0.41	0.50	0.35	24.13
328	Laurasiatheria	Chiroptera	Furipteridae	Amorphochilus_schnablii	3.30	19.01	2.82	1.12	2.57	1.10	33.76	1.91	1.12	2.03	1.02	32.48	0.98	0.56	0.92	0.66	4.32	0.95	0.45	0.61	0.39	25.53
329	Laurasiatheria	Chiroptera	Phyllostomidae	Vampyrum_spectrum	171.61	64.71	9.04	3.95	12.03	3.78	103.32	8.15	3.43	8.37	3.31	76.21	4.14	1.77	3.08	1.88	43.66	2.94	1.57	1.85	1.45	124.37
330	Laurasiatheria	Chiroptera	Phyllostomidae	Chrotopterus_auritus	78.26	44.17	6.54	2.90	8.93	2.67	75.22	5.27	2.39	5.69	2.26	58.05	2.60	1.32	2.02	1.30	30.24	2.02	0.95	1.14	1.08	87.08
331	Laurasiatheria	Chiroptera	Phyllostomidae	Lophostoma_brasiliense	9.76	21.77	3.17	1.32	3.78	1.26	31.49	2.64	1.16	2.70	1.17	26.15	1.14	0.67	1.01	0.63	11.00	1.09	0.56	0.65	0.54	31.68
332	Laurasiatheria	Chiroptera	Phyllostomidae	Phyllostomus_discolor	36.70	33.46	5.49	2.13	5.80	2.31	56.07	3.99	2.03	4.23	1.65	56.63	1.91	1.01	1.50	1.00	12.80	1.75	0.92	1.08	0.80	51.79
333	Laurasiatheria	Chiroptera	Phyllostomidae	Macrophyllum_macrophyllum	8.02	21.10	3.12	1.38	3.60	1.34	33.36	2.50	1.30	3.04	1.04	34.44	1.22	0.72	1.35	0.61	14.08	1.30	0.56	0.65	0.44	38.10
334	Laurasiatheria	Chiroptera	Phyllostomidae	Mimon_cozumelae	23.00	29.86	4.75	2.03	5.32	2.04	52.73	3.48	1.71	3.82	1.73	48.31	2.06	0.95	1.35	0.97	19.81	1.58	0.82	0.83	0.75	59.35
335	Laurasiatheria	Chiroptera	Phyllostomidae	Trachops_cirrhosus	36.90	30.98	5.15	2.06	5.99	2.00	51.89	3.72	1.73	4.60	1.67	42.45	2.45	1.02	1.65	1.05	18.00	1.55	0.79	0.93	0.88	56.24
336	Laurasiatheria	Chiroptera	Phyllostomidae	Carollia_brevicauda	14.85	23.64	3.44	1.41	3.90	1.52	34.56	2.65	1.39	3.17	1.27	34.51	1.53	0.88	1.37	0.77	15.42	1.24	0.64	0.82	0.63	43.75
337	Laurasiatheria	Chiroptera	Phyllostomidae	Rhinophylla_pumilio	9.58	19.45	3.03	1.40	3.63	1.33	31.24	2.45	1.24	2.86	1.18	33.09	1.17	0.82	1.10	0.57	14.76	1.24	0.52	0.63	0.55	43.59
338	Laurasiatheria	Chiroptera	Phyllostomidae	Uroderma_bilobatum	16.28	24.83	4.30	1.89	4.95	1.74	41.68	3.36	1.59	3.79	1.50	43.17	1.72	0.86	1.18	0.89	15.64	1.42	0.69	0.83	0.61	50.33
339	Laurasiatheria	Chiroptera	Phyllostomidae	Vampyressa_pusilla	8.77	19.82	3.32	1.35	3.67	1.40	32.48	2.54	1.27	2.86	1.31	34.80	1.36	0.73	1.05	0.78	14.78	1.19	0.55	0.64	0.57	43.94
340	Laurasiatheria	Chiroptera	Phyllostomidae	Mesophylla_macconnelli	6.86	16.62	2.80	1.17	3.25	1.22	27.64	2.27	1.11	2.37	1.01	27.64	1.17	0.59	0.84	0.60	11.63	0.82	0.45	0.55	0.48	33.06
341	Laurasiatheria	Chiroptera	Phyllostomidae	Platyrrhinus_helleri	13.44	22.58	3.89	1.70	4.43	1.70	35.97	3.06	1.40	3.33	1.44	37.72	1.83	0.83	1.19	0.76	12.60	1.30	0.71	0.82	0.54	47.37
342	Laurasiatheria	Chiroptera	Phyllostomidae	Vampyrodes_caraccioli	35.89	29.46	4.86	2.14	5.49	2.04	48.61	3.84	1.76	4.57	1.69	51.87	2.32	1.02	1.33	1.00	16.50	1.57	0.75	0.96	0.72	58.66
343	Laurasiatheria	Chiroptera	Phyllostomidae	Chiroderma_villosum	23.81	30.06	4.79	2.21	5.52	2.14	45.73	3.99	1.81	4.26	1.91	47.30	2.11	1.05	1.66	1.13	17.99	1.62	0.74	0.99	0.88	61.48
344	Laurasiatheria	Chiroptera	Phyllostomidae	Enchisthenes_hartii	16.99	26.70	3.86	1.58	4.18	1.60	38.79	2.89	1.42	3.11	1.46	40.84	1.65	0.78	1.15	0.83	15.13	1.12	0.63	0.68	0.65	48.31
345	Laurasiatheria	Chiroptera	Phyllostomidae	Ectophylla_alba	5.55	16.99	2.55	0.97	2.71	1.02	25.17	2.00	0.90	2.24	0.91	24.60	1.10	0.49	0.90	0.55	7.99	0.85	0.41	0.51	0.40	26.48
346	Laurasiatheria	Chiroptera	Phyllostomidae	Ardops_nichollsi	19.23	31.40	4.20	2.00	5.21	2.01	47.53	3.75	1.67	3.96	1.60	48.69	2.20	0.97	1.37	0.99	17.09	1.28	0.83	0.89	0.76	58.02
347	Laurasiatheria	Chiroptera	Phyllostomidae	Phyllops_falcatus	19.50	25.82	3.80	1.69	4.42	1.59	37.65	3.19	1.43	3.18	1.42	38.69	1.78	0.80	1.26	0.75	16.46	1.39	0.70	0.76	0.57	46.98
348	Laurasiatheria	Chiroptera	Phyllostomidae	Stenoderma_rufum	21.10	28.89	4.05	1.68	4.62	1.68	44.96	3.29	1.61	3.26	1.41	46.66	2.01	0.92	1.59	0.90	16.36	1.67	0.73	0.83	0.68	56.97
349	Laurasiatheria	Chiroptera	Phyllostomidae	Ametrida_centurio	10.61	23.76	3.32	1.50	3.87	1.38	29.48	2.66	1.07	2.51	1.22	29.65	1.21	0.51	1.20	0.78	10.60	0.98	0.46	0.64	0.55	35.15
350	Laurasiatheria	Chiroptera	Phyllostomidae	Pygoderma_bilabiatum	18.50	26.10	4.15	1.93	4.66	1.79	37.86	3.21	1.62	4.00	1.26	41.20	1.94	0.89	1.46	0.80	18.22	1.56	0.74	1.06	0.72	57.99
351	Laurasiatheria	Chiroptera	Phyllostomidae	Centurio_senex	23.09	26.57	4.16	1.80	4.60	1.73	39.88	3.21	1.44	3.42	1.44	38.16	1.81	0.70	1.38	0.96	16.81	1.27	0.56	0.78	0.63	50.53
352	Laurasiatheria	Chiroptera	Phyllostomidae	Artibeus_planirostris	54.50	34.57	6.29	2.21	6.49	2.38	57.14	4.83	2.15	4.91	2.07	55.29	2.34	1.07	1.68	1.20	18.26	1.84	0.97	1.17	0.91	64.16
353	Laurasiatheria	Chiroptera	Phyllostomidae	Sturnira_ludovici	21.00	24.67	4.07	1.61	4.48	1.54	41.39	3.27	1.57	3.38	1.46	43.49	1.97	0.93	1.38	0.92	15.96	1.17	0.69	0.82	0.73	48.40
354	Laurasiatheria	Chiroptera	Phyllostomidae	Lionycteris_spurrelli	8.85	21.00	3.27	1.23	3.47	1.35	33.22	2.42	1.19	2.20	1.02	34.96	1.38	0.67	0.83	0.59	10.42	0.91	0.46	0.64	0.48	34.46

						Humerus					Radius					Metacarpal					Phalanx					
	Superord. group	Order	Family	Species	Mass	L	PW	MW	DW	H	L	PW	MW	DW	H	L	PW	MW	DW	H	L	PW	MW	DW	H	DL
304	Laurasiatheria	Chiroptera	Vespertilionidae	Glischropus_tylopus	4.59	17.01	2.53	1.04	2.53	0.97	25.14	1.87	1.03	2.32	0.89	25.87	0.80	0.63	1.07	0.45	13.43	0.97	0.42	0.58	0.39	26.00
305	Laurasiatheria	Chiroptera	Vespertilionidae	Vespertilio_murinus	15.42	26.89	3.67	1.48	2.84	1.53	42.58	2.28	1.43	2.70	1.45	41.37	0.94	0.86	1.16	0.78	17.33	1.12	0.57	0.77	0.70	29.46
306	Laurasiatheria	Chiroptera	Vespertilionidae	Neoromicia_nana	3.88	18.52	2.48	1.06	2.28	0.98	29.78	1.69	0.99	2.13	0.95	29.53	0.59	0.61	0.82	0.55	10.93	0.70	0.35	0.59	0.41	20.31
307	Laurasiatheria	Chiroptera	Vespertilionidae	Nyctophilus_geoffroyi	8.90	18.12	2.49	0.94	2.17	0.94	30.00	1.71	0.94	2.01	0.79	28.98	0.60	0.46	0.79	0.58	11.20	0.77	0.36	0.48	0.39	22.38
308	Laurasiatheria	Chiroptera	Vespertilionidae	Vespadelus_sp	5.05	18.45	2.60	1.03	2.20	0.98	30.12	1.71	1.09	2.08	0.93	28.72	0.63	0.59	0.83	0.57	10.30	0.81	0.40	0.52	0.47	18.74
309	Laurasiatheria	Chiroptera	Vespertilionidae	Chalinolobus_gouldii	14.24	27.42	3.90	1.59	2.96	1.68	41.65	2.51	1.43	2.67	1.50	43.81	0.96	0.69	1.15	0.78	18.27	1.23	0.54	0.81	0.59	33.78
310	Laurasiatheria	Chiroptera	Vespertilionidae	Eptesicus_fuscus	17.49	26.98	3.59	1.47	3.18	1.46	40.34	2.52	1.48	2.93	1.40	39.87	0.90	0.68	1.12	0.78	14.97	1.08	0.54	0.67	0.54	27.86
311	Laurasiatheria	Chiroptera	Vespertilionidae	Histiotus_velatus	11.32	25.52	3.52	1.49	2.98	1.53	43.71	2.63	1.40	3.02	1.33	43.20	0.86	0.66	1.03	0.80	13.67	1.04	0.56	0.66	0.51	28.75
312	Laurasiatheria	Chiroptera	Vespertilionidae	Lasionycteris_noctivagans	11.02	25.24	3.42	1.22	2.84	1.38	37.91	2.19	1.37	2.60	1.30	38.01	0.73	0.73	0.93	0.76	14.86	0.94	0.48	0.64	0.54	27.28
313	Laurasiatheria	Chiroptera	Vespertilionidae	Euderma_maculatum	16.17	28.67	3.82	1.49	3.31	1.61	47.38	2.57	1.52	2.96	1.37	43.87	0.82	0.66	1.08	0.65	13.95	1.08	0.54	0.79	0.58	33.78
314	Laurasiatheria	Chiroptera	Vespertilionidae	Plecotus_auritus	8.19	23.62	3.22	1.31	2.99	1.27	39.65	2.23	1.14	2.67	0.93	36.68	0.86	0.55	0.91	0.56	13.71	0.93	0.36	0.58	0.47	27.70
315	Laurasiatheria	Chiroptera	Vespertilionidae	Barbastella_barbastellus	8.31	23.86	2.99	1.41	2.77	1.27	36.23	2.08	1.20	2.52	1.24	35.58	0.79	0.64	0.90	0.55	12.38	0.99	0.39	0.56	0.53	27.08
316	Laurasiatheria	Chiroptera	Vespertilionidae	Rhogeessa_tumida	4.58	17.82	2.75	1.10	2.55	1.09	28.60	2.08	1.05	2.37	0.94	28.68	0.67	0.57	0.84	0.54	10.51	0.78	0.42	0.48	0.43	20.79
317	Laurasiatheria	Chiroptera	Vespertilionidae	Antrozous_pallidus	22.24	31.16	4.63	1.75	4.37	1.77	50.82	3.17	1.72	3.73	1.54	46.71	1.13	0.87	1.31	0.63	14.60	1.15	0.60	0.65	0.55	28.45
318	Laurasiatheria	Chiroptera	Vespertilionidae	Lasiurus_borealis	12.33	24.77	3.27	1.39	2.56	1.31	35.88	2.55	1.21	2.50	1.16	41.06	1.04	0.65	0.91	0.56	16.61	1.01	0.42	0.53	0.51	32.99
319	Laurasiatheria	Chiroptera	Vespertilionidae	Scotophilus_kuhlii	20.31	31.71	4.63	1.58	3.42	1.66	48.03	2.82	1.61	3.37	1.50	49.93	1.00	0.78	1.32	0.74	16.07	1.40	0.52	0.73	0.62	28.52
320	Laurasiatheria	Chiroptera	Vespertilionidae	Nycticeius_humeralis	9.12	22.58	3.14	1.18	2.60	1.16	35.57	1.92	1.19	2.59	1.02	34.34	0.80	0.59	0.97	0.66	12.99	0.92	0.45	0.55	0.45	24.91
321	Laurasiatheria	Chiroptera	Vespertilionidae	Kerivoula_picta	4.50	19.31	2.79	1.20	2.69	1.08	32.83	2.21	1.06	2.70	0.96	36.70	0.91	0.85	1.29	0.45	15.68	1.24	0.51	0.60	0.40	35.85
322	Laurasiatheria	Chiroptera	Vespertilionidae	Myotis_lucifugus	7.80	21.69	2.92	1.17	2.63	1.13	34.96	2.10	1.23	2.55	0.99	34.70	0.76	0.57	0.88	0.63	11.14	0.84	0.35	0.52	0.46	21.70
323	Laurasiatheria	Chiroptera	Miniopteridae	Miniopterus_australis	7.40	19.78	3.00	0.90	2.17	1.08	34.06	2.10	1.02	2.01	0.92	31.83	0.81	0.49	0.97	0.62	8.39	1.06	0.40	0.67	0.44	32.18
324	Laurasiatheria	Chiroptera	Myzopodidae	Myzopoda_aurita	9.10	24.04	3.26	1.47	3.82	1.26	45.74	2.61	1.39	3.07	1.26	39.67	1.11	0.50	1.31	0.80	17.68	1.26	0.47	0.71	0.63	48.02
325	Laurasiatheria	Chiroptera	Thyropteridae	Thyroptera_tricolor	4.52	17.13	2.41	1.02	2.66	0.93	33.85	1.96	0.90	2.64	0.89	34.34	1.20	0.53	0.97	0.49	13.82	1.06	0.36	0.48	0.33	26.46
326	Laurasiatheria	Chiroptera	Noctilionidae	Noctilio_albiventris	31.46	33.06	5.20	2.19	5.57	2.06	59.16	3.81	2.08	4.06	1.82	57.71	2.48	1.31	1.81	1.19	13.82	2.06	0.97	1.22	0.71	54.83
327	Laurasiatheria	Chiroptera	Furipteridae	Furipterus_horrens	3.15	18.33	2.87	0.99	2.45	0.91	33.69	1.85	1.02	1.74	0.82	31.99	0.98	0.46	0.88	0.57	5.44	0.84	0.41	0.50	0.35	24.13
328	Laurasiatheria	Chiroptera	Furipteridae	Amorphochilus_schnablii	3.30	19.01	2.82	1.12	2.57	1.10	33.76	1.91	1.12	2.03	1.02	32.48	0.98	0.56	0.92	0.66	4.32	0.95	0.45	0.61	0.39	25.53
329	Laurasiatheria	Chiroptera	Phyllostomidae	Vampyrum_spectrum	171.61	64.71	9.04	3.95	12.03	3.78	103.32	8.15	3.43	8.37	3.31	76.21	4.14	1.77	3.08	1.88	43.66	2.94	1.57	1.85	1.45	124.37
330	Laurasiatheria	Chiroptera	Phyllostomidae	Chrotopterus_auritus	78.26	44.17	6.54	2.90	8.93	2.67	75.22	5.27	2.39	5.69	2.26	58.05	2.60	1.32	2.02	1.30	30.24	2.02	0.95	1.14	1.08	87.08
331	Laurasiatheria	Chiroptera	Phyllostomidae	Lophostoma_brasiliense	9.76	21.77	3.17	1.32	3.78	1.26	31.49	2.64	1.16	2.70	1.17	26.15	1.14	0.67	1.01	0.63	11.00	1.09	0.56	0.65	0.54	31.68
332	Laurasiatheria	Chiroptera	Phyllostomidae	Phyllostomus_discolor	36.70	33.46	5.49	2.13	5.80	2.31	56.07	3.99	2.03	4.23	1.65	56.63	1.91	1.01	1.50	1.00	12.80	1.75	0.92	1.08	0.80	51.79
333	Laurasiatheria	Chiroptera	Phyllostomidae	Macrophyllum_macrophyllum	8.02	21.10	3.12	1.38	3.60	1.34	33.36	2.50	1.30	3.04	1.04	34.44	1.22	0.72	1.35	0.61	14.08	1.30	0.56	0.65	0.44	38.10
334	Laurasiatheria	Chiroptera	Phyllostomidae	Mimon_cozumelae	23.00	29.86	4.75	2.03	5.32	2.04	52.73	3.48	1.71	3.82	1.73	48.31	2.06	0.95	1.35	0.97	19.81	1.58	0.82	0.83	0.75	59.35
335	Laurasiatheria	Chiroptera	Phyllostomidae	Trachops_cirrhosus	36.90	30.98	5.15	2.06	5.99	2.00	51.89	3.72	1.73	4.60	1.67	42.45	2.45	1.02	1.65	1.05	18.00	1.55	0.79	0.93	0.88	56.24
336	Laurasiatheria	Chiroptera	Phyllostomidae	Carollia_brevicauda	14.85	23.64	3.44	1.41	3.90	1.52	34.56	2.65	1.39	3.17	1.27	34.51	1.53	0.88	1.37	0.77	15.42	1.24	0.64	0.82	0.63	43.75
337	Laurasiatheria	Chiroptera	Phyllostomidae	Rhinophylla_pumilio	9.58	19.45	3.03	1.40	3.63	1.33	31.24	2.45	1.24	2.86	1.18	33.09	1.17	0.82	1.10	0.57	14.76	1.24	0.52	0.63	0.55	43.59
338	Laurasiatheria	Chiroptera	Phyllostomidae	Uroderma_bilobatum	16.28	24.83	4.30	1.89	4.95	1.74	41.68	3.36	1.59	3.79	1.50	43.17	1.72	0.86	1.18	0.89	15.64	1.42	0.69	0.83	0.61	50.33
339	Laurasiatheria	Chiroptera	Phyllostomidae	Vampyressa_pusilla	8.77	19.82	3.32	1.35	3.67	1.40	32.48	2.54	1.27	2.86	1.31	34.80	1.36	0.73	1.05	0.78	14.78	1.19	0.55	0.64	0.57	43.94
340	Laurasiatheria	Chiroptera	Phyllostomidae	Mesophylla_macconnelli	6.86	16.62	2.80	1.17	3.25	1.22	27.64	2.27	1.11	2.37	1.01	27.64	1.17	0.59	0.84	0.60	11.63	0.82	0.45	0.55	0.48	33.06
341	Laurasiatheria	Chiroptera	Phyllostomidae	Platyrrhinus_helleri	13.44	22.58	3.89	1.70	4.43	1.70	35.97	3.06	1.40	3.33	1.44	37.72	1.83	0.83	1.19	0.76	12.60	1.30	0.71	0.82	0.54	47.37
342	Laurasiatheria	Chiroptera	Phyllostomidae	Vampyrodes_caraccioli	35.89	29.46	4.86	2.14	5.49	2.04	48.61	3.84	1.76	4.57	1.69	51.87	2.32	1.02	1.33	1.00	16.50	1.57	0.75	0.96	0.72	58.66
343	Laurasiatheria	Chiroptera	Phyllostomidae	Chiroderma_villosum	23.81	30.06	4.79	2.21	5.52	2.14	45.73	3.99	1.81	4.26	1.91	47.30	2.11	1.05	1.66	1.13	17.99	1.62	0.74	0.99	0.88	61.48
344	Laurasiatheria	Chiroptera	Phyllostomidae	Enchisthenes_hartii	16.99	26.70	3.86	1.58	4.18	1.60	38.79	2.89	1.42	3.11	1.46	40.84	1.65	0.78	1.15	0.83	15.13	1.12	0.63	0.68	0.65	48.31
345	Laurasiatheria	Chiroptera	Phyllostomidae	Ectophylla_alba	5.55	16.99	2.55	0.97	2.71	1.02	25.17	2.00	0.90	2.24	0.91	24.60	1.10	0.49	0.90	0.55	7.99	0.85	0.41	0.51	0.40	26.48
346	Laurasiatheria	Chiroptera	Phyllostomidae	Ardops_nichollsi	19.23	31.40	4.20	2.00	5.21	2.01	47.53	3.75	1.67	3.96	1.60	48.69	2.20	0.97	1.37	0.99	17.09	1.28	0.83	0.89	0.76	58.02
347	Laurasiatheria	Chiroptera	Phyllostomidae	Phyllops_falcatus	19.50	25.82	3.80	1.69	4.42	1.59	37.65	3.19	1.43	3.18	1.42	38.69	1.78	0.80	1.26	0.75	16.46	1.39	0.70	0.76	0.57	46.98
348	Laurasiatheria	Chiroptera	Phyllostomidae	Stenoderma_rufum	21.10	28.89	4.05	1.68	4.62	1.68	44.96	3.29	1.61	3.26	1.41	46.66	2.01	0.92	1.59	0.90	16.36	1.67	0.73	0.83	0.68	56.97
349	Laurasiatheria	Chiroptera	Phyllostomidae	Ametrida_centurio	10.61	23.76	3.32	1.50	3.87	1.38	29.48	2.66	1.07	2.51	1.22	29.65	1.21	0.51	1.20	0.78	10.60	0.98	0.46	0.64	0.55	35.15
350	Laurasiatheria	Chiroptera	Phyllostomidae	Pygoderma_bilabiatum	18.50	26.10	4.15	1.93	4.66	1.79	37.86	3.21	1.62	4.00	1.26	41.20	1.94	0.89	1.46	0.80	18.22	1.56	0.74	1.06	0.72	57.99
351	Laurasiatheria	Chiroptera	Phyllostomidae	Centurio_senex	23.09	26.57	4.16	1.80	4.60	1.73	39.88	3.21	1.44	3.42	1.44	38.16	1.81	0.70	1.38	0.96	16.81	1.27	0.56	0.78	0.63	50.53
352	Laurasiatheria	Chiroptera	Phyllostomidae	Artibeus_planirostris	54.50	34.57	6.29	2.21	6.49	2.38	57.14	4.83	2.15	4.91	2.07	55.29	2.34	1.07	1.68	1.20	18.26	1.84	0.97	1.17	0.91	64.16
353	Laurasiatheria	Chiroptera	Phyllostomidae	Sturnira_ludovici	21.00	24.67	4.07	1.61	4.48	1.54	41.39	3.27	1.57	3.38	1.46	43.49	1.97	0.93	1.38	0.92	15.96	1.17	0.69	0.82	0.73	48.40
354	Laurasiatheria	Chiroptera	Phyllostomidae	Lionycteris_spurrelli	8.85	21.00	3.27	1.23	3.47	1.35	33.22	2.42	1.19	2.20	1.02	34.96	1.38	0.67	0.83	0.59	10.42	0.91	0.46	0.64	0.48	34.46

						Humerus					Radius					Metacarpal					Phalanx					
	Superord. group	Order	Family	Species	Mass	L	PW	MW	DW	H	L	PW	MW	DW	H	L	PW	MW	DW	H	L	PW	MW	DW	H	DL
406	Laurasiatheria	Chiroptera	Pteropodidae	Sphaerias_blanfordi	28.88	30.43	4.74	2.07	5.59	1.90	47.64	3.63	1.62	4.46	1.56	36.53	1.50	0.95	1.89	0.92	24.57	1.37	0.79	1.15	0.83	52.19
407	Euarchontoglires	Scandentia	Cynocephalidae	Galeopterus_variegatus	1112.20	106.19	12.64	6.08	13.74	5.78	145.45	9.10	4.14	8.95	3.42	27.97	1.64	1.55	3.44	1.50	16.09	2.74	2.06	2.25	2.24	46.40
408	Euarchontoglires	Scandentia	Cynocephalidae	Cynocephalus_volans	1250.00	94.87	11.21	5.47	13.83	4.93	117.10	10.12	4.31	8.71	4.03	26.36	3.33	1.67	2.05	1.67	15.13	3.01	1.86	1.83	2.29	51.50
409	Euarchontoglires	Scandentia	Ptilocercidae	Ptilocercus_lowii	42.50	22.07	3.87	2.04	5.12	2.14	23.51	1.93	1.50	2.53	1.16	6.07	0.96	0.63	1.11	0.72	4.69	1.25	0.62	0.90	0.66	9.99
410	Euarchontoglires	Scandentia	Tupaiidae	Tupaia_sp	156.27	28.32	4.33	2.32	5.53	2.15	25.18	2.50	1.50	2.74	1.43	8.46	1.08	0.83	1.30	0.85	4.49	1.52	0.81	0.99	0.80	10.65
411	Euarchontoglires	Scandentia	Tupaiidae	Tupaia_dorsalis	168.05	28.51	4.76	2.32	5.85	2.50	29.19	2.93	1.53	2.82	1.31	9.44	1.21	0.84	1.41	0.86	5.07	1.52	0.79	0.94	0.80	11.55
412	Euarchontoglires	Primates	Lorisidae	Nycticebus_pygmaeus	342.32	50.50	7.74	4.00	10.94	4.57	55.54	4.21	2.55	5.75	2.84	9.62	2.15	1.49	2.13	1.66	10.89	2.24	1.54	1.93	1.45	20.53
413	Euarchontoglires	Primates	Lorisidae	Nycticebus_coucang	924.55	71.97	11.71	6.60	16.65	6.68	74.47	6.14	3.85	8.25	4.60	13.43	3.01	2.17	2.89	2.27	15.06	3.30	2.50	2.38	2.22	27.61
414	Euarchontoglires	Primates	Lorisidae	Loris_tardigradus	249.22	53.22	6.79	2.92	7.45	2.73	61.45	2.55	1.84	4.03	1.90	8.17	1.76	1.02	1.62	1.08	8.40	2.14	1.12	1.51	1.10	15.15
415	Euarchontoglires	Primates	Galagidae	Galagoides_demidovii	66.04	27.57	4.56	2.11	6.26	2.26	30.71	2.36	1.56	3.21	1.55	6.31	1.24	0.77	1.18	0.93	6.68	1.42	0.79	0.94	0.86	12.88
416	Euarchontoglires	Primates	Galagidae	Galago_senegalensis	215.20	30.79	5.36	2.63	7.99	2.96	32.85	2.73	2.18	3.92	1.70	8.27	1.61	1.00	1.46	1.10	7.91	1.67	1.07	1.31	1.00	15.58
417	Euarchontoglires	Primates	Galagidae	Sciurocheirus_alleni	266.03	21.73	3.11	1.75	5.29	1.93	25.91	1.76	1.36	2.33	1.30	5.19	1.06	0.68	1.08	0.77	5.94	1.12	0.68	0.89	0.71	11.46
418	Euarchontoglires	Primates	Galagidae	Otolemur_garnettii	811.17	56.15	8.95	4.89	15.52	4.51	62.02	4.66	3.83	6.74	3.05	14.19	2.94	1.64	2.78	2.04	13.38	3.24	1.94	2.46	1.91	25.28
419	Euarchontoglires	Primates	Galagidae	Euoticus_elegantulus	295.48	40.61	6.55	2.95	10.48	3.60	43.46	3.60	2.10	5.66	2.47	11.07	2.13	1.37	2.08	1.60	11.85	2.68	1.13	1.87	1.46	22.08
420	Euarchontoglires	Primates	Lorisidae	Perodicticus_potto	1081.81	60.50	10.17	5.48	18.03	6.94	60.26	6.40	3.95	9.21	3.55	12.37	3.46	1.81	3.06	2.75	13.88	3.52	2.48	2.78	2.09	26.04
421	Euarchontoglires	Primates	Lorisidae	Arctocebus_calabarensis	258.01	52.81	6.60	3.04	9.22	3.51	52.80	3.86	2.16	5.44	2.48	7.90	1.55	0.99	1.63	1.47	9.56	2.03	1.17	1.58	1.28	18.26
422	Euarchontoglires	Primates	Lorisidae	Arctocebus_aureus	234.16	51.78	6.66	3.49	9.60	3.75	53.56	3.83	2.24	5.63	2.35	8.03	1.91	1.09	1.32	1.33	6.73	1.70	1.09	1.07	1.12	13.12
423	Euarchontoglires	Primates	Daubentoniidae	Daubentonia_madagascariensis	2731.37	90.74	15.88	8.28	25.46	7.13	90.91	7.78	5.47	11.64	5.17	36.65	4.19	2.22	2.46	2.50	44.26	2.81	1.84	1.68	2.06	69.14
424	Euarchontoglires	Primates	Indriidae	Indri_indri	8565.48	116.81	18.85	8.82	28.18	7.83	147.82	12.27	5.28	14.18	5.76	48.04	4.28	3.43	5.42	2.99	41.63	4.69	3.40	5.39	3.39	76.87
425	Euarchontoglires	Primates	Indriidae	Propithecus_verreauxi	3588.26	92.19	12.36	6.69	20.07	6.44	97.08	8.25	5.01	10.98	3.95	27.73	3.20	3.27	4.93	2.95	27.90	5.24	3.31	4.76	2.56	53.22
426	Euarchontoglires	Primates	Indriidae	Avahi_laniger	1092.28	60.68	10.48	5.58	14.90	5.22	72.89	6.72	3.88	7.54	3.32	21.03	2.52	1.71	2.78	2.03	16.40	3.11	2.23	2.69	1.93	31.90
427	Euarchontoglires	Primates	Lemuridae	Varecia_variegata	3849.99	101.80	17.42	8.47	24.05	9.58	101.04	8.74	5.42	13.48	7.22	27.28	4.93	3.50	4.86	3.60	24.50	5.64	4.37	4.61	3.27	47.80
428	Euarchontoglires	Primates	Lemuridae	Lemur_catta	2626.48	79.77	10.00	6.04	16.16	6.81	84.90	5.86	3.79	7.14	3.60	20.29	3.13	2.04	2.91	2.56	15.71	3.60	2.55	2.92	2.07	30.32
429	Euarchontoglires	Primates	Lemuridae	Hapalemur_griseus	916.00	54.85	9.79	4.96	12.35	4.84	62.33	4.28	3.14	7.13	2.64	15.62	2.15	1.52	2.54	1.80	13.71	2.92	1.69	2.16	1.65	25.97
430	Euarchontoglires	Primates	Lemuridae	Eulemur_coronatus	1699.85	77.82	11.56	6.39	16.35	6.34	81.36	6.39	4.72	8.40	4.40	20.16	2.96	2.27	3.30	2.31	16.27	3.27	2.68	3.04	2.38	31.33
431	Euarchontoglires	Primates	Lepilemuridae	Lepilemur_mustelinus	669.03	46.49	7.57	4.04	11.90	4.69	49.88	4.33	3.14	5.79	2.74	13.14	2.23	1.69	2.16	1.75	12.74	2.52	1.86	1.95	1.33	25.19
432	Euarchontoglires	Primates	Cheirogaleidae	Cheirogaleus_medius	196.76	25.95	5.54	2.63	8.41	2.83	25.80	3.08	1.88	3.92	2.02	7.38	1.46	0.95	1.61	1.22	6.64	1.77	1.25	1.54	0.87	13.17
433	Euarchontoglires	Primates	Cheirogaleidae	Mirza_zaza	280.90	37.76	6.65	3.39	10.10	3.19	40.30	3.46	2.09	4.93	2.42	9.54	1.71	1.18	1.94	1.32	9.16	2.29	1.52	1.78	1.07	17.81
434	Euarchontoglires	Primates	Cheirogaleidae	Microcebus_murinus	69.00	23.74	4.29	1.98	5.70	1.88	26.54	1.93	1.25	2.90	1.38	5.48	0.89	0.68	0.96	0.84	5.13	1.10	0.70	0.76	0.70	10.07
435	Euarchontoglires	Primates	Tarsiidae	Tarsius_sp	139.79	29.94	5.48	2.50	8.23	2.58	38.21	2.67	1.88	3.80	1.76	11.83	1.61	1.21	1.78	1.40	14.73	2.19	1.08	1.42	1.25	28.09
436	Euarchontoglires	Primates	Tarsiidae	Carlito_syrichta	115.91	30.96	5.54	2.30	8.69	2.33	36.89	3.09	1.65	3.53	1.70	10.65	1.70	1.15	1.76	1.39	12.38	2.31	1.08	1.44	1.19	24.53
437	Euarchontoglires	Primates	Pitheciidae	Cheracebus_torquatus	1209.57	168.52	25.78	12.48	30.74	12.35	168.48	14.71	11.15	19.79	8.85	39.56	6.66	4.76	7.65	4.02	29.49	8.60	4.65	5.93	3.23	NA
438	Euarchontoglires	Primates	Pitheciidae	Pithecia_pithecia	1667.19	99.38	10.32	7.55	16.73	7.15	91.60	6.74	4.76	8.29	4.09	20.04	3.93	2.58	4.75	2.48	19.10	4.53	3.05	3.45	2.35	40.55
439	Euarchontoglires	Primates	Pitheciidae	Chiropotes_sp	2967.27	111.81	14.39	7.80	21.27	7.44	96.45	9.18	5.34	11.78	5.64	22.58	4.33	3.21	4.16	3.74	20.14	4.72	3.46	3.43	2.63	40.15
440	Euarchontoglires	Primates	Pitheciidae	Cacajao_calvus	3421.04	100.54	12.75	6.17	18.05	6.64	85.42	7.93	4.81	10.40	3.64	21.33	4.69	3.13	4.61	2.53	20.06	4.82	3.29	3.63	3.53	41.25
441	Euarchontoglires	Primates	Cebidae	Saguinus_sp	493.42	53.34	7.59	4.04	11.22	4.03	46.43	4.23	2.37	5.12	2.63	14.12	2.01	1.43	2.11	1.43	10.68	2.40	1.41	1.78	1.32	23.48
442	Euarchontoglires	Primates	Cebidae	Callithrix_sp	345.22	31.77	5.37	2.49	7.00	2.67	29.50	2.57	2.24	3.47	1.39	8.24	1.24	0.86	1.46	0.89	6.43	1.73	0.96	1.12	0.94	15.69
443	Euarchontoglires	Primates	Cebidae	Callithrix_jacchus	290.21	42.83	6.32	2.89	9.00	3.04	37.98	4.33	2.12	4.47	1.79	11.68	1.43	1.29	2.35	1.19	10.14	2.34	1.41	2.00	1.70	19.64
444	Euarchontoglires	Primates	Cebidae	Callimico_goeldii	558.00	54.01	7.84	3.91	10.69	4.24	48.71	4.30	2.50	5.07	2.48	14.70	2.21	1.41	2.21	1.51	11.61	2.53	1.54	1.82	1.51	25.89
445	Euarchontoglires	Primates	Cebidae	Leontopithecus_rosalia	592.52	61.75	8.44	4.36	9.61	4.50	63.10	4.48	2.96	5.34	2.55	22.36	2.09	1.54	2.47	1.70	14.97	2.47	1.54	1.67	1.87	32.35
446	Euarchontoglires	Primates	Cebidae	Saimiri_sciureus	749.47	75.60	9.34	4.63	13.40	4.86	67.21	5.86	3.04	7.43	3.25	15.03	3.03	2.33	4.00	2.32	12.71	3.81	2.25	2.65	1.78	27.17
447	Euarchontoglires	Primates	Cebidae	Sapajus_apella	2758.38	106.87	14.62	6.41	19.61	6.68	97.82	8.78	4.99	11.40	3.89	22.80	3.72	2.58	4.20	2.32	19.83	4.63	2.83	3.33	2.21	42.64
448	Euarchontoglires	Primates	Cebidae	Cebus_albifrons	2509.68	109.13	16.10	8.40	22.04	8.74	98.84	8.64	6.36	11.49	4.40	23.03	3.35	2.78	4.81	2.68	20.29	5.11	3.39	3.52	2.39	44.12
449	Euarchontoglires	Primates	Cebidae	Aotus_trivirgatus	912.40	75.10	10.23	5.45	14.12	4.56	66.17	6.04	3.85	7.88	2.98	17.83	2.75	2.00	3.74	1.85	17.65	3.95	1.87	3.10	1.67	33.52
450	Euarchontoglires	Primates	Atelidae	Ateles_fusciceps	9067.94	206.27	19.06	11.40	26.70	11.84	214.49	11.79	8.13	16.86	8.90	57.63	6.24	3.97	6.88	5.12	43.10	7.74	5.70	6.54	4.87	91.54
451	Euarchontoglires	Primates	Atelidae	Ateles_belzebuth	6692.42	197.40	16.27	11.10	30.67	10.48	185.44	11.09	6.76	12.92	7.48	46.72	7.01	4.50	6.24	4.55	35.44	7.60	5.91	6.39	4.63	73.30
452	Euarchontoglires	Primates	Atelidae	Lagothrix_sp	6263.69	162.05	17.05	9.01	24.66	9.73	132.19	10.52	6.50	13.81	6.98	31.99	5.36	3.87	5.25	4.41	29.29	5.74	5.62	5.07	3.47	60.61
453	Euarchontoglires	Primates	Atelidae	Alouatta_seniculus	6398.31	160.47	15.63	9.01	24.05	9.84	130.57	8.03	6.66	12.54	6.03	29.53	6.15	4.02	5.14	4.52	33.12	5.75	4.18	4.75	3.73	71.46
454	Euarchontoglires	Primates	Hylobatidae	Symphalangus_syndactylus	10839.00	229.33	14.88	9.44	26.35	11.28	254.16	11.73	6.21	15.11	7.41	58.91	5.22	4.02	6.15	4.60	43.29	6.62	6.67	5.88	4.18	85.74
455	Euarchontoglires	Primates	Hylobatidae	Hylobates_sp	5757.16	187.86	14.39	8.09	24.10	7.52	203.41	9.08	4.97	13.53	5.25	42.83	3.95	2.98	5.28	3.46	35.05	6.04	5.05	5.88	3.36	72.72
456	Euarchontoglires	Primates	Hylobatidae	Nomascus_concolor	6410.47	227.24	20.57	9.36	32.49	10.95	255.91	14.46	6.67	18.96	5.90	54.14	5.42	4.46	8.22	4.37	43.92	7.95	6.39	6.82	4.60	88.49

						Humerus					Radius					Metacarpal					Phalanx					
	Superord. group	Order	Family	Species	Mass	L	PW	MW	DW	H	L	PW	MW	DW	H	L	PW	MW	DW	H	L	PW	MW	DW	H	DL
457	Euarchontoglires	Primates	Hylobatidae	Hoolock_leuconedys	6699.00	229.89	19.85	9.97	26.51	10.37	259.83	13.01	6.56	15.66	7.01	53.34	4.96	3.92	6.04	4.22	41.82	6.36	6.42	8.03	4.43	87.86
458	Euarchontoglires	Primates	Hominidae	Pongo_pygmaeus	53408.29	466.27	51.72	28.90	81.27	33.79	381.51	28.18	23.83	51.00	18.55	106.31	13.32	8.74	19.33	15.16	86.88	19.49	16.63	17.84	11.87	157.75
459	Euarchontoglires	Primates	Hominidae	Pan_paniscus	35119.95	267.99	35.39	20.25	61.06	23.42	248.49	19.62	14.54	33.40	12.99	86.31	11.46	9.22	14.17	11.44	59.73	15.50	12.74	12.24	8.75	127.17
460	Euarchontoglires	Primates	Hominidae	Homo_sapiens	58540.63	342.56	45.43	20.48	58.94	23.90	248.22	20.50	15.16	33.96	11.25	62.87	12.55	7.04	15.27	9.34	42.52	14.99	9.54	11.18	7.26	90.70
461	Euarchontoglires	Primates	Hominidae	Gorilla_gorilla	112588.99	368.43	58.71	36.61	86.98	39.04	300.45	29.67	20.97	45.02	22.87	86.54	14.57	12.35	21.40	16.39	56.82	21.10	19.57	15.73	10.82	121.39
462	Euarchontoglires	Primates	Cercopithecidae	Trachypithecus_phayrei	7681.72	150.44	18.90	9.92	27.67	10.18	143.95	13.45	7.00	15.87	6.54	36.39	5.14	4.05	5.44	3.68	31.25	6.30	4.45	5.49	3.68	61.24
463	Euarchontoglires	Primates	Cercopithecidae	Semnopithecus_entellus	12679.29	123.86	17.21	8.03	23.16	9.72	136.02	12.24	6.59	13.10	5.43	38.45	5.79	4.08	6.07	3.80	26.05	6.67	4.47	5.55	3.81	49.92
464	Euarchontoglires	Primates	Cercopithecidae	Presbytis_sp	6419.29	106.45	12.04	6.94	19.13	7.00	114.01	8.75	5.17	11.99	5.02	33.61	4.30	3.35	4.39	3.38	25.91	5.52	3.92	4.40	2.80	52.90
465	Euarchontoglires	Primates	Cercopithecidae	Nasalis_larvatus	12265.65	185.24	23.80	11.96	29.65	11.05	183.49	16.77	7.91	17.31	7.13	44.05	5.53	4.48	6.98	4.18	38.52	8.62	5.09	6.74	3.74	77.93
466	Euarchontoglires	Primates	Cercopithecidae	Piliocolobus_badius	8430.40	140.87	17.57	10.14	25.17	9.81	139.61	11.62	6.69	13.37	5.86	36.72	5.00	3.83	5.84	3.67	27.14	6.41	4.83	5.52	3.34	56.93
467	Euarchontoglires	Primates	Cercopithecidae	Procolobus_verus	3977.86	156.85	19.50	10.67	26.85	10.54	151.64	13.01	6.54	14.37	6.01	40.75	5.17	3.95	5.52	3.73	32.15	6.98	5.34	5.45	3.50	65.77
468	Euarchontoglires	Primates	Cercopithecidae	Colobus_polykomos	8797.29	156.53	19.04	10.70	28.67	11.13	147.93	13.37	7.27	15.50	6.69	40.79	6.54	4.31	6.67	4.44	32.94	7.77	4.59	6.29	3.84	69.02
469	Euarchontoglires	Primates	Cercopithecidae	Macaca_mulatta	6455.19	138.14	21.11	10.55	25.80	10.66	136.16	12.03	7.83	16.16	8.14	34.90	6.09	4.45	6.23	4.59	25.52	7.31	5.45	5.43	3.83	52.80
470	Euarchontoglires	Primates	Cercopithecidae	Cercocebus_atys	6941.24	130.12	17.10	8.29	25.10	8.42	126.43	10.72	7.07	13.70	5.47	32.41	5.46	3.91	5.71	3.55	26.11	6.62	4.59	5.21	3.79	51.50
471	Euarchontoglires	Primates	Cercopithecidae	Mandrillus_leucophaeus	14253.30	165.26	22.08	10.86	29.11	11.26	173.56	14.42	8.38	16.75	7.25	33.62	4.71	4.08	6.94	3.95	19.89	6.74	4.66	5.35	3.89	40.67
472	Euarchontoglires	Primates	Cercopithecidae	Lophocebus_aterrimus	6510.37	143.93	18.89	8.79	26.96	9.14	145.19	9.46	7.31	21.75	5.42	34.21	5.21	4.13	6.68	3.48	27.31	7.48	5.16	5.74	3.97	52.49
473	Euarchontoglires	Primates	Cercopithecidae	Papio_sp	16662.66	197.60	28.06	14.16	36.22	14.90	196.85	14.39	12.15	22.00	8.93	40.22	8.99	5.95	8.83	5.86	21.44	9.49	6.53	5.81	4.52	46.40
474	Euarchontoglires	Primates	Cercopithecidae	Erythrocebus_patas	7966.30	122.85	20.10	10.29	21.21	8.31	135.89	10.58	8.18	14.95	5.84	29.15	5.36	3.41	5.95	3.09	16.98	5.50	3.49	4.15	2.77	32.90
475	Euarchontoglires	Primates	Cercopithecidae	Chlorocebus_pygerythrus	3695.99	87.92	14.97	8.71	19.17	7.14	101.45	8.42	6.50	11.36	5.50	22.45	3.64	3.23	4.50	2.85	16.97	5.06	3.44	4.07	3.03	34.87
476	Euarchontoglires	Primates	Cercopithecidae	Cercopithecus_albogularis	5033.33	107.90	14.68	7.96	16.80	7.19	102.74	8.04	6.71	11.28	4.07	21.28	3.29	2.73	4.67	2.46	18.69	5.09	3.23	5.67	3.09	38.60
477	Euarchontoglires	Primates	Cercopithecidae	Miopithecus_talapoin	1248.86	84.64	12.00	6.02	14.38	5.39	87.36	7.32	4.82	8.50	3.84	19.85	2.87	2.50	3.67	2.03	16.33	4.49	2.57	3.44	1.77	35.24
478	Euarchontoglires	Rodentia	Gliridae	Glis_glis	128.09	25.26	4.62	2.53	7.09	3.48	24.06	2.90	2.05	2.56	1.55	6.27	1.02	0.83	1.28	1.00	4.95	1.59	0.83	0.89	0.75	10.50
479	Euarchontoglires	Rodentia	Gliridae	Muscardinus_avellanarius	29.19	12.06	2.79	1.18	3.89	1.37	14.28	1.53	0.97	1.38	0.73	3.48	0.47	0.48	0.55	0.53	3.00	0.74	0.42	0.42	0.42	6.03
480	Euarchontoglires	Rodentia	Gliridae	Dryomys_nitedula	29.50	14.51	3.07	1.47	4.09	1.72	15.58	1.75	1.00	1.61	0.83	3.93	0.55	0.49	0.85	0.47	2.94	0.88	0.43	0.56	0.46	6.36
481	Euarchontoglires	Rodentia	Gliridae	Eliomys_sp	107.49	19.38	3.76	1.84	5.28	2.35	18.95	1.94	1.46	1.85	1.12	4.85	0.82	0.62	0.95	0.56	3.21	1.03	0.50	0.68	0.54	7.09
482	Euarchontoglires	Rodentia	Gliridae	Graphiurus_murinus	20.07	12.55	2.66	1.38	3.82	1.70	13.35	1.44	0.96	1.34	0.86	3.65	0.51	0.52	0.66	0.48	2.67	0.76	0.42	0.48	0.46	5.68
483	Euarchontoglires	Rodentia	Aplodontiidae	Aplodontia_rufa	806.21	NA	10.45	4.97	15.31	8.54	39.08	6.03	3.35	6.05	3.51	11.68	3.02	1.97	3.04	2.00	6.56	3.63	1.94	2.07	1.96	21.82
484	Euarchontoglires	Rodentia	Sciuridae	Ratufa_indica	1060.00	64.53	11.29	5.06	16.42	6.52	52.71	6.49	3.56	7.29	2.61	14.97	2.41	1.85	3.64	1.55	13.41	3.30	1.72	3.05	1.70	33.00
485	Euarchontoglires	Rodentia	Sciuridae	Funambulus_pennantii	102.49	23.64	3.88	1.85	5.70	2.31	21.67	2.31	1.30	2.51	1.24	6.70	0.88	0.68	1.15	0.67	5.11	1.26	0.65	0.67	0.63	11.37
486	Euarchontoglires	Rodentia	Sciuridae	Lariscus_insignis	174.41	33.26	5.81	2.84	8.04	3.54	29.49	3.63	2.18	3.42	1.50	9.84	1.27	1.04	1.64	0.94	7.12	1.91	0.97	1.08	0.94	16.01
487	Euarchontoglires	Rodentia	Sciuridae	Tamiops_maritimus	66.77	21.53	3.82	1.94	5.33	2.42	21.93	2.18	1.49	2.29	1.12	6.08	0.84	0.66	1.02	0.72	5.30	1.20	0.63	0.76	0.76	12.57
488	Euarchontoglires	Rodentia	Sciuridae	Dremomys_pernyi	198.63	35.20	6.75	3.03	8.89	3.68	31.79	3.91	2.25	3.75	1.70	9.97	1.48	1.12	1.60	1.23	7.49	1.84	0.97	1.25	1.15	17.13
489	Euarchontoglires	Rodentia	Sciuridae	Prosciurillus_leucomus	158.27	27.82	4.29	2.51	7.25	2.79	26.56	3.33	2.07	2.93	1.33	8.71	1.25	0.95	1.53	0.94	6.95	1.86	0.99	1.04	1.06	16.13
490	Euarchontoglires	Rodentia	Sciuridae	Rubrisciurus_rubriventer	688.10	49.57	9.05	4.01	13.23	4.55	45.13	5.57	3.07	5.75	2.21	14.80	2.05	1.63	2.49	1.54	10.80	2.89	1.50	1.64	1.51	24.15
491	Euarchontoglires	Rodentia	Sciuridae	Hyosciurus_heinrichi	296.00	33.26	6.50	3.12	9.50	3.52	32.82	4.13	2.21	4.15	1.91	11.02	1.61	1.30	2.01	1.20	6.53	2.38	1.19	1.41	1.14	16.56
492	Euarchontoglires	Rodentia	Sciuridae	Callosciurus_notatus	209.49	34.90	5.55	3.34	8.71	3.62	32.05	4.03	2.53	3.80	1.64	9.32	1.27	1.06	1.66	1.06	8.27	1.94	1.05	1.11	1.24	18.69
493	Euarchontoglires	Rodentia	Sciuridae	Spermophilopsis_leptodactylus	600.00	37.41	7.61	3.75	11.45	4.74	34.82	5.10	2.29	4.97	2.57	12.48	2.19	1.80	2.23	1.75	8.06	2.61	1.59	1.82	1.75	23.19
494	Euarchontoglires	Rodentia	Sciuridae	Xerus_erythropus	602.23	39.94	8.40	3.38	10.04	4.88	36.72	4.84	2.61	5.22	2.40	12.18	2.57	1.69	2.51	1.45	6.79	2.72	1.98	2.04	1.41	20.14
495	Euarchontoglires	Rodentia	Sciuridae	Paraxerus_cepapi	222.85	22.51	5.36	2.35	6.60	2.80	19.33	2.94	1.86	3.18	1.84	8.53	1.18	1.05	1.52	1.26	6.74	1.66	1.11	1.07	1.14	14.95
496	Euarchontoglires	Rodentia	Sciuridae	Heliosciurus_rufobrachium	332.88	28.47	5.29	2.64	7.81	3.08	24.99	3.14	1.83	3.37	1.72	9.73	1.50	1.08	1.67	1.12	7.85	1.96	1.04	1.12	1.11	17.29
497	Euarchontoglires	Rodentia	Sciuridae	Funisciurus_anerythrus	223.54	30.88	5.33	2.56	7.07	3.08	29.51	3.06	1.88	3.24	1.53	7.78	1.24	1.09	1.51	0.94	6.28	1.68	0.99	1.07	0.97	13.96
498	Euarchontoglires	Rodentia	Sciuridae	Tamias_striatus	154.00	22.33	4.14	2.29	5.63	2.37	19.66	2.33	1.34	2.61	1.29	6.69	0.98	0.84	1.37	0.87	4.70	1.53	1.07	1.15	0.86	11.03
499	Euarchontoglires	Rodentia	Sciuridae	Spermophilus_sp	353.19	28.22	5.85	2.63	8.26	3.14	24.89	3.33	1.88	3.81	1.83	9.65	1.77	1.30	2.07	1.22	5.14	2.38	1.33	1.40	1.18	14.52
500	Euarchontoglires	Rodentia	Sciuridae	Cynomys_ludovicianus	797.05	40.39	9.96	4.77	12.46	7.37	36.49	5.40	4.17	6.79	2.70	11.61	3.01	1.93	3.33	1.82	6.31	2.84	2.02	2.93	1.33	17.88
501	Euarchontoglires	Rodentia	Sciuridae	Marmota_marmota	4059.15	67.93	16.02	7.27	22.15	8.79	57.49	8.19	5.64	10.10	4.04	18.60	4.43	2.91	4.67	2.38	11.76	4.60	3.00	3.76	2.72	32.41
502	Euarchontoglires	Rodentia	Sciuridae	Sciurus_vulgaris	333.00	38.41	6.02	2.80	9.07	3.28	36.63	4.10	2.23	4.01	1.88	11.39	1.30	1.23	1.84	1.15	8.87	2.24	1.20	1.39	1.27	21.88
503	Euarchontoglires	Rodentia	Sciuridae	Tamiasciurus_hudsonicus	200.24	34.14	6.17	3.06	9.01	3.43	31.22	3.73	2.40	4.13	1.75	9.50	1.36	1.13	1.56	1.09	7.29	2.01	1.07	1.07	1.04	17.12
504	Euarchontoglires	Rodentia	Sciuridae	Glaucomys_volans	71.90	24.72	3.40	1.67	4.47	1.84	28.53	2.71	1.31	2.35	1.47	5.32	0.73	0.61	0.95	0.59	4.85	1.09	0.50	0.63	0.66	10.45
505	Euarchontoglires	Rodentia	Sciuridae	Belomys_pearsonii	217.00	43.03	5.54	2.61	6.89	3.03	44.64	3.82	2.52	4.25	1.96	6.76	1.06	1.13	1.49	1.00	6.66	1.72	1.01	1.18	1.11	15.09
506	Euarchontoglires	Rodentia	Sciuridae	Petaurista_petaurista	1533.84	80.90	9.95	3.84	12.42	4.70	81.02	6.66	3.45	7.34	2.67	15.74	2.62	2.08	2.62	1.75	12.65	2.71	1.63	2.24	1.65	30.83
507	Euarchontoglires	Rodentia	Diatomyidae	Laonastes_aenigmamus	374.00	36.09	6.25	2.69	7.56	3.78	31.09	3.39	1.93	3.70	1.71	9.31	1.66	1.24	1.94	1.13	5.52	2.18	1.30	1.36	1.07	11.58

						Humerus					Radius					Metacarpal					Phalanx					
	Superord. group	Order	Family	Species	Mass	L	PW	MW	DW	H	L	PW	MW	DW	H	L	PW	MW	DW	H	L	PW	MW	DW	H	DL
508	Euarchontoglires	Rodentia	Ctenodactylidae	Ctenodactylus_sp	231.01	29.05	5.95	2.54	6.99	3.69	24.91	3.20	1.73	3.14	1.24	8.44	1.63	1.24	1.80	1.02	4.74	2.09	1.01	1.14	0.94	10.04
509	Euarchontoglires	Rodentia	Ctenodactylidae	Massoutiera_mzabi	194.00	27.57	6.03	2.12	5.61	3.79	25.02	2.96	1.66	3.38	1.17	6.33	1.27	1.02	1.68	0.85	4.20	1.73	1.01	1.30	0.91	8.61
510	Euarchontoglires	Rodentia	Ctenodactylidae	Felovia_vae	205.00	26.60	4.51	2.19	6.24	3.39	21.74	2.83	1.56	2.79	1.35	7.40	1.37	1.14	1.54	0.97	4.66	1.73	0.97	1.12	0.91	9.80
511	Euarchontoglires	Rodentia	Ctenodactylidae	Pectinator_spekei	169.70	26.85	5.69	2.09	5.34	3.45	21.40	3.26	1.57	2.44	1.15	6.46	0.91	0.78	1.35	0.79	3.99	1.43	0.78	0.82	0.72	8.50
512	Euarchontoglires	Rodentia	Hystricidae	Trichys_fasciculata	1750.00	68.42	12.28	5.12	15.41	5.39	64.63	7.03	2.97	8.31	3.26	24.30	2.93	1.96	3.13	2.03	9.11	3.75	2.00	2.13	1.86	24.58
513	Euarchontoglires	Rodentia	Hystricidae	Atherurus_macrourus	2000.00	48.44	11.20	4.63	14.35	8.18	34.28	6.17	3.73	6.79	2.56	15.29	3.80	2.45	3.93	2.15	7.84	4.05	3.09	2.78	2.02	17.49
514	Euarchontoglires	Rodentia	Hystricidae	Hystrix_cristata	13406.27	101.91	26.65	12.05	30.42	21.14	74.89	13.97	5.54	15.48	7.60	26.58	7.79	4.85	8.11	4.10	12.20	6.44	5.67	6.86	4.23	36.23
515	Euarchontoglires	Rodentia	Heterocephalidae	Heterocephalus_glaber	39.36	15.89	3.90	1.80	4.38	2.29	10.81	1.65	1.04	1.74	1.00	4.88	1.02	0.66	1.22	0.72	3.21	1.33	0.67	0.78	0.63	6.81
516	Euarchontoglires	Rodentia	Bathyergidae	Heliophobius_argenteocinereus	159.46	21.18	5.36	2.76	6.08	4.31	17.15	2.49	1.60	3.19	1.20	8.11	1.45	0.89	1.65	0.98	4.25	1.73	0.95	1.18	0.85	9.68
517	Euarchontoglires	Rodentia	Bathyergidae	Fukomys_mechowi	271.54	25.52	7.24	2.32	7.90	5.64	21.66	3.11	1.62	3.69	1.56	8.42	1.65	1.19	2.11	1.25	4.29	2.11	1.09	1.31	0.97	9.97
518	Euarchontoglires	Rodentia	Bathyergidae	Cryptomys_hottentotus	75.13	17.66	5.11	1.96	5.79	4.92	16.42	2.22	1.17	2.73	1.10	6.30	1.26	0.92	1.44	0.72	3.29	1.31	0.78	0.93	0.64	7.28
519	Euarchontoglires	Rodentia	Bathyergidae	Georychus_capensis	188.36	21.80	5.43	1.88	6.24	4.69	19.19	2.51	1.38	2.84	0.92	6.86	1.32	0.67	1.31	0.78	3.62	1.39	0.78	0.93	0.69	8.04
520	Euarchontoglires	Rodentia	Bathyergidae	Bathyergus_suillus	777.38	38.87	11.91	4.85	14.38	9.50	35.33	5.00	3.17	6.52	2.18	12.27	2.04	1.93	2.60	2.05	6.07	1.94	1.54	2.38	2.74	25.66
521	Euarchontoglires	Rodentia	Cuniculidae	Cuniculus_taczanowskii	8999.95	75.29	12.97	6.47	17.80	10.10	58.54	9.25	4.40	8.39	5.47	23.46	4.66	3.60	5.46	2.86	9.49	5.66	3.99	4.56	2.58	NA
522	Euarchontoglires	Rodentia	Cuniculidae	Cuniculus_paca	1590.57	89.83	18.76	6.84	20.71	12.21	68.68	10.57	5.83	11.06	4.73	24.32	4.43	4.29	6.45	3.61	9.32	5.83	4.57	5.04	4.51	26.08
523	Euarchontoglires	Rodentia	Dasyproctidae	Myoprocta_acouchy	954.87	56.53	8.86	3.71	9.78	5.13	54.65	5.72	3.29	5.48	2.44	18.67	2.52	2.36	3.65	1.66	6.48	3.19	2.27	2.70	2.42	17.63
524	Euarchontoglires	Rodentia	Dasyproctidae	Dasyprocta_prymnolopha	2900.00	70.59	11.54	4.23	12.25	6.12	63.41	7.94	4.16	7.42	3.14	23.00	3.71	3.00	4.28	2.41	7.41	3.97	2.85	3.19	3.02	19.65
525	Euarchontoglires	Rodentia	Dasyproctidae	Dasyprocta_punctata	2309.12	80.48	13.99	5.90	14.33	7.49	69.45	7.96	4.38	8.54	4.10	27.17	4.28	3.20	4.76	2.55	8.72	4.46	3.12	3.55	2.27	NA
526	Euarchontoglires	Rodentia	Caviidae	Kerodon_rupestris	799.15	45.47	8.17	3.75	8.52	4.79	33.33	5.25	2.76	5.48	1.84	13.09	2.21	1.92	3.03	1.54	7.80	2.67	1.59	1.81	1.47	14.30
527	Euarchontoglires	Rodentia	Caviidae	Hydrochoerus_hydrochaeris	48144.91	160.25	37.71	11.73	37.03	21.10	123.41	24.74	10.69	25.25	9.51	61.31	12.12	9.97	14.68	6.04	21.24	14.37	11.56	12.82	6.26	51.04
528	Euarchontoglires	Rodentia	Caviidae	Dolichotis_patagonum	8000.00	105.90	17.76	7.97	17.82	13.47	141.26	14.51	8.98	16.70	6.61	37.98	5.93	4.25	6.29	4.28	9.76	5.07	3.48	3.76	3.31	27.05
529	Euarchontoglires	Rodentia	Caviidae	Galea_musteloides	386.64	26.25	4.68	2.10	4.77	2.87	21.36	2.97	1.71	2.50	1.06	7.19	1.91	1.27	1.68	1.03	3.48	1.75	1.15	1.14	1.01	8.75
530	Euarchontoglires	Rodentia	Caviidae	Cavia_fulgida	282.50	31.70	5.21	2.55	5.74	3.01	25.34	3.61	1.84	3.66	1.32	9.73	2.03	1.29	2.13	1.19	4.70	1.98	1.21	1.23	1.08	11.61
531	Euarchontoglires	Rodentia	Erethizontidae	Coendou_prehensilis	4116.20	73.80	17.93	8.50	21.08	11.43	64.30	8.83	6.38	10.62	3.84	15.64	3.16	2.22	3.86	2.32	10.49	3.98	2.66	3.20	2.42	32.20
532	Euarchontoglires	Rodentia	Chinchillidae	Lagidium_sp	1814.00	53.86	13.14	5.14	14.61	9.71	56.84	7.39	4.40	7.23	3.26	12.21	3.08	2.62	4.04	2.25	7.75	3.65	2.87	3.40	2.76	17.68
533	Euarchontoglires	Rodentia	Chinchillidae	Chinchilla_lanigera	480.28	35.85	6.21	2.95	6.79	4.10	40.73	3.98	2.28	3.75	1.77	10.54	1.85	1.47	1.91	1.20	4.88	2.06	1.22	1.41	1.06	10.26
534	Euarchontoglires	Rodentia	Echimyidae	Isothrix_bistriata	444.99	35.33	6.14	2.99	8.50	6.15	31.93	4.16	2.13	3.77	1.81	8.15	1.98	1.39	2.31	1.24	6.46	2.19	1.55	1.65	1.08	15.85
535	Euarchontoglires	Rodentia	Echimyidae	Myocastor_coypus	6361.55	74.50	19.91	7.09	21.05	9.83	79.60	10.37	4.72	10.19	5.49	18.41	4.27	3.24	5.29	3.34	11.34	5.73	3.70	3.66	2.76	29.93
536	Euarchontoglires	Rodentia	Echimyidae	Phyllomys_brasiliensis	312.49	28.61	5.00	2.57	7.10	3.60	24.48	3.60	1.79	3.41	1.65	7.07	1.66	1.29	1.84	1.22	4.96	2.13	1.47	1.56	0.98	11.96
537	Euarchontoglires	Rodentia	Echimyidae	Makalata_didelphoides	398.66	27.95	5.12	2.40	6.26	3.45	23.45	3.10	1.80	2.86	1.58	7.44	1.43	1.01	1.76	0.98	5.10	1.98	1.31	1.40	0.82	11.71
538	Euarchontoglires	Rodentia	Echimyidae	Lonchothrix_emiliae	138.20	19.07	3.81	1.68	5.57	2.62	16.05	2.60	1.38	2.26	1.19	5.71	1.11	0.95	1.36	0.82	4.01	1.55	1.08	1.06	0.72	9.01
539	Euarchontoglires	Rodentia	Echimyidae	Hoplomys_gymnurus	281.42	37.17	7.16	3.46	8.06	4.26	34.79	4.50	2.51	4.35	2.00	11.67	2.18	1.88	2.55	1.68	6.62	2.58	1.64	1.71	1.57	15.97
540	Euarchontoglires	Rodentia	Echimyidae	Proechimys_semispinosus	353.32	25.08	4.26	1.91	5.59	2.63	23.84	2.64	1.46	2.34	0.95	8.08	1.65	1.17	1.51	1.02	4.67	1.69	1.20	1.16	0.96	10.71
541	Euarchontoglires	Rodentia	Echimyidae	Proechimys_guyannensis	314.03	29.38	5.19	2.58	5.89	3.28	26.19	3.24	1.69	2.94	1.18	8.64	1.59	1.04	1.59	0.91	4.64	1.72	0.99	1.15	0.90	10.43
542	Euarchontoglires	Rodentia	Capromyidae	Capromys_pilorides	5200.00	65.06	15.07	6.41	17.04	14.71	58.74	7.80	4.33	8.03	4.66	17.77	3.79	3.21	5.20	2.40	10.43	5.08	3.17	3.70	2.43	27.31
543	Euarchontoglires	Rodentia	Ctenomyidae	Ctenomys_maulinus	215.00	17.42	4.08	2.04	5.43	2.31	16.16	2.10	0.98	2.15	1.33	5.19	1.22	0.96	1.50	0.99	2.41	1.58	0.96	1.16	0.91	9.15
544	Euarchontoglires	Rodentia	Octodontidae	Octodon_degus	203.27	24.59	4.81	2.12	5.88	2.73	22.87	2.79	1.64	2.49	1.39	6.47	1.51	1.00	1.42	1.04	3.41	1.79	1.00	1.14	0.92	9.14
545	Euarchontoglires	Rodentia	Octodontidae	Spalacopus_cyanus	100.86	19.68	3.88	1.59	5.35	1.76	17.28	2.49	1.18	2.19	1.08	6.16	1.30	0.89	1.39	0.84	3.25	1.59	0.86	1.11	0.85	9.54
546	Euarchontoglires	Rodentia	Abrocomidae	Abrocoma_cinerea	193.64	27.63	5.75	2.44	5.78	4.54	25.92	2.98	1.94	2.78	1.38	6.19	1.13	0.94	1.52	0.84	2.96	1.53	0.90	1.04	0.66	7.14
547	Euarchontoglires	Rodentia	Anomaluridae	Anomalurus_beecrofti	479.07	61.90	7.41	3.83	7.97	4.15	52.49	3.86	2.43	3.71	1.76	8.57	1.29	1.34	1.93	1.16	8.42	2.00	1.61	1.16	1.15	22.39
548	Euarchontoglires	Rodentia	Anomaluridae	Anomalurus_sp	250.00	46.57	5.74	3.05	6.81	3.26	42.78	3.14	2.21	3.17	1.82	7.59	1.05	1.01	1.54	0.92	7.25	1.60	1.25	0.99	0.96	19.49
549	Euarchontoglires	Rodentia	Anomaluridae	Idiurus_zenkeri	100.00	13.79	1.92	1.02	2.73	1.23	14.84	1.09	0.72	1.19	0.55	2.79	0.36	0.32	0.47	0.27	2.67	0.53	0.36	0.35	0.34	6.67
550	Euarchontoglires	Rodentia	Zenkerellidae	Zenkerella_insignis	200.00	30.48	5.10	2.77	6.91	3.71	29.68	2.88	1.96	2.72	1.63	10.19	0.96	0.81	1.25	0.89	7.68	1.20	0.68	0.75	1.03	19.12
551	Euarchontoglires	Rodentia	Spalacidae	Nannospalax_ehrenbergi	164.35	20.75	5.05	2.02	6.75	5.77	16.42	3.30	1.46	2.57	0.95	4.87	1.67	0.93	1.67	0.90	2.85	1.65	1.04	1.39	0.71	7.92
552	Euarchontoglires	Rodentia	Spalacidae	Spalax_leucodon	188.67	23.84	5.62	2.23	7.66	6.48	19.23	3.73	2.03	2.51	1.34	4.76	2.01	1.15	1.86	1.21	3.26	2.00	1.35	1.53	0.94	9.20
553	Euarchontoglires	Rodentia	Spalacidae	Myospalax_myospalax	356.50	31.48	9.43	4.92	14.31	9.49	20.38	5.64	2.40	5.57	2.96	6.43	3.70	2.97	3.72	3.09	2.01	4.64	4.34	4.00	2.55	25.67
554	Euarchontoglires	Rodentia	Spalacidae	Tachyoryctes_splendens	218.57	27.80	6.59	3.23	8.31	6.50	24.88	3.47	2.10	3.05	1.66	7.20	1.88	1.35	1.92	1.16	3.86	2.05	1.21	1.51	1.11	10.04
555	Euarchontoglires	Rodentia	Muridae	Pachyuromys_duprasi	47.50	15.10	3.55	1.60	4.25	1.72	19.59	1.65	0.96	1.60	0.95	3.89	0.75	0.59	0.87	0.58	1.71	0.92	0.55	0.60	0.53	5.02
556	Euarchontoglires	Rodentia	Muridae	Meriones_tamariscinus	120.00	22.64	4.57	1.95	5.62	2.63	23.99	2.55	1.43	2.25	1.46	5.30	1.17	0.94	1.45	0.92	2.80	1.63	0.88	0.97	0.86	8.97
557	Euarchontoglires	Rodentia	Muridae	Rhombomys_opimus	192.50	23.46	4.67	2.03	6.07	2.77	23.97	2.55	1.47	2.23	1.54	4.96	1.07	0.89	1.36	0.98	2.75	1.64	0.87	0.93	0.90	8.42
558	Euarchontoglires	Rodentia	Muridae	Psammomys_obesus	102.15	22.90	4.37	2.06	5.99	2.37	23.77	2.33	1.25	2.24	1.16	5.94	1.52	0.88	1.51	1.02	2.48	1.36	0.80	0.79	0.69	7.32

						Humerus					Radius					Metacarpal					Phalanx					
	Superord. group	Order	Family	Species	Mass	L	PW	MW	DW	H	L	PW	MW	DW	H	L	PW	MW	DW	H	L	PW	MW	DW	H	DL
559	Euarchontoglires	Rodentia	Muridae	Taterillus_emini	52.50	15.69	2.98	1.32	3.58	1.68	17.36	1.63	1.09	1.45	0.84	3.63	0.80	0.65	0.84	0.57	1.72	0.92	0.56	0.64	0.56	5.19
560	Euarchontoglires	Rodentia	Muridae	Gerbillus_gerbillus	26.99	12.39	2.48	0.99	3.05	1.22	14.61	1.23	0.72	1.28	0.67	3.28	0.67	0.49	0.75	0.44	1.87	0.89	0.47	0.52	0.42	5.52
561	Euarchontoglires	Rodentia	Muridae	Sekeetamys_calurus	56.61	16.08	3.15	1.36	3.86	1.71	18.88	1.68	1.07	1.55	0.79	3.95	0.71	0.64	0.83	0.59	2.37	1.01	0.55	0.62	0.53	6.09
562	Euarchontoglires	Rodentia	Muridae	Gerbilliscus_kempi	100.83	21.30	3.88	1.65	5.05	2.26	21.05	2.09	1.32	2.08	1.25	4.41	0.97	0.73	1.17	0.72	2.19	1.27	0.76	0.83	0.72	7.69
563	Euarchontoglires	Rodentia	Muridae	Desmodillus_auricularis	54.81	16.90	3.28	1.42	4.23	1.98	17.84	1.72	0.92	1.44	1.01	3.79	0.73	0.55	0.77	0.56	1.81	0.96	0.49	0.60	0.48	5.18
564	Euarchontoglires	Rodentia	Muridae	Tatera_indica	138.28	21.08	4.45	1.94	4.68	2.11	22.30	2.07	1.40	1.84	1.20	3.95	0.90	0.83	0.98	0.89	2.12	1.15	0.69	0.82	0.78	5.46
565	Euarchontoglires	Rodentia	Muridae	Deomys_ferrugineus	57.60	18.24	2.79	1.44	3.55	1.79	19.79	1.50	1.04	1.46	0.87	5.67	0.99	0.63	0.98	0.55	2.82	0.96	0.59	0.68	0.57	6.02
566	Euarchontoglires	Rodentia	Muridae	Acomys_cahirinus	41.16	14.67	2.81	1.32	3.55	1.76	14.47	1.31	0.78	1.55	0.76	3.29	0.63	0.48	0.80	0.53	2.50	0.78	0.48	0.67	0.48	4.74
567	Euarchontoglires	Rodentia	Muridae	Lophuromys_flavopunctatus	57.07	12.27	2.50	1.23	3.69	1.66	12.05	1.62	0.89	1.20	0.61	4.29	1.06	0.63	0.87	0.66	2.25	1.04	0.62	0.66	0.54	5.65
568	Euarchontoglires	Rodentia	Muridae	Micromys_minutus	6.99	7.47	1.48	0.66	2.09	0.79	8.23	0.85	0.45	0.74	0.43	2.42	0.48	0.33	0.45	0.33	1.66	0.53	0.27	0.33	0.25	3.65
569	Euarchontoglires	Rodentia	Muridae	Melasmothrix_naso	47.70	13.90	4.07	1.62	5.40	1.92	15.68	2.32	1.11	1.93	0.84	4.23	1.23	0.77	1.18	0.69	2.74	1.34	0.75	0.86	0.69	7.54
570	Euarchontoglires	Rodentia	Muridae	Paraleptomys_wilhelmina	33.68	15.84	2.68	1.39	3.84	1.46	18.11	1.71	0.91	1.63	0.68	5.31	0.93	0.60	0.97	0.53	2.66	1.09	0.54	0.68	0.50	5.92
571	Euarchontoglires	Rodentia	Muridae	Leopoldamys_sabanus	347.61	30.02	5.42	2.55	7.77	4.23	26.75	3.22	1.95	2.56	1.77	9.10	1.86	1.14	1.81	1.15	5.25	2.04	1.02	1.21	1.05	10.99
572	Euarchontoglires	Rodentia	Muridae	Niviventer_rapit	79.73	19.19	3.48	1.65	4.78	2.06	19.04	1.95	1.19	1.81	1.09	5.72	1.05	0.72	1.11	0.64	3.62	1.28	0.66	0.77	0.58	7.64
573	Euarchontoglires	Rodentia	Muridae	Paruromys_dominator	325.31	30.76	5.58	2.50	8.42	2.92	29.87	3.90	1.79	3.11	1.62	10.00	1.83	1.10	1.89	1.03	5.58	2.24	0.98	1.28	0.97	12.45
574	Euarchontoglires	Rodentia	Muridae	Taeromys_celebensis	252.70	26.23	5.72	2.33	7.26	2.83	26.15	3.33	1.79	3.01	1.38	9.06	1.58	1.04	1.83	1.11	5.13	2.06	0.97	1.23	0.98	10.41
575	Euarchontoglires	Rodentia	Muridae	Sundamys_muelleri	356.48	24.76	5.20	2.25	7.14	3.07	24.04	3.23	1.82	2.52	1.37	7.75	1.58	1.13	1.71	1.05	4.93	1.80	1.05	1.23	0.96	11.23
576	Euarchontoglires	Rodentia	Muridae	Rattus_norvegicus	282.89	24.50	4.94	2.37	7.05	2.90	21.33	3.11	1.56	2.47	1.46	7.36	1.54	1.15	1.57	1.06	4.63	1.91	1.05	1.23	0.89	10.05
577	Euarchontoglires	Rodentia	Muridae	Nesokia_indica	178.08	24.26	5.44	2.43	7.18	3.51	21.49	2.85	1.63	2.31	1.70	7.31	1.65	1.16	1.62	1.11	4.64	1.98	1.03	1.20	0.91	10.46
578	Euarchontoglires	Rodentia	Muridae	Bandicota_bengalensis	226.99	21.41	4.32	1.86	6.19	2.32	21.24	2.67	1.46	2.20	0.89	7.06	1.26	0.82	1.27	0.83	4.04	1.54	0.67	0.94	0.69	8.78
579	Euarchontoglires	Rodentia	Muridae	Otomys_irroratus	114.45	17.81	3.62	1.54	4.88	1.99	18.45	2.22	1.07	2.34	1.00	4.72	1.29	0.91	1.06	0.86	3.20	1.37	0.79	0.81	0.74	7.46
580	Euarchontoglires	Rodentia	Muridae	Oenomys_hypoxanthus	89.84	19.90	3.52	1.70	4.41	2.48	19.15	1.91	1.06	1.81	1.08	5.20	0.94	0.71	1.08	0.65	3.69	1.26	0.57	0.76	0.63	13.85
581	Euarchontoglires	Rodentia	Muridae	Hybomys_univittatus	54.46	17.98	2.74	1.27	3.84	1.76	17.96	1.65	0.90	1.75	0.84	5.68	0.99	0.63	1.01	0.53	3.70	1.10	0.60	0.70	0.53	7.56
582	Euarchontoglires	Rodentia	Muridae	Desmomys_yaldeni	47.00	16.69	2.78	1.19	3.66	1.95	15.71	1.66	0.93	1.65	0.83	5.12	0.92	0.73	1.07	0.56	3.00	1.19	0.61	0.72	0.48	6.70
583	Euarchontoglires	Rodentia	Muridae	Pelomys_fallax	120.46	19.86	3.70	1.78	5.01	2.23	18.48	2.11	1.46	1.79	0.88	4.81	1.09	0.84	1.20	0.77	2.75	1.19	0.67	0.77	0.56	6.81
584	Euarchontoglires	Rodentia	Muridae	Arvicanthis_niloticus	95.80	23.99	4.60	2.00	5.99	2.73	20.51	2.52	1.44	2.23	1.51	6.29	1.32	0.98	1.57	0.92	3.57	1.61	0.92	0.96	0.81	8.46
585	Euarchontoglires	Rodentia	Muridae	Lenothrix_canus	150.00	24.92	4.86	2.51	6.07	3.44	23.33	2.66	1.74	2.94	1.67	6.06	1.31	1.19	1.63	0.93	4.27	1.62	1.31	1.21	0.83	9.29
586	Euarchontoglires	Rodentia	Muridae	Rhabdomys_pumilio	40.73	13.68	2.50	1.14	3.23	1.57	13.64	1.31	0.79	1.15	0.61	3.73	0.72	0.49	0.68	0.51	2.05	0.85	0.48	0.51	0.43	5.08
587	Euarchontoglires	Rodentia	Muridae	Dasymys_incomtus	127.75	19.20	3.48	1.74	4.59	2.13	19.67	2.04	1.21	2.28	0.97	5.18	1.07	0.79	1.13	0.83	3.16	1.29	0.79	0.85	0.75	7.97
588	Euarchontoglires	Rodentia	Muridae	Micaelamys_namaquensis	57.10	15.99	2.78	1.18	3.40	1.64	15.60	1.48	0.88	1.44	0.64	3.89	0.71	0.53	0.78	0.47	2.43	0.87	0.43	0.54	0.48	5.51
589	Euarchontoglires	Rodentia	Muridae	Grammomys_dolichurus	41.85	16.27	3.01	1.42	4.04	1.76	16.55	1.85	0.89	1.66	0.82	4.32	0.93	0.58	1.05	0.59	3.07	1.16	0.60	0.70	0.59	6.71
590	Euarchontoglires	Rodentia	Muridae	Thallomys_sp	101.10	17.57	3.07	1.32	4.19	1.72	16.72	1.74	0.93	1.45	0.80	4.41	0.80	0.55	0.88	0.56	2.94	1.05	0.55	0.64	0.43	6.24
591	Euarchontoglires	Rodentia	Muridae	Golunda_ellioti	60.73	15.44	2.76	1.22	3.73	1.74	15.48	1.57	1.05	1.30	0.72	4.39	0.85	0.58	0.88	0.55	2.58	0.96	0.49	0.57	0.46	5.88
592	Euarchontoglires	Rodentia	Muridae	Millardia_meltada	67.17	15.69	2.71	1.36	4.06	2.94	15.86	1.60	1.04	1.35	0.75	4.37	0.90	0.58	0.94	0.64	2.41	0.96	0.54	0.63	0.61	5.48
593	Euarchontoglires	Rodentia	Muridae	Mus_musculus	19.30	9.30	1.79	0.81	2.49	1.06	9.35	1.04	0.61	0.81	0.49	2.78	0.59	0.42	0.57	0.39	1.85	0.66	0.39	0.45	0.34	4.12
594	Euarchontoglires	Rodentia	Muridae	Praomys_sp	37.75	11.50	1.90	1.04	2.70	1.25	12.24	1.00	0.71	0.81	0.66	3.00	0.46	0.40	0.56	0.34	2.07	0.64	0.41	0.42	0.33	4.12
595	Euarchontoglires	Rodentia	Muridae	Colomys_goslingi	62.50	13.37	2.54	1.27	3.89	1.32	16.28	1.62	0.84	1.39	0.81	4.76	0.86	0.65	0.87	0.54	2.77	1.13	0.60	0.64	0.57	5.96
596	Euarchontoglires	Rodentia	Muridae	Mastomys_sp	51.56	12.81	2.07	1.12	3.20	1.41	13.69	1.34	0.82	1.18	0.59	3.93	0.67	0.56	0.74	0.58	2.18	0.79	0.46	0.55	0.49	4.90
597	Euarchontoglires	Rodentia	Muridae	Stenocephalemys_albocaudata	144.00	20.43	3.24	1.61	4.84	2.18	20.46	1.88	1.05	1.39	0.82	5.33	1.00	0.65	1.03	0.62	2.90	1.04	0.58	0.69	0.57	6.75
598	Euarchontoglires	Rodentia	Muridae	Stenocephalemys_griseicauda	85.75	20.55	3.44	1.72	4.43	2.20	21.05	1.88	1.25	1.66	0.94	4.78	1.04	0.73	1.04	0.64	2.70	1.13	0.64	0.82	0.59	6.39
599	Euarchontoglires	Rodentia	Muridae	Hylomyscus_stella	18.99	11.90	2.02	1.03	3.12	1.24	12.10	1.27	0.67	0.94	0.59	3.15	0.62	0.46	0.64	0.42	2.40	0.80	0.41	0.48	0.41	5.02
600	Euarchontoglires	Rodentia	Muridae	Tokudaia_muenninki	148.40	21.08	4.22	1.79	6.03	2.40	22.19	2.53	1.49	2.14	1.18	6.43	1.27	0.89	1.38	0.93	3.64	1.58	0.87	0.99	0.69	8.91
601	Euarchontoglires	Rodentia	Muridae	Apodemus_agrarius	21.11	12.52	2.10	0.92	2.86	1.17	11.62	1.27	0.70	1.01	0.62	3.54	0.68	0.40	0.68	0.44	2.00	0.73	0.38	0.56	0.38	4.75
602	Euarchontoglires	Rodentia	Muridae	Malacomys_longipes	95.64	17.73	3.05	1.24	3.78	1.57	18.60	1.78	0.99	1.31	0.63	5.95	0.86	0.54	0.90	0.53	3.33	1.09	0.46	0.69	0.44	6.78
603	Euarchontoglires	Rodentia	Muridae	Chiropodomys_gliroides	23.68	12.69	2.35	1.15	3.29	1.58	12.52	1.43	0.88	1.31	0.68	3.23	0.59	0.39	0.67	0.43	2.37	0.75	0.36	0.45	0.38	5.01
604	Euarchontoglires	Rodentia	Muridae	Lorentzimys_nouhuysi	14.44	12.14	2.33	1.09	3.17	1.19	14.32	1.30	0.87	1.36	0.62	3.37	0.55	0.42	0.71	0.42	2.74	0.82	0.43	0.48	0.41	6.02
605	Euarchontoglires	Rodentia	Muridae	Pogonomys_loriae	95.39	18.95	3.42	1.65	4.99	2.22	20.73	2.05	1.20	2.06	0.93	5.08	1.00	0.64	1.10	0.65	3.67	1.34	0.62	0.69	0.58	8.12
606	Euarchontoglires	Rodentia	Muridae	Vandeleuria_oleracea	10.00	9.12	1.67	0.90	2.57	1.03	9.84	1.11	0.58	1.06	0.56	2.53	0.55	0.49	0.60	0.40	2.27	0.72	0.38	0.50	0.34	4.66
607	Euarchontoglires	Rodentia	Muridae	Hydromys_chrysogaster	626.17	29.19	5.97	3.00	8.12	4.65	25.60	3.29	1.86	3.61	1.94	8.81	1.70	1.32	2.16	1.18	5.16	2.29	1.21	1.39	1.03	11.60
608	Euarchontoglires	Rodentia	Muridae	Tateomys_rhinogradoides	86.50	16.08	5.17	2.13	7.20	2.91	19.19	2.93	1.42	2.74	1.28	5.70	1.42	0.98	1.47	1.01	3.55	1.73	1.06	1.20	0.90	8.88
609	Euarchontoglires	Rodentia	Muridae	Zyzomys_argurus	40.42	13.34	2.66	1.26	3.20	1.73	12.47	1.51	0.78	1.30	0.74	3.44	0.61	0.42	0.77	0.41	2.28	0.82	0.38	0.52	0.40	4.80

						Humerus					Radius					Metacarpal					Phalanx					
	Superord. group	Order	Family	Species	Mass	L	PW	MW	DW	H	L	PW	MW	DW	H	L	PW	MW	DW	H	L	PW	MW	DW	H	DL
610	Euarchontoglires	Rodentia	Muridae	Pseudomys_higginsi	63.16	18.39	3.60	1.55	4.24	1.94	20.69	2.08	1.19	2.10	0.95	5.53	1.03	0.78	1.16	0.76	3.46	1.38	0.73	0.81	0.65	7.87
611	Euarchontoglires	Rodentia	Muridae	Mastacomys_fuscus	125.72	20.19	3.72	1.47	4.97	1.72	21.63	2.41	1.07	1.90	0.93	5.81	1.28	0.72	1.21	0.82	3.51	1.34	0.62	0.91	0.64	8.04
612	Euarchontoglires	Rodentia	Muridae	Pseudomys_hermannsburgensis	13.38	10.26	1.96	0.78	2.29	0.98	10.82	1.07	0.63	1.06	0.48	2.81	0.50	0.40	0.55	0.35	1.54	0.59	0.33	0.40	0.29	3.64
613	Euarchontoglires	Rodentia	Muridae	Leggadina_forresti	23.88	11.62	2.13	0.88	2.84	1.11	11.27	1.41	0.71	1.07	0.63	3.35	0.64	0.39	0.61	0.43	1.95	0.70	0.33	0.46	0.36	6.91
614	Euarchontoglires	Rodentia	Muridae	Melomys_burtoni	71.29	15.55	3.12	1.58	4.49	1.79	14.57	1.84	0.99	1.58	0.79	4.90	0.98	0.62	1.05	0.56	3.55	1.06	0.61	0.72	0.49	7.48
615	Euarchontoglires	Rodentia	Muridae	Uromys_sp	628.46	39.98	7.12	3.61	10.84	5.59	35.91	5.07	3.30	4.16	2.25	12.13	2.49	1.68	2.61	1.59	7.17	2.97	1.84	1.98	1.44	15.81
616	Euarchontoglires	Rodentia	Muridae	Hapalomys_longicaudatus	70.00	21.40	4.18	2.16	5.56	2.59	20.46	2.42	1.47	2.39	1.39	5.43	1.13	0.90	1.39	0.92	4.13	1.54	0.81	0.90	0.87	8.67
617	Euarchontoglires	Rodentia	Muridae	Rhynchomys_isarogensis	122.29	21.63	4.38	1.91	6.34	3.95	23.40	2.69	1.41	2.42	0.97	6.24	1.24	0.98	1.35	0.87	3.20	1.41	0.98	0.96	0.89	8.00
618	Euarchontoglires	Rodentia	Muridae	Chrotomys_whiteheadi	54.33	17.44	2.77	1.32	3.72	1.62	17.24	1.66	0.96	1.38	0.89	4.99	0.88	0.62	1.01	0.55	3.02	1.05	0.61	0.65	0.54	6.23
619	Euarchontoglires	Rodentia	Muridae	Chrotomys_gonzalesi	140.20	19.96	4.01	1.84	6.23	2.43	19.50	2.52	1.32	2.32	1.00	6.72	1.24	0.90	1.39	0.87	3.77	1.51	0.84	0.96	0.71	9.00
620	Euarchontoglires	Rodentia	Muridae	Apomys_littoralis	30.95	12.49	2.27	1.13	3.51	1.31	12.72	1.54	0.83	1.27	0.66	4.53	0.80	0.47	0.83	0.56	3.15	1.04	0.52	0.61	0.51	6.28
621	Euarchontoglires	Rodentia	Cricetidae	Prometheomys_schaposchnikowi	75.00	15.63	3.14	1.85	5.27	2.00	15.39	1.84	1.24	1.76	0.76	4.51	1.24	0.84	1.38	0.94	2.55	1.53	0.86	1.04	0.77	9.15
622	Euarchontoglires	Rodentia	Cricetidae	Dicrostonyx_richardsoni	62.50	14.13	2.97	1.36	4.58	1.69	13.81	1.72	0.83	1.68	1.21	3.57	1.07	1.06	1.27	0.87	2.23	1.35	0.90	1.09	0.89	6.47
623	Euarchontoglires	Rodentia	Cricetidae	Ondatra_zibethicus	991.31	34.80	8.14	3.39	11.35	5.55	37.42	4.70	2.70	4.65	2.20	9.38	2.37	1.35	2.13	1.88	6.11	2.42	1.50	1.56	1.66	16.50
624	Euarchontoglires	Rodentia	Cricetidae	Neofiber_alleni	265.38	22.36	4.26	2.02	5.46	2.95	21.04	2.34	1.38	2.23	1.06	5.70	1.15	0.74	1.19	0.69	3.52	1.35	0.77	0.83	0.60	7.93
625	Euarchontoglires	Rodentia	Cricetidae	Lemmus_sibiricus	53.81	17.69	3.17	1.54	4.76	1.90	14.91	2.06	1.01	1.96	0.96	4.51	1.04	0.78	1.20	0.81	2.01	1.13	0.84	0.87	0.78	6.07
626	Euarchontoglires	Rodentia	Cricetidae	Lemmus_lemmus	67.62	16.55	3.01	1.43	4.38	1.64	14.55	1.73	0.97	1.77	0.87	3.99	0.96	0.61	1.02	0.86	1.94	0.98	0.72	0.76	0.76	6.14
627	Euarchontoglires	Rodentia	Cricetidae	Myopus_schisticolor	29.99	12.71	2.20	0.97	2.74	1.02	13.09	1.21	0.64	1.35	0.55	3.24	0.71	0.38	0.64	0.53	1.55	0.74	0.37	0.52	0.49	4.11
628	Euarchontoglires	Rodentia	Cricetidae	Chionomys_nivalis	42.01	15.59	2.50	1.14	3.41	1.47	14.68	1.50	0.78	1.17	0.81	3.67	0.79	0.51	0.85	0.50	2.19	0.92	0.46	0.62	0.46	5.39
629	Euarchontoglires	Rodentia	Cricetidae	Microtus_afghanus	30.00	13.18	2.43	1.10	3.26	1.48	12.08	1.34	0.65	1.02	0.70	2.79	0.75	0.48	0.93	0.50	1.68	0.87	0.41	0.58	0.41	4.56
630	Euarchontoglires	Rodentia	Cricetidae	Microtus_chrotorrhinus	38.99	12.47	2.43	0.97	3.02	1.26	11.78	1.43	0.64	1.05	0.53	3.99	0.83	0.46	0.79	0.54	2.18	0.86	0.43	0.56	0.46	5.29
631	Euarchontoglires	Rodentia	Cricetidae	Lasiopodomys_brandtii	46.05	13.21	2.73	1.24	3.88	1.44	12.34	1.64	0.79	1.34	0.76	3.69	0.82	0.59	0.90	0.54	2.13	0.97	0.53	0.64	0.56	6.19
632	Euarchontoglires	Rodentia	Cricetidae	Ellobius_alaicus	60.00	16.80	3.89	1.64	5.12	3.18	15.65	2.04	1.04	1.69	0.88	5.50	1.00	0.69	1.23	0.70	3.43	1.26	0.64	0.97	0.57	7.03
633	Euarchontoglires	Rodentia	Cricetidae	Arvicola_amphibius	120.00	17.58	3.82	1.59	5.18	2.22	16.16	2.21	1.02	1.68	1.04	4.64	1.15	0.69	1.06	0.69	2.93	1.19	0.63	0.72	0.65	7.21
634	Euarchontoglires	Rodentia	Cricetidae	Lemmiscus_curtatus	20.60	10.11	2.10	0.99	2.73	1.05	9.53	1.10	0.63	1.01	0.61	2.37	0.52	0.48	0.64	0.50	1.27	0.63	0.43	0.45	0.46	3.62
635	Euarchontoglires	Rodentia	Cricetidae	Eolagurus_luteus	26.00	17.51	3.59	1.58	4.91	1.79	15.93	1.99	1.03	1.82	1.10	4.06	1.01	0.73	1.16	0.66	2.44	1.12	0.63	0.86	0.72	6.94
636	Euarchontoglires	Rodentia	Cricetidae	Hyperacrius_wynnei	52.60	13.38	3.06	1.23	4.04	1.53	12.49	1.64	0.95	1.30	0.78	3.75	0.79	0.63	0.89	0.77	2.21	1.05	0.57	0.76	0.67	6.12
637	Euarchontoglires	Rodentia	Cricetidae	Alticola_argentatus	37.69	13.85	2.79	1.15	3.40	1.41	13.80	1.36	0.78	1.31	0.74	4.04	0.70	0.53	0.83	0.55	2.51	0.84	0.49	0.61	0.48	5.55
638	Euarchontoglires	Rodentia	Cricetidae	Myodes_rutilus	19.94	12.45	2.02	0.91	2.92	1.11	11.70	1.22	0.56	0.95	0.60	3.73	0.68	0.45	0.75	0.50	2.03	0.75	0.41	0.50	0.40	4.93
639	Euarchontoglires	Rodentia	Cricetidae	Eothenomys_melanogaster	19.59	10.89	2.19	0.79	2.63	0.97	10.22	1.13	0.62	0.90	0.50	2.95	0.64	0.40	0.63	0.43	1.95	0.72	0.35	0.48	0.39	4.51
640	Euarchontoglires	Rodentia	Cricetidae	Phodopus_roborovskii	21.00	13.71	2.43	1.18	3.61	1.34	14.24	1.33	0.85	1.36	0.71	2.93	0.58	0.45	0.69	0.46	1.47	0.66	0.40	0.44	0.41	3.71
641	Euarchontoglires	Rodentia	Cricetidae	Cricetus_cricetus	428.95	35.42	6.45	3.54	10.36	4.30	30.71	3.61	3.21	3.18	2.09	8.13	1.90	1.32	2.10	1.31	4.89	2.13	1.29	1.36	1.22	11.95
642	Euarchontoglires	Rodentia	Cricetidae	Allocricetulus_eversmanni	50.00	15.19	2.35	1.50	4.00	1.71	15.31	1.50	1.03	1.34	0.88	3.40	0.75	0.48	0.76	0.43	1.93	0.81	0.42	0.56	0.39	4.55
643	Euarchontoglires	Rodentia	Cricetidae	Cricetulus_barabensis	33.50	13.82	2.28	1.13	3.48	1.35	13.84	1.44	0.74	1.30	0.75	3.66	0.73	0.47	0.78	0.43	1.92	0.82	0.44	0.55	0.48	4.73
644	Euarchontoglires	Rodentia	Cricetidae	Neotoma_mexicana	203.00	22.59	3.95	1.95	5.68	2.30	22.96	2.36	1.31	2.21	1.19	5.75	1.11	0.73	1.17	0.74	3.65	1.31	0.66	0.86	0.65	7.90
645	Euarchontoglires	Rodentia	Cricetidae	Hodomys_alleni	367.59	28.56	5.57	2.80	7.49	3.45	25.64	3.10	1.68	2.66	1.54	7.07	1.31	1.00	1.54	1.02	4.52	1.65	1.03	1.07	0.83	9.82
646	Euarchontoglires	Rodentia	Cricetidae	Ochrotomys_nuttalli	22.81	12.12	2.26	1.04	3.44	1.24	12.86	1.35	0.73	1.21	0.65	3.64	0.60	0.46	0.71	0.48	2.48	0.80	0.42	0.51	0.41	5.19
647	Euarchontoglires	Rodentia	Cricetidae	Reithrodontomys_megalotis	10.72	9.31	1.63	0.85	2.34	0.90	10.86	0.89	0.53	0.87	0.44	2.54	0.46	0.30	0.50	0.32	1.72	0.54	0.25	0.32	0.24	3.67
648	Euarchontoglires	Rodentia	Cricetidae	Onychomys_leucogaster	30.00	14.81	2.78	1.36	4.34	1.63	15.32	1.59	0.95	1.56	0.82	4.14	0.95	0.62	1.02	0.61	2.57	1.11	0.63	0.73	0.60	6.68
649	Euarchontoglires	Rodentia	Cricetidae	Osgoodomys_banderanus	49.99	12.93	2.35	1.25	3.42	1.40	12.64	1.45	0.80	1.25	0.73	3.90	0.70	0.42	0.81	0.52	2.51	0.96	0.46	0.55	0.46	5.23
650	Euarchontoglires	Rodentia	Cricetidae	Peromyscus_leucopus	18.07	11.85	2.22	1.22	3.35	1.26	12.33	1.44	0.81	1.24	0.65	3.92	0.65	0.49	0.77	0.55	2.46	0.86	0.48	0.67	0.50	5.02
651	Euarchontoglires	Rodentia	Cricetidae	Peromyscus_truei	27.00	12.79	2.31	1.07	3.36	1.31	14.57	1.32	0.80	1.16	0.59	3.43	0.71	0.41	0.70	0.40	2.20	0.73	0.40	0.51	0.37	5.03
652	Euarchontoglires	Rodentia	Cricetidae	Habromys_lepturus	84.99	16.65	2.78	1.37	4.35	1.78	17.35	1.65	1.06	1.59	0.75	4.79	0.89	0.52	0.89	0.60	2.92	1.01	0.59	0.64	0.51	6.53
653	Euarchontoglires	Rodentia	Cricetidae	Neotomodon_alstoni	44.64	14.75	2.70	1.42	4.10	1.82	16.54	1.61	0.92	1.34	0.76	4.36	0.87	0.56	0.86	0.62	2.42	0.95	0.53	0.67	0.52	5.82
654	Euarchontoglires	Rodentia	Cricetidae	Podomys_floridanus	30.74	13.56	2.38	1.08	3.30	1.23	14.13	1.37	0.78	1.15	0.60	3.71	0.77	0.45	0.77	0.57	2.21	0.80	0.46	0.51	0.49	4.96
655	Euarchontoglires	Rodentia	Cricetidae	Megadontomys_thomasi	110.52	19.43	3.24	1.69	5.20	1.89	20.65	2.11	0.98	1.87	1.08	6.08	0.97	0.61	1.04	0.67	3.50	1.19	0.68	0.79	0.59	7.49
656	Euarchontoglires	Rodentia	Cricetidae	Scotinomys_teguina	11.59	9.75	1.86	0.91	2.85	0.97	10.24	1.05	0.54	0.93	0.46	2.97	0.60	0.40	0.70	0.38	1.98	0.73	0.37	0.49	0.37	4.53
657	Euarchontoglires	Rodentia	Cricetidae	Baiomys_taylori	7.43	8.02	1.48	0.70	2.26	0.92	8.25	0.88	0.56	0.85	0.43	2.26	0.41	0.34	0.50	0.35	1.46	0.61	0.33	0.40	0.31	3.59
658	Euarchontoglires	Rodentia	Cricetidae	Ototylomys_phyllotis	86.94	21.52	3.35	1.90	4.68	2.34	18.73	1.90	1.03	1.80	1.08	4.88	0.90	0.72	1.13	0.59	3.21	1.15	0.67	0.82	0.56	6.55
659	Euarchontoglires	Rodentia	Cricetidae	Nyctomys_sumichrasti	59.99	16.29	2.97	1.72	4.55	2.10	16.69	1.90	1.37	1.56	0.86	4.14	0.90	0.60	0.92	0.60	3.33	0.93	0.52	0.62	0.53	7.01
660	Euarchontoglires	Rodentia	Cricetidae	Sigmodon_hispidus	110.65	23.07	3.74	1.86	5.18	3.59	21.51	2.08	1.27	1.72	1.10	5.13	1.04	0.77	1.17	0.68	3.01	1.23	0.70	0.77	0.66	7.68

						Humerus					Radius					Metacarpal					Phalanx					
	Superord. group	Order	Family	Species	Mass	L	PW	MW	DW	H	L	PW	MW	DW	H	L	PW	MW	DW	H	L	PW	MW	DW	H	DL
610	Euarchontoglires	Rodentia	Muridae	Pseudomys_higginsi	63.16	18.39	3.60	1.55	4.24	1.94	20.69	2.08	1.19	2.10	0.95	5.53	1.03	0.78	1.16	0.76	3.46	1.38	0.73	0.81	0.65	7.87
611	Euarchontoglires	Rodentia	Muridae	Mastacomys_fuscus	125.72	20.19	3.72	1.47	4.97	1.72	21.63	2.41	1.07	1.90	0.93	5.81	1.28	0.72	1.21	0.82	3.51	1.34	0.62	0.91	0.64	8.04
612	Euarchontoglires	Rodentia	Muridae	Pseudomys_hermannsburgensis	13.38	10.26	1.96	0.78	2.29	0.98	10.82	1.07	0.63	1.06	0.48	2.81	0.50	0.40	0.55	0.35	1.54	0.59	0.33	0.40	0.29	3.64
613	Euarchontoglires	Rodentia	Muridae	Leggadina_forresti	23.88	11.62	2.13	0.88	2.84	1.11	11.27	1.41	0.71	1.07	0.63	3.35	0.64	0.39	0.61	0.43	1.95	0.70	0.33	0.46	0.36	6.91
614	Euarchontoglires	Rodentia	Muridae	Melomys_burtoni	71.29	15.55	3.12	1.58	4.49	1.79	14.57	1.84	0.99	1.58	0.79	4.90	0.98	0.62	1.05	0.56	3.55	1.06	0.61	0.72	0.49	7.48
615	Euarchontoglires	Rodentia	Muridae	Uromys_sp	628.46	39.98	7.12	3.61	10.84	5.59	35.91	5.07	3.30	4.16	2.25	12.13	2.49	1.68	2.61	1.59	7.17	2.97	1.84	1.98	1.44	15.81
616	Euarchontoglires	Rodentia	Muridae	Hapalomys_longicaudatus	70.00	21.40	4.18	2.16	5.56	2.59	20.46	2.42	1.47	2.39	1.39	5.43	1.13	0.90	1.39	0.92	4.13	1.54	0.81	0.90	0.87	8.67
617	Euarchontoglires	Rodentia	Muridae	Rhynchomys_isarogensis	122.29	21.63	4.38	1.91	6.34	3.95	23.40	2.69	1.41	2.42	0.97	6.24	1.24	0.98	1.35	0.87	3.20	1.41	0.98	0.96	0.89	8.00
618	Euarchontoglires	Rodentia	Muridae	Chrotomys_whiteheadi	54.33	17.44	2.77	1.32	3.72	1.62	17.24	1.66	0.96	1.38	0.89	4.99	0.88	0.62	1.01	0.55	3.02	1.05	0.61	0.65	0.54	6.23
619	Euarchontoglires	Rodentia	Muridae	Chrotomys_gonzalesi	140.20	19.96	4.01	1.84	6.23	2.43	19.50	2.52	1.32	2.32	1.00	6.72	1.24	0.90	1.39	0.87	3.77	1.51	0.84	0.96	0.71	9.00
620	Euarchontoglires	Rodentia	Muridae	Apomys_littoralis	30.95	12.49	2.27	1.13	3.51	1.31	12.72	1.54	0.83	1.27	0.66	4.53	0.80	0.47	0.83	0.56	3.15	1.04	0.52	0.61	0.51	6.28
621	Euarchontoglires	Rodentia	Cricetidae	Prometheomys_schaposchnikowi	75.00	15.63	3.14	1.85	5.27	2.00	15.39	1.84	1.24	1.76	0.76	4.51	1.24	0.84	1.38	0.94	2.55	1.53	0.86	1.04	0.77	9.15
622	Euarchontoglires	Rodentia	Cricetidae	Dicrostonyx_richardsoni	62.50	14.13	2.97	1.36	4.58	1.69	13.81	1.72	0.83	1.68	1.21	3.57	1.07	1.06	1.27	0.87	2.23	1.35	0.90	1.09	0.89	6.47
623	Euarchontoglires	Rodentia	Cricetidae	Ondatra_zibethicus	991.31	34.80	8.14	3.39	11.35	5.55	37.42	4.70	2.70	4.65	2.20	9.38	2.37	1.35	2.13	1.88	6.11	2.42	1.50	1.56	1.66	16.50
624	Euarchontoglires	Rodentia	Cricetidae	Neofiber_alleni	265.38	22.36	4.26	2.02	5.46	2.95	21.04	2.34	1.38	2.23	1.06	5.70	1.15	0.74	1.19	0.69	3.52	1.35	0.77	0.83	0.60	7.93
625	Euarchontoglires	Rodentia	Cricetidae	Lemmus_sibiricus	53.81	17.69	3.17	1.54	4.76	1.90	14.91	2.06	1.01	1.96	0.96	4.51	1.04	0.78	1.20	0.81	2.01	1.13	0.84	0.87	0.78	6.07
626	Euarchontoglires	Rodentia	Cricetidae	Lemmus_lemmus	67.62	16.55	3.01	1.43	4.38	1.64	14.55	1.73	0.97	1.77	0.87	3.99	0.96	0.61	1.02	0.86	1.94	0.98	0.72	0.76	0.76	6.14
627	Euarchontoglires	Rodentia	Cricetidae	Myopus_schisticolor	29.99	12.71	2.20	0.97	2.74	1.02	13.09	1.21	0.64	1.35	0.55	3.24	0.71	0.38	0.64	0.53	1.55	0.74	0.37	0.52	0.49	4.11
628	Euarchontoglires	Rodentia	Cricetidae	Chionomys_nivalis	42.01	15.59	2.50	1.14	3.41	1.47	14.68	1.50	0.78	1.17	0.81	3.67	0.79	0.51	0.85	0.50	2.19	0.92	0.46	0.62	0.46	5.39
629	Euarchontoglires	Rodentia	Cricetidae	Microtus_afghanus	30.00	13.18	2.43	1.10	3.26	1.48	12.08	1.34	0.65	1.02	0.70	2.79	0.75	0.48	0.93	0.50	1.68	0.87	0.41	0.58	0.41	4.56
630	Euarchontoglires	Rodentia	Cricetidae	Microtus_chrotorrhinus	38.99	12.47	2.43	0.97	3.02	1.26	11.78	1.43	0.64	1.05	0.53	3.99	0.83	0.46	0.79	0.54	2.18	0.86	0.43	0.56	0.46	5.29
631	Euarchontoglires	Rodentia	Cricetidae	Lasiopodomys_brandtii	46.05	13.21	2.73	1.24	3.88	1.44	12.34	1.64	0.79	1.34	0.76	3.69	0.82	0.59	0.90	0.54	2.13	0.97	0.53	0.64	0.56	6.19
632	Euarchontoglires	Rodentia	Cricetidae	Ellobius_alaicus	60.00	16.80	3.89	1.64	5.12	3.18	15.65	2.04	1.04	1.69	0.88	5.50	1.00	0.69	1.23	0.70	3.43	1.26	0.64	0.97	0.57	7.03
633	Euarchontoglires	Rodentia	Cricetidae	Arvicola_amphibius	120.00	17.58	3.82	1.59	5.18	2.22	16.16	2.21	1.02	1.68	1.04	4.64	1.15	0.69	1.06	0.69	2.93	1.19	0.63	0.72	0.65	7.21
634	Euarchontoglires	Rodentia	Cricetidae	Lemmiscus_curtatus	20.60	10.11	2.10	0.99	2.73	1.05	9.53	1.10	0.63	1.01	0.61	2.37	0.52	0.48	0.64	0.50	1.27	0.63	0.43	0.45	0.46	3.62
635	Euarchontoglires	Rodentia	Cricetidae	Eolagurus_luteus	26.00	17.51	3.59	1.58	4.91	1.79	15.93	1.99	1.03	1.82	1.10	4.06	1.01	0.73	1.16	0.66	2.44	1.12	0.63	0.86	0.72	6.94
636	Euarchontoglires	Rodentia	Cricetidae	Hyperacrius_wynnei	52.60	13.38	3.06	1.23	4.04	1.53	12.49	1.64	0.95	1.30	0.78	3.75	0.79	0.63	0.89	0.77	2.21	1.05	0.57	0.76	0.67	6.12
637	Euarchontoglires	Rodentia	Cricetidae	Alticola_argentatus	37.69	13.85	2.79	1.15	3.40	1.41	13.80	1.36	0.78	1.31	0.74	4.04	0.70	0.53	0.83	0.55	2.51	0.84	0.49	0.61	0.48	5.55
638	Euarchontoglires	Rodentia	Cricetidae	Myodes_rutilus	19.94	12.45	2.02	0.91	2.92	1.11	11.70	1.22	0.56	0.95	0.60	3.73	0.68	0.45	0.75	0.50	2.03	0.75	0.41	0.50	0.40	4.93
639	Euarchontoglires	Rodentia	Cricetidae	Eothenomys_melanogaster	19.59	10.89	2.19	0.79	2.63	0.97	10.22	1.13	0.62	0.90	0.50	2.95	0.64	0.40	0.63	0.43	1.95	0.72	0.35	0.48	0.39	4.51
640	Euarchontoglires	Rodentia	Cricetidae	Phodopus_roborovskii	21.00	13.71	2.43	1.18	3.61	1.34	14.24	1.33	0.85	1.36	0.71	2.93	0.58	0.45	0.69	0.46	1.47	0.66	0.40	0.44	0.41	3.71
641	Euarchontoglires	Rodentia	Cricetidae	Cricetus_cricetus	428.95	35.42	6.45	3.54	10.36	4.30	30.71	3.61	3.21	3.18	2.09	8.13	1.90	1.32	2.10	1.31	4.89	2.13	1.29	1.36	1.22	11.95
642	Euarchontoglires	Rodentia	Cricetidae	Allocricetulus_eversmanni	50.00	15.19	2.35	1.50	4.00	1.71	15.31	1.50	1.03	1.34	0.88	3.40	0.75	0.48	0.76	0.43	1.93	0.81	0.42	0.56	0.39	4.55
643	Euarchontoglires	Rodentia	Cricetidae	Cricetulus_barabensis	33.50	13.82	2.28	1.13	3.48	1.35	13.84	1.44	0.74	1.30	0.75	3.66	0.73	0.47	0.78	0.43	1.92	0.82	0.44	0.55	0.48	4.73
644	Euarchontoglires	Rodentia	Cricetidae	Neotoma_mexicana	203.00	22.59	3.95	1.95	5.68	2.30	22.96	2.36	1.31	2.21	1.19	5.75	1.11	0.73	1.17	0.74	3.65	1.31	0.66	0.86	0.65	7.90
645	Euarchontoglires	Rodentia	Cricetidae	Hodomys_alleni	367.59	28.56	5.57	2.80	7.49	3.45	25.64	3.10	1.68	2.66	1.54	7.07	1.31	1.00	1.54	1.02	4.52	1.65	1.03	1.07	0.83	9.82
646	Euarchontoglires	Rodentia	Cricetidae	Ochrotomys_nuttalli	22.81	12.12	2.26	1.04	3.44	1.24	12.86	1.35	0.73	1.21	0.65	3.64	0.60	0.46	0.71	0.48	2.48	0.80	0.42	0.51	0.41	5.19
647	Euarchontoglires	Rodentia	Cricetidae	Reithrodontomys_megalotis	10.72	9.31	1.63	0.85	2.34	0.90	10.86	0.89	0.53	0.87	0.44	2.54	0.46	0.30	0.50	0.32	1.72	0.54	0.25	0.32	0.24	3.67
648	Euarchontoglires	Rodentia	Cricetidae	Onychomys_leucogaster	30.00	14.81	2.78	1.36	4.34	1.63	15.32	1.59	0.95	1.56	0.82	4.14	0.95	0.62	1.02	0.61	2.57	1.11	0.63	0.73	0.60	6.68
649	Euarchontoglires	Rodentia	Cricetidae	Osgoodomys_banderanus	49.99	12.93	2.35	1.25	3.42	1.40	12.64	1.45	0.80	1.25	0.73	3.90	0.70	0.42	0.81	0.52	2.51	0.96	0.46	0.55	0.46	5.23
650	Euarchontoglires	Rodentia	Cricetidae	Peromyscus_leucopus	18.07	11.85	2.22	1.22	3.35	1.26	12.33	1.44	0.81	1.24	0.65	3.92	0.65	0.49	0.77	0.55	2.46	0.86	0.48	0.67	0.50	5.02
651	Euarchontoglires	Rodentia	Cricetidae	Peromyscus_truei	27.00	12.79	2.31	1.07	3.36	1.31	14.57	1.32	0.80	1.16	0.59	3.43	0.71	0.41	0.70	0.40	2.20	0.73	0.40	0.51	0.37	5.03
652	Euarchontoglires	Rodentia	Cricetidae	Habromys_lepturus	84.99	16.65	2.78	1.37	4.35	1.78	17.35	1.65	1.06	1.59	0.75	4.79	0.89	0.52	0.89	0.60	2.92	1.01	0.59	0.64	0.51	6.53
653	Euarchontoglires	Rodentia	Cricetidae	Neotomodon_alstoni	44.64	14.75	2.70	1.42	4.10	1.82	16.54	1.61	0.92	1.34	0.76	4.36	0.87	0.56	0.86	0.62	2.42	0.95	0.53	0.67	0.52	5.82
654	Euarchontoglires	Rodentia	Cricetidae	Podomys_floridanus	30.74	13.56	2.38	1.08	3.30	1.23	14.13	1.37	0.78	1.15	0.60	3.71	0.77	0.45	0.77	0.57	2.21	0.80	0.46	0.51	0.49	4.96
655	Euarchontoglires	Rodentia	Cricetidae	Megadontomys_thomasi	110.52	19.43	3.24	1.69	5.20	1.89	20.65	2.11	0.98	1.87	1.08	6.08	0.97	0.61	1.04	0.67	3.50	1.19	0.68	0.79	0.59	7.49
656	Euarchontoglires	Rodentia	Cricetidae	Scotinomys_teguina	11.59	9.75	1.86	0.91	2.85	0.97	10.24	1.05	0.54	0.93	0.46	2.97	0.60	0.40	0.70	0.38	1.98	0.73	0.37	0.49	0.37	4.53
657	Euarchontoglires	Rodentia	Cricetidae	Baiomys_taylori	7.43	8.02	1.48	0.70	2.26	0.92	8.25	0.88	0.56	0.85	0.43	2.26	0.41	0.34	0.50	0.35	1.46	0.61	0.33	0.40	0.31	3.59
658	Euarchontoglires	Rodentia	Cricetidae	Ototylomys_phyllotis	86.94	21.52	3.35	1.90	4.68	2.34	18.73	1.90	1.03	1.80	1.08	4.88	0.90	0.72	1.13	0.59	3.21	1.15	0.67	0.82	0.56	6.55
659	Euarchontoglires	Rodentia	Cricetidae	Nyctomys_sumichrasti	59.99	16.29	2.97	1.72	4.55	2.10	16.69	1.90	1.37	1.56	0.86	4.14	0.90	0.60	0.92	0.60	3.33	0.93	0.52	0.62	0.53	7.01
660	Euarchontoglires	Rodentia	Cricetidae	Sigmodon_hispidus	110.65	23.07	3.74	1.86	5.18	3.59	21.51	2.08	1.27	1.72	1.10	5.13	1.04	0.77	1.17	0.68	3.01	1.23	0.70	0.77	0.66	7.68

						Humerus					Radius					Metacarpal					Phalanx					
	Superord. group	Order	Family	Species	Mass	L	PW	MW	DW	H	L	PW	MW	DW	H	L	PW	MW	DW	H	L	PW	MW	DW	H	DL
712	Euarchontoglires	Rodentia	Dipodidae	Dipus_sagitta	89.00	13.37	3.47	1.39	4.31	1.65	16.81	2.02	1.09	1.76	0.98	3.71	0.81	0.79	0.95	0.88	2.76	1.19	0.70	0.81	0.81	6.60
713	Euarchontoglires	Rodentia	Dipodidae	Jaculus_jaculus	59.80	11.83	3.04	1.32	4.00	1.70	15.36	1.82	1.04	1.37	0.90	3.09	0.66	0.63	0.86	0.75	2.14	0.92	0.69	0.76	0.76	6.81
714	Euarchontoglires	Rodentia	Dipodidae	Stylodipus_andrewsi	75.32	12.20	3.52	1.32	4.04	1.47	15.00	1.93	0.98	1.51	0.82	3.19	0.84	0.78	0.86	0.73	2.05	1.07	0.83	0.77	0.77	6.48
715	Euarchontoglires	Rodentia	Dipodidae	Pygeretmus_pumilio	52.24	11.75	3.10	1.21	3.48	1.53	14.51	1.75	0.91	1.42	0.73	3.16	0.59	0.50	0.75	0.60	1.98	0.88	0.60	0.64	0.54	5.27
716	Euarchontoglires	Rodentia	Dipodidae	Allactaga_elater	59.00	10.94	2.79	1.16	3.12	1.38	14.01	1.69	0.94	1.37	1.00	2.59	0.66	0.54	0.75	0.60	2.06	0.85	0.61	0.55	0.66	5.39
717	Euarchontoglires	Rodentia	Zapodidae	Zapus_hudsonius	18.43	10.70	1.97	0.83	2.58	1.11	10.97	1.29	0.66	0.96	0.48	3.52	0.67	0.42	0.67	0.41	2.44	0.80	0.42	0.54	0.35	5.60
718	Euarchontoglires	Rodentia	Zapodidae	Napaeozapus_insignis	22.25	11.29	2.35	0.99	2.78	1.16	12.06	1.47	0.63	1.07	0.55	4.30	0.79	0.45	0.68	0.44	2.77	0.87	0.43	0.58	0.40	6.00
719	Euarchontoglires	Rodentia	Heteromyidae	Microdipodops_megacephalus	12.30	8.74	2.31	0.87	2.82	1.05	12.09	1.19	0.60	1.13	0.54	2.66	0.53	0.44	0.57	0.45	1.35	0.73	0.38	0.48	0.43	4.81
720	Euarchontoglires	Rodentia	Heteromyidae	Dipodomys_deserti	107.63	15.58	2.99	1.14	4.87	1.78	20.55	1.69	1.00	1.50	1.11	3.47	0.78	0.73	0.85	0.66	2.12	1.12	0.72	0.75	0.62	7.61
721	Euarchontoglires	Rodentia	Heteromyidae	Dipodomys_merriami	37.91	12.24	2.82	1.00	3.67	1.31	16.76	1.36	0.75	1.28	0.73	2.74	0.56	0.48	0.64	0.51	1.49	0.78	0.46	0.70	0.54	5.40
722	Euarchontoglires	Rodentia	Geomyidae	Thomomys_mazama	93.07	17.56	4.64	1.65	6.92	2.60	16.55	2.74	1.32	2.44	1.48	5.09	1.44	0.90	1.95	1.15	2.08	1.84	1.34	1.35	0.98	11.13
723	Euarchontoglires	Rodentia	Geomyidae	Geomys_pinetis	201.15	18.73	3.88	1.73	5.06	2.44	18.44	1.91	1.00	1.88	1.11	4.51	1.12	0.73	1.15	0.80	2.15	1.34	0.77	0.87	0.84	7.33
724	Euarchontoglires	Rodentia	Geomyidae	Cratogeomys_castanops	266.83	26.46	6.59	2.86	9.91	6.60	26.68	4.05	1.94	3.87	2.62	6.87	2.27	1.78	2.79	1.70	2.81	2.81	1.90	2.15	1.81	15.63
725	Euarchontoglires	Rodentia	Heteromyidae	Heteromys_nelsoni	67.55	18.27	3.44	1.43	4.73	1.77	17.12	2.13	1.02	1.93	0.79	5.72	0.87	0.68	1.03	0.73	3.49	1.24	0.71	0.87	0.62	7.73
726	Euarchontoglires	Rodentia	Heteromyidae	Perognathus_fasciatus	11.29	9.34	1.89	0.80	2.53	1.08	9.71	1.10	0.50	0.95	0.59	2.36	0.54	0.38	0.60	0.40	1.41	0.71	0.36	0.44	0.34	4.07
727	Euarchontoglires	Rodentia	Heteromyidae	Chaetodipus_penicillatus	15.57	11.17	2.19	0.91	2.57	1.12	10.76	1.22	0.65	1.25	0.56	3.13	0.45	0.50	0.62	0.44	1.63	0.78	0.42	0.52	0.39	4.54
728	Euarchontoglires	Rodentia	Castoridae	Castor_fiber	19000.00	82.06	22.20	9.80	29.33	14.83	91.14	12.07	6.91	12.05	4.54	21.50	6.67	4.06	7.12	3.42	11.04	7.22	4.75	5.46	3.52	33.82
729	Euarchontoglires	Rodentia	Castoridae	Castor_canadensis	18124.41	53.36	18.02	7.17	22.11	11.70	57.13	8.90	3.67	9.43	4.33	16.28	4.45	3.34	5.24	2.86	8.70	5.82	3.99	3.70	3.43	24.43
730	Euarchontoglires	Lagomorpha	Ochotonidae	Ochotona_alpina	150.00	25.96	6.12	1.83	5.16	2.64	20.50	3.24	1.63	2.50	0.82	7.43	1.39	1.01	1.53	0.86	3.55	1.71	0.89	1.01	0.89	9.64
731	Euarchontoglires	Lagomorpha	Leporidae	Pronolagus_rupestris	2249.99	57.09	8.56	3.97	8.29	5.16	47.19	5.77	3.04	5.29	1.96	17.78	2.93	1.96	2.79	1.88	7.38	2.86	1.84	1.91	1.57	NA
732	Euarchontoglires	Lagomorpha	Leporidae	Nesolagus_netscheri	1511.67	58.35	9.57	3.95	7.77	4.07	54.14	6.88	2.84	5.10	1.91	17.79	2.45	2.10	2.88	1.93	7.57	2.69	1.74	2.39	1.67	18.89
733	Euarchontoglires	Lagomorpha	Leporidae	Poelagus_marjorita	2509.70	69.68	13.39	4.88	9.74	6.70	62.22	6.87	4.21	6.77	3.23	21.25	4.39	2.52	3.57	2.59	7.69	3.14	2.29	2.66	2.48	20.27
734	Euarchontoglires	Lagomorpha	Leporidae	Lepus_sp	2554.35	99.31	17.58	6.05	11.87	7.24	100.29	8.47	6.52	10.60	3.89	33.56	4.34	3.00	4.64	2.48	16.30	4.76	2.37	3.19	2.70	33.35
735	Euarchontoglires	Lagomorpha	Leporidae	Sylvilagus_bachmani	714.53	47.86	7.28	3.50	6.92	4.53	45.05	5.05	2.89	5.26	2.17	15.01	2.19	1.58	2.51	1.56	6.95	2.43	1.26	1.66	1.40	15.01
736	Euarchontoglires	Lagomorpha	Leporidae	Pentalagus_furnessi	2240.00	65.27	13.48	5.34	11.76	7.79	58.21	7.49	4.13	7.29	3.37	18.72	3.35	2.62	4.34	2.33	7.36	4.32	3.09	3.28	2.34	NA
737	Euarchontoglires	Lagomorpha	Leporidae	Oryctolagus_cuniculus	1590.57	64.50	12.30	4.15	9.23	5.05	57.18	5.70	3.76	6.19	2.42	18.81	2.47	2.13	3.16	1.99	9.17	3.15	1.84	2.42	2.07	22.07
738	Euarchontoglires	Lagomorpha	Leporidae	Romerolagus_diazi	465.58	41.75	8.54	3.00	6.36	4.44	36.75	4.18	2.38	4.31	1.60	12.40	1.99	1.43	2.13	1.10	4.20	2.11	1.37	1.61	1.17	11.00
739	Xenarthra	Cingulata	Dasypodidae	Dasypus_sp	4149.37	42.48	11.43	5.83	15.19	5.80	28.81	5.77	3.54	7.09	3.93	14.73	6.68	4.47	5.35	4.17	5.04	5.10	4.99	5.08	3.36	22.27
740	Xenarthra	Cingulata	Chlamyphoridae	Euphractus_sexcinctus	4731.16	38.40	11.49	6.10	14.87	5.29	24.89	4.70	2.41	5.60	3.29	13.47	4.41	2.49	3.83	3.67	2.94	4.19	4.10	3.90	4.36	22.86
741	Xenarthra	Cingulata	Chlamyphoridae	Chaetophractus_villosus	4372.80	53.56	19.75	15.17	26.72	14.31	39.07	10.55	4.06	11.45	5.82	14.36	6.24	4.29	6.75	5.29	3.94	6.27	6.29	6.57	5.17	33.80
742	Xenarthra	Cingulata	Chlamyphoridae	Chlamyphorus_truncatus	83.53	17.97	6.17	4.01	11.19	4.11	10.76	2.79	1.36	3.74	1.86	4.27	2.72	1.59	2.09	2.20	2.61	1.94	1.85	1.53	1.85	15.28
743	Xenarthra	Cingulata	Chlamyphoridae	Tolypeutes_matacus	1303.47	36.75	10.07	4.13	13.67	6.21	26.08	6.71	2.34	5.32	3.10	5.00	5.90	4.47	4.82	4.65	4.67	3.55	3.74	3.83	3.59	25.67
744	Xenarthra	Cingulata	Chlamyphoridae	Priodontes_maximus	40641.89	110.14	36.54	12.63	53.85	28.39	61.89	23.00	7.66	17.56	11.42	14.80	21.38	18.23	22.40	12.22	17.16	18.27	13.99	12.28	13.77	104.19
745	Xenarthra	Cingulata	Chlamyphoridae	Cabassous_chacoensis	1490.01	42.80	12.15	9.26	18.15	8.99	23.90	5.89	3.35	5.82	5.11	9.26	4.97	4.10	5.16	4.52	6.10	4.49	4.10	3.60	4.24	29.03
746	Xenarthra	Pilosa	Myrmecophagidae	Tamandua_tetradactyla	4800.00	87.45	22.58	23.46	39.82	11.75	71.93	11.09	7.51	15.71	7.14	18.06	13.90	6.34	12.69	6.69	6.48	12.40	11.85	12.02	9.94	61.27
747	Xenarthra	Pilosa	Myrmecophagidae	Myrmecophaga_tridactyla	29531.83	191.62	51.94	57.50	96.03	29.93	211.76	23.18	24.63	41.52	16.47	60.36	22.95	13.21	20.39	17.33	10.08	22.02	20.53	20.81	16.00	101.41
748	Xenarthra	Pilosa	Cyclopedidae	Cyclopes_didactylus	263.95	26.69	7.18	4.61	12.90	3.67	20.59	4.36	2.98	5.53	2.15	6.36	5.98	4.64	4.89	3.17	6.20	4.96	3.74	2.72	3.17	23.01
749	Xenarthra	Pilosa	Megalonychidae	Choloepus_didactylus	6646.50	180.02	26.35	14.58	40.88	14.04	218.07	13.60	12.27	23.15	7.57	41.09	10.15	6.04	8.58	7.38	5.18	8.96	9.21	8.97	9.28	109.19
750	Xenarthra	Pilosa	Bradypodidae	Bradypus_tridactylus	4375.80	148.70	19.94	8.98	32.50	9.07	143.36	11.67	6.59	17.04	5.50	20.47	7.36	3.69	4.40	6.32	28.00	5.63	4.74	6.18	6.07	83.01
751	Afrotheria	Sirenia	Trichechidae	Trichechus_senegalensis	454000.00	171.81	61.10	26.65	59.17	28.33	122.89	37.02	19.53	29.90	21.38	66.78	16.80	8.87	19.50	8.24	34.52	19.17	12.50	19.21	8.06	69.23
752	Afrotheria	Sirenia	Dugongidae	Dugong_dugon	295000.00	122.66	58.33	18.36	56.92	32.80	100.93	27.25	16.46	26.65	13.68	63.61	13.94	8.94	18.45	9.44	24.92	14.73	10.31	14.05	8.16	49.31
753	Afrotheria	Proboscidea	Elephantidae	Loxodonta_africana	3824539.93	865.54	205.36	78.48	221.42	124.72	674.55	97.05	41.89	131.15	39.88	157.99	59.90	58.61	71.47	42.39	69.54	57.11	50.61	51.69	32.45	116.37
754	Afrotheria	Proboscidea	Elephantidae	Elephas_maximus	3269794.34	700.78	168.14	83.78	181.60	81.97	547.66	65.85	35.53	94.88	34.47	122.46	49.09	49.64	62.62	26.36	59.26	46.06	39.42	45.86	27.74	83.81
755	Afrotheria	Hyracoidea	Procaviidae	Procavia_capensis	2952.48	65.81	14.33	6.12	11.39	8.96	44.04	6.84	4.06	8.22	2.49	16.01	3.70	2.92	4.61	2.59	7.83	4.32	3.24	3.64	2.51	16.52
756	Afrotheria	Hyracoidea	Procavidae	Heterohyrax_brucei	2453.66	64.54	15.82	5.08	12.38	7.62	42.08	7.36	3.08	7.58	3.93	14.20	3.93	2.87	4.67	2.51	7.91	3.90	3.39	3.56	2.81	NA
757	Afrotheria	Hyracoidea	Procavidae	Dendrohyrax_arboreus	2981.11	66.33	17.04	6.38	15.16	8.04	44.96	8.11	3.58	8.63	2.95	16.22	4.72	3.05	5.30	2.70	8.67	4.66	3.50	3.46	2.54	14.48
758	Afrotheria	Tubulidentata	Orycteropodidae	Orycteropus_afer	56175.20	141.83	34.83	17.17	56.12	20.97	100.91	19.41	10.12	27.32	15.61	54.23	17.57	10.06	11.26	9.95	40.88	10.34	9.12	10.28	9.77	98.05
759	Afrotheria	Macroscelidea	Macroscelididae	Rhynchocyon_petersi	423.99	37.55	7.53	2.95	7.41	4.46	36.81	4.42	2.58	4.16	1.90	16.74	2.04	2.12	2.35	1.50	6.08	2.45	1.41	1.73	1.50	16.98
760	Afrotheria	Macroscelidea	Macroscelididae	Macroscelides_micus	38.64	13.80	2.62	1.12	2.69	1.54	19.55	1.68	1.04	1.91	0.93	5.25	0.84	0.57	0.71	0.51	1.99	0.73	0.44	0.57	0.47	4.56
761	Afrotheria	Macroscelidea	Macroscelididae	Macroscelides_proboscideus	38.64	17.66	3.97	1.38	3.17	2.06	22.81	1.90	1.19	2.55	1.37	5.04	0.91	0.71	0.87	0.64	2.10	1.02	0.62	0.58	0.61	5.82
762	Afrotheria	Macroscelidea	Macroscelididae	Petrosaltator_rozeti	43.07	17.72	3.48	1.45	2.98	1.81	22.34	1.87	1.26	2.42	1.01	5.35	0.81	0.62	0.76	0.51	1.92	0.88	0.44	0.48	0.47	4.93

						Humerus					Radius					Metacarpal					Phalanx					
	Superord. group	Order	Family	Species	Mass	L	PW	MW	DW	H	L	PW	MW	DW	H	L	PW	MW	DW	H	L	PW	MW	DW	H	DL
763	Afrotheria	Macroscelidea	Macroscelididae	Petrodromus_tetradactylus	201.00	24.39	4.64	2.20	4.57	2.28	31.18	2.79	1.87	4.01	1.57	8.82	1.10	0.98	1.26	0.86	4.04	1.37	0.89	1.01	0.87	8.90
764	Afrotheria	Macroscelidea	Macroscelididae	Elephantulus_brachyrhynchus	45.11	16.91	3.42	1.29	3.02	1.98	17.45	1.92	1.18	2.18	1.05	4.85	0.64	0.52	0.78	0.52	1.90	0.80	0.41	0.50	0.52	5.01
765	Afrotheria	Afrosoricida	Potamogalidae	Potamogale_velox	670.99	26.60	5.80	2.81	7.04	3.06	17.55	3.22	1.47	2.98	1.73	9.53	1.66	1.08	1.96	1.22	5.97	1.85	0.99	1.32	1.05	11.90
766	Afrotheria	Afrosoricida	Potamogalidae	Micropotamogale_ruwenzorii	109.13	18.41	4.60	2.01	6.01	3.24	14.33	2.17	1.10	2.33	1.01	7.21	1.18	0.73	1.27	0.84	4.59	1.39	0.74	1.05	0.81	10.02
767	Afrotheria	Afrosoricida	Tenrecidae	Microgale_mergulus	76.86	16.39	3.64	2.16	5.68	1.90	14.84	1.75	1.00	1.91	1.12	6.48	0.77	0.66	1.02	0.64	4.08	1.03	0.57	0.76	0.61	9.68
768	Afrotheria	Afrosoricida	Tenrecidae	Nesogale_sp	42.84	19.05	3.06	1.49	4.81	1.75	17.18	1.90	1.14	1.83	0.82	6.68	1.09	0.67	1.26	0.56	3.72	1.16	0.57	0.83	0.55	7.81
769	Afrotheria	Afrosoricida	Tenrecidae	Microgale_longicaudata	8.08	9.55	1.93	0.95	2.44	0.95	10.96	0.91	0.60	0.94	0.59	3.51	0.46	0.37	0.61	0.42	2.38	0.59	0.38	0.52	0.35	4.61
770	Afrotheria	Afrosoricida	Tenrecidae	Oryzorictes_tetradactylus	35.99	13.61	3.65	1.68	6.23	2.53	11.34	1.83	0.91	1.93	1.04	3.52	1.39	0.81	1.28	0.88	2.20	1.38	0.84	1.16	0.93	9.01
771	Afrotheria	Afrosoricida	Tenrecidae	Geogale_aurita	6.69	9.64	1.80	0.96	2.14	0.89	8.13	0.92	0.57	1.05	0.55	3.50	0.48	0.34	0.60	0.32	2.08	0.55	0.29	0.43	0.31	4.38
772	Afrotheria	Afrosoricida	Tenrecidae	Tenrec_ecaudatus	887.59	38.84	8.57	4.13	12.29	5.12	30.70	4.42	3.08	6.30	2.91	12.16	2.49	1.97	3.06	1.68	5.49	2.95	1.87	2.21	1.50	15.43
773	Afrotheria	Afrosoricida	Tenrecidae	Hemicentetes_semispinosus	134.00	13.88	4.51	2.59	6.00	1.67	11.57	2.18	1.17	3.02	1.50	6.22	1.64	1.04	1.76	1.02	3.18	1.65	1.05	1.42	0.86	8.99
774	Afrotheria	Afrosoricida	Tenrecidae	Setifer_setosus	185.00	25.53	5.29	3.06	6.95	2.29	20.60	3.44	1.58	3.15	1.58	8.04	1.39	1.07	1.75	0.91	4.42	1.65	0.98	1.32	0.87	10.60
775	Afrotheria	Afrosoricida	Tenrecidae	Echinops_telfairi	152.25	18.57	4.03	2.71	5.16	1.74	16.12	2.13	1.32	2.56	1.31	5.43	1.17	0.75	1.28	0.70	3.19	1.45	0.79	1.04	0.67	8.19
776	Afrotheria	Afrosoricida	Chrysochloridae	Eremitalpa_granti	22.04	10.99	4.50	2.06	7.29	1.50	8.03	1.74	1.18	2.40	1.03	1.61	2.56	1.92	1.44	0.77	NA	NA	NA	NA	NA	7.25
777	Afrotheria	Afrosoricida	Chrysochloridae	Huetia_leucorhina	41.00	10.46	4.06	2.14	7.41	1.83	6.84	1.83	1.26	2.51	0.97	2.60	2.56	1.91	1.75	0.94	NA	NA	NA	NA	NA	6.22
778	Afrotheria	Afrosoricida	Chrysochloridae	Chrysochloris_asiatica	37.16	12.84	5.11	2.58	9.88	2.23	9.40	2.06	1.42	2.74	1.20	2.61	2.96	2.20	1.91	0.88	NA	NA	NA	NA	NA	8.16
779	Afrotheria	Afrosoricida	Chrysochloridae	Amblysomus_hottentotus	62.60	12.28	4.96	2.95	11.64	2.15	8.67	2.08	1.48	2.77	0.83	2.83	3.04	2.03	1.52	1.15	NA	NA	NA	NA	NA	9.83
780	Marsupialia	Paucituberculata	Caenolestidae	Rhyncholestes_raphanurus	21.94	12.82	3.07	1.18	4.35	1.58	15.31	1.48	0.82	1.47	0.86	3.89	0.94	0.64	0.93	0.59	2.33	1.19	0.65	0.75	0.57	5.99
781	Marsupialia	Paucituberculata	Caenolestidae	Lestoros_inca	23.07	13.81	3.22	1.20	3.96	1.82	15.03	1.43	0.98	1.59	0.94	4.37	0.67	0.49	1.00	0.48	2.79	1.10	0.50	0.71	0.44	6.65
782	Marsupialia	Paucituberculata	Caenolestidae	Caenolestes_fuliginosus	28.64	12.22	2.75	1.28	4.01	1.50	14.27	1.40	0.76	1.75	0.83	4.44	0.83	0.56	0.96	0.49	2.81	1.25	0.63	0.85	0.39	6.53
783	Marsupialia	Didelphimorphia	Didelphidae	Glironia_venusta	114.00	16.78	3.06	1.69	4.42	2.13	17.51	1.58	1.05	1.26	1.12	3.73	0.88	0.63	1.06	0.59	2.84	1.12	0.65	0.75	0.56	5.89
784	Marsupialia	Didelphimorphia	Didelphidae	Monodelphis_domestica	93.45	24.69	4.72	2.28	7.40	4.01	22.51	2.14	1.28	2.49	1.82	5.50	1.00	0.75	1.24	0.85	3.39	1.32	0.79	0.86	0.70	7.73
785	Marsupialia	Didelphimorphia	Didelphidae	Marmosa_robinsoni	60.57	23.39	4.20	2.14	6.64	3.16	23.56	2.19	1.29	2.01	2.00	4.86	1.22	0.91	1.49	0.93	4.97	1.66	0.99	1.20	0.84	9.50
786	Marsupialia	Didelphimorphia	Didelphidae	Gracilinanus_agilis	22.03	14.67	2.95	1.49	4.60	2.30	17.04	1.32	0.94	1.52	1.14	3.41	0.78	0.46	0.79	0.49	3.07	0.87	0.52	0.60	0.47	6.18
787	Marsupialia	Didelphimorphia	Didelphidae	Thylamys_venustus	17.80	16.63	3.24	1.68	4.65	2.29	17.61	1.50	0.98	1.49	1.10	3.71	0.73	0.46	0.96	0.58	2.83	1.07	0.52	0.65	0.52	5.93
788	Marsupialia	Didelphimorphia	Didelphidae	Marmosops_incanus	59.88	18.71	3.61	1.77	5.34	2.15	22.49	1.52	0.95	1.82	1.27	4.51	0.78	0.47	1.11	0.61	3.69	1.16	0.60	0.75	0.55	7.20
789	Marsupialia	Didelphimorphia	Didelphidae	Metachirus_nudicaudatus	363.77	41.22	7.92	3.94	9.75	6.22	40.28	3.44	2.90	3.65	2.68	10.49	1.61	1.50	2.48	1.37	5.54	2.41	1.38	1.63	1.11	11.30
790	Marsupialia	Didelphimorphia	Didelphidae	Lutreolina_crassicaudata	554.77	35.49	6.40	2.76	9.34	4.24	32.92	3.31	2.09	3.78	2.92	9.75	1.85	1.20	2.31	1.47	5.88	2.68	1.41	1.58	1.11	12.56
791	Marsupialia	Didelphimorphia	Didelphidae	Philander_opossum	425.81	47.19	8.62	3.81	12.27	5.62	47.01	4.23	2.63	4.13	3.24	11.54	2.42	1.57	2.73	1.54	7.64	2.76	1.50	1.75	1.21	15.03
792	Marsupialia	Didelphimorphia	Didelphidae	Didelphis_sp	1428.30	42.09	8.02	4.50	12.13	5.30	43.38	4.42	2.53	4.54	3.13	10.35	1.87	1.55	2.80	1.40	7.40	2.84	1.45	1.87	1.21	14.94
793	Marsupialia	Didelphimorphia	Didelphidae	Chironectes_minimus	974.33	50.23	9.12	3.75	12.78	5.10	54.40	4.29	2.59	5.23	2.91	15.60	2.17	2.00	3.24	1.92	11.31	3.22	1.77	2.47	1.68	23.05
794	Marsupialia	Didelphimorphia	Didelphidae	Caluromysiops_irrupta	257.48	46.89	10.54	4.89	14.86	7.94	51.51	4.99	5.50	5.73	3.90	9.89	2.40	1.67	3.02	1.74	9.95	3.79	2.29	1.99	1.55	20.25
795	Marsupialia	Didelphimorphia	Didelphidae	Caluromys_sp	307.84	37.43	7.10	3.58	11.23	3.50	40.49	3.29	3.26	3.60	1.95	8.43	2.19	1.51	2.57	1.44	7.68	2.44	1.64	1.95	1.08	14.63
796	Marsupialia	Didelphimorphia	Didelphidae	Caluromys_derbianus	326.72	41.22	6.54	3.45	11.10	4.09	42.69	3.77	2.43	3.91	3.81	8.70	2.04	1.43	2.06	1.15	8.48	2.66	1.30	1.76	1.12	17.46
797	Marsupialia	Microbiotheria	Microbiotheriidae	Dromiciops_gliroides	25.00	14.39	2.89	1.33	4.24	1.66	16.97	1.35	0.92	1.51	0.88	3.79	0.76	0.55	0.94	0.53	3.46	1.13	0.49	0.70	0.47	6.85
798	Marsupialia	Notoryctemorphia	Notoryctidae	Notoryctes_typhlops	55.00	12.95	4.37	2.57	8.21	3.26	7.88	2.57	1.52	3.04	1.36	5.41	2.63	1.15	2.19	1.77	11.82	NA	NA	NA	NA	11.82
799	Marsupialia	Peramelemorphia	Thylacomyidae	Macrotis_lagotis	1229.58	41.00	9.83	3.45	11.53	7.07	46.59	4.77	3.86	6.55	2.44	15.30	3.76	2.81	3.93	2.30	5.41	3.62	2.96	2.70	3.50	19.85
800	Marsupialia	Peramelemorphia	Peramelidae	Isoodon_obesulus	824.76	40.35	8.65	3.44	11.16	5.58	32.54	4.14	4.56	5.05	2.70	11.58	3.78	2.53	3.34	1.91	4.48	3.34	2.26	2.40	2.13	17.24
801	Marsupialia	Peramelemorphia	Peramelidae	Perameles_nasuta	720.26	39.01	7.33	2.76	10.11	5.41	35.58	5.05	3.91	4.90	2.30	13.47	3.50	2.56	3.50	1.55	5.71	3.70	2.31	2.61	1.92	19.45
802	Marsupialia	Peramelemorphia	Peramelidae	Echymipera_kalubu	825.16	34.54	7.38	2.97	9.57	4.36	26.18	3.36	3.51	4.70	2.30	10.27	3.80	2.81	3.28	1.75	4.66	3.31	2.41	2.33	1.83	13.99
803	Marsupialia	Peramelemorphia	Peramelidae	Peroryctes_raffrayana	905.63	43.41	9.62	2.81	11.24	5.71	45.15	4.15	4.41	5.92	1.94	16.46	3.67	2.11	4.29	1.70	7.90	4.17	2.13	2.66	1.47	22.65
804	Marsupialia	Dasyuromorpha	Thylacidae	Thylacinus_cynocephalus	29999.99	150.67	31.21	13.20	28.42	15.58	148.78	13.18	10.34	17.30	5.84	38.44	6.63	5.26	8.64	6.29	16.54	9.03	6.17	7.18	4.87	39.71
805	Marsupialia	Dasyuromorpha	Myrmecobiidae	Myrmecobius_fasciatus	511.44	30.65	7.19	2.89	10.53	5.62	31.53	3.54	2.33	4.62	2.66	11.16	1.85	1.60	2.48	1.58	3.05	2.48	1.99	1.98	1.15	14.36
806	Marsupialia	Dasyuromorpha	Dasyuridae	Sminthopsis_crassicaudata	15.98	11.77	2.09	0.77	2.64	1.12	14.69	1.08	0.60	1.12	0.74	2.65	0.44	0.29	0.55	0.40	1.31	0.62	0.32	0.41	0.34	3.26
807	Marsupialia	Dasyuromorpha	Dasyuridae	Antechinomys_laniger	25.57	14.09	2.07	0.96	2.26	1.14	19.99	1.02	0.76	1.13	0.76	2.97	0.49	0.38	0.62	0.37	1.41	0.68	0.37	0.47	0.36	4.10
808	Marsupialia	Peramelemorphia	Chaeropodidae	Chaeropus_ecaudatus	219.51	28.89	5.75	2.09	5.11	2.81	35.18	2.53	1.95	3.52	1.97	13.93	2.62	1.55	2.21	1.15	5.35	2.23	1.25	1.62	1.17	10.94
809	Marsupialia	Dasyuromorpha	Dasyuridae	Sarcophilus_harrisii	8202.25	111.91	24.25	9.26	28.75	15.36	110.20	11.72	7.18	14.14	5.87	30.19	4.45	3.68	7.77	3.62	12.10	6.37	4.01	5.21	2.57	NA
810	Marsupialia	Dasyuromorpha	Dasyuridae	Dasyurus_maculatus	3284.15	72.86	15.14	5.52	19.12	10.01	64.25	5.58	4.16	8.15	3.66	15.31	2.98	2.43	3.80	2.33	9.52	4.43	2.83	3.27	2.09	24.08
811	Marsupialia	Dasyuromorpha	Dasyuridae	Dasyuroides_byrnei	109.47	26.32	4.66	1.83	5.17	2.02	32.36	2.09	1.36	2.65	1.34	7.25	0.85	0.76	1.28	0.70	3.20	1.53	0.78	1.01	0.66	9.02
812	Marsupialia	Dasyuromorpha	Dasyuridae	Dasycercus_cristicauda	99.54	19.77	3.63	1.55	5.31	1.87	20.86	1.75	0.96	2.28	1.17	5.09	0.75	0.64	1.04	0.64	2.47	1.27	0.68	0.83	0.62	7.34
813	Marsupialia	Dasyuromorpha	Dasyuridae	Phascogale_pirata	179.88	35.16	6.14	2.66	5.45	3.22	38.28	2.63	1.99	2.79	1.37	8.55	0.83	0.85	1.77	1.10	5.68	1.70	1.04	1.51	1.07	13.55

						Humerus					Radius					Metacarpal					Phalanx					
	Superord. group	Order	Family	Species	Mass	L	PW	MW	DW	H	L	PW	MW	DW	H	L	PW	MW	DW	H	L	PW	MW	DW	H	DL
814	Marsupialia	Dasyuromorpha	Dasyuridae	Antechinus_stuartii	29.01	15.11	2.81	1.29	3.59	1.72	18.36	1.27	0.95	1.62	0.88	3.48	0.60	0.49	0.82	0.44	1.92	0.81	0.55	0.70	0.45	5.46
815	Marsupialia	Diprotodontia	Phascolarctidae	Phascolarctos_cinereus	6528.74	112.10	29.88	12.63	39.04	16.71	127.78	12.34	9.36	16.01	6.41	30.71	8.70	6.54	9.58	4.99	19.86	10.01	6.42	6.38	5.38	53.97
816	Marsupialia	Diprotodontia	Vombatidae	Vombatus_ursinus	26000.00	116.69	37.34	11.22	45.53	21.57	106.82	12.03	10.67	22.47	6.95	23.73	9.73	4.86	9.28	5.33	8.72	10.03	6.92	6.41	4.44	34.82
817	Marsupialia	Diprotodontia	Vombatidae	Lasiorhinus_latifrons	26163.80	114.92	40.94	13.31	50.47	24.28	101.54	13.69	11.09	21.65	7.99	22.13	10.44	6.62	10.78	4.87	8.73	10.24	8.16	7.88	5.32	35.27
818	Marsupialia	Diprotodontia	Burramyidae	Cercartetus_concinnus	15.96	10.74	2.23	1.08	3.26	1.20	13.41	0.99	0.57	1.20	0.79	2.30	0.53	0.38	0.67	0.38	2.16	0.78	0.37	0.46	0.33	4.19
819	Marsupialia	Diprotodontia	Phalangeridae	Trichosurus_vulpecula	2685.39	47.00	8.63	4.75	13.09	5.16	47.61	4.62	2.38	5.29	3.75	8.90	2.70	1.87	2.77	1.60	8.61	3.28	2.10	2.54	1.41	17.64
820	Marsupialia	Diprotodontia	Phalangeridae	Spilocuscus_maculatus	4060.46	77.87	15.62	6.20	21.82	7.21	79.86	6.56	4.46	8.56	4.05	14.73	4.18	2.65	4.09	2.69	13.14	5.07	2.97	3.03	2.32	NA
821	Marsupialia	Diprotodontia	Phalangeridae	Strigocuscus_pelengensis	1000.00	48.51	10.51	5.02	15.77	7.75	45.45	4.76	4.86	5.44	4.09	9.94	2.66	1.77	2.93	1.71	9.09	3.63	2.07	2.81	1.48	NA
822	Marsupialia	Diprotodontia	Phalangeridae	Phalanger_orientalis	2487.50	54.23	11.31	5.11	17.50	6.41	53.03	5.09	4.24	6.92	3.14	11.32	3.38	2.26	3.48	2.09	9.66	3.97	2.67	2.62	2.04	21.76
823	Marsupialia	Diprotodontia	Phalangeridae	Ailurops_ursinus	10000.00	102.10	20.06	9.58	32.75	9.73	102.14	9.52	6.83	14.04	5.12	20.39	5.68	4.77	8.35	3.77	18.72	8.47	5.32	6.70	4.19	48.53
824	Marsupialia	Diprotodontia	Hypsiprymnodontidae	Hypsiprymnodon_moschatus	534.25	38.84	7.80	3.49	10.88	5.46	44.08	3.52	2.99	4.13	2.11	12.00	2.14	1.52	2.60	1.28	6.43	2.88	1.66	2.02	1.02	13.52
825	Marsupialia	Diprotodontia	Macropodidae	Onychogalea_fraenata	4952.05	59.54	14.30	5.20	20.04	8.32	66.40	6.23	4.00	8.08	3.25	9.85	4.39	2.75	4.03	2.61	6.79	4.52	3.36	3.55	2.51	21.30
826	Marsupialia	Diprotodontia	Macropodidae	Dorcopsis_muelleri	5370.79	81.88	13.79	5.47	19.28	10.42	99.24	6.69	4.83	9.06	3.47	12.82	5.86	3.00	5.52	2.42	7.55	5.73	4.07	5.54	2.25	NA
827	Marsupialia	Diprotodontia	Macropodidae	Thylogale_stigmatica	4511.47	72.27	15.73	6.92	20.16	12.11	91.32	6.53	5.22	7.67	3.62	12.13	4.40	3.00	4.94	2.73	8.19	5.50	3.65	4.05	2.55	21.60
828	Marsupialia	Diprotodontia	Macropodidae	Petrogale_penicillata	6931.60	64.31	13.47	6.03	18.05	8.47	72.59	6.14	3.90	8.85	3.39	12.88	4.74	2.50	3.97	3.14	8.29	4.23	2.79	3.59	3.31	21.66
829	Marsupialia	Diprotodontia	Macropodidae	Dendrolagus_lumholtzi	6649.97	97.57	17.04	10.02	29.12	12.81	107.89	10.19	8.46	13.16	4.80	19.31	6.53	4.07	7.96	4.05	16.69	8.67	4.76	6.78	3.87	53.78
830	Marsupialia	Diprotodontia	Macropodidae	Macropus_giganteus	33409.89	214.23	36.04	23.22	56.27	26.99	273.96	18.06	13.08	22.50	10.64	39.46	11.75	8.55	14.10	6.23	23.48	13.47	8.38	10.74	6.14	68.27
831	Marsupialia	Diprotodontia	Macropodidae	Notamacropus_parryi	12629.83	86.58	17.43	7.07	22.08	9.94	113.11	4.28	5.72	11.41	4.50	17.83	7.75	4.69	6.30	3.01	10.02	5.39	4.16	5.29	3.30	34.08
832	Marsupialia	Diprotodontia	Macropodidae	Wallabia_bicolor	14999.95	94.90	17.81	9.66	26.89	13.97	125.54	9.78	8.14	13.02	5.01	20.90	5.95	4.50	7.20	3.41	12.03	7.84	5.50	6.03	3.11	36.57
833	Marsupialia	Diprotodontia	Macropodidae	Setonix_brachyurus	3027.67	60.32	13.75	6.23	18.81	9.26	70.85	6.97	6.39	7.86	3.97	13.74	3.94	2.73	4.94	2.79	7.68	4.81	3.26	3.86	2.14	21.95
834	Marsupialia	Diprotodontia	Potoroidae	Aepyprymnus_rufescens	2810.31	41.35	9.39	4.04	14.64	8.20	42.90	3.78	2.70	5.69	4.74	11.25	4.55	2.28	3.32	2.76	4.12	3.24	2.90	3.00	2.67	21.81
835	Marsupialia	Diprotodontia	Potoroidae	Bettongia_gaimardi	1667.55	25.78	5.91	2.34	8.47	4.28	27.40	2.92	2.52	4.68	1.94	8.74	3.43	2.16	2.76	2.21	3.68	2.79	2.67	2.56	2.30	16.46
836	Marsupialia	Diprotodontia	Potoroidae	Potorous_tridactylus	1054.67	35.34	7.36	2.94	9.33	5.26	42.13	3.23	2.36	4.57	2.25	10.22	3.12	1.71	2.65	1.94	3.28	2.73	1.84	1.97	1.42	NA
837	Marsupialia	Diprotodontia	Tarsipedidae	Tarsipes_rostratus	9.66	12.81	2.26	0.86	3.15	1.05	13.22	1.09	0.63	1.28	0.85	2.60	0.49	0.38	0.67	0.41	1.90	0.66	0.44	0.53	0.53	3.74
838	Marsupialia	Diprotodontia	Pseudocheiridae	Pseudocheirus_peregrinus	895.22	45.72	9.76	3.96	12.75	4.91	46.59	4.53	2.85	4.96	2.61	8.34	2.26	1.57	2.25	1.57	7.54	3.05	1.51	1.89	1.55	17.27
839	Marsupialia	Diprotodontia	Pseudocheiridae	Petauroides_volans	1257.17	74.44	10.46	4.49	13.13	4.90	63.81	4.86	3.09	5.99	2.94	10.22	2.75	2.17	2.80	1.79	12.46	3.64	1.74	1.99	1.99	27.11
840	Marsupialia	Diprotodontia	Pseudocheiridae	Hemibelideus_lemuroides	993.59	53.88	10.40	5.08	15.11	5.01	52.65	5.05	3.34	6.33	3.01	9.54	2.88	2.20	2.93	1.88	10.04	3.53	2.00	2.20	2.04	22.53
841	Marsupialia	Diprotodontia	Petauridae	Petaurus_breviceps	120.76	28.69	5.07	2.17	6.92	2.36	33.79	2.19	1.95	2.78	1.13	5.80	1.30	0.82	1.42	0.84	5.41	1.81	0.88	0.93	0.82	12.37
842	Marsupialia	Diprotodontia	Petauridae	Dactylopsila_trivirgata	413.41	37.41	9.34	4.20	13.04	7.17	41.67	4.37	2.82	4.63	2.65	9.18	2.12	1.23	2.08	1.31	9.31	2.47	1.15	1.55	1.57	20.84
843	Marsupialia	Diprotodontia	Acrobatidae	Acrobates_pygmaeus	13.84	12.44	2.15	1.07	3.26	1.11	14.02	1.08	0.78	1.36	0.73	2.66	0.60	0.44	0.71	0.42	2.69	0.84	0.42	0.54	0.39	5.56

S1.1. References

Afflerbaugh, K. (2002). *"Conepatus chinga" (On-line)*. Animal Diversity Web. https://animaldiversity.org/accounts/Conepatus_chinga/

Aguilar, S. (2011). *"Peromyscus leucopus" (On-line)*. Animal Diversity Web. https://animaldiversity.org/accounts/Peromyscus_leucopus/

Allen, D. (2000). *"Notiosorex crawfordi" (On-line)*. Animal Diversity Web. https://animaldiversity.org/accounts/Notiosorex_crawfordi/

Amador, L. I., & Giannini, N. P. (2016). Phylogeny and evolution of body mass in didelphid marsupials (Marsupialia: Didelphimorphia: Didelphidae). *Organisms Diversity and Evolution*, *16*(3), 641–657. https://doi.org/10.1007/s13127-015-0259-x

Ambrose, L. (2013). *Euoticus elegantulus* Southern Needle-clawed Galago (Elegant Galago). In J. Kingdon, D. C. D. Happold, T. M. Butynski, M. Hoffman, M. Happold, & J. Kalina (Eds.), *Mammals of Africa Volume II: Primates* (pp. 442–444). Bloomsbury.

Anna Toenjes, N. (2014). *"Felis catus" (On-line)*. Animal Diversity Web. https://animaldiversity.org/accounts/Felis_catus/

Aplin, K. P., Rhind, S. G., Ten Have, J., & Chesser, R. T. (2015). Taxonomic revision of *Phascogale tapoatafa* (Meyer, 1793) (Dasyuridae; Marsupialia), including descriptions of two new subspecies and confirmation of *P. pirata* Thomas, 1904 as a "Top End" endemic. *Zootaxa*, *4055*(1), 1–73. https://doi.org/10.11646/zootaxa.4055.1.1

Aulagnier, S., & Vogel, P. (2013). *Crocidura russula* Greater Shrew (Greater White-toothed Shrew). In *Mammals of Africa Volume IV: Hedgehogs, shrews and bats* (pp. 129–130). Bloomsbury.

Ávila-Palma, H. D., Turcios-Casco, M. A., Bautista, D. J. O., Martínez, M., & Ordoñez-Mazier, D. I. (2019). First records of *Mimon cozumelae goldman*, 1914 (Chiroptera, phyllostomidae) in the Río Plátano biosphere reserve in northeastern Honduras. *Check List*, *15*(6), 1113–1118. https://doi.org/10.15560/15.6.1113

Ballenger, L. (1999). *"Hemiechinus auritus."* Animal Diversity Web. https://animaldiversity.org/accounts/Hemiechinus_auritus/

Barrière, P., & Hutterer, R. (2013). *Congosorex verheyeni* Lesser Congo Shrew. In J. Kingdon, D. C. D. Happold, T. M. Butynski, M. Hoffman, M. Happold, & J. Kalina (Eds.), *Mammals of Africa Volume IV: Hedgehogs, shrews and bats* (pp. 53–53). Bloomsbury.

Barry, R. E., & Hoeck, H. N. (2013). *Heterohyrax brucei* Bush Hyrax (Yellow-spotted Hyrax). In J. Kingdon, D. C. D. Happold, T. M. Butynski, M. Hoffman, M. Happold, & J. Kalina (Eds.), *Mammals of Africa Volume I: Introductory chapters and Afrotheria* (pp. 161–165).

Benstead, J. P., Barnes, K. H., & Pringle, C. M. (2011). Diet, activity patterns, foraging movement and responses to deforestation of the aquatic tenrec *Limnogale mergulus* (Lipotyphla: Tenrecidae) in eastern Madagascar. *Journal of Zoology*, *1*, 119–129.

Blessing, S. (2002). *"Amorphochilus schnablii" (On-line)*. Animal Diversity Web. https://animaldiversity.org/accounts/Amorphochilus_schnablii/

Bronner, G. N. (2013). Family CHRYSOCHLORIDAE. In J. Kingdon, D. C. D. Happold, T. M. Butynski, M. Hoffman, M. Happold, & J. Kalina (Eds.), *Mammals of Africa Volume I: Introductory chapters and Afrotheria* (pp. 223–256). Bloomsbury.

Cason, M. (2009). *"Tachyglossus aculeatus" (On-line)*. Animal Diversity Web. https://animaldiversity.org/accounts/Tachyglossus_aculeatus/

Cassola, F. (2016a). *Cryptotis mexicana*. The IUCN Red List of Threatened Species. https://dx.doi.org/10.2305/IUCN.UK.2016-2.RLTS.T41374A22286065.en

Cassola, F. (2016b). *Hyosciurus heinrichi*. The IUCN Red List of Threatened Species. https://dx.doi.org/10.2305/IUCN.UK.2016-2.RLTS.T10635A22262335.en

Cassola, F. (2016c). *Melanomys caliginosus (errata version published in 2017)*. The IUCN Red List of Threatened Species. https://dx.doi.org/10.2305/IUCN.UK.2016-3.RLTS.T13046A22344255.en.

Cheng, F., Kai, H. E., Chen, Z. Z., Zhang, B., Wan, T., Li, J. T., Zhang, B. W., & Jiang, X. L. (2017). Phylogeny and systematic revision of the genus *Typhlomys* (Rodentia, Platacanthomyidae), with description of a new species. *Journal of Mammalogy*, *98*(3), 731–743. https://doi.org/10.1093/jmammal/gyx016

Chen, M., & Wilson, G. P. (2015). A multivariate approach to infer locomotor modes in Mesozoic mammals. *Paleobiology*, *21*(2), 280–312. https://doi.org/10.5061/dryad.870j3

Clark, S. T., Odell, D. K., & Lacinak, C. T. (2000). Aspects of growth in captive killer whales (*Orcinus orca*). *Marine Mammal Science*, *16*(1), 110–123. https://doi.org/10.1111/j.1748-7692.2000.tb00907.x

Contreras-Medina, R., Santiago-Alvarado, M., Espinosa, D., Rivas, G., & Luna-Vega, I. (2022). Distributional patterns and conservation of the genus *Habromys* (Rodentia: Cricetidae) in Mesoamerica. *Studies on Neotropical Fauna and Environment*. https://doi.org/10.1080/01650521.2022.2085071

Cooper, C. E., & Withers, P. C. (2002). Metabolic physiology of the numbat (*Myrmecobius fasciatus*). *Journal of Comparative Physiology B: Biochemical, Systemic, and Environmental Physiology*, *172*(8), 669–675. https://doi.org/10.1007/s00360-002-0294-8

Cover, S. (2000). *"Caperea marginata" (On-line)*. Animal Diversity Web. https://animaldiversity.org/accounts/Caperea_marginata/

Tavares, V. da C., & Mancina, C. A. (2008). *Phyllops falcatus* (Chiroptera: Phyllostomidae). *Mammalian Species*, *811*, 1–7. https://doi.org/10.1644/811.1

Desbiez, A. L. J., Santos, S. A., Alvarez, J. M., & Tomas, W. M. (2011). Forage use in domestic cattle (*Bos indicus*), capybara (*Hydrochoerus hydrochaeris*) and pampas deer (*Ozotoceros bezoarticus*) in a seasonal Neotropical wetland. *Mammalian Biology*, *76*(3), 351–357. https://doi.org/10.1016/j.mambio.2010.10.008

Dumbacher, J. P., Rathbun, G. B., Osborne, T. O., Griffin, M., & Eiseb, S. J. (2014). A new species of round-eared sengi (genus *Macroscelides*) from Namibia. *Journal of Mammalogy*, *95*(3), 443–454. https://doi.org/10.1644/13-MAMM-A-159

Dunnum, J., Vargas, J., Bernal, N., Zeballos, H., & Vivar, E. (2016). *Auliscomys pictus (errata version published in 2017)*. The IUCN Red List of Threatened Species. https://dx.doi.org/10.2305/IUCN.UK.2016-3.RLTS.T2397A22337332.en

Emmons, L. H., Leite, Y. L. R., Kock, D., & Costa, L. P. (2002). A review of the named forms of *Phyllomys* (Rodentia: Echimyidae) with the description of a new species from coastal Brazil. *American Museum Novitates*, 1–40. https://doi.org/10.1206/0003-0082(2002)380<0001:AROTNF>2.0.CO;2

Esselstyn, J. A., Achmadi, A. S., Handika, H., & Rowe, K. C. (2015). A hog-nosed shrew rat (Rodentia: Muridae) from Sulawesi Island, Indonesia. *Journal of Mammalogy*, *96*(5), 895–907. https://doi.org/10.1093/jmammal/gyv093

Fabre, A.-C., Cornette, R., Goswami, A., & Peigné, S. (2015). Do constraints associated with the locomotor habitat drive the evolution of forelimb shape? A case study in musteloid carnivorans. *Journal of Anatomy*, *226*(6), 596–610. https://doi.org/10.1111/joa.12315

Fabre, P. H., Reeve, A. H., Fitriana, Y. S., Aplin, K. P., & Helgen, K. M. (2018). A new species of Halmaheramys (Rodentia: Muridae) from Bisa and Obi Islands (North Maluku Province, Indonesia). *Journal of Mammalogy*, *99*(1), 187–208. https://doi.org/10.1093/jmammal/gyx160

Frederick, B. (2002). *"Miopithecus talapoin" (On-line)*. Animal Diversity Web. https://animaldiversity.org/accounts/Miopithecus_talapoin/

Freudenthal, M., & Suárez, E. M. (2013). Estimating body mass of fossil rodents. *Scripta Geologica*, *145*, 1–513. https://www.researchgate.net/publication/288556361

García, M. J., Medici, E. P., Naranjo, E. J., Novarino, W., & Leonardo, R. S. (2012). Distribution, habitat and adaptability of the genus tapirus. In *Integrative Zoology* (Vol. 7, Issue 4, pp. 346–355). https://doi.org/10.1111/j.1749-4877.2012.00317.x

GBIF Secretariat. (2022a). *Blarina brevicauda (Say, 1823)*. GBIF Backbone Taxonomy. https://doi.org/10.15468/39omei

GBIF Secretariat. (2022b). *Manis gigantea Illiger, 1815*. GBIF Backbone Taxonomy. https://doi.org/10.15468/39omei

GBIF Secretariat. (2022c). *Manis pentadactyla Linnaeus, 1758*. GBIF Backbone Taxonomy. https://doi.org/10.15468/39omei

GBIF Secretariat. (2022d). *Manis tricuspis Rafinesque, 1821*. GBIF Backbone Taxonomy. https://doi.org/10.15468/39omei

GBIF Secretariat. (2022e). *Poelagus marjorita (St.Leger, 1929)*. GBIF Backbone Taxonomy. https://doi.org/10.15468/39omei

GBIF Secretariat. (2022f). *Rhynchomys isarogensis Musser & Freeman, 1981*. GBIF Backbone Taxonomy. https://doi.org/10.15468/39omei

GBIF Secretariat. (2022g). *Stenocephalemys albocaudata Frick, 1914*. GBIF Backbone Taxonomy.

GBIF Secretariat. (2022h). *Sylvilagus bachmani (Waterhouse, 1839)*. GBIF Backbone Taxonomy. https://doi.org/10.15468/39omei

Gillette, C. (2005). *"Poiana richardsonii" (On-line)*. Animal Diversity Web. https://animaldiversity.org/accounts/Poiana_richardsonii/

Gochis, E. (2002). *"Neurotrichus gibbsii" (On-line)*. Animal Diversity Web. https://animaldiversity.org/accounts/Neurotrichus_gibbsii/

Gómez-Laverde, M., & Pino, J. (2016). *Transandinomys bolivaris*. The IUCN Red List of Threatened Species. https://dx.doi.org/10.2305/IUCN.UK.2016-2.RLTS.T15588A22332894.en.

Goodman, S. M., Jansen Van Vuuren, B., & Bowie, R. C. K. (2008). Specific status of populations in the Mascarene Islands referred to *Mormopterus acetabulosus* (Chiroptera: Molossidae), with description of a new species. *Journal or Mammalogy*, *89*(5), 1316–1327. https://doi.org/10.1644/07-MAMM-A-232.1

Granatosky, M. C. (2018). A review of locomotor diversity in mammals with analyses exploring the influence of substrate use, body mass and intermembral index in primates. *Journal of Zoology, 306*(4): 207–216. https://doi.org/10.1111/jzo.12608

Green, E. (2006). *"Lasiorhinus latifrons" (On-line)*. Animal Diversity Web. https://animaldiversity.org/accounts/Lasiorhinus_latifrons/

Gregg, M. (2013). *"Galictis vittata" (On-line)*. Animal Diversity Web. https://animaldiversity.org/accounts/Galictis_vittata/

Guichón, M. L., Benítez, V. B., Abba, A., Borgnia, M., & Cassini, M. H. (2003). Foraging behaviour of coypus Myocastor coypus: Why do coypus consume aquatic plants? *Acta Oecologica*, *24*(5–6), 241–246. https://doi.org/10.1016/j.actao.2003.08.001

Gumas, J. (2004). *"Peromyscus truei" (On-line)*. Animal Diversity Web. https://animaldiversity.org/accounts/Peromyscus_truei/

Happold, D. C. D. (2013a). *Atelerix albiventris* White-bellied Hedgehog (Four-toed Hedgehog). In J. Kingdon, D. C. D. Happold, T. M. Butynski, M. Hoffman, M. Happold, & J. Kalina (Eds.), *Mammals of Africa Volume VI: Hedgehogs, shrews and bats* (pp. 31–32). Bloomsbury.

Happold, D. C. D. (2013b). *Surdisorex norae* Aberdare Mole-shrew. In J. Kingdon, D. C. D. Happold, T. M. Butynski, M. Hoffman, M. Happold, & J. Kalina (Eds.), *Mammals of Africa Volume IV: Hedgehogs, shrews and bats* (pp. 183–184). Bloomsbury.

Hart, J. A. (2013). *Hyemoschus aquaticus* Water Chevrotain. In J. Kingdon, D. C. D. Happold, T. M. Butynski, M. Hoffman, M. Happold, & J. Kalina (Eds.), *Mammals of Africa Volume VI: Pigs, hippopotamuses, chevrotain, giraffes, deer and bovids* (pp. 88–92). Bloomsbury.

Hayssen, V. (2008). Patterns of body and tail length and body mass in Sciuridae. *Journal of Mammalogy*, *89*(4), 852–873. https://doi.org/10.1644/07-MAMM-A-217.1

Hayssen, V. (2011). *Tamandua tetradactyla* (Pilosa: Myrmecophagidae). *Mammalian Species*, *43*, 64–74. https://doi.org/10.1644/875.1

Heaney, L. R., Tabaranza, B. R., Rickart, E. A., Danilo S, Ingle, & Nina R. (2006). The mammals of Mt. Kitanglad Nature Park, Mindanao, Philippines. *Fieldiana: Zoology*, *112*, 1–63. https://doi.org/10.3158/0015

Hoffman, E. (2014). *"Lama guanicoe" (On-line)*. Animal Diversity Web. https://animaldiversity.org/accounts/Lama_guanicoe/

Hollis, L. (2005). Artibeus planirostris. *Mammalian Species*, *775*, 1–6. https://doi.org/10.1644/1545-1410(2005)775[0001:ap]2.0.co;2

Hood, G. A. (2020). *Semi-aquatic mammals: Ecology and biology*. John Hopkins University Press.

Hopkins, S. S. B., & Davis, E. B. (2009). Quantitative morphological proxies for the fossoriality in small mammals. *Journal of Mammalogy*, *90*(6), 1449–1460. https://doi.org/10.1644/08-MAMM-A-262R1.1

Horst, G. R., Hoagland, D. B., & Kilpatrick, C. W. (2001). The mongoose in the West Indies: The biogeography and population biology of an introduced species. In *Biogeography of the West Indies* (pp. 409–424). CRC Press. https://doi.org/10.1201/9781420039481-21

Howell, A. B. (1970). *Aquatic mammals: Their adaptations to life in the water*. Dover Publication Inc.

Hrouzková, E., Dvořáková, V., Jedlička, P., & Šumbera, R. (2013). Seismic communication in demon African mole rat *Tachyoryctes daemon* from Tanzania. *Journal of Ethology*, *31*(3), 255–259. https://doi.org/10.1007/s10164-013-0374-0

Isbell, L. A. (2013). *Erythrocebus patas* Patas Monkey (Hussar Monkey, Nisnas). In J. Kingdon, D. C. D. Happold, T. M. Butynski, M. Hoffman, M. Happold, & J. Kalina (Eds.), *Mammals of Africa Volume II: Primates* (pp. 257–263). Bloomsbury.

Isbell, L. A., & Jaffe, K. L. E. (2013). *Chlorocebus pygerythrus* Vervet Monkey. In J. Kingdon, D. C. D. Happold, T. M. Butynski, M. Hoffman, M. Happold, & J. Kalina (Eds.), *Mammals of Africa Volume II: Primates* (pp. 277–284). Bloomsbury.

Jackson, S. M. (2000). Glide angle in the genus Petaurus and a review of gliding in mammals. *Mammal Review*, *30*(1), 9–30. https://doi.org/10.1046/j.1365-2907.2000.00056.x

Jacobs, D. S., Barclay, R. M. R., & Walker, M. H. (2007). The allometry of echolocation call frequencies of insectivorous bats: Why do some species deviate from the pattern? *Oecologia*, *152*(3), 583–594. https://doi.org/10.1007/s00442-007-0679-1

Jenkins, P. D., Kilpatrick, W. C., Robinson, M. F., & Timmins, R. J. (2005a). Morphological and molecular investigations of a new family, genus and species of rodent (Mammalia: Rodentia: Hystricognatha) from lao PDR. *Systematics and Biodiversity*, *2*(4), 419–454. https://doi.org/10.1017/S1477200004001549

Jenkins, P. D., Kilpatrick, W. C., Robinson, M. F., & Timmins, R. J. (2005b). Morphological and molecular investigations of a new family, genus and species of rodent (Mammalia: Rodentia: Hystricognatha) from lao PDR. *Systematics and Biodiversity*, *2*(4), 419–454. https://doi.org/10.1017/S1477200004001549

John, J. (2005). *"Arvicanthis niloticus" (On-line)*. Animal Diversity Web. https://animaldiversity.org/accounts/Arvicanthis_niloticus/

Kroll, M. (2013). *"Tamias striatus" (On-line)*. Animal Diversity Web. https://animaldiversity.org/accounts/Tamias_striatus/

Lavrenchenko, L. A. (2003). A contribution to the systematics of *Desmomys* Thomas, 1910 (Rodentia, Muridae) with the description of a new species. *Bonner Zoologische Beiträge*, *50*(4), 313–327. https://www.researchgate.net/publication/335392202

Law, C. J. (2021). Ecological drivers of carnivoran body shape evolution. *The American Naturalist*, *198*(3), 406–420. https://doi.org/10.5061/dryad.pg4f4qrpm

Lutz, J. (2003). *"Herpestes javanicus" (On-line)*. Animal Diversity Web. https://animaldiversity.org/accounts/Herpestes_javanicus/

Makhasi, N. (2013). *Morphological and genetic variation in samango monkeys (*Cercopithecus albogularis*) in southern Africa* [Master's dissertation]. University of Fort Hare.

Malek, K. (2003). *"Lyncodon patagonicus" (On-line)*. Animal Diversity We. https://animaldiversity.org/accounts/Lyncodon_patagonicus/

Mancina, C. A. (2010). *Phyllonycteris poeyi* (Chiroptera: Phyllostomidae). *Mammalian Species*, *42*(852), 41–48. https://doi.org/10.1644/852.1

Martinez, Q., Lebrun, R., Achmadi, A. S., Esselstyn, J. A., Evans, A. R., Heaney, L. R., Miguez, R. P., Rowe, K. C., & Fabre, P. H. (2018). Convergent evolution of an extreme dietary specialisation, the olfactory system of worm-eating rodents. *Scientific Reports*, *8*(1). https://doi.org/10.1038/s41598-018-35827-0

McGraw, W. S. (2013). *Cercocebus atys* Sooty Mangabey (Smoky Mangabey). In J. Kingdon, D. C. D. Happold, T. M. Butynski, M. Hoffman, M. Happold, & J. Kalina (Eds.), *Mammals of Africa Volume II: Primates* (pp. 180–182). Bloomsbury.

Middlebrook, C. (2007). *"Vulpes lagopus" (On-line)*. Animal Diversity Web. https://animaldiversity.org/accounts/Vulpes_lagopus/

Milner, J. M., & Gaylard, A. (2013). *Dendrohyrax arboreus* Southern Tree Hyrax (Southern Tree Dassie). In J. Kingdon, D. C. D. Happold, T. M. Butynski, M. Hoffman, M. Happold, & J. Kalina (Eds.), *Mammals of Africa Volume I: Introductory chapters and Afrotheria* (pp. 152–155). Bloomsbury.

Moe, B. (2007). *"Strigocuscus celebensis" (On-line)*. Animal Diversity Web. https://animaldiversity.org/accounts/Strigocuscus_celebensis/

Molur, S. (2016a). *Blanfordimys afghanus*. The IUCN Red List of Threatened Species. https://dx.doi.org/10.2305/IUCN.UK.2016-2.RLTS.T2823A22383332.en

Molur, S. (2016b). *Episoriculus caudatus*. The IUCN Red List of Threatened Species. https://dx.doi.org/10.2305/IUCN.UK.2016-2.RLTS.T41428A22293617.en

Nielsen, T. (2005). *"Geogale aurita" (On-line)*. Animal Diversity Web. https://animaldiversity.org/accounts/Geogale_aurita/

Normile, R. (1999). *"Chaeropus ecaudatus" (On-line)*. Animal Diversity Web. https://animaldiversity.org/accounts/Chaeropus_ecaudatus/

Nowak, R. M. (1999). *Walker's mammals of the world*. Johns Hopkins University Press.

Okihiro, A. (2011). *"Nectomys squamipes" (On-line)*. Animal Diversity Web. https://animaldiversity.org/accounts/Nectomys_squamipes/

Owens, R. (2014). *"Setifer setosus" (On-line)*. Animal Diversity Web. https://animaldiversity.org/accounts/Setifer_setosus/

Pacheco, V. (2016). *Thomasomys aureus*. The IUCN Red List of Threatened Species. https://dx.doi.org/10.2305/IUCN.UK.2016-2.RLTS.T96801180A22366616.en

Patterson, B. D., Meserve, P. L., & Lang, B. K. (1990). Quantitative habitat associations of small mammals along an elevational transect in temperate rainforests of Chile. *Journal of Mammalogy*, *71*(4), 620–633. https://doi.org/10.2307/1381803

Patton, J., Catzeflis, F., Weksler, M., Percequillo, A., D'Elia, G., & Pardinas, U. (2017). *Thaptomys nigrita*. The IUCN Red List of Threatened Species. https://dx.doi.org/10.2305/IUCN.UK.2017-2.RLTS.T750A22333428.en

Perrin, M. (2013). *Elephantulus brachyrhynchus* Short-snouted Sengi (Shortsnouted Elephant-shrew). In J. Kingdon, D. C. D. Happold, T. M. Butynski, M. Hoffman, M. Happold, & J. Kalina (Eds.), *Mammals of Africa Volume I: Introductory chapters and Afrotheria* (pp. 263–265). Bloomsbury.

Perrin, M., & Rathbun, G. B. (2013a). *Elephantulus rozeti* North African Sengi (North African Elephant-shrew). In J. Kingdon, D. C. D. Happold, T. M. Butynski, M. Hoffman, M. Happold, & J. Kalina (Eds.), *Mammals of Africa Volume I: Introductory chapters and Afrotheria* (pp. 272–273). Bloomsbury.

Perrin, M., & Rathbun, G. B. (2013b). *Macroscelides proboscideus* Round-eared Sengi (Roundeared Elephant-shrew). In J. Kingdon, D. C. D. Happold, T. M. Butynski, M. Hoffman, M. Happold, & J. Kalina (Eds.), *Mammals of Africa Volume I: Introductory chapters and Afrotheria* (pp. 277–279). Bloomsbury.

Peterhans, J. C. K., Hutterer, R., Kaliba, P., & Mazibuko, L. (2008). First record of *Myosorex* (Mammalia: Soricidae) from Malawi with description ds d new species, *Myosorex gnoskei*. *Journal of East African Natural History*, *97*(1), 19–32. https://doi.org/10.2982/0012-8317(2008)97[19:fromms]2.0.co;2

Poole, J., Kahambu, P., & Whyte, I. (2013). *Loxodonta africana* Savanna Elephant (African Bush Elephant). In J. Kingdon, D. C. D. Happold, T. M. Butynski, M. Hoffman, M. Happold, & J. Kalina (Eds.), *Mammals of Africa Volume I: Introductory chapters and Afrotheria* (pp. 181–195). Bloomsbury.

Poor, A. (2005). *"Myospalacinae" (On-line)*. Animal Diversity Web. https://animaldiversity.org/accounts/Myospalacinae/

Pronga, A. (2017). *"Paraxerus cepapi" (On-line)*. Animal Diversity Web. https://animaldiversity.org/accounts/Paraxerus_cepapi/

Rasmussen, A. (2007). *"Podogymnura truei" (On-line)*. Animal Diversity Web. https://animaldiversity.org/accounts/Podogymnura_truei/

Rathbun, G. B. (2013). *Rhynchocyon petersi* Black-and-rufous Giant Sengi (Blackand- rufous Elephant-shrew). In J. Kingdon, D. C. D. Happold, T. M. Butynski, M. Hoffman, M. Happold, & J. Kalina (Eds.), *Mammals of Africa Volume I: Introductory chapters and Afrotheria* (pp. 286–287). Bloomsbury.

Ray, J. C., & Hutterer, R. (2013). *Paracrocidura schoutedeni* Schouteden's Large-headed Shrew (Lesser Large-headed Shrew). In J. Kingdon, D. C. D. Happold, T. M. Butynski, M. Hoffman, M. Happold, & J. Kalina (Eds.), *Mammals of Africa Volume IV: Hedgehogs, shrews and bats*. Bloomsbury.

Raynor, S. (2000). *"Manis pentadactyla" (On-line)*. Animal Diversity Web.

Reister, A. (2006). *"Trichys fasciculata" (On-line)*. Animal Diversity Web. https://animaldiversity.org/accounts/Trichys_fasciculata/

Rode-Margono, E. J., Nekaris, K. A. I., Kappeler, P. M., & Schwitzer, C. (2015). The largest relative testis size among primates and aseasonal reproduction in a nocturnal lemur, *Mirza zaza* . *American Journal of Physical Anthropology*, *158*(1), 165–169. https://doi.org/10.1002/ajpa.22773

Rowe, K. C., Achmadi, A. S., & Esselstyn, J. A. (2016). A new genus and species of omnivorous rodent (Muridae: Murinae) from Sulawesi, nested within a clade of endemic carnivores. *Journal of Mammalogy*, *97*(3), 978–991. https://doi.org/10.1093/jmammal/gyw029

Rowe, K., & Kennerley, R. (2019). *Hyorhinomys stuempkei*. The IUCN Red List of Threatened Species. https://dx.doi.org/10.2305/IUCN.UK.2019-1.RLTS.T92441853A92441855.en

Samuels, J. X., Meachen, J. A., & Sakai, S. A. (2013). Postcranial morphology and the locomotor habits of living and extinct carnivorans. *Journal of Morphology*, *274*(2), 121–146. https://doi.org/10.1002/jmor.20077

Samuels, J. X., & Van Valkenburgh, B. (2008). Skeletal indicators of locomotor adaptations in living and extinct rodents. *Journal of Morphology*, *269*(11), 1387–1411. https://doi.org/10.1002/jmor.10662

Santoro, K. (2004). *"Lonchophylla thomasi" (On-line)*. Animal Diversity Web. https://animaldiversity.org/accounts/Lonchophylla_thomasi/

Schaaf, C. D., Gadsby, E. L., & Butynski, T. M. (2013). *Mandrillus leucophaeus* Drill. In J. Kingdon, D. C. D. Happold, T. M. Butynski, M. Hoffman, M. Happold, & J. Kalina (Eds.), *Mammals of Africa Volume I: Introductory chapters and Afrotheria* (pp. 197–203). Bloomsbury.

Seaton, T. (2002). *"Ailurops ursinus" (On-line)*. Animal Diversity Web. https://animaldiversity.org/accounts/Ailurops_ursinus/

Semke, R. (2011). *"Semnopithecus entellus" (On-line)*. Animal Diversity Web. https://animaldiversity.org/accounts/Semnopithecus_entellus/

Severud, W. J., Windels, S. K., Belant, J. L., & Bruggink, J. G. (2013). The role of forage availability on diet choice and body condition in American beavers (*Castor canadensis*). *Mammalian Biology*, *2*, 87–93. https://doi.org/10.1016/j.mambio.2012.12.001

Shenbrot, G., Bannikova, A., Giraudoux, P., Quéré, J. P., Raoul, F., & Lebedev, V. (2017). A new recent genus and species of three-toed jerboas (Rodentia: Dipodinae) from China: A living fossil? *Journal of Zoological Systematics and Evolutionary Research*, *55*(4), 356–368. https://doi.org/10.1111/jzs.12182

Siciliano Martina, L. (2013). *"Lestoros inca" (On-line)*. Animal Diversity Web. https://animaldiversity.org/accounts/Lestoros_inca/

Smith, A. T. (2017). *Typhlomys cinereus*. The IUCN Red List of Threatened Species. https://dx.doi.org/10.2305/IUCN.UK.2017-2.RLTS.T22605A22240953.en

Smith, F. A., Smith, R. E. E., Lyons, S. K., & Payne, J. L. (2018). Body size downgrading of mammals over the late Quaternary. *Science*, *360*(6386), 310–313. https://doi.org/10.1126/science.aao5987

Smith, J. (1999). *"Zapus hudsonius" (On-line)*. Animal Diversity Web. https://animaldiversity.org/accounts/Zapus_hudsonius/

Speakman, J., Stephenson, P. J., Speakman, J. R., & Racey, P. A. (1994). Related papers Field metabolic rate in two species of shrew-tenrec, *Microgale dobsoni* and *M. talazaci*. *Comparative Biochemistry and Physiology*, *107*(2), 283–287. https://doi.org/10.1016/0300-9629(94)90382-4

Stalder, J. (2009). *"Funambulus pennantii" (On-line)*. Animal Diversity Web. https://animaldiversity.org/accounts/Funambulus_pennantii/

Stanley, W. T. (2013a). *Myosorex kihaulei* Kihaule's Mouse Shrew. In J. Kingdon, D. C. D. Happold, T. M. Butynski, M. Hoffman, M. Happold, & J. Kalina (Eds.), *Mammals of Africa Volume IV: Hedgehogs, shrews and bats* (pp. 155–156). Bloomsbury.

Stanley, W. T. (2013b). *Sylvisorex howelli* Howell's Forest Shrew (Uluguru Forest Shrew). In J. Kingdon, D. C. D. Happold, T. M. Butynski, M. Hoffman, M. Happold, & J. Kalina (Eds.), *Mammals of Africa Volume IV: Hedgehogs, shrews and bats* (pp. 188–189). Bloomsbury.

Stanley, W. T., Rogers, M. A., & Hutterer, R. (2005). A new species of *Congosorex* from the Eastern Arc Mountains, Tanzania, with significant biogeographical implications. *Journal of Zoology*, *265*(3), 269–280. https://doi.org/10.1017/S0952836904006314

Stubbe, A., Stubbe, B., Batsajchan, N., Samjaa, R., Driechciarz, E., Driechciarz, R., Schonert, A., & Winter, M. (2007). *<i>Euchoreutes naso<ii> Sclater, 1890-ein Säugetier-Endemit Zentralasiens*. *10*, 471–486. https://www.researchgate.net/publication/237725258

Tchabovsky, A., & Bazykin, G. (2004). Females delay dispersal and breeding in a solitary gerbil, *Meriones tamariscinus*. *Journal of Mammalogy*, *85*(1), 105–112. https://doi.org/10.1644/1545-1542(2004)085<0105:FDDABI>2.0.CO;2

Timm, R., Matson, J., Tirira, D., Boada, C., Weksler, M., Anderson, R. P., Rivas, B., Delgado, C., & Gómez-Laverde, M. (2016). *Handleyomys alfaroi (errata version published in 2017)*. The IUCN Red List of Threatened Species.

Tschapka, M., Sperr, E. B., Caballero-Martinez, L. A., Marti´nez, M., Medelli´n, R. A., & Medelli´n, M. (2008). Diet and cranial morphology of *Musonycteris harrisoni*, a highly specialized nectar-feeding bat in western Mexico. *Journal of Mammalogy*, *89*(4), 924–932. https://doi.org/10.1644/07-MAMM-A-038.1

Turbill, C., & Geiser, F. (2006). Thermal physiology of pregnant and lactating female and male long-eared bats, *Nyctophilus geoffroyi* and *N. gouldi*. *Journal of Comparative Physiology B: Biochemical, Systemic, and Environmental Physiology*, *176*(2), 165–172. https://doi.org/10.1007/s00360-005-0038-7

Ushakova, M. V., Feoktistova, N. Y., Petrovskii, D. V., Gureeva, A. V., Naidenko, S. V., & Surov, A. V. (2012). Hibernation in the Eversman hamster (*Allocricetulus eversmanni* Brandt, 1859) from the Saratov Trans-Volga region. *Biology Bulletin*, *39*(10), 846–851. https://doi.org/10.1134/S1062359012100111

van Staaden, M. (1994). *Suricata suricatta*. *Mammalian Species*, *483*, 1–8. https://doi.org/10.2307/3504085.

Velazco, P. M., Cadenillas, R., Centty, O., Huamaní, L., & Zamora, H. (2013). New records of *Platalina genovensium* (Chiroptera, Phyllostomidae) and *Tomopeas ravus* (Chiroptera, Molossidae). *Mastozoología Neotropical*, *20*(2), 425–434. http://www.sarem.org.ar

Verde Arregoitia, L. D., Fisher, D. O., & Schweizer, M. (2017). Morphology captures diet and locomotor types in rodents. *Royal Society Open Science*, *4*(1). https://doi.org/10.1098/rsos.160957

Verts, B. J., Carraway, L. N., & Kinlaw, A. (2001). *Spilogale gracilis*. *Mammalian Species*. https://doi.org/10.2307/0.674.1

Warburton, N. M., Grégoire, L., Jacques, S., & Flandrin, C. (2013). Adaptations for digging in the forelimb muscle anatomy of the southern brown bandicoot (*Isoodon obesulus*) and bilby (Macrotis lagotis). *Australian Journal of Zoology*, *61*(5), 402–419. https://doi.org/10.1071/ZO13086

Weisbecker, V., & Schmid, S. (2007). Autopodial skeletal diversity in hystricognath rodents: Functional and phylogenetic aspects. *Mammalian Biology*, *72*(1), 27–44. https://doi.org/10.1016/j.mambio.2006.03.005

Wilson, D. E., Mittermeier, R. A., & Lacher Jr, T. E. (2017). Muridae. In *Handbook of the Mammals of the World: Vol. 7 Rodents II* (pp. 536–884). Lynx Edicions. https://doi.org/10.5281/zenodo.6887260

Woinarski, J., Rhind, S., & Oakwood, M. (2019). *Phascogale pirata*. The IUCN Red List of Threatened Species. https://dx.doi.org/10.2305/IUCN.UK.2019-2.RLTS.T16889A21944455.en

Woltanski, A. (2004). *"Nasalis larvatus" (On-line)*. Animal Diversity Web. https://animaldiversity.org/accounts/Nasalis_larvatus/

Yamada, F., & Cervantes, F. A. (2005). *Pentalagus furnessi*. *Mammalian Species*, *782*, 1–5. https://doi.org/10.2307/3504397

Yamada, F., Kawauchi, N., Nakata, K., Abe, S., Kotaka, N., Takashima, A., Murata, C., & Kuroiwa, A. (2010). Rediscovery after thirty years since the last capture of the critically endangered Okinawa spiny rat *Tokudaia muenninki* in the northern part of Okinawa Island. In *Mammal Study* (Vol. 35).

Zhang, X. Y., & Wang, D. H. (2006). Energy metabolism, thermogenesis and body mass regulation in Brandt's voles (*Lasiopodomys brandtii*) during cold acclimation and rewarming. *Hormones and Behavior*, *50*(1), 61–69. https://doi.org/10.1016/j.yhbeh.2006.01.005

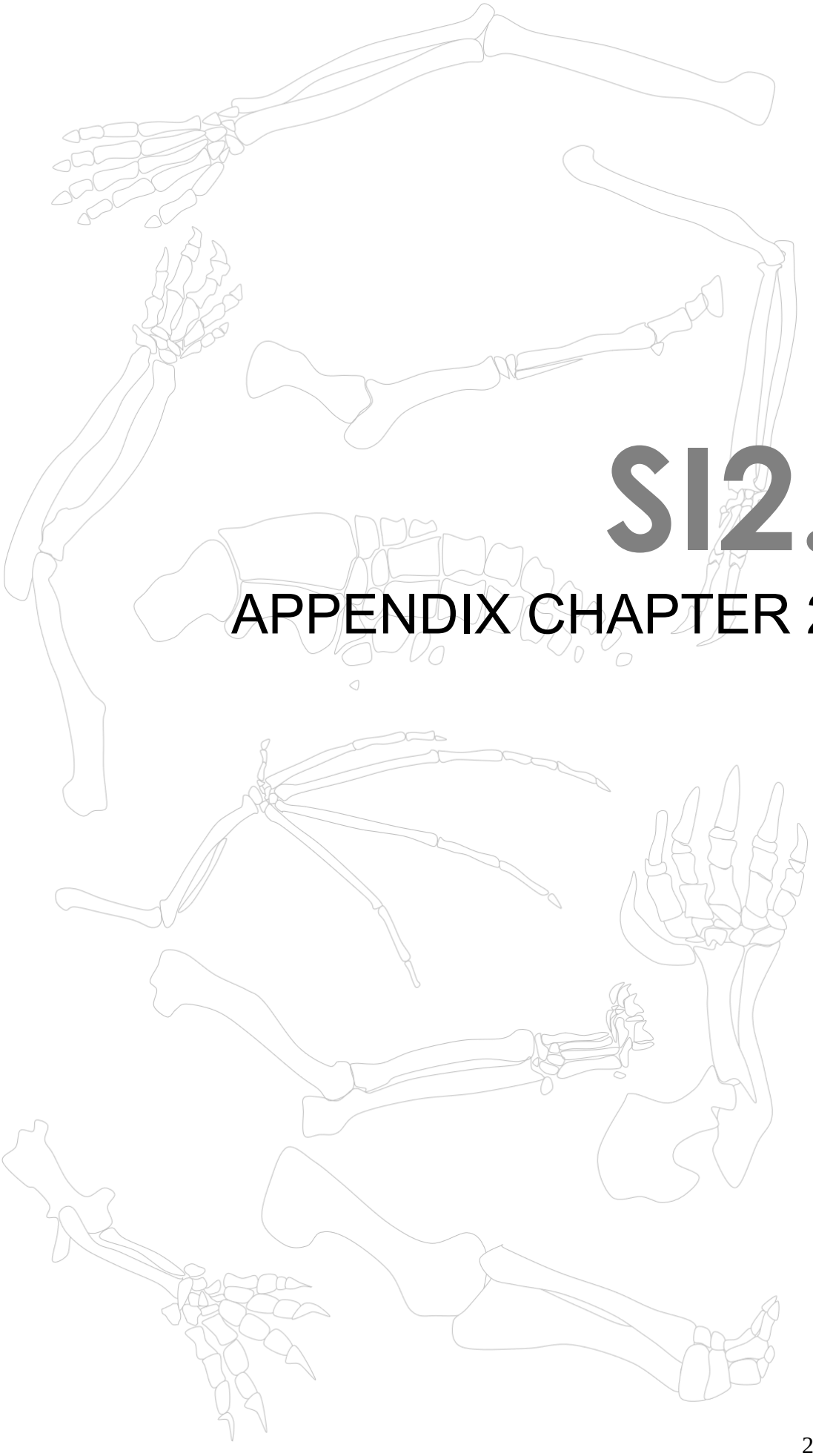

SI2.

APPENDIX CHAPTER 2

Table S2.1. Fits of linear models of evolution for each bone. In bold, the best model fitted according to generalized information criterion (GIC) and loglikelihood (logLik). σ^2 = mean evolutionary rate, α = attraction toward optimum, stat.var. = mean stationary variance.

	Best-fit model rank	GIC	lnL	σ^2	α	stat. var.
Humerus	**OU**	**-3494.708**	**1796.783**	**1.59E-03**	**0.020**	**0.039**
	BM	-3158.830	1647.660	1.13E-03	-	-
	EB	-3156.829	1647.660	1.13E-03	-	-
Radius	**OU**	**-3244.176**	**1660.549**	**1.83E-03**	**0.022**	**0.041**
	BM	-2374.789	1239.853	1.28E-03	-	-
	EB	-2845.109	1468.898	1.28E-03	-	-
Metacarpal	**OU**	**-2645.917**	**1382.228**	**2.02E-03**	**0.017**	**0.060**
	BM	-2374.789	1239.853	1.49E-03	-	-
	EB	-2372.786	1239.851	1.49E-03	-	-
Phalanx	**OU**	**-2767.643**	**1444.173**	**2.70E-03**	**0.024**	**0.055**
	BM	-2333.077	1227.580	1.64E-03	-	-
	EB	-2331.071	1227.576	1.64E-03	-	-

Table S2.2. Empirical values from PGLS regression computing for body mass in the geometric means.

	Determinant	Trace	Integration	Stat. variance (MCC tree)
humerus	0.0015	0.0079	0.175	0.039
radius	0.0016	0.0091	0.058	0.041
metacarpal	0.0017	0.0101	0.226	0.060
phalanx	0.0019	0.0135	0.356	0.055

Table S2.3. Empirical values from PGLS regression without body mass in the geometric means.

	Determinant	Trace	Integration	Stat. variance (MCC tree)
humerus	0.0013	0.0075	0.226	0.038
radius	0.0016	0.0090	0.057	0.040
metacarpal	0.0017	0.0103	0.231	0.060
phalanx	0.0019	0.0135	0.363	0.056

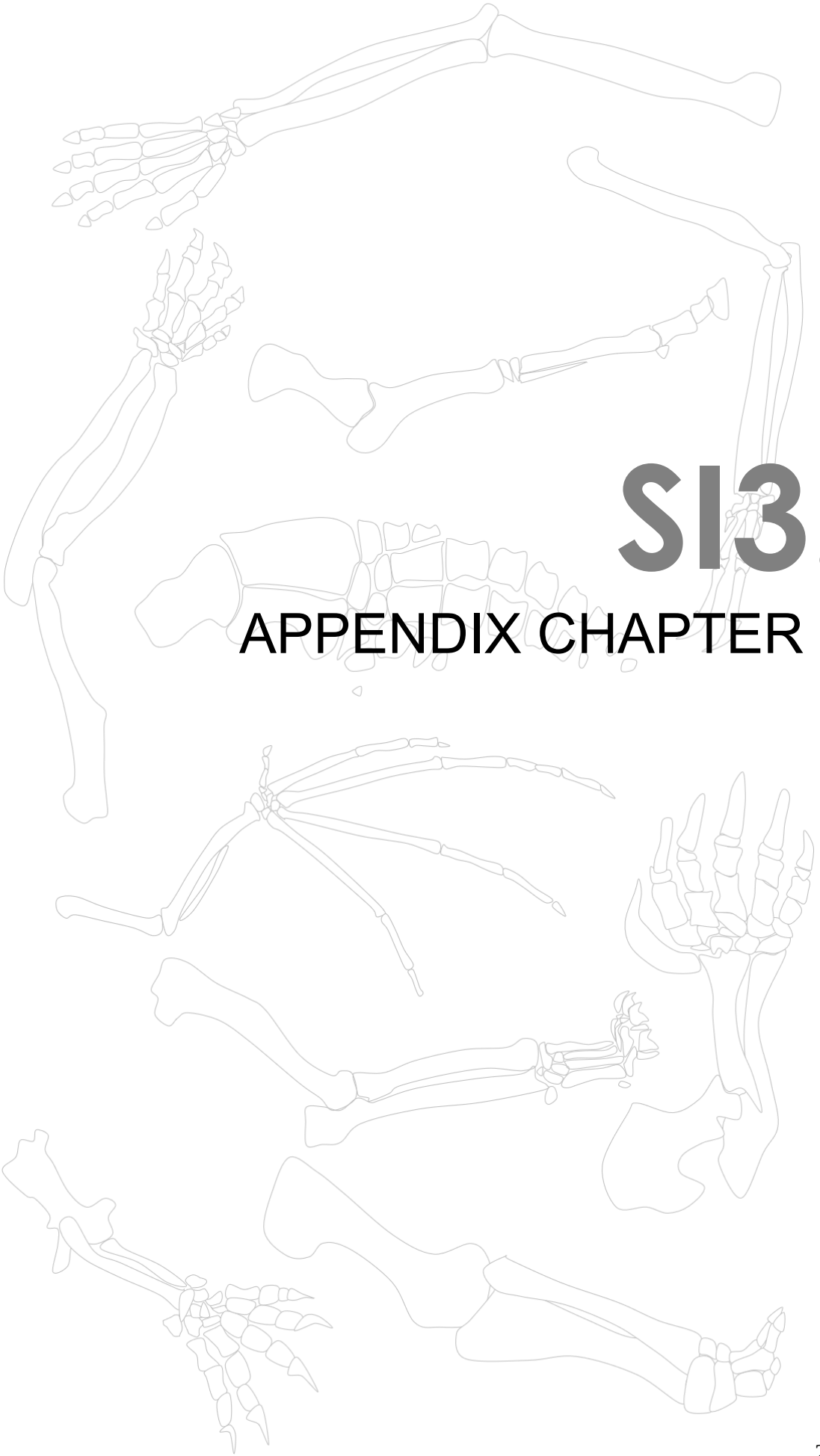

SI3.

APPENDIX CHAPTER 3

Table S3.1. **Fits of linear models of evolution for the whole limb and for each bone separately.** The best model fitted is highlighted in bold, according to generalized information criterion (GIC) and log-likelihood (logLik). σ^2 = mean evolutionary rate, α = attraction to optimum.

		raw (absolute size)				size residuals			
		GIC	logLik	σ^2	α	GIC	logLik	σ^2	α
whole limb									
	BM	-11688.6	21682.7	0.049	-	-49174.6	25148.9	5.20E-03	-
	OU	**-3743.7**	**22500.1**	**0.080**	**0.020**	**-50985.7**	**25967.2**	**7.97E-03**	**0.022**
	EB	-11688.0	21682.7	0.049	-	-49172.6	25148.9	5.20E-03	-
humerus									
	BM	-8688.3	4391.7	0.014	-	-11914.3	6007.2	1.06E-03	-
	OU	**-9037.3**	**4559.9**	**0.019**	**0.017**	**-12314.3**	**6208.9**	**1.35E-03**	**0.019**
	EB	-8686.3	4391.7	0.014	-	-11912.3	6007.2	1.06E-03	-
radius									
	BM	-7701.3	3902.0	0.014	-	-11121.6	5607.3	1.30E-03	-
	OU	**-8182.7**	**4132.0**	**0.022**	**0.021**	**-11692.7**	**5884.8**	**1.81E-03**	**0.024**
	EB	-7699.3	3902.0	0.014	-	-11119.6	5607.3	1.30E-03	-
metacarpal									
	BM	-6756.4	3563.8	0.014	-	-10251.4	5207.3	1.69E-03	-
	OU	**-7142.8**	**3739.3**	**0.020**	**0.017**	**-10718.9**	**5419.8**	**2.37E-03**	**0.020**
	EB	-6754.4	3563.8	0.014	-	-10249.4	5207.3	1.69E-03	-
phalanx									
	BM	-6126.9	3880.7	0.014	-	-10590.6	5363.6	1.66E-03	-
	OU	**-6560.1**	**4054.5**	**0.020**	**0.017**	**-11155.3**	**5632.0**	**2.56E-03**	**0.024**
	EB	-6124.8	3880.7	0.014	-	-10588.6	5363.6	1.66E-03	-

Table S3.2. Morphological differences of limb elements between ecological categories. Manova results from phylogenetic generalized least squares regression indicating whether limb morphology elements differ between locomotor media.

	raw (absolute size)		size residuals	
	Tstat	*p*	Tstat	*p*
whole limb	0.920	**0.001**	0.984	**0.001**
humerus	0.210	**0.001**	0.211	**0.001**
radius	0.242	**0.001**	0.329	**0.001**
metacarpal	0.401	**0.001**	0.502	**0.001**
phalanx	0.298	**0.001**	0.433	**0.001**

Table S3.3. Body mass variation across ecological regimes. Adjusted p-values indicating the similarity and differences of body mass per group (significant values in bold). The diagonal indicates the average body mass in the category (log-transformed values in linear scale).

	aerial	aquatic	semi-aerial	semi-aquatic	terrestrial
aerial	0.401				
aquatic	**0.010**	1.870			
semi-aerial	1.000	**0.050**	0.816		
semi-aquatic	0.510	**0.020**	1.000	1.040	
terrestrial	0.570	**0.020**	1.000	1.000	0.975

Table S3.4. Phylogenetic principal component loadings of each bone measured.

		raw (absolute size)					size residuals				
		pPC1	pPC2	pPC3	pPC4	pPC5	pPC1	pPC2	pPC3	pPC4	pPC5
humerus	length	0.402	0.853	-0.218	-0.249	0.035	0.176	0.975	0.027	0.075	-0.113
	proximal width	0.451	0.016	0.237	0.654	0.558	-0.342	0.172	-0.275	-0.811	0.345
	mid-shaft width	0.461	-0.261	0.560	-0.624	0.128	-0.563	0.094	-0.618	0.524	0.132
	distal width	0.448	-0.040	0.164	0.327	-0.815	-0.276	-0.034	-0.148	-0.233	-0.920
	heigth	0.471	-0.450	-0.745	-0.115	0.084	-0.677	0.103	0.721	0.089	0.061
	eigen	0.01825	0.00035	0.00025	0.00020	0.00016	0.00049	0.00027	0.00025	0.00019	0.00015
	% var	94.99%	1.82%	1.30%	1.04%	0.85%	36.04%	20.34%	18.32%	14.15%	11.15%
radius	length	0.387	0.864	0.308	0.084	-0.039	0.977	0.153	0.146	-0.016	-0.006
	proximal width	0.455	-0.109	-0.011	-0.667	0.580	0.001	-0.012	-0.002	-0.416	0.909
	mid-shaft width	0.467	-0.032	-0.617	0.571	0.273	0.159	-0.931	-0.049	0.299	0.124
	distal width	0.472	-0.118	-0.273	-0.321	-0.765	0.039	-0.320	-0.036	-0.859	-0.397
	heigth	0.450	-0.476	0.671	0.346	-0.033	-0.136	-0.081	0.987	-0.015	-0.006
	eigen	0.02041	0.00053	0.00038	0.00027	0.00019	0.00062	0.00040	0.00037	0.00022	0.00021
	% var	93.73%	2.46%	1.73%	1.23%	0.85%	34.06%	21.92%	20.49%	12.04%	11.50%
metacarpal	length	0.369	0.912	-0.173	0.000	0.053	0.922	-0.351	0.030	-0.163	0.003
	proximal width	0.491	-0.300	-0.522	-0.628	0.042	-0.279	-0.884	0.125	0.353	-0.014
	mid-shaft width	0.464	-0.228	-0.002	0.520	0.680	-0.231	-0.242	-0.028	-0.798	-0.500
	distal width	0.457	-0.162	-0.103	0.473	-0.729	-0.139	-0.167	-0.153	-0.441	0.857
	heigth	0.445	-0.021	0.829	-0.335	-0.051	-0.021	0.090	0.979	-0.132	0.121
	eigen	0.01793	0.00104	0.00037	0.00031	0.00019	0.00114	0.00043	0.00034	0.00027	0.00018
	% var	90.37%	5.24%	1.88%	1.56%	0.95%	48.18%	18.27%	14.42%	11.62%	7.51%
phalanx	length	0.368	0.912	0.009	-0.016	-0.179	0.841	-0.471	0.180	-0.128	-0.150
	proximal width	0.453	-0.051	-0.328	-0.451	0.694	-0.129	-0.406	-0.214	-0.502	0.721
	mid-shaft width	0.475	-0.329	-0.048	-0.472	-0.664	-0.396	-0.331	0.047	-0.568	-0.639
	distal width	0.476	-0.186	-0.445	0.734	-0.057	-0.264	-0.698	-0.188	0.636	-0.054
	heigth	0.456	-0.148	0.832	0.187	0.207	-0.223	-0.126	0.940	0.066	0.215
	eigen	0.01802	0.00105	0.00038	0.00019	0.00012	0.00135	0.00050	0.00040	0.00018	0.00014
	% var	91.15%	5.35%	1.93%	0.94%	0.63%	52.68%	19.46%	15.49%	7.08%	5.29%

Table S3.5. A**ssociations between the absolute limb size (scores from raw pPC1), body mass (bm), and media use.** Terrestrial taxa were set as the intercept.

	value	SE	t-value	*p*
intercept (terrestrial)	-4.231	0.212	-19.914	< **0.001**
body mass	4.769	0.064	74.993	< **0.001**
aerial	1.513	0.215	7.043	< **0.001**
aquatic	0.611	0.371	1.648	0.100
semi-aerial	-0.468	0.413	-1.134	0.257
semi-aquatic	-0.207	0.138	-1.502	0.134
bm:aerial	-0.322	0.254	-1.267	0.206
bm:aquatic	-0.699	0.201	-3.478	**0.001**
bm:semi-aerial	0.464	0.492	0.942	0.346
bm:semi-aquatic	-0.005	0.127	-0.042	0.966

Table S3.6. Linear model fit with different interactions among ecological categories. Results obtained from different linear regressions of the absolute limb size (x = raw pPC1 scores) combining or not body mass (bm) and the different categories of media use. For 'media', it means that all ecological categories (terrestrial, aquatic, aerial, semi-aquatic, and semi-aerial) were fitted in the linear model. RSE = residual standard error; λ = phylogenetic signal. Best model fit to the raw pPC1 data combines body mass and all media categories (AICc in bold).

linear model	RSE	R^2	λ	logLik	AICc
x ~ bm	0.616	0.979	0.848	-244.51	497.07
x ~ bm * media	0.484	0.981	0.715	-205.79	**435.97**
x ~ aquatic | not aquatic	2.397	0.855	0.981	-1018.44	2044.93
x ~ bm + aquatic | not aquatic	0.591	0.980	0.830	-237.28	484.63
x ~ aerial | not aerial	2.412	0.855	0.981	-1020.90	2049.85
x ~ bm + aerial | not aerial	0.553	0.980	0.794	-229.38	468.83
x ~ terrestrial | not terrestrial	2.385	0.857	0.981	-1014.07	2036.20
x ~ bm + terrestrial | not terrestrial	0.616	0.980	0.852	-239.73	489.53
x ~ semi-aquatic | not semi-aquatic	2.404	0.858	0.983	-1012.09	2032.22
x ~ bm + semi-aquatic | not semi-aquatic	0.612	0.979	0.847	-241.14	492.36
x ~ semi-aerial | not semi-aerial	2.457	0.854	0.985	-1021.14	2050.33
x ~ bm + semi-aerial | not semi-aerial	0.619	0.979	0.852	-243.67	497.41
x ~ aquatic | not aquatic + aerial | not aerial	2.378	0.856	0.980	-1016.25	2042.57
x ~ bm + aquatic | not aquatic + aerial | not aerial	0.511	0.981	0.745	-219.33	450.77

Table S3.7. Limb morphological similarity between locomotor media. Significance was calculated for the first two raw and residual phylogenetic principal components, for the whole limb and per bone. Below the diagonal, adjusted p-values from pPC1 scores and above diagonal the adjusted p-values from the pPC2 scores (95% CI).

	raw (absolute size)					size residuals				
	aerial	aquatic	semi-aerial	semi-aquatic	terrestrial	aerial	aquatic	semi-aerial	semi-aquatic	terrestrial
whole limb										
aerial	-	**0.001**	**0.001**	**0.001**	**0.001**	-	0.292	**0.010**	0.093	0.052
aquatic	**0.009**	-	**0.010**	0.119	**0.029**	**0.001**	-	**0.100**	0.609	0.401
semi-aerial	0.881	**0.011**	-	**0.012**	**0.033**	**0.001**	**0.007**	-	**0.047**	0.063
semi-aquatic	0.442	**0.007**	0.516	-	0.072	**0.001**	0.271	**0.009**	-	0.314
terrestrial	0.450	**0.008**	0.460	0.985	-	**0.001**	0.066	**0.029**	0.062	-
humerus										
aerial	-	**0.001**	0.829	**0.008**	**0.030**	-	**0.001**	0.097	0.468	0.918
aquatic	**0.008**	-	**0.001**	**0.001**	**0.001**	**0.001**	-	**0.001**	**0.001**	**0.001**
semi-aerial	0.548	**0.014**	-	**0.001**	**0.005**	**0.024**	0.178	-	**0.002**	**0.002**
semi-aquatic	0.176	**0.011**	0.453	-	**0.001**	**0.001**	0.498	0.175	-	**0.050**
terrestrial	0.180	**0.008**	0.468	0.764	-	**0.004**	0.117	0.650	**0.010**	-
radius										
aerial	-	**0.001**	0.525	**0.001**	**0.009**	-	**0.001**	0.343	0.852	0.369
aquatic	**0.008**	-	**0.001**	**0.003**	**0.001**	**0.002**	-	**0.001**	**0.001**	**0.001**
semi-aerial	0.837	**0.015**	-	**0.001**	**0.006**	0.604	**0.001**	-	0.202	0.598
semi-aquatic	0.511	**0.003**	0.671	-	**0.003**	**0.001**	0.171	**0.001**	-	**0.025**
terrestrial	0.478	**0.002**	0.606	0.892	-	**0.005**	**0.011**	**0.001**	**0.001**	-
metacarpal										
aerial	-	**0.001**	**0.001**	**0.001**	**0.001**	-	**0.003**	**0.001**	**0.003**	**0.002**
aquatic	**0.014**	-	0.406	0.429	0.195	**0.001**	-	0.291	0.529	0.576
semi-aerial	0.893	**0.01**	-	0.688	0.907	**0.001**	0.446	-	**0.006**	**0.005**
semi-aquatic	0.479	**0.008**	0.284	-	0.152	**0.001**	0.431	0.740	-	0.790
terrestrial	0.486	**0.006**	0.258	0.860	-	**0.001**	0.193	0.872	0.155	-
phalanx										
aerial	-	**0.001**	**0.004**	**0.001**	**0.001**	-	0.656	0.237	0.625	0.460
aquatic	**0.009**	-	0.254	0.895	0.959	**0.001**	-	0.110	0.266	0.161
semi-aerial	0.798	**0.016**	-	**0.042**	**0.036**	**0.003**	0.221	-	0.238	0.293
semi-aquatic	0.301	**0.006**	0.404	-	0.517	**0.001**	0.878	**0.037**	-	0.418
terrestrial	0.350	**0.005**	0.359	0.873	-	**0.001**	0.926	**0.028**	0.495	-

Table S3.8. Limb disparity for different locomotor media. Above the diagonal are represented the p-values from pairwise disparity comparisons generated by a PERMANOVA significance test. All values are significant ($p<0.05$). The diagonal highlighted in dark grey indicates the average disparity for each locomotor medium.

	raw (absolute size)					size residuals				
	aerial	aquatic	semi-aerial	semi-aquatic	terrestrial	aerial	aquatic	semi-aerial	semi-aquatic	terrestrial
whole limb										
aerial	0.480					0.252				
aquatic	**<0.001**	0.860				**<0.001**	0.490			
semi-aerial	**<0.001**	1.000	0.891			1.000	**<0.001**	0.254		
semi-aquatic	**<0.001**	**<0.001**	**<0.001**	1.673		**<0.001**	**<0.001**	0.203	0.267	
terrestrial	**<0.001**	**<0.001**	**<0.001**	**<0.001**	1.902	**<0.001**	**<0.001**	**<0.001**	**<0.001**	0.342
humerus										
aerial	0.213					0.088				
aquatic	**<0.001**	0.424				**<0.001**	0.228			
semi-aerial	**<0.001**	0.963	0.453			**<0.001**	**1.1E-100**	0.108		
semi-aquatic	**<0.001**	**<0.001**	**<0.001**	0.851		**<0.001**	**<0.001**	**<0.001**	0.142	
terrestrial	**<0.001**	**<0.001**	**<0.001**	1.000	0.860	**<0.001**	**<0.001**	**<0.001**	**<0.001**	0.152
radius										
aerial	0.208					0.094				
aquatic	**<0.001**	0.448				**<0.001**	0.185			
semi-aerial	**<0.001**	0.393	0.489			**<0.001**	**<0.001**	0.137		
semi-aquatic	**<0.001**	**<0.001**	**<0.001**	0.895		**<0.001**	**<0.001**	0.373	0.131	
terrestrial	**<0.001**	**<0.001**	**<0.001**	0.144	0.933	**<0.001**	**<0.001**	1.000	**<0.001**	0.138
metacarpal										
aerial	0.247					0.144				
aquatic	**<0.001**	0.430				**<0.001**	0.233			
semi-aerial	**<0.001**	**0.003**	0.502			1.000	**<0.001**	0.142		
semi-aquatic	**<0.001**	**<0.001**	**<0.001**	0.934		**<0.001**	**<0.001**	**<0.001**	0.121	
terrestrial	**<0.001**	**<0.001**	**<0.001**	1.000	0.936	**<0.001**	**<0.001**	**<0.001**	**<0.001**	0.179
phalanx										
aerial	0.259					0.125				
aquatic	**<0.001**	0.420				**<0.001**	0.227			
semi-aerial	**<0.001**	0.291	0.459			**<0.001**	**<0.001**	0.112		
semi-aquatic	**<0.001**	**<0.001**	**<0.001**	0.918		1.000	**<0.001**	**<0.001**	0.124	
terrestrial	**<0.001**	**<0.001**	**<0.001**	1.000	0.937	**<0.001**	**<0.001**	**<0.001**	**<0.001**	0.157

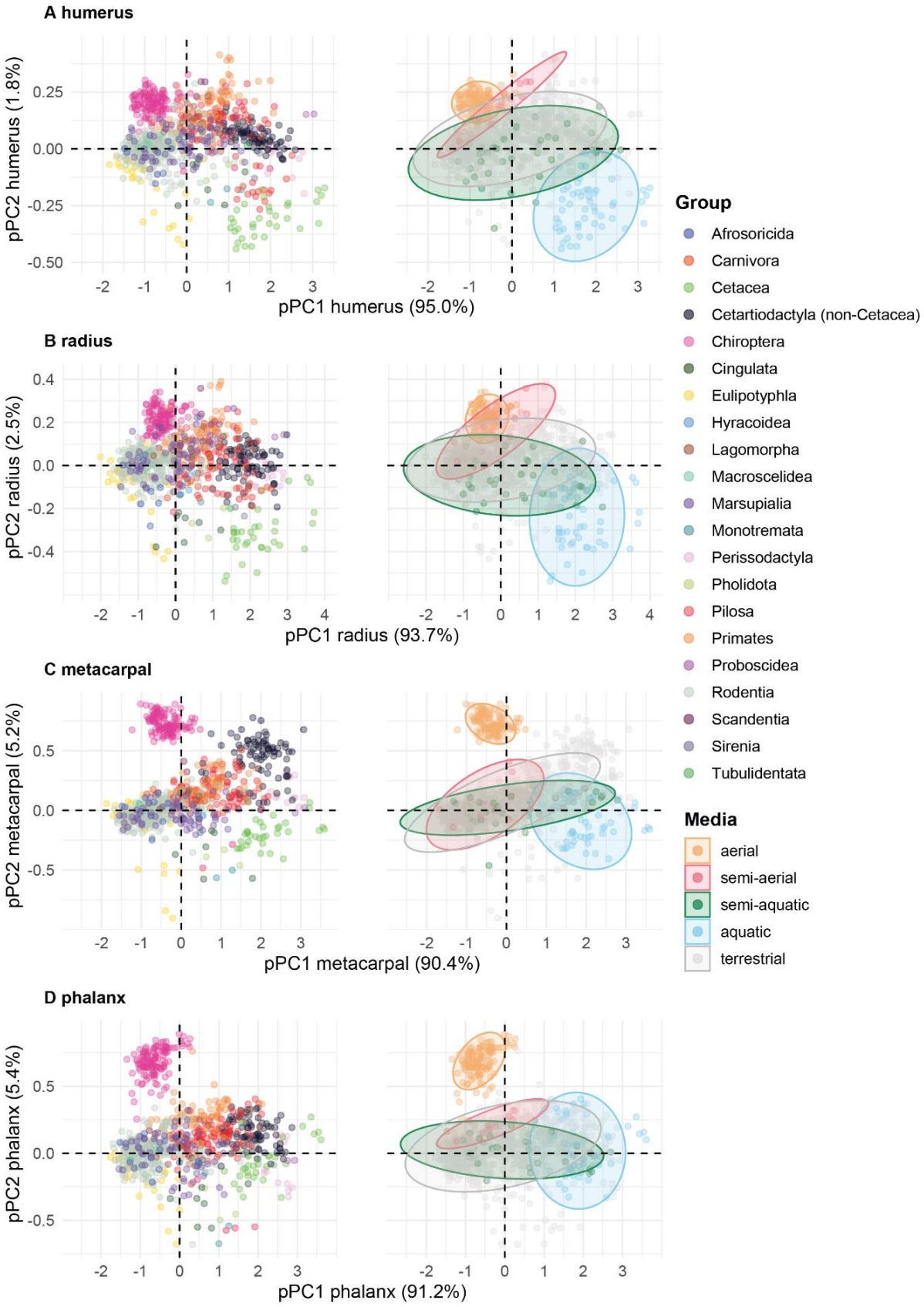

Figure S3.1. Morphospaces of absolute forelimb and bone sizes. Morphospace generated by the raw pPCA of each bone measured (size included), indicating the taxonomic classification and the medium used for locomotion. **A)** humerus; **B)** radius; **C)** metacarpal; **D)** phalanx.

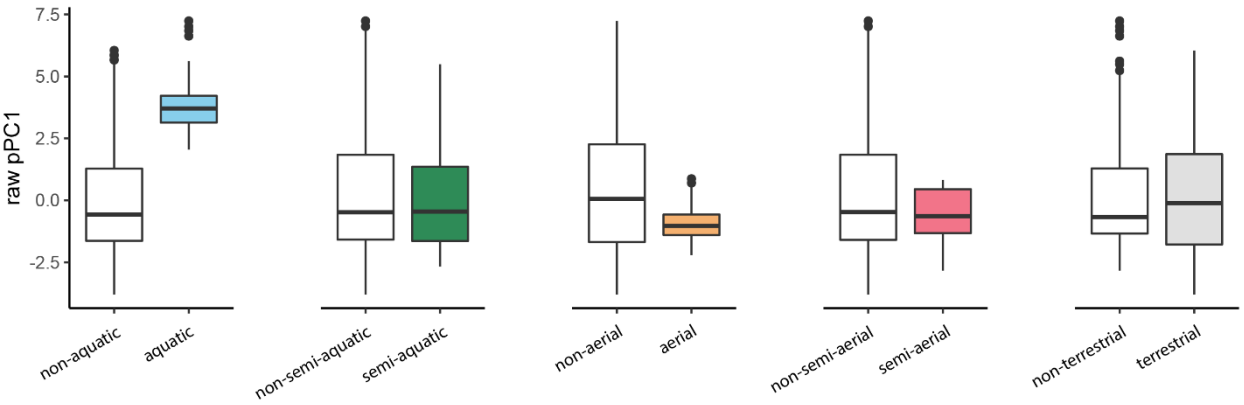

Figure S3.2. Absolute forelimb size variation. Box plot representations of the model output provided in Table S3.3 indicating the differences and similarities in absolute limb size (raw pPC1) between each media category (colored boxes) and all other species that do not belong to that group (white boxes).

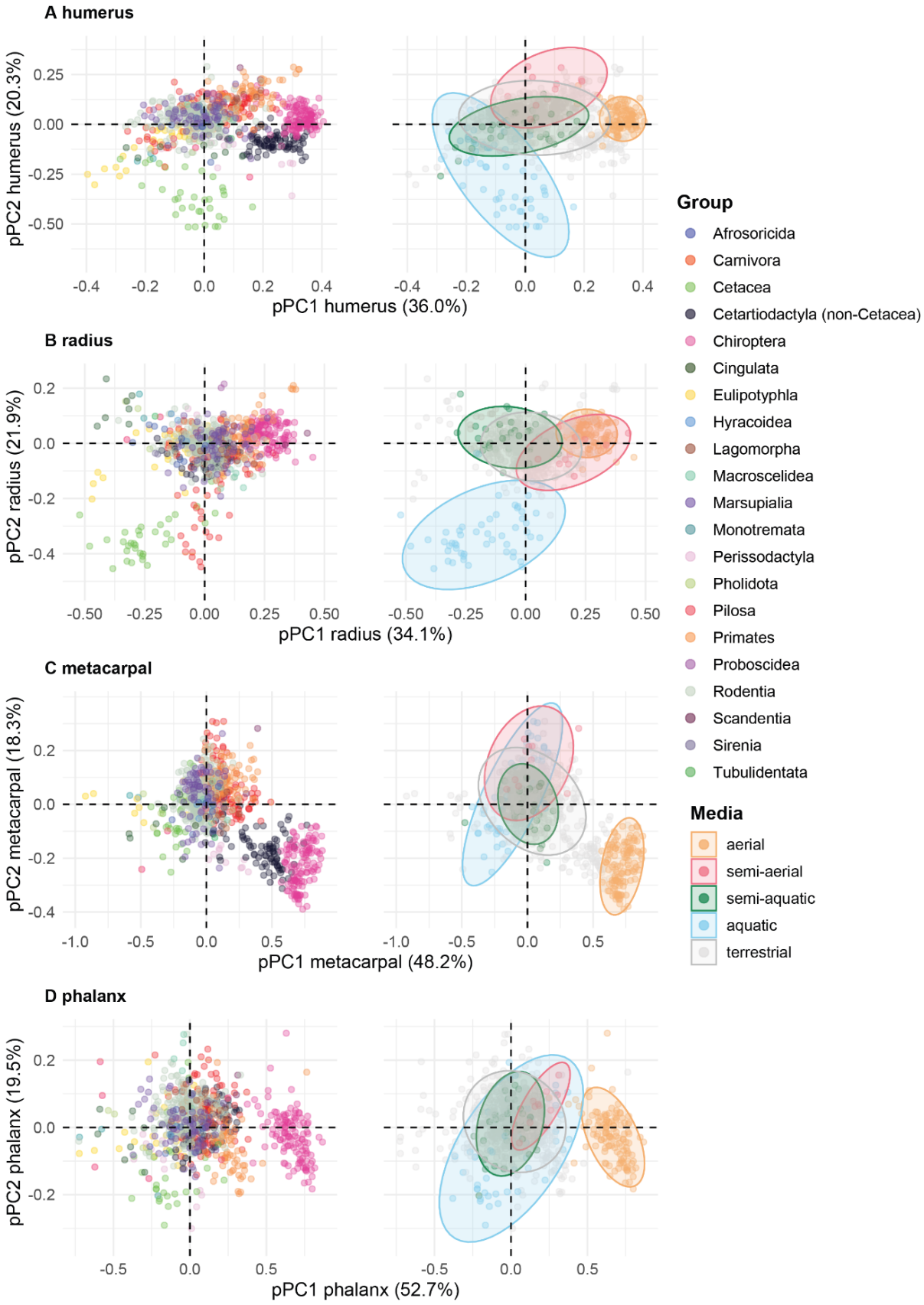

Figure S3.3. Morphospaces of forelimb and bone shapes. Morphospace generated by the residual pPCA of each bone measured (size removed), indicating the higher taxonomic classification and the medium used for locomotion. **A)** humerus; **B)** radius; **C)** metacarpal; **D)** phalanx.

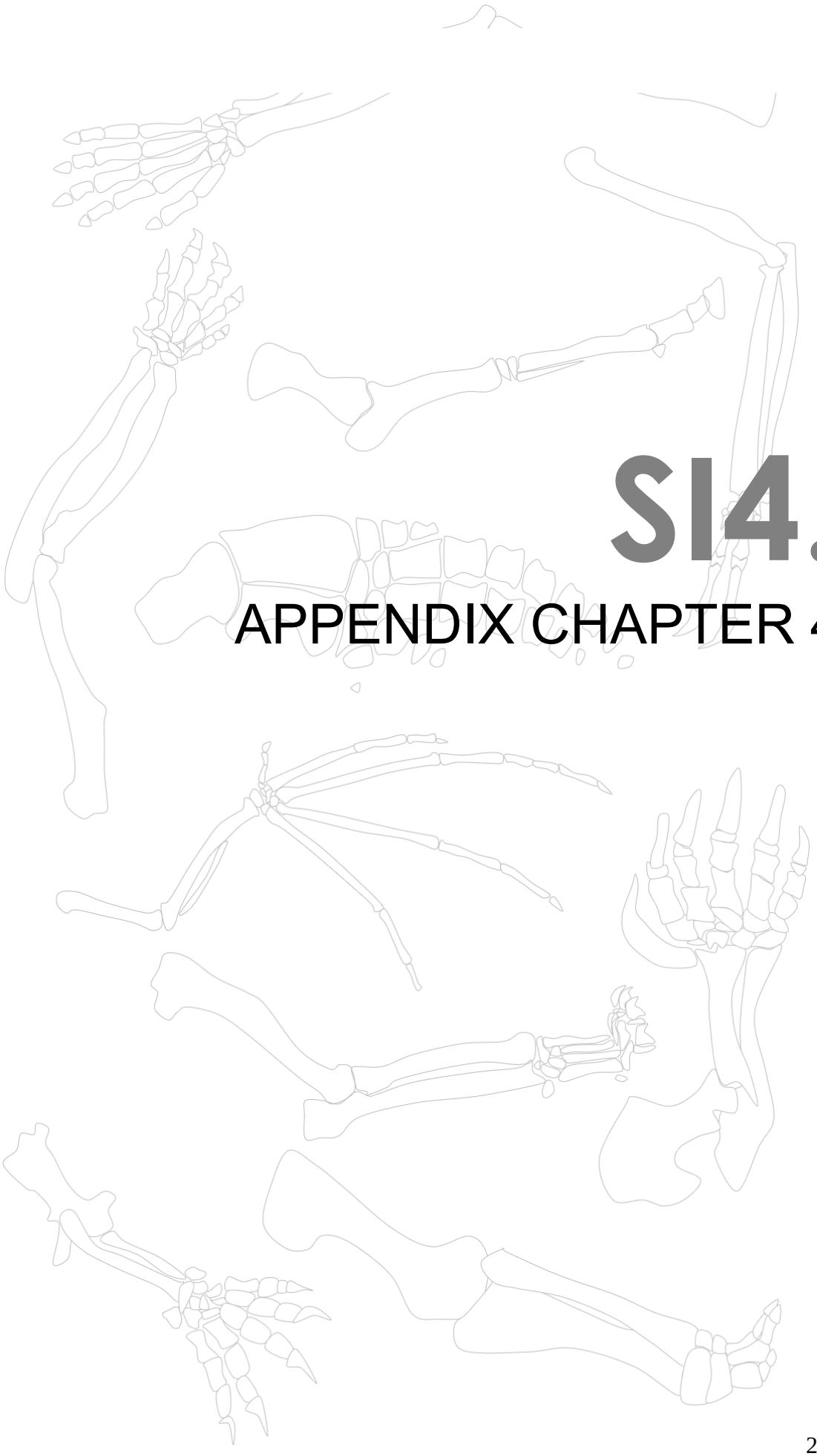

SI4.
APPENDIX CHAPTER 4

Table S4.1. Body mass comparison. Adjusted p-values from a phylogenetic ANOVA comparing body mass across locomotor modes (significant values in bold). The diagonal indicates the average body mass in the category (log-transformed g values in linear scale).

	aquatic	arboreal	flight	fossorial	gliding	scansorial	semiaquatic	semifossorial	terrestrial biped	terrestrial quadruped
aquatic	1.87									
arboreal	**0.002**	0.921								
flight	**0.001**	0.105	0.401							
fossorial	**0.001**	0.186	0.398	0.675						
gliding	**0.001**	0.63	0.295	0.609	0.816					
scansorial	**0.001**	0.905	0.083	0.115	0.644	0.939				
semiaquatic	**0.001**	0.389	**0.03**	**0.011**	0.337	0.276	1.06			
semifossorial	**0.001**	0.58	0.164	0.262	0.922	0.345	**0.034**	0.842		
terrestrial biped	**0.021**	0.995	0.248	0.487	0.707	0.948	0.671	0.807	0.919	
terrestrial quadruped	**0.001**	0.383	**0.020**	**0.022**	0.335	0.288	0.925	0.061	0.674	1.07

Table S4.2. Evolutionary model fit. Fits of linear models of evolution for the absolute limb values, including body mass (raw), and the size residual limb distances. The best model fitted is highlighted in bold, according to generalized information criterion (GIC) and log-likelihood (logLik). *Average GIC and log-likelihood from 100 regressions using different simmap trees.

	body mass + raw limb traits		size residual limb traits	
	GIC	**logLik**	**GIC**	**logLik**
BM	-25152.97	12863.34	-27797.62	14162.81
OU	-25950.66	13224.67	-28684.59	14565.1
EB	-25150.97	12863.34	-27795.62	14162.81
BMM*	-26392.24	13460.60	-28927.32	14710.81
OUM*	**-27410.27**	**14078.55**	**-30089.21**	**15382.1**

Table S4.3. Adaptive optima sums compared between modes of locomotion (95% CI). Pair-wise comparisons are listed in descending order of absolute difference between optima means (inferred as the modulus of the difference). |Diff| = modulus of the difference between means; Diff = difference between means; Lwr = lower end point of the interval; Upr = upper end point of the interval; P-adj = adjusted p-value.

raw						residual					
	|Diff|	Diff	Lwr	Upr	P-adj		|Diff|	Diff	Lwr	Upr	P-adj
flight-aquatic	19.62	-19.62	-20.14	-19.09	< 0.001	fossorial-flight	1.72	-1.72	-1.74	-1.70	< 0.001
fossorial-aquatic	18.30	-18.30	-18.83	-17.78	< 0.001	flight-aquatic	1.51	1.51	1.49	1.53	< 0.001
gliding-aquatic	17.04	-17.04	-17.56	-16.51	< 0.001	semifossorial-flight	1.37	-1.37	-1.39	-1.34	< 0.001
terrestrial biped-aquatic	16.90	-16.90	-17.42	-16.37	< 0.001	semiaquatic-flight	1.33	-1.33	-1.35	-1.31	< 0.001
semifossorial-aquatic	16.73	-16.73	-17.26	-16.21	< 0.001	terrestrial biped-flight	1.26	-1.26	-1.28	-1.23	< 0.001
scansorial-aquatic	16.70	-16.70	-17.22	-16.17	< 0.001	terrestrial quadruped-flight	1.15	-1.15	-1.17	-1.13	< 0.001
arboreal-aquatic	15.86	-15.86	-16.38	-15.33	< 0.001	scansorial-flight	1.11	-1.11	-1.13	-1.08	< 0.001
terrestrial quadruped-aquatic	15.38	-15.38	-15.90	-14.85	< 0.001	gliding-fossorial	1.03	1.03	1.01	1.06	< 0.001
semiaquatic-aquatic	10.13	-10.13	-10.66	-9.61	< 0.001	flight-arboreal	0.92	0.92	0.90	0.95	< 0.001
semiaquatic-flight	9.49	9.49	8.96	10.01	< 0.001	gliding-aquatic	0.82	0.82	0.80	0.84	< 0.001
semiaquatic-fossorial	8.17	8.17	7.64	8.69	< 0.001	fossorial-arboreal	0.80	-0.80	-0.82	-0.78	< 0.001
semiaquatic-gliding	6.90	6.90	6.38	7.43	< 0.001	gliding-flight	0.69	-0.69	-0.71	-0.67	< 0.001
terrestrial biped-semiaquatic	6.77	-6.77	-7.29	-6.24	< 0.001	semifossorial-gliding	0.68	-0.68	-0.70	-0.66	< 0.001
semifossorial-semiaquatic	6.60	-6.60	-7.12	-6.07	< 0.001	semiaquatic-gliding	0.64	-0.64	-0.67	-0.62	< 0.001
semiaquatic-scansorial	6.57	6.57	6.04	7.09	< 0.001	scansorial-fossorial	0.62	0.62	0.59	0.64	< 0.001
semiaquatic-arboreal	5.72	5.72	5.20	6.25	< 0.001	arboreal-aquatic	0.59	0.59	0.56	0.61	< 0.001
terrestrial quadruped-semiaquatic	5.24	-5.24	-5.77	-4.72	< 0.001	terrestrial quadruped-fossorial	0.57	0.57	0.55	0.59	< 0.001
terrestrial quadruped-flight	4.24	4.24	3.72	4.77	< 0.001	terrestrial biped-gliding	0.57	-0.57	-0.59	-0.55	< 0.001
flight-arboreal	3.76	-3.76	-4.29	-3.24	< 0.001	terrestrial biped-fossorial	0.47	0.47	0.44	0.49	< 0.001
terrestrial quadruped-fossorial	2.92	2.92	2.40	3.45	< 0.001	terrestrial quadruped-gliding	0.46	-0.46	-0.48	-0.44	< 0.001
scansorial-flight	2.92	2.92	2.40	3.44	< 0.001	semifossorial-arboreal	0.44	-0.44	-0.46	-0.42	< 0.001
semifossorial-flight	2.89	2.89	2.36	3.41	< 0.001	scansorial-gliding	0.42	-0.42	-0.44	-0.40	< 0.001
terrestrial biped-flight	2.72	2.72	2.20	3.24	< 0.001	semiaquatic-arboreal	0.41	-0.41	-0.43	-0.39	< 0.001
gliding-flight	2.58	2.58	2.06	3.11	< 0.001	scansorial-aquatic	0.40	0.40	0.38	0.43	< 0.001
fossorial-arboreal	2.44	-2.44	-2.97	-1.92	< 0.001	semiaquatic-fossorial	0.39	0.39	0.37	0.41	< 0.001
terrestrial quadruped-gliding	1.66	1.66	1.14	2.18	< 0.001	terrestrial quadruped-aquatic	0.36	0.36	0.34	0.38	< 0.001
scansorial-fossorial	1.60	1.60	1.08	2.13	< 0.001	semifossorial-fossorial	0.36	0.36	0.33	0.38	< 0.001
semifossorial-fossorial	1.57	1.57	1.05	2.09	< 0.001	terrestrial biped-arboreal	0.33	-0.33	-0.35	-0.31	< 0.001
terrestrial quadruped-terrestrial biped	1.52	1.52	1.00	2.05	< 0.001	semifossorial-scansorial	0.26	-0.26	-0.28	-0.24	< 0.001
terrestrial biped-fossorial	1.40	1.40	0.88	1.93	< 0.001	terrestrial biped-aquatic	0.25	0.25	0.23	0.28	< 0.001
terrestrial quadruped-semifossorial	1.35	1.35	0.83	1.88	< 0.001	gliding-arboreal	0.24	0.24	0.21	0.26	< 0.001
terrestrial quadruped-scansorial	1.32	1.32	0.80	1.85	< 0.001	semiaquatic-scansorial	0.23	-0.23	-0.25	-0.20	< 0.001
fossorial-flight	1.32	1.32	0.79	1.84	< 0.001	terrestrial quadruped-arboreal	0.23	-0.23	-0.25	-0.20	< 0.001
gliding-fossorial	1.26	1.26	0.74	1.79	< 0.001	terrestrial quadruped-semifossorial	0.22	0.22	0.19	0.24	< 0.001
gliding-arboreal	1.18	-1.18	-1.70	-0.66	< 0.001	fossorial-aquatic	0.21	-0.21	-0.23	-0.19	< 0.001
terrestrial biped-arboreal	1.04	-1.04	-1.57	-0.52	< 0.001	terrestrial quadruped-semiaquatic	0.18	0.18	0.16	0.21	< 0.001
semifossorial-arboreal	0.88	-0.88	-1.40	-0.35	< 0.001	scansorial-arboreal	0.18	-0.18	-0.20	-0.16	< 0.001
scansorial-arboreal	0.84	-0.84	-1.37	-0.32	< 0.001	semiaquatic-aquatic	0.18	0.18	0.16	0.20	< 0.001
terrestrial quadruped-arboreal	0.48	0.48	-0.05	1.00	0.107	terrestrial biped-scansorial	0.15	-0.15	-0.17	-0.13	< 0.001
scansorial-gliding	0.34	0.34	-0.19	0.86	0.569	semifossorial-aquatic	0.14	0.14	0.12	0.17	< 0.001
semifossorial-gliding	0.31	0.31	-0.22	0.83	0.705	terrestrial biped-semifossorial	0.11	0.11	0.09	0.13	< 0.001
terrestrial biped-scansorial	0.20	-0.20	-0.72	0.32	0.970	terrestrial quadruped-terrestrial biped	0.11	0.11	0.08	0.13	< 0.001
terrestrial biped-semifossorial	0.17	-0.17	-0.69	0.36	0.991	terrestrial biped-semiaquatic	0.08	0.08	0.05	0.10	< 0.001
terrestrial biped-gliding	0.14	0.14	-0.39	0.66	0.998	terrestrial quadruped-scansorial	0.04	-0.04	-0.07	-0.02	< 0.001
semifossorial-scansorial	0.03	-0.03	-0.56	0.49	1.000	semifossorial-semiaquatic	0.03	-0.03	-0.06	-0.01	< 0.001

Table S4.4. Principal components of trait optima. First four PC loadings of each morphological trait optimum (raw data).

	PC1	PC2	PC3	PC4
Humerus length	-0.169	0.124	-0.519	0.109
Humerus width	-0.329	-0.089	0.135	-0.259
Humerus height	-0.315	-0.185	0.203	-0.052
Radius length	-0.146	0.269	-0.569	0.024
Radius width	-0.356	0.031	0.017	-0.493
Radius height	-0.297	0.022	-0.022	-0.067
Metacarpal length	-0.147	0.560	0.268	0.590
Metacarpal width	-0.297	-0.135	0.148	0.219
Metacarpal height	-0.280	-0.151	0.186	0.213
Phalanx length	-0.206	0.527	0.022	-0.196
Phalanx width	-0.295	-0.225	0.070	0.215
Phalanx height	-0.251	-0.192	-0.107	0.275
Digit length	-0.175	0.361	0.279	-0.257
Body mass	-0.342	-0.137	-0.352	0.049
Eigenvalue	2.360	0.274	0.031	0.017
Var explained %	87.48	10.17	1.153	0.613

Table S4.5. Models of evolutionary transition between locomotor modes. Aqua = aquatic; Arb = arboreal; Fos = fossorial; Glid = gliding; Scan = scansorial; SemiAqua = semiaquatic; SemiFos = semi-fossorial; TB = terrestrial biped; TQ = terrestrial quadruped. Arrows indicate the direction of transitions that are allowed to occur.

Model of evolution	Transition rates	Transition pairs
ER	All rates equal	Transitions between all pairs allowed, in a same rate
Symmetric	Symmetric rates equal	Transitions between all pairs allowed
ARD	All rates different	Transitions between all pairs allowed, in different rates
Directional 1	All rates different	TQ → SemiAqua → Aqua TQ → SemiFos → Fos TQ → Scan → Arb → Glid → Flight TQ → TB
Directional 2	All rates different	TQ ←→ SemiAqua ←→ Aqua TQ ←→ SemiFos ←→ Fos TQ ←→ Scan ←→ Arb ←→ Glid ←→ Flight TQ ←→ TB
Directional 3	All rates different	TQ ←→ SemiAqua ←→ Aqua TQ ←→ SemiFos ←→ Fos TQ ←→ Scan ←→ Arb ←→ Glid ←→ Flight TQ ←→ TB SemiAqua ←→ SemiFos SemiAqua ←→ Scan SemiFos ←→ Scan

Table S4.6. Rates of morphological evolution per locomotor category (σ^2). The diagonals in grey indicate the average evolutionary rate for each locomotor mode, calculated with a multi-rate Brownian motion model (BMM). All evolutionary rates are multiplied by 100 to facilitate interpretation. Adjusted p-values from pairwise comparisons (Tukey test, 95% CI) are indicated and highlighted in bold when significant ($p<0.05$).

		aquatic	arboreal	flight	fossorial	gliding	scansorial	semiaquatic	semifossorial	terrestrial biped	terrestrial quadruped
raw	aquatic	0.954									
	arboreal	**<0.001**	0.188								
	flight	**<0.001**	**<0.001**	0.117							
	fossorial	**<0.001**	**<0.001**	**<0.001**	0.244						
	gliding	**<0.001**	**<0.001**	**<0.001**	0.992	0.248					
	scansorial	**<0.001**	**<0.001**	**<0.001**	**<0.001**	**<0.001**	0.216				
	semiaquatic	**<0.001**	**<0.001**	**<0.001**	0.704	0.123	**<0.001**	0.236			
	semifossorial	**<0.001**	**<0.001**	**<0.001**	**<0.001**	**<0.001**	0.867	**0.030**	0.222		
	terrestrial biped	**<0.001**	0.900	**<0.001**	**<0.001**	**<0.001**	**<0.001**	**<0.001**	**<0.001**	0.195	
	restrial quadruped	**<0.001**	**<0.001**	**<0.001**	0.026	**0.001**	0.028	0.878	0.734	**<0.001**	0.230
residual	aquatic	0.118									
	arboreal	**<0.001**	0.023								
	flight	**<0.001**	**<0.001**	0.015							
	fossorial	**<0.001**	**<0.001**	**<0.001**	0.030						
	gliding	**<0.001**	**0.005**	**<0.001**	**<0.001**	0.025					
	scansorial	**<0.001**	**<0.001**	**<0.001**	**<0.001**	0.769	0.025				
	semiaquatic	**<0.001**	**<0.001**	**<0.001**	**<0.001**	**<0.001**	**<0.001**	0.028			
	semifossorial	**<0.001**	**<0.001**	**<0.001**	**<0.001**	**<0.001**	0.132	**0.005**	0.027		
	terrestrial biped	**<0.001**	0.839	**<0.001**	**<0.001**	0.450	0.003	**<0.001**	**<0.001**	0.024	
	restrial quadruped	**<0.001**	**<0.001**	**<0.001**	**<0.001**	**<0.001**	**<0.001**	1.000	0.009	**<0.001**	0.028

Table S4.7. MCMC chain convergence with a Gelman and Rubin's diagnostic. Convergence was estimated between two among ten chains ran for the body size and limb shape evolution. Point est. = the points estimate; Upper CI = upper confidence limit; Multivariate psfr = point-estimate of the multivariate potential scale reduction factor.

	body mass		limb shape	
	Point est.	Upper CI	Point est.	Upper CI
Lh	1.00	1.00	1.02	1.10
Lh...Prior	1.00	1.00	1.00	1.00
No.Pram	1.00	1.00	1.00	1.02
Alpha	1.00	1.00	1.01	1.05
Sigma.2	1.06	1.09	1.00	1.02
Multivariate psrf		1.01		1.08

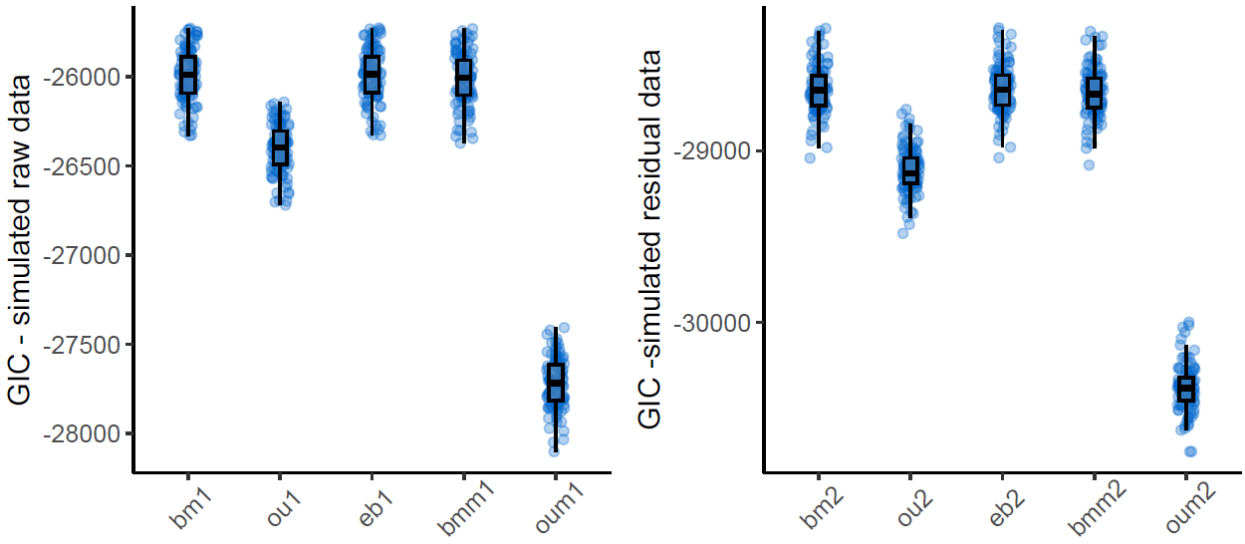

Figure S4.1. GIC scores from simulated data under Brownian motion evolution. The simulated traits were calculated using the parameters generated by the best fitted evolutionary model (OUM).

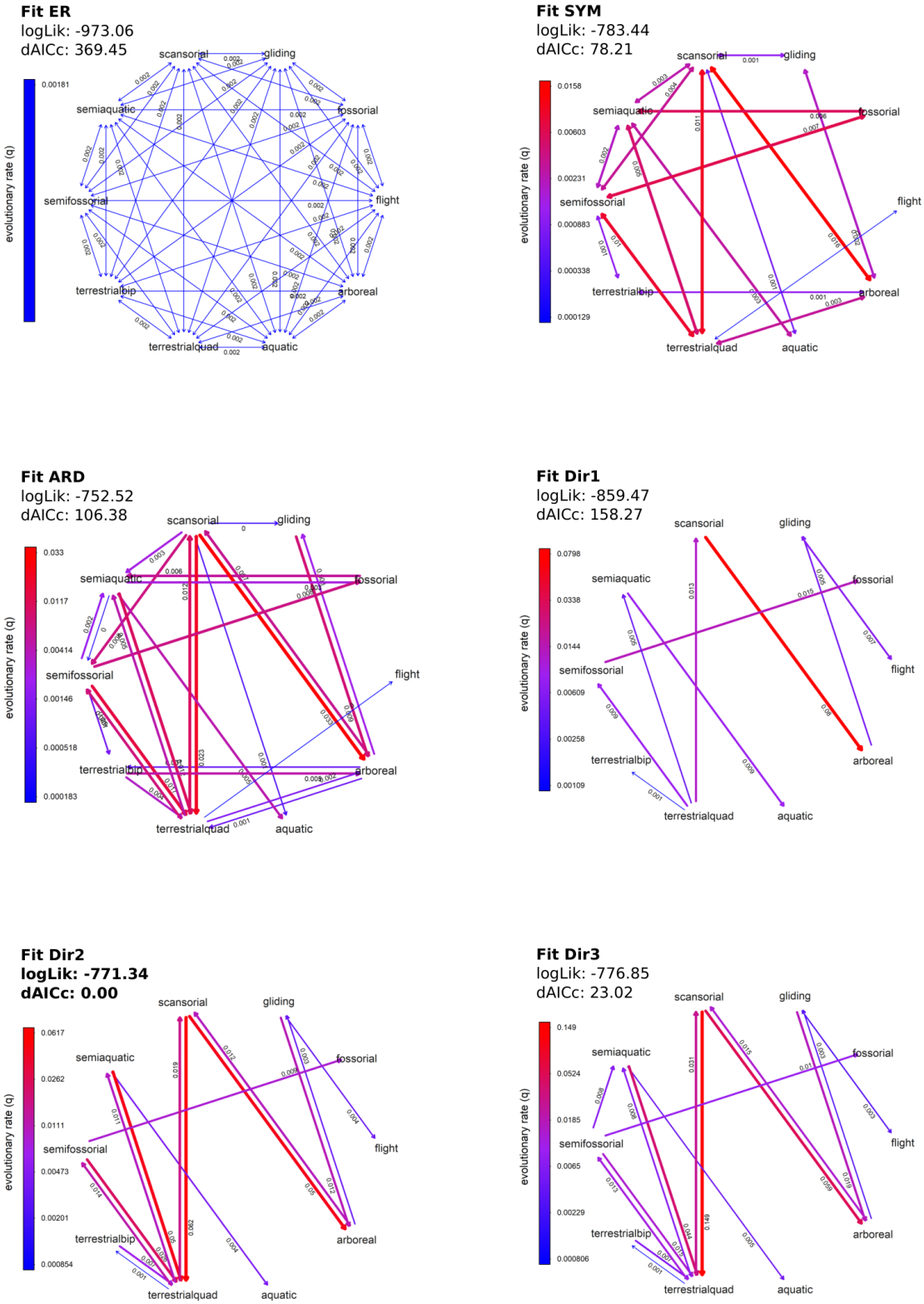

Figure S4.2. Fitted models of character transition. Evolutionary rate transitions (q) between locomotor modes calculated using different mapped states of character evolution, indicating the log likelihood (logLik) and the delta of the adjusted Akaike information criteria (dAICc). ER = equal-rates model; SYM = symmetrical model; ARD = all-rates-different model; Dir1 = directional model 1; Dir2 = directional model 2; Dir3 = directional model 3.

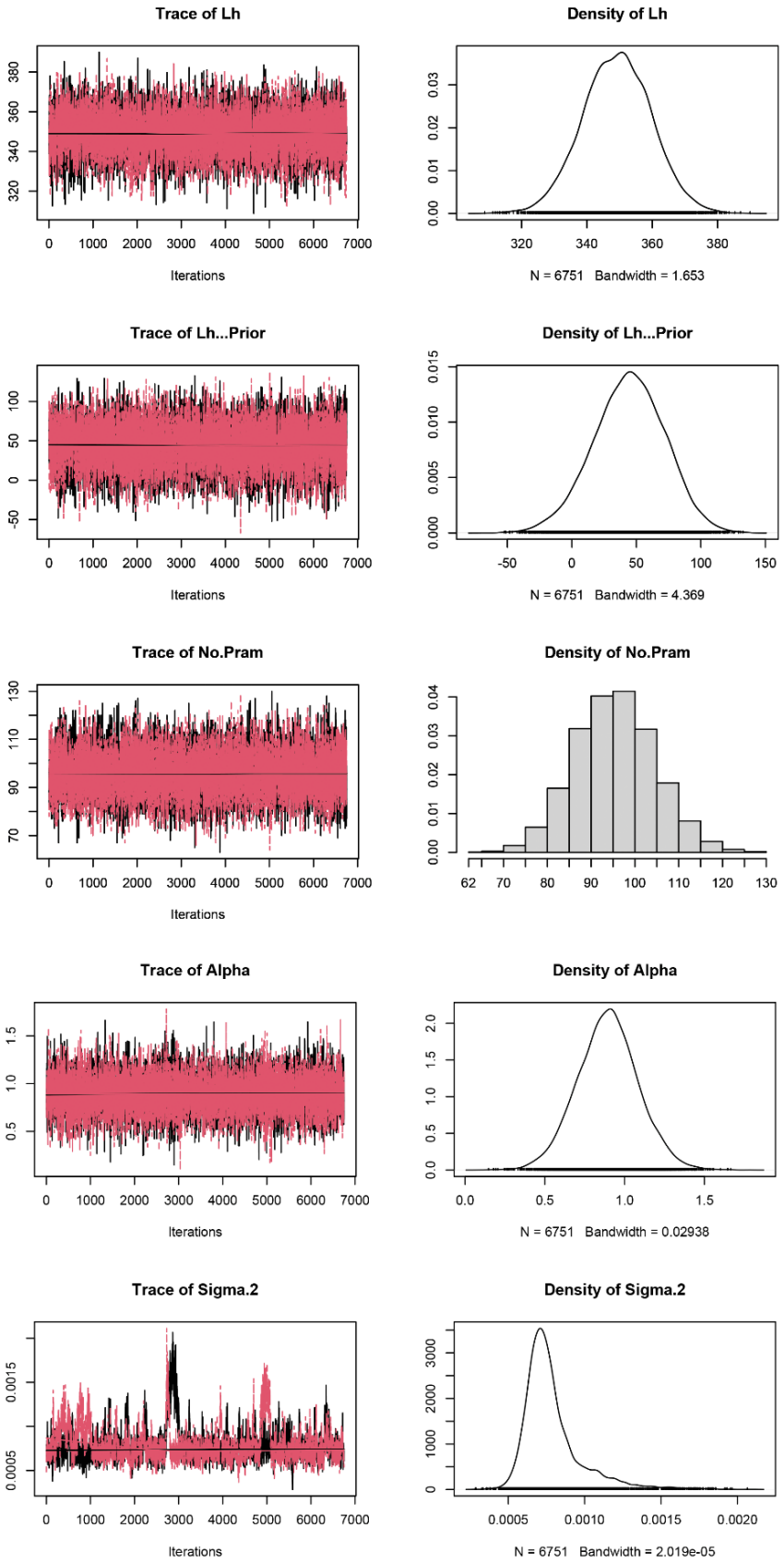

Figure S4.3. Trace plots for diagnosing MCMC chain convergence of the rates of body mass evolution. Comparison of the outputs of the two runs (black and red lines) with multivariate potential scale reduction factor closer to 1.0.

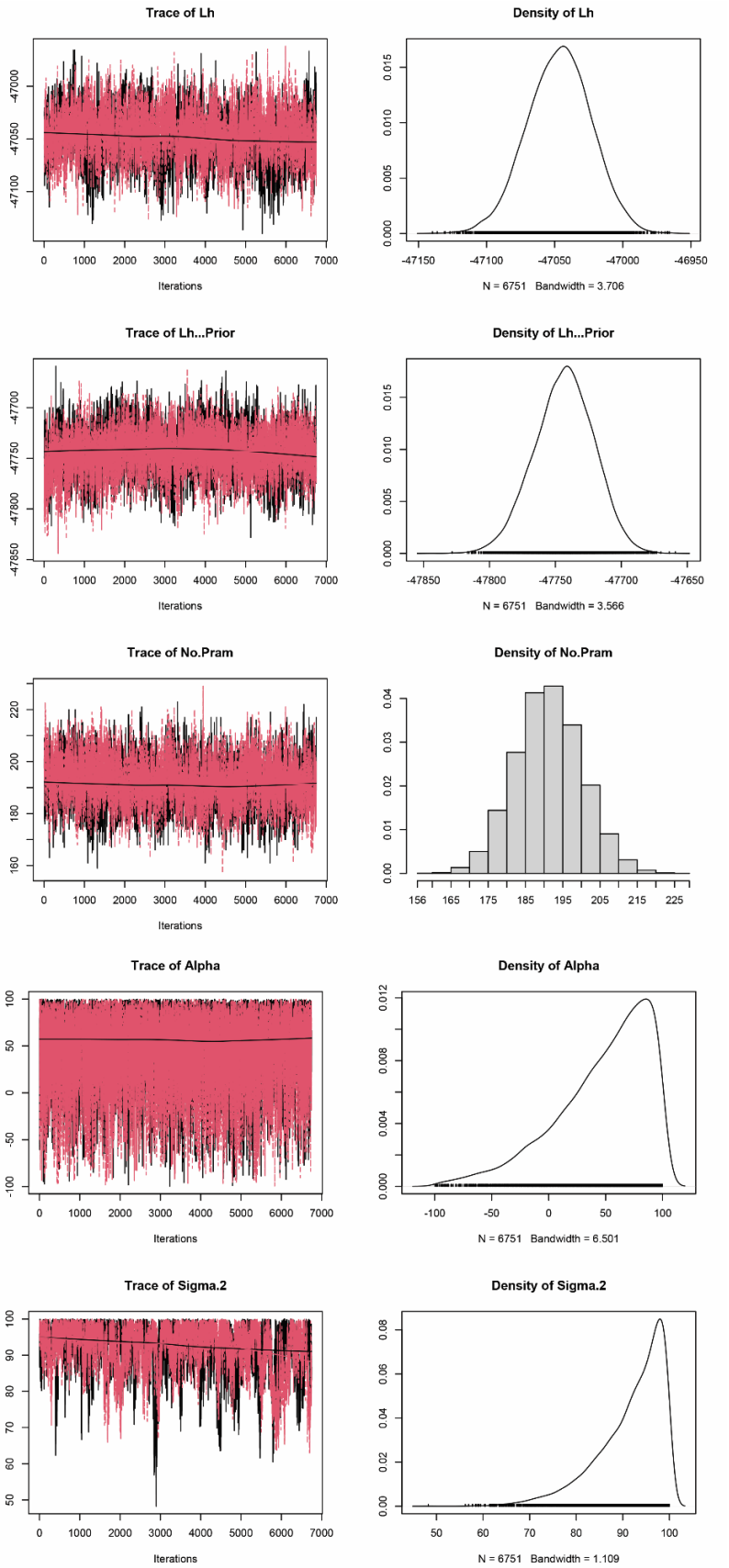

Figure S4.4. Trace plots for diagnosing MCMC chain convergence of the rates of limb shape evolution. Comparison of the outputs of the two runs (black and red lines) with multivariate potential scale reduction factor closer to 1.0.